June 20, 2025

Dear Reader,

The State of Washington Joint Legislative Task Force on Water Supply identified development of information on groundwater as a major gap limiting management of water resources in the Skagit River basin (Basin). Subsequently, the Washington State Water Research Center (WRC) conducted a synthesis study covering water resources availability and use in the Basin and developed specific knowledge gaps associated with various disciplines, including groundwater (Yoder et al. 2021). This study was developed with the goal of partially filling knowledge gaps identified in that synthesis study. Specifically, the study was intended to produce a more complete understanding of groundwater resources (relevant to future water supply and demand), how baseflow can best be characterized in the context of a basin water budget, and how groundwater is related to surface streamflow (and therefore aquatic habitat) in their watershed.

Western Washington University and HDR Engineering, Inc. (HDR) conducted the Skagit River Basin Groundwater Study (Study) in three parts, seeking to evaluate groundwater resources with a focus on the lower Skagit River valley, between Sedro-Woolley and Birdsview, in Skagit County. This reach was selected as a focal area because it has substantial groundwater resources and is in a part of the Basin likely facing future development pressure.  The first part of the Study evaluated the subsurface geology and aquifer characterization (Tasks 200 and 500) and documented this work in a MS thesis (Williams 2025). Although the MS thesis was produced by Henry Willaims at Western Washington University, his thesis advisor, Robert Mitchell, and committee member Jon Riedel serve as coauthors for this first part of the study. The second part of the study evaluated groundwater-surface water interactions via seepage run surveys and hydraulic gradients at paired gaging stations in a subset of the Part 1 Study area (Task 400). The third part of the Study assessed groundwater baseflow via hydrograph separation (Task 300).

Key Findings

- Aquifer characterization (Williams 2025) suggests the area is made up of complex geology. Data and monitoring validate aquifer continuity from the glacial outwash deposits in the eastern portion of the study area recharging Skagit River floodplain aquifers and the Skagit River. There may be no truly isolated aquifers in the upland area that would serve as an alternative water supply.

- The evaluation of groundwater/ surface water interaction indicate that both Grandy and Muddy Creeks gain flow from groundwater in their respective watersheds and then discharge flow to the aquifer associated with the Skagit River floodplain during the low-flow period. Both Grandy Creek and Muddy Creek gain flow from groundwater discharge from outwash deposits. Grandy gains more flow. Differences in groundwater gains were due to the presence and thickness of glacial outwash. Both streams lose flow on the Skagit River floodplain because of seepage into the alluvial aquifer.

- Hydrograph separation efforts (Task 300) used 44 gaging stations of daily streamflow data collected between 1908 and 2021 throughout the Basin, partitioning it into quickflow and baseflow (the latter is a proxy for groundwater discharge). From these and other data, this work offers a details and summary statistics of a wide set of water supply data, from precipitation to basin runoff, including components partitioned into groundwater recharge, and streamflow, and the portion of streamflow moving through the groundwater system and emerging in streams as baseflow, including the ratio of total baseflow to total streamflow (baseflow index; BFI). Two separate baseflow estimation techniques were evaluated and compared. Mean BFI values are 0.61 and 0.50 using the Baseflow Separation Model and Lyne-Hollick method (with alpha parameter equal to 0.98), respectively. Rather large differences in estimated groundwater discharge between subbasins and across the annual hydrograph are elucidated. About 85 percent of the subbasins analyzed have estimated groundwater discharge rates that are higher than the groundwater recharge rates derived from the Synthesis Study (Yoder et al. 2021).

The hydrogeologic framework and aquifer characterization serve as a basis for the region, although more detailed studies will be necessary to inform water resource management decisions going forward in the lower Skagit River Valley. Water resource managers should consider the documented connectivity among the upland aquifers, local streamflow, and subsequent discharge to the Skagit River alluvial aquifer. Finally, future Basin water balance models should consider these estimated baseflow rates when estimating recharge and when modeling supply and demand scenarios.

Sincerely,

Chad Wiseman (HDR)
Bob Mitchell (WWU)
Henry Williams (WWU)
John Riedel (WWU)
Nathan Rossman (HDR)

# Table of Contents

Spring 2025

# Aquifer Characterization in the lower Skagit River Valley, Northwest Washington State

Henry O. Williams
*Western Washington University*, hwms97@gmail.com

**Aquifer Characterization in the lower Skagit River Valley, Northwest Washington State**

By

Henry O. Williams

Accepted in Partial Completion

of the Requirements for the Degree

Master of Science

ADVISORY COMMITTEE

Dr. Robert Mitchell, Chair

Dr. Jon L. Riedel

Dr. Doug Clark

GRADUATE SCHOOL

David L. Patrick, Dean

**Aquifer Characterization in the lower Skagit River Valley, Northwest Washington State**

A Thesis

Presented to

The Faculty of

Western Washington University

In Partial Fulfillment

Of the Requirements for the Degree

Master of Science

By

Henry O. Williams

May 2025

**Abstract**

The Skagit River, its tributaries, and groundwater are important water resources for salmon habitat, agriculture, municipalities, and industries in the lower Skagit River basin. Unfortunately, these resources are threatened by receding glaciers and reduced meltwater due to a warming climate, compounded by increasing groundwater withdrawals driven by development and agricultural practices in the lowlands. Floodplain aquifers have been identified as a source of groundwater for the Skagit River and research has demonstrated that groundwater extracted from the floodplain reduces baseflow to the river which is problematic considering the instream flow rules established in 2001 for the Skagit River. Other potential sources for groundwater in the lower Skagit region are glacial outwash and glacial upland deposits north of the floodplain identified by recent geologic mapping. For water resources management purposes, it is important to characterize the aquifers in the glacial terraces and uplands and determine their connection to the floodplain and the Skagit River.

To characterize the hydrogeologic framework in the lower Skagit Valley, I synthesized well log data, gravel pit and natural stream exposures, recent geomorphic mapping and hydrogeologic studies, borehole data, and LiDAR data and developed two-dimensional (2D) cross sections and 3D conceptual models between Sedro-Woolley and Birdsview, WA. My results reveal a complex geology that differentiates six different hydrogeologic units. Glacial deposits dominate most of the upland aquifers, with lahars and alluvium composing most of the floodplain, with sedimentary and metamorphic rocks at higher elevations. My hydrogeologic framework indicates that glacial outwash deposits in the eastern portion of the study area are connected to and recharging Skagit floodplain aquifers and the Skagit River. The aquifer continuity in the east is also validated by groundwater monitoring data and seepage runs results. There are likely low rates of groundwater flow from the low-conductive units in the uplands to the floodplain deposits in the western half of the study area, meaning that there may be no truly isolated aquifers in the upland area that would serve as an alternative water supply. The hydrogeologic framework serves as a basis for the region, however, more detailed studies will be necessary to inform water resource management decisions going forward in the lower Skagit River Valley, i.e., more extensive well monitoring, long-term pump tests, and groundwater modeling to constrain recharge rates and groundwater flow directions and rates in the study area.

**Acknowledgements**

Funding for this project came from the State of Washington Joint Legislative Task Force on Water Supply though the Washington State Department of Ecology in collaboration with Western Washington University and HDR, Inc. I was also supported for two years by a teaching assistantship from the Geology Department and a Nadine L. Romero Graduate Scholarship from the 2024 Washington Hydrogeology Symposium allowed me to continue my work through the summer of 2024. The financial assistance allowed me to focus on this research and the incredible learning experience it has afforded me.

I have many to thank for all their guidance and support during this two-year journey. A huge thank you to my thesis advisor Dr. Robert J. Mitchell for his relentless efforts during my thesis process. He was always ready to respond to me whether he was on sabbatical or was busy grading at the end of a semester. The time and attention he provided was amazing, especially with the writing of this thesis. I have learned so much from him and will always be truly blessed to have learned from someone who is committed to research and this field as much as him. I also want to thank my committee including Doug Clark for sharing his glacial knowledge (and awesome field trips) and Jon Riedel for sharing his extensive knowledge of the Skagit Valley's glacial history. I also thank them for their comments and suggestions in the writing of my thesis. I also really appreciated the support and attention my project received from Chad Wiseman at HDR, Inc.  My research was also supported by three landowners in the Skagit Valley who tolerated our intrusions and donated their precious water usage data every month for well monitoring.

A big thanks also to my fellow graduate students in the Western Washington University Geology Department, particularly Brian Pinke, Jonathan Chan, Taylor McCombs, Josh Sayre, Carlos Jimenez-Diaz, Teagan Maher, and everyone who shared your friendship and comradery on campus and on Friday "Happy Hours" in Bellingham. You helped me stay sane and always encouraged me. I also want to give special thanks to all my students in GEOL 213 whose questions pushed me to expand my understanding of ArcGIS. A final thanks to my parents Greg and Susan, and my sister Kate for always believing in me and for being there during my darkest days. They know when to encourage me and when I need to be reminded to "just deal with it." They also shared their own graduate school experiences, proofing, organization, and graphic design skills. They all modeled that strong midwestern work ethic that propelled me to get these hours of work completed. I also cannot forget to thank Louie, our little family rescue dog who always gets excited just hearing my voice and loses his mind with delight when he sees me, whether I am gone for 2 months or 15 minutes! Thank you all. I could not have done it without all of you!

## Table of Contents

## List of Tables

## List of Figures

## 1.0 Introduction

My study was motivated by the State of Washington Joint Legislative Task Force on Water Supply, which identified groundwater impacts on regulated instream flows as a major gap limiting management of water resources in the lower Skagit River basin. The Skagit River, its tributaries, and groundwater are important water resources for salmon habitat, agriculture, municipalities, and industries in the lower Skagit basin between Sedro Wolley and Birdsview, WA (Figure 1). These resources, however, are threatened by receding glaciers, receding snowpack and reduced meltwater due to a warming climate, compounded by increasing groundwater withdrawals driven by development and agricultural practices in the basin (Frans, et al., 2018). Prior research by the United States Geological Survey (USGS) and others demonstrate that groundwater extracted near the Skagit River floodplain reduces baseflow to the river (Savoca et al., 2009a and 2009b; HDR 2017; HDR 2019). This is problematic because since 2001, the Skagit River has been under instream flow rules that restrict groundwater and surface water usage (WADOE, 2023a). Instream flow rules were established in part to ensure adequate streamflow to support salmon habitat and the guaranteed fishing rights of the Samish Indian Nation, Upper Skagit and Swinomish Indian Tribes in the Skagit Valley. Floodplain aquifers have been identified as a source of groundwater for the Skagit River and geologic mapping has also identified glacial outwash deposits in the glacial terraces and uplands just north of the floodplain that likely conduct water (Figure 1; Dragovich et al., 1999; Hidaka, 1973). However, the connection between these aquifer systems is poorly understood. For management purposes, it is important to understand how such aquifers that are perched above the alluvial deposits in the floodplain contribute to the Skagit River and its tributaries and whether those aquifers are inter-connected.

In this study, I developed a hydrogeologic framework to better characterize the groundwater resources in the lower Skagit Valley. I synthesized well-log data, gravel pit and natural stream exposures, recent geomorphic mapping and hydrogeologic studies, borehole data, and LiDAR data to create two-dimensional (2D) cross sections and three-dimensional (3D) conceptual models of the hydrogeologic framework to characterize the glacial terraces, glacial upland, and floodplain deposits east of Sedro-Woolley to Birdsview, WA (Figure 1). I used the framework to constrain the connection between glacial and floodplain aquifers and to test the hypothesis that the glacial aquifers are disconnected from the floodplain aquifers and can be used as a water resource without negatively impacting tributary and river streamflows.

## 2.0 Background

### 2.1 Study Area

The study area compromises the lower Skagit Valley, ranging from east of Sedro-Woolley to Birdsview, WA (Figure 1). The lower Skagit Valley is developed with several small communities and private residences and is used intensively for agriculture. The Skagit River and surrounding landscape have been altered from their natural, original conditions by the installation of hydroelectric dams, erosion control structures, levees, and extensive logging. My study focuses on a sequence of mostly glaciated uplands, glacial outwash terraces, and alluvial deposits just north of the Skagit River floodplain in the northern part of the study area (Figure 1 and Figure 2).

It should also be noted that Figure 2 has some spatial inaccuracies in the geologic units and is used to illustrate the general surficial geology of the study area (WADNR, 2016). More refined geologic interpretations are illustrated in my 2D cross sections and 3D conceptual models in the model boundaries in my results section (Figure 3). Also, to simplify glacial landforms, northwestern glacial deposits within Boundaries A and B are referred to as glacial uplands due to high elevation, uneven, sub-glacial fluted till surfaces, and being underlain by bedrock. Areas in the northeastern glacial deposits within Boundaries C and D are dominated by glacial outwash terraces and include some elevated sub-glacial fluted till surfaces and some moraines (i.e. glacial terraces; Figure 1 and Figure 2). When referring to both glacial terraces and glacial uplands, I will use glacial area or glacial aquifer. Finally, valley walls include everything at higher elevations above the glacial uplands or glacial terraces. The glacial uplands and glacial terraces exist between the northern valley walls and the southern floodplain.

### 2.2 Climate and Hydrologic Conditions

The Skagit River basin drains 3,115 square miles in Canada and northwestern Washington State, and discharges into Skagit Bay west of Mt Vernon (Figure 1). Relief in the watershed varies from sea level at the mouth to 10,786 ft at the top of Mt. Baker and 10,541 ft at the top of Glacier Peak. Flow in the Skagit River is supported by glacier meltwater, seasonal precipitation, runoff, and groundwater, and is managed by five major dams (Gorge, Diablo, Ross, Upper and Lower Baker). The average annual river discharge near Mt. Vernon, WA is about 16,500 cfs, with an average annual minimum of 10,500 cfs, and average annual maximum of 23,140 cfs (USACE, 2013; Drost and Lombard, 1978). The hydrologic conditions of the river support five species of salmon that pass through the river annually. In particular, the Skagit River supports the largest run of Chinook Salmon in the Puget Sound and the largest runs of Pink and Chum Salmon in the United States (Connor and Pflug, 2004). Some species of salmon like Chinook are threatened in the watershed because of agricultural, fishing, pollution, and civil works (Lee and Hamlet, 2011).

The Skagit River basin has a maritime climate with wet, cool, humid winters, and mild, dry summers in lower elevations, and higher elevations have colder climates that support glaciers. Sedro-Woolley, west of my study area, has a 30-year average annual precipitation of 46.6 inches, and about 75% occurs between October-April (Table 1). Due to orographic effects, the higher elevations can receive 140 to >180 inches of precipitation according to the 1991-2020 normal (PRISM, 2024). Savoca et al. (2009a) suggest that about 35% of the annual precipitation in the Nookachamps region (east of Mount Vernon and south of Sedro-Woolley (Figure 1) goes to surface runoff, 32% is lost from evapotranspiration, and 33% becomes groundwater recharge.

The Skagit basin is located in the North Cascade Mountain range which has about 72 square miles of glaciers (Fountain et al., 2023). Glaciers and groundwater are critical river base-flow sources to the Skagit River during the relatively dry summers as snow melt diminishes. All the glacier runoff is a combination of seasonal snow, firn, and glacial ice (Riedel and Larrabee, 2016). Of concern is that glaciers have been receding in the Skagit basin. Between 1959 to 2009, glacier recession due to a warming climate has caused a 24% decrease in glacier contributions to summer streamflow- resulting in higher reliance on groundwater to support baseflows (Riedel and Larrabee, 2016). Furthermore, a projected warming climate will cause glaciers to recede by as much as 50% by 2050 (Bandaragoda et al., 2015; Frans et at., 2018). Precipitation is also projected to decrease by five to 20 percent in summers by 2050, further decreasing future summer streamflow which will place a strain on Indigenous communities, farmers, salmon runs, and other municipal and industrial water users, coincident with groundwater withdrawal increases due to projected development (Frans et al., 2018; Roop et al., 2020).

### 2.3 Geological and Glacial History

Although the majority of the surface and subsurface of the study area is dominated by glacial deposits from the late Quaternary, bedrock, including the Jurassic Darrington Phyllite and the Eocene Chuckanut Formation, also influences the groundwater (WADNR, 2016). The Darrington Phyllite underwent subduction-related blueschist metamorphism (Dunham, 2010). The Darrington phyllite covers all the northern valley walls within the study area (Figure 2). The Chuckanut Formation (sandstone, shale, siltstone, and coal beds) deposited ~50 Ma makes up a majority of the sedimentary bedrock underlying the glacial uplands below the valley walls (Mustoe and Gannaway, 1997; WADNR, 2024). Sedimentary rocks of the Chuckanut Formation are located on the west side of the glacial uplands between east Sedro-Wolley and Lyman and are mostly covered by glacial deposits with some isolated surficial exposure (Figure 2).

Pleistocene glaciation in the North Cascades likely began sometime in the early Quaternary after 2.6 Ma (Haugerud and Tabor, 2009). During this time, glacial erosion and deposition altered the western Cascades and created the modern Skagit River watershed (Riedel et al., 2007). The valley, as it exists today, was strongly shaped between ~29-11.7 ka during the last major glaciation that included both alpine glaciers and the Cordilleran ice sheet (Riedel, 2017). The alpine glaciers and continental ice sheets had separate accumulation zones and advanced and receded in two different stades (Armstrong et al., 1965). Glacier fluctuations and the advance of alpine glaciers blocked the valley resulting in a large glacier lake forming in the lower Skagit Valley floor (Riedel et al., 2010). The advance of the continental ice sheet especially influenced the complex sequence of glacial deposits on the north side of the valley within the study area mantling the glacial uplands in drift and forming extensive glacial outwash terraces (Figure 1). The eastern portion of the glacial terrace (Figure 2) is a result of the damming and glaciation of the valley by the Cordilleran ice sheet (Riedel, 2017). Overall, however, nearly all the glacial geology in my study area is a result of the Cordilleran ice sheet on both east and west sides of the study area.

Starting about 29 ka and during the Evans Creek Stade, alpine glaciers dominated most of the valley's mountain area outside my study area but started to retreat by 21 ka and were absent from the lower Skagit by the time the continental ice sheet arrived during the subsequent Vashon Stade (Riedel et al., 2010). Between 18-16 ka, the Cordilleran ice sheet advanced into the basin (initially from the west), depositing advanced glaciolacustrine, advanced glacial outwash, and glacial till, and by 15 ka began to retreat from the valley leaving behind a complex sequence of basal till and recessional outwash (Armstrong et al., 1965; Riedel, 2017). Outwash and till are exposed on the east side of the glacial terraces (Figure 2). Glaciolacustrine deposits are found in driller well logs in the sub-surface, lower Grandy Creek, along Skagit River near Cape Horn, and road cuts on Highway 20. The western portion of glacial area, known as the glacial uplands, is quite different including glaciolacustrine deposits as well as glaciomarine deposits from the marine waters that flooded the valley to elevations of ~100 m 13.6 ka (Dethier et al., 1995).

The Skagit floodplain also developed with Holocene alluvium. During this development of the floodplain, the Skagit River cut through the glacial deposits at the end of the ice age likely from outburst floods (Riedel et al., 2020). In addition to the modern valley shaped by erosion and deposition related to two episodes of glaciation, the Skagit Valley was also affected by Glacier Peak volcanic eruptions and lahars. About 13,700 years ago, a lahar discharged to the Puget Sound via the Stillaguamish River, but did not flow into the Skagit River (Vallance, 2015). Over the past 6,000 years, there have been two more lahars, one occurring around 6,000 years ago, rerouting the Sauk River to the Skagit River and depositing ~50 ft of lahar deposits and another one 2,000 years ago depositing ~30 ft of lahar deposits (Beget, 1982; Dragovich and McKay, 2000; Dragovich et al., 2002). Mt Baker erupted 13,000 and 9,500 years ago, but these had little apparent effect on the recent history of the Skagit River (Scott et al., 2020).

### 2.4 Recent Hydrogeologic Studies

Due to the concerns of groundwater withdrawals on instream flows in the basin, several hydrogeologic studies were conducted near the study area to better characterize groundwater movement and groundwater-surface water interactions (HDR, 2017 and 2019; Savoca et al., 2009a; Geoengineers 2003; Hidaka 1973). Due to the 2001 instream flow rule, the basin is closed to new groundwater wells unless the State Department of Ecology approves a plan for mitigation or a plan for reliance on an alternative water source during times when the minimum instream flow requirements are not met. Regardless of how small the effects, new wells could be denied by the state if they impair minimum instream flows.

HDR (2017) examined the lower Skagit River basin floodplain in the eastern half of my study area (Lyman to Grandy Creek) and tested groundwater depletion via a streamflow model developed to determine streamflow depletion from groundwater pumping to help aid in Washington State Department of Ecology's (WADOE) water rights mitigation program (Figure 2). They also used well logs and cross sections to help aid in the development of the groundwater flow numerical model. HDR (2017) identified two hydrogeologic units in the floodplain, a surface-level unconfined aquifer defined by near surface alluvial deposits and deeper unconfined aquifers mostly of sand and gravel and reaching 0-100 ft in depth and about 100 ft thick; and deep confining unit or confined aquifer defined by fine grained silt-clay lacustrine deposit that is about 100 ft thick. Nearly all wells simulated in their grounwater model, pumped water from the unconfined aquifers. HDR (2017) suggested that pumping water 600 ft away from the Skagit River can result in about 90% of the pumped water being redirected from flowing into the Skagit River. Wells further away from the Skagit River can pull about 75% of their water from the Skagit River if no tributaries are nearby, while wells near tributaries get 50-75% of capture from the tributary (HDR, 2017).

HDR (2019) examined the floodplain near the river to determine if aquifers in the floodplain and potentially in the glacial terraces are connected to the Skagit River. They created five cross sections, one near Grandy Creek (Figure 2), and the other cross sections farther east outside my study area. HDR (2019) reported that the Grandy Creek aquifers in both the floodplain and glacial terraces, and the four other cross sections are moderately connected, and do not have large lateral gaps. They concluded that even deeper confined aquifers, though more disconnected, could still add to some streamflow loss due to leaky confining units (HDR, 2019).

Savoca et al. (2009a) examined the glacial terraces and the floodplain just southwest of Sedro-Woolley in the Nookachamps sub-basin (Figure 1). They defined many of the same glacial units found in my study area and created a hydrogeologic framework. Their defined hydrogeologic units included: 1) unconsolidated aquifers alluvium, advance glacial outwash, recessional glacial outwash, glaciomarine outwash, and alluvial fan (Figure 2), which typically consist of moderately to well-sorted alluvial and glacial outwash deposits composed of sand and cobble gravel, with minor lenses of silt and clay and high hydraulic conductivities; and 2) confining units that serve as aquitards typically consist of units having low hydraulic conductivities such as unconsolidated poorly sorted compacted glacial till, and glaciolacustrine containing mostly fine grained material such as clay and silt with limited sand and gravel and (3) igneous and metamorphic bedrock unit, that serve as aquicludes and 4) sedimentary aquifer units consisting of cobble conglomerate and medium coarse grain sandstone with intervals of fine grained shale, siltstone and even mudstone (Savoca et al., 2009a).

Savoca et al. (2009a) calculated hydraulic conductivities for these units, with unconsolidated aquifers ranging from 47-48 ft per day, confining units ranging from 13-26 ft per day, bedrock units about 0.13 ft per day, and sedimentary bedrock aquifer units 0.27 ft per day. They also determined that the average annual recharge was about 18 inches per year from precipitation. Of that recharge, about 65% discharges to streams, 32% to the Skagit River and three percent extracted from wells. They also suggested that large contributions of water from tributaries to major creeks is groundwater discharging from aquifers overlying shallow bedrock that exist in the glacial uplands (Savoca et al., 2009a).

Geoengineers (2003) examined the hydrogeology of the Samish River sub-basin northwest of Sedro-Woolley and determined the groundwater-surface water interaction, evaluated streamflow conditions, and modeled different types of water usage (Figure 1). They defined six hydrogeologic units and found that most of the wells tap an unconfined outwash and alluvium aquifer that is about 10-100 ft thick. They also determined that 80% of water demand comes from groundwater pumping and is mostly used for irrigation purposes. In particular, higher elevation areas (glacial uplands) had less groundwater use, while the lower elevation basin (floodplains) experienced more groundwater usage and instances of streamflow depletion. Geoengineers (2003) concluded that increased groundwater usage will significantly decrease Samish River instream flows.

Hidaka (1973) examined streams across Puget Sound to determine how low flow conditions occur and how geologic, climate, and topographic characteristics can lead to low flow conditions. Multiple streams were examined using multiple different methods to determine these characteristics. One of these streams includes Alder Creek in my study area (Figure 2). Hidaka (1973) determined Alder Creek had groundwater contributing to inflows in the late summer due to permeable glacial deposits in the subsurface. Precipitation could also easily infiltrate the surface due to these permeable glacial deposits that were also unconsolidated at and below the surface. Hidaka (1973) also determined Alder Creek's head of the stream is found at high altitudes with a abundance of precipitation contributing to its flows.

### 2.5 Project Objective

The purpose of my project is to build upon these previous studies in the lower Skagit River basin to further characterize alluvial aquifers and glacial aquifers in the glacial deposits forming the glacial uplands and glacial terraces between Sedro-Woolley and Birdsview, WA (Figure 1 and Figure 2). My findings will serve as a basis to guide future studies regarding water resource management decisions to sustain instream flows, especially as the climate warms. Glacial aquifers may be recharging the floodplain aquifers, so groundwater withdrawals in the glacial aquifers could influence baseflows in adjacent tributaries and the Skagit River. Conversely, isolated confined glacial aquifers may not influence surface water and may serve as possible groundwater resources.

## 3.0 Methodologies

To characterize the aquifer system in the lower Skagit Valley and to determine the connection between floodplain aquifers and the glacial terrace aquifers, I developed a hydrogeologic framework using driller well-log data, surficial geologic maps, recent geomorphic mapping and hydrogeologic studies, deep borehole data, LiDAR, and ArcGIS software tools. I took these steps to build the framework:

- Created a well log database that includes thoroughly selected and relocated well logs from the Washington State Department of Ecology database (WADOE, 2023b).
- Characterized the glacial terraces and glacial uplands using related literature and field visits and the well-log database.
- Located a site for the drilling of a new 310-foot monitoring well installed to improve stratigraphic interpretation of the sub-surface.
- Estimated hydraulic conductivity of various geologic and glacial deposits from well log pump-test data.
- Identified geologic units and hydrogeologic units.

- Created 2D cross sections and 3D hydrogeologic conceptual models using hydrogeologic units developed from geologic units.
- Monitored water levels in wells in the glacial terraces and floodplain to observe water table changes over time.
- Approximated annual recharge of various hydrogeologic units and landcovers throughout the study area.
- Characterized streams as gaining or losing streams based on seepage run and stream piezometer data.

3.1 Well Log Database

Most of the sub-surface geology was interpreted from driller well logs acquired from the well log database maintained by the WADOE (WADOE, 2023b). A shapefile of Washington State well locations was downloaded from Ecology's Geographic Information System (GIS) Data Download website (WADOE, 2022) and imported into ArcGIS Pro. The WADOE Well Report Viewer was used to download well reports (logs) that provide the location, ownership, construction details, and logs of formation materials (grain size) encountered at depths during drilling (WADOE, 2023b). Some well logs also contain information including screen length, pumping rate, and drawdown which is useful for estimating the hydraulic conductivities of the glacial and alluvial deposits.

There is a range of well depths in the floodplain, glacial uplands and glacial terraces and I attempted to identify as many deep wells as possible to characterize the underlying stratigraphy. Wells in the floodplain ranged from 10 to 200 ft deep, with an average depth of ~20 ft. Wells in the glacial terraces and uplands vary from 30-500 ft deep with an average depth of ~60 ft. The deepest wells selected in the floodplain are greater than 40 ft deep, while the deepest wells selected in the glacial terraces and uplands are greater than 100 ft deep.

Information collected from each well log included the well ID number, year drilled, name of owner, depth of well, geology, and grain size at specified depths. Each well log in the database was checked for locational accuracy by first looking at the township section and range (TSR) which display the location of a well within a quarter mile square. Each well log also contains information on the well owner at the time the well was drilled, and some well logs also include address information. The WADOE used the TSR from the well log to place wells on GIS maps

(WADOE, 2023b). Unfortunately, the TSR recorded well locations were commonly incorrect by a few feet to thousands of yards from their actual locations. Some wells were even located in the wrong county. To mitigate these locational errors, addresses from the well logs were used instead of the TSR. The Skagit County survey site was used to identify the address of each well log where possible (Skagit County, 2024a). Once an address was located, it was cross referenced with the tax parcel on the Skagit County IMap tool (Skagit County, 2024b). Once the address was confirmed, the well location was accurately recorded in ArcGIS Pro for conceptual modeling (Figure 2).

After verifying locational accuracy and relocating the wells in ArcGIS Pro, the updated spatial information was included in the database. Wells with incomplete information or material interpretations, illegible information, or unverifiable locations were not included in the database. Wells used for hydraulic conductivity estimates (Figure 3) were not relocated due to the overwhelming number of wells used in these calculations. The well data were then placed in GIS software overlaying mosaiced 2017 Puget Sound LiDAR digital terrain model (DTM) raster data (Lowe, 2017), the most recent bare-earth DEM data available. Well elevations were then recorded using this DTM. Material descriptions were further simplified into different grain sizes, including gravel, sand, silt, clay, gravel sand, gravel clay, sand clay, and bedrock.

### 3.2 Field Work and New 310-foot Well

Well logs provided most of the data for the study area, but some locations lacked domestic well information, particularly in the glacial area between Lyman and Hamilton, WA (Figure 2). Additional field work was required to better characterize the geology of these areas. Between April-June 2024, I collected field observations with Jon Riedel to characterize the sub-surface via exposures along the streams and the glacial area, observations from available surface map data, gravel pits, and proximity with the other wells.

There were very few deep wells in the glacial terraces of the study area (Figure 2). Fortunately, the state research budget allowed for the drilling of a new deep well to inform stratigraphic interpretations and water-level observations. Based on initial ArcGIS screening, ease of access, and field visits, a location was chosen on Washington State Department of Natural Resources (WADNR) land near Alder Creek in the central portion of the study area where deep-well information was lacking (Figure 2). A WADNR permit was secured, and a 310-

foot-deep monitoring well was hydraulically drilled in late March 2023. The wellhead is at 300 ft elevation (estimated from LiDAR), placing the bottom of the well 10 ft below sea level and 100 ft below the Skagit River. A professional geologist was on site during the drilling and produced a highly detailed geological well log (Appendix C) that was later classified into interpreted hydro stratigraphic units based on textural descriptions (e.g., gravel, sand, silt, and clay). The well log interpretation is explained in the results.

### 3.3 Hydraulic Conductivity Estimates

I estimated the hydraulic conductivities of different geologic deposits to group deposits into hydrogeologic units. When long-term pump test data are not available, an economic approach is to use drillers pump test data from domestic well logs and the relations below commonly used by the USGS in regional studies (e.g., Kahle and Olsen, 1995; Gendaszek, 2014). The pump test data from driller well logs (used to estimate specific capacity) were used in a modified Theis equation (Ferris et al., 1962) to estimate the horizontal hydraulic conductivity in the vicinity of a well. Well logs in Ecology's database that contained pump-test data, i.e., drawdown, pumping rate, and duration; and well screen length and radius were used in the analysis. The modified Theis equation is given as:

$$s = \frac{Q}{4\pi T} \ln \frac{2.25Tt}{r^2 S} \qquad (1)$$

where s = drawdown (ft), Q = pumping rate (cfm), t = time (minutes), r = well radius (ft), S = storativity (dimensionless) and T is the aquifer transmissivity ($ft^2$/minute). Equation (1) is algebraically transcendental, so T is iteratively determined using a root solver in a Python script (Mitchell, 2023) given an estimated value for the storativity (S). I used well log material descriptions and whether the well was in an unconfined or confined aquifer to determine the storativity. Generally, confined aquifers have a storativity coefficient of 0.0001 to 0.001 if substantial clay or other confining units (like shale or sandstone) are present. Unconfined aquifers have a storativity coefficient ranging between 0.01 to 0.1 and have sand and gravel grain sizes throughout the well logs with little clay. The horizonal hydraulic conductivity was determined from the iteratively resolved T value using the relation below.

$$K_h = \frac{T}{b} 1440 \qquad (2)$$

$K_h$ = horizontal hydraulic conductivity (ft/day), T = transmissivity ($ft^2$/minute), b = length of well screen (ft), 1440 = minutes in a day (Kahle and Olsen, 1995).

If no well screen is given in the well log, then the expression below was used to estimate the horizontal hydraulic conductivity for wells with openings at the end of the well (Bear, 1979).

$$K_h = \frac{Q}{4\pi sr} 1440 \qquad (3)$$

$K_h$ = horizontal hydraulic conductivity (ft/day), Q = discharge (cfm), s = drawdown (ft), r = radius of the well (ft), 1440 = minutes in a day. Storativity and time are not required for this equation and this equation assumes that vertical and horizontal conductivity are the same, which is not likely with unconsolidated deposits (Kahle and Olsen, 1995).

To reduce the influence of outlying K values, geometric means were used for the generalized mean hydraulic conductivity of a geologic unit. Wells were then mapped and symbolized based on the geologic unit in which the pump tests were completed (Figure 3).

### 3.4 Creating Geologic Units and Hydrogeologic Units

Well data were put into the Aquaveo Arc-Hydro Groundwater Subsurface Analyst (3.5.0) and geologic units were created using well-log interpreted grain sizes (Aquaveo, 2024). These geologic units were further refined to include similar elevations and depths and the surficial deposit descriptions on the surficial maps (Dragovich et al., 1999, Riedel 2024a). Following Freeze and Cherry (1979), multiple geologic units having similar lithologies and hydraulic conductivities, stratigraphic position, and depth (confined or unconfined) were combined into hydrogeologic units. Note that the hydrogeologic units will not necessarily match the geologic units because groundwater flow is determined by grain size (hydraulic conductivity), not by the geologic unit.

### 3.5 2D Cross Sections and 3D Hydrogeologic Conceptual Models

I used Aquaveo Arc-Hydro Groundwater Subsurface Analyst (3.5.0) to develop 2D cross sections and 3D conceptual models of the hydrostratigraphy in the study area. Aquaveo Arc-Hydro Groundwater Subsurface Analyst is an add-on tool for ESRI's ArcMap (10.8) that allows well information to be placed in a 3D environment that can be formatted to display 3D aquifer units after 2D cross sections are created to connect the well-log stratigraphy (Aquaveo, 2024).

The final product is a series of 3D conceptual models of the hydrogeologic framework of the study area. Aquaveo has other add-on tools including MODFLOW (USGS, 2025) that is a 3D numerical groundwater flow model, but groundwater modeling is beyond the scope of my study. Below are the steps used to create the conceptual models.

Data for conceptual modeling were gathered and placed into different programs from the well log database. Three MS Excel files were created that included locational data on each well, characteristics from each well, and defined hydrogeologic units. In ArcGIS Pro, I created raster and vector datasets using the North Puget 2017 DTM survey including a point shapefile of the wells with information on location, elevation, and depth of the well. The data sets were then placed in an ArcScene project (Lowe, 2017). The tutorial provided by Aquaveo was followed to place the wells and display their units by depth. Wells were examined and 2D cross sections pathways were manually created in ArcMap using wells along a desired pathway. The similar units between the wells were connected in the cross sections and then the 2D cross sections were placed back into ArcScene as 3D fence diagrams. The 3D conceptual models showing various hydrogeologic units and their extents were created by interpolating the 2D cross sections. I did this for four model boundaries across my study area (Figure 2). These boundaries include: Sedro-Woolley to Cokedale (Boundary A), Cokedale to Lyman (Boundary B), Lyman to West Muddy Creek (Boundary C), and East Muddy Creek to Grandy Creek (Boundary D; Figure 2). I created multiple 2D cross sections in each model boundary, about 40 in total. However, only the key most descriptive cross sections will be discussed further in the results. More information on the specifics of this process can be found in Aquaveo tutorials (Aquaveo, 2024).

### 3.6 Well Monitoring

Between April 2023 and May 2024, water levels were measured monthly in four domestic drinking-water wells volunteered by private landowners. The wells are located along Grandy Creek with three wells (Monitoring well A-C) in the floodplain, and one (Monitoring well D) in a glacial terrace (Figure 2). The wells were assumed to be completed in the same aquifer and were chosen on that basis. The surface elevation, latitude, and longitude of the wells were determined using the WWU Geology Department's Emlid Reach RS2+, a survey-grade GPS.

The depths to the water surface were determined using a standard engineering measuring tape with a sensor. In contrast to static water levels from well logs, these monthly data were used to show monthly changes between the floodplain and glacial terrace water tables. The monthly monitoring data were also compared to the AgWeatherNet Concrete daily rainfall data for better understanding of the recharge response times of both areas to major rainfall events and seasonal changes (WSU, 2024). Additionally, water levels were monitored and measured using a pressure transducer in the new 310-foot well (Figure 2). Deep well surface elevation and latitude and longitude was gathered from the 2017 Puget Sound DTM raster data (Lowe, 2017).

### 3.7 Recharge

I roughly estimated groundwater recharge to generally illustrate its variability in the study area, not for a thorough water budget or to predict groundwater flow. Recharge in the lowlands is the amount of precipitation that supplies an aquifer system and is an important element in estimating water budgets. Recharge is estimated by removing evapotranspiration, soil storage, and surface runoff from the gross precipitation. Infiltration and runoff are highly controlled by the hydraulic conductivities of the overlying soils and surficial geologic units. I used recharge to demonstrate how different hydrogeologic units may respond to rainfall throughout the different conceptual model boundaries. I used a 30-year normal precipitation with a raster that is set at 800-meter resolution from the PRISM climate group data from Oregon State University for the annual rainfall within the lower Skagit River Valley (PRISM, 2024). I placed this raster into ArcGIS and analyzed these values with the surrounding surficial hydrogeology. While recharge can include water from rivers, streams and glaciers, these factors were not included in my recharge estimates.

There are multiple methods that can be used to calculate recharge. Some methods are more complex with numerical based modeling, while others use simplified equations. I used methods developed by Bidlake and Payne (2001) and used estimates from Vaccaro et al., (1998) and Pitz (2005). Bidlake and Payne (2001) developed a method for estimating annual recharge by splitting areas up into individual soil and land-cover groups and using different linear regression equations for each. Equations are used for each individual soil and land-cover group and can be found on Table 2. Due to the simplicity of the recharge estimates, runoff from the valley wall could not be estimated.

### 3.8 Seepage Run and Stream Piezometers

Seepage run data can provide insight about whether a stream is a gaining stream (groundwater is supplying the stream) or is a losing stream (water from the stream is seeping into the ground). On September 12 and September 15, 2023, seepage run tests were conducted at Muddy and Grandy Creek by two HDR, Inc. teams: one team downstream, and another team upstream. Both mechanical (propellor) and electronic streamflow devices were used with a tested 1.5% relative difference between devices. Measurements were taken and the location of the measurements were recorded with an elevation-less GPS device. Mid-September was selected as this is typically the driest month of the year, when baseflow conditions are most prevalent in the Skagit Valley. These results provided some insight into groundwater connectivity between the glacial terraces and floodplain.

HDR also gathered data from March 2023 through November 2024 from three piezometers and staff gauge pairs installed in the streambed of Grandy Creek and four pairs in Muddy Creek. Details of the construction, placement, monitoring, and analyses can be found in HDR (2024). Vertical hydraulic gradients determined from the piezometers and staff gauge pairs were used to validate the seepage run results. Generally, if the hydraulic head in the stream piezometer is higher than the stream level stage (upward vertical gradient) the groundwater is discharging to the stream (gaining; HDR, 2024).

## 4.0 Results

### 4.1 Well-Log Database

While there were some exposures found on the surface across the valley including gravel pits and stream exposures, the only source of subsurface information used in this study were the driller well logs. Well logs can contain valuable information including well depth and radius, screen length, location, pump test data and stratigraphic descriptions (e.g., grain sizes) throughout the depth. There are over 1000 wells sourced from the WADOE within my study area, and 133 of those wells were used in the 2D cross sections and the 3D conceptual modeling (Figure 2; Appendix A). Most of the wells used in conceptual modeling are between Hamilton and east Sedro-Woolley. Of the 133 wells, about 50 wells from the glacial area and 83 from the floodplain (Figure 2). Nearly all wells removed from consideration were less than 40 ft deep in the floodplain or less than 100 ft deep in the glacial area. Some were also removed because of missing important locational data. About 198 wells were used for hydraulic conductivity calculations (Figure 3; Appendix B), with 137 wells located in the floodplain and the rest in the glacial area.

4.2 Field Investigation:

My field investigations with Jon Riedel were limited to April-May 2024. The areas explored include the glacial terraces north of the town of Hamilton and the glacial uplands north of Lyman to eastern Sedro-Woolley (Figure 2). Exposures were limited to steam banks along the glacial terrace that were mostly vegetated. My observations indicate that the surface of the glacial terraces north of Hamilton (Boundary C) grades from till and some recessional outwash on the far west side of the glacial terraces to glacial till in the middle and then to outwash on the far east side of the glacial terraces (Figure 2). In addition, an east facing exposure at Muddy Creek revealed that till is overlain by recessional outwash. Further upstream on Muddy Creek, there is fine-grained glaciolacustrine exposed near the surface which also occurs further north at Muddy Creek (Figure 2). The Hamilton glacial terraces (Boundary C) are similar to the glacial terraces in Boundary D but differ from Boundary D because of the Hamilton moraine and extensive ICSD. Large portions of the southern part of the glacial uplands from Lyman to eastern Sedro-Woolley (Boundary B to A) are covered with till or glaciomarine drift instead of outwash as indicated by many ponds that formed during a moderate intensity rainfall event. Also, during an observation on the floodplain near the glacial uplands, I noted that all the inclines and steep slopes leading up from the floodplain to the top of the glacial uplands had exposed Chuckanut Formation at Boundary B. Based on these observations of the glacial uplands in the area (Boundary B and A) there appears to be significant amounts of till at the surface, and the Chuckanut Formation runs down from the glacial uplands down to and below the lower elevations of the floodplain.

The new 310 ft monitoring well near Alder Creek provided higher quality well-log information as compared to other wells in the valley. The well log includes a foot-by-foot description of the geologic material recorded by a professional geologist (Figure 4; Appendix C). The overall sequence of glacial deposits based on depth below the ground surface was recessional outwash (0-70 ft), glacial till (70-80 ft), advance outwash (80-261 ft), and glaciolacustrine (261>310 ft; Riedel 2024a; Figure 4). The 310-foot well is one of the few wells that reached the glaciolacustrine deposit beneath the glacial terraces and floodplain and is also one of few wells in the glacial terraces near Alder and Grandy creeks (Figure 2). There were also three tree bark wood samples collected from this well that were radiocarbon dated. The results of these radiocarbon dates indicate the calibrated age of these deposits to be 29,237-29,894 BP at depth of 266 ft, 29,481-30,041 BP at depth of 277 ft, 30,872-31,158 BP at depth of 288 ft (Figure 4). Overall, there is a coarsening up sequence from glaciolacustrine to distal outwash (sand) to proximal outwash (gravel) and then till, ending in recessional outwash (Figure 4).

### 4.3 Geologic Units

I used surficial geologic maps (e.g., Dragovich et al., 1999; Savoca et al., 2009a; WADNR, 2016, Riedel, 2024a), exposures in gravel pits along Boundaries C and D (Figure 2), and driller well logs to aid in my geologic interpretations. Most driller well log stratigraphic descriptions vary in quality. Driller well logs are not constructed by geologists, except for the 310-foot well drilled for this project. This required me to make interpretations of the deposits based on my own judgment. Also because of the limited number of wells in the glacial terraces and some areas of the glacial uplands, I had to interpolate interpretations across substantial distance between wells in many locations. As stated in my Background section, when referring to both glacial terraces and glacial uplands, I will use glacial area or glacial aquifer. Valley walls include everything at higher elevations above the glacial uplands or glacial terraces. The glacial uplands and glacial terraces exist between the northern valley walls and the southern floodplain. For completeness and for further reference, all the geologic symbols I use in the following descriptions are those used by Dragovich et al. (1999).

#### 4.3.1 Late Holocene Skagit River Alluvium

Late Holocene Skagit River alluvium (Qa) is a surficial deposit located within the floodplain area deposited from the Skagit River and covers most of the area from Birdsview to Sedro-Woolley (Dragovich et al., 1999; Figure 2). The alluvium mostly contains sand and gravel with minor silt and clay. Gravel occurs near Birdsview which grades into sand, silt, and clay, towards Sedro-Woolley (Riedel, 2023). Alluvium tends to get finer grained farther from the river. The thickness of this deposit ranges from 5-35 ft and is present at the surface of the floodplain (Figure 1).

#### 4.3.2 Alluvial Fan

Alluvial fan (Qaf) is a Holocene tributary stream deposit found between Hamilton and Sedro-Woolley and is located on both the glacial uplands and floodplain of this area at the base of drainages (Figure 2). The fans were mostly debris flow and fluvial deposits from the creeks draining the uplands onto and through the glacial landforms. While this unit is mostly Holocene in origin, some alluvial fan deposits can be from the late Pleistocene and located higher in elevation on the glacial uplands (Dragovich et al., 1999). These deposits occur at the northern edge of the floodplain and glacial upland areas and are usually composed of poorly sorted gravel, silt, and sand (Savoca et al., 2009a). The well logs show the unit is usually composed of gravel or gravel with sand with some instances of sand with clay. Thickness ranges from 5-20 ft.

#### 4.3.3 Lahar Deposit or Older Alluvium Deposit

The lahar deposits (Qvl and Qoa) are Holocene deposits sourced from volcanic mudflows that deposited in the Skagit Valley in the Holocene from Glacier Peak (Dragovich et al., 1999). Lahar deposits occur mainly on the northern edge of the floodplain near the glacial uplands between Hamilton and Sedro-Woolley (Figure 2). The towns of Lyman and Sedro-Woolley are built on lahar deposits. Although well logs do not describe lahar material, the unit is fine sand with gravel and includes muddy silt and clay runout in these areas (Dragovich et al., 1999). The lahar deposits are believed to be as thick as 50 ft thick at Sedro-Woolley from the 6.0 ka Glacier Peak eruption (Dragovich and McKay, 2000). WADNR (2016) describes it as an older alluvium deposit (Qoa) but mentions nothing of the volcanic origin, while Dragovich et al., (1999) describes it as a post volcanic alluvium that is intermixed with the lahar deposit. It is hard to distinguish between the lahar and older alluvium deposits, but I will refer to it as lahar herein.

#### 4.3.4 Glaciomarine Outwash

Glaciomarine outwash (Qgom(e)) occurs between Sedro-Woolley and Lyman at the surface of the glacial uplands (Figure 2). It is exposed on the glacial uplands between the mapped northern recessional outwash and mapped southern till. It is mostly composed of gravel, sand, and silty sand. It also occurs below 400 ft in elevation at the late glacial marine limit (Dragovich et al., 1999). This is a thin unit ranging from a couple of feet thick to about 25 ft thick. Due to its similar characteristics to recessional glacial outwash, I interpret that this outwash is glacial outwash deposited in marine waters during the Skagit Marine Embayment.

4.3.5 Glaciomarine Drift

Glaciomarine drift (Qgdm(e)) is mapped exclusively north in the glacial upland of Sedro-Woolley, is mostly exposed at the surface, (Figure 2) and is primarily composed of clay and silt with local gravel and sand (Dragovich et al., 1999). The unit is somewhat finer-textured than till as it has less sand and more silt and clay present but has similar elevations and characteristics to till. It is also present in the lower elevations of the glacial uplands, about 50-100 ft lower in elevation, yet overlays the glacial till unit (Figure 2). The thickness of this unit ranges from 50-100 ft. This unit was also deposited in the Everson interstade.

4.3.6 Recessional Glacial Outwash

Recessional glacial outwash (Qgo) was deposited over a period of several hundred years at the end of the ice age as the ice sheet retreated east up Skagit Valley. Much of the outwash was deposited by ice-marginal streams flowing between the ice sheet and the north valley wall. Some of that outwash was deposited into marine waters (Riedel, 2025a). Recessional glacial outwash extends from Sedro-Woolley to Birdsview in the glacial terrace and glacial upland area (Figure 2). Deposits occurred between ~14,000 years ago and 12,000 years ago, and consist of loose sand and gravel, with some instances of boulders, cobbles, and lenses of silt (Savoca et al., 2009a; WADNR, 2016). The thickness of the outwash deposits varies. Outwash ranges from 10-80 ft thick and is typically present on the surface of the glacial terrace between Hamilton and Birdsview. Outwash can range from only 10-30 ft thick on the surface in the glacial area between Hamilton and Sedro-Woolley (Figure 2). It is difficult to determine the outwash thickness in the glacial terraces between Lyman and Hamilton due to limited well log information, but it could be thicker in this area compared to the area between Lyman and Sedro-Woolley. Also based on field investigations, the outwash in the glacial terraces above Hamilton likely has the same characteristics as in Boundary D.

4.3.7 Glacial Till

Glacial till (Qgt) is usually located directly underneath or adjacent to recessional outwash (Figure 2). It was likely deposited during the continental ice sheet advance and retreat. It is composed mostly of silt and clay, with some gravel and sand (Savoca et al., 2009a). Well logs indicate that till grain sizes vary depending on location, with till on the east side of the glacial terraces composed of mostly silt and sand with minimal clay while glacial till on the west side (glacial uplands) has silt and clay with minimal sand and gravel. There are multiple exposures of this unit between Sedro-Woolley and Lyman north and south of the recessional outwash deposits. It also is exposed north of the recessional outwash deposits between Hamilton and Birdsview (Figure 2). The till thickness can range from 10 to 80 ft (Dragovich et al., 1999). It also could be stratigraphically below the alluvium and recessional outwash in the floodplain near the glacial area but would be thin. It should also be noted that based on LiDAR (Figure 3), most of the surface of the glacial terrace and glacial uplands is occupied by basal till due to the fluted structures.

#### 4.3.8 Advance Glacial Outwash

Advance glacial outwash (Qga) is located directly beneath the till deposits and is composed of gravel, sand, silt, and some clay. The unit was likely deposited by ice marginal streams during the advance of the Cordilleran ice sheet (Dragovich et al., 1999). While there are some exposures of this unit on the southern edge of the glacial uplands at Lyman, the unit almost exclusively occurs in the sub-surface of the glacial uplands and glacial terraces between Lyman and Grandy Creek (Figure 2). The unit ranges from 5-130 ft in thickness, with units at ~130 ft thick near Alder Creek and on the east side but thin at Lyman with about 5-10 ft in thickness. This unit is also located directly below alluvium and till deposits in the floodplain based on the well log data, and ranges from 5-50 ft in thickness.

#### 4.3.9 Glaciolacustrine

Glaciolacustrine (Qgl) deposits are located stratigraphically directly below the advanced outwash between eastern Lyman and Birdsview and directly below the till just east of Sedro-Woolley (Figure 2). This unit has silty clay, clayey silt, and silty sand (Dragovich et al., 1999). This description matches the grains occurring in the well logs near Sedro-Woolley, but this unit seems to exclusively be silt between the glacial terrace at Jackson and Grandy Creek (Figure 2). The deposit in the glacial uplands north of Sedro-Woolley is 50-150 ft thick while on the east side it could range from 30 ft to 130 ft or more thick (Appendix C). It also is in the floodplain below the advanced outwash and is dominated by clay or silt. It is one of the few units to go below modern sea level. The glaciolacustrine is likely a result of sediments being deposited into pro-glacial lakes before the advance of the Cordilleran ice sheet, potentially from alpine glaciers (Riedel, 2025a).

4.3.10 Chuckanut Formation

The Chuckanut Formation (Ec(cb)) bedrock underlies glacial uplands between Sedro-Woolley and Jackson Creek, but outcrops at the surface in boundaries A and B (Figure 2). It is composed of shale, sandstone, and siltstone. It is unknown how thick the unit truly is as no wells extend through the Chuckanut Formation. In particular, shale is common near Jackson Creek, but it is mostly sandstone and some siltstone west of Jackson Creek (Figure 2). There is also some fracturing noted in the well logs, which serve as a secondary porosity and avenues for groundwater transmittance.

4.3.11 Darrington Phyllite Bedrock

Darrington Phyllite bedrock, a Jurasic-age (Jph) metamorphosed mudstone, is located on the walls and top of the glacial valley walls (Figure 2; Dragovich et al., 1999). No wells were completed in this geologic deposit.

4.4 Hydraulic Conductivity Estimates

About 198 wells were used for hydraulic conductivity calculations (Figure 3; Appendix B), with 137 wells located in the floodplain and 61 in the glacial terraces and uplands. There were many usable wells between Sedro-Wolley and Lyman (Boundary A and B) where outwash, till, lacustrine, marine and lahar deposits are common (Figure 3). The area with the least number of well logs available is on the east side (Boundary C and D) of the study area where recessional glacial outwash is found because it is undeveloped state forest land (Figure 3). Using a Python script (Mitchell, 2023) and the equations described above in section 3.3, I estimated the hydraulic conductivities at the well location, catalogued the values into the specific deposits and took geometric means to define a single average hydraulic conductivity for each deposit (Table 3). My values are consistent with hydraulic conductivities measured in similar glacial and alluvial deposits in Puget Sound aquifers (e.g., Kahle and Olsen, 1995; AESI, 2016; Gendaszek, 2014).

The average hydraulic conductivities of deposits in the floodplain are higher than all the glacial and bedrock deposits and range from a high of 569 ft/day between Alder and Muddy Creek to as low as 171 ft/day between Alder and Grandy Creek. Alluvial fan deposits averaged about 288 ft/day, and lahar deposits averaged about 518 ft/day (Table 3; Figure 3). Average hydraulic conductivities of deposits in the glacial area have a range of values. Advance glacial outwash (eastside) average 267 ft/day and average 38 ft/day on the westside. Recessional glacial outwash does not have any measured values but is likely high (>100 ft/day) since it is mostly composed of gravel and sand. All other deposits have generally low conductivities. The conductivity of continental glacial till and glaciomarine drift is 9 ft/day, glaciolacustrine is 8 ft/day (Table 3; Figure 3). I estimated the hydraulic conductivity of the Chuckanut Formation to be about 2 ft/day based on values in Whatcom County (Sullivan, 2005; Associated Earth Sciences, Inc, 2016) and from my own estimates (Table 3). The hydraulic conductivity of the Darrington Phyllite is assumed to be zero (impermeable) due to not having any wells to measure this unit, being a metamorphosed mudstone.

### 4.5 Hydrogeologic Units

Following Freeze and Cherry (1979), multiple geologic units having similar lithologies, hydraulic conductivities, stratigraphic position, and depth (confined or unconfined) can be combined to form hydrogeologic units (Table 4). These units range from high hydraulic conductivity units (100ft/day; aquifers), low conductivity units (10ft/day; aquitard) to very low conductivity units (1 ft/day; aquiclude). Arc Hydro Groundwater uses “horizons” to distinguish each hydrogeologic unit and are ranked so the largest number is the “aquifer” at the highest elevation and the lower the number, the lower down the unit is placed beneath the subsurface.

#### 4.5.1 H5: Recessional Outwash, Glaciomarine Outwash, Alluvial Fan and Coarse Alluvium Surficial Aquifers

The recessional outwash, glaciomarine outwash, alluvial fan, and coarse alluvium surficial aquifers are all exposed on the surface. The hydrogeologic conductivity of these units can range from 40-400 ft/day, the highest conductivities in the study area. While I have no calculations for the recessional outwash, it likely has similar conductivity since the grain sizes are coarse sand and gravel dominated. H5 also includes all coarse-grained materials (sand or gravel) in the alluvial fan, alluvium, and lahar deposits (Table 4). These units were lumped and make up the coarse alluvium. The aquifers on the surface of the glacial uplands are about 5-50 ft thick between Lyman and Sedro-Woolley and are 50-110 ft thick in the glacial terraces between Lyman and Grandy Creek (Figure 2). The coarse alluvium aquifers are located on the surface of the floodplain ranging from 5-50 ft in thickness throughout the entire study area (Figure 2).

### 4.5.2 H4: Glacial Till, Glaciomarine Drift and Fine Alluvium Aquitards

The glacial till and glaciomarine drift (GMD) both occur in similar locations in Sedro-Woolley in the sub-surface (below the recessional outwash or H5) and on the surface. The glacial till unit dominates most of H4 as it appears throughout most of the glacial area, unlike the GMD that is limited in extent to near Sedro-Woolley (Figure 2). The mean hydraulic conductivity of the till and GMD is about 9 ft/day, representing aquitards. Both units have relatively similar grain sizes, with a fine-grained matrix mostly of clay and silt with some cobbles and dropstones present (although the GMD does seem to have more clay). Glacial till and GMD range from about 10-100 ft thick on the west side to ~50-120 ft thick on the east side. Although they are aquitards, water can still infiltrate them, but at lower rates compared to the aquifers directly above and directly below them. H4 also includes all fine grained (silt or clay) alluvial fan, alluvium, and lahar deposits. These units were lumped into the fine alluvium in H4 (Table 4). Fine alluvium is also present at the surface and subsurface of the floodplain (Figure 2) and ranges from 10-50 ft thick but is not nearly as confining in the floodplain compared to other H4 units in the glacial area.

### 4.5.3 H3: Advance Glacial Outwash Confined Aquifer

The advanced glacial outwash confined aquifer is solely the advanced glacial outwash geologic unit (Table 4). The unit is located between west Lyman (Boundary B) and Birdsview (Boundary D) and usually occurs in the subsurface below till (H4), but there are some exposures north of the study area on the east side, and above Lyman, where it is exposed on the surface (Figure 2). The hydraulic conductivity is about 38 ft/day on the westside (although it is likely higher, it is likely this low due to limited well calculations available) and is about 267 ft/day on the east side (Table 4). This unit is also usually located between the H4 and H2 aquitards. It also occurs only in the subsurface of the floodplain below the fine alluvium (H4) and is likely connecting the glacial area with the floodplain. The thickness ranges from 1-10 ft around Lyman to 80-150 ft between Jones creek and Grandy Creek in the glacial terraces (Figure 2). In the floodplain subsurface, it is 5-50 ft thick.

### 4.5.4 H2: Glaciolacustrine Aquitard

The glaciolacustrine aquitard is exclusively composed of the geologic unit dominated by silt and clay. It exists mostly in the subsurface of the glacial uplands near Sedro-Woolley and the glacial terraces between Jones Creek and Grandy Creek and is directly beneath the entire floodplain in the study area. There are also surface exposures along Grandy Creek, Muddy Creek, Cape Horn and other areas along the Skagit River. It is located only in the sub-surface and usually located directly beneath advance outwash between Jones Creek and Grandy Creek and is located underneath till in Sedro-Woolley (Figure 2). The glaciolacustrine unit has a similar hydraulic conductivity to till and glaciomarine drift at about 8 ft/day (Table 4). However, this aquitard is separate from the glaciomarine drift and till aquitard because it usually occurs below advance outwash. The unit has a thickness between 20-100 ft from the well logs, but it is likely much deeper. It is also located below the advance outwash in the floodplain. The glaciolacustrine aquitard likely has more clay on the west side and more silt than clay on the east side based on field observations.

#### 4.5.5 H1: Chuckanut Formation Aquitard

The Chuckanut Formation aquitard is composed of three main rock types, sandstone and siltstone between eastern Sedro-Woolley and western Lyman (Boundary A and B), and shale in middle and eastern Lyman (Boundary B) Figure 2). This unit is also below till or advance outwash in this area and underlays the whole glacial uplands. While the unfractured rock matrix does not transmit water, the fractures in the formation can transmit water and I defined the hydraulic conductivity to be at 2 ft/day based on values in Whatcom County (Sullivan, 2005; Associated Earth Sciences, Inc, 2016). If my estimate is valid, this unit has the lowest conductivity out of all measurable units (not including the Darrington Phyllite) and can be considered an aquitard or potentially an aquiclude (Table 4). The degree of fracturing is unknown and likely transmits water from the glacial uplands to the floodplain.

#### 4.5.6 H0: Darington Phyllite Bedrock Aquiclude

The Darrington Phyllite aquiclude exclusively defines the northern sections at elevations above the glacial area in the valley walls (Figure 2 and 3). Because no wells encounter this unit in my study area, I assume that the hydraulic conductivity is negligible since it is a metamorphosed mudstone (Table 4). I also assume most of the precipitation runoff flows down the valley walls into conductive deposits in the glacial area.

## 4.6 Hydrogeologic Conceptual Modeling

I used the six hydrogeologic units described above to develop 2D cross sections and 3D conceptual models using the Aquaveo Arc-Hydro Groundwater Subsurface Analyst (Figure 5). The model domain was divided into four different areas: Sedro-Woolley to Cokedale (Boundary A), Cokedale to Lyman (Boundary B), Lyman to West Muddy Creek (Boundary C), and East Muddy Creek to Grandy Creek (Boundary D; Figure 5). The conceptual models include both the glacial areas and the northern part of the floodplain to illustrate the connections between deposits and the Skagit River. The four boundaries were also split into smaller subsections due to the complex spatial geology and hydrostratigraphy in the glacial terraces, glacial uplands and floodplain. A distribution of wells was selected in the glacial area and floodplain to capture the spatial variability of the hydrogeologic system. In some cases, pseudo (fictitious) wells were created where wells were nonexistent so that hydrogeologic units could be interpolated in the absence of wells (wells bolded in Appendix A). All wells in the Darrington Phyllite bedrock are pseudo wells (Figure 2). Some hydrogeologic unit depths were extended beyond their actual well depths like glaciolacustrine and Chuckanut Formations as these wells did not extend into these units (highlighted in red in Appendix A). Question marks are placed next to pseudo wells and assumed conditions in cross sections and in some conceptual models. The following is an explanation of both 2D cross section and 3D conceptual model key observations.

### 4.6.1 2D Cross Sections

I created multiple 2D cross sections for each model boundary that included as many deep wells as available, and as much of the glacial terraces, glacial uplands, and nearby floodplain as possible. About 38 cross sections were developed in total, but only 11 were selected for viewing in this thesis. These 11 cross sections show the best general hydrogeologic characteristics found in each boundary. Each boundary contains at least one cross section that goes from the glacial area to the floodplain, while one cross section goes longitudinally across the glacial terraces or glacial uplands. Below I discuss these key 2D cross sections within each model boundary that highlight the most important hydrogeologic variation through space (Figure 5). The cross sections are vertically exaggerated by 20x to illustrate subtle topographic variations and thicknesses.

Boundary A covers the area from Sedro-Woolley to Cokedale, or west of Wiseman Creek (Figure 6). Cross section A indicates a thick sequence with H1 (Chuckanut Formation) incorporating much of the glacial uplands subsurface which is about 300-500 ft thick in the middle of the cross section. H1 is bounded to the east and west by H2 (glaciolacstrine) which ranges between 100-200 ft thick. The surface of cross section A is mostly dominated by H4 (glacial till and drift) and is thick on the west side (70-120 ft) and gradually thins to the east side to about 20 ft thick. H5 (recessional and glaciomarine outwash) covers the surface in the middle of the cross section and is about 65 ft thick (Figure 6). Cross section B illustrates the connection between the glacial uplands with the floodplain and the lack of highly conductive glacial uplands deposits in the subsurface in contact with the floodplain (Figure 6). The floodplain is dominated by H2 at depth (150 ft thick), H3 (advance outwash) lies below H4 (fine alluvium; 20-60 ft thick; thicker away from glacial uplands), followed by H4 (20-50 ft thick; thicker near the glacial uplands) with H5 (coarse alluvium) at the surface at about 20 ft thick.

I selected four cross sections to illustrate the geologic complexity in Boundary B, the area between Cokedale and Lyman (Figure 7). Cross section C has a consistent glacial upland subsurface dominated by H1 (Chuckanut Formation) that ranges between 300 ft and 500 ft thick (Figure 7). The west side contains a thin H5 unit (recessional and glaciomarine outwash) at the surface and is about 5-15 ft thick. Both H5 and H4 (glacial till and glaciomarine drift) units form thin (30 ft) surface deposits in the middle and east side of cross section C (Figure 7). Cross section D is similar to cross section C but illustrates thicker surface units of H4 and H5. Across the profile, H4 ranges between 50-100 ft thick and H5 is thinner at 5 to 50 ft. A 10-20 ft thick section of H3 (advance outwash) exists between H1 and H4 in the eastern portion of cross section D (Figure 7).

Cross sections E and F illustrate the connection between the glacial uplands and the floodplain in Boundary B and the thick sequence of H1 below the glacial uplands. H5 (recessional and glaciomarine outwash) is present at the surfaces at 30 ft thick and H4 (glacial till and glaciomarine drift) is 70 ft thick below it. Both thin closer to the glacial uplands edge with H4 found at the edge of the glacial uplands in cross section E, while in cross section F, a transition into a thick sequence of H3 (advance outwash; 10-50 ft thick) occurs near the edge. H1 (Chuckanut Formation) potentially serves as a groundwater recharge source through fractures to the floodplain deposits in this region, although the exposure of the glaciolacustrine (H2) and till (H4) at the flanks of H1 would have an impact on the rate of recharge to the more conductive H3 and H5 deposits in the floodplain, especially in the areas in the vicinity of cross section F.

Boundary C is an area between eastern Lyman and Hamilton which I illustrate with three cross sections (Figure 8). Many units have thickness derived from assumptions inferred from field visits. Cross section G is dominated directly below all units by what is believed to be 150 ft of H2 (glaciolacustrine) throughout the glacial terraces followed by a thickening and thinning H3 (advance outwash) above it from west to east (believed to be 300- ft thick). H4 (glacial till) appears to dominate the glacial terrace on the west side believed to be thick (125-250 ft thick), but thins out to 125 ft thick below H5 (recessional outwash) which appears to dominate the surface on the eastside (10-50 ft thick). Cross section H is similar to cross section G but with thinner H3-H5 units located on the floodplain (Figure 8). The H3 is thick in the middle (50-75 ft) but thins out on both east and west sides (5-10 ft). H4 (fine alluvium) maintains a relatively consistent thickness (25-75 ft thick) below H5, while the thin H5 (coarse alluvium; 5-10 ft thick) leaves H4 exposed on some areas of eastern side cross section H (Figure 8). Cross section I illustrates a potential strong connection between the glacial terraces and floodplain through H3 in the subsurface (Figure 8). Floodplain and glacial terraces units are similar to those on the east sides of cross sections G and H. H3 is located in the subsurface of the floodplain and glacial terraces and connects both areas at similar elevations. H3 is likely a groundwater recharge source between the glacial terraces and floodplain due to its high conductivity and continuity between the glacial terraces and floodplain (Figure 8). H4 (glacial till in terrace and fine alluvium in floodplain) is also at similar elevations in both glacial terraces and floodplain but likely does not transmit as much water due to its lower hydraulic conductivity.

Boundary D covers Grandy Creek to Muddy Creek (Figure 9). Cross section J has a consistent subsurface in the glacial terraces with H2 (glaciolacustrine) dominating the bottom of the glacial terrace at 50-100 ft thick. H3 (advance outwash) overlays H4 and is thick on the west side (75-150 ft thick) and thins out on the east side (10-30 ft). H4 (glacial till) overlays H3 and is thick on the west side and the middle (60-150 ft) but thins on the east side to 25-30 ft thick in the glacial terraces. The surface of the glacial terraces is dominated by H5 (recessional outwash) which is thin in the middle and west side of the glacial terraces (10-30 ft) but thickens on the east side near Grandy Creek (50-125 ft; Figure 9). Cross section K illustrates a strong continuity of the glacial terraces with the floodplain, particularly through the hydraulically conductive H3 unit (Figure 9). At depth, the floodplain is dominated by H2 (glaciolacustrine;150 ft thick) and is overlain by H3 (advance outwash; 25 ft thick), H4 (fine alluvium; 10 ft thick), and H5 (coarse alluvium) at the surface at about 25 ft thick. The area that transitions from floodplain to glacial terraces is composed of no H5 (coarse alluvium on the surface and instead 50 ft of H4 (fine alluvium) present on the surface that extends up from to floodplain to the glacial terraces H4 (till). Only further north on the glacial terraces is a thin H5 (glacial outwash; 5 ft thick) found on the surface. The conductive H3 is located at similar elevations in the floodplain and glacial terraces and likely acts as a recharge source between the glacial terraces and floodplain, displaying strong subsurface connectivity. H4 (glacial till and fine alluvium) is also at similar elevations in both glacial terraces and floodplain and on the surface seen in the transition area between floodplain and glacial terraces in cross section K (Figure 9). H3 likely transmits groundwater at high rates between the glacial terraces and floodplain due to its high hydraulic conductivity and gradient. H4 in the east likely transmits groundwater to the outwash at a slower rate than H3, but higher than the till (H4) on the west side, due to the east side till (H4) being coarser grained and likely having a higher hydraulic conductivity.

4.6.2 3D Hydrogeologic Conceptual Models

The 3D conceptual models developed in the Aquaveo software in ArcGIS ArcScene provide a better visual representation of the surface hydrogeologic features and the spatial variability. The drawback of ArcScene is the lack of a tool to define horizontal and vertical axes. As such I added numbers to the 3D images to indicate unit thicknesses. Each conceptual model is composed of multiple cross sections and sub-boundaries and these sub-boundaries were created due to the spatially varying hydrogeologic sequences and topographic differences. Figure 10 displays all four boundaries used for the 3D conceptual models. Unlike the cross sections, each 3D model is expanded further north to include the valley walls. Consequently, there are also more pseudo wells added to the north because no wells exist in this part of the lower Skagit Valley.

The impermeable H0 (phyllite) defines the valley walls north and above the glacial uplands in Boundary A that transitions into the H1 (Chuckanut Formation) and H2 (glaciolacustrine) at depth toward the floodplain (3D models and 2D cross sections in Figures 11-13). These units are capped with a conductive recessional and glaciomarine outwash (H5) on the surface of the flanks of the glacial uplands that overlies a less conductive glacial till and glaciomarine drift (H4). The H4 unit dominates the surface on the lower portion of the glacial uplands and on the western section of the floodplain as fine alluvium, but is overlain by H5 (coarse alluvium) in the eastern portion of the floodplain of Boundary A. It is possible that the H4 (glacial till and glaciomarine drift) is recharged by direct precipitation and by shallow groundwater from the overlying H5 (recessional and glaciomarine outwash) unit on the glacial uplands and may provide low rates of groundwater recharge to the H5 unit (coarse alluvium) on the floodplain that likely transmits groundwater along with tributary streams discharging the glacial area to the Skagit River.

H0 (Darington Phyllite) dominates the northern valley walls of Boundary B but transitions to H1 (Chuckanut Formation) at the base of the glacial uplands to H2 (glaciolacustrine) beneath the floodplain at depth (Figure 14-16). The northern half of the glacial uplands is overlain by H5 (recessional and glaciomarine outwash) with some H4 (glacial till and glaciomarine drift) below it that extends to the southern edges of the east and western edges of Boundary B. H4 however, dominates the middle and western southern half of the glacial uplands with H1 partially exposed on the surface but primarily exposed on the incline between the glacial uplands and the floodplain. H5 and H3 (advance outwash) dominate the eastern edges of the glacial upland, with the floodplain overlain by H4 (fine alluvium). The highly conductive H5 and H3 outwashes on the east side of the glacial uplands in Boundary B is likely providing surface water and groundwater to the floodplain, and H4 on the west side of the glacial uplands might be providing limited low rates of recharge to the floodplain as well. In the southern middle of the glacial uplands of Boundary B, the very low conductive H1 unit is likely not providing much recharge to the floodplain due to its low conductivity and the overlaying H4 slowly providing recharge to H1. However, runoff from the surface of H1 may be providing some recharge to the floodplain. Baseflow to the Skagit is likely supported mostly by the floodplain deposits with limited connection to the glacial uplands in Boundary B.

H0 (Darrington Phyllite) dominates the northern valley walls of Boundary C with H5 (recessional outwash) and H4 (glacial till) on the surfaces of the glacial terraces, followed by H3 (advance outwash) directly below it, with H2 (glaciolacustrine) at depth in the glacial terraces and floodplain (Figure 17 and Figure 18). The glacial terraces and floodplain have the same units at the same elevations only varying with H4 (glacial till) dominating the surface in the western half and H5 dominating the surface in the eastern half. It is likely that the conductive H5 unit in the glacial terraces on east side of Boundary C is supplying shallow groundwater directly to the H5 (coarse alluvium) on the floodplain below, while the less conductive H4 (glacial till) is transmitting water on the westside down to the floodplain's H4 (fine alluvium) but at a much-lower rate. The conductive sub-surface H3 also is likely supplying groundwater from the glacial terraces where it is connected to the floodplain Boundary C. Baseflow to the Skagit River is likely supported by the floodplain and glacial terraces and stream runoff in this region.

H0 (Darrington Phyllite) dominates the northern valley walls of Boundary D with H4 (glacial till) and H3 (advance outwash) on the surface of the southern flank of the valley wall (Figure 19-21). Some H2 (glaciolacustrine) is exposed at the surface, dominating the subsurface base in both the glacial terraces and the floodplain. The glacial terraces are fairly consistent with H5 (recessional outwash) on the surface throughout, H4 below it, followed by H3 and H2. However, there are areas such as shown in cross section K that till (H4) might dominate the surface of the glacial terraces at its edges (Figure 9). The units on the floodplain vary, with H4 (fine alluvium) at the surface in the middle, far west, and east edges of the floodplain while H5 (coarse alluvium) dominates the rest of the surface of the floodplain. Some groundwater is likely transmitted between the H4 (till and fine alluvium) units as well, but at lower rates compared to H3. Most subsurface groundwater that is transmitted between glacial terraces and floodplain is likely transmitted from the highly connected H3 unit. Groundwater likely is sourced from rainfall recharge mainly into H5 (recessional outwash) and H4 (glacial till), but recharge could also be from the H3 and H2 units higher near the H0. The baseflow to the Skagit River is supported by the floodplain and heavily supported by aquifers in the glacial terraces and stream runoff in this region.

### 4.7 Groundwater Monitoring Data

I measured water levels monthly between April 2023 and May 2024 in four domestic wells using a water-level tape. Wells MWA-C are in the Skagit alluvial floodplain and MWD is in the glacial terrace near Grandy Creek in the eastern portion of the study area (Table 5; Figures

2 and 22). The four wells are assumed to be completed in the H3 unit (advance outwash; Figure 24). Water levels in the newly installed 310-foot monitoring well west of Grandy Creek in a glacial terrace (Figure 2) were measured by HDR using a pressure sensor and data logger that recorded the water table depth three times a day. The well was also screened in the H3 unit.

The water levels in the monitoring wells in the alluvial aquifer floodplain (MWA, B & C) follow a similar seasonal pattern in response to regional rainfall and were generally highest in April and lowest in November mimicking rainfall recharge (Table 6; Figure 22 and Figure 23). MWA has a different pattern than the other two alluvial wells (MWB & C) which may be the result of MWA being completed in a different hydrogeologic unit, or due to its closer proximity to the Skagit River. i.e., responding to river stage fluctuations. Although the water levels in MWD in glacial terrace are more erratic, its overall trend is similar to those in the floodplain wells and is likely in the same H3 hydrogeologic unit (Cross section L; Figure 24). Note that this section of the floodplain is mostly covered by H4 (fine alluvium) on the surface and contains a H3 unit that extends in the subsurface from the glacial terrace to the floodplain. Implications of this will be covered in the discussion section.

The 310-foot well that is also located in a glacial terrace to the west in Boundary C had the lowest overall water level fluctuation and responded three or more months after other wells began to change patterns. The 310-foot well did not begin to sense recharge until February 2024 and water levels continued to rise through May 2024, likely because it is screened between 200—220 ft in the advanced outwash deposit (H3) which is slow to respond to recharge (Table 6, Figure 22).

## 4.8 Recharge Results

I roughly estimated groundwater recharge to generally illustrate its variability in the study area, not for a thorough water budget or to predict groundwater flow. Aquifer recharge occurs primarily between October and April when rainfall exceeds evapotranspiration rates. I used 30-yr average gridded precipitation data (800 m) from PRISM and applied the relations developed by Bidlake and Payne (2001), Vaccaro et al. (1998), and Pitz (2005), to estimate recharge (Table 2). Recharge values are influenced spatially due to elevation impacts on rainfall (orographic effect) and by the hydraulic conductivity (infiltration capacity) of the soils and surficial geology type (Table 2; Figure 25 and Figure 26). Because of the higher elevations of the valley walls and the orographic effect, the Darrington Phyllite bedrock unit receives significant precipitation (up to 125 in/yr) but has no or minimal recharge (Vaccaro et al., 1998). The Chuckanut Formation is believed to be more permeable through its secondary porosity (fractures) than the Darrington Phyllite yet is overlain mostly by till and is assumed to have a recharge rate of 2 in/yr (Pitz, 2005). Glacial till units receive moderately high rainfall in some areas (up to 88 in/yr) but only have about ~18 in/yr of recharge because of its low hydraulic conductivity. Exposed outwash and glaciomarine outwash in the study area receive slightly less rainfall than glacial till (up to 75 in/yr), but average ~36 in/yr of recharge. The higher conductive floodplain alluvium and outwash units receive the least rainfall (up to 56 in/yr) and averages 30 in/yr of recharge (Table 7, Figure 25).

The Boundary B and Boundary C regions receive the most precipitation and recharge via H5 (outwash) located in glacial areas higher in elevations than in other boundaries (Table 7, Figure 24). Based on the averages for each conceptual model boundaries (without Darrington Phyllite bedrock and Chuckanut Formation), Boundary D has the highest recharge rate and precipitation along with Boundary B (Figure 25). Because of the Boundary D overall high recharge rate and connection to the floodplain aquifers, water levels in the monitoring wells have similar trends. Boundary A and C have the lowest recharge rate and precipitation (Figure 25).

Overall recharge is higher on the east side of the study area and in areas with higher glacial terrace or upland elevations and lower on the west side and in areas of lower glacial terrace or upland elevations and less conductive deposits (Figure 25). Some runoff from the Darrington Phyllite bedrock may contribute recharge to glacial aquifers along with the Chuckanut Formation such as at Boundary B and Boundary A (Figure 25) but this would require further study.

### 4.9 Seepage Run and Stream Piezometer Results

The seepage run data gathered on September 12 and September 15, 2023, by HDR, Inc., indicate variable surface-groundwater interactions (HDR, 2024; Table 8 and Table 9, Figure 27). It was a relatively dry summer with about 1.3 inches of rain recorded between July 1 and Sept 15 at the Concrete WSU AgWeatherNet station (WSU, 2024). About half of this (0.75 in) occurred during a single rain event in late August. For the profile illustrated in Figure 25, Grandy Creek drops about 620 ft to 112 ft over a 3.75-mile distance, resulting in a gradient of about 0.03.

Along the flanks of the glacial terraces, Grandy Creek is mostly gaining groundwater from the outwash deposits (H5 and H3). The only area that is not a gaining stream is between the river miles of 3.25 and 3.79 (Table 8, Figure 27). This could possibly be because there are fine grained lacustrine deposits exposed on the walls of the glacial terraces that reduce infiltration along this section of the stream. Between the river miles of 3.25 and 1.66, the stream was a gaining stream and was also likely supported by baseflow. The gaining stream could be a result of the advance outwash being exposed at or near the surface of the stream from the glacial terraces walls allowing water to seep into the stream. Further evidence was supported by water observed actively seeping out of the glacial terrace walls on the western edges of Grandy Creek (HDR, 2024). Below river miles of 1.66 where the stream enters the floodplain, the stream is either neutral or losing water. This could indicate that the stream water is supplying water to the Skagit River or aquifer, as water from here is likely not being seeped out of the saturated glacial terraces and instead is infiltrating into coarse floodplain deposits (Table 8, Figure 27). Grandy Creek also appears to flow into the Skagit all year long. This is likely due to the water table being lower than the stream depth in the floodplain, compared to the water table of the surrounding glacial terraces which was much higher than the streams depth at higher river miles.

The Muddy Creek profile (Figure 27) is about 3.0-miles and drops 945 ft from the top measuring point to the floodplain resulting in a gradient of 0.06—twice that of Grandy Creek. Within the glacial terraces, between river miles of 3.67 and 2.31, the stream is neutral (Figure 26). The stream could be gaining water or losing water. This is also an area where both advance outwash, till and lacustrine could be exposed and provide both seepage to the stream through the advance outwash, and a lack of flow in other areas due to lacustrine blocking water access, causing water to infiltrate back into the soil. At river miles 2.31 and 2.11, the stream is gaining and likely being supported by baseflow from the advance outwash. From river miles 2.11 and 1.2, the stream is a neutral stream again, which could be caused by till providing both baseflow in some areas and infiltration in other areas that are completely dry and unsaturated. Within the floodplain and from the river miles 1.2 and 0.1, the stream is a losing stream, thus stream water is supplying the aquifer (Figure 27). Baseflow is likely supplying a lot of water to the Skagit River via glacial terraces at Muddy Creek, but it is likely not as much as at Grandy Creek due to the large neutral stream river miles of Muddy Creek. Based on these results, it appears Grandy and Muddy Creek both are losing streams within the floodplain, however, Grandy Creek is overall a gaining creek within the glacial terraces, while Muddy Creek is neutral in the glacial terraces (Table 9, Figure 27). Muddy Creek also has more till and lacustrine exposed near the surface on the stream banks with the outwash, balancing out water going both into the stream and infiltrating back into the aquifer. It should also be noted that Muddy Creek was far less accessible in the glacial terraces to do measurements (in particular between 2.31 and 3.2 river miles), resulting in potential data gaps. These issues did not exist at Grandy Creek.

Piezometer data were also gathered by HDR at both Grandy and Muddy Creeks between March 2023 and continued until November 2024 (HDR, 2024; Figure 28 and Figure 29). However, due to numerous instrument errors the piezometer results were inconclusive- neither confirming nor denying the seepage run results. For example, a piezometer placed at about river mile 2.5 at Grandy Creek showed it having a negative head, negative hydraulic gradient, and having low temperatures despite the seepage run results showing it to be a gaining stream (HDR, 2024; Figure 27 and Figure 28). As this data did not confirm, but only created inconsistencies, these piezometer measures were disregarded.

## 5.0 Discussion

My primary objective was to characterize the aquifer systems in the lower Skagit River Valley and to determine the hydrogeologic connection between Skagit River floodplain aquifers and aquifers in the northern uplands and glacial terraces. My 2D cross sections and 3D conceptual models reveal complex subsurface conditions that define a series of aquifers and aquitards (Table 4). Predominant throughout the study area are hydrogeologic units H5 (recessional outwash, glaciomarine outwash, alluvial fan and coarse alluvium) on the surface which functions as a thin unconfined aquifer, H4 (glacial till, glaciomarine drift and fine alluvium) on the surface and in the subsurface acting as an aquitard, and H2 (glaciolacustrine) in the subsurface which also serves as an aquitard. Less common throughout the study area is H3 (advance outwash) found in the subsurface serving as an aquifer, H1 (Chuckanut Formation) found mostly in the subsurface acting as an aquitard or low-yield aquifer, and H0 (Darrington Phyllite) acting as an aquiclude. All six hydrogeologic units influence the groundwater connectivity between the glacial area and the floodplain throughout all four model boundaries in the study area.

### 5.1 Glacial Deposits

The surface and subsurface hydrogeologic units are dominated by glacial deposits that correspond to the glacial history of my study area. Around 29 ka, the valley walls outside my study area were mostly dominated by alpine glaciers that began to retreat around 21 ka and were absent before the Cordilleran ice sheet arrived ca 18ka (Riedel et al., 2010). Between 18-16 ka, the ice sheet deposited advance glaciolacustrine, advance glacial outwash, and glacial till. By 15 ka, the ice sheet was retreating leaving behind basal till and recessional outwash (Armstrong et al., 1965; Riedel, 2017). While this sequence is mostly consistent throughout the study area, some of my results suggest some deviations. The new 310-foot monitoring well revealed the Cordilleran ice sheet depositional pattern in the eastern glacial terrace area (Figure 2 and Figure 4). Radiocarbon dating of wood samples found near the bottom of the 310-foot well, the same depth as the glaciolacustrine deposit, denote a calibrated age range of 29,000-31,000 BP. It is possible that the lacustrine deposit is not associated with the Cordilleran ice sheet and is a fluvial-lacustrine or an alpine glacier lake deposit. However, this is speculative as there is no moraine present to support this (Riedel, 2025b). The glacial upland was also influenced by glaciomarine deposits from marine waters flooding the area about 13.6 ka leaving behind glaciomarine drift (Dethier et al., 1995). While the glaciomarine till is relatively extensive spatially, the glaciomarine outwash is nearly non-existent at the surface, likely being a few feet thick instead of tens of feet thick, unlike Dragovich (1999) which reports thicker glaciomarine outwash. Also, the well logs suggest that the entire floodplain in the study areas appears to have a glaciolacustrine base 50-100 feet below the surface and 25 feet above sea level. This glaciolacustrine unit is at similar elevations to the glaciolacustrine found in the 310-foot well in the glacial area. However, unlike the glacial area glaciolacustrine, the floodplain glaciolacustrine could be a mix of older glaciolacustrine and floodplain deposits at deeper depths (25 -27 ka) and advanced glaciolacustrine from the Cordilleran ice sheet at shallower depths (18-16 ka; Armstrong et al., 1965; Riedel, 2017).

### 5.2 Hydrogeology of the Skagit River Floodplain

Generally, the stratigraphic sequence in the Skagit River floodplain includes discontinuous H5 (coarse alluvium) on the surface, H4 (fine alluvium) on both surface and in the subsurface underlain by H3 (advance outwash) with H2 (glaciolacustrine) at the base (Figures 6-21). Unlike the glacial area, H4 is mostly fine alluvium and is consistent throughout the floodplain (either at the surface, or in the subsurface below H5) having silt and sandy with limited clay, making it a semi-confining unit. The Boundary A region (between east Sedro-Woolley and Cokedale) has the finest grained surface conditions, with H4 prevalent through most of this area's floodplain surface (Figure 6 and Figure 13). Boundary B (between Cokedale and east Lyman) is similar but mostly has H4 remaining prevalent through most areas (Figure 7 and Figure 14). Boundary C (Hamilton area) has coarser grained surface conditions with H5 found more frequently at the surface (Figure 8 and Figure 17). In Boundary D (between east Hamilton and Grandy Creek) the coarse grained H5 is found more commonly at the surface than H4 (Figure 9 and Figure 19). Thus, where H5 is found on the surface, it is an unconfined aquifer, with H4 below it being a semi-confining unit, H3 being the confined aquifer, and H2 at the base serving as an aquitard.

All areas of the floodplain appear hydrogeologically connected to the Skagit River through the H5 (coarse alluvium) surficial aquifer or through the confined H3 (advance outwash) aquifer. While there are areas that appear completely unconfined (H5 exposures), most of the floodplain in the study area is semi-confined, as boundaries like Boundary A and B have high amounts of H4 (fine alluvium) at the surface (Figure 6 and Figure 7). This is supported by HDR (2017) which reported that pumping in the floodplain reduces the groundwater flowing into the Skagit River. HDR (2017) also concluded there are three units in the floodplain; a surficial aquifer H5, underlain by a 100 ft thick deeper aquifer H3 and a deeper confining unit or confined aquifer H2 (glaciolacustrine). I define the H2 as an aquitard, but HDR (2017) stated that it could be a confined aquifer because there are small lenses of sand within this unit in Boundary D (Figure 9). However, unlike the clay and silt that define H2, the sand was mostly absent or very thin (1-5 feet) in many of the well logs I examined. Based on these findings, I view H2 as an aquitard or confining unit instead of a deep aquifer.

Recharge to the floodplain aquifers varies spatially because rainfall magnitudes increase eastward, and the surface units vary in infiltration capacity. In the western portion of the study area (Boundary A-C areas), where there is less precipitation and the lower conductive H4 (fine alluvium) is exposed at the surface, the 30-yr annual recharge is about 26-28 inches (Table 7 and Figure 25). Further east in the Boundary D area where the more conductive H5 (coarse alluvium) is exposed at the surface and there is more rainfall due to the orographic effect, the 30-yr annual recharge is about 36 inches (Table 7 and Figure 25). The monitoring well data in the floodplain in Boundary D validates the winter-time recharge by documenting a rise in the water table from November through April (Table 6). It is also likely that the floodplain aquifers are being recharged by connecting hydrogeologic units from the glacial area, but quantifying the recharge rate and magnitude is beyond the scope of my study. In general, groundwater flow in floodplain aquifers is toward the Skagit River and has a westward component down valley through the H5 and H3 (advance outwash) units.

### 5.3 Hydrogeology of the Glacial Terraces and Glacial Uplands

The hydrostratigraphic sequence of the glacial area varies both between model boundaries and within the model boundary. Consistent at higher elevations above the glacial area is H0, the Darrington Phyllite which outcrops on the valley walls and acts as an aquiclude. The H4 in Boundaries C and D is glacial till that is coarse with sand, silt, with limited clay, making H4 less of an aquitard and more conductive to groundwater movement. In the western Boundaries A and B, H4 is glacial till with a finer-grained matrix and glaciomarine drift and is an aquitard. Also, H5 is mostly just recessional outwash on the east side, with glaciomarine outwash on the surface of the west side. Regardless, H5 is still very coarse and conductive in all boundary areas.

Boundary D has a sequence that contains H5 (recessional outwash) on the surface, followed by H4 (glacial till), H3 (advance outwash), and H2 (glaciolacustrine) in the subsurface, at the base (Figures 3, 9 and 19). Boundary C has a very similar hydrostratigraphic sequence to Boundary D, with the eastern part containing more H5 on the surface and the western surface containing H4 on the surface (Figure 8 and Figure 17). Thus, both boundaries have the sequence of an unconfined aquifer at the surface (H5), semi-confining unit below (H4), a confined aquifer (H3) below that, and a low conductive aquitard at the base (H2). HDR (2019) illustrates relatively similar surface and subsurface characteristics in their cross section near Grandy Creek. However, HDR (2019) also reported in their cross section significant amounts of clay and silt in the subsurface of the glacial terrace, mostly at depths occupied by H4 (Figure 9). HDR (2019) likely derived these results from older well logs in the glacial terrace in Boundary D. These well logs near the 310-foot well describe the subsurface as being all clay, or a gravel to clay gradient, but this is likely a result of observation error (e.g., well log 84572 in Appendix A). The subsurface of this area, especially within the H4 depth range had significantly more sand and silt in the geologist-logged 310-foot well rather than silt and clay in the older logs (Figure 4; Appendix C). Given that the 310-foot well stratigraphy is more accurate and detailed, much of the subsurface in Boundaries C and D is likely silt and sand with limited clay, instead of mostly silt and clay. However, there is a possibility that some areas in the glacial terrace area near the 310-foot well might have thicker recessional outwash, and other areas that might have thicker silt and clay units due to glacial erosion causing uneven hilly surface (Riedel, 2025c).

The drift mantled bedrock uplands areas of Boundaries A and B (east Sedro-Woolley to Lyman) have far more complex hydrostratigraphy due to their geologic setting and history. Both contain varying degrees of the hydrogeologic units found in C and D, however, instead of an H2 (glaciolacustrine) base, H1 (Chuckanut Formation) defines much of the base of the glacial uplands. There is limited information about the hydraulic conductivity of H1. I assigned H1 a low K value of about 2 ft/day (Table 3) based on evidence from hydrogeologic studies in Whatcom County (Pitz, 2005; Sullivan, 2005; Associated Earth Sciences, Inc, 2016) and define it as an aquitard. This value could be higher depending on the fracture network in the Chuckanut and could be slowly transmitting groundwater to adjacent glacial deposits. Savoca et al. (2009a) also reported a very low hydraulic conductivity of 0.27 ft/day and referred to the Chuckanut Formation as a confining unit when overlain by other hydrogeologic units similar to what is found in Boundaries A and B.

In the Boundary A area, the surface is mostly dominated by H4 (glacial till and glaciomarine drift) surficial aquitard on the eastern and western locations with H1 (Chuckanut Formation) as the base. The H5 unit (recessional outwash and glaciomarine outwash) is only found on the surface and is of limited areal extent in the middle of the boundary and serves as an unconfined aquifer (Figure 6 and Figure 11). H5 aquifers dominate the surface of the eastern, northern, and west sides of Boundary B, with an H4 aquitard subsurface and an aquitard H1 base (Figure 7 and Figure 14-16). There is an H3 (advance outwash) aquifer present on the surface and subsurface along the east side of Boundary B as well (Figure 16). However, the southern parts of the boundary area are dominated by H4 on the surface followed by H1 in the sub-surface (Figure 7 and Figure 14). The hydraulic conductivities and cross sections described in Savoca et al. (2009a) are similar to what I found in the boundary A area, with an outwash surface, till surface or subsurface, advance outwash confined aquifer, and glaciolacustrine below that. While they found additional units below (older outwash, older till, etc.), their study area had a different glacial history at the end of the ice age, explaining the differences with boundaries C and D.

Like the floodplain, recharge to the aquifers in the glacial area varies spatially because rainfall magnitudes increase eastward and with elevation, and the surface units vary in infiltration capacity. Because H0 (Darrington Phyllite) outcrops at the highest elevations, it receives higher rainfall than the floodplain but is assumed to be impermeable with no recharge (Table 7, Figure 25). However, precipitation runoff is likely providing some recharge to adjacent H4 and H5 units. Recharge to H1 is also minimal, I used a value of 2.0 in/yr estimated by Pitz (2005) for Chuckanut Formation. The 30-yr annual average recharge to the till and outwash in the glacial area ranged from 22-39 inches (Table 7 and Figure 25). My recharge estimates match Savoca et al. (2009a) estimates, as I used the same approach (Bidlake and Payne, 2003; Figure 25).

### 5.4 Hydrogeologic Spatial Continuity

The hydrogeologic continuity between the glacial terraces, glacial uplands, and the floodplain is not necessarily controlled by the floodplain as it has a relatively uniform hydrostratigraphy throughout the study area (at least based on my modeling near glacial area). Instead, the variability of the hydraulic conductivity of the deposits in the glacial uplands and terraces significantly influences the groundwater exchange between both areas. The coarse-grained outwash deposits in the terraces in Boundaries C and D and parts of Boundaries A and B provide high rates of groundwater recharge to the floodplain aquifers. Upland locations in Boundaries A and B with lower conductive units likely deliver lower rates of groundwater to the floodplain.

#### 5.4.1 3D Conceptual Model and 2D Cross Section Evidence

The 3D conceptual models and the 2D cross sections reveal that H3 (advance outwash) is the most important hydrogeologic unit connecting to the floodplain in the glacial terrace in Boundaries C and D. The terraces in Boundaries C and D have fairly conductive surficial units that enhance recharge, and both have thick conductive H3 units that cover the entire lower subsurface that extend down to the same elevations as the valley floor, contributing groundwater to the H5 (recessional outwash and coarse alluvium) and H3 (advance outwash) units in the floodplain (Figure 8-9 and Figure 17-21). Also, the H4 unit (glacial till and fine alluvium) in Boundaries C and D is more coarsely grained, thinner, and more conductive than in the western portions of the study area and is likely slowly recharging deposits in the floodplain. However, due to more of H4 found at the surface of Boundary C, there is likely a lower overall contribution of groundwater transported to the floodplain in this boundary than in Boundary D, with maybe slightly more surface runoff in Boundary C than in D. Despite this, the hydrogeologic units in both boundaries appear to be very well connected to the floodplain units.

Some parts of the glacial uplands in Boundary A and B appear moderately hydrogeologically connected to the floodplain. The south middle area of Boundary A has groundwater connectivity between the glacial uplands and the floodplain, mostly occurring through the H5 unit on the surface. H5 (recessional outwash and glaciomarine outwash) is relatively thick and extends down from the glacial uplands to the floodplain. Much of the groundwater likely reaches the floodplain from the H5 unit in the glacial uplands, with some coming from the lower conductive H4 (glacial till and glaciomarine drift) unit (Figure 11). This is also true for the upper northern side and the east side of Boundary B, as conductive H5 is found on the surface along with conductive H3 (advance outwash) units that extend down to the floodplain. Although the H1 (Chuckanut Formation) aquitard is at the base of the glacial uplands in this region, the high hydraulic gradients due to the large elevation difference between the floodplain and the glacial uplands may cause some recharge to the floodplain deposits through the fracture network in the Chuckanut Formation (H1; Figure 16). The H5 surficial aquifer on the northwest side of Boundary B is likely supplying western streams that could be supporting recharge in the floodplain aquifers (Figure 14).

The east and west sides of the Boundary A glacial uplands have low connectivity to the floodplain due to the presence of the low conductive finer-grained H4 (glacial till and glaciomarine drift) unit on the surface and the H1 (Chuckanut formation) aquitard in the subsurface. Both units are found at the edge of the boundary at the same elevations as the floodplain. While some groundwater might be seeping from the H4 unit to the floodplain, it is likely moving very slowly (Figure 13). As described above, the Chuckanut Formation (H1), may be also slowly recharging the floodplain aquifers through fractures. A similar connectivity occurs on the southwest side of Boundary B as low conductive H4 is found on the surface and H1 aquitard is found in the subsurface (Figure 15). The south middle area of glacial uplands in Boundary B is likely very disconnected with the floodplain because H1 extends 100-300 feet above the floodplain and the H4 unit does not reach the floodplain. It is likely that surface-water runoff is supporting more recharge to the floodplain, than is discharging through the Chuckanut Formation (Figure 14). As a result, the south middle area of Boundary B appears to have the slowest flow between the glacial area and the floodplain.

5.4.2 Seepage Run and Groundwater Monitoring Evidence

Although I found HDR's stream piezometer data to be relatively inconclusive, seepage run data collected in Muddy and Grandy Creeks in Boundaries C and D support some connectivity between the glacial terrace area via the streams and the floodplain. Seepage run data indicate that both creeks are losing water discharged from the upland terraces to the coarse deposits on the floodplain that deliver water to the Skagit River. Where it cuts through the glacial outwash terraces, Grandy Creek is a gaining stream via the unconfined H5 (recessional outwash) unit that extends down from the terrace to the stream along with Alder Creek nearby. The advance outwash (H3) at higher elevations in the glacial terrace as seen with cross sections J and K (Figure 9) also could be supplying some groundwater along the incline between the floodplain and the glacial terrace (HDR, 2024). This can also be seen with WADNR (2016) mapping exposed advanced outwash along the higher elevation regions of Boundary D (Figure 2). Although seepage run data indicates that Muddy Creek is nearly all neutral from the top of the stream to the southern edge of the glacial terrace, it must be gaining water along some reaches to support its flow—possibly along some reaches that were inaccessible to HDR data collectors, e.g., river mile 3.2 and 2.3 (Table 8 Figure 8 and Figure 27). Another reason for the neutral stream results could be the limited exposure of the H5 and H3 units along the glacial terrace walls to supply water. This is further supported with WADNR (2016) mapping showing minimal advance outwash exposed along Muddy Creek (Figure 2). There also could be larger amounts of glacial till or glaciolacustrine along the stream, limiting the water that is seeping into the stream. While no seepage run or stream piezometer data were gathered from Alder Creek, Boundary C, or the five other creeks discharging the uplands in Boundaries A and B (Figure 2), they too are likely losing water to the floodplain aquifers that support flow to the Skagit River. This is supported by Hidaka (1973) as he reported that Alder Creek is a gaining stream with water supplied from precipitation accumulated on the valley peaks during the fall and winter, groundwater supplying inflow to the stream during the dry summer, and water infiltrating into the glacial deposits due to having coarse surficial conditions. These are similar characteristics to what is found in Grandy Creek, so it would be reasonable to assume similar conditions for both areas.

The four domestic wells that I monitored all showed similar seasonal patterns, suggesting that they are all in the H3 unit connecting the upland terrace to the floodplain in Boundary D (Figure 24). In general, the water levels increased with seasonal rainfall and decreased during the dry season. MWD in the glacial terrace had the fastest response time to seasonal changes, and the largest fluctuations in groundwater depth (Figure 22). MWD's response to precipitation is relatively quick—possibly due to higher rainfall rates infiltrating rapidly into H3 exposures at higher elevation valley walls. For example, MWD suddenly increased in water le depth in December due to November rainfalls, while the response in the wells in the floodplain was delayed due to the transport time required to reach the floodplain (Figure 2 and Figure 22). The erratic water levels observed in some of the wells could have resulted from rainfall recharge fluctuations, human or instrument error, or a delayed well recovery because some wells were used for irrigation purposes. Although landowners were notified prior to field visits they may have been operating their wells prior to the measurements.

The 310-foot well responded very slowly to seasonal changes and its water levels fluctuated minimally (Figure 22). The well is screened in the H3 unit between 200-220 feet below the ground surface and may be slower to respond to recharge due to the lower conductive deposits above the screened interval. Because of its depth and the complex geology, it is difficult to say what controls the recharge and water-level response. Despite this, it is apparent groundwater is moving from the glacial outwash terraces to the floodplain in Boundary D and presumably along Boundary C from H5 in the surface and H3 in the subsurface.

## 6. Conclusions and Recommendations

I used information from over 133 driller well logs, geologic mapping, and field visits to develop 2D cross sections and 3D conceptual models of the aquifer systems of the lower Skagit River valley. To fully characterize the hydrogeologic framework I also estimated aquifer hydraulic parameters and annual recharge and identified regions where aquifers in the glacial uplands and glacial terraces are connected to and recharging floodplain aquifers. Although my hydrogeologic framework is the most extensive to date, I recommend more detailed studies before groundwater management choices are made regarding water resources in the lower Skagit River Valley.

Although my well-log database is extensive, a limitation of my 2D cross sections, 3D conceptual models, and interpretations is the inconsistent spatial distribution of drinking-water wells and the quality of the driller well logs. Boundaries A and B have a significant number of wells, whereas Boundaries C and D have limited well information due to the lack of housing development, and some areas being on undeveloped state forest land, hence the decision to drill the 310-foot monitoring well near Alder Creek. While my project benefited from a new 310-foot well that provided useful stratigraphic information in Boundary D, the same cannot be said for Boundary C which has no wells in the glacial terraces (Figure 2, Appendix A). This limited my interpretations to above ground field observations and the use of pseudo wells in the modeling software to interpolate between wells. I had to use pseudo wells and infer depths in other areas due to the lack of wells to support my interpretations (as seen with the ?? on the cross sections).

To better characterize the hydrogeology, I recommend more extensive well monitoring, long-term pump tests, and groundwater modeling to constrain recharge rates and groundwater flow directions and rates in the study area. While I am confident that the sub-surface conditions at Boundary C are similar to Boundary D, drilling some deep wells in the Hamilton glacial terrace area would confirm my interpretations of the hydrogeologic characteristics and connectivity of Boundary C's glacial terrace and the floodplain. Drilling some deep wells in the floodplain would help determine the extent and thickness of the glaciolacustrine deposit as in some wells, it appears extraordinarily thick (150+ feet thick). Based on regional geologic evidence there are likely Olympia and Whidbey interglacial deposits beneath the lacustrine layer that may serve as alternative aquifers (e.g., Vaccaro et al., 1998; AESI, 2016). Also, performing some strategically located, long duration well-pumping tests in both the glacial area and adjacent floodplain areas would validate groundwater connections in the glacial area to the floodplain and refine the hydraulic attributes of the aquifers, especially in areas where connections are more suspect.

Another major limitation resulted from the lack of seepage run and well monitoring data in Boundaries A and B. There are likely low rates of groundwater flow from the low-conductive H4 (till and drift) and H1 (fractured Chuckanut Formation) to floodplain deposits in the western half of the study area, meaning that there may be no truly isolated aquifers in the upland area that would serve as an alternative water supply. Seepage runs, well monitoring, and pump tests in Boundaries A and B would help validate this. This is especially true in the in areas where the Chuckanut Formation (H1) is connected to the floodplain deposits. It remains unclear how the fracture network is transmitting water but some domestic wells are completed in the formation, so it has some permeability.

My detailed conceptual models not only provide some evidence of the continuity between the glacial and alluvial deposits, but they may also serve as a basis for assessing the location of potential managed aquifer recharge (MAR) sites. The idea of MAR is to enhance groundwater storage by diverting river water during high-flow periods into engineered detention sites that infiltrate into unconfined aquifers that connect to the river. With the proper detention volumes, infiltration rates, aquifer hydraulic conductivity, and travel length, the enhanced groundwater recharge can augment river flow during the drier, low-flow periods in summer months (e.g., Parker et al., 2022).

In terms of modeling, I used Aquaveo's Arc-Hydro Groundwater Subsurface Analyst to develop 2D cross sections and 3D conceptual models of the hydrostratigraphy in the study area. Groundwater modeling would be the next logical step for examining the continuity of the aquifer systems and for determining recharge rates and groundwater flow directions and rates in the study area. However, applying Aquaveo's MODFLOW (USGS, 2025) extension to model groundwater flow would be challenging using my conceptual framework. I chose to break up the study area into four separate boundaries to capture and illustrate the complex nature of the hydrostratigraphy, whereas MODFLOW requires a single modeling domain. Also, the version of the Subsurface Analyst that I used to develop the conceptual models requires ESRI's ArcMap which is being phased out by ESRI. My conceptual models would have to be rebuilt using my well database and the ArcGIS Pro version of Aquaveo's Arc-Hydro Groundwater Subsurface Analyst.

## 7. References


Armstrong, J.E., D.R. Crandell, D.J. Easterbrook, and J.B. Noble. 1965. Late Pleistocene Stratigraphy and Chronology in Southwestern British Columbia and Northwestern Washington, GSA Bulletin, https://pubs.geoscienceworld.org/gsa/gsabulletin/article-abstract/76/3/321/5867/Late-Pleistocene-Stratigraphy-and-Chronology-in (accessed June 2023).

Aquaveo Arc Hydro Groundwater. 2024. https://www.aquaveo.com/software/ahgw-archydro-groundwater-introduction (accessed June 2024).

Associated Earth Sciences, Inc (AESI). 2016. Final Draft Technical Report Phase 2 – Data Collection and Conceptual Model Development, Whatcom County, Washington. Prepared for Whatcom County

Bandaragoda, C., C. Evans, E. Istanbulluoglu, C. Raymond, and L. Wasserman. 2015. Hydrologic Impacts of Climate Change in the Skagit River Basin: Skagit Climate Science, http://www.skagitclimatescience.org/wp-content/uploads/2016/04/UW-SC2_SkagitDHSVM-glacierModel_FinalReport_2015.pdf (accessed May 2023).

Bear, J. 1979. Hydraulics of Groundwater, McGraw-Hill Series in Water Resources and Environmental Engineering. McGraw-Hill, New York.

Beget, J.E. 1982. Postglacial Volcanic Deposits at Glacier Peak, Washington, and Potential Hazards from Future Eruptions; Open-File Report, doi: 10.3133/ofr82830.

Bidlake, W.R., and K.L. Payne. 2001. Estimating Recharge to Ground Water from Precipitation at Naval Submarine Base Bangor and Vicinity, Kitsap County, Washington: Water-Resources Investigations Report, https://doi.org/10.3133/wri014110 (accessed June 2024).

Connor, E.J., and D.E. Pflug. 2004. Changes in the Distribution and Density of Pink, Chum, and Chinook Salmon Spawning in the Upper Skagit River in Response to Flow Management Measures, North American Journal of Fisheries Management, v. 24, p. 835–852, doi: 10.1577/m03-066.1.

Dethier, D.P., F. Pessl, R.F. Keuler, M.A. Balzarini, and D.R. Pevear. 1995. Late Wisconsinan Glaciomarine Deposition and isostatic rebound, northern Puget Lowland, Washington, Geological Society of America Bulletin, v. 107, p. 1288–1303, doi: 10.1130/0016-7606(1995)107<1288:lwgdai>2.3.co;2.

Dragovich, J.D., D.K. Norman, T.J. Lapen, and G. Anderson. 1999. Geologic Map of the Sedro-Woolley North and Lyman 7.5-minute Quadrangles, Western Skagit County, Washington, Washington Division of Geology and Earth Resources, Open-File Report.

Dragovich, J.D, and D.T. Mckay. 2000. Holocene Glacier Peak Lahar Deposits in the Lower Skagit River Valley, Washington, Washington Geology, vol. 28, no. 1-2, https://www.dnr.wa.gov/publications/ger_washington_geology_2000_v28_no1-2.pdf (accessed October 2024).

Dragovich, J. D., L.A. Gilbertson, W.S. Lingley Jr., M. Polenz, and J. Glenn. 2002. Geologic Map of the Darrington 7.5-minute Quadrangle, Skagit and Snohomish Counties, Washington, WA DGER OFR 2002-7, 1 sheet, 1:24,000.

Drost, B.W., and R.E. Lombard. 1978. Water in the Skagit River Basin, Washington, Water-Supply Bulletin 47.

Dunham, R.E., 2010, Kink band development in the Darrington Phyllite on Samish Island, northwestern Washington: WWU Graduate School Collection. 66, https://cedar.wwu.edu/wwuet/66 (accessed November 2024).

Ferris, J.G., D.B. Knowles, R.H. Brown, and R.W. Stallman. 1962. Theory of Aquifer Tests: U.S. Geological Survey Water-Supply Paper 1536-E.

Fountain, A.G., Glenn, B., and Mcneil, C., 2023, Inventory of glaciers and perennial snowfields of the Conterminous USA: Earth System Science Data, v. 15, p. 4077–4104, doi: 10.5194/essd-15-4077-2023.

Frans, C., E. Istanbulluoglu, D.P. Lettenmaier, A.G. Fountain, and J. Riedel. 2018. Glacier Recession and the Response of Summer Streamflow in the Pacific Northwest United States, 1960–2099, Water Resources Research, v. 54, p. 6202–6225, doi: 10.1029/2017wr021764.

Freeze, R.A., J.A. and Cherry. 1979. Groundwater. Englewood Cliffs, New Jersey, Prentice-Hall, 604 p.

Gendaszek, A. S. 2014. Hydrogeologic framework and groundwater/surface-water interactions of the South Fork Nooksack River Basin, northwestern Washington. USGS Scientific Investigations Report No. 2014-5221. DOI: 10.3133/sir20145221

GeoEngineers. 2003. Lower and Upper Skagit Watershed Plan Samish River Sub-Basin, Ground Water Hydrology Evaluation, File no. 7291-001-00-1180, 175 p.

Haugerud, R. A., and R.W. Tabor. 2009. Geologic Map of the North Cascade Range, Washington, USGS Publications Warehouse, https://pubs.usgs.gov/sim/2940/ (accessed March 2023).

Hidaka, F.T. 1973. Low-flow Characteristics of streams in the Puget Sound region, U.S. Geological Survey Open File Report to Washington Department of Ecology, doi: 10.3133/ofr72163.

HDR. 2017. Middle Skagit Valley Hydrogeologic Assessment, prepared for the Washington State Department of Ecology Technical Memorandum, 126 p., https://wsuniv.maps.arcgis.com/sharing/rest/content/items/1bdeabd03bd34124adafd009629a65e0/data.

HDR. 2019. Middle and Upper Skagit River Valley Hydrostratigraphy Characterization, prepared for the Washington State Department of Ecology, 124 p., https://apps.ecology.wa.gov/publications/parts/1911088part3.pdf.

HDR. 2024. Surface Water and Groundwater Interaction: Skagit River Basin Groundwater Study, Report prepared for Washington State University.

Kahle, S.C., and T.D. Olsen. 1995. Hydrogeology and Quality of Ground Water on Guemes Island, Skagit County, Washington, Report, USGS Series No. 94-4236. doi: 10.3133/wri944236.

Lee, S-Y., and A.F. Hamlet. 2011. Skagit River Basin Climate Science Report, a summary report prepared for Skagit County and the Envision Skagit Project by the Department of Civil and Environmental Engineering and The Climate Impacts Group, University of Washington, Seattle. (accessed January 2023)

Lowe, A, 2017, Western Washington 3DEP 2016 LIDAR Technical Data Report: Quantum Spatial, originally contracted by United States Geological Survey. (accessed January 2024 at https://lidarportal.dnr.wa.gov/#)

Mitchell, R.J. 2023. Hydraulic Conductivity Python Script, Personal Communication.

Mustoe, G.E., and Gannaway, W.L. 1997. Paleogeography and paleontology of the early tertiary chuckanut formation, Northwest Washington: Olympia, Wash, Washington State Dept. of Natural Resources, v. 25, p. 3-18.

Parker, T. K., W. M. Alley, and C. A. Jobs. 2022. Managed Aquifer Recharge: A Proven Technology for Water Supply Resilience. Groundwater. https://doi.org/10.1111/gwat.13222

Pitz, C.F. 2005. Lake Whatcom Total Maximum Daily Load Groundwater Study, https://apps.ecology.wa.gov/publications/documents/0503001.pdf.

PRISM Climate Group, Oregon State University, https://prism.oregonstate.edu/ (accessed August 2024).

Riedel, J. 2007. Late Pleistocene Glacial and Environmental History of the Skagit Valley, Washington and British Columbia: Summit Research Repository, https://summit.sfu.ca/item/8099 (accessed June 2023).

Riedel, J.L. 2017. Deglaciation of the North Cascade Range, Washington, and British Columbia, from the Last Glacial Maximum to the Holocene, Cuadernos de Investigación Geográfica, v. 43, p. 467–496, doi:10.18172/cig.3236.

Riedel, J.L. 2023. Formation of Skagit Valley Glacial Terrace, Personal Communication.

Riedel, J.L. 2024a. Geomorphic Map of the Lower Skagit Valley, Personal Communication.

Riedel, J.L. 2024b. 310-Foot Well Log Stratigraphic Interpretation, Personal Communication.

Riedel, J.L. 2025a. Glacial Deposit Interpretation, Personal Communication.

Riedel, J.L. 2025b. Glaciolacustrine Event Timeline, Personal Communication.

Riedel, J.L. 2025c. Possible Glacial Erosion in Glacial Terrace Area, Personal Communication

Riedel, J.L., J.J. Clague, and B.C. Ward. 2010. Timing and extent of early Marine Oxygen Isotope Stage 2 Alpine glaciation in Skagit Valley, Washington, Quaternary Research, v. 73, p. 313–323, doi: 10.1016/j.yqres.2009.10.004.

Riedel, J.L., and M.A. Larrabee. 2016. Impact of Recent Glacial Recession on Summer Streamflow in the Skagit River, Northwest Science, v. 90, p. 5–22, doi:10.3955/046.090.0103.

Roop, H.A., G.S. Mauger, H. Morgan, A.K. Snover, and M. Krosby. 2020. Shifting Snowlines and Shorelines: The Intergovernmental Panel on Climate Change's Special Report on the Ocean and Cryosphere and Implications for Washington State, Climate Impacts Group, University of Washington, Seattle, https://cig.uw.edu/projects/shifting-snowlines-and-shorelines/ (accessed May 2023).

Savoca, M.E., K.H. Johnson, S.S. Sumioka, T.D. Olsen, E.T. Fasser, and R.L. Huffman. 2009a. Hydrogeologic Framework, Groundwater Movement, and Water Budget in Tributary Subbasins and Vicinity, Lower Skagit River Basin, Skagit and Snohomish Counties, Washington: U.S. Geological Survey, p. 1–46, doi: 10.3133/sir20095270.

Savoca, M.E., K.H. Johnson, and E.T. Fasser. 2009b. Shallow Groundwater Movement in the Skagit River Delta Area, Skagit County, Washington: Scientific Investigations Report, doi: 10.3133/sir20095208.

Scott, K.M., D.S. Tucker, J.L. Riedel, C.A. Gardner, and J.P. McGeehin. 2020. Latest Pleistocene to Present Geology of Mount Baker Volcano, Northern Cascade Range, Washington: Professional Paper, https://pubs.er.usgs.gov/publication/pp1865 (accessed June 2023).

Sedro-Woolley, Washington. Period of Record Monthly Climate Summary, https://wrcc.dri.edu/cgi-bin/cliMAIN.pl?wa7507 (accessed May 2023).

Skagit County. 2024a. Well Search by Address, https://skagitcounty.net/Search/wells/ (accessed June 2024).

Skagit County. 2024b. iMap Skagit County Government Home Page, https://skagitcounty.net/maps/imap/ (accessed June 2024).

Sullivan, William M. 2005. The Hydrogeology of North Lummi Island, Washington. WWU Graduate School Collection. 459.https://cedar.wwu.edu/wwuet/459 (accessed January 2025).

US Army Corps of Engineer (USACE). 2013. Hydrology Technical Documentation - Skagit County, Washington: Skagit County, https://www.skagitcounty.net/PublicWorksSalmonRestoration/Documents/Skagit%20River%20Hydrology%20Technical%20Doc_Final_August2013.pdf (accessed May 2023).

United States Geological Survey (USGS). MODFLOW 6: USGS modular hydrologic model. https://www.usgs.gov/mission-areas/water-resources/science/modflow-and-related-programs (accessed March 2025).

Vaccaro, J.J., A. J. Hansen, and M. A. Jones. 1998. Hydrogeologic Framework of the Puget Sound Aquifer System, Washington and British Columbia: Professional Paper, doi: 10.3133/pp1424d.

Vallance, J.W., Van Eaton, A.R., and Ramsey, D.W. 2015. Late Pleistocene and Holocene Geology and Hazards at Glacier Peak Volcano, Washington: AGU, https://ui.adsabs.harvard.edu/abs/2015AGUFM.V33B3088V/abstract (accessed March 2025).

Washington State Department of Ecology (Ecology). 2022. Well Reports (Well Logs), https://geo.wa.gov/datasets/waecy::well-reports-well-logs/about (accessed August 2022).

Washington State Department of Ecology (Ecology). 2023a. Skagit River Basin, https://ecology.wa.gov/Water-Shorelines/Water-supply/Protecting-stream-flows/Instream-flow-implementation/Skagit-River-basin#:~:text=In%202001%2C%20we%20adopted%20WAC,while%20protecting%20existing%20water%20rights (accessed January 2023).

Washington State Department of Ecology (Ecology). 2023b. Washington State Well Report Viewer Well Report Search Options, https://appswr.ecology.wa.gov/wellconstruction/map/WCLSWebMap/default.aspx (accessed May 2023).

Washington State Department of Natural Resources (DNR). 2016. 100k_Surface_Geology: https://gis.dnr.wa.gov/site1/rest/services/Public_Geology/100k_Surface_Geology/MapServer (accessed April 2023).

Washington State Department of Natural Resources (DNR). 2024. Chuckanut Mountains: WA100, https://wa100.dnr.wa.gov/north-cascades/chuckanut-mountains (accessed June 2024).

Washington State University (WSU). 2024. AgWeatherNet, Concrete Weather Station, https://weather.wsu.edu/?p=88650 (accessed September 2024).

## 8. Tables

Table 1: Temperature (°F) and precipitation (inches) for the 1981 – 2020 normal recorded at the Sedro-Woolley 1 E, WA Coop weather station, Skagit River Valley (Sedro Woolley).

| | Jan | Feb | Mar | Apr | May | Jun | Jul | Aug | Sep | Oct | Nov | Dec | Annual |
|---|---|---|---|---|---|---|---|---|---|---|---|---|---|
| Temp | 40.9 | 42.4 | 46.1 | 50.1 | 55.5 | 59.8 | 63.5 | 63.9 | 59.1 | 51.6 | 44.7 | 39.6 | 51.5 |
| Prec | 5.9 | 3.6 | 4.4 | 3.8 | 3.2 | 2.8 | 1.5 | 1.7 | 2.6 | 4.8 | 7.3 | 5.0 | 46.5 |

Temp = Mean Temperature

Prec = Precipitation

Table 2: Recharge equations used with the associated geologic units and landcover type. Equations derived from Bidlake and Payne, 2001, Vaccaro et al., 1998, and Pitz, 2005.

| Landcover type | Equation | Geologic Units |
|---|---|---|
| "nonforest vegetation on soils formed on glacial outwash and other alluvium" | $R = 0.806P - 8.87$ (Bidlake and Payne, 2001) | Alluvium |
| "forest vegetation and soils formed on glacial outwash and other alluvium" | $R = 0.633P - 6.96$ (Bidlake and Payne, 2001) | Recessional Outwash<br>Advance Outwash<br>Glaciomarine Outwash |
| "forest and nonforest vegetation on soils formed on glacial till or fine-grained sediments" | $R = 0.388P - 4.27$ (Bidlake and Payne, 2001) | Glacial Till<br>Glaciomarine Drift |
| Chuckanut Formation | $R = 2$ (Pitz, 2005) | Chuckanut Formation |
| Bedrock | $R = 0$ (Vaccaro et al., 1998) | Darrington Phyllite |

R = Recharge (in/yr)

P = Precipitation (in/yr)

Table 3: Geometric means of hydraulic conductivity (K) estimates of geologic units in the Skagit River Valley (n = number of wells used in the analysis).

| Geologic Unit | K (ft/day) |
|---|---|
| Alluvium between Alder and Muddy Creek | 569 (n = 10) |
| Alluvium at Hamilton | 543 (n = 12) |
| Lahar | 518 (n = 24) |
| Alluvium West of Hamilton | 437 (n = 7) |
| Alluvium East of Grandy Creek | 293 (n = 37) |
| Alluvial Fan | 288 (n = 7) |
| Advance Glacial Outwash (East side) | 267 (n = 3) |
| Alluvium between Alder and Grandy Creek | 171 (n = 40) |
| Advance Glacial Outwash (West side) | 38 (n = 7) |
| Till and Glaciomarine Drift | 9 (n = 21) |
| Glaciolacustrine | 8 (n = 16) |
| Chuckanut Formation | 2 (n = 14) |

Table 4: Hydrogeologic units in the Skagit River Valley Hydraulic conductivity (K) values are approximate.

| Hydrogeologic Unit | Geologic Units | K (ft/day) |
|---|---|---|
| H5 | Recessional Glacial Outwash, Glaciomarine Outwash, Coarse Alluvium | 171-569 |
| H4 | Glacial Till, Glaciomarine Drift, Fine Alluvium | 9 |
| H3 | Advance Glacial Outwash | 38-267 |
| H2 | Glaciolacustrine | 8 |
| H1 | Chuckanut Formation | 2 |
| H0 | Jurassic Darrington Phyllite | NA |

Table 5: Well and spatial data of the monitoring wells in the Skagit River Valley.

| Well | Elevation (ft) | Depth (ft) | Screen Length (ft) | Longitude | Latitude |
|---|---|---|---|---|---|
| MWA | 156.66 | 60 | 5 | -121.8952 | 48.5253 |
| MWB | 178.10 | 70 | Open Interval | -121.8924 | 48.5304 |
| MWC | 186.08 | 78? | Unknown | -121.8928 | 48.5288 |
| MWD | 354.67 | 125-130 | Open Interval | -121.8858 | 48.5382 |
| 310-Foot Well | 300 | 310 | 20 | -121.9402 | 48.5346 |

Table 6: Monthly water level data from the monitoring wells in the Skagit River Valley.

| | MWA | | MWB | | MWC | | MWD | | 310-foot well | |
|---|---|---|---|---|---|---|---|---|---|---|
| Date | Depth from Surface (ft) | Change in Depth (ft) | Depth from Surface (ft) | Change in Depth (ft) | Depth from Surface (ft) | Change in Depth (ft) | Depth from Surface (ft) | Change in Depth (ft) | Depth from Surface (ft) | Change in Depth (ft) |
| 4/26/23 | 0.00 | 0.00 | 35.30 | 0.00 | 35.10 | 0.00 | 83.70 | -3.80 | 131.83 | -0.41 |
| 5/23/23 | 33.50 | -0.10 | 38.50 | -3.20 | 38.80 | -3.70 | 84.50 | -4.60 | 131.86 | -0.44 |
| 6/21/23 | 34.80 | -1.40 | 37.40 | -2.10 | 40.05 | -4.95 | 86.40 | -6.50 | 132.37 | -0.95 |
| 7/20/23 | 36.05 | -2.65 | 38.45 | -3.15 | 41.50 | -6.45 | 87.60 | -7.70 | 132.78 | -1.36 |
| 8/24/23 | 37.40 | -4.00 | 39.90 | -4.60 | 43.00 | -7.90 | 88.70 | -8.80 | 133.57 | -2.15 |
| 9/22/23 | 38.10 | -4.70 | 40.90 | -5.60 | 44.10 | -9.00 | 90.40 | -10.50 | 133.30 | -1.88 |
| 10/23/23 | 38.60 | -5.20 | 41.60 | -6.30 | 45.00 | -9.90 | 91.30 | -11.40 | 133.99 | -2.57 |
| 11/29/23 | 38.60 | -5.20 | 42.10 | -6.80 | 45.80 | -10.70 | 86.10 | -6.20 | 134.61 | -3.18 |
| 12/20/23 | 36.40 | -3.00 | 41.70 | -6.40 | 45.60 | -10.50 | 87.90 | -8.00 | 134.55 | -3.13 |
| 1/24/24 | 35.30 | -1.90 | 40.85 | -5.55 | 44.80 | -9.70 | 82.00 | -2.10 | 135.27 | -3.85 |
| 2/24/24 | 34.82 | -1.44 | 39.80 | -4.50 | 43.46 | -8.36 | 82.20 | -2.30 | 135.25 | -3.83 |
| 3/19/24 | 33.40 | 0.00 | 38.10 | -2.80 | 41.80 | -6.70 | 79.90 | 0.00 | 134.70 | -3.28 |
| 4/30/24 | 34.70 | -1.30 | 38.10 | -2.80 | 41.05 | -5.95 | 80.80 | -0.90 | 134.26 | -2.84 |

Table 7: Recharge and precipitation estimates in geologic units within the Skagit River Valley.

| Location | | Glacial Till (in/yr) | Alluvium (in/yr) | Outwash (in/yr) | Chuckanut Formation (in/yr) | Darrington Phyllite Bedrock (in/yr) |
|---|---|---|---|---|---|---|
| Boundary A | Precipitation | 53.0 | 44.0 | 75.0 | 53.0 | 125.0 |
| | Recharge | 16.3 | 26.6 | 40.5 | 2.0 | 0.0 |
| Boundary B | Precipitation | 68.0 | 45.0 | 72.0 | 68.0 | 115.0 |
| | Recharge | 22.1 | 27.4 | 38.6 | 2.0 | 0.0 |
| Boundary C | Precipitation | 60.0 | 46.0 | 62.0 | 0.0 | 100.0 |
| | Recharge | 19.0 | 28.2 | 32.3 | 0.0 | 0.0 |
| Boundary D | Precipitation | 88.0 | 56.0 | 65.0 | 0.0 | 105.0 |
| | Recharge | 29.9 | 36.3 | 34.2 | 0.0 | 0.0 |

Table 8: Seepage run data of Grandy Creek in the Skagit River Valley (from HDR, 2024).

| Reach Begin (River Mile) | Reach End (River Mile) | Inferred Groundwater Gain/Loss (cfs) | Inferred Groundwater Gain/Loss rate (cfs per river mile) | Gaining or losing |
|---|---|---|---|---|
| 5.30 | 5.20 | 0.03 | | |
| 5.18 | 4.85 | 4.53 | 13.73 | Gaining |
| 4.85 | 4.23 | 1.08 | 1.75 | Gaining |
| 4.23 | 3.79 | 0.21 | 0.48 | Gaining |
| 3.79 | 3.25 | -2.23 | -4.13 | Losing |
| 3.25 | 2.88 | 0.86 | 2.33 | Gaining |
| 2.88 | 2.84 | -0.10 | 0.00 | Neutral |
| 2.84 | 2.30 | 1.09 | 2.01 | Gaining |
| 2.30 | 1.66 | 3.87 | 6.04 | Gaining |
| 1.66 | 1.10 | -3.93 | -7.02 | Losing |
| 1.10 | 0.30 | 0.16 | 0 | Neutral |

Table 9: Seepage run data of Muddy Creek in the Skagit River Valley (from HDR, 2024).

| Reach Begin (River Mile) | Reach End (River Mile) | Inferred Groundwater Gain/Loss (cfs) | Inferred Groundwater Gain/Loss rate (cfs per river mile) | Gaining or losing |
|---|---|---|---|---|
| 3.7 | 3.61 | 0.01 | 0.00 | Neutral |
| 3.61 | 3.20 | -0.05 | 0.00 | Neutral |
| 3.20 | 2.31 | 0.10 | 0.00 | Neutral |
| 2.31 | 2.11 | 1.20 | 5.99 | Gaining |
| 2.11 | 1.53 | 0.00 | 0.00 | Neutral |
| 1.53 | 1.20 | -0.06 | 0.00 | Neutral |
| 1.20 | 0.98 | -0.33 | -1.52 | Losing |
| 0.98 | 0.67 | -0.48 | -1.55 | Losing |
| 0.67 | 0.10 | -0.46 | -0.81 | Losing |

# 9. Figures

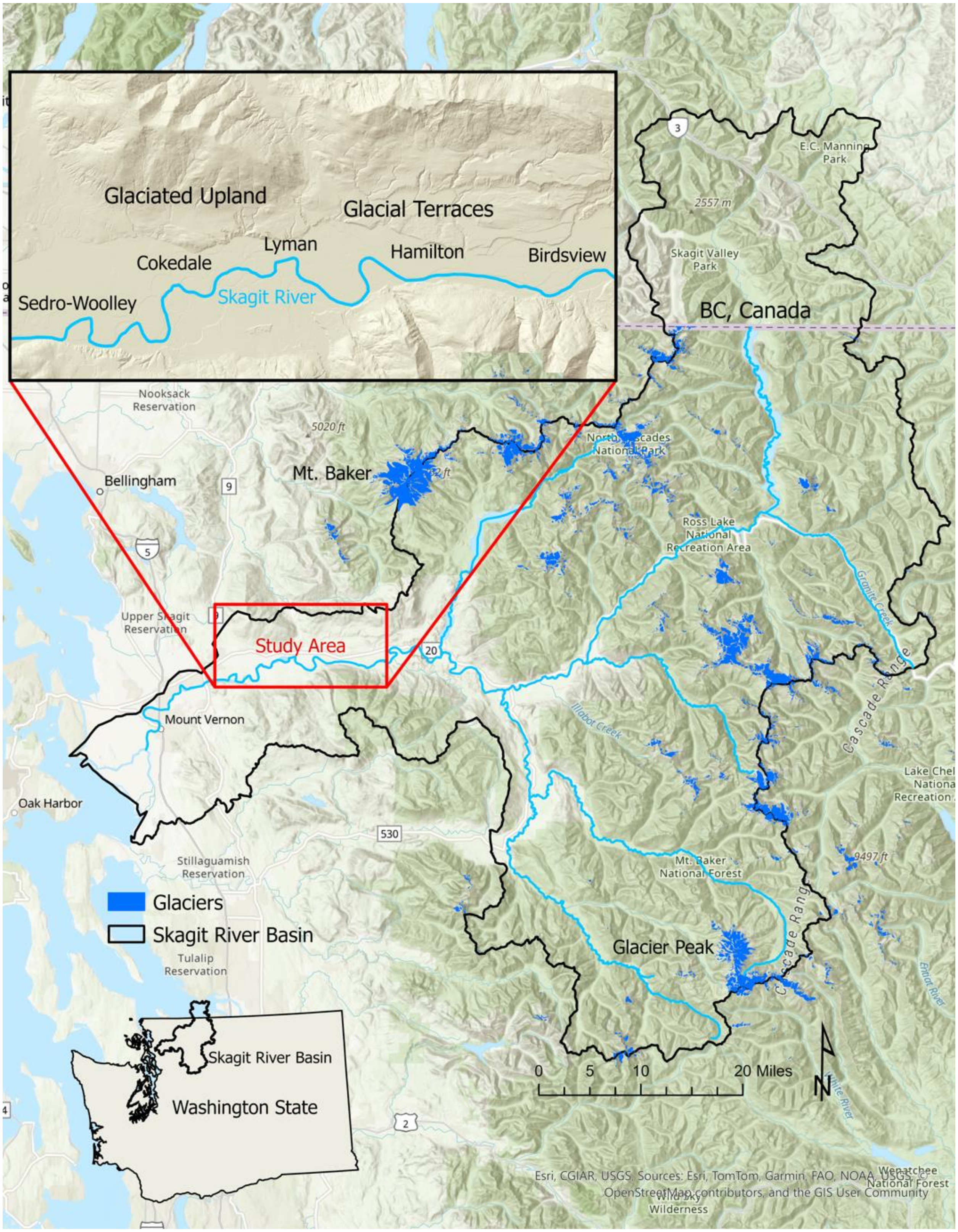


Figure 1: Map of the Skagit River basin and study area in northwest Washington State.

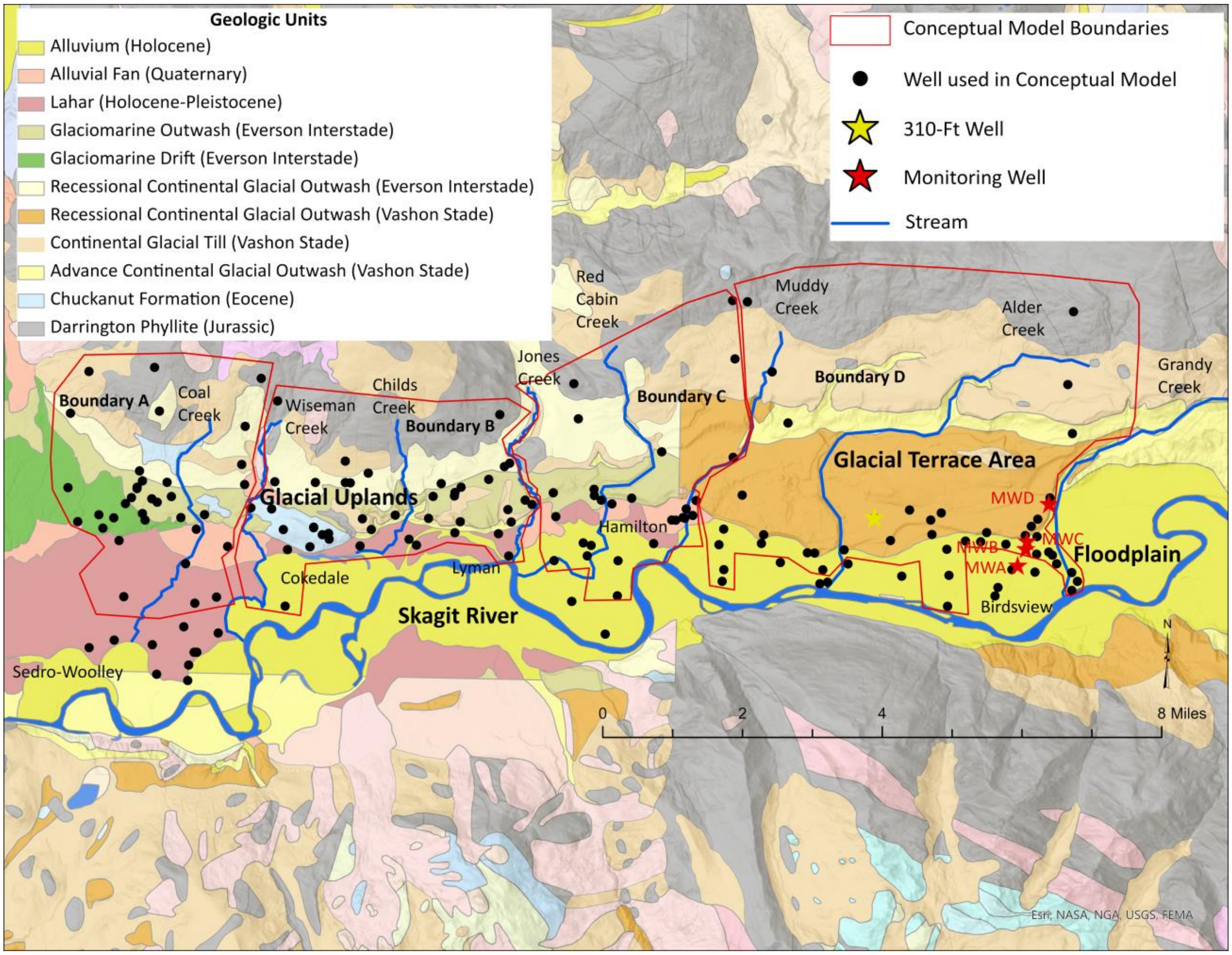


Figure 2: Map of the surficial geology in the lower Skagit River Valley study area, including the conceptual model Boundaries A-D, wells used in the conceptual model, and monitoring wells (geology modified from WADNR, 2016, 100k Surface Geology).

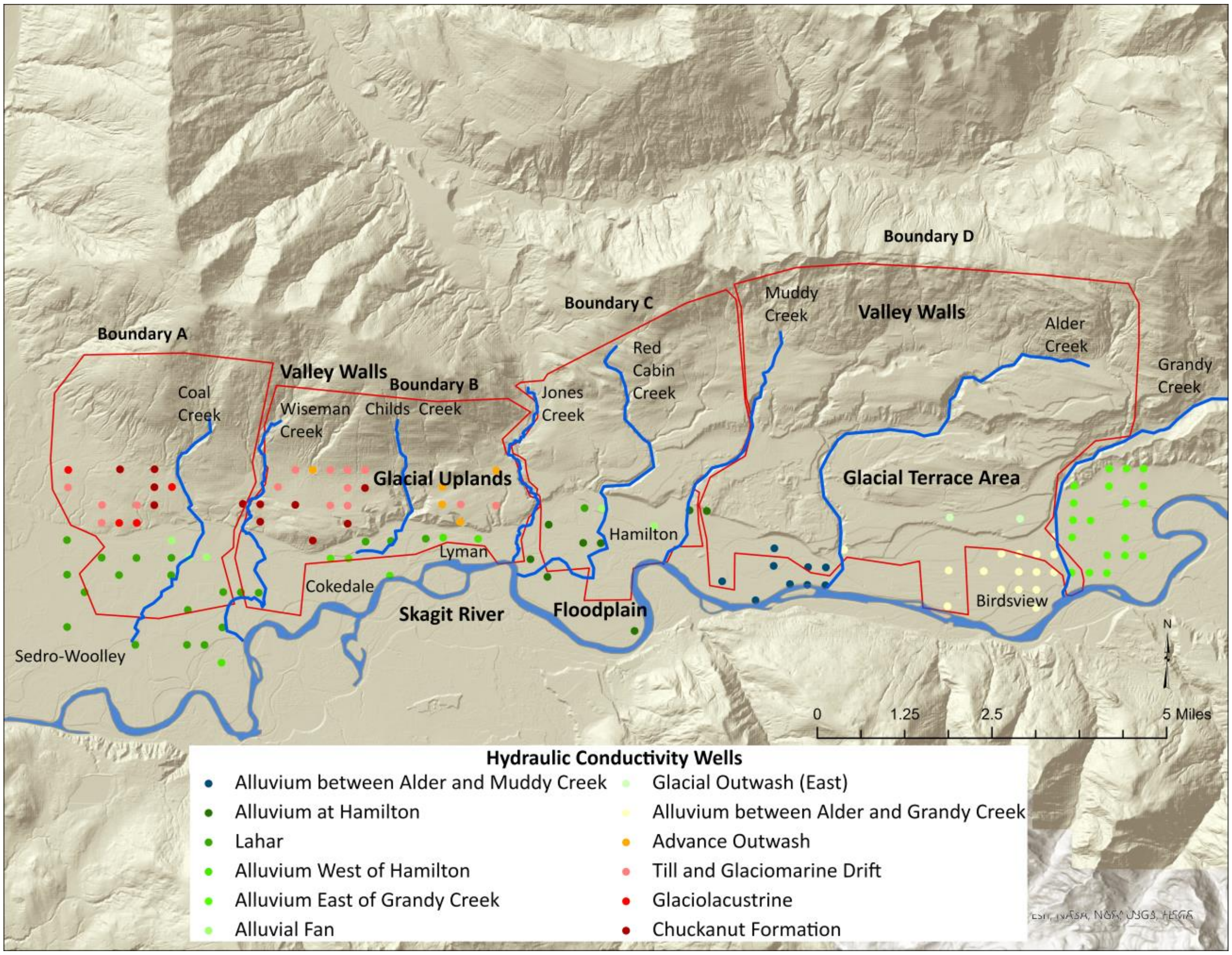


Figure 3: LiDAR map of the lower Skagit River Valley study area, including the conceptual model Boundaries A-D, and wells used to estimate hydraulic conductivity values (LiDAR hillshade from Lowe, 2017, Puget Sound LiDAR digital terrain model).

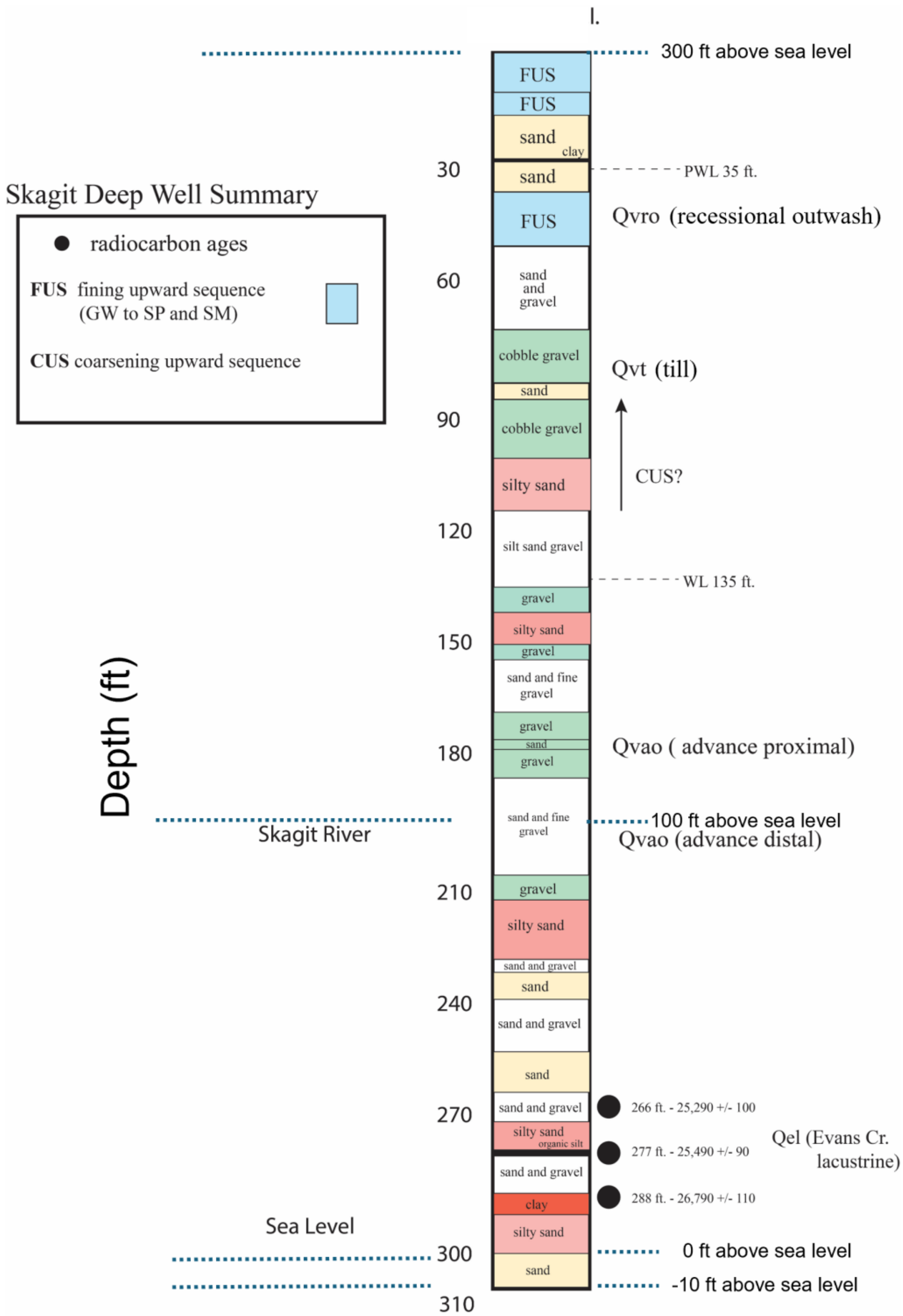


Figure 4: New 310-foot well stratigraphic sequence. Important glacial deposits, sea level elevations and grain sizes displayed in the image. Source: Riedel 2024b.

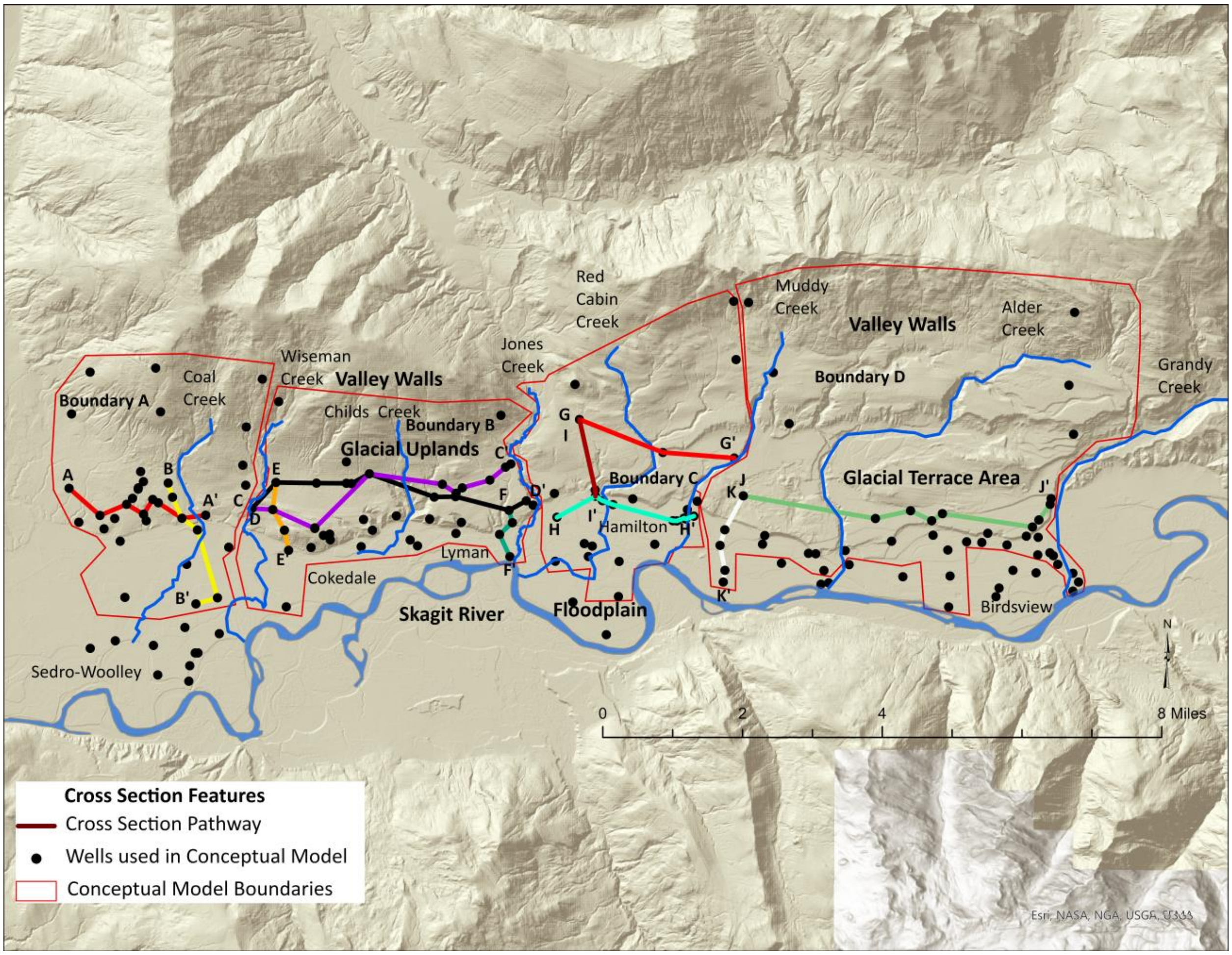


Figure 5: LiDAR map of the conceptual model Boundaries A-D, wells used in the conceptual models and selected cross sections in each boundary (LiDAR hillshade from Lowe, 2017, Puget Sound LiDAR digital terrain model).

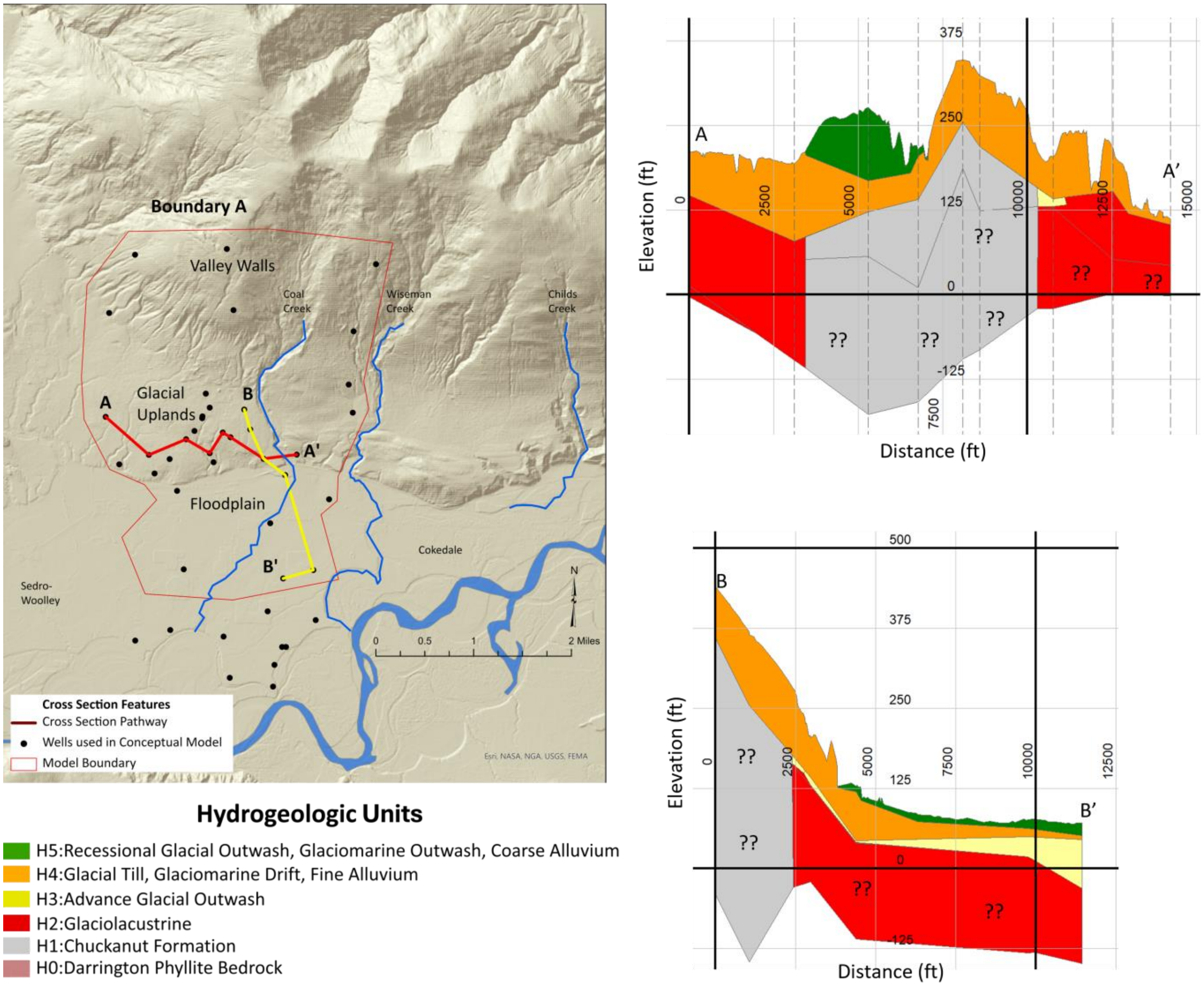


Figure 6: LiDAR map and hydrogeology of the selected cross sections in conceptual model Boundary A in the lower Skagit River Valley study area. Cross sections A-B are vertically exaggerated by 20x to better display topographic changes (LiDAR hillshade from Lowe, 2017, Puget Sound LiDAR digital terrain model).

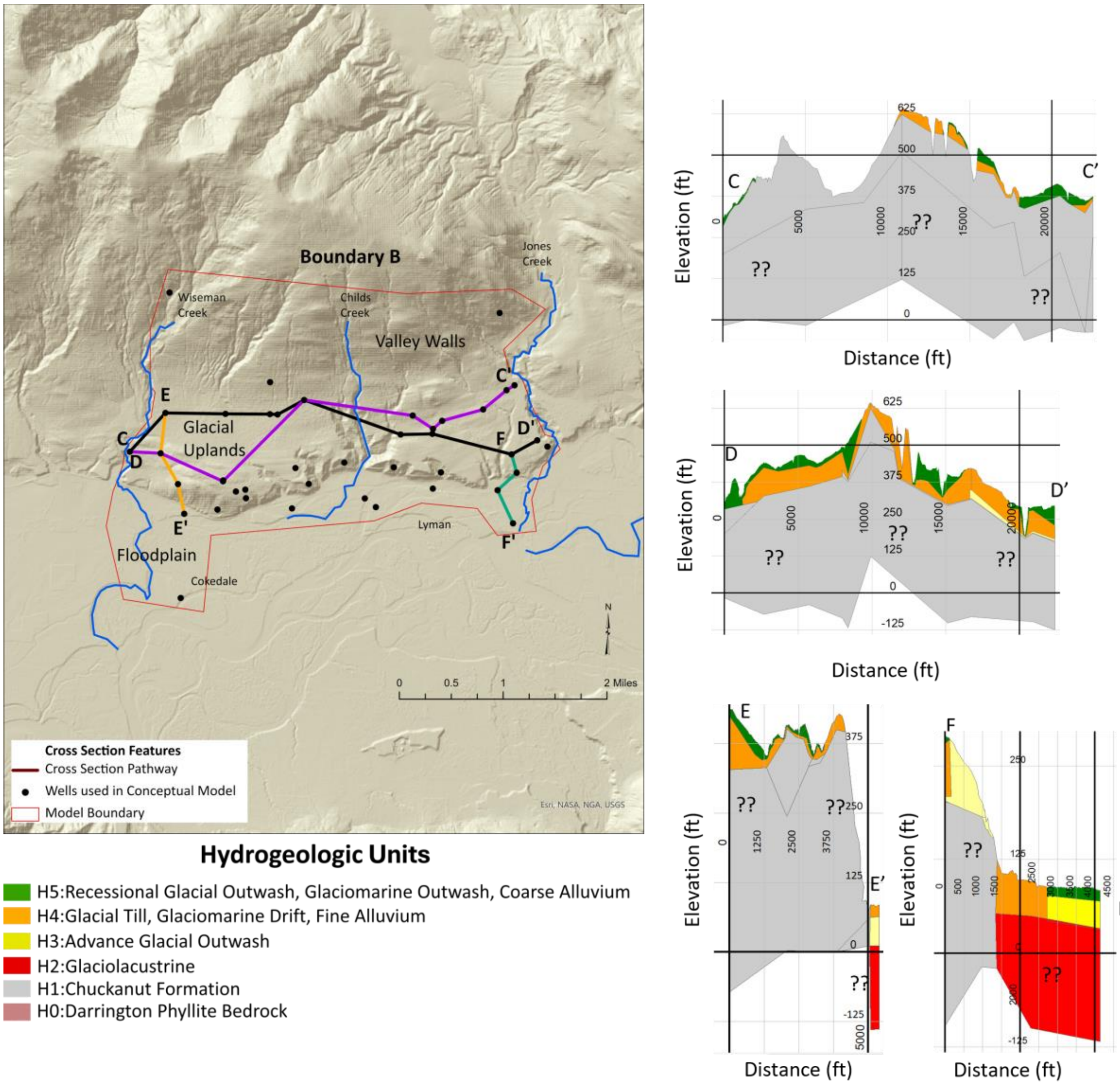


Figure 7: LiDAR map and hydrogeology of the selected cross sections in conceptual model Boundary B in the lower Skagit River Valley study area. Cross sections C-F are vertically exaggerated by 20x to better display topographic changes (LiDAR hillshade from Lowe, 2017, Puget Sound LiDAR digital terrain model).

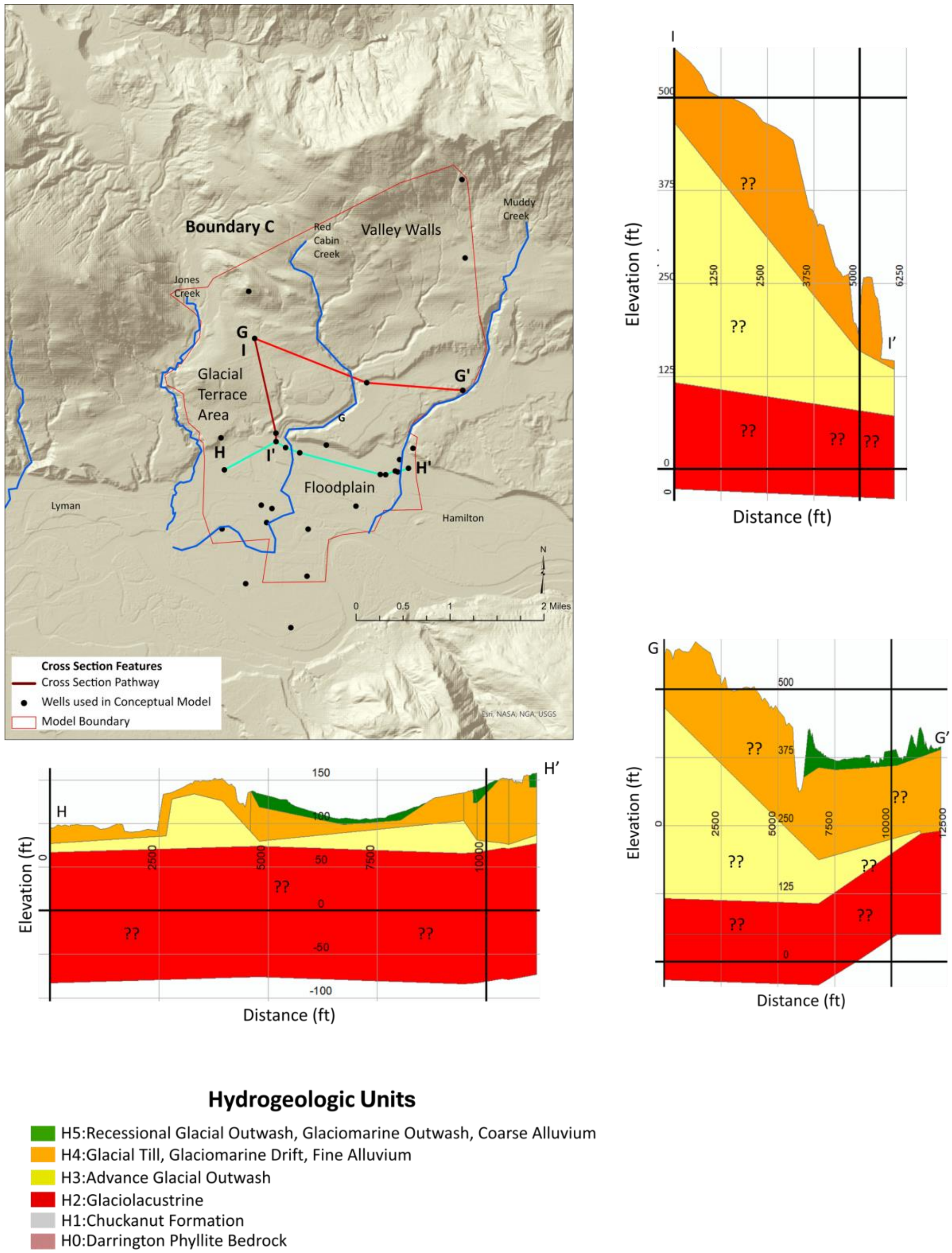


Figure 8: LiDAR map and hydrogeology of the selected cross sections in conceptual model Boundary C in the lower Skagit River Valley study area. Cross sections G-I are vertically exaggerated by 20x to better display topographic changes (LiDAR hillshade from Lowe, 2017, Puget Sound LiDAR digital terrain model).

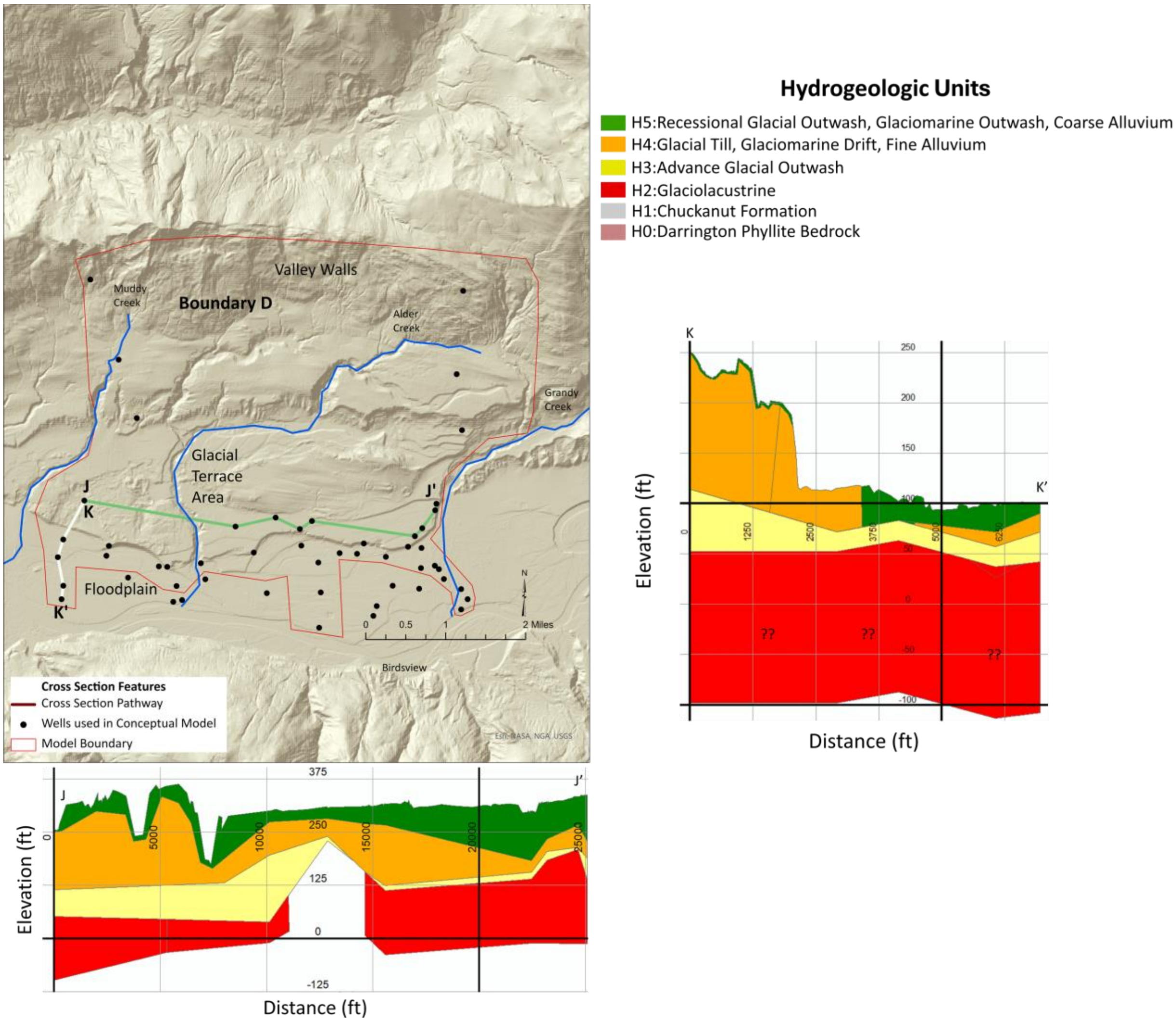


Figure 9: LiDAR map and hydrogeology of the selected cross sections in conceptual model Boundary D in the lower Skagit River Valley study area. Cross sections J-K are vertically exaggerated by 20x to better display topographic changes. Note, Cross section J is on the Hamilton moraine on its west side, explaining the uneven topography. (LiDAR hillshade from Lowe, 2017, Puget Sound LiDAR digital terrain model).

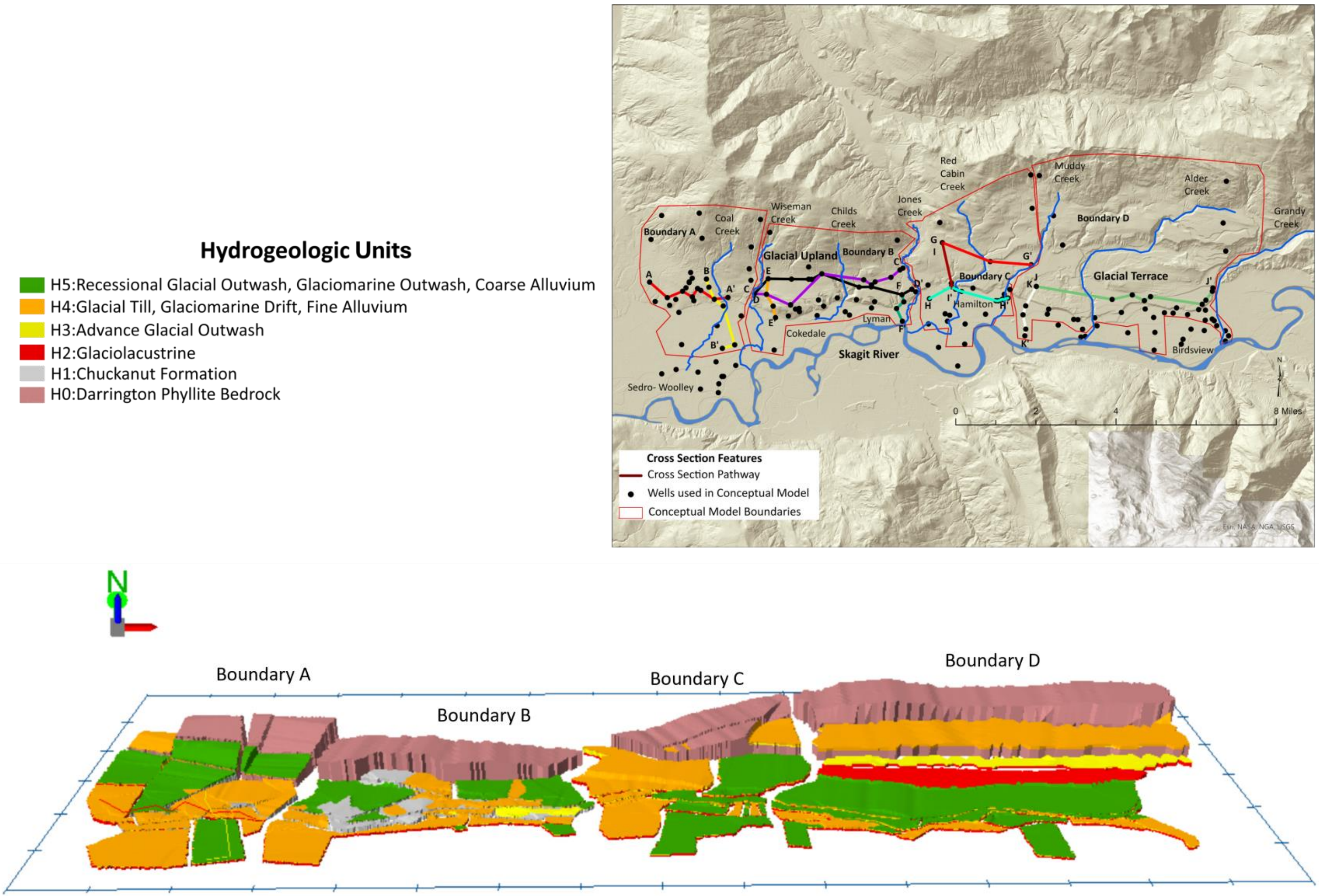


Figure 10: Full extent of 3D conceptual model of the lower Skagit River Valley, including the hydrogeologic units and conceptual model Boundaries A-D (LiDAR hillshade from Lowe, 2017, Puget Sound LiDAR digital terrain model).

.

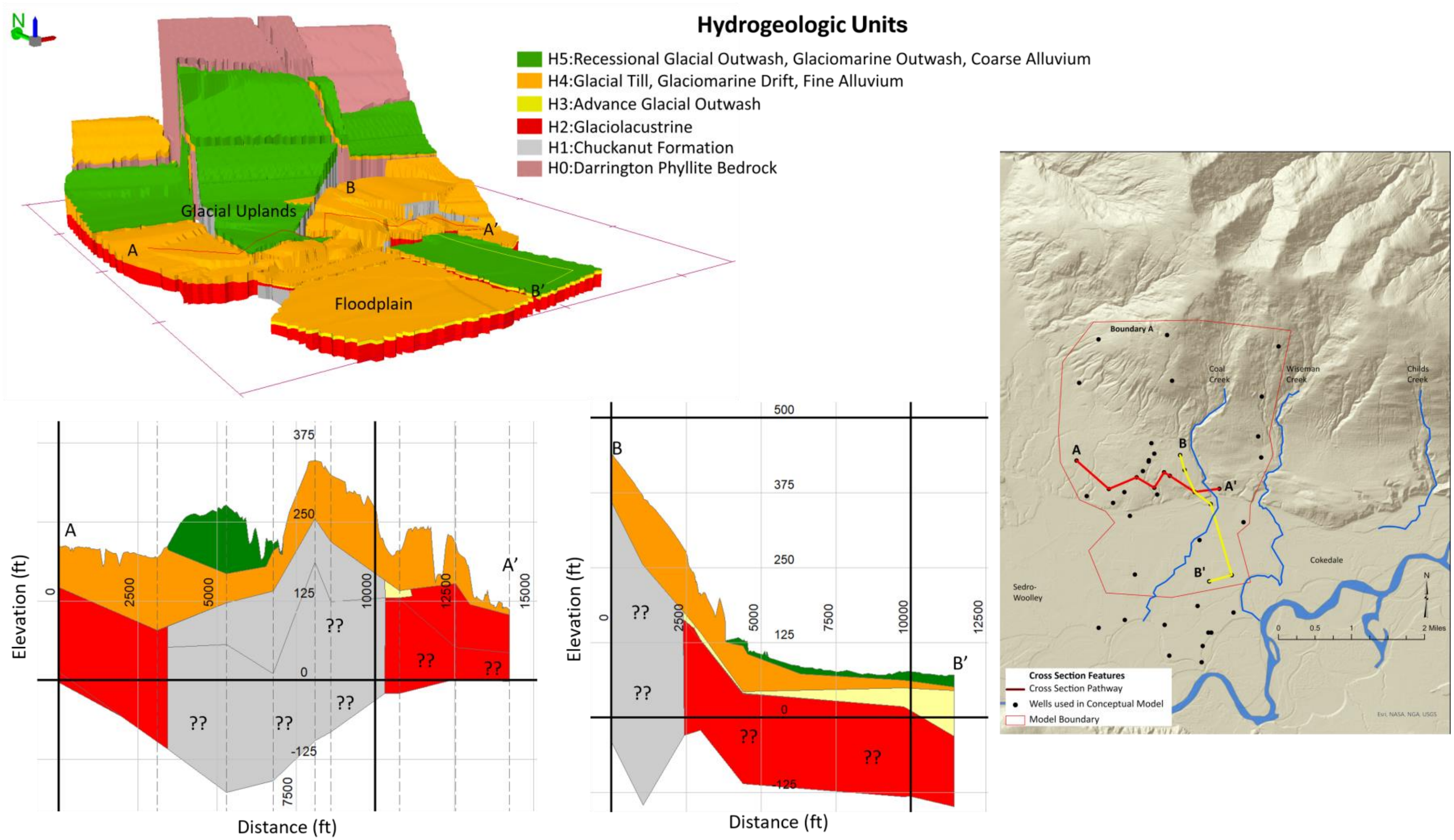


Figure 11: 3D conceptual model of Boundary A in the lower Skagit River Valley, including the hydrogeologic units and selected cross sections A and B. Conceptual model is vertically exaggerated by 3x and cross sections A and B are vertically exaggerated by 20x to better display topographic changes (LiDAR hillshade from Lowe, 2017, Puget Sound LiDAR digital terrain model).

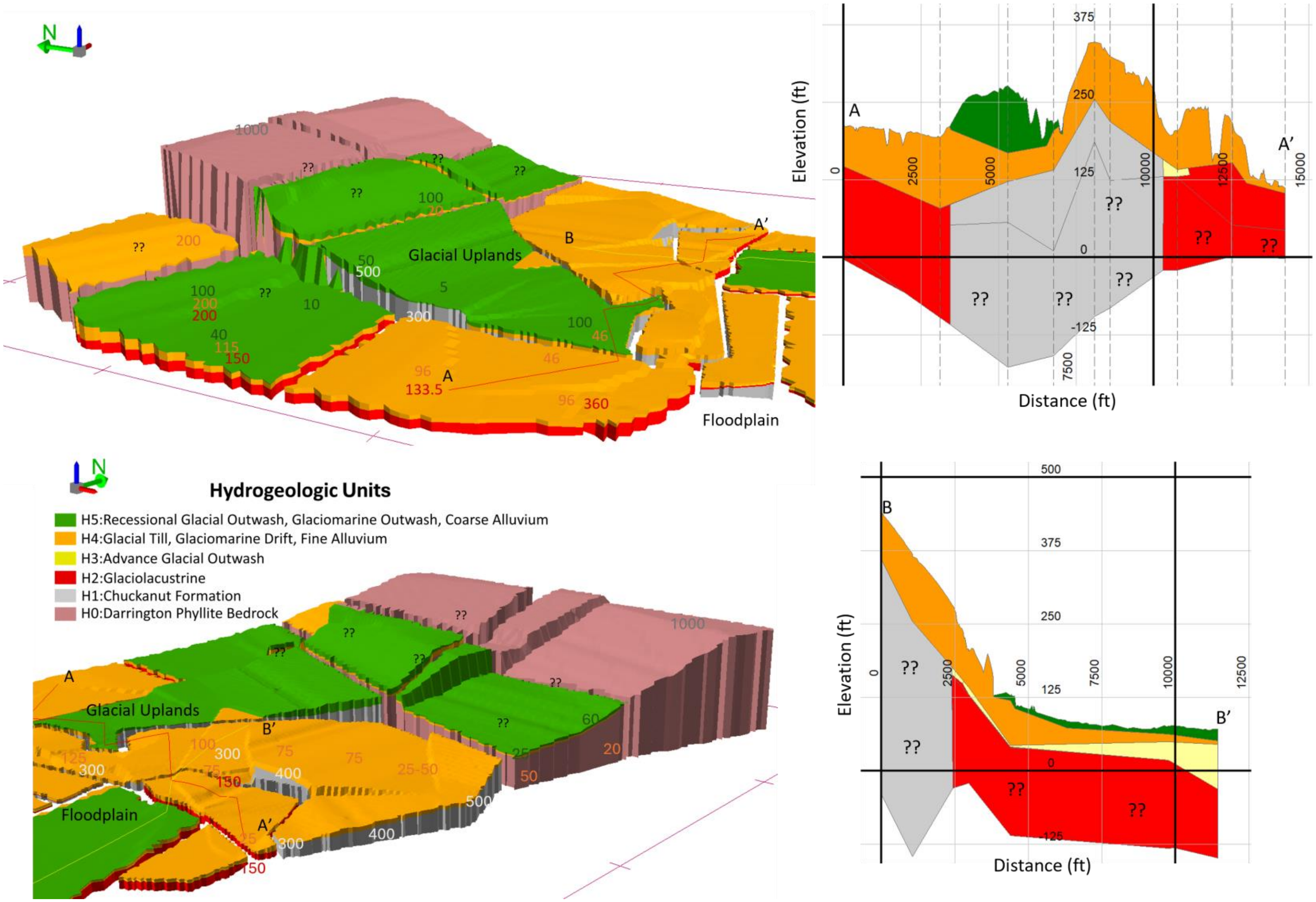


Figure 12: Eastern and western perspectives of the 3D conceptual model of Boundary A in the lower Skagit River Valley, including the hydrogeologic units and selected cross sections A and B. Cross sections A and B are vertically exaggerated by 20x to better display topographic changes. Colored numbers on the conceptual model represent thickness for each individual hydrogeologic unit.

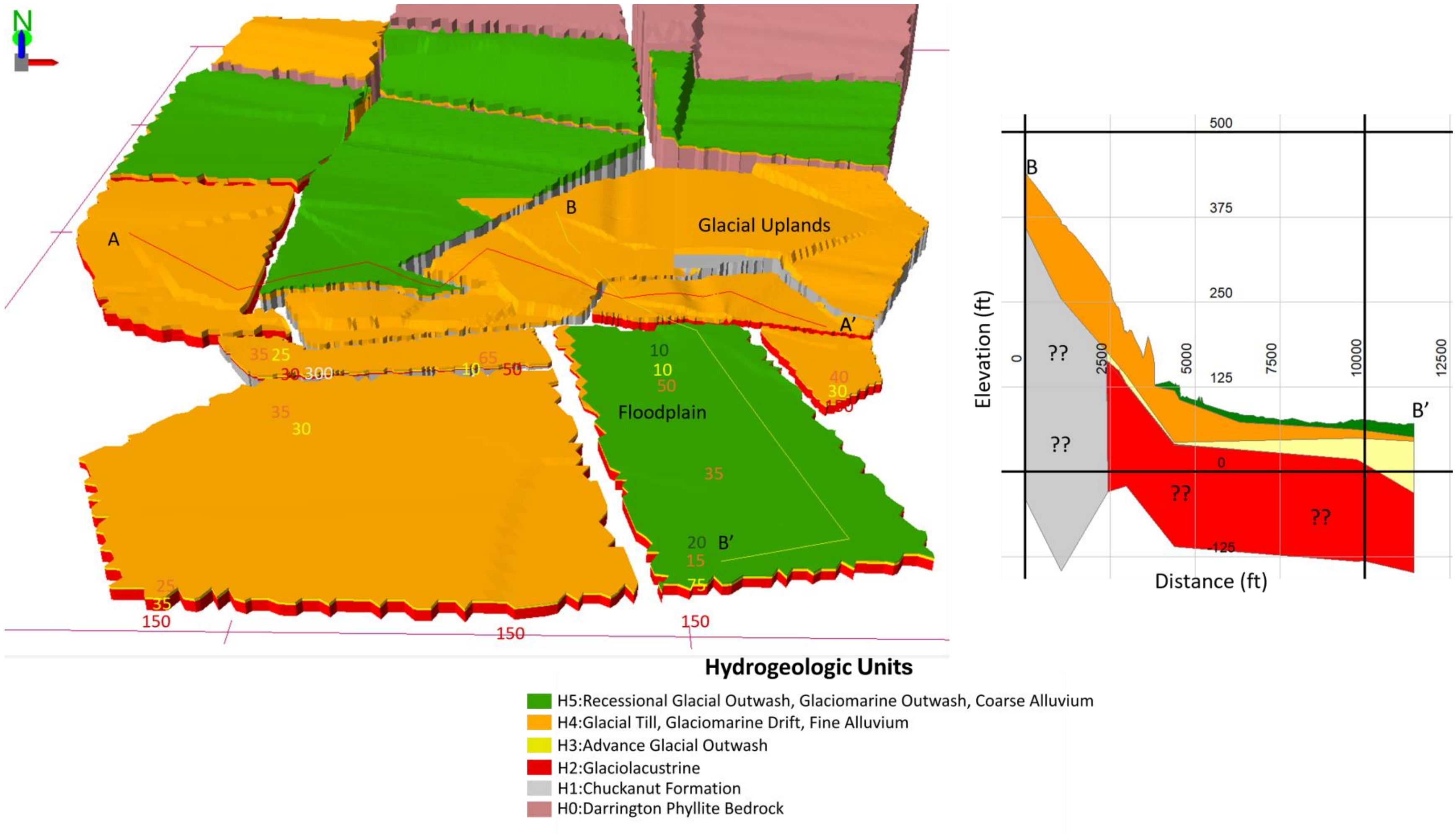


Figure 13: Southern perspective of the 3D conceptual model of Boundary A in the lower Skagit River Valley, including the hydrogeologic units and selected cross sections A and B. Cross sections A and B are vertically exaggerated by 20x to better display topographic changes. Colored numbers on the conceptual model represent thickness for each individual hydrogeologic unit.

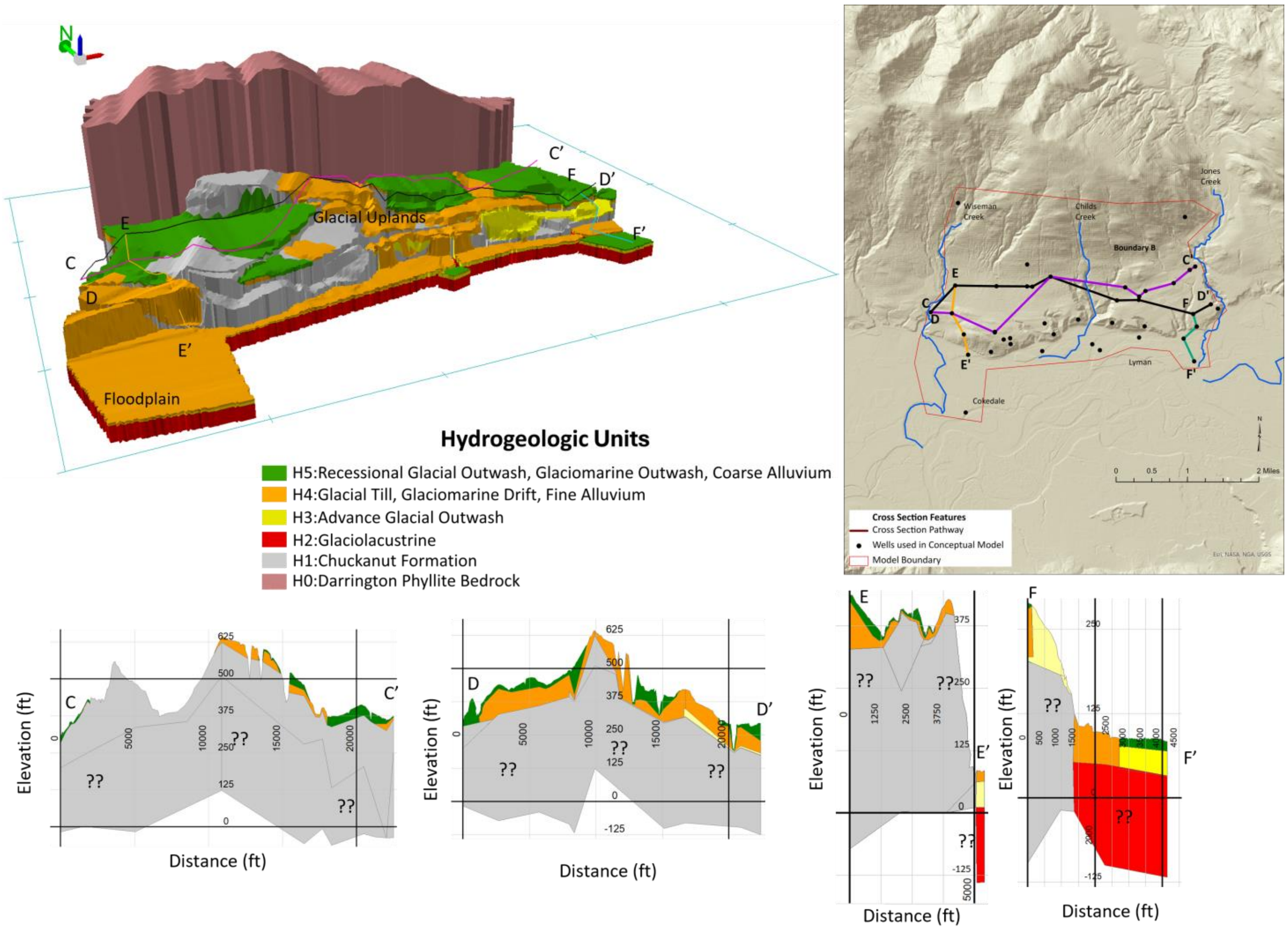


Figure 14: 3D conceptual model of Boundary B in the lower Skagit River Valley, including the hydrogeologic units and selected cross sections C-F. Conceptual model is vertically exaggerated by 3x and cross sections C-F are vertically exaggerated by 20x to better display topographic changes (LiDAR hillshade from Lowe, 2017, Puget Sound LiDAR digital terrain model).

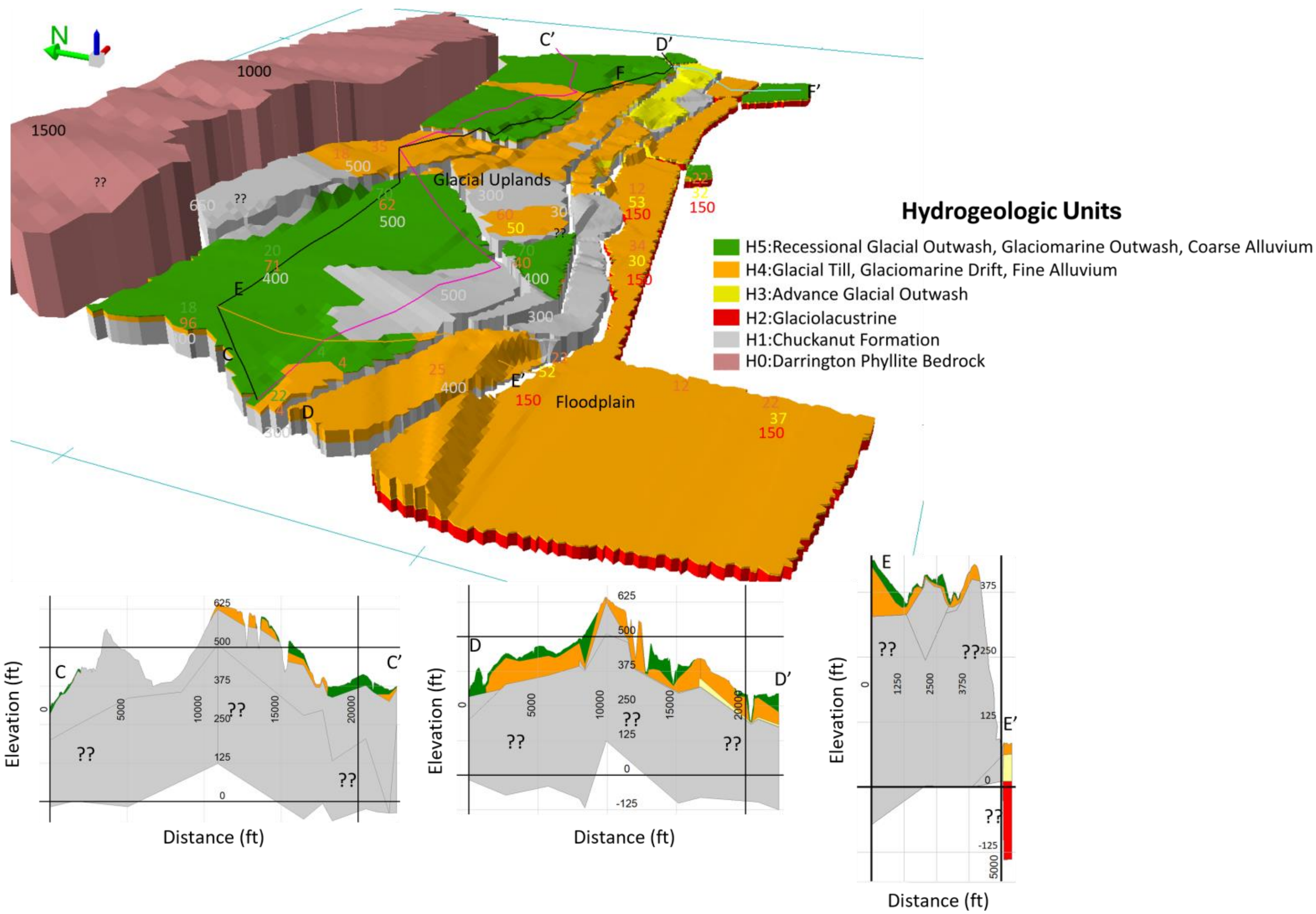


Figure 15: Western perspective of the 3D conceptual model of Boundary B in the lower Skagit River Valley, including the hydrogeologic units and selected cross sections C-F. Cross sections C-F are vertically exaggerated by 20x to better display topographic changes. Colored numbers on the conceptual model represent thickness for each individual hydrogeologic unit.

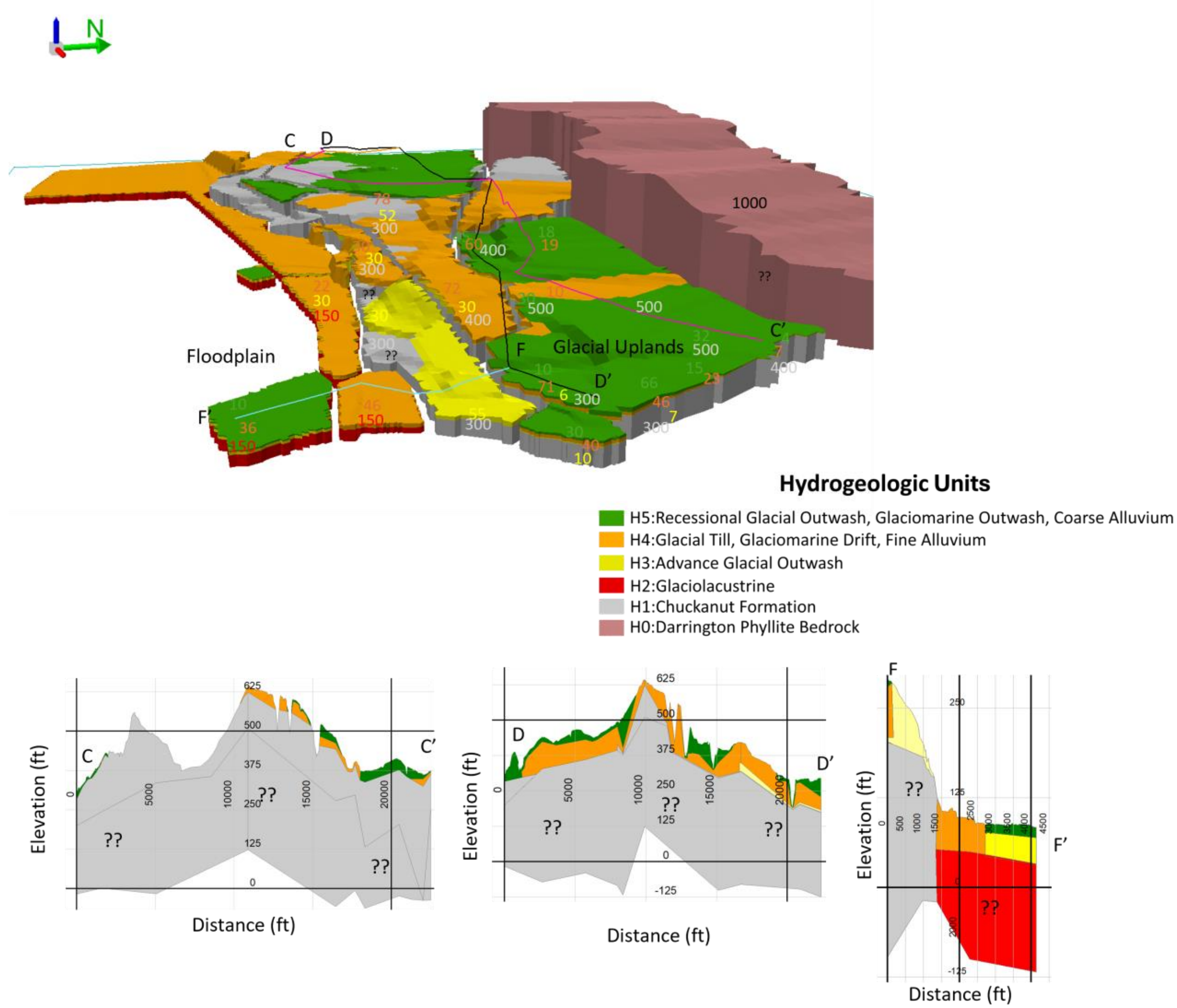


Figure 16: Eastern perspective of the 3D conceptual model of Boundary B in the lower Skagit River Valley, including the hydrogeologic units and selected cross sections C-F. Cross sections C-F are vertically exaggerated by 20x to better display topographic changes. Colored numbers on the conceptual model represent thickness for each individual hydrogeologic unit.

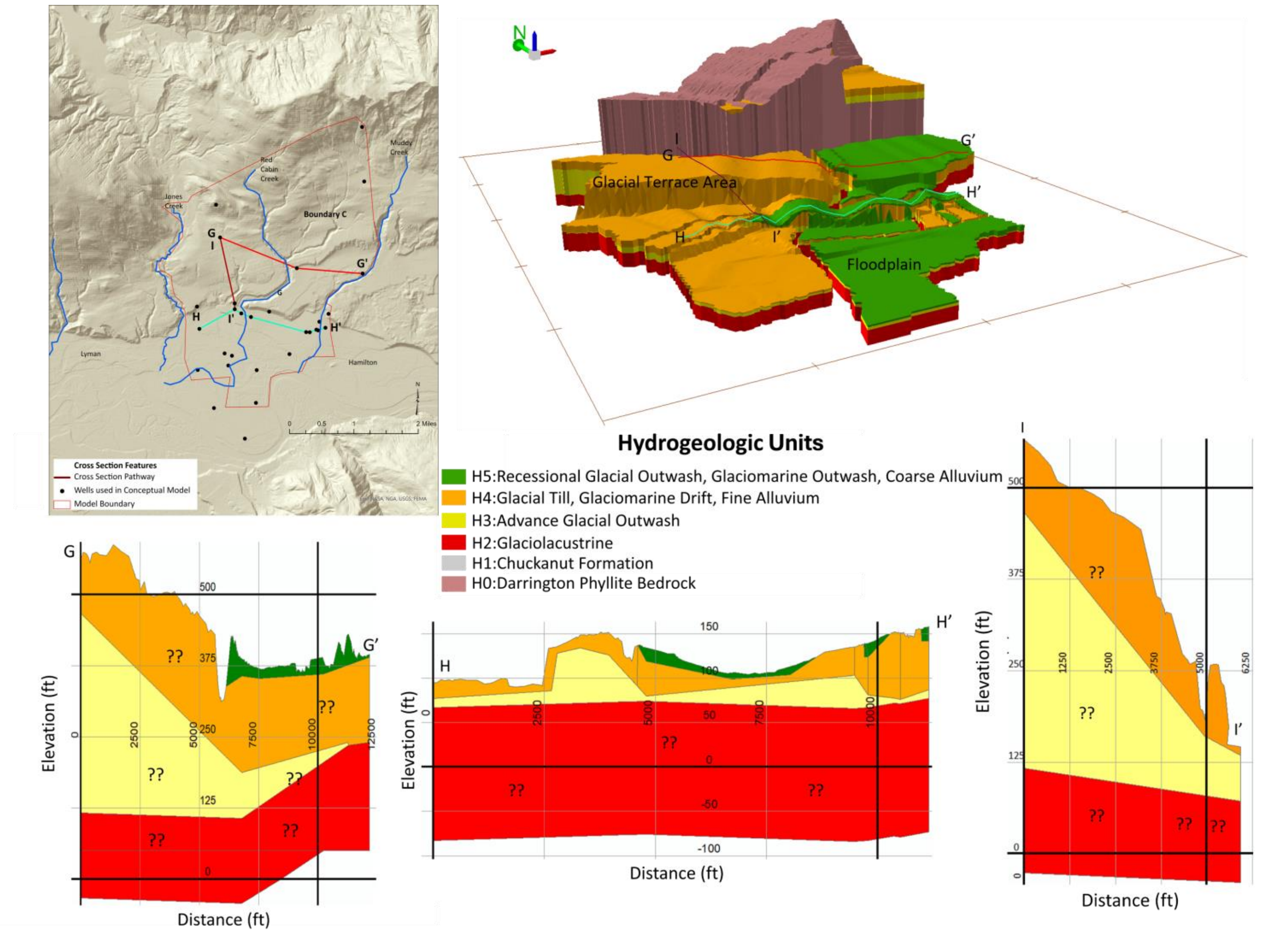


Figure 17: 3D conceptual model of Boundary C in the lower Skagit River Valley, including the hydrogeologic units and selected cross sections G-I. Conceptual model is vertically exaggerated by 3x and cross sections G-I are vertically exaggerated by 20x to better display topographic changes (LiDAR hillshade from Lowe, 2017, Puget Sound LiDAR digital terrain model).

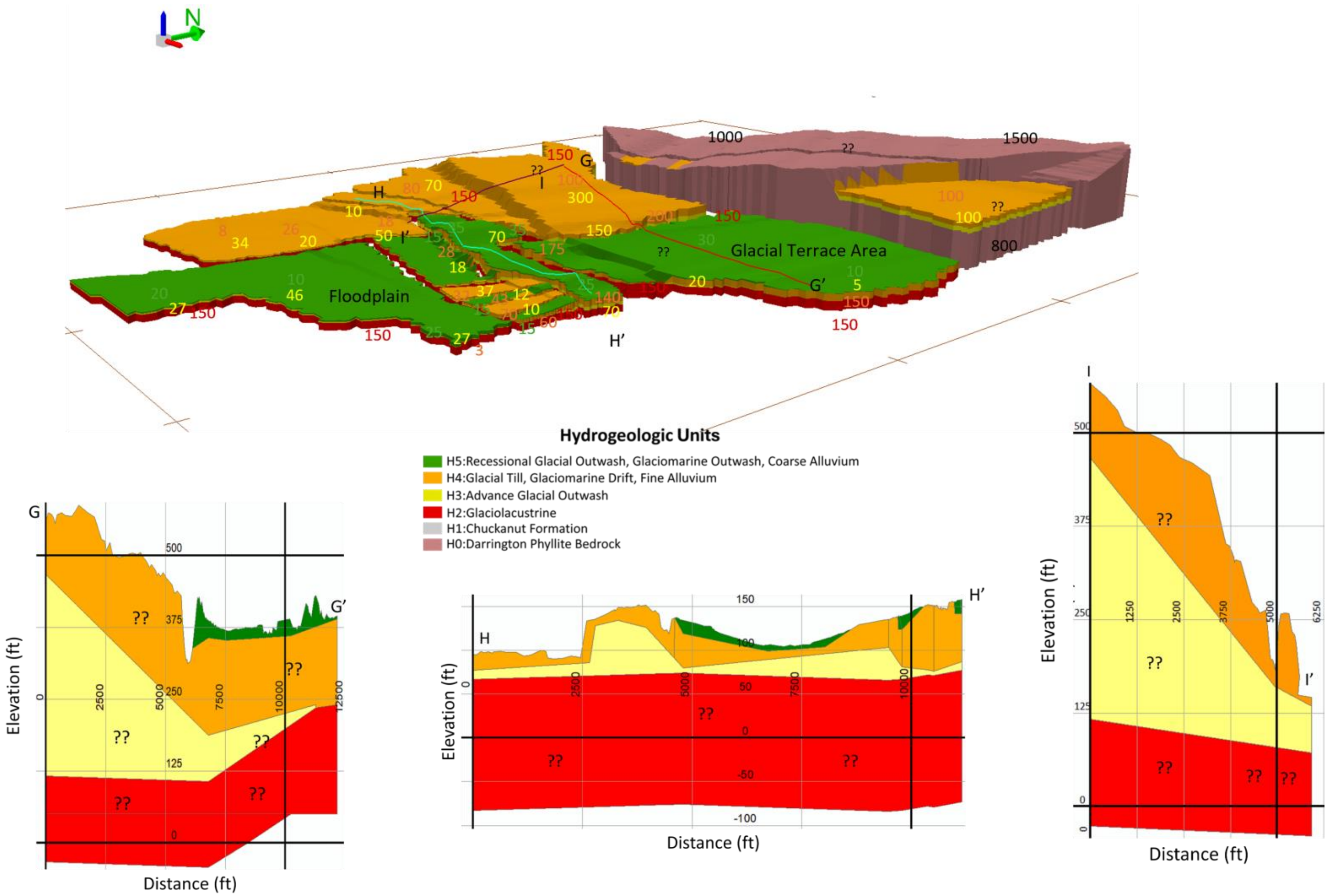


Figure 18: Eastern perspective of the 3D conceptual model of Boundary C in the lower Skagit River Valley, including the hydrogeologic units and selected cross sections G-I. Cross sections G-I are vertically exaggerated by 20x to better display topographic changes. Colored numbers on the conceptual model represent thickness for each individual hydrogeologic unit.

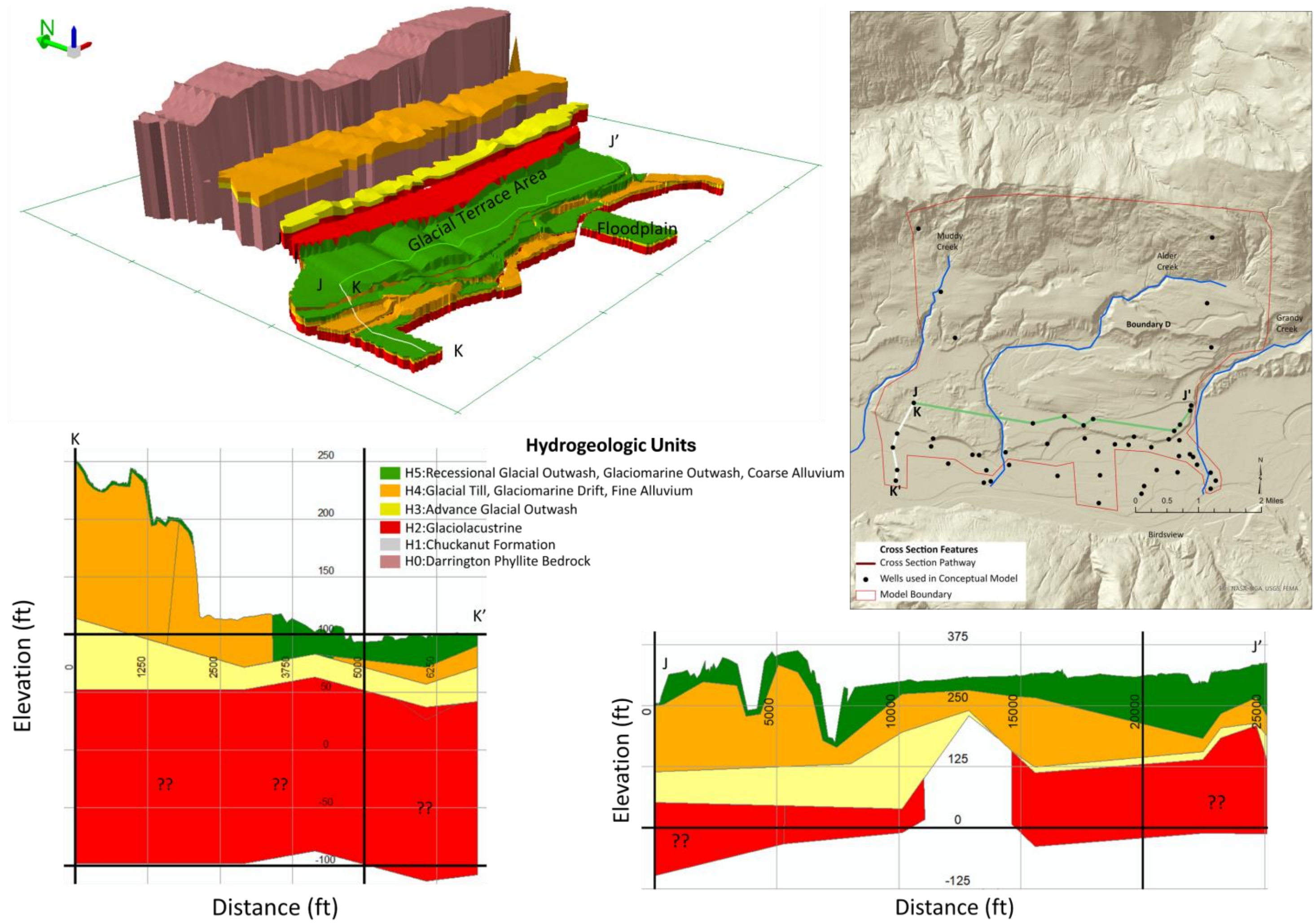


Figure 19: 3D conceptual model of Boundary D in the lower Skagit River Valley, including the hydrogeologic units and selected cross sections J and K. Conceptual model is vertically exaggerated by 3x and cross sections J and K are vertically exaggerated by 20x to better display topographic changes (LiDAR hillshade from Lowe, 2017, Puget Sound LiDAR digital terrain model).

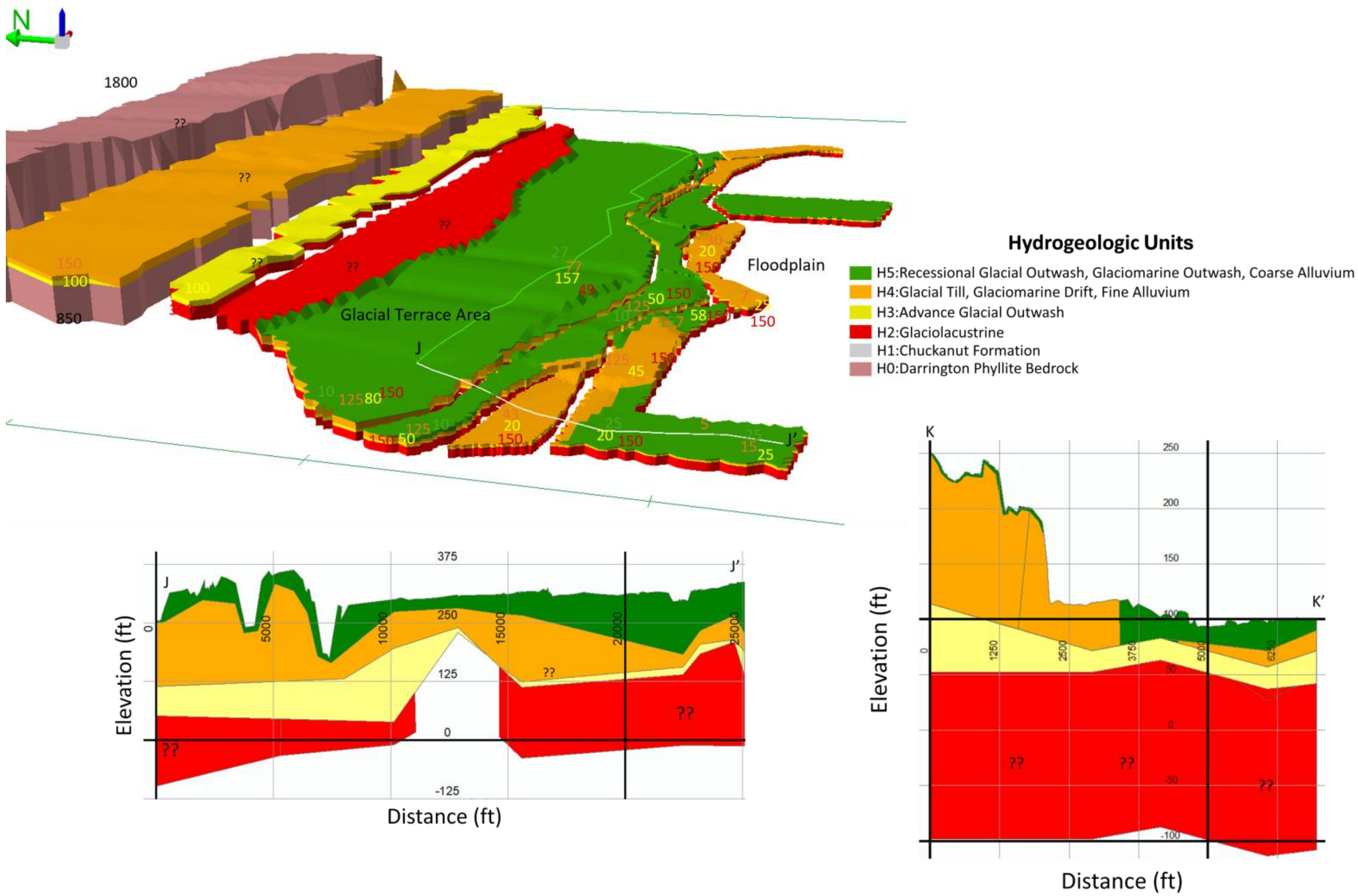


Figure 20: Western perspective of the 3D conceptual model of Boundary D in the lower Skagit River Valley, including the hydrogeologic units and selected cross sections J and K. Cross sections J and K are vertically exaggerated by 20x to better display topographic changes. Colored numbers on the conceptual model represent thickness for each individual hydrogeologic unit.

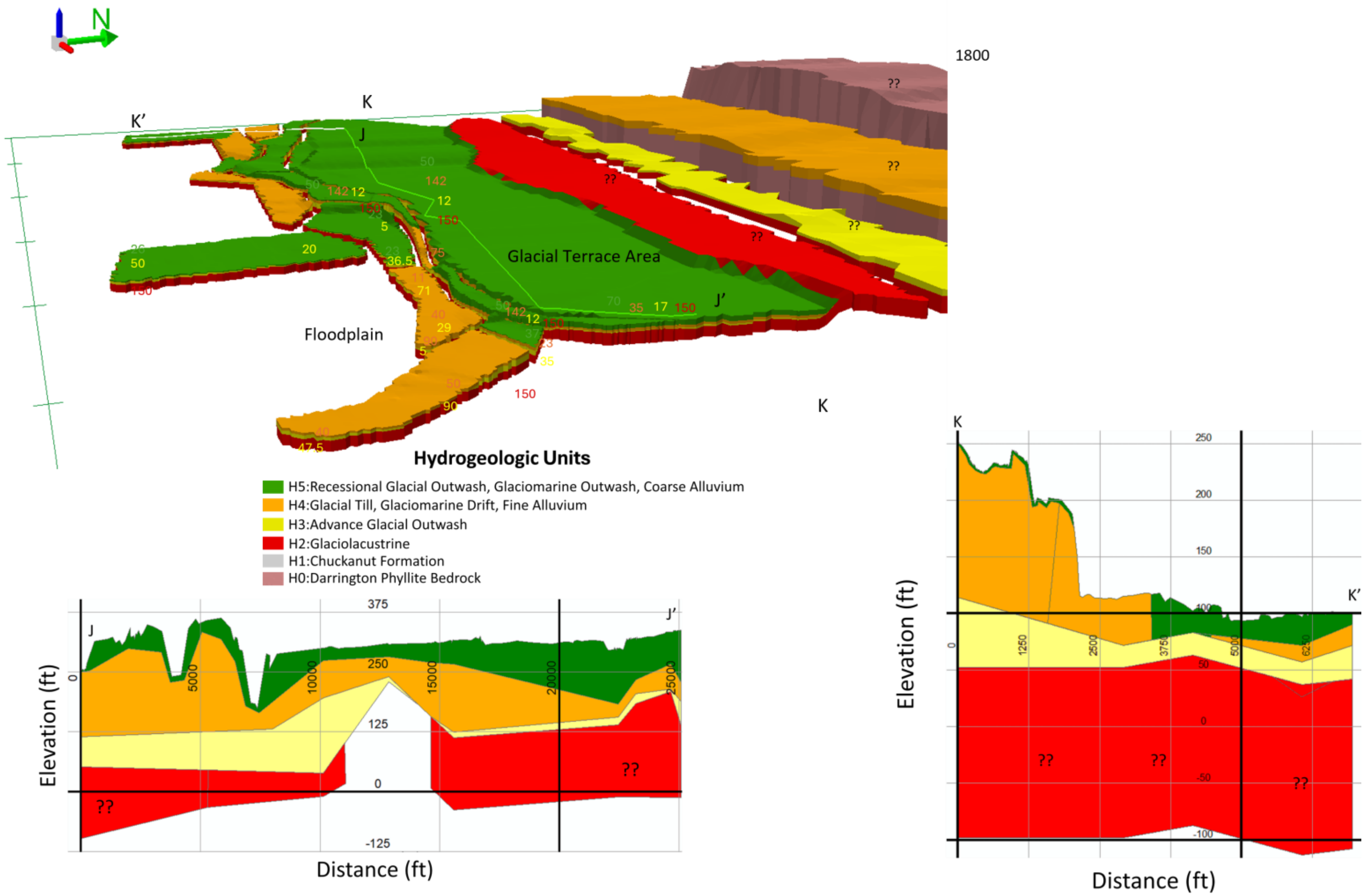


Figure 21: Eastern perspective of the 3D conceptual model of Boundary D in the lower Skagit River Valley, including the hydrogeologic units and selected cross sections J and K. Cross sections are vertically exaggerated by 20x to better display topographic changes. Colored numbers on the conceptual model represent thickness for each individual hydrogeologic unit.

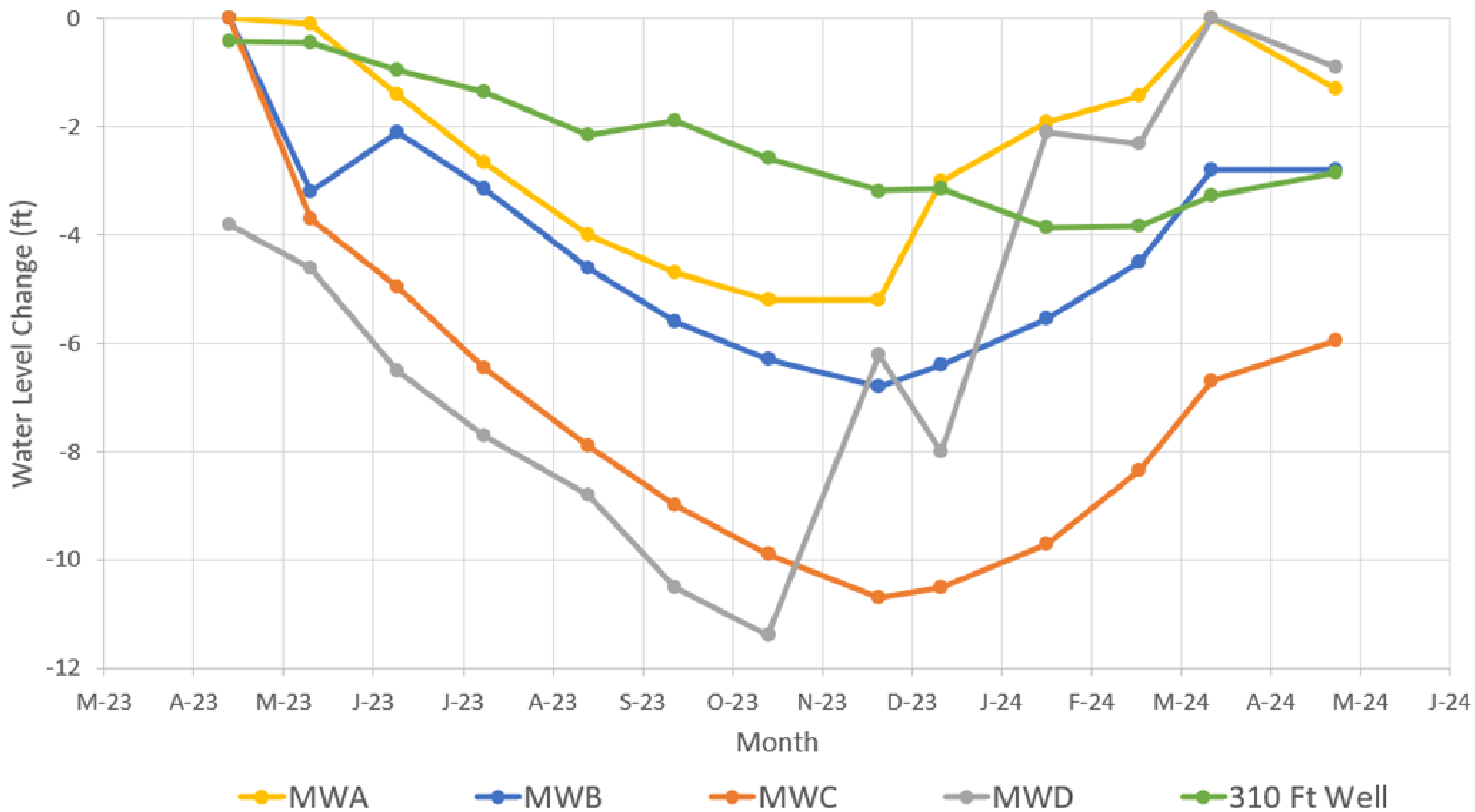


Figure 22: Groundwater levels from monitoring wells near the lower Skagit River Valley. Water level changes that are more negative represent an increase in depth of the water table.

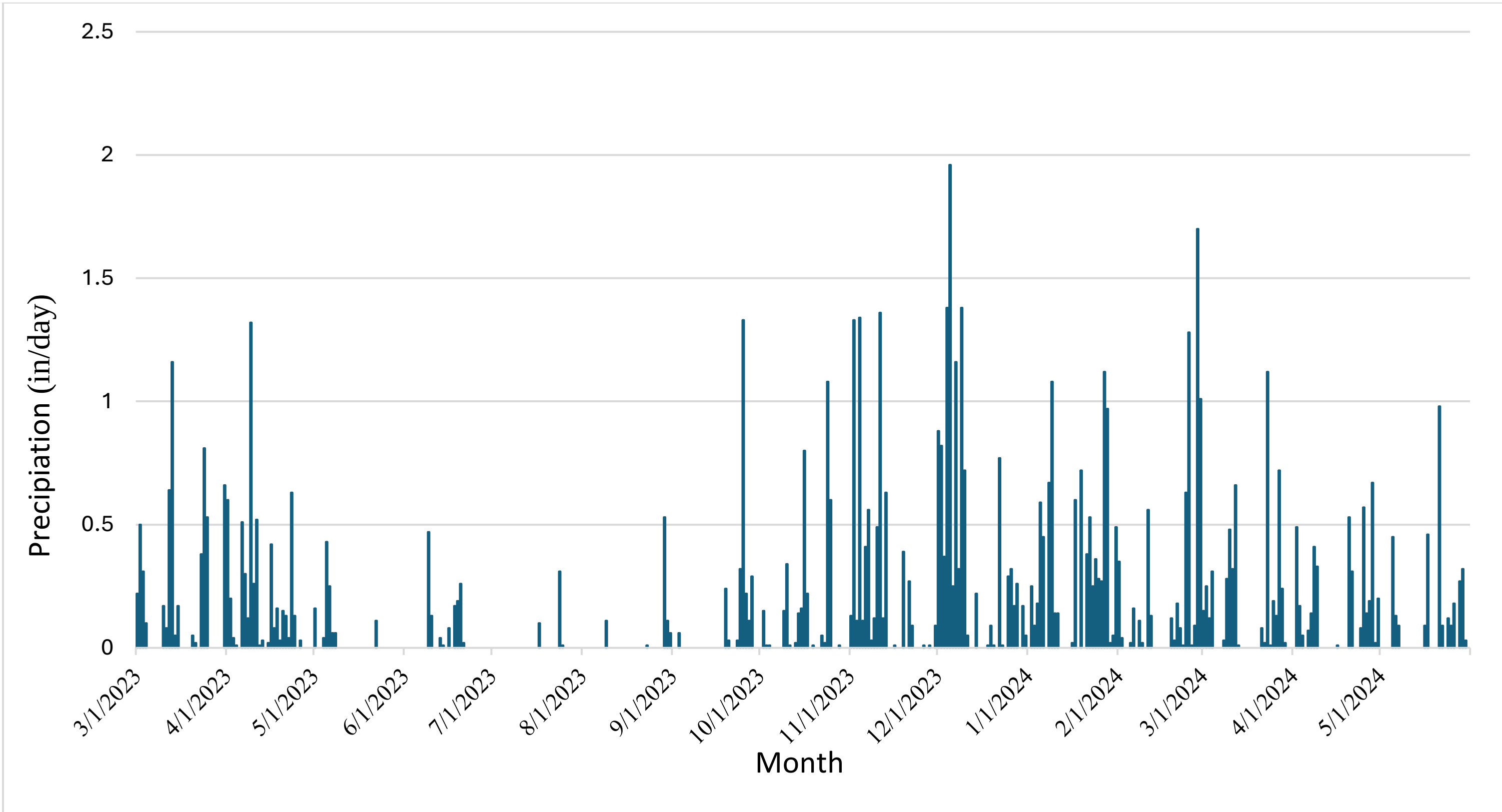


Figure 23: Daily precipitation values at the Concrete Weather Station in the lower Skagit River Basin (Data obtained from Concrete WSU, 2024, AgWeatherNet station)

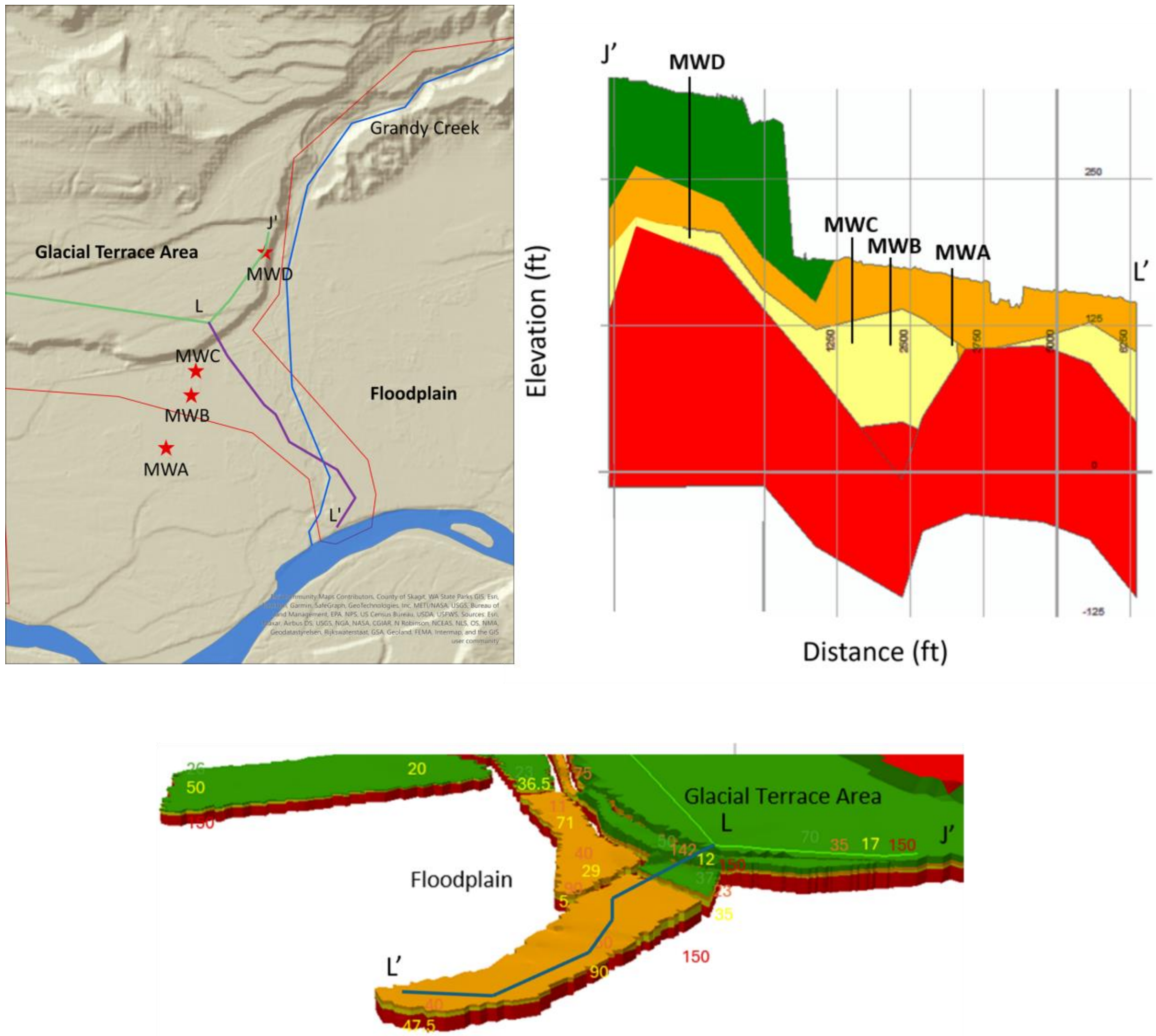


Figure 24: Additional Cross Section L. Map view of Cross Section L, 3D models and screenshot along with Cross Section J included as well (but mirrored to show more of the glacial terrace that is absent in the Cross Section J pathway). Used for further evidence of connectivity and groundwater monitoring interpretations (Lidar hillshade from Lowe, 2017, Puget Sound lidar digital terrain model).

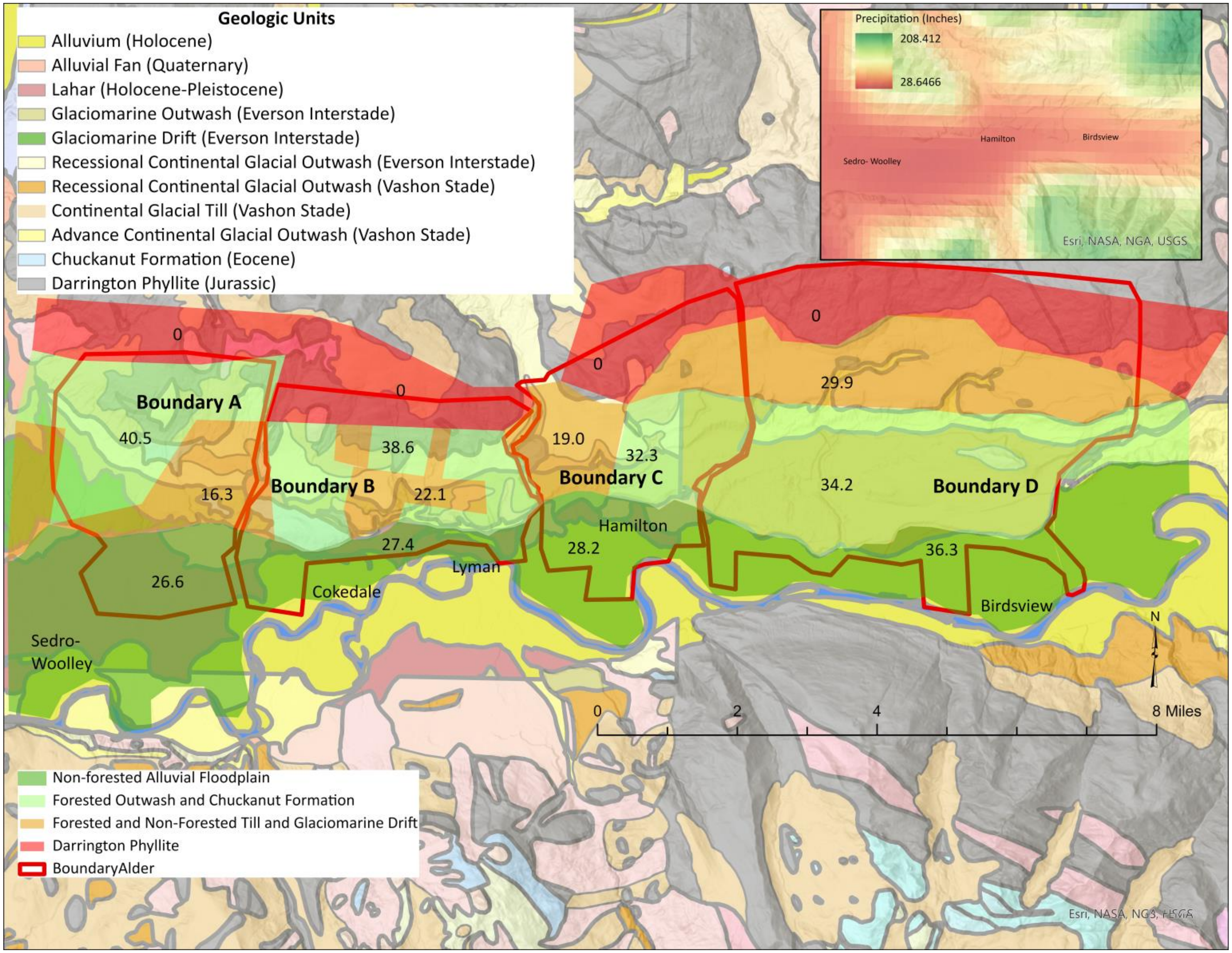


Figure 25: Map of recharge estimates in the lower Skagit River Valley (geology modified from WADNR, 2016, 100k Surface Geology). The inset map shows precipitation values (Precipitation raster modified from PRISM, 2024, 800m spatial resolution).

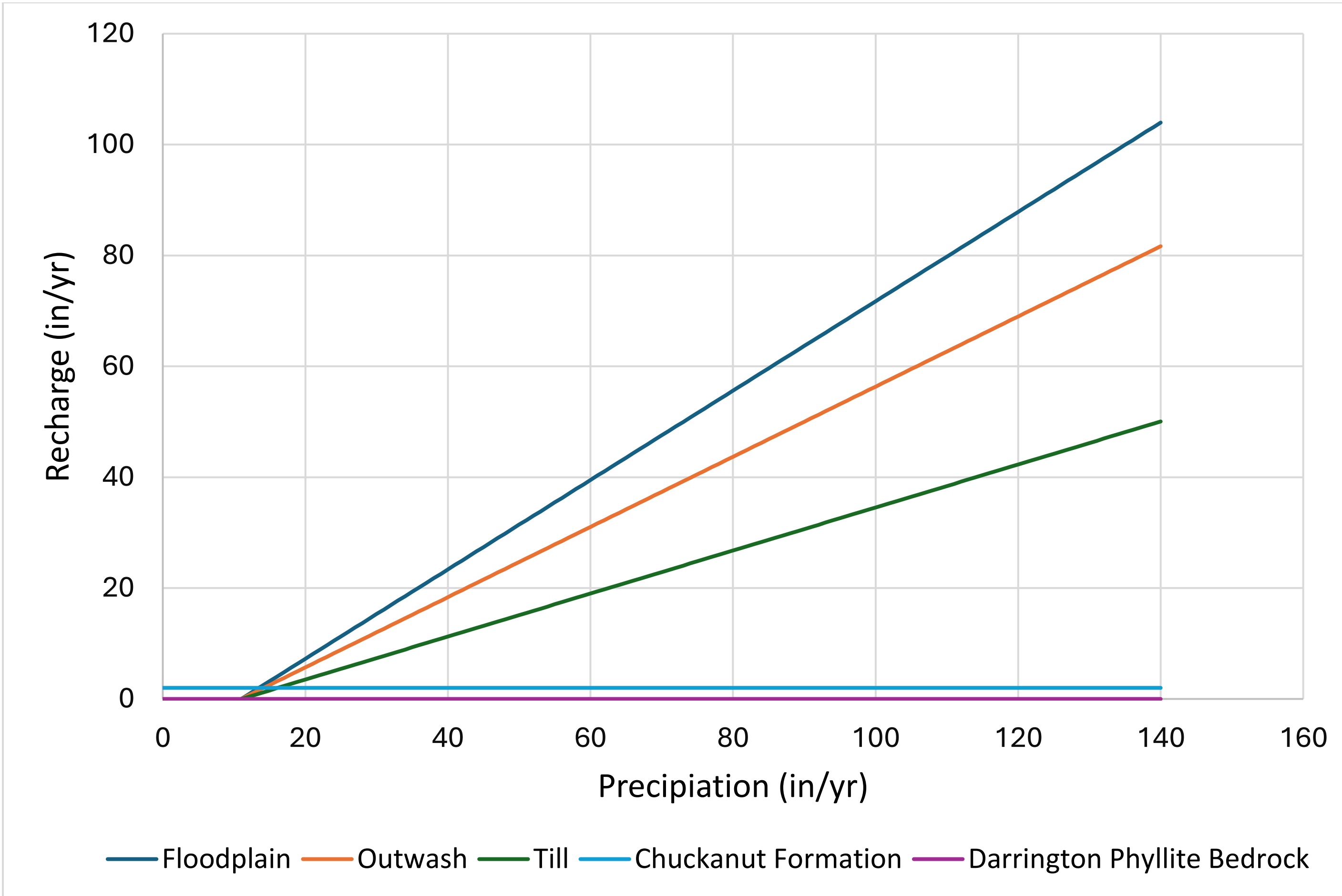


Figure 26: Recharge of various geologic deposits based on Bidlake and Payne, 2001, Vaccaro et al., 1998, and Pitz, 2005.

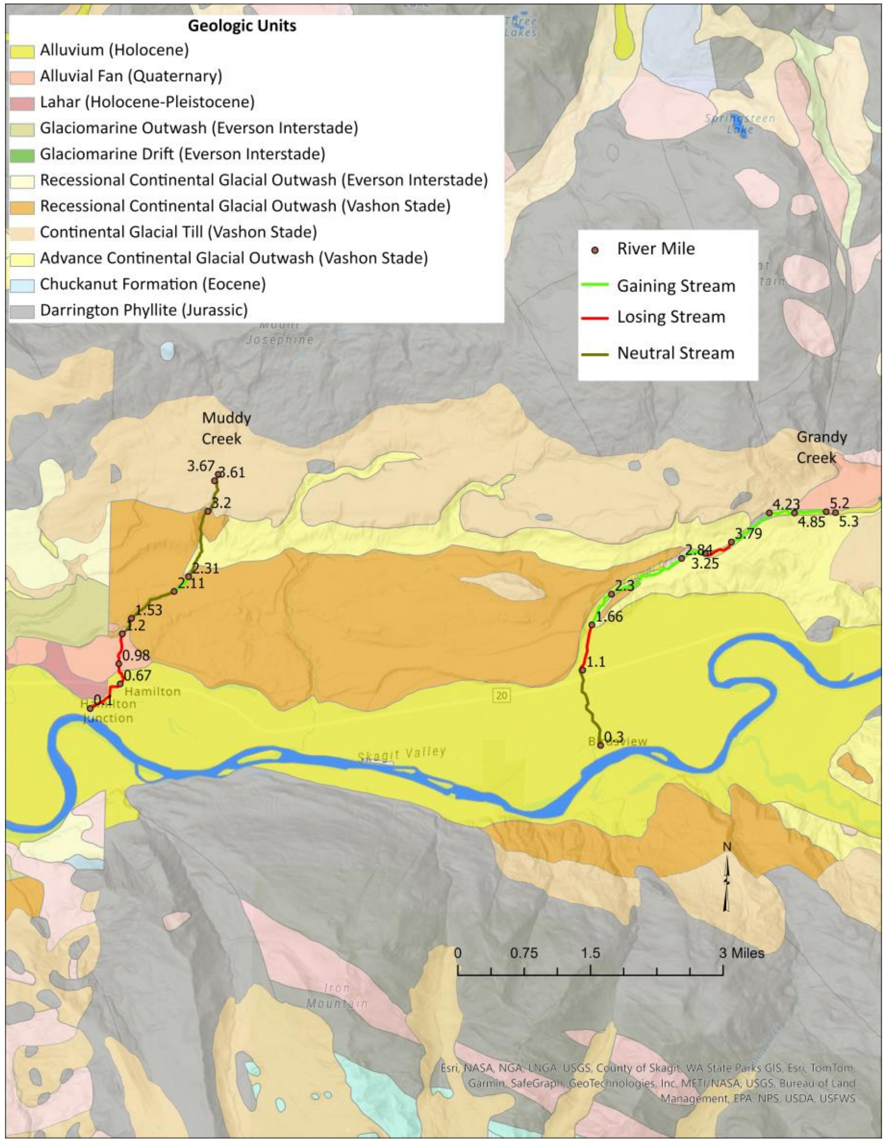


Figure 27: Geologic map of the lower Skagit Valley with seepage run results from Muddy and Grandy Creek displayed (geology modified from WADNR, 2016, 100k Surface Geology).

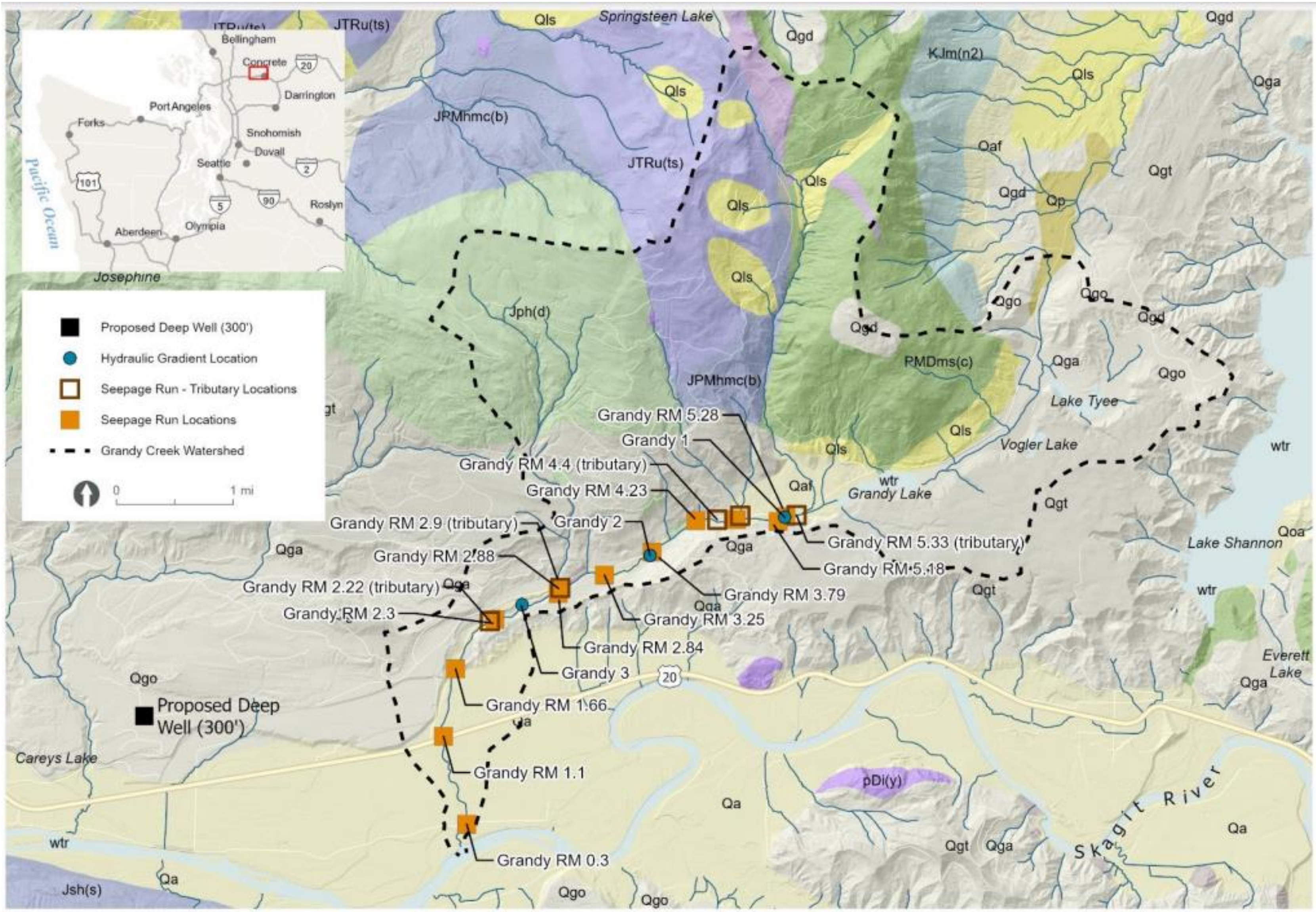


Figure 28: Grandy Creek monitoring locations. Proposed deep well already installed (modified from HDR 2024).

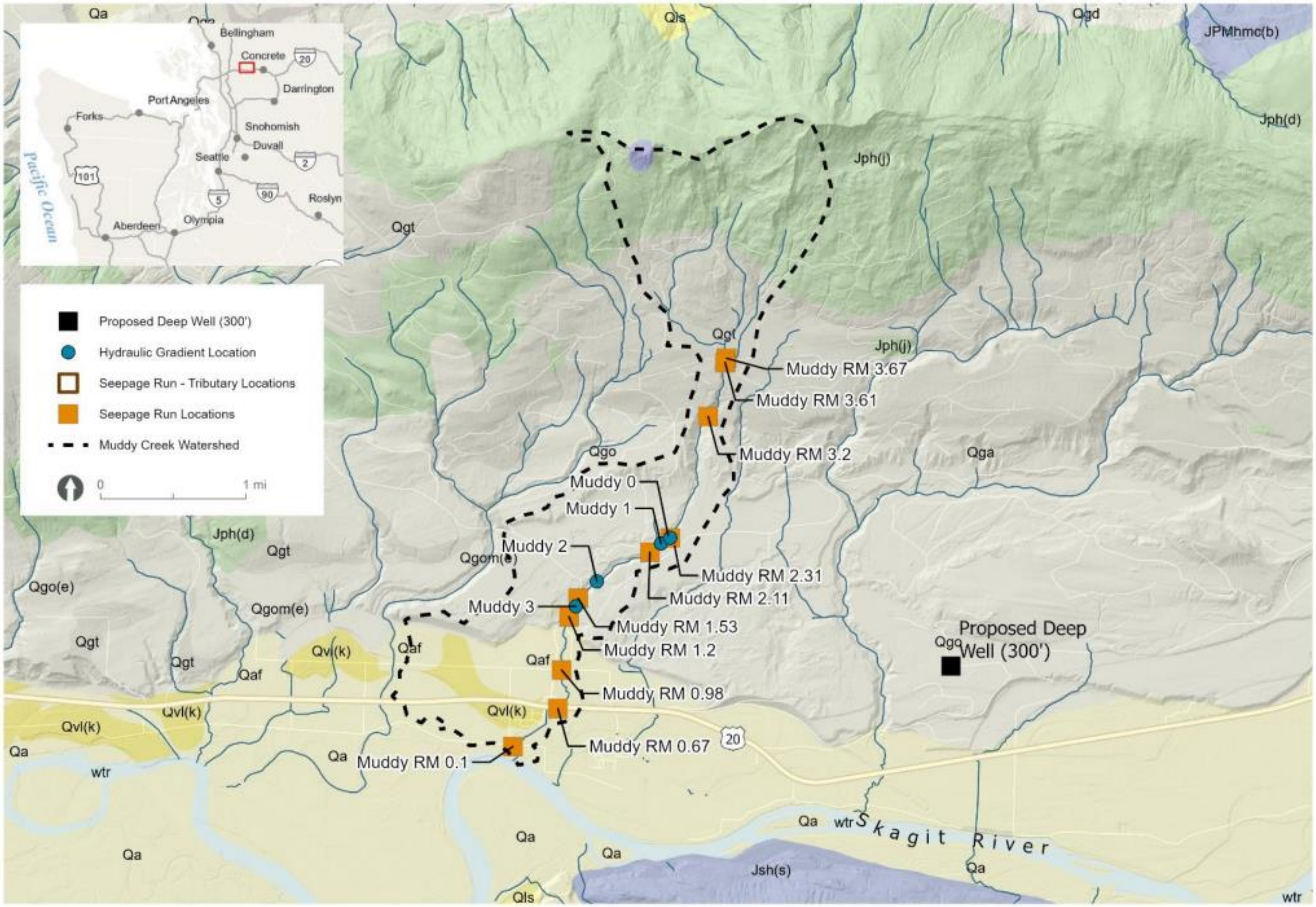


Figure 29: Muddy Creek monitoring locations. Proposed deep well is already installed (modified from HDR 2024).

## Appendix A: Conceptual Model Wells

Well logs used in conceptual modeling in model Boundary A within Skagit River Valley. Rows in red are wells with modified depths and bolded wells are pseudo wells used for extrapolation purposes. The horizon number is the hydrogeologic unit.

| Log ID | Top (ft) | Bottom (ft) | Thickness (ft) | Longitude | Latitude | Elevation (ft) | Horizon |
|---|---|---|---|---|---|---|---|
| 84972 | 0 | 110 | 110 | 122.1595 | 48.53624 | 364 | 4 |
| 84972 | 110 | 510 | 400 | 122.1595 | 48.53624 | 364 | 1 |
| 74328 | 0 | 77 | 77 | 122.1609 | 48.53916 | 436 | 4 |
| 74328 | 77 | 477 | 400 | 122.1609 | 48.53916 | 436 | 1 |
| 453953 | 0 | 62 | 62 | 122.1564 | 48.53193 | 204 | 4 |
| 453953 | 62 | 74 | 12 | 122.1564 | 48.53193 | 204 | 3 |
| 453953 | 74 | 75 | 1 | 122.1564 | 48.53193 | 204 | 2 |
| 453953 | 75 | 225 | 150 | 122.1564 | 48.53193 | 204 | 2 |
| 405696 | 0 | 55 | 55 | 122.1367 | 48.53903 | 413 | 4 |
| 405696 | 55 | 455 | 400 | 122.1367 | 48.53903 | 413 | 1 |
| 74349 | 0 | 31 | 31 | 122.1629 | 48.49939 | 66 | 5 |
| 74349 | 31 | 34 | 3 | 122.1629 | 48.49939 | 66 | 4 |
| 74349 | 34 | 58 | 24 | 122.1629 | 48.49939 | 66 | 3 |
| 74349 | 58 | 208 | 150 | 122.1629 | 48.49939 | 66 | 2 |
| 74419 | 0 | 20 | 20 | 122.1514 | 48.51426 | 71 | 5 |
| 74419 | 20 | 26 | 6 | 122.1514 | 48.51426 | 71 | 4 |
| 74419 | 26 | 103 | 77 | 122.1514 | 48.51426 | 71 | 3 |
| 74419 | 103 | 220 | 117 | 122.1514 | 48.51426 | 71 | 2 |
| 77980 | 0 | 9 | 9 | 122.1514 | 48.52958 | 128 | 5 |
| 77980 | 9 | 85 | 76 | 122.1514 | 48.52958 | 128 | 4 |
| 77980 | 85 | 88 | 3 | 122.1514 | 48.52958 | 128 | 3 |
| 77980 | 88 | 89 | 1 | 122.1514 | 48.52958 | 128 | 2 |
| 77980 | 89 | 239 | 150 | 122.1514 | 48.52958 | 128 | 2 |
| 79374 | 0 | 34 | 34 | 122.1644 | 48.50548 | 66 | 4 |
| 79374 | 34 | 57 | 23 | 122.1644 | 48.50548 | 66 | 3 |

| | | | | | | | |
|---|---|---|---|---|---|---|---|
| 79374 | 57 | 207 | 150 | 122.1644 | 48.50548 | 66 | 2 |
| 80259 | 0 | 10 | 10 | 122.1513 | 48.50411 | 72 | 5 |
| 80259 | 10 | 33 | 23 | 122.1513 | 48.50411 | 72 | 4 |
| 80259 | 33 | 57 | 24 | 122.1513 | 48.50411 | 72 | 3 |
| 80259 | 57 | 207 | 150 | 122.1513 | 48.50411 | 72 | 2 |
| 83477 | 0 | 45 | 45 | 122.1416 | 48.52613 | 99 | 4 |
| 83477 | 45 | 66 | 21 | 122.1416 | 48.52613 | 99 | 3 |
| 83477 | 66 | 216 | 150 | 122.1416 | 48.52613 | 99 | 2 |
| 85231 | 0 | 25 | 25 | 122.1532 | 48.49822 | 73 | 5 |
| 85231 | 25 | 42 | 17 | 122.1532 | 48.49822 | 73 | 4 |
| 85231 | 42 | 56 | 14 | 122.1532 | 48.49822 | 73 | 3 |
| 85231 | 56 | 206 | 150 | 122.1532 | 48.49822 | 73 | 2 |
| 190220 | 0 | 10 | 10 | 122.1546 | 48.5224 | 77 | 4 |
| 190220 | 10 | 60 | 50 | 122.1546 | 48.5224 | 77 | 3 |
| 190220 | 60 | 210 | 150 | 122.1546 | 48.5224 | 77 | 2 |
| 1038821 | 0 | 42 | 42 | 122.1763 | 48.50627 | 60 | 4 |
| 1038821 | 42 | 61 | 19 | 122.1763 | 48.50627 | 60 | 3 |
| 1038821 | 61 | 211 | 150 | 122.1763 | 48.50627 | 60 | 2 |
| 367256 | 0 | 33 | 33 | 122.1547 | 48.50934 | 71 | 4 |
| 367256 | 33 | 74 | 41 | 122.1547 | 48.50934 | 71 | 3 |
| 367256 | 74 | 224 | 150 | 122.1547 | 48.50934 | 71 | 2 |
| 369262 | 0 | 27 | 27 | 122.1736 | 48.51531 | 73 | 4 |
| 369262 | 27 | 60 | 33 | 122.1736 | 48.51531 | 73 | 3 |
| 369262 | 60 | 210 | 150 | 122.1736 | 48.51531 | 73 | 2 |
| 422154 | 0 | 39 | 39 | 122.153 | 48.50144 | 70 | 4 |
| 422154 | 39 | 53 | 14 | 122.153 | 48.50144 | 70 | 3 |
| 422154 | 53 | 203 | 150 | 122.153 | 48.50144 | 70 | 2 |
| 436502 | 0 | 96 | 96 | 122.1806 | 48.52941 | 143 | 4 |
| 436502 | 96 | 100 | 4 | 122.1806 | 48.52941 | 143 | 3 |
| 436502 | 100 | 125 | 25 | 122.1806 | 48.52941 | 143 | 2 |
| 436502 | 125 | 250 | 125 | 122.1806 | 48.52941 | 143 | 2 |

| | | | | | | | |
|---|---|---|---|---|---|---|---|
| 436687 | 0 | 34 | 34 | 122.1755 | 48.52691 | 73 | 4 |
| 436687 | 34 | 58 | 24 | 122.1755 | 48.52691 | 73 | 3 |
| 436687 | 58 | 88 | 30 | 122.1755 | 48.52691 | 73 | 2 |
| 436687 | 88 | 91 | 3 | 122.1755 | 48.52691 | 72.5 | 1 |
| 436687 | 91 | 391 | 300 | 122.1755 | 48.52691 | 72.5 | 1 |
| 441240 | 0 | 17 | 17 | 122.144 | 48.5082 | 75 | 5 |
| 441240 | 17 | 35 | 18 | 122.144 | 48.5082 | 75 | 4 |
| 441240 | 35 | 55 | 20 | 122.144 | 48.5082 | 75 | 3 |
| 441240 | 55 | 56 | 1 | 122.144 | 48.5082 | 75 | 2 |
| 441240 | 56 | 206 | 150 | 122.144 | 48.5082 | 75 | 2 |
| 451887 | 0 | 40 | 40 | 122.1505 | 48.50413 | 72 | 4 |
| 451887 | 40 | 57 | 17 | 122.1505 | 48.50413 | 72 | 3 |
| 451887 | 57 | 207 | 150 | 122.1505 | 48.50413 | 72 | 2 |
| 462712 | 0 | 14 | 14 | 122.1447 | 48.51561 | 76 | 5 |
| 462712 | 14 | 27 | 13 | 122.1447 | 48.51561 | 76 | 4 |
| 462712 | 27 | 58 | 31 | 122.1447 | 48.51561 | 76 | 3 |
| 462712 | 58 | 208 | 150 | 122.1447 | 48.51561 | 76 | 2 |
| 1710326 | 0 | 48 | 48 | 122.1841 | 48.5046 | 64 | 4 |
| 1710326 | 48 | 71 | 23 | 122.1841 | 48.5046 | 64 | 3 |
| 1710326 | 71 | 72 | 1 | 122.1841 | 48.5046 | 64 | 2 |
| 1710326 | 72 | 222 | 150 | 122.1841 | 48.5046 | 64 | 2 |
| 256219 | 0 | 65 | 65 | 122.149 | 48.53265 | 218 | 4 |
| 256219 | 65 | 166 | 101 | 122.149 | 48.53265 | 218 | 2 |
| 256219 | 166 | 216 | 50 | 122.149 | 48.53265 | 218 | 2 |
| 304014 | 0 | 5 | 5 | 122.1702 | 48.53801 | 378 | 5 |
| 304014 | 5 | 120 | 115 | 122.1702 | 48.53801 | 378 | 1 |
| 304014 | 120 | 405 | 285 | 122.1702 | 48.53801 | 378 | 1 |
| 304018 | 0 | 108 | 3 | 122.1737 | 48.53457 | 277 | 5 |
| 304018 | 108 | 154 | 46 | 122.1737 | 48.53457 | 277 | 4 |
| 304018 | 154 | 220 | 66 | 122.1737 | 48.53457 | 277 | 1 |
| 304018 | 220 | 454 | 234 | 122.1737 | 48.53457 | 277 | 1 |

| | | | | | | | |
|---|---|---|---|---|---|---|---|
| 457607 | 0 | 105 | 105 | 122.1638 | 48.53501 | 324 | 4 |
| 457607 | 105 | 200 | 95 | 122.1638 | 48.53501 | 324 | 1 |
| 457607 | 200 | 405 | 205 | 122.1638 | 48.53501 | 324 | 1 |
| 481861 | 0 | 115 | 115 | 122.1819 | 48.53214 | 194 | 4 |
| 481861 | 115 | 291 | 176 | 122.1819 | 48.53214 | 194 | 2 |
| 579452 | 0 | 22 | 22 | 122.1686 | 48.53934 | 406 | 5 |
| 579452 | 22 | 220 | 198 | 122.1686 | 48.53934 | 406 | 1 |
| 579452 | 220 | 522 | 302 | 122.1686 | 48.53934 | 406 | 1 |
| 620346 | 0 | 61 | 61 | 122.1773 | 48.53159 | 226 | 4 |
| 620346 | 61 | 124 | 63 | 122.1773 | 48.53159 | 226 | 1 |
| 620346 | 124 | 361 | 237 | 122.1773 | 48.53159 | 226 | 1 |
| 1972918 | 0 | 65 | 65 | 122.1917 | 48.53764 | 212 | 4 |
| 1972918 | 65 | 198.5 | 133.5 | 122.1917 | 48.53764 | 212 | 2 |
| 1972918 | 198.5 | 215 | 16.5 | 122.1917 | 48.53764 | 212 | 2 |
| 75612 | 0 | 17 | 17 | 122.1695 | 48.5414 | 452 | 5 |
| 75612 | 17 | 224 | 207 | 122.1695 | 48.5414 | 452 | 1 |
| 75612 | 224 | 517 | 293 | 122.1695 | 48.5414 | 452 | 1 |
| 76389 | 0 | 2 | 2 | 122.1702 | 48.53775 | 367 | 5 |
| 76389 | 2 | 182 | 180 | 122.1702 | 48.53775 | 367 | 1 |
| 76389 | 182 | 402 | 220 | 122.1702 | 48.53775 | 367 | 1 |
| 76767 | 0 | 62 | 62 | 122.1719 | 48.53584 | 314 | 5 |
| 76767 | 62 | 182 | 120 | 122.1719 | 48.53584 | 314 | 1 |
| 76767 | 182 | 462 | 280 | 122.1719 | 48.53584 | 314 | 1 |
| 83689 | 0 | 60 | 60 | 122.1885 | 48.53065 | 117 | 4 |
| 83689 | 60 | 420 | 360 | 122.1885 | 48.53065 | 117 | 2 |
| 84433 | 0 | 10 | 10 | 122.1684 | 48.53259 | 215 | 5 |
| 84433 | 10 | 74 | 64 | 122.1684 | 48.53259 | 215 | 4 |
| 84433 | 74 | 204 | 130 | 122.1684 | 48.53259 | 215 | 1 |
| 84433 | 204 | 374 | 170 | 122.1684 | 48.53259 | 215 | 1 |
| 86110 | 0 | 92 | 92 | 122.1656 | 48.53569 | 347 | 4 |
| 86110 | 92 | 160 | 68 | 122.1656 | 48.53569 | 347 | 1 |

| | | | | | | | |
|---|---|---|---|---|---|---|---|
| 86110 | 160 | 442 | 282 | 122.1656 | 48.53569 | 347 | 1 |
| **11111** | **0** | **21** | **21** | **122.1675** | **48.53127** | **161** | **4** |
| **11111** | **21** | **171** | **150** | **122.1675** | **48.53127** | **161** | **1** |
| **11142** | **0** | **55** | **55** | **122.1369** | **48.55108** | **1185** | **5** |
| **11142** | **55** | **85** | **30** | **122.1369** | **48.55108** | **1185** | **4** |
| **11142** | **85** | **1085** | **1000** | **122.1369** | **48.55108** | **1185** | **0** |
| **11143** | **0** | **50** | **50** | **122.1377** | **48.54318** | **646** | **4** |
| **11143** | **50** | **650** | **600** | **122.1377** | **48.54318** | **646** | **1** |
| **11144** | **0** | **40** | **40** | **122.1915** | **48.55303** | **427** | **5** |
| **11144** | **40** | **240** | **200** | **122.1915** | **48.55303** | **427** | **4** |
| **11144** | **240** | **440** | **200** | **122.1915** | **48.55303** | **427** | **2** |
| **11145** | **0** | **200** | **200** | **122.186** | **48.56175** | **1250** | **4** |
| **11145** | **200** | **1200** | **1000** | **122.186** | **48.56175** | **1250** | **0** |
| **11146** | **0** | **2500** | **2500** | **122.1655** | **48.56288** | **2580** | **0** |
| **11147** | **0** | **25** | **25** | **122.1638** | **48.55385** | **1766** | **5** |
| **11147** | **25** | **125** | **100** | **122.1638** | **48.55385** | **1766** | **4** |
| **11147** | **125** | **1625** | **1500** | **122.1638** | **48.55385** | **1766** | **0** |
| **11148** | **0** | **2400** | **2400** | **122.1322** | **48.56108** | **2417** | **0** |

Well logs used in conceptual modeling in model Boundary B within Skagit River Valley. Rows in red are wells with modified depths and bolded wells are pseudo wells used for extrapolation purposes. The horizon number is the hydrogeologic unit.

| Log ID | Top (ft) | Bottom (ft) | Thickness (ft) | Longitude | Latitude | Elevation (ft) | Horizon |
|---|---|---|---|---|---|---|---|
| 86084 | 0 | 6 | 6 | 122.1122 | 48.529 | 437 | 5 |
| 86084 | 6 | 64 | 58 | 122.1122 | 48.529 | 437 | 4 |
| 86084 | 64 | 72 | 8 | 122.1122 | 48.529 | 437 | 1 |
| 86084 | 72 | 464 | 392 | 122.1122 | 48.529 | 437 | 1 |
| 477679 | 0 | 34 | 34 | 122.1003 | 48.52681 | 90 | 4 |
| 477679 | 34 | 60 | 26 | 122.1003 | 48.52681 | 90 | 3 |
| 477679 | 60 | 210 | 150 | 122.1003 | 48.52681 | 90 | 2 |
| 760446 | 0 | 6 | 6 | 122.0827 | 48.52723 | 82 | 5 |
| 760446 | 6 | 28 | 22 | 122.0827 | 48.52723 | 82 | 4 |
| 760446 | 28 | 60 | 32 | 122.0827 | 48.52723 | 82 | 3 |
| 760446 | 60 | 80 | 20 | 122.0827 | 48.52723 | 82 | 2 |
| 760446 | 80 | 210 | 130 | 122.0827 | 48.52723 | 82 | 2 |
| 82864 | 0 | 12 | 12 | 122.0851 | 48.5284 | 90 | 4 |
| 82864 | 12 | 65 | 53 | 122.0851 | 48.5284 | 90 | 3 |
| 82864 | 65 | 66 | 1 | 122.0851 | 48.5284 | 90 | 2 |
| 82864 | 66 | 216 | 150 | 122.0851 | 48.5284 | 90 | 2 |
| 75904 | 0 | 15 | 15 | 122.0539 | 48.52535 | 84 | 5 |
| 75904 | 15 | 51 | 36 | 122.0539 | 48.52535 | 84 | 3 |
| 75904 | 51 | 52 | 1 | 122.0539 | 48.52535 | 84 | 2 |
| 75904 | 52 | 202 | 150 | 122.0539 | 48.52535 | 84 | 2 |
| 954129 | 0 | 46 | 46 | 122.0573 | 48.52992 | 96 | 4 |
| 954129 | 46 | 196 | 150 | 122.0573 | 48.52992 | 96 | 2 |
| 74422 | 0 | 4 | 4 | 122.0709 | 48.52996 | 77 | 4 |
| 74422 | 4 | 39 | 35 | 122.0709 | 48.52996 | 77 | 3 |
| 74422 | 39 | 189 | 150 | 122.0709 | 48.52996 | 77 | 2 |
| 747895 | 0 | 22 | 22 | 122.1229 | 48.52575 | 85 | 4 |

| | | | | | | | |
|---|---|---|---|---|---|---|---|
| 747895 | 22 | 74 | 52 | 122.1229 | 48.52575 | 85 | 3 |
| 747895 | 74 | 224 | 150 | 122.1229 | 48.52575 | 85 | 2 |
| 78410 | 0 | 21 | 21 | 122.1233 | 48.51404 | 74 | 4 |
| 78410 | 21 | 58 | 37 | 122.1233 | 48.51404 | 74 | 3 |
| 78410 | 58 | 208 | 150 | 122.1233 | 48.51404 | 74 | 2 |
| 820529 | 0 | 22 | 22 | 122.1346 | 48.53424 | 305 | 5 |
| 820529 | 22 | 105 | 83 | 122.1346 | 48.53424 | 305 | 1 |
| 820529 | 105 | 322 | 217 | 122.1346 | 48.53424 | 305 | 1 |
| 394181 | 0 | 78 | 78 | 122.0998 | 48.53243 | 395 | 4 |
| 394181 | 78 | 130 | 52 | 122.0998 | 48.53243 | 395 | 3 |
| 394181 | 130 | 430 | 300 | 122.0998 | 48.53243 | 395 | 1 |
| 622925 | 0 | 1 | 1 | 122.1281 | 48.53411 | 407 | 5 |
| 622925 | 1 | 5 | 4 | 122.1281 | 48.53411 | 407 | 4 |
| 622925 | 5 | 163 | 158 | 122.1281 | 48.53411 | 407 | 1 |
| 622925 | 163 | 405 | 242 | 122.1281 | 48.53411 | 407 | 1 |
| 78010 | 0 | 65 | 65 | 122.1149 | 48.53052 | 484 | 5 |
| 78010 | 65 | 87 | 22 | 122.1149 | 48.53052 | 484 | 4 |
| 78010 | 87 | 93 | 6 | 122.1149 | 48.53052 | 484 | 3 |
| 78010 | 93 | 493 | 400 | 122.1149 | 48.53052 | 484 | 1 |
| 82972 | 0 | 18 | 18 | 122.1273 | 48.53973 | 442 | 5 |
| 82972 | 18 | 114 | 96 | 122.1273 | 48.53973 | 442 | 4 |
| 82972 | 114 | 514 | 400 | 122.1273 | 48.53973 | 442 | 1 |
| 85215 | 0 | 20 | 20 | 122.1147 | 48.53978 | 451 | 5 |
| 85215 | 20 | 91 | 71 | 122.1147 | 48.53978 | 451 | 4 |
| 85215 | 91 | 491 | 400 | 122.1147 | 48.53978 | 451 | 1 |
| 86161 | 0 | 18 | 18 | 122.0982 | 48.54193 | 642 | 4 |
| 86161 | 18 | 132 | 114 | 122.0982 | 48.54193 | 642 | 1 |
| 86161 | 132 | 518 | 386 | 122.0982 | 48.54193 | 642 | 1 |
| 86169 | 0 | 148 | 148 | 122.1149 | 48.53039 | 484 | 1 |
| 86169 | 148 | 500 | 352 | 122.1149 | 48.53039 | 484 | 1 |
| 86923 | 0 | 107 | 107 | 122.1038 | 48.53983 | 509 | 5 |

| | | | | | | | |
|---|---|---|---|---|---|---|---|
| 86923 | 107 | 127 | 20 | 122.1038 | 48.53983 | 509 | 4 |
| 86923 | 127 | 132 | 5 | 122.1038 | 48.53983 | 509 | 1 |
| 86923 | 132 | 627 | 495 | 122.1038 | 48.53983 | 509 | 1 |
| 87302 | 0 | 16 | 16 | 122.1054 | 48.53986 | 493 | 5 |
| 87302 | 16 | 78 | 62 | 122.1054 | 48.53986 | 493 | 4 |
| 87302 | 78 | 100 | 22 | 122.1054 | 48.53986 | 493 | 1 |
| 87302 | 100 | 578 | 478 | 122.1054 | 48.53986 | 493 | 1 |
| 372361 | 0 | 10 | 10 | 122.0545 | 48.53495 | 290 | 5 |
| 372361 | 10 | 81 | 71 | 122.0545 | 48.53495 | 290 | 4 |
| 372361 | 81 | 87 | 6 | 122.0545 | 48.53495 | 290 | 3 |
| 372361 | 87 | 88 | 1 | 122.0545 | 48.53495 | 290 | 1 |
| 372361 | 88 | 387 | 299 | 122.0545 | 48.53495 | 290 | 1 |
| 467261 | 0 | 66 | 66 | 122.0492 | 48.53697 | 294 | 5 |
| 467261 | 66 | 112 | 46 | 122.0492 | 48.53697 | 294 | 4 |
| 467261 | 112 | 119 | 7 | 122.0492 | 48.53697 | 294 | 3 |
| 467261 | 119 | 121 | 2 | 122.0492 | 48.53697 | 294 | 1 |
| 467261 | 121 | 419 | 298 | 122.0492 | 48.53697 | 294 | 1 |
| 84239 | 0 | 15 | 15 | 122.0558 | 48.54386 | 363 | 5 |
| 84239 | 15 | 38 | 23 | 122.0558 | 48.54386 | 363 | 4 |
| 84239 | 38 | 400 | 362 | 122.0558 | 48.54386 | 363 | 1 |
| 285101 | 0 | 18 | 18 | 122.0754 | 48.54007 | 480 | 5 |
| 285101 | 18 | 37 | 19 | 122.0754 | 48.54007 | 480 | 4 |
| 285101 | 37 | 200 | 163 | 122.0754 | 48.54007 | 480 | 1 |
| 285101 | 200 | 537 | 337 | 122.0754 | 48.54007 | 480 | 1 |
| 479791 | 0 | 36 | 36 | 122.0692 | 48.53941 | 374 | 5 |
| 479791 | 36 | 242 | 206 | 122.0692 | 48.53941 | 374 | 1 |
| 479791 | 242 | 436 | 194 | 122.0692 | 48.53941 | 374 | 1 |
| 84238 | 0 | 2 | 2 | 122.0558 | 48.54386 | 363 | 5 |
| 84238 | 2 | 20 | 18 | 122.0558 | 48.54386 | 363 | 4 |
| 84238 | 20 | 205 | 185 | 122.0558 | 48.54386 | 363 | 1 |
| 84238 | 205 | 420 | 215 | 122.0558 | 48.54386 | 363 | 1 |

| | | | | | | | |
|---|---|---|---|---|---|---|---|
| 1949988 | 0 | 32 | 32 | 122.0606 | 48.54111 | 409 | 5 |
| 1949988 | 32 | 205 | 173 | 122.0606 | 48.54111 | 409 | 1 |
| 1949988 | 205 | 432 | 227 | 122.0606 | 48.54111 | 409 | 1 |
| 84237 | 0 | 8 | 8 | 122.0558 | 48.54386 | 363 | 5 |
| 84237 | 8 | 34 | 26 | 122.0558 | 48.54386 | 363 | 4 |
| 84237 | 34 | 140 | 106 | 122.0558 | 48.54386 | 363 | 1 |
| 84237 | 140 | 434 | 294 | 122.0558 | 48.54386 | 363 | 1 |
| 315155 | 0 | 4 | 4 | 122.0542 | 48.54456 | 375 | 5 |
| 315155 | 4 | 11 | 7 | 122.0542 | 48.54456 | 375 | 4 |
| 315155 | 11 | 120 | 109 | 122.0542 | 48.54456 | 375 | 1 |
| 315155 | 120 | 411 | 291 | 122.0542 | 48.54456 | 375 | 1 |
| 1057400 | 0 | 9 | 9 | 122.0711 | 48.53827 | 403 | 4 |
| 1057400 | 9 | 106 | 97 | 122.0711 | 48.53827 | 403 | 1 |
| 1057400 | 106 | 409 | 303 | 122.0711 | 48.53827 | 403 | 1 |
| 493345 | 0 | 50 | 50 | 122.0779 | 48.53739 | 400 | 5 |
| 493345 | 50 | 101 | 51 | 122.0779 | 48.53739 | 400 | 4 |
| 493345 | 101 | 106 | 5 | 122.0779 | 48.53739 | 400 | 1 |
| 493345 | 106 | 501 | 395 | 122.0779 | 48.53739 | 400 | 1 |
| 814463 | 0 | 72 | 72 | 122.0712 | 48.53757 | 421 | 4 |
| 814463 | 72 | 102 | 30 | 122.0712 | 48.53757 | 421 | 3 |
| 814463 | 102 | 104 | 2 | 122.0712 | 48.53757 | 421 | 1 |
| 814463 | 104 | 502 | 398 | 122.0712 | 48.53757 | 421 | 1 |
| 76732 | 0 | 87 | 87 | 122.1102 | 48.52929 | 408 | 5 |
| 76732 | 87 | 96 | 9 | 122.1102 | 48.52929 | 408 | 4 |
| 76732 | 96 | 487 | 391 | 122.1102 | 48.52929 | 408 | 1 |
| **11112** | **0** | **23** | **23** | **122.1243** | **48.52988** | **423** | **4** |
| **11112** | **23** | **423** | **400** | **122.1243** | **48.52988** | **423** | **1** |
| **11113** | **0** | **300** | **300** | **122.116** | **48.52644** | **238** | **1** |
| **11114** | **0** | **350** | **350** | **122.11** | **48.5281** | **343** | **1** |
| **11115** | **0** | **30** | **30** | **122.0969** | **48.53027** | **320** | **4** |
| **11115** | **30** | **330** | **300** | **122.0969** | **48.53027** | **320** | **1** |

| | | | | | | | |
|---|---|---|---|---|---|---|---|
| 11116 | 0 | 30 | 30 | 122.0896 | 48.53333 | 352 | 4 |
| 11116 | 30 | 60 | 30 | 122.0896 | 48.53333 | 352 | 3 |
| 11116 | 60 | 360 | 300 | 122.0896 | 48.53333 | 352 | 1 |
| 11117 | 0 | 30 | 30 | 122.0792 | 48.53282 | 298 | 4 |
| 11117 | 30 | 60 | 30 | 122.0792 | 48.53282 | 298 | 3 |
| 11117 | 60 | 360 | 300 | 122.0792 | 48.53282 | 298 | 1 |
| 11118 | 0 | 30 | 30 | 122.0692 | 48.53225 | 149 | 3 |
| 11118 | 30 | 230 | 200 | 122.0692 | 48.53225 | 149 | 1 |
| 11119 | 0 | 20 | 20 | 122.0534 | 48.5324 | 202 | 3 |
| 11119 | 20 | 220 | 200 | 122.0534 | 48.5324 | 202 | 1 |
| 11120 | 0 | 30 | 30 | 122.047 | 48.53612 | 266 | 5 |
| 11120 | 30 | 70 | 40 | 122.047 | 48.53612 | 266 | 4 |
| 11120 | 70 | 80 | 10 | 122.047 | 48.53612 | 266 | 3 |
| 11120 | 80 | 330 | 250 | 122.047 | 48.53612 | 266 | 1 |
| 11139 | 0 | 1000 | 1000 | 122.0576 | 48.55458 | 1054 | 0 |
| 11140 | 0 | 70 | 70 | 122.1055 | 48.54431 | 887 | 4 |
| 11140 | 70 | 700 | 630 | 122.1055 | 48.54431 | 887 | 1 |
| 11141 | 0 | 1500 | 1500 | 122.127 | 48.55648 | 1684 | 0 |

Well logs used in conceptual modeling in model Boundary C within Skagit River Valley. Rows in red are wells with modified depths and bolded wells are pseudo wells used for extrapolation purposes. The horizon number is the hydrogeologic unit.

| Log ID | Top (ft) | Bottom (ft) | Thickness (ft) | Longitude | Latitude | Elevation (ft) | Horizon |
|---|---|---|---|---|---|---|---|
| 315160 | 0 | 15 | 15 | 122.034 | 48.51622 | 86 | 4 |
| 315160 | 15 | 53 | 38 | 122.034 | 48.51622 | 86 | 3 |
| 315160 | 53 | 108 | 55 | 122.034 | 48.51622 | 86 | 2 |
| 315160 | 108 | 203 | 95 | 122.034 | 48.51622 | 86 | 2 |
| 78784 | 0 | 7 | 7 | 121.9989 | 48.5358 | 167 | 5 |
| 78784 | 7 | 21 | 14 | 121.9989 | 48.5358 | 167 | 4 |
| 78784 | 21 | 94 | 73 | 121.9989 | 48.5358 | 167 | 3 |
| 78784 | 94 | 244 | 150 | 121.9989 | 48.5358 | 167 | 2 |
| 74851 | 0 | 74 | 74 | 121.9998 | 48.53402 | 152 | 4 |
| 74851 | 74 | 80 | 6 | 121.9998 | 48.53402 | 152 | 3 |
| 74851 | 80 | 230 | 150 | 121.9998 | 48.53402 | 152 | 2 |
| 85489 | 0 | 75 | 75 | 121.9993 | 48.53388 | 151 | 4 |
| 85489 | 75 | 80 | 5 | 121.9993 | 48.53388 | 151 | 3 |
| 85489 | 80 | 230 | 150 | 121.9993 | 48.53388 | 151 | 2 |
| 86008 | 0 | 15 | 15 | 121.9968 | 48.53448 | 157 | 5 |
| 86008 | 15 | 70 | 55 | 121.9968 | 48.53448 | 157 | 4 |
| 86008 | 70 | 80 | 10 | 121.9968 | 48.53448 | 157 | 3 |
| 86008 | 80 | 230 | 150 | 121.9968 | 48.53448 | 157 | 2 |
| 334092 | 0 | 25 | 25 | 122.0254 | 48.5373 | 151 | 4 |
| 334092 | 25 | 78 | 53 | 122.0254 | 48.5373 | 151 | 3 |
| 334092 | 78 | 228 | 150 | 122.0254 | 48.5373 | 151 | 2 |
| 235250 | 0 | 3 | 3 | 122.0276 | 48.5382 | 149 | 5 |
| 235250 | 3 | 15 | 12 | 122.0276 | 48.5382 | 149 | 4 |
| 235250 | 15 | 77 | 62 | 122.0276 | 48.5382 | 149 | 3 |
| 235250 | 77 | 227 | 150 | 122.0276 | 48.5382 | 149 | 2 |
| 77211 | 0 | 15 | 15 | 122.0021 | 48.53343 | 139 | 5 |
| 77211 | 15 | 58 | 43 | 122.0021 | 48.53343 | 139 | 4 |

| | | | | | | | |
|---|---|---|---|---|---|---|---|
| 77211 | 58 | 72 | 14 | 122.0021 | 48.53343 | 139 | 3 |
| 77211 | 72 | 222 | 150 | 122.0021 | 48.53343 | 139 | 2 |
| 190520 | 0 | 32 | 32 | 122.0033 | 48.53345 | 135 | 4 |
| 190520 | 32 | 69 | 37 | 122.0033 | 48.53345 | 135 | 3 |
| 190520 | 69 | 219 | 150 | 122.0033 | 48.53345 | 135 | 2 |
| 83754 | 0 | 15 | 15 | 122.0221 | 48.53654 | 134 | 5 |
| 83754 | 15 | 54 | 39 | 122.0221 | 48.53654 | 134 | 4 |
| 83754 | 54 | 60 | 6 | 122.0221 | 48.53654 | 134 | 3 |
| 83754 | 60 | 210 | 150 | 122.0221 | 48.53654 | 134 | 2 |
| 78897 | 0 | 19 | 19 | 122.0198 | 48.51756 | 91 | 5 |
| 78897 | 19 | 22 | 3 | 122.0198 | 48.51756 | 91 | 4 |
| 78897 | 22 | 49 | 27 | 122.0198 | 48.51756 | 91 | 3 |
| 78897 | 49 | 199 | 150 | 122.0198 | 48.51756 | 91 | 2 |
| 366218 | 0 | 5 | 5 | 122.0234 | 48.50959 | 90 | 4 |
| 366218 | 5 | 54 | 49 | 122.0234 | 48.50959 | 90 | 3 |
| 366218 | 54 | 204 | 150 | 122.0234 | 48.50959 | 90 | 2 |
| 487474 | 0 | 25 | 25 | 122.0294 | 48.52571 | 89 | 4 |
| 487474 | 25 | 41 | 16 | 122.0294 | 48.52571 | 89 | 3 |
| 487474 | 41 | 45 | 4 | 122.0294 | 48.52571 | 89 | 2 |
| 487474 | 45 | 191 | 146 | 122.0294 | 48.52571 | 89 | 2 |
| 77414 | 0 | 28 | 28 | 122.0088 | 48.52849 | 94 | 5 |
| 77414 | 28 | 49 | 21 | 122.0088 | 48.52849 | 94 | 3 |
| 77414 | 49 | 199 | 150 | 122.0088 | 48.52849 | 94 | 2 |
| 1955145 | 0 | 8 | 8 | 122.0398 | 48.5246 | 83 | 4 |
| 1955145 | 8 | 42 | 34 | 122.0398 | 48.5246 | 83 | 3 |
| 1955145 | 42 | 44 | 2 | 122.0398 | 48.5246 | 83 | 2 |
| 1955145 | 44 | 192 | 148 | 122.0398 | 48.5246 | 83 | 2 |
| 1029542 | 0 | 18 | 18 | 122.0395 | 48.53369 | 95 | 4 |
| 1029542 | 18 | 28 | 10 | 122.0395 | 48.53369 | 95 | 3 |
| 1029542 | 28 | 178 | 150 | 122.0395 | 48.53369 | 95 | 2 |
| 190222 | 0 | 18 | 18 | 122.0308 | 48.52836 | 86 | 5 |

| | | | | | | | |
|---|---|---|---|---|---|---|---|
| 190222 | 18 | 40 | 22 | 122.0308 | 48.52836 | 96 | 3 |
| 190222 | 40 | 190 | 150 | 122.0308 | 48.52836 | 96 | 2 |
| 982843 | 0 | 11 | 11 | 122.0283 | 48.52788 | 87 | 4 |
| 982843 | 11 | 35 | 24 | 122.0283 | 48.52788 | 87 | 3 |
| 982843 | 35 | 36 | 1 | 122.0283 | 48.52788 | 87 | 2 |
| 982843 | 36 | 185 | 149 | 122.0283 | 48.52788 | 87 | 2 |
| 823221 | 0 | 10 | 10 | 122.0198 | 48.5248 | 88 | 5 |
| 823221 | 10 | 56 | 46 | 122.0198 | 48.5248 | 88 | 3 |
| 823221 | 56 | 206 | 150 | 122.0198 | 48.5248 | 88 | 2 |
| **111** | **0** | **100** | **100** | **122.0331** | **48.55404** | **566.5** | **4** |
| **111** | **100** | **450** | **350** | **122.0331** | **48.55404** | **566.5** | **3** |
| **111** | **450** | **516.5** | **66.5** | **122.0331** | **48.55404** | **566.5** | **2** |
| **111** | **516.5** | **600** | **83.5** | **122.0331** | **48.55404** | **566.5** | **2** |
| **222** | **0** | **30** | **30** | **122.0069** | **48.54754** | **387** | **5** |
| **222** | **30** | **200** | **170** | **122.0069** | **48.54754** | **387** | **4** |
| **222** | **200** | **280** | **80** | **122.0069** | **48.54754** | **387** | **3** |
| **222** | **280** | **337** | **57** | **122.0069** | **48.54754** | **387** | **2** |
| **222** | **337** | **430** | **93** | **122.0069** | **48.54754** | **387** | **2** |
| **333** | **0** | **5** | **5** | **121.9846** | **48.54666** | **395** | **5** |
| **333** | **5** | **155** | **150** | **121.9846** | **48.54666** | **395** | **4** |
| **333** | **155** | **345** | **190** | **121.9846** | **48.54666** | **395** | **2** |
| **11121** | **0** | **80** | **80** | **122.0404** | **48.53862** | **204** | **4** |
| **11121** | **80** | **160** | **80** | **122.0404** | **48.53862** | **204** | **3** |
| **11121** | **160** | **310** | **150** | **122.0404** | **48.53862** | **204** | **2** |
| **11122** | **0** | **30** | **30** | **122.0277** | **48.5395** | **258** | **5** |
| **11122** | **30** | **100** | **70** | **122.0277** | **48.5395** | **258** | **4** |
| **11122** | **100** | **200** | **100** | **122.0277** | **48.5395** | **258** | **3** |
| **11122** | **200** | **350** | **150** | **122.0277** | **48.5395** | **258** | **2** |
| **11123** | **0** | **10** | **10** | **122.016** | **48.53781** | **185** | **5** |
| **11123** | **10** | **90** | **80** | **122.016** | **48.53781** | **185** | **4** |
| **11123** | **90** | **160** | **70** | **122.016** | **48.53781** | **185** | **3** |

| | | | | | | | |
|---|---|---|---|---|---|---|---|
| **11123** | **160** | **310** | **150** | **122.016** | **48.53781** | **185** | **2** |
| **11124** | **0** | **5** | **5** | **121.9959** | **48.53758** | **242** | **5** |
| **11124** | **5** | **150** | **145** | **121.9959** | **48.53758** | **242** | **4** |
| **11124** | **150** | **220** | **70** | **121.9959** | **48.53758** | **242** | **3** |
| **11124** | **220** | **370** | **150** | **121.9959** | **48.53758** | **242** | **2** |
| **11136** | **0** | **100** | **100** | **121.9846** | **48.56705** | **1135** | **4** |
| **11136** | **100** | **200** | **100** | **121.9846** | **48.56705** | **1135** | **3** |
| **11136** | **200** | **1000** | **800** | **121.9846** | **48.56705** | **1135** | **0** |
| **11137** | **0** | **1800** | **1800** | **121.9857** | **48.57912** | **1913** | **0** |
| **11138** | **0** | **1000** | **1000** | **122.0347** | **48.56126** | **1193** | **0** |

Well logs used in conceptual modeling in model Boundary D within Skagit River Valley. Rows in red are wells with modified depths and bolded wells are pseudo wells used for extrapolation purposes. The horizon number is the hydrogeologic unit.

| Log ID | Top (ft) | Bottom (ft) | Thickness (ft) | Longitude | Latitude | Elevation (ft) | Horizon |
|---|---|---|---|---|---|---|---|
| 472381 | 0 | 30 | 30 | 121.9495 | 48.52794 | 160 | 4 |
| 472381 | 30 | 54 | 24 | 121.9495 | 48.52794 | 160 | 3 |
| 472381 | 54 | 204 | 150 | 121.9495 | 48.52794 | 160 | 2 |
| 86839 | 0 | 28 | 28 | 121.9482 | 48.52505 | 143 | 5 |
| 86839 | 28 | 35 | 7 | 121.9482 | 48.52505 | 143 | 4 |
| 86839 | 35 | 57 | 22 | 121.9482 | 48.52505 | 143 | 3 |
| 86839 | 57 | 207 | 150 | 121.9482 | 48.52505 | 143 | 2 |
| 1038808 | 0 | 10 | 10 | 121.956 | 48.52373 | 112 | 4 |
| 1038808 | 10 | 40 | 30 | 121.956 | 48.52373 | 112 | 3 |
| 1038808 | 40 | 190 | 150 | 121.956 | 48.52373 | 112 | 2 |
| 285270 | 0 | 14 | 14 | 121.9544 | 48.52121 | 112 | 4 |
| 285270 | 14 | 19 | 5 | 121.9544 | 48.52121 | 112 | 3 |
| 285270 | 19 | 169 | 150 | 121.9544 | 48.52121 | 112 | 2 |
| 79907 | 0 | 6 | 6 | 121.9117 | 48.53022 | 149 | 5 |
| 79907 | 6 | 42.5 | 36.5 | 121.9117 | 48.53022 | 149 | 3 |
| 79907 | 42.5 | 43.5 | 1 | 121.9117 | 48.53022 | 149 | 2 |
| 79907 | 43.5 | 192.5 | 149 | 121.9117 | 48.53022 | 149 | 2 |
| 315211 | 0 | 11 | 11 | 121.9069 | 48.53014 | 153 | 4 |
| 315211 | 11 | 82 | 71 | 121.9069 | 48.53014 | 153 | 3 |
| 315211 | 82 | 85 | 3 | 121.9069 | 48.53014 | 153 | 2 |
| 315211 | 85 | 232 | 147 | 121.9069 | 48.53014 | 153 | 2 |
| 372155 | 0 | 40 | 40 | 121.8991 | 48.5297 | 150 | 4 |
| 372155 | 40 | 69 | 29 | 121.8991 | 48.5297 | 150 | 3 |
| 372155 | 69 | 219 | 150 | 121.8991 | 48.5297 | 150 | 2 |
| 87698 | 0 | 42 | 42 | 121.8971 | 48.52449 | 148 | 5 |
| 87698 | 42 | 45 | 3 | 121.8971 | 48.52449 | 148 | 4 |
| 87698 | 45 | 95 | 50 | 121.8971 | 48.52449 | 148 | 3 |

| | | | | | | | |
|---|---|---|---|---|---|---|---|
| 87698 | 95 | 245 | 150 | 121.8971 | 48.52449 | 148 | 2 |
| 81381 | 0 | 30 | 30 | 121.9022 | 48.51898 | 147 | 5 |
| 81381 | 30 | 31 | 1 | 121.9022 | 48.51898 | 147 | 4 |
| 81381 | 31 | 83 | 52 | 121.9022 | 48.51898 | 147 | 3 |
| 81381 | 83 | 233 | 150 | 121.9022 | 48.51898 | 147 | 2 |
| 800269 | 0 | 25 | 25 | 121.9013 | 48.52075 | 147 | 4 |
| 800269 | 25 | 78 | 53 | 121.9013 | 48.52075 | 147 | 3 |
| 800269 | 78 | 228 | 150 | 121.9013 | 48.52075 | 147 | 2 |
| 81224 | 0 | 32 | 32 | 121.9313 | 48.52273 | 127 | 4 |
| 81224 | 32 | 40 | 8 | 121.9313 | 48.52273 | 127 | 3 |
| 81224 | 40 | 190 | 150 | 121.9313 | 48.52273 | 127 | 2 |
| 542322 | 0 | 90 | 90 | 121.8894 | 48.52778 | 165 | 4 |
| 542322 | 90 | 95 | 5 | 121.8894 | 48.52778 | 165 | 3 |
| 542322 | 95 | 245 | 150 | 121.8894 | 48.52778 | 165 | 2 |
| 403191 | 0 | 6 | 6 | 121.8898 | 48.52404 | 155 | 5 |
| 403191 | 6 | 67 | 61 | 121.8898 | 48.52404 | 155 | 4 |
| 403191 | 67 | 86 | 19 | 121.8898 | 48.52404 | 155 | 2 |
| 403191 | 86 | 217 | 131 | 121.8898 | 48.52404 | 155 | 2 |
| 84560 | 0 | 25 | 25 | 121.9169 | 48.51667 | 135 | 5 |
| 84560 | 25 | 75 | 50 | 121.9169 | 48.51667 | 135 | 3 |
| 84560 | 75 | 153 | 78 | 121.9169 | 48.51667 | 135 | 2 |
| 84560 | 153 | 225 | 72 | 121.9169 | 48.51667 | 135 | 2 |
| 75973 | 0 | 15 | 15 | 121.9166 | 48.52306 | 135 | 5 |
| 75973 | 15 | 38 | 23 | 121.9166 | 48.52306 | 135 | 3 |
| 75973 | 38 | 188 | 150 | 121.9166 | 48.52306 | 135 | 2 |
| 83221 | 0 | 26 | 26 | 121.9174 | 48.52848 | 143 | 5 |
| 83221 | 26 | 48 | 22 | 121.9174 | 48.52848 | 143 | 3 |
| 83221 | 48 | 198 | 150 | 121.9174 | 48.52848 | 143 | 2 |
| 85521 | 0 | 23 | 23 | 121.9222 | 48.53145 | 141 | 5 |
| 85521 | 23 | 27 | 4 | 121.9222 | 48.53145 | 141 | 3 |
| 85521 | 27 | 35 | 8 | 121.9222 | 48.53145 | 141 | 2 |

| | | | | | | | |
|---|---|---|---|---|---|---|---|
| 85521 | 35 | 177 | 142 | 121.9222 | 48.53145 | 141 | 2 |
| 85860 | 0 | 40 | 40 | 121.8783 | 48.52041 | 143 | 4 |
| 85860 | 40 | 100 | 60 | 121.8783 | 48.52041 | 143 | 3 |
| 85860 | 100 | 250 | 150 | 121.8783 | 48.52041 | 143 | 2 |
| 342227 | 0 | 24 | 24 | 121.8766 | 48.5223 | 152 | 4 |
| 342227 | 24 | 59 | 35 | 121.8766 | 48.5223 | 152 | 3 |
| 342227 | 59 | 209 | 150 | 121.8766 | 48.5223 | 152 | 2 |
| 76609 | 0 | 40 | 40 | 121.8784 | 48.5241 | 155 | 4 |
| 76609 | 40 | 47 | 7 | 121.8784 | 48.5241 | 155 | 3 |
| 76609 | 47 | 197 | 150 | 121.8784 | 48.5241 | 155 | 2 |
| 87268 | 0 | 60 | 60 | 121.8831 | 48.52587 | 165 | 4 |
| 87268 | 60 | 210 | 150 | 121.8831 | 48.52587 | 165 | 2 |
| 441246 | 0 | 41 | 41 | 121.8845 | 48.52764 | 172 | 4 |
| 441246 | 41 | 125 | 84 | 121.8845 | 48.52764 | 172 | 3 |
| 441246 | 125 | 178 | 53 | 121.8845 | 48.52764 | 172 | 2 |
| 441246 | 178 | 275 | 97 | 121.8845 | 48.52764 | 172 | 2 |
| 454844 | 0 | 35 | 35 | 121.8857 | 48.52825 | 174 | 4 |
| 454844 | 35 | 131 | 96 | 121.8857 | 48.52825 | 174 | 3 |
| 454844 | 131 | 180 | 49 | 121.8857 | 48.52825 | 174 | 2 |
| 454844 | 180 | 281 | 101 | 121.8857 | 48.52825 | 174 | 2 |
| 81670 | 0 | 37 | 37 | 121.8894 | 48.53142 | 182 | 5 |
| 81670 | 37 | 60 | 23 | 121.8894 | 48.53142 | 182 | 4 |
| 81670 | 60 | 95 | 35 | 121.8894 | 48.53142 | 182 | 3 |
| 81670 | 95 | 245 | 150 | 121.8894 | 48.53142 | 182 | 2 |
| 372700 | 0 | 15 | 15 | 121.9609 | 48.52721 | 103 | 5 |
| 372700 | 15 | 22 | 7 | 121.9609 | 48.52721 | 103 | 4 |
| 372700 | 22 | 80 | 58 | 121.9609 | 48.52721 | 103 | 3 |
| 372700 | 80 | 100 | 20 | 121.9609 | 48.52721 | 103 | 2 |
| 372700 | 100 | 230 | 130 | 121.9609 | 48.52721 | 103 | 2 |
| 419463 | 0 | 16 | 16 | 121.9568 | 48.52086 | 112 | 5 |
| 419463 | 16 | 60 | 44 | 121.9568 | 48.52086 | 112 | 3 |

| | | | | | | | |
|---|---|---|---|---|---|---|---|
| 419463 | 60 | 210 | 150 | 121.9568 | 48.52086 | 112 | 2 |
| 76276 | 0 | 22 | 22 | 121.9752 | 48.52896 | 99 | 5 |
| 76276 | 22 | 40 | 18 | 121.9752 | 48.52896 | 99 | 3 |
| 76276 | 40 | 190 | 150 | 121.9752 | 48.52896 | 99 | 2 |
| 80464 | 0 | 13 | 13 | 121.9692 | 48.52508 | 105 | 5 |
| 80464 | 13 | 40 | 27 | 121.9692 | 48.52508 | 105 | 3 |
| 80464 | 40 | 190 | 150 | 121.9692 | 48.52508 | 105 | 2 |
| 285103 | 0 | 10 | 10 | 121.9872 | 48.52096 | 100 | 5 |
| 285103 | 10 | 28 | 18 | 121.9872 | 48.52096 | 100 | 4 |
| 285103 | 28 | 58 | 30 | 121.9872 | 48.52096 | 100 | 3 |
| 285103 | 58 | 208 | 150 | 121.9872 | 48.52096 | 100 | 2 |
| 87030 | 0 | 19 | 19 | 121.9885 | 48.52854 | 102 | 5 |
| 87030 | 19 | 39 | 20 | 121.9885 | 48.52854 | 102 | 3 |
| 87030 | 39 | 189 | 150 | 121.9885 | 48.52854 | 102 | 2 |
| 83642 | 0 | 43 | 43 | 121.9871 | 48.53177 | 115 | 4 |
| 83642 | 43 | 63 | 20 | 121.9871 | 48.53177 | 115 | 3 |
| 83642 | 63 | 213 | 150 | 121.9871 | 48.53177 | 115 | 2 |
| 1883595 | 0 | 25 | 25 | 121.9868 | 48.52339 | 97 | 5 |
| 1883595 | 25 | 40 | 15 | 121.9868 | 48.52339 | 97 | 4 |
| 1883595 | 40 | 60 | 20 | 121.9868 | 48.52339 | 97 | 3 |
| 1883595 | 60 | 71 | 11 | 121.9868 | 48.52339 | 97 | 2 |
| 1883595 | 71 | 210 | 139 | 121.9868 | 48.52339 | 97 | 2 |
| 190506 | 0 | 1 | 1 | 121.9815 | 48.53888 | 251 | 5 |
| 190506 | 1 | 137 | 136 | 121.9815 | 48.53888 | 251 | 4 |
| 190506 | 137 | 199 | 62 | 121.9815 | 48.53888 | 251 | 3 |
| 190506 | 199 | 349 | 150 | 121.9815 | 48.53888 | 251 | 2 |
| 310 | 0 | 27 | 27 | 121.9402 | 48.53469 | 300 | 5 |
| 310 | 27 | 104 | 77 | 121.9402 | 48.53469 | 300 | 4 |
| 310 | 104 | 261 | 157 | 121.9402 | 48.53469 | 300 | 3 |
| 310 | 261 | 310 | 49 | 121.9402 | 48.53469 | 300 | 2 |
| 611775 | 0 | 26 | 26 | 121.9293 | 48.53644 | 308 | 5 |
| 611775 | 26 | 68 | 42 | 121.9293 | 48.53644 | 308 | 4 |

| | | | | | | | |
|---|---|---|---|---|---|---|---|
| 611775 | 68 | 78 | 10 | 121.9293 | 48.53644 | 308 | 3 |
| 77349 | 0 | 40 | 40 | 121.9226 | 48.53445 | 310 | 5 |
| 77349 | 40 | 153 | 113 | 121.9226 | 48.53445 | 310 | 4 |
| 77349 | 153 | 163 | 10 | 121.9226 | 48.53445 | 310 | 3 |
| 77349 | 163 | 313 | 150 | 121.9226 | 48.53445 | 310 | 2 |
| 87284 | 0 | 109 | 109 | 121.8855 | 48.53947 | 337 | 5 |
| 87284 | 109 | 149 | 40 | 121.8855 | 48.53947 | 337 | 4 |
| 87284 | 149 | 199 | 50 | 121.8855 | 48.53947 | 337 | 3 |
| 87284 | 199 | 349 | 150 | 121.8855 | 48.53947 | 337 | 2 |
| 403 | 0 | 68 | 68 | 121.8858 | 48.53829 | 334 | 5 |
| 403 | 68 | 120 | 52 | 121.8858 | 48.53829 | 334 | 4 |
| 403 | 120 | 125 | 5 | 121.8858 | 48.53829 | 334 | 3 |
| 256214 | 0 | 88 | 88 | 121.8893 | 48.535 | 322 | 5 |
| 256214 | 88 | 117 | 29 | 121.8893 | 48.535 | 322 | 4 |
| 256214 | 117 | 138 | 21 | 121.8893 | 48.535 | 322 | 3 |
| 2014318 | 0 | 116 | 116 | 121.8912 | 48.53353 | 299 | 5 |
| 2014318 | 116 | 143 | 27 | 121.8912 | 48.53353 | 299 | 4 |
| 2014318 | 143 | 160 | 17 | 121.8912 | 48.53353 | 299 | 3 |
| 2014318 | 160 | 310 | 150 | 121.8912 | 48.53353 | 299 | 2 |
| 84572 | 0 | 50 | 50 | 121.9194 | 48.53594 | 316 | 5 |
| 84572 | 50 | 192 | 142 | 121.9194 | 48.53594 | 316 | 4 |
| 84572 | 192 | 204 | 12 | 121.9194 | 48.53594 | 316 | 3 |
| 84572 | 204 | 362 | 150 | 121.9194 | 48.53594 | 316 | 2 |
| **11125** | **0** | **5** | **5** | **121.9746** | **48.53076** | **239** | **5** |
| **11125** | **5** | **100** | **95** | **121.9746** | **48.53076** | **239** | **4** |
| **11125** | **100** | **180** | **80** | **121.9746** | **48.53076** | **239** | **3** |
| **11125** | **180** | **330** | **150** | **121.9746** | **48.53076** | **239** | **2** |
| **11126** | **0** | **5** | **5** | **121.9586** | **48.52717** | **242** | **5** |
| **11126** | **5** | **100** | **95** | **121.9586** | **48.52717** | **242** | **4** |
| **11126** | **100** | **180** | **80** | **121.9586** | **48.52717** | **242** | **3** |
| **11126** | **180** | **330** | **150** | **121.9586** | **48.52717** | **242** | **2** |
| **11127** | **0** | **20** | **20** | **121.9351** | **48.53005** | **263** | **5** |

| | | | | | | | |
|---|---|---|---|---|---|---|---|
| 11127 | 20 | 100 | 80 | 121.9351 | 48.53005 | 263 | 4 |
| 11127 | 100 | 220 | 120 | 121.9351 | 48.53005 | 263 | 3 |
| 11127 | 220 | 370 | 150 | 121.9351 | 48.53005 | 263 | 2 |
| 11128 | 0 | 20 | 20 | 121.9051 | 48.53205 | 253 | 5 |
| 11128 | 20 | 100 | 80 | 121.9051 | 48.53205 | 253 | 4 |
| 11128 | 100 | 220 | 120 | 121.9051 | 48.53205 | 253 | 3 |
| 11128 | 220 | 370 | 150 | 121.9051 | 48.53205 | 253 | 2 |
| 11129 | 0 | 70 | 70 | 121.8931 | 48.5316 | 261 | 5 |
| 11129 | 70 | 150 | 80 | 121.8931 | 48.5316 | 261 | 4 |
| 11129 | 150 | 250 | 100 | 121.8931 | 48.5316 | 261 | 3 |
| 11129 | 250 | 400 | 150 | 121.8931 | 48.5316 | 261 | 2 |
| 11130 | 0 | 100 | 100 | 121.8789 | 48.55286 | 777 | 3 |
| 11130 | 100 | 400 | 300 | 121.8789 | 48.55286 | 777 | 2 |
| 11131 | 0 | 100 | 100 | 121.8806 | 48.56299 | 1219 | 4 |
| 11131 | 100 | 200 | 100 | 121.8806 | 48.56299 | 1219 | 3 |
| 11131 | 200 | 1200 | 1000 | 121.8806 | 48.56299 | 1219 | 0 |
| 11132 | 0 | 2500 | 2500 | 121.8792 | 48.57808 | 2548 | 0 |
| 11133 | 0 | 100 | 100 | 121.9677 | 48.55399 | 618 | 3 |
| 11133 | 100 | 400 | 300 | 121.9677 | 48.55399 | 618 | 2 |
| 11134 | 0 | 100 | 100 | 121.9729 | 48.5645 | 1074 | 4 |
| 11134 | 100 | 200 | 100 | 121.9729 | 48.5645 | 1074 | 3 |
| 11134 | 200 | 1000 | 800 | 121.9729 | 48.5645 | 1074 | 0 |
| 11135 | 0 | 1800 | 1800 | 121.981 | 48.5789 | 1857 | 0 |

**Appendix B: Wells and well data used to estimate hydraulic conductivities.**

Chuckanut Formation

| Well ID | Diameter (in) | Screen Length (ft) | Pumping Rate (gpm) | Drawdown (ft) | Time (hr) | Storativity (0.1-0.0001) | Screened Hydraulic Conductivity (ft/day) | Open End Hydraulic Conductivity (ft/day) |
|---|---|---|---|---|---|---|---|---|
| 85684 | 6 | 44-48 | 1.5 | 23 | 6 | 0.0001 | 3.51 | |
| 75172 | 6 | 195-198 | 1.3 | 8 | 1 | 0.0001 | 10.87 | |
| 655490 | 6 | 140-150 | 24 | 130 | 0.5 | 0.0001 | 3.53 | |
| 86161 | 6 | 94-98 | 3 | 74.6 | 6 | 0.0001 | 2.08 | |
| 820529 | 6 | 90-105 | 8.2 | 80 | 3 | 0.0001 | 1.44 | |
| 86110 | 6 | 96-100 | 5 | 126 | 6 | 0.0001 | 2.05 | |
| 80338 | 6 | - | 0.09 | 39 | 1 | - | | 0.14 |
| 579452 | 6 | 210-220 | 4 | 180 | 12 | 0.0001 | 0.46 | |
| 235246 | 6 | 116-128 | 5 | 123 | 0.5 | 0.0001 | 0.56 | |
| 669830 | 6 | - | 0.5 | 56 | 1 | - | | 0.55 |
| 457607 | 6 | 150-160 | 1 | 51 | 15 | 0.01 | 0.41 | |
| 87302 | 6 | - | 0.5 | 12 | 2 | - | | 2.55 |
| 80266 | 6 | - | 3 | 10 | 8 | - | | 18.38 |
| 412092 | 6 | 28-32 | 2 | 26 | 4 | 0.001 | 4.06 | |
| | | | Number of Wells | | | | 10 | 4 |
| | | | Arthrometric Mean | | | | 2.90 | 5.41 |
| | | | Arthrometric Mean Combined | | | | 3.61 | |
| | | | Geometric Mean | | | | 1.80 | 1.38 |
| | | | Geometric Mean Combined | | | | 1.67 | |

gpm= gallons per minute

| Till and Glaciomarine Drift | | | | | | | | |
|---|---|---|---|---|---|---|---|---|
| Well ID | Diameter (in) | Screen Length (ft) | Pumping Rate (gpm) | Drawdown (ft) | Time (hr) | Storativity (0.1-0.0001) | Screened Hydraulic Conductivity (ft/day) | Open End Hydraulic Conductivity (ft/day) |
| 77084 | 6 | 38-43 | 4.5 | 25 | 6 | 0.0001 | 8.35 | |
| 78010 | 6 | 82-92 | 6 | 22 | 6 | 0.01 | 4.43 | |
| 235249 | 6 | 21-26 | 10 | 17 | 1 | 0.01 | 17.04 | |
| 87632 | 6 | 33-38 | 12 | 18 | 2 | 0.01 | 21.17 | |
| 441234 | 6 | 67.5-72.5 | 1.5 | 7 | 1 | 0.001 | 7.15 | |
| 814463 | 6 | 99-102 | 5 | 16 | 2 | 0.001 | 19.25 | |
| 481861 | 6 | 52-56 | 1.5 | 26 | 8 | 0.0001 | 3.14 | |
| 1940179 | 6 | 47-51 | 3 | 36 | 3 | 0.001 | 3.53 | |
| 83284 | 6 | 60-69 | 15 | 20 | 6 | 0.0001 | 21.27 | |
| 84086 | 6 | 55-60 | 7.6 | 31.04 | 4 | 0.001 | 9.42 | |
| 315145 | 6 | 60-70 | 1 | 7.5 | 4 | 0.001 | 2.43 | |
| 86919 | 6 | 64-66 | 10 | 82 | .75 | 0.001 | 9.29 | |
| 86168 | 6 | 95-100 | 12 | 1 | 8 | 0.0001 | 731.61 | |
| 1571080 | 6 | 36-41 | 9 | 35 | 1 | 0.001 | 8.74 | |
| 372361 | 6 | 82-87 | 6.5 | 32 | 1.5 | 0.001 | 7.02 | |
| 86172 | 6 | 27-37 | 12 | 30 | 1 | 0.0001 | 8.62 | |
| 79460 | 6 | - | 17 | 7 | 1 | | | 148.81 |
| 86915 | 6 | 33-38 | 1 | 36 | 6 | 0.001 | 0.90 | |
| 87649 | 6 | 18-22.5 | 0.38 | 7.2 | 2 | 0.001 | 1.81 | |
| 86923 | 6 | - | 10 | 80 | .67 | | | 7.66 |
| 82972 | 6 | 108-118 | 5 | 35 | 8 | 0.001 | 2.78 | |
| | | | Number of Wells | | | | 19 | 2 |
| | | | Arthrometric Mean | | | | 46.73 | 78.23 |
| | | | Arthrometric Mean Combined | | | | 49.73 | |

| | | |
|---|---|---|
| Geometric Mean | 8.05 | 33.76 |
| Geometric Mean Combined | 9.22 | |

| Advance Glacial Outwash (Westside) | | | | | | | | |
|---|---|---|---|---|---|---|---|---|
| Well ID | Diameter (in) | Screen Length (ft) | Pumping Rate (gpm) | Drawdown (ft) | Time (hr) | Storativity (0.1-0.0001) | Screened Hydraulic Conductivity (ft/day) | Open End Hydraulic Conductivity (ft/day) |
| 304025 | 6 | 18-20 | 8 | 11 | 2 | 0.001 | 58.28 | |
| 377643 | 6 | 28-33 | 4 | 5 | 2 | 0.01 | 25.91 | |
| 792802 | 6 | 40-42 | 1 | 1.89 | 24 | 0.001 | 62.05 | |
| 530984 | 6 | 39-44 | 18 | 18 | 1 | 0.001 | 38.52 | |
| 357499 | 6 | 42-47 | 15 | 14 | 2 | 0.001 | 43.99 | |
| 315205 | 6 | 32-37 | 18 | 20 | 2 | 0.01 | 29.50 | |
| 315206 | 6 | 41-49 | 3.75 | 3 | 2 | 0.01 | 26.47 | |
| | | | Number of Wells | | | | 7 | - |
| | | | Arthrometric Mean | | | | 40.67 | - |
| | | | Arthrometric Mean Combined | | | | 40.67 | |
| | | | Geometric Mean | | | | 38.44 | - |
| | | | Geometric Mean Combined | | | | 38.44 | |

| Well ID | Diameter (in) | Screen Length (ft) | Pumping Rate (gpm) | Glaciolacustrine<br>Drawdown (ft) | Time (hr) | Storativity (0.1-0.0001) | Screened Hydraulic Conductivity (ft/day) | Open End Hydraulic Conductivity (ft/day) |
|---|---|---|---|---|---|---|---|---|
| 457606 | 6 | 70-80 | 5 | 26 | 9 | 0.001 | 3.88 | |
| 457608 | 6 | 70-75 | 7 | 29 | 1 | 0.0001 | 10.00 | |
| 481865 | 6 | 314-319 | 10 | 260 | 1 | 0.001 | 1.06 | |
| 514404 | 6 | 78-83 | 14 | 9 | 0.5 | 0.001 | 58.62 | |
| 452816 | 6 | 74-79 | 15 | 50 | 2 | 0.001 | 11.05 | |
| 452818 | 6 | 112-117 | 20 | 40 | 3 | 0.001 | 19.94 | |
| 452820 | 6 | 153-158 | 18 | 90 | 2 | 0.001 | 7.09 | |
| 1972918 | 6 | 188-199 | 16 | 118 | 1.5 | 0.001 | 2.05 | |
| 315149 | 6 | - | 4.5 | 32 | 4 | - | | 8.62 |
| 75309 | 6 | 90-95 | 18 | 22.5 | 2 | 0.01 | 25.90 | |
| 315146 | 6 | 89-94 | 12 | 17 | 4 | 0.001 | 29.62 | |
| 315148 | 6 | 102-97 | 2 | 24 | 4 | 0.001 | 2.90 | |
| 84084 | 6 | 110-115 | 15.5 | 63.8 | 4.5 | 0.001 | 9.43 | |
| 84085 | 6 | 205-210 | 15 | 80 | 5 | 0.001 | 7.18 | |
| 84083 | 6 | 142-147 | 6.5 | 33.25 | 4.5 | 0.001 | 7.45 | |
| 85455 | 8 | 328-336 | 50 | 222.5 | 18 | 0.001 | 5.79 | |
| | | | Number of Wells | | | | 15 | 1 |
| | | | Arthrometric Mean | | | | 13.46 | 8.62 |
| | | | Arthrometric Mean Combined | | | | 10.03 | |
| | | | Geometric Mean | | | | 8.19 | 8.62 |
| | | | Geometric Mean Combined | | | | 8.22 | |

| Advance Glacial Outwash (east side) | | | | | | | | |
|---|---|---|---|---|---|---|---|---|
| Well ID | Diameter (in) | Screen Length (ft) | Pumping Rate (gpm) | Drawdown (ft) | Time (hr) | Storativity (0.1-0.0001) | Screened Hydraulic Conductivity (ft/day) | Open End Hydraulic Conductivity (ft/day) |
| 373546 | 6 | - | 12 | 6 | 2 | | | 122.55 |
| 84572 | 6 | - | 126 | 17.5 | 6 | | | 441.18 |
| 84548 | 6 | 15 | 75 | 3.75 | 4 | 0.001 | 352.81 | |
| Number of Wells | | | | | | | 1 | 2 |
| Arthrometric Mean | | | | | | | 352.81 | 281.86 |
| Arthrometric Mean Combined | | | | | | | 90.67 | |
| Geometric Mean | | | | | | | 352.81 | 232.52 |
| Geometric Mean Combined | | | | | | | 267.19 | |

| Alluvium west of Hamilton | | | | | | | | |
|---|---|---|---|---|---|---|---|---|
| Well ID | Diameter (in) | Screen Length (ft) | Pumping Rate (gpm) | Drawdown (ft) | Time (hr) | Storativity (0.1-0.0001) | Screened Hydraulic Conductivity (ft/day) | Open End Hydraulic Conductivity (ft/day) |
| 87736 | 6 | 33-38 | 18 | 3 | 2 | 0.1 | 188.40 | |
| 80731 | 6 | 25-30 | 10 | 6 | 2 | 0.01 | 58.08 | |
| 84075 | 6 | 45-50 | 25 | 1 | 2 | 0.01 | 1096.27 | |
| 760446 | 6 | no | 50 | 15 | 2 | | | 204.25 |
| 87283 | 6 | | 10 | 3 | 2 | | | 204.25 |
| 1661863 | 6 | 32-37 | 15 | 0.4 | 1.5 | 0.1 | 1372.64 | |
| 451887 | 6 | 52-57 | 12 | 0.15 | 2 | 0.001 | 4413.79 | |
| Number of Wells | | | | | | | 5 | 2 |
| Arthrometric Mean | | | | | | | 1425.84 | 204.25 |
| Arthrometric Mean Combined | | | | | | | 1076.81 | |
| Geometric Mean | | | | | | | 591.95 | 204.25 |
| Geometric Mean Combined | | | | | | | 436.77 | |

| Well ID | Diameter (in) | Screen Length (ft) | Pumping Rate (gpm) | Lahar Drawdown (ft) | Time (hr) | Storativity (0.1-0.0001) | Screened Hydraulic Conductivity (ft/day) | Open End Hydraulic Conductivity (ft/day) |
|---|---|---|---|---|---|---|---|---|
| 1682014 | 6 | 21-26 | 16 | 0.5 | 1 | 0.01 | 1356.12 | |
| 74391 | 6 | 28-33 | 14 | 8 | 1 | 0.01 | 57.19 | |
| 315150 | 6 | - | 10 | 3 | 2 | | | 204.25 |
| 463265 | 6 | 33-38 | 20 | 1 | 1 | 0.01 | 816.49 | |
| 760535 | 6 | - | 10 | 1 | 2 | | | 612.74 |
| 760475 | 6 | - | 10 | 1 | 2 | | | 612.74 |
| 86838 | 6 | - | 10 | 1 | 2 | | | 612.74 |
| 1940032 | 6 | 32-37 | 17 | 0.5 | 1 | 0.1 | 1187.17 | |
| 462712 | 6 | 48-58 | 40 | 1 | 1 | 0.001 | 1013.28 | |
| 81379 | 6 | - | 20 | 2 | 1 | | | 612.74 |
| 190220 | 6 | - | 10 | 2 | 2 | | | 306.37 |
| 86510 | 6 | 33-38 | 15 | 3 | 0.5 | 0.01 | 169.41 | |
| 837460 | 6 | 33-38 | 15 | 10 | 1 | 0.001 | 59.81 | |
| 235252 | 6 | | 10 | 6 | 2 | | | 102.12 |
| 335374 | 6 | - | 60 | 4 | 2 | | | 919.12 |
| 351444 | 8 | screen? | 80 | 3 | 1 | 0.001 | 904.00 | |
| 430325 | 6 | - | 75 | 3 | 2 | | | 1531.86 |
| 303897 | 6 | 32-37 | 20 | 1 | 1.5 | 0.01 | 843.31 | |
| 450955 | 6 | 32-37 | 30 | 2 | 1 | 0.001 | 711.88 | |
| 441240 | 6 | 49-54 | 20 | 2 | 1 | 0.001 | 461.30 | |
| 1681981 | 6 | 33-38 | 17 | 1 | 1 | 0.001 | 813.77 | |
| 1025473 | 6 | 32-37 | 18 | 3 | 1 | 0.001 | 266.71 | |

| | | | | | | | | | |
|---|---|---|---|---|---|---|---|---|---|
| 892569 | 6 | 32-37 | 13 | 0.5 | 1 | 0.01 | 1084.01 | | |
| 2120755 | 6 | 33-38 | 16.5 | 0.3 | 1 | 0.01 | 2429.05 | | |
| | | | Number of Wells | | | | 15 | | 9 |
| | | | Arthrometric Mean | | | | 811.57 | | 612.74 |
| | | | Arthrometric Mean Combined | | | | | 737.01 | |
| | | | Geometric Mean | | | | 544.76 | | 476.58 |
| | | | Geometric Mean Combined | | | | | 518.12 | |

| Alluvial Fan | | | | | | | | |
|---|---|---|---|---|---|---|---|---|
| Well ID | Diameter (in) | Screen Length (ft) | Pumping Rate (gpm) | Drawdown (ft) | Time (hr) | Storativity (0.1-0.0001) | Screened Hydraulic Conductivity (ft/day) | Open End Hydraulic Conductivity (ft/day) |
| 79732 | 6 | 55-60 | 10 | 2 | 1 | 0.001 | 219.25 | |
| 482978 | 6 | 49-54 | 17 | 12 | 1.5 | 0.01 | 47.22 | |
| 86174 | 6 | 29-34 | 12 | 2.5 | 8 | 0.01 | 206.31 | |
| 392159 | 6 | 33.2-38.2 | 7.9 | 0.5 | 0.5 | 0.001 | 716.62 | |
| 385654 | 6 | - | 10 | 1.5 | 6 | | | 408.50 |
| 346680 | 6 | - | 10 | 3 | 2 | | | 204.25 |
| 424813 | 6 | 32-38 | 15 | 0.48 | 1 | 0.001 | 1298.40 | |
| | | Number of Wells | | | | | 5 | 2 |
| | | Arthrometric Mean | | | | | 497.56 | 306.37 |
| | | Arthrometric Mean Combined | | | | | 442.94 | |
| | | Geometric Mean | | | | | 288.18 | 288.85 |
| | | Geometric Mean Combined | | | | | 288.37 | |

| Alluvium between Alder and Muddy | | | | | | | | |
|---|---|---|---|---|---|---|---|---|
| Well ID | Diameter (in) | Screen Length (ft) | Pumping Rate (gpm) | Drawdown (ft) | Time (hr) | Storativity (0.1-0.0001) | Closed Hydraulic Conductivity (ft/day) | Open Hydraulic Conductivity (ft/day) |
| 1007517 | 6 | 33-37 | 15 | 1.5 | 1 | 0.01 | 481.54 | |
| 351464 | 8? | 34-39 | 100 | 4 | 4 | 0.1 | 915.09 | |
| 285103 | 8 | | 24 | 3 | 6 | | | 367.65 |
| 87281 | 6 | - | 20 | 1 | 2 | | | 1225.49 |
| 235497 | 6 | - | 20 | 4 | 2 | | | 306.37 |
| 80051 | 6 | - | 45 | 3 | 1 | | | 919.12 |
| 304027 | 6 | - | 10 | 7.5 | 2 | | | 81.70 |
| 760506 | 6 | - | 20 | 3 | 2 | | | 408.50 |
| 83196 | 6 | - | 20 | 3.5 | 2 | | | 350.14 |
| 351489 | 8 | - | 108 | 1.7 | 3 | | | 2919.55 |
| | | | Number of Wells | | | | 2 | 8 |
| | | | Arthrometric Mean | | | | 698.31 | 822.31 |
| | | | Arthrometric Mean Combined | | | | 797.51 | |
| | | | Geometric Mean | | | | 663.81 | 506.45 |
| | | | Geometric Mean Combined | | | | 568.73 | |

| Alluvium Between Alder and Grandy | | | | | | | | |
|---|---|---|---|---|---|---|---|---|
| Well ID | Diameter (in) | Screen Length (ft) | Pumping Rate (gpm) | Drawdown (ft) | Time (hr) | Storativity (0.1-0.0001) | Hydraulic Conductivity (ft/day) | Open Interval Conductivity (ft/day) |
| 441246 | 6 | 71-76 | 20 | 0.5 | 1 | 0.001 | 2026.56 | |
| 450951 | 6 | 176-181 | 20 | 32 | 4.5 | 0.001 | 26.22 | |
| 86846 | 6 | - | 10 | 2 | 3 | | | 306.37 |
| 2140884 | 6 | 53-57 | 15 | 6.5 | 1 | 0.01 | 96.96 | |
| 76291 | 6 | - | 7 | 20 | 2 | | | 21.45 |
| 561270 | 6 | 53-58 | 17.5 | 1.25 | 4 | 0.1 | 512.24 | |
| 304036 | 6 | - | 30 | 7 | 2 | | | 262.60 |
| 87698 | 6 | - | 40 | 21 | 2 | | | 116.71 |
| 76795 | 6 | 50-55 | 10 | 5 | 3 | 0.001 | 88.90 | |
| 87279 | 6 | - | 10 | 2.5 | 2 | | | 245.10 |
| 87280 | 6 | - | 10 | 2 | 2 | | | 306.37 |
| 304038 | 6 | - | 20 | 8 | 2 | | | 153.19 |
| 701796 | 6 | - | 30 | 3 | 2 | | | 612.74 |
| 256216 | 6 | - | 20 | 2 | 2 | | | 612.74 |
| 285271 | 6 | - | 20 | 1.1 | 2 | | | 1114.08 |
| 2184513 | 6 | 53-58 | 15 | 4 | 1 | 0.01 | 132.17 | |
| 2184524 | 6 | 53-58 | 15 | 11 | 1 | 0.01 | 43.41 | |
| 2184550 | 6 | 52-57 | 15 | 5.3 | 1 | 0.01 | 97.08 | |
| 304033 | 6 | - | 30 | 6 | 2 | | | 306.37 |
| 235259 | 6 | 55-60 | 10 | 10 | 2 | 0.01 | 33.13 | |
| 349582 | 6 | 152.1-155.1 | 15 | 3.7 | 2 | 0.01 | 255.57 | |

| | | | | | | | | | |
|---|---|---|---|---|---|---|---|---|---|
| 304037 | 6 | - | 30 | 11 | 1 | | | | 167.11 |
| 315163 | 6 | - | 10 | 3.5 | 2 | | | | 175.07 |
| 2142364 | 6 | 52.5-57.5 | 9 | 1 | 1 | 0.01 | 343.55 | | |
| 79913 | 6 | - | 10 | 1 | 2 | | | | 612.74 |
| 342228 | 6 | - | 26 | 3 | 2 | | | | 531.05 |
| 87049 | 6 | - | 10 | 3 | 2 | | | | 204.25 |
| 87298 | 6 | - | 10 | 1.5 | 2 | | | | 408.50 |
| 403191 | 6 | - | 15 | 7 | 2 | | | | 131.30 |
| 342844 | 6 | - | 10 | 8 | 2 | | | | 76.59 |
| 81039 | 6 | - | 70 | 20 | 2 | | | | 214.46 |
| 414241 | 6 | - | 10 | 1 | 1 | | | | 612.74 |
| 83571 | 6 | - | 10 | 7.5 | 3 | | | | 81.70 |
| 760515 | 6 | - | 25 | 4 | 2 | | | | 382.97 |
| 1972916 | 6 | 72-77 | 18.6 | 5.7 | 1 | 0.01 | 113.49 | | |
| | | | | | | 0.001 | 2.16 | | |
| 84560 | 8 | 141-150 | 12 | 105 | 4 | | | | |
| 796585 | 6 | 53-58 | 16 | 15.5 | 1 | 0.1 | 23.66 | | |
| 800269 | 6 | - | 15 | 0.7 | 1 | | | | 1313.02 |
| 87268 | 6 | - | 10 | 6 | 2 | | | | 102.12 |
| 472381 | 6 | 53-58 | 32 | 14 | 1 | 0.01 | 76.76 | | |
| | | Number of Wells | | | | | 15 | | 25 |
| | | Arthrometric Mean | | | | | 258.12 | | 362.85 |
| | | Arthrometric Mean Combined | | | | | | 328.97 | |
| | | Geometric Mean | | | | | 88.82 | | 253.90 |
| | | Geometric Mean Combined | | | | | | 171.24 | |

| Alluvium east of Grandy Creek | | | | | | | | |
|---|---|---|---|---|---|---|---|---|
| Well ID | Diameter (in) | Screen Length (ft) | Pumping Rate (gpm) | Drawdown (ft) | Time (hr) | Storativity (0.1-0.0001) | Closed Hydraulic Conductivity (ft/day) | Open Hydraulic Conductivity (ft/day) |
| 343745 | 8 | - | 30 | 4 | 2 | | | 344.67 |
| 342211 | 6 | - | 10 | 2 | 2 | | | 306.37 |
| 87029 | 6 | - | 30 | 4 | 3 | | | 459.56 |
| 304034 | 8 | - | 10 | 1.5 | 2.5 | | | 306.37 |
| 379471 | 6 | - | 30 | 15 | 1 | | | 122.55 |
| 87036 | 6 | 325 tto 335 | 15 | 2.6 | 1 | 0.001 | 127.852 | |
| 86856 | 6 | - | 20 | 7 | 2 | | | 175.07 |
| 235257 | 6 | - | 10 | 4.5 | 2 | | | 136.17 |
| 256082 | 6 | - | 15 | 3.5 | 2 | | | 262.6 |
| 256083 | 6 | - | 10 | 7 | 2 | | | 87.535 |
| 256215 | 6 | 39-44 | 10 | 3 | 1 | 0.01 | 116.167 | |
| 338588 | 6 | - | 3 | 8 | 4 | | | 22.978 |
| 407118 | 6 | - | 10 | 6 | 2 | | | 102.12 |
| 407119 | 6 | - | 50 | 6 | 1 | | | 510.62 |
| 79178 | 6 | 121-126 | 60 | 6 | 3 | 0.01 | 421.65 | |
| 386468 | 6 | - | 20 | 10 | 2 | | | 122.55 |
| 79305 | 6 | - | 12 | 2.5 | 4 | | | 294.12 |
| 79397 | 6 | 73-78 | 15 | 0.85 | 1 | 0.001 | 846.89 | |
| 315214 | 6 | 33-38 | 10 | 0.25 | 1 | 0.01 | 1724.51 | |
| 453436 | 6 | 72-77 | 20 | 1 | 4 | 0.001 | 1058.42 | |
| 368654 | 6 | - | 22 | 2.5 | 2 | | | 539.22 |

| | | | | | | | | |
|---|---|---|---|---|---|---|---|---|
| 81007 | 6 | - | 10 | 2 | 1 | | | 306.37 |
| 625200 | 6 | 32.5-37.5 | 30 | 0.5 | 1 | 0.001 | 3119.11 | |
| 304032 | 6 | - | 10 | 3.5 | 1.5 | | | 175.07 |
| 116585 | 6 | - | 10 | 3 | 6 | | | 204.25 |
| 86976 | 6 | - | 30 | 6 | 2 | | | 306.37 |
| 83474 | 6 | - | 15 | 1.5 | 1 | | | 612.74 |
| 87282 | 6 | - | 10 | 1 | 2 | | | 612.74 |
| 87294 | 6 | - | 10 | 7 | 2 | | | 87.535 |
| 87262 | 6 | - | 10 | 7 | 4 | | | 87.535 |
| 315209 | 6 | - | 14 | 4.5 | 2 | | | 190.63 |
| 87026 | 6 | - | 10 | 3 | 1 | | | 204.25 |
| 85793 | 6 | - | 10 | 3 | 5 | | | 204.25 |
| 86864 | 6 | - | 10 | 3 | 2 | | | 204.25 |
| 87303 | 6 | - | 10 | 4 | 2 | | | 153.19 |
| 190568 | 6 | 53-58 | 20 | 0.25 | 1 | 0.01 | 3631.74 | |
| 190569 | 6 | 52.9-57.9 | 20 | 0.3 | 1 | 0.01 | 2986.5 | |
| | | Number of Wells | | | | | 9 | 28 |
| | | Arthrometric Mean | | | | | 1559.20 | 255.06 |
| | | Arthrometric Mean Combined | | | | | 572.28 | |
| | | Geometric Mean | | | | | 883.35 | 205.30 |
| | | Geometric Mean Combined | | | | | 292.79 | |

| Well ID | Diameter (in) | Screen Length (ft) | Pumping Rate (gpm) | Hamilton Alluvium<br>Drawdown (ft) | Time (hr) | Storativity (0.1-0.0001) | Closed Hydraulic Conductivity (ft/day) | Open Hydraulic Conductivity (ft/day) |
|---|---|---|---|---|---|---|---|---|
| 504757 | 6 | 32-37 | 15 | 0.5 | 1 | 0.01 | 1264.97 | |
| 982843 | 6 | 29-34 | 18 | 4 | 1 | 0.01 | 161.36 | |
| 1955145 | 6 | 36.5-41.5 | 18 | 0.2 | 1 | 0.01 | 4120.53 | |
| 190222 | 6 | - | 10 | 3 | 2 | | | 204.25 |
| 2120021 | 6 | 32-37 | 15 | 2 | 1 | 0.1 | 223.50 | |
| 1055237 | 6 | 32-37 | 16 | 0.5 | 1 | 0.01 | 1356.12 | |
| 246996 | 6 | 52-57 | 30 | 3 | 1 | 0.001 | 461.30 | |
| 1029542 | 6 | 23-28 | 14 | 0.5 | 1 | 0.01 | 1174.25 | |
| 407257 | 6 | 69-74 | 16 | 2 | 1 | 0.001 | 363.17 | |
| 372701 | 6 | - | 10 | 4.5 | 2 | | | 136.17 |
| 79398 | 6 | 32-37 | 15 | 0.5 | 1.5 | 0.001 | 1531.44 | |
| 342212 | 6 | - | 10 | 2 | 2 | | | 306.37 |
| | | Number of Wells | | | | | 9 | 3 |
| | | Arthrometric Mean | | | | | 1184.07 | 215.60 |
| | | Arthrometric Mean Combined | | | | | 941.95 | |
| | | Geometric Mean | | | | | 751.88 | 204.25 |
| | | Geometric Mean Combined | | | | | 542.82 | |

# Appendix C: 310-foot Well Log

CANYON ENVIRONMENTAL GROUP

## GROUNDWATER LOG BH01 GW

| | | |
|---|---|---|
| **PROJECT NUMBER** C2022013_HDR_SR_GW | **Drilling Date** 3/28/2023 - 3/30/2023 | **COORDINATES** 48.53469, -121.94020 |
| **PROJECT NAME** Skagit River Basin GW Study | **Total Depth** 310-feet | **COORD SYS** NAD83 (HARN) |
| **CLIENT** WSU-WDOE & HDR Inc. | **Depth To Water** 135.06-feet | **COMPLETION** Casing Installed on 3/31/2023 |
| **DRILLER** Holt Drilling | **CASING** Schedule 80 PVC (2" diameter) | **SURFACE ELEVATION** 300-ft NAVD88 |
| **DRILLING EQUIPMENT** Sonic (1200 PS5A64) | **SCREEN** 0.010 | **WDOE Unique Tag** BPW070 |

**COMMENTS** On the southern side of a corner on the DNR Rd ~1.28 miles from gate at the end of Ohara Road, Hamilton WA.

**LOGGED BY** Jeff Ninnemann, LHG
**CHECKED BY** Ryan Cooper

| Soil Samples | Core Interval | Moisture | Depth (ft) | USCS | Material Description | Well Diagram | Elevation (ft) |
|---|---|---|---|---|---|---|---|
| | #1 | Dry | 0 | OL | Organic SILTS, some Fine to Coarse Sands and Fine Gravels, light brown to dark brown, dry, loose, roots, no odor/weathering top soil. | concrete seal | |
| | | Dry | 1 | SW-SM | Silty Fine to Medium SAND with Fine to Coarse Gravel, light brown, dry, loose, roots, no odor/weathering | | 299 |
| | | Dry | 2.5 | SP | Fine SAND with Fine Gravel, light brown to greenish grey, dry, loose, no organics/odor/weathering | | 298 |
| | #2 | | 5 | | | | 295 |
| | | Dry | 6 | GW -GM | Fine to Coarse Sandy Silty Fine to Coarse GRAVEL, light brown to dark brown, dry, loose, no organics/odor, some redoximorphic (redox) features, cobble. | backfill (quick grout) | 294 |
| | | Dry | 9 | SW | Fine to Coarse SAND with Fine Gravels, olive grey, moist, loose, no organics/odor/weathering. | | 291 |
| | #3 | Dry | 10 | SP | Clean Fine to Medium SAND, olive grey, dry, loose, no organics/odor/weathering. Grading from fine to medium clean sand than back to fine sand. | | 290 |
| | | Dry | 12 | GW | Fine to Medium Sandy Fine to Coarse GRAVEL, light grey to reddish tan, dry, loose, no organics/odor, some weathering (redox). | | 288 |
| | | | 15 | | | | 285 |

Depth scale (ft): 1, 2, 3, 4, 5, 6, 7, 8, 9, 10, 11, 12, 13, 14, 15

Elevation scale (ft): 299, 298, 297, 296, 295, 294, 293, 292, 291, 290, 289, 288, 287, 286, 285

**Disclaimer** This bore log is intended for environmental not geotechnical purposes.

Page 1 of 18

produced by ESlog.ESdat.net on 19 Apr 2023

CANYON ENVIRONMENTAL GROUP

## GROUNDWATER LOG BH01 GW

| Soil Samples | Core Interval | % Recovery | Moisture | Depth (ft) | Graphic Log | USCS | Material Description | Well Diagram | Elevation (ft) |
|---|---|---|---|---|---|---|---|---|---|
| | | | | 16 | | | | | 284 |
| SRGW SS#1 | | | Dry<br>M<br>W | 17<br>18<br>19 | | SW | Fine to Coarse Gravelly Fine to Coarse SAND with Cobbles, olive grey to tan, dry to moist, loose, no organics/odor, some weathering (redox), moist @18-ft, wet @ 18.9-ft. | | 283<br>282<br>281 |
| | #4 | | W | 20 | | ML | SILT with Fine Sands, tan to yellowish orange, wet, medium stiff, Pocket Penetrometer (PP)=0.5-ton/sqft, no organics/odor/weathering. | | 280 |
| | | | W | 21<br>22<br>23<br>24<br>25<br>26 | | SM/ML | Silty Fine SAND to Sandy SILT, tan to yellowish orange, wet, medium stiff (PP=0.75-ton/sqft), no organics/odor/weathering, silt content variable throughout layer. | backfill (quick grout) | 279<br>278<br>277<br>276<br>275<br>274 |
| | | | Dry -M | 27 | | CL | Lean CLAY, tan, dry to moist, medium stiff (PP=0.9-ton/sqft), no organics/odor/weathering. | | 273 |
| | | | Dry | 28<br>29 | | SP | Fine SAND with clasts of clay/silt (2-4" chucks), tan to olive grey, dry, loose, no organics/odor/weathering. | | 272<br>271 |
| | #5 | | W | 30<br>31<br>32 | | SP -SM | Silty Fine SAND, tan to light brown, wet, loose, no organics/odor/weathering,<br><br>Perched groundwater from 30.5 to 32.8-feet. | | 270<br>269<br>268 |

**Disclaimer** This bore log is intended for environmental not geotechnical purposes.



produced by ESlog.ESdat.net on 19 Apr 2023

# GROUNDWATER LOG BH01 GW

CANYON ENVIRONMENTAL GROUP

| Soil Samples | Core Interval | % Recovery | Moisture | Depth (ft) | Graphic Log | USCS | Material Description | Well Diagram | Elevation (ft) |
|---|---|---|---|---|---|---|---|---|---|
| | | | Dry | 33–35 | | SP-SM | Silty Fine SAND with Fine to Coarse Gravel, tan to light brown, dry, dense very compact/cemented, no organics/odor/weathering. | | 267–265 |
| | | | Dry | 35–39.5 | | SP -SM | Silty Fine SAND with Fine to Coarse Gravel, tan to light brown, dry, loose, no organics/odor/weathering. | | 265–260.5 |
| | #6 | | Dry | 39.5–41 | | SP -SM | Silty Fine SAND with Fine to Coarse Gravel, tan to light brown, dry, medium dense, no organics/odor/weathering. | | 260.5–259 |
| | | | Dry | 41–43.25 | | SP | Fine SAND with Trace Silts, tan to light grey, dry, loose, no organics/odor/weathering. | backfill (quick grout) | 259–256.75 |
| | | | Dry | 43.25–47.75 | | GW /SW | Fine to Coarse Sandy Fine to Coarse GRAVEL, (gravel clasts are sub-rounded) tan to light grey, dry, loose, no organics/odor/weathering.<br>@ 46-ft some moisture and redox weathering. | | 256.75–252.25 |
| | #7 | | Dry | 47.75–51 | | GW /SW | Fine to Coarse Sandy Fine to Coarse GRAVEL, (gravel clasts are sub-angular possibly broken from sonic drilling), light grey to whitish, dry, likely cemented before sonic drilling, no organics/odor/weathering. | | 252.25–249 |

**Disclaimer** This bore log is intended for environmental not geotechnical purposes.

produced by ESlog.ESdat.net on 19 Apr 2023

**GROUNDWATER LOG** BH01 GW

CANYON ENVIRONMENTAL GROUP

| Soil Samples | Core Interval | % Recovery | Moisture | Depth (ft) | Graphic Log | USCS | Material Description | Well Diagram | Elevation (ft) |
|---|---|---|---|---|---|---|---|---|---|
| | | | Dry -M | 51–55 | | SP -SM | Fine Gravelly, Silty, Fine SAND, (gravel clasts are sub-rounded) tan to light grey, dry to moist, loose to medium dense, no organics/odor/weathering. Silts content increases to 25%-30% than decrease again to less than 5%. | | 249–245 |
| | | | Dry | 55 | | SP -SM | Fine Gravelly Fine SAND with silts, (gravel clasts are sub-rounded) tan to light grey, dry, dense, no organics/odor/weathering. | | 245 |
| SRGW SS#2 | | | Dry | 56–60 | | SP | Fine Gravelly Fine SAND with silts, (gravel clasts are sub-rounded) tan to light grey, dry, loose, no organics/odor/weathering. | | 244–240 |
| | #8 | | Dry | 60–68 | | SP | Fine Gravelly Fine SAND with silts, (gravel clasts are sub-rounded/sub-angular) tan to light grey, dry, loose, no organics/odor/weathering.<br>Cobble @ 66-ft. | backfill (quick grout) | 240–232 |
| | | | Dry | 68 | | SP | Fine Gravelly Fine SAND with silts, (gravel clasts are sub-rounded/sub-angular) tan to light grey, dry, dense, no organics/odor/weathering. | | 232 |

**Disclaimer** This bore log is intended for environmental not geotechnical purposes.

produced by ESlog.ESdat.net on 19 Apr 2023

CANYON
ENVIRONMENTAL GROUP

# GROUNDWATER LOG BH01 GW

| Soil Samples | Core Interval | % Recovery | Moisture | Depth (ft) | Graphic Log | USCS | Material Description | Well Diagram | Elevation (ft) |
|---|---|---|---|---|---|---|---|---|---|
| | | | | 69 | | | | | 231 |
| | #9 | | | 70 | | | | | 230 |
| | | | | 71 | | | | | 229 |
| | | | Dry | 72 | | SW /GP | Fine Gravelly Fine to Coarse SAND, (gravel clasts are sub-rounded) tan to light grey, dry, loose, no organics/odor/weathering. | | 228 |
| | | | | 73 | | | | | 227 |
| | | | | 74 | | | | | 226 |
| | | | | 75 | | | | | 225 |
| | | | | 76 | | | | | 224 |
| | | | | 77 | | | | | 223 |
| | | | | 78 | | | | backfill (quick grout) | 222 |
| | | | | 79 | | | @ 79.5 to 80.5 (Start of new day and top of sample contained sluff. Collapse from previous night may have disrupted the sequence. Difficulty with drilling due to density. | | 221 |
| | #10 | | | 80 | | | | | 220 |
| | | | Dry | 81 | | GW /SP | Coarse Sandy Fine to Coarse GRAVEL with Silts, (gravel clasts are sub-rounded/sub-angular) whitish to light grey, dry, cemented, no organics/odor/weathering. | | 219 |
| | | | | 82 | | | Cobbles at 82.5-ft | | 218 |
| | | | | 83 | | | Increasing fines with depth. | | 217 |
| | | | | 84 | | | Grades into: | | 216 |
| | | | | 85 | | SW -SM | Fine to Coarse Gravelly Silty Fine to Coarse SAND, (gravel clasts are sub-rounded/sub-angular) whitish to light grey, dry, cemented, no organics/odor/weathering. | | 215 |
| | | | | 86 | | | | | 214 |
| | | | M | | | | | | |

**Disclaimer** This bore log is intended for environmental not geotechnical purposes.

produced by ESlog.ESdat.net on 19 Apr 2023

CANYON ENVIRONMENTAL GROUP

# GROUNDWATER LOG BH01 GW

| Depth (ft) | Core Interval | Moisture | USCS | Material Description | Elevation (ft) |
|---|---|---|---|---|---|
| 87 | | | SW -SM | Fine to Coarse Gravelly Silty Fine to Coarse SAND, (gravel clasts are sub-rounded/sub-angular), whitish to light grey, moist, loose, no organics/odor/weathering. | 213 |
| 88 | | M | GW -GM | Fine to Coarse Sandy Silty Fine to Coarse GRAVEL, (gravel clasts are sub-rounded/sub-angular) whitish to light grey, dry, cemented, no organics/odor/weathering.<br>Note: Difficulty drilling in this interval, sub-angular is likely due to breaking through hard layers.<br>Bag blew out and lost Sample 90-100-feet. Spill pile looks similar to sample above.<br>Some of the core was dropped down the borehole and re-drilled, size and stratigraphy suspect. | 212 |
| 90 | #11 | | | | 210 |
| 94 | | | SW -SM | Silty Fine to Medium SAND w Fine Gravels, (gravel clasts are sub-rounded) whitish to light grey, dry, loose, no organics/odor/weathering.<br>Lost sample | 206 |
| 99 | | M | SW -SM | Silty Fine to Coarse SAND w Fine Gravels, (gravel clasts are sub-rounded), tan to light grey, moist, dense almost cement for ~0.5-ft than loosens, no organics/odor/weathering. | 201 |
| 100 | #12 | M | GP -GM | Fine to Coarse Sandy Fine GRAVEL with Silts, (gravel clasts are sub-rounded), tan to olive grey, moist, loose to medium dense, no organics/odor/weathering. | 200 |
| 103 | | M | SP -SM | Fine SAND with Silts and Fine Gravels, (gravel clasts are sub-rounded), tan to olive grey, moist, medium dense, no organics/odor, some weathering (redox). | 197 |
| 104 | | M | SW /GW | | 196 |

Well Diagram: backfill (quick grout)

Disclaimer This bore log is intended for environmental not geotechnical purposes.

produced by ESlog.ESdat.net on 19 Apr 2023

# GROUNDWATER LOG BH01 GW

CANYON ENVIRONMENTAL GROUP

| Soil Samples | Core Interval | % Recovery | Moisture | Depth (ft) | USCS | Material Description | Well Diagram | Elevation (ft) |
|---|---|---|---|---|---|---|---|---|
| | | | | 105<br>106<br>107 | | Fine to Coarse Gravelly Fine to Coarse SAND with Cobbles, (gravel clasts are sub-rounded to sub-angular), tan to light grey, moist, medium dense/fractured clasts, no organics/odor, some weathering (redox). | | 195<br>194<br>193 |
| | | | M-D | 108<br>109 | SW-SM /GW-GM | Silty Fine to Coarse Gravelly Fine to Coarse SAND, (gravel clasts are sub-rounded), tan to light grey, moist to damp, medium dense, no organics/odor, weathered (redox).<br><br>On 3/29/2023 the depth to water was measured at 109.35-ft, however this was interpreted as not the regional groundwater table and more likely reflects a small perched saturated zone. | | 192<br>191 |
| | #17 | | D-W | 110<br>111<br>112<br>113<br>114 | SW-SM | Silty Fine to Medium SAND with Fine Gravels, (gravel clasts are sub-rounded), tan to olive grey, damp to wet, medium dense, no organics/odor, some weathering (redox). | backfill (quick grout) | 190<br>189<br>188<br>187<br>186 |
| | | | M | 115 | SW-SM | Silty Fine Gravelly Fine to Coarse SAND, (gravel clasts are sub-rounded), tan to light grey, moist, loose, no organics/odor/weathering. | | 185 |
| | #18 | | D | 116<br>117<br>118 | SW/GP | Gravelly Fine to Coarse SAND with Silts and Cobbles, (gravel clasts are sub-rounded), dark grey to olive grey, damp, medium dense, no organics/odor/weathering.<br><br>Grading to coarse sand than back to medium sand. | | 184<br>183<br>182 |
| | | | D | | SP/GP | Gravelly Medium SAND with Silts, (gravel clasts are sub-rounded),dark grey to olive grey, damp, medium dense, no organics/odor/weathering. | | |
| | | | D | 119 | SW-SM | Silty Fine to Coarse SAND with Fine Gravels, (gravel clasts are sub-rounded), dark grey to olive grey, damp, loose, no organics/odor, some weathering (redox). Embedded clasts of medium clean sand. | | 181 |
| | #19 | | | 120<br>121 | | | | 180<br>179 |
| | | | D-M | 122 | SP-SM | Medium SAND with Silts, (gravel clasts are sub-rounded), olive grey, moist to damp, loose, no | | 178 |

**Disclaimer** This bore log is intended for environmental not geotechnical purposes.



produced by ESlog.ESdat.net on 19 Apr 2023

CANYON
ENVIRONMENTAL GROUP

## GROUNDWATER LOG BH01 GW

| Soil Samples | Core Interval | % Recovery | Moisture | Depth (ft) | Graphic Log | USCS | Material Description | Well Diagram | Elevation (ft) |
|---|---|---|---|---|---|---|---|---|---|
| | | | | 123–124 | | | organics/odor/weathering. | | 177–176 |
| | | | M | 125–130 | | SW-SM /GW | Silty Fine to Coarse Gravelly Fine to Coarse SAND, (gravel clasts are sub-rounded), olive grey, moist to damp, loose, no organics/odor/weathering. | | 175–170 |
| | #20 | | M-D | 131 | | SP | Clean Medium SAND lense, olive grey, moist to damp, loose, no organics/odor/weathering. | | 169 |
| | | | M-D | 131–135 | | SW-SM /GW-GM | Silty Fine to Coarse Gravelly Fine to Coarse SAND, (gravel clasts are sub-rounded), olive grey, moist to damp, loose, no organics/odor, with some weathering (redox) in the lower portion of the unit. | backfill (quick grout) | 169–165 |
| | | | D | 135–138 | | SP/GP | Fine Gravelly Medium SAND, (gravel clasts are sub-rounded), olive grey, damp, loose, no organics/odor/weathering.<br><br>Groundwater was measure @ 135.06 on the 4/3/23, after the well had stabilized over the weekend. | | 165–162 |
| | #21 | | M | 138–140 | | GW-GM | Fine to Coarse Sandy Fine to Coarse GRAVEL with Silts, (gravel clasts are sub-rounded),olive grey, moist to wet (@141-ft, loose, no organics/odor/weathering.<br><br>Fractured cobble. | | 162–160 |

**Disclaimer** This bore log is intended for environmental not geotechnical purposes.

produced by ESlog.ESdat.net on 19 Apr 2023

## GROUNDWATER LOG BH01 GW

| Soil Samples | Core Interval | % Recovery | Moisture | Depth (ft) | Graphic Log | USCS | Material Description | Well Diagram | Elevation (ft) |
|---|---|---|---|---|---|---|---|---|---|
| | | | | 141 | | | Some weathering (redox). | | 159 |
| | | | D-W | 142 | | SP-SM | Fine to Coarse Gravelly Medium SAND with Silts, (gravel clasts are sub-rounded), olive grey, damp-wet, loose, no organics/odor, some weathering (redox). | | 158 |
| | | | | 143 | | | | | 157 |
| | | | D-W | 144 | | SP-SM | Silty Fine to Coarse Gravelly Medium to Coarse SAND, (gravel clasts are sub-rounded), olive grey, damp-wet, loose, no organics/odor, some weathering (redox). Gravel and moisture increasing around 146-ft.. | | 156 |
| | | | | 145 | | | | | 155 |
| | | | | 146 | | | | | 154 |
| | | | | 147 | | | | | 153 |
| | | | | 148 | | | | | 152 |
| | | | | 149 | | GW-GM | Medium to Coarse Sandy Fine to Coarse GRAVEL with Silts, (gravel clasts are sub-rounded), olive grey to reddish and light grey, damp to wet, loose, no organics/odor, some weathering (redox). | backfill (quick grout) | 151 |
| | #22 | | | 150 | | | | | 150 |
| | | | | 151 | | | Grading Coarser | | 149 |
| | | | | 152 | | GW-GM /SP-SM | Coarse Sandy Fine to Coarse GRAVEL with Silts, (gravel clasts are sub-rounded), olive grey to tan, wet, loose, no organics/odor, some weathered (redox). | | 148 |
| | | | W | 153 | | SP | Medium SAND with Fine Gravels (Clean), (gravel clasts are sub-rounded), light grey, wet, loose, no organics/odor/weathering. | | 147 |
| | | | D | 154 | | SP | Fine SAND (Clean), tan-olive grey, damp, loose, no organics/odor/weathering. | | 146 |
| SRGW SS#3 | | | | 155 | | | | | 145 |
| | | | | 156 | | | Layer of medium dense, damp to wet. | | 144 |
| | | | | 157 | | | | | 143 |
| | | | | 158 | | | | | 142 |

**Disclaimer** This bore log is intended for environmental not geotechnical purposes.

Page 9 of 18

produced by ESlog.ESdat.net on 19 Apr 2023

CANYON ENVIRONMENTAL GROUP

## GROUNDWATER LOG BH01 GW

| Soil Samples | Core Interval | % Recovery | Moisture | Depth (ft) | Graphic Log | USCS | Material Description | Well Diagram | Elevation (ft) |
|---|---|---|---|---|---|---|---|---|---|
| | | | | 159 | | | | | 141 |
| | #23 | | | 160 | | | | | 140 |
| | | | W | 161 | | SW-SM | Coarse Gravelly Medium to Coarse SAND with Silts, (gravel clasts are sub-rounded), light grey- olive grey, wet, loose, no organics/odor, some weathering. | | 139 |
| | | | | 162 | | | | | 138 |
| | | | | 163 | | | Grades to | | 137 |
| SRGW SS#4 | | | | 164 | | GW-GM | Medium to Coarse Sandy Fine to Coarse GRAVEL with Silts, (gravel clasts are sub-rounded), light grey- olive grey, damp to wet, loose, no organics/odor, some weathering (redox). | | 136 |
| | | | | 165 | | | | | 135 |
| | | | D | 166 | | SP-SM | Silty Coarse Gravelly Fine SAND, (gravels are sub-rounded), dark grey- olive grey, damp, medium dense, no organics/odor/weathering. (strongly gleyed layer) | | 134 |
| | | | | 167 | | | | | 133 |
| | | | D-W | 168 | | GW-GM | Medium to Coarse Sandy Fine to Coarse GRAVEL with Silts, (gravels are sub-rounded), light grey- dark grey, damp-wet, loose, no organics/odor, some weathering (redox). | backfill (quick grout) | 132 |
| | | | | 169 | | | | | 131 |
| | #24 | | | 170 | | | | | 130 |
| | | | D | 171 | | SP | Clean Medium SAND, (gravels are sub-rounded), olive grey, damp, loose, no organics/odor/ weathering. | | 129 |
| | | | D | 172 | | | | | 128 |
| | | | D | 173 | | SP | Clean Fine SAND, (gravels are sub-rounded), olive grey, damp, medium dense, no organics/odor/weathering. | | 127 |
| | | | | 174 | | | | | 126 |
| | | | D | 175 | | GP | Coarse GRAVEL with Coarse Sands and Trace Silts, (gravels are sub-rounded), light grey, damp, loose, no organics/odor/weathering. | | 125 |
| | | | | 176 | | | | | 124 |

**Disclaimer** This bore log is intended for environmental not geotechnical purposes.



produced by ESlog.ESdat.net on 19 Apr 2023

CANYON
ENVIRONMENTAL GROUP

## GROUNDWATER LOG BH01 GW

| Soil Samples | Core Interval | % Recovery | Moisture | Depth (ft) | Graphic Log | USCS | Material Description | Well Diagram | Elevation (ft) |
|---|---|---|---|---|---|---|---|---|---|

SRGW SS#5

#25

#26

D-W

Depth (ft): 177, 178, 179, 180, 181, 182, 183, 184, 185, 186, 187, 188, 189, 190, 191, 192, 193, 194

Elevation (ft): 123, 122, 121, 120, 119, 118, 117, 116, 115, 114, 113, 112, 111, 110, 109, 108, 107, 106

GW-GM /SW — Fine to Coarse Sandy Fine to Coarse GRAVEL with Silts, (gravels are sub-rounded), light grey- olive grey, damp, loose, no organics/odor, some weathering (redox).

@182.5 damp to wet

Grading into

SW/GW — Fine to Coarse Gravelly Fine to Coarse SAND with trace Silts, (gravels are sub-rounded), light grey- olive grey, wet, loose, no organics/odor/weathering.

@186.5 weathering (redox)

backfill (quick grout)

**Disclaimer** This bore log is intended for environmental not geotechnical purposes.

produced by ESlog.ESdat.net on 19 Apr 2023

CANYON ENVIRONMENTAL GROUP

# GROUNDWATER LOG BH01 GW

| Soil Samples | Core Interval | % Recovery | Moisture | Depth (ft) | Graphic Log | USCS | Material Description | Well Diagram | Elevation (ft) |
|---|---|---|---|---|---|---|---|---|---|
| | | | | 195 | | | | backfill (quick grout) | 105 |
| | | | | 196 | | | | | 104 |
| | | | W | 197 | | SW-SM | Fine to Coarse Gravelly Fine to Coarse SAND with trace Silts, (gravel clasts are sub-rounded), light grey- olive grey, wet, loose, no organics/odor/weathering. | | 103 |
| | | | | 198 | | | Decreasing fines with depth. | | 102 |
| SRGW SS#6 | | | W | 199 | | SW | Fine to Coarse Gravelly Medium to Coarse SAND with trace Silts, (gravel clasts aresub-rounded), olive grey, wet, loose, no organics/odor/weathering. | | 101 |
| | #27 | | | 200 | | | | | 100 |
| | | | | 201 | | | @201 weathering (redox) | | 99 |
| | | | | 202 | | | | | 98 |
| | | | | 203 | | | Varying medium to coarse sand quantities. Generally coarse sand with a lense of medium sand between 203-ft and 204-ft. | | 97 |
| | | | | 204 | | | | | 96 |
| | | | | 205 | | | @ 205 saturated | filter pack (12/20) | 95 |
| | | | | 206 | | | | | 94 |
| | | | | 207 | | | | | 93 |
| | | | W | 208 | | GM /ML | Silty Fine to Coarse Sandy Fine to Coarse GRAVEL, (gravel clasts are sub-rounded), olive grey, wet, medium dense/medium stiff (PP=0.5), no organics/odor, some weathering (redox). | | 92 |
| | | | | 209 | | | | | 91 |
| | | | | 210 | | | | | 90 |
| | | | | 211 | | | | | 89 |
| | #28 | | | 212 | | | | | 88 |

**Disclaimer** This bore log is intended for environmental not geotechnical purposes.



produced by ESlog.ESdat.net on 19 Apr 2023

CANYON ENVIRONMENTAL GROUP

# GROUNDWATER LOG BH01 GW

| Soil Samples | Core Interval | % Recovery | Moisture | Depth (ft) | Graphic Log | USCS | Material Description | Well Diagram | Elevation (ft) |
|---|---|---|---|---|---|---|---|---|---|
| | | | | 213 | | | | | 87 |
| | | | W | 214–220 | | SW-SM /GW-GM | Fine to Coarse Gravelly Fine to Coarse SAND with Silts, (gravel clasts are sub-rounded), greenish grey- olive grey, wet, loose, no organics/odor, some weathering (redox). | filter pack (12/20) | 86–80 |
| | | | W-D | 221–225 | | SP | Clean Fine Gravelly Medium SAND, (gravel clasts are sub-rounded), light grey, wet to damp, loose, no organics/odor/weathering. | collapsed | 79–75 |
| SRGW SS#7 | #29 | | W-D | 226–230 | | SW/GW | Clean Fine to Coarse Gravelly Fine to Coarse SAND, (gravel clasts are sub-rounded), greenish grey- olive grey, wet to damp, loose, no organics/odor/weathering.<br><br>Beds of higher sand content are inter-bedded within the layer.<br><br>@228 (bed ~0.5-ft thick)<br><br>@229.3 (bed~0.4-ft thick) | | 74–70 |

**Disclaimer** This bore log is intended for environmental not geotechnical purposes.



produced by ESlog.ESdat.net on 19 Apr 2023

## GROUNDWATER LOG BH01 GW

| Soil Samples | Core Interval | % Recovery | Moisture | Depth (ft) | USCS | Material Description | Well Diagram | Elevation (ft) |
|---|---|---|---|---|---|---|---|---|
| | | | | 231 | | Gravel content decreases and grades into a Fine to Coarse Sand. | | 69 |
| | | | W-D | 232 | SW | Clean Fine to Coarse SAND, greenish grey- olive grey, wet to damp, loose, no organics/odor/weathering. | | 68 |
| | | | | 233 | | | | 67 |
| | | | | 234 | | | | 66 |
| | | | | 235 | | | | 65 |
| | | | | 236 | | | | 64 |
| | | | | 237 | | | | 63 |
| | | | | 238 | | | | 62 |
| SRGW SS#8 | | | W | 239 | SP | Fine SAND with trace Silts, greenish grey (gleyed), wet, medium dense, no organics/odor/weathering. | collapsed | 61 |
| | #30 | | | 240 | | | | 60 |
| | | | | 241 | | Grading to | | 59 |
| | | | | 242 | SP-SM | Silty Fine SAND, greenish grey (gleyed), wet, medium dense, no organics/odor, some weathering (redox). | | 58 |
| | | | | 243 | | | | 57 |
| | | | | 244 | | | | 56 |
| | | | D-W | 245 | SP | Clean Fine Gravelly Fine to Medium SAND, (gravel clasts are sub-rounded), tan-light brown, damp-wet, loose, no organics/odor, with weathering (redox). | | 55 |
| | | | | 246 | | | | 54 |
| | | | D-W | 247 | SP/GW | Clean Fine to Coarse Gravelly Fine to Medium SAND, (gravel clasts are sub-rounded0, light grey to greenish grey, damp-wet, loose, no organics/odor, with weathering (redox). | | 53 |
| | | | D | 248 | SP | Clean Fine Gravelly Fine to Medium SAND, (gravel clasts are sub-rounded), tan-light brown, damp, loose, no organics/odor, with weathering (redox). | | 52 |

**Disclaimer** This bore log is intended for environmental not geotechnical purposes.



produced by ESlog.ESdat.net on 19 Apr 2023

CANYON ENVIRONMENTAL GROUP

# GROUNDWATER LOG BH01 GW

| Soil Samples | Core Interval | % Recovery | Moisture | Depth (ft) | Graphic Log | USCS | Material Description | Well Diagram | Elevation (ft) |
|---|---|---|---|---|---|---|---|---|---|
| | | | D | 249 – 250 | | SP/GP | Clean Fine Gravelly Fine to Medium SAND, gravel clasts are sub-rounded, light grey-greenish grey, damp, loose, no organics, with sulfuric odor and weathering (redox). | | 51 – 50 |
| | #31 | | | 250 – 255 | | SW/GW | Grading to<br>Clean Fine to Coarse Gravelly Fine to Coarse SAND, gravel clasts are sub-rounded, olive grey-greenish grey, damp, loose, no organics, with sulfuric odor and weathering (redox). | | 50 – 45 |
| | | | | 255 – 260 | | SW-SM /GW | Grading to<br>Fine Coarse Gravelly Fine to Medium SAND with Silts, sub-rounded, light grey-greenish grey, damp, loose, no organics, with sulfuric odor and weathering (redox).<br>Grades to | collapsed | 45 – 40 |
| | #32 | | | 260 – 261 | | SP | Clean Fine SAND with Fine Gravels, gravel clasts are sub-rounded, light grey-greenish grey, damp, loose, no organics/odor/weathering. | | 40 – 39 |
| | | | D | 261 – 266 | | SP | Clean Fine SAND, light grey-dark grey, damp, loose-low/medium dense, no organics, with sulfuric odor and weathering (redox).<br>@ 266 organic debris found | | 39 – 34 |

Depth (ft) scale: 249, 250, 251, 252, 253, 254, 255, 256, 257, 258, 259, 260, 261, 262, 263, 264, 265, 266

Elevation (ft) scale: 51, 50, 49, 48, 47, 46, 45, 44, 43, 42, 41, 40, 39, 38, 37, 36, 35, 34

**Disclaimer** This bore log is intended for environmental not geotechnical purposes.

produced by ESlog.ESdat.net on 19 Apr 2023

CANYON ENVIRONMENTAL GROUP

## GROUNDWATER LOG BH01 GW

| Soil Samples | Core Interval | % Recovery | Moisture | Depth (ft) | Graphic Log | USCS | Material Description | Well Diagram | Elevation (ft) |
|---|---|---|---|---|---|---|---|---|---|
| | | | | 267 | | | Increasing fines with depth. | | 33 |
| | | | | 268 | | | | | 32 |
| SRGW SS#9 | | | | 269 | | | | | 31 |
| | #33 | | | 270 | | SP-SM | Fine SAND with Silts, light grey-dark grey, wet, loose-low medium dense, no organics, with sulfuric odor and weathering (redox). | | 30 |
| | | | | 271 | | | | | 29 |
| | | | | 272 | | | Increasing fines with depth. | | 28 |
| | | | | 273 | | | | | 27 |
| | | | | 274 | | | | | 26 |
| | | | | 275 | | | @275 organic debris found | collapsed | 25 |
| | | | | 276 | | SM | @277 organic debris found<br>Silty Fine SAND, light grey-dark grey, wet-damp, loose-low medium dense, no organics, with sulfuric odor and weathering (redox)<br>@278 organic debris found | | 24 |
| | | | | 277 | | | | | 23 |
| | | | | 278 | | | | | 22 |
| | | | D | 279 | | SP | Clean Medium SAND, gravel clasts are sub-rounded, dark grey, damp, loose, no organics/weathering, sulfuric odor. | | 21 |
| | #34 | | | 280 | | | | | 20 |
| | | | | 281 | | | | | 19 |
| | | | | 282 | | | | | 18 |
| | | | | 283 | | | | | 17 |
| | | | | 284 | | | | | 16 |

**Disclaimer** This bore log is intended for environmental not geotechnical purposes.



produced by ESlog.ESdat.net on 19 Apr 2023

CANYON
ENVIRONMENTAL GROUP

## GROUNDWATER LOG BH01 GW

| Soil Samples | Core Interval | % Recovery | Moisture | Depth (ft) | Graphic Log | USCS | Material Description | Well Diagram | Elevation (ft) |
|---|---|---|---|---|---|---|---|---|---|
| | | | D | 285 | | CL | Silty Clay, light grey, damp, very stiff to hard (PP=+5.0), organics, weathering (redox), and sulfuric odor. | | 15 |
| | | | | 286 | | | | | 14 |
| | | | | 287 | | | | | 13 |
| | | | | 288 | | | @288 Organic debris | | 12 |
| | | | | 289 | | | | | 11 |
| | #35 | | | 290 | | | | | 10 |
| | | | | 291 | | | | | 9 |
| | | | W | 292 | | SM | Silty Fine SAND, light grey- dark grey, wet, dense, organics, weathering (redox), and sulfuric odor. | | 8 |
| | | | | 293 | | | | collapsed | 7 |
| | | | | 294 | | | Fines decrease with depth. | | 6 |
| | | | D | 295 | | SP | Fine SAND with trace Silts, light to dark grey, damp, low to medium dense, organics, weathering (redox), and sulfuric odor. | | 5 |
| | | | | 296 | | | Fines decrease with depth | | 4 |
| | | | D | 297 | | SM | Silty Fine SAND, light to dark grey, damp, upper medium dense with density decreasing with depth, organics, weathering (redox), and sulfuric odor. | | 3 |
| | | | | 298 | | | | | 2 |
| | | | | 299 | | | | | 1 |
| | #36 | | | 300 | | | | | 0 |
| | | | | 301 | | | | | -1 |
| | | | | 302 | | | | | -2 |

**Disclaimer** This bore log is intended for environmental not geotechnical purposes.

produced by ESlog.ESdat.net on 19 Apr 2023

## GROUNDWATER LOG BH01 GW

| Soil Samples | Core Interval | % Recovery | Moisture | Depth (ft) | Graphic Log | USCS | Material Description | Well Diagram | Elevation (ft) |
|---|---|---|---|---|---|---|---|---|---|
| | | | D | 303 | | SP | Fine to Medium SAND with inclusions of very fine Sand and Silts, dark grey to greenish grey, damp, loose to medium dense, organics, weathering (redox), and sulfuric odor. | | -3 |
| | | | | 304 | | | @ 304.3 Organic debris. | | -4 |
| | | | | 305 | | | | | -5 |
| | | | | 306 | | | Clean Medium Sand | collapsed | -6 |
| | | | | 307 | | | | | -7 |
| | | | | 308 | | | | | -8 |
| | | | D | 309 | | SW | Medium to Coarse SAND with Fine Gravels, gravel clasts are sub-rounded, light to dark grey, damp, loose, no organics/weathering/odor. | | -9 |
| | | | | 310 | | | Termination Depth at: 310-ft | | -10 |
| | | | | 311 | | | | | -11 |
| | | | | 312 | | | | | -12 |
| | | | | 313 | | | | | -13 |
| | | | | 314 | | | | | -14 |
| | | | | 315 | | | | | -15 |
| | | | | 316 | | | | | -16 |
| | | | | 317 | | | | | -17 |
| | | | | 318 | | | | | -18 |
| | | | | 319 | | | | | -19 |
| | | | | 320 | | | | | -20 |

# Surface Water and Groundwater Interaction

Skagit River Basin Groundwater Study

Lower Skagit River Valley from Sedro-Woolley to Birdsview, Washington

*Skagit County, Washington*

June 13, 2025

*This page intentionally left blank*

# Surface Water and Groundwater Interaction

# Skagit River Basin Groundwater Study

June 13, 2025

Prepared for:

Washington State University

Prepared by:

Chad Wiseman (HDR Engineering, Inc.)
Jeff Ninnemann (Canyon Environmental Group)

*This page intentionally left blank*

# Contents



# Tables



# Figures

## Abbreviations

| | |
|---|---|
| Basin | Skagit River Basin |
| cfs | cubic foot/feet per second |
| Ecology | Washington State Department of Ecology |
| GPS | Global Positioning System |
| GW | groundwater |
| HDR | HDR Engineering, Inc. |
| RM | river mile |
| SW | surface water |
| USGS | United States Geological Survey |

## Appendices

# 1 Introduction

The Washington State Joint Legislative Task Force on Water Supply identified information on groundwater (GW) resources as a major gap limiting management of water resources in the Skagit River Basin (Basin). The Washington State University, Water Research Center (WRC) conducted a synthesis study covering water-resources availability and use in the Basin and developed specific knowledge gaps associated with various disciplines, including GW (Yoder et al. 2021). As an outcome of the synthesis study recommendations, the WRC authorized Western Washington University and HDR Engineering, Inc., (HDR) to conduct a three-part study seeking to gain understanding of GW resources with a focus on the lower Skagit River Valley, between Sedro-Woolley and Cape Horn, in Skagit County (Figure 1). This study area was selected because of its significant GW resources and future development pressure.

Only a few GW studies have been undertaken in Skagit County upstream of Sedro-Woolley. Glacial outwash terraces suspected to contain abundant GW (aquifers) are common in the Skagit River Valley between Sedro-Woolley and Cape Horn, but the largest accumulations of sand and gravel, and therefore potential aquifers, are located on the north side of the valley (Riedel 2017). A study by the United States Geological Survey (USGS) (Hidaka 1973) identified Day and Alder Creeks as having significant GW input from large glacial outwash terrace aquifers during low-flow periods in late summer. It is suspected that other tributary streams are also fed by these aquifers, including Muddy, Red Cabin, Jones, and Grandy Creeks, but data characterizing these interactions and their hydraulic dynamics are limited.

The first part of the study is to characterize aquifers in the upland glacial outwash deposits in the study area by evaluating well records and constructing hydrogeologic cross-sections and a three-dimensional framework (Tasks 200 and 500). The second part of the study is to quantify baseflow by comparing existing streamflow gage records (Task 300). The third part of the study is to evaluate surface water (SW) and GW interaction in a subset of the aquifer characterization study area. This report pertains to this third part of the study, the evaluation of SW and GW interaction.

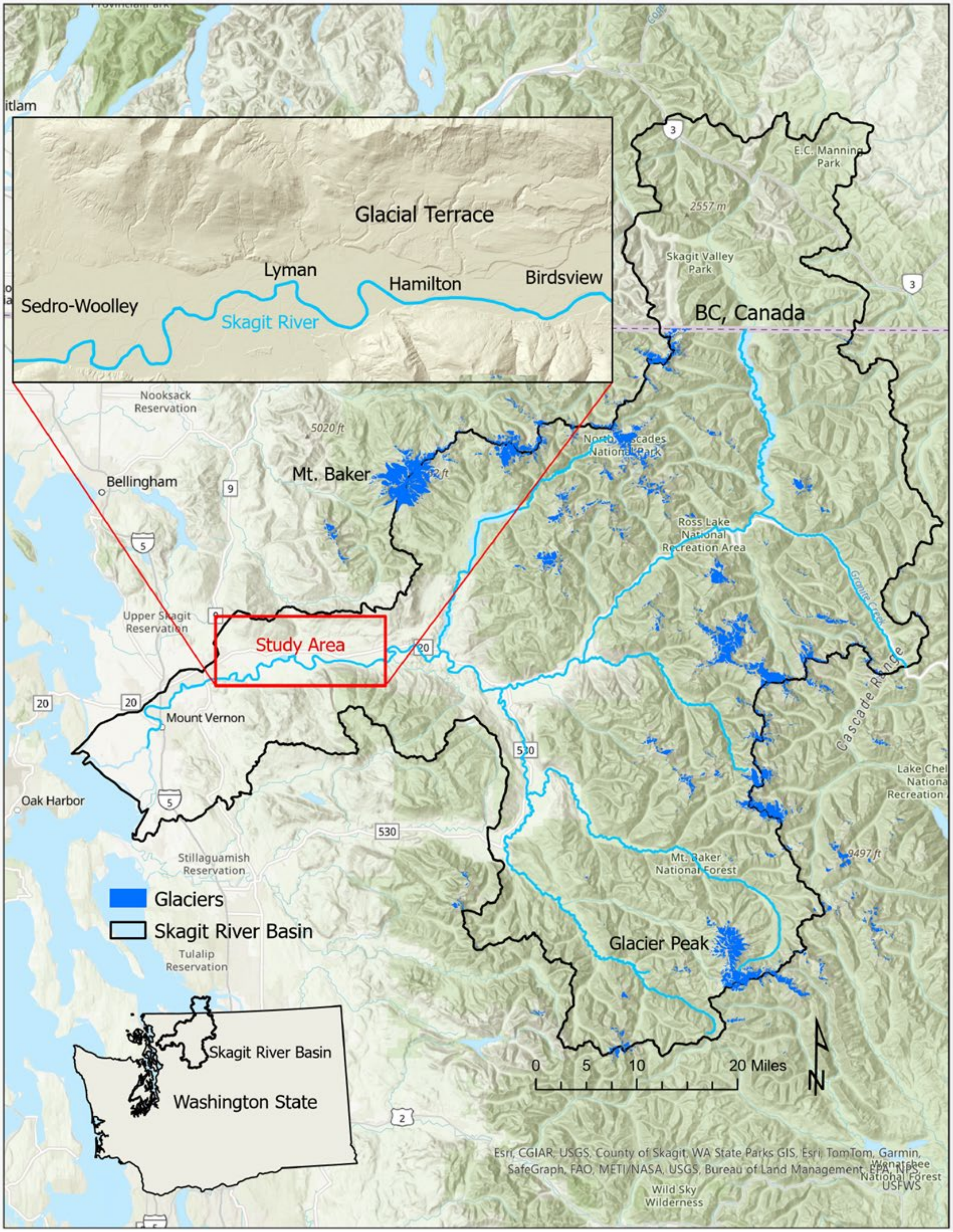


**Figure 1. Study area**

## 1.1 Study Goals and Objectives

The goal of this study is to evaluate GW-SW interactions on select Skagit River tributary streams within the focus area between Sedro-Woolley and Cape Horn, in conjunction with the local aquifer characterization. These GW-SW interactions were evaluated by measuring the hydraulic gradient between paired GW (instream piezometer with level logger) and SW (stream gage with level logger) elevations over the course of at least one month during the low flow season (i.e., late summer and early fall) at select tributary locations. The GW-SW interactions along these select Skagit River tributary streams were also evaluated with seepage run (synoptic stream discharge) surveys. These results will be compared to previous findings within the Lower Skagit River basin. The objectives of this study are to develop the following information:

- Infer reaches gaining flow, reaches losing flow, and overall SW flow balance in tributary streams with synoptic seepage run surveys
- Develop continuous hydraulic gradient estimates at up to six locations in tributary streams that are also undergoing seepage run evaluation

# 2 Methods

This section describes the study design, seepage run, and hydraulic gradient materials and methods, and the evaluation.

## 2.1 Study Design

The study paired hydraulic gradient measurements with seepage run surveys along two tributary streams to the Skagit River. Streams selected for the study were limited to those discharging to the north bank of the Skagit River between Sedro-Woolley and Concrete, where a glacial terrace occurs. Grandy and Muddy Creeks were selected because they were relevant for fisheries and where hydrogeologic cross-sections were being constructed (part 1 of the overall study, as described in Section 1). Cross-sections were developed in the eastern portion of the study area in the Grandy Creek, Alder Creek, and Muddy Creek watersheds. The eastern portion of the glacial terrace is where the glacial outwash deposits (Qgo) are the most prevalent and thick. Furthermore, the streams must have access that accommodates meaningful seepage run measurements. Grandy and Muddy Creeks met this criterion, but Alder Creek was ruled out because of poor access for conducting a seepage run. Therefore, Grandy and Muddy Creeks were selected for hydraulic gradient and seepage run measurements.

Seepage run surveys occurred during periods of relatively low flow during fall 2023. The seepage run study extent was from the upstream extent of the glacial outwash deposits (Qgo) to the confluence with the Skagit River. Mainstem (Grandy and Muddy Creeks) and associated tributary flows were measured. These measurements allowed for development of a water balance so that GW gain or loss could be inferred.

Hydraulic gradient measurements were made between seepage run locations, to confirm the inferred streamflow gain or loss from the seepage run surveys. The hydraulic gradient measurements quantified local GW head over time. Hydraulic gradient measurements were made with paired instream piezometer and stream gage monitoring stations to collect time series of shallow GW levels and paired stream SW elevations. Results were analyzed for a continuous record of hydraulic gradients between shallow GW and SW to assess durations of losing or gaining conditions at each established monitoring site. Hydraulic gradient was measured with installation of instream piezometers and paired stream gage, in proximity to each other. Reconnaissance surveys in September 2022 and January 2023 identified hydraulic gradient monitoring locations for Grandy Creek (Figure 2) and Muddy Creek (Figure 3). Three locations per stream were selected and located between proposed seepage run flow measurement locations.

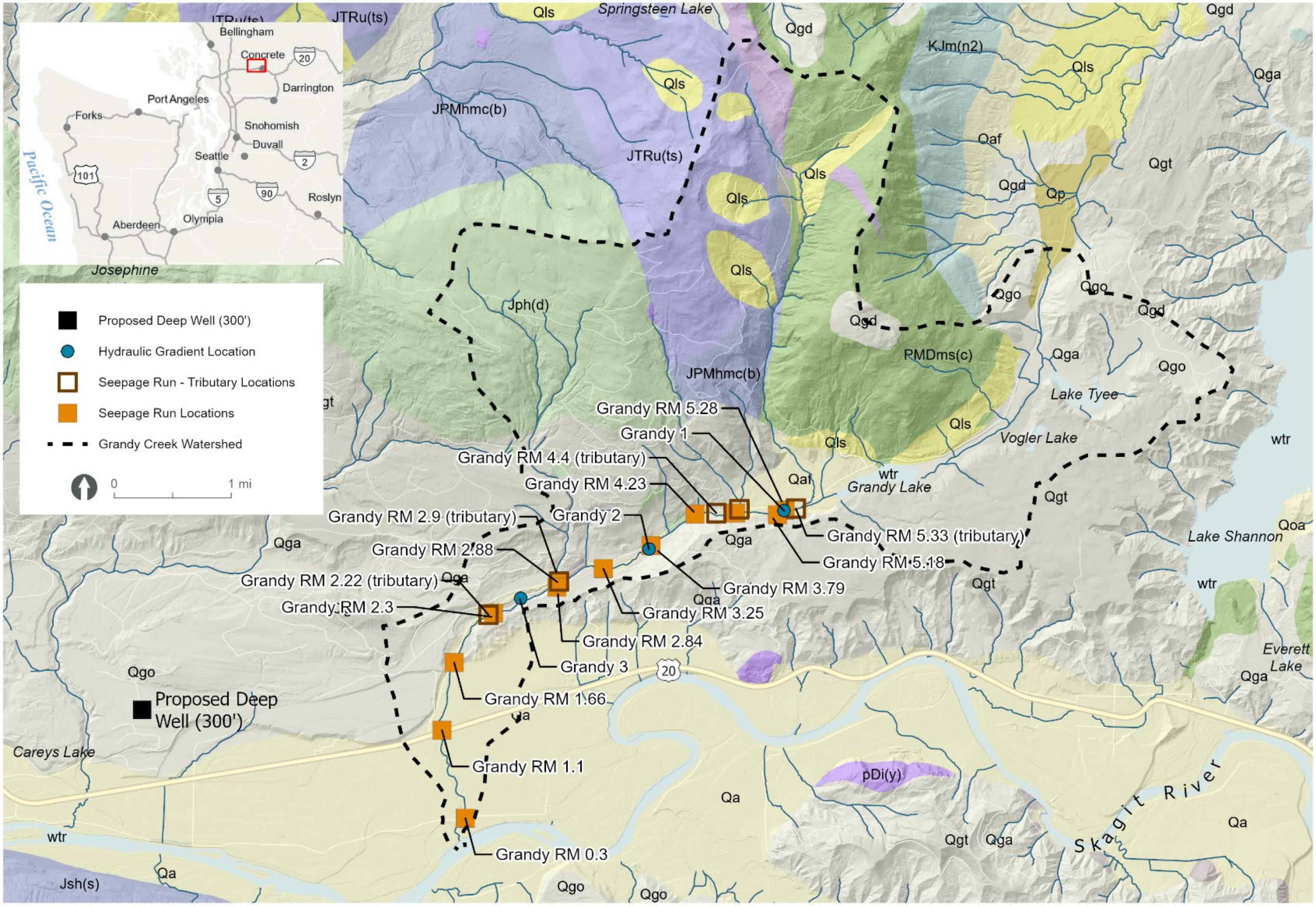


**Figure 2. Grandy Creek monitoring locations**

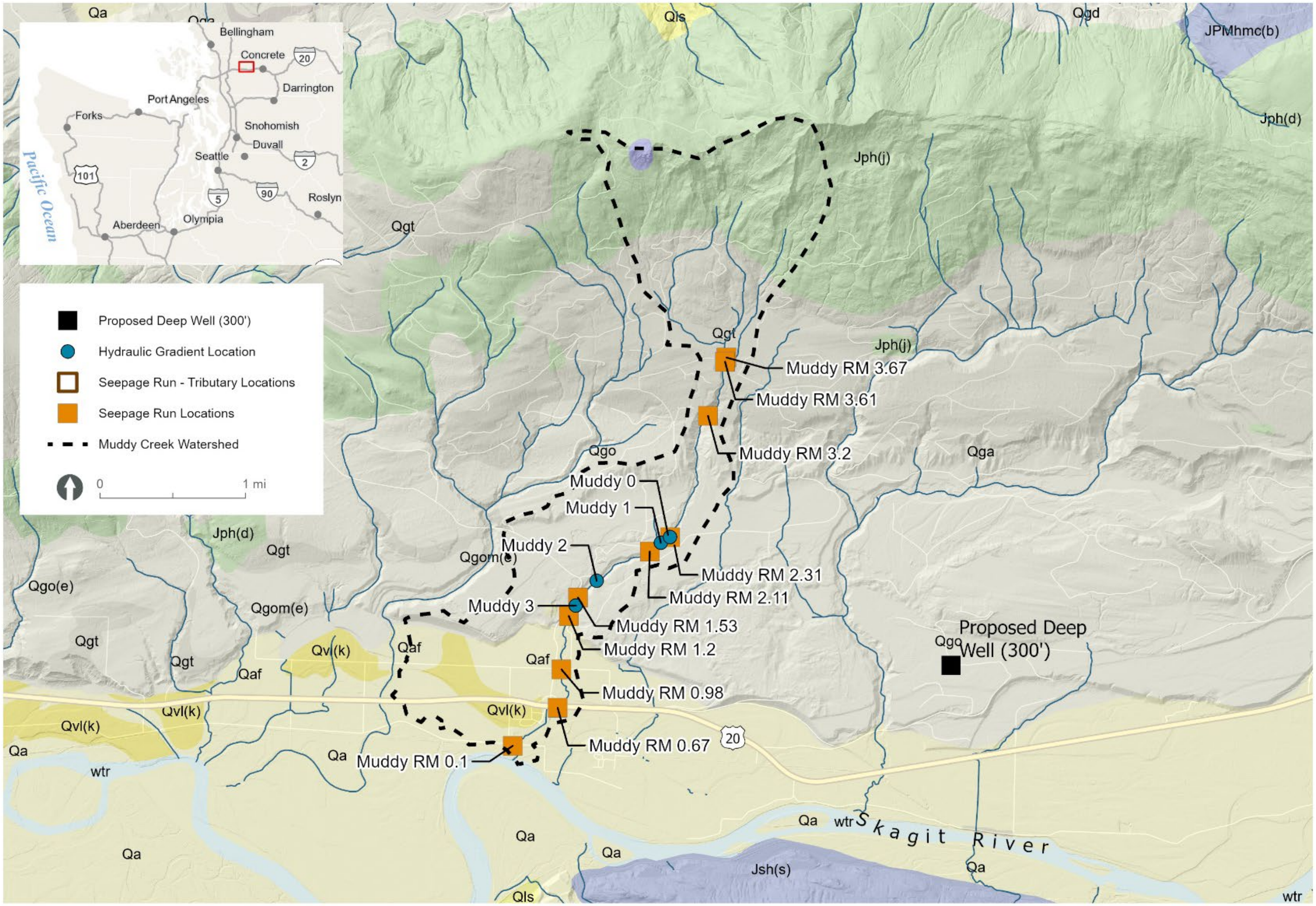


Figure 3. Muddy Creek monitoring locations

## 2.2 Seepage Run

Synoptic seepage run (or stream discharge) surveys at Grandy and Muddy Creeks occurred from the upstream extent of the glacial outwash (Qgo) formation to near the confluence with the Skagit River. Flows were measured during one synoptic survey at Grandy Creek and one at Muddy Creek to infer GW gain or loss between monitoring locations. Flows at tributaries were measured and accounted for in the analysis of reach gains/losses. GW gain was inferred when stream discharge is higher at downstream transects than discharge at the upstream transects. GW loss was inferred when stream discharge is higher at upstream transects than discharge at the downstream transects. Neutral water balance was inferred with the difference.

Seepage run survey data can provide insight about whether a stream is a gaining stream (GW is supplying the stream) or a losing stream (water from the stream is seeping into the ground). On September 12 and September 15, 2023, two teams conducted seepage run tests at Muddy and Grandy Creeks: one team downstream and another team upstream. Both mechanical (propeller) and electronic streamflow devices were used with a tested 1.5 percent relative difference between devices. Measurements were recorded and the locations of the measurements were recorded with a Global Positioning System (GPS) device. Mid-September was selected as this was the driest month of the year, and when baseflow conditions were most prevalent. These results will provide some insight into GW connectivity between the glacial terraces and floodplain.

### 2.2.1 Seepage Run (Stream Discharge) Locations

The locations on the mainstem of Grandy and Muddy Creeks were spaced apart systematically and located within the constraints of access. All tributaries defined on a 1:24,000 quad map were measured. Grandy Creek seepage run measurements were started downstream of the outlet of Grandy Lake and ended near the confluence with the Skagit River (Figure 2; Table 1). Muddy Creek seepage run measurements were started at the upper Medford Road crossing and ended near the confluence with the Skagit River (Figure 3; Table 1). Two teams collected the measured flow concurrently for each stream, respectively. Grandy Creek flow measurements were collected on September 12, 2023. Muddy Creek flow measurements were collected on September 15, 2023.

**Table 1. Seepage run monitoring locations**

| Watershed | Location | Type | Mainstem river mile | Latitude | Longitude |
|---|---|---|---|---|---|
| Grandy | 5.30 | Mainstem | 5.28 | 48.560867 | -121.821056 |
| Grandy | 5.33 (tributary) | Tributary | 5.33 | 48.561076 | -121.819035 |
| Grandy | 5.20 | Mainstem | 5.18 | 48.560264 | -121.822489 |
| Grandy | 4.90 (tributary) | Tributary | 4.90 | 48.560882 | -121.829586 |
| Grandy | 4.90 | Mainstem | 4.85 | 48.560402 | -121.83029 |
| Grandy | 4.04 (tributary) | Tributary | 4.40 | 48.560346 | -121.833853 |
| Grandy | 4.20 | Mainstem | 4.23 | 48.560174 | -121.837815 |
| Grandy | 3.80 | Mainstem | 3.79 | 48.5562 | -121.845945 |
| Grandy | 3.30 | Mainstem | 3.25 | 48.553247 | -121.854756 |

| Watershed | Location | Type | Mainstem river mile | Latitude | Longitude |
|---|---|---|---|---|---|
| Grandy | 2.90 | Mainstem | 2.88 | 48.551552 | -121.862967 |
| Grandy | 2.90 (tributary) | Tributary | 2.90 | 48.551552 | -121.862967 |
| Grandy | 2.80 | Mainstem | 2.84 | 48.550854 | -121.863333 |
| Grandy | 2.30 | Mainstem | 2.30 | 48.54748629 | -121.8750747 |
| Grandy | 2.22 (tributary) | Tributary | 2.22 | 48.547281 | -121.876007 |
| Grandy | 1.70 | Mainstem | 1.66 | 48.541293 | -121.88225 |
| Grandy | 1.10 | Mainstem | 1.10 | 48.532889 | -121.884298 |
| Grandy | 0.30 | Mainstem | 0.30 | 48.522053 | -121.879657 |
| Muddy | 3.70 | Mainstem | 3.67 | 48.564907 | -121.974695 |
| Muddy | 3.60 | Mainstem | 3.61 | 48.564485 | -121.974893 |
| Muddy | 3.20 | Mainstem | 3.20 | 48.55907921 | -121.9772939 |
| Muddy | 2.30 | Mainstem | 2.31 | 48.546951 | -121.982619 |
| Muddy | 2.10 | Mainstem | 2.11 | 48.545487 | -121.985622 |
| Muddy | 1.50 | Mainstem | 1.53 | 48.54078 | -121.996236 |
| Muddy | 1.20 | Mainstem | 1.20 | 48.538926 | -121.997559 |
| Muddy | 1.00 | Mainstem | 0.98 | 48.533611 | -121.998515 |
| Muddy | 0.70 | Mainstem | 0.67 | 48.529792 | -121.998968 |
| Muddy | 0.10 | Mainstem | 0.10 | 48.52592674 | -122.0055841 |

### 2.2.2 Methods for Measuring Stream Discharge

Stream discharge was measured at each location using the mid-section method (Ecology 2018a). Each discharge measurement was conducted with two field staff in wadable locations that have relatively laminar flow, are single-thread channels, are free from obstructions with no eddies, and have no undercut banks. A cross-section perpendicular to flow was defined with a measuring tape and secured to each bank with stakes. Detailed methods are defined in the Study Plan (HDR 2023). Flow was calculated according to the following equation:

$$Q = \Sigma(a \times v)$$

where:

Q = total measured discharge
a = area of individual cell
v = mean velocity of individual cell, normal to the cross-section

A water balance spreadsheet was developed that subtracts the flow of each mainstem station from the next downstream station. Positive differences indicate reaches with gaining GW conditions. Negative differences indicate reaches with losing GW conditions. Differences in flow equal to or less than field duplicate measurements were considered neutral. Tributary flow between mainstem stations was included in the upstream flow term. This water balance is represented by the following:

$$S = Qd - Qu - SUM(T) + SUM(W)$$

where:

S = net seepage loss/gain

Qd = downstream flow

Qu = upstream flow

T = tributary inputs

W = known water withdrawals (out-of-stream diversions)

## 2.3 Hydraulic Gradient

Hydraulic gradient measurements were made with instream piezometers and paired stream stage gaging sites at three locations in Grandy Creek and Muddy Creek, respectively. The piezometers were driven at least 3 to 5 feet below the streambed mud line. The piezometers were screened within the bottom 6 inches. This screened depth below the streambed was assumed to represent the local GW and therefore a positive or negative hydraulic pressure would result in a greater or lesser water surface elevation in the piezometer, relative to the adjacent stream water surface elevation. Gaging sites were selected in a fluvial geomorphic area where it was suspected that hyporheic influence would be at a minimum, i.e. areas of large drops directly upstream or directly downstream were avoided, when possible. The piezometers and stream gages had level loggers installed that measured and recorded pressure, that equates to water depth above the loggers. Pressure and depth were corrected with local barometers. Hourly depths from the paired piezometer and stream gage level loggers were used to calculate their relative water surface elevations. The relative water surface elevations between piezometer and stream gage depth data were calculated by measuring the water surface elevation in the piezometer and stream gage relative to a common benchmark while the level loggers were recording depths. Subsequent depth measurements were then transformed to relative elevations, based on the same relationship. The GW and tributary stream level elevation data were continuously monitored for at least 1 month during the low-flow season. Some sites were also measured in the spring.

### 2.3.1 Hydraulic Gradient Locations

At Grandy Creek, the most upstream piezometer and staff gage pair (Grandy 1) was installed at the upstream extent of the seepage run survey, at river mile (RM) 5.3 (Figure 2, Table 2). The second-most upstream piezometer and staff gage pair (Grandy 2) was installed between seepage run sites at RM 3.7. The most downstream piezometer and staff gage pair (Grandy 3) was installed between seepage run sites at RM 2.5. All locations will be in reaches surrounded by uplands of glacial outwash (Qgo).

At Muddy Creek, the most upstream piezometer and staff gage pair (Muddy 0) was installed at RM 2.3, at a seepage run site and at the upstream extent of the Qgo in the stream valley (Figure 3, Table 2). The next pair (Muddy 1) was installed between seepage run sites at RM 2.1. The next pair (Muddy 2) was installed between seepage run sites at RM 1.69. The most downstream pair (Muddy 3) was installed between seepage run sites at RM 1.46. Muddy 3 was located near the entrance of the Muddy

Creek Valley and confluence with the Skagit River floodplain. All locations were in reaches surrounded by uplands of glacial outwash.

**Table 2. Approximate piezometer and stream gage locations proposed for hydraulic gradient measurements**

| Hydraulic site location | River mile | Latitude | Longitude | Monitoring period(s) |
|---|---|---|---|---|
| Grandy 1 | 5.30 | 48.56080221 | -121.8212789 | 3/2023–8/2023 |
| Grandy 2 | 3.74 | 48.55575696 | -121.8463 | 3/2023–9/2023 |
| Grandy 3 | 2.53 | 48.54936411 | -121.8700853 | 3/2023–7/2023<br>8/2024–9/2024 |
| Muddy 0 | 2.30 | 48.546951 | -121.982619 | 8/2024–9/2024 |
| Muddy 1 | 2.20 | 48.54637057 | -121.9839896 | 3/2023–8/2023 |
| Muddy 2 | 1.69 | 48.54249327 | -121.9934914 | 3/2023–7/2023 |
| Muddy 3 | 1.46 | 48.53997621 | -121.9965304 | 8/2024–9/2024 |

### 2.3.2 Hydraulic Gradient Field Methods

Piezometers were installed directly into the streambed, within a few feet of the paired stream gages, respectively. Each piezometer was installed with 6-inch drive-point piezometer tip and 1-inch coupled piping. The piezometers were driven into the streambed by hand with a piezometer drive-head assembly and slide hammer. The piezometer tip was driven at least 3 to 5 feet into the streambed. Once each piezometer was installed, pre-launched level loggers were installed (Ecology 2019). Solinst Levelogger 5 units were installed inside the piping by suspending the unit with braided metal cable near the piezometer tip and attached to the cap.

Stream gages were installed instream, within a few feet of the instream piezometers. The gages were installed in a stable pool or cut bank. A T-post or rebar was driven into the streambed or fixed onto woody debris. A 1-inch-diameter polyvinyl chloride (PVC) pipe was attached to the T-post or rebar. Solinst Levelogger 5 units were installed inside the piping by suspending the unit with braided metal cable at the bottom of the pipe and attached to the cap.

For each pair of piezometers and stream gages, the relative elevations were surveyed, without tying them to an elevation datum. The vertical difference between the top of the piezometer casing and the staff gage PVC pipe casing was surveyed with a transit, relative to a common station elevation (Figure 4). The vertical distances from the top of the casing to the water level in the piezometer and outside of the piezometer were measured during survey and while the level logger was recording (Ecology 2018b).

### 2.3.3 Hydraulic Gradient Calculations

Field measurements defined the vertical distance from the top of the casing to the level logger for both the piezometer and stream gage, respectively, according to the following relationship:

*Distance from TOC to level logger = DTW + Di*

*where:*

*TOC = top of casing*

*DTW = depth to water from TOC*

*$D_i$ = depth of water measured above the level logger*

Once this relationship was established, the DTW could be calculated with unattended monitoring of the depth of water over the level logger (Dx) using the following equation:

*DTW = distance from TOC to level logger - Dx*

*where:*

*$D_x$ = depth of water measured above the level logger hourly while unattended*

The relative difference in SW elevation between the piezometer and stream gage (dh) was calculated by accounting for the relative difference in height between the piezometer and stream gage top of casing:

*dh = (station - TOCp - DTWp) - (station - TOCg - DTWg)*

*where:*

*dh = hydraulic head; elevation difference between the stream water level and monitoring well water level*

*Station = common benchmark elevation defined by transit during installation*

*TOCp = top of casing of piezometer*

*DTWp = depth to water in piezometer*

*TOCg = top of casing in stream gage*

*DTWg = depth to water in stream gage*

Vertical hydraulic gradients ($i_v$) were derived by dividing the hydraulic head (dh) by the vertical distance between the streambed elevation and the elevation of the screened piezometer tip (dl). Converting raw field measurements to hydraulic gradient values normalizes for differences in screen depth and screen interval length, thereby enabling direct comparisons to be drawn among paired gage sites. This relationship assumes that the bed level does not significantly change over the course of the monitoring period. The following equation was used to calculate vertical hydraulic gradients:

*$i_v$ = dh / dl*

*where:*

*$i_v$ = vertical hydraulic gradient*

*dh = difference in head between the stream water level and monitoring well water level*

*dl = distance from the streambed surface to the midpoint of the monitoring well screen*

Continuous water levels were periodically downloaded from the level loggers installed in each piezometer and staff gage. During each download, the distances from the surveyed top of piezometer and gage casings to their respective water levels were measured. The level loggers were inspected, cleaned, and checked for battery life. Some manufacturing errors in the firmware and hardware caused some of the data to be corrupted during the 2023 monitoring period. As a result of these issues, some additional monitoring was done for a month in 2024 at Grandy 3, Muddy 0, and Muddy 3. The results were compared to the calculated results from the level logger results as a quality control check.

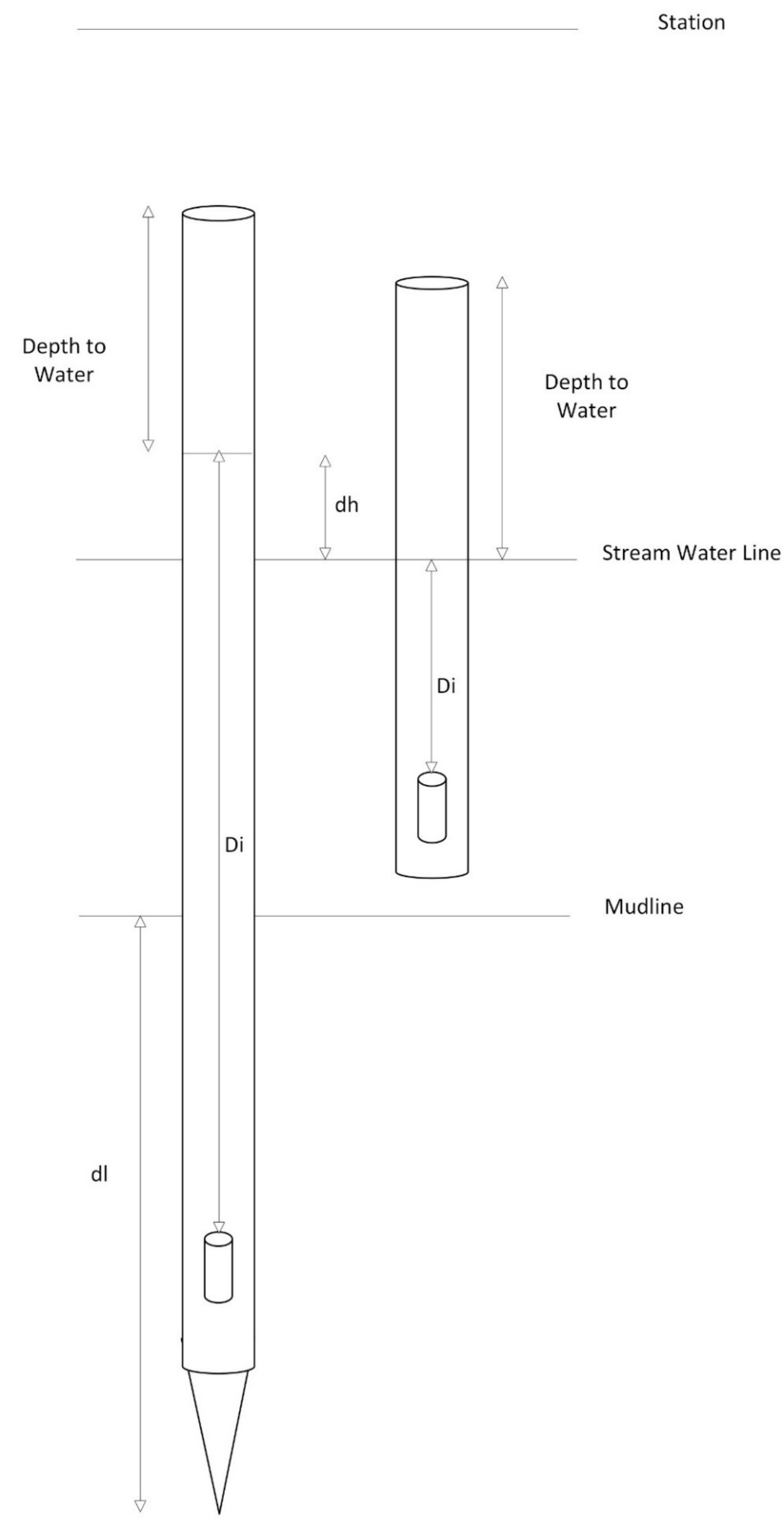


Figure 4. Piezometer and stream gage setup

# 3 Results

This section describes the seepage run and hydraulic gradient results for Grandy Creek and Muddy Creek, respectively.

## 3.1 Quality Control

Discharge field duplicate measurements were within 0.1 cubic foot per second (cfs) of each other (Appendix A), suggesting that longitudinal seepage run measurements less than 0.1 cfs difference are unlikely to be actual measurable differences.

Hydraulic gradient estimates were compared between those derived from manual tape-down measurements (i.e., measurements from top of casing to the static water level) and those derived from level logger measurements collected at the same time (Appendix A). These paired measurements generally corresponded well, indicating that the site setup, level logger measurements, and calculations were functioning as intended.

## 3.2 Grandy Creek

On September 12, 2023, Grandy Creek had a dry stream channel with residual wetted pools downstream of Grandy Lake to approximately RM 5.2, where flow was first detected (Table 3; Figure 5; Appendix B). The dry channel conditions were presumably due to zero flow being allowed to discharge from Grandy Lake at that time. The creek then gained flow to the entrance of the Grandy Creek Valley at approximately RM 1.7, except for a 0.5-mile-long losing reach between RM 3.8 and RM 3.3. After exiting the valley and entering the Skagit River Valley floodplain alluvium, Grandy Creek lost streamflow and then had a neutral reach, before discharging to the Skagit River.

**Table 3. Seepage run data of Grandy Creek in the Skagit River Valley**

| Reach begin (RM) | Reach end (RM) | Inferred GW gain/loss (cfs) | Inferred GW gain/loss rate (cfs per RM) | Gaining or losing |
|---|---|---|---|---|
| 5.3 | 5.2 | 0.0 | | |
| 5.2 | 4.9 | 4.5 | 13.7 | Gaining |
| 4.9 | 4.2 | 1.1 | 1.7 | Gaining |
| 4.2 | 3.8 | 0.2 | 0.5 | Gaining |
| 3.8 | 3.3 | -2.2 | -4.1 | Losing |
| 3.3 | 2.9 | 0.9 | 2.3 | Gaining |
| 2.9 | 2.8 | -0.1 | 0.0 | Neutral |
| 2.8 | 2.3 | 1.1 | 2.0 | Gaining |
| 2.3 | 1.7 | 3.9 | 6.0 | Gaining |
| 1.7 | 1.1 | -3.9 | -7.0 | Losing |
| 1.1 | 0.3 | 0.2 | 0.0 | Neutral |

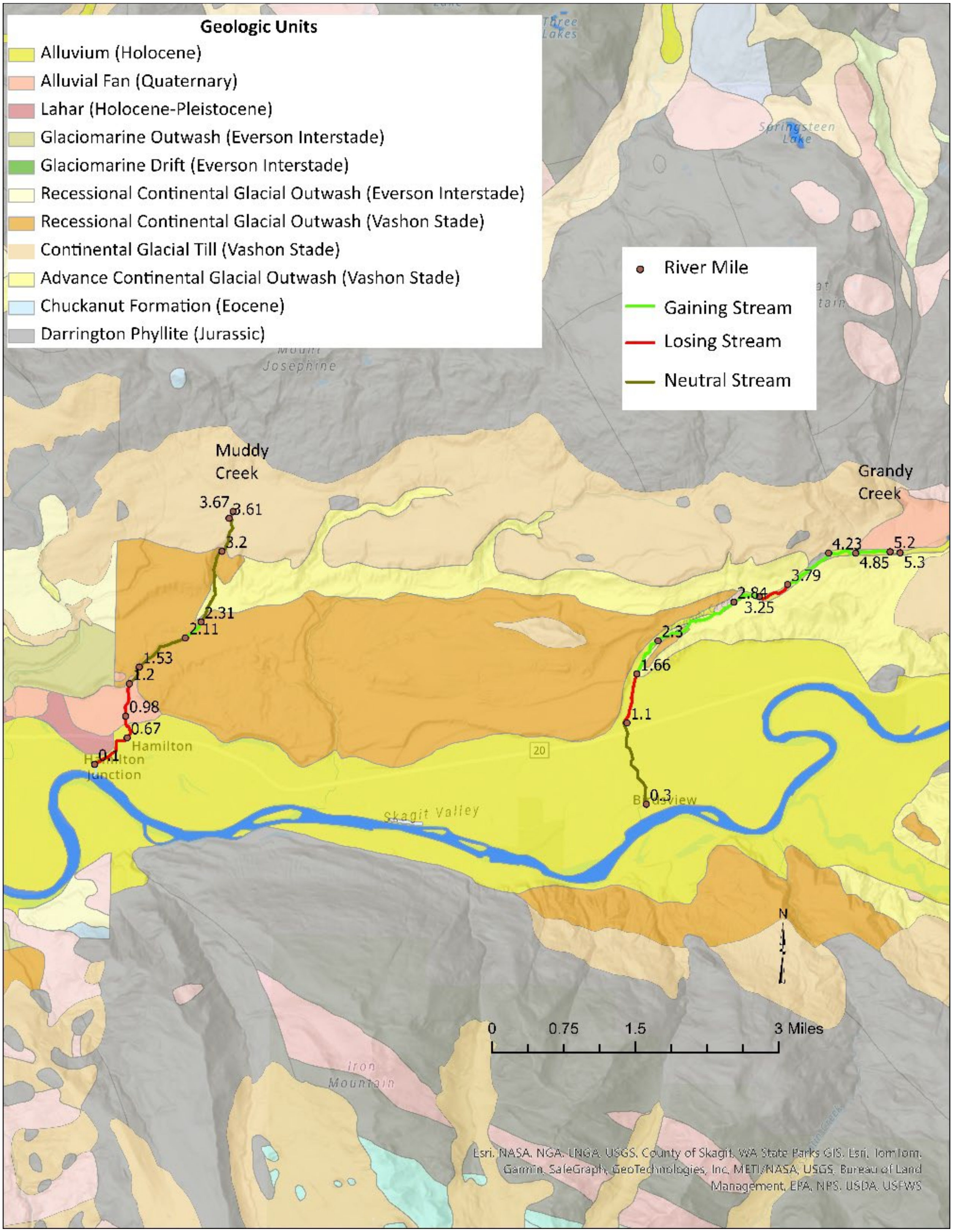


**Figure 5. Geologic map of the Lower Skagit River Valley with seepage run results from Muddy and Grandy Creeks displayed (geology modified from DNR 2016, 100k Surface Geology)**

Hydraulic gradient measurements generally corroborated with inferred seepage run results, with limitations. Grandy 1 (RM 5.3) had a positive hydraulic gradient in the spring and early summer of 2023, indicating a gaining reach, which matched the seepage run (Figure 6: Appendix C; Appendix D). However, when the stream went dry in late summer, the hydraulic gradient could not be calculated. It is possible that some flow was hyporheic, but that was not measured or it was below our piezometer.

Grandy 2 was located in a losing reach, as indicated by the seepage run results, and had a negative hydraulic gradient from spring through fall, which matches the seepage results.

Grandy 3 did not agree with the seepage run results. Grandy 3 was in a gaining reach for the seepage study, but had negative hydraulic gradient results for the gradient study, indicating a losing location. The Grandy 3 piezometer was reinstalled three times because the depth to water measurements indicated very little water occupying the piezometer, suggesting that water may not be entering the piezometer. Possibly the only water to get enter the piezometer was during the installation of the pipe. However, corroborating results with all three installations suggest that this location has a very negative hydraulic gradient, the screen was clogged, or the location sediments did not allow for GW communication (i.e., clay).

Water temperature results at all hydraulic gradient locations indicate that water in the piezometer generally tracked SW but with muted variation, indicating a representation of more hyporheic conditions (Figure 7). Grandy 2’s temperature did not show the muted variation, likely indicating that this station was more influenced by SW than GW.

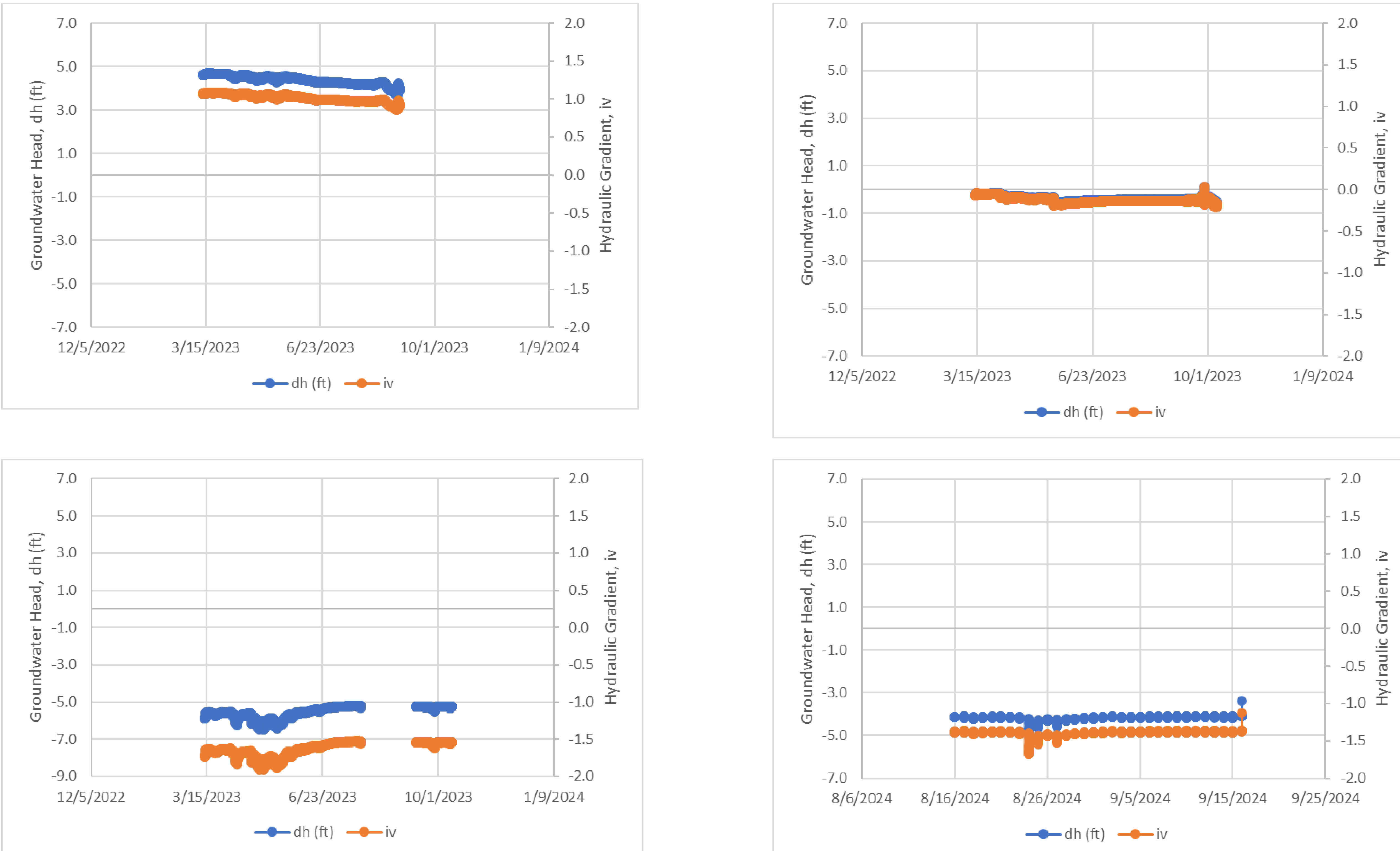


**Figure 6. Groundwater head (dh) and hydraulic gradient (iv) at locations Grandy 1 (top left), Grandy 2 (top right), and Grandy 3 (bottom left and bottom right)**

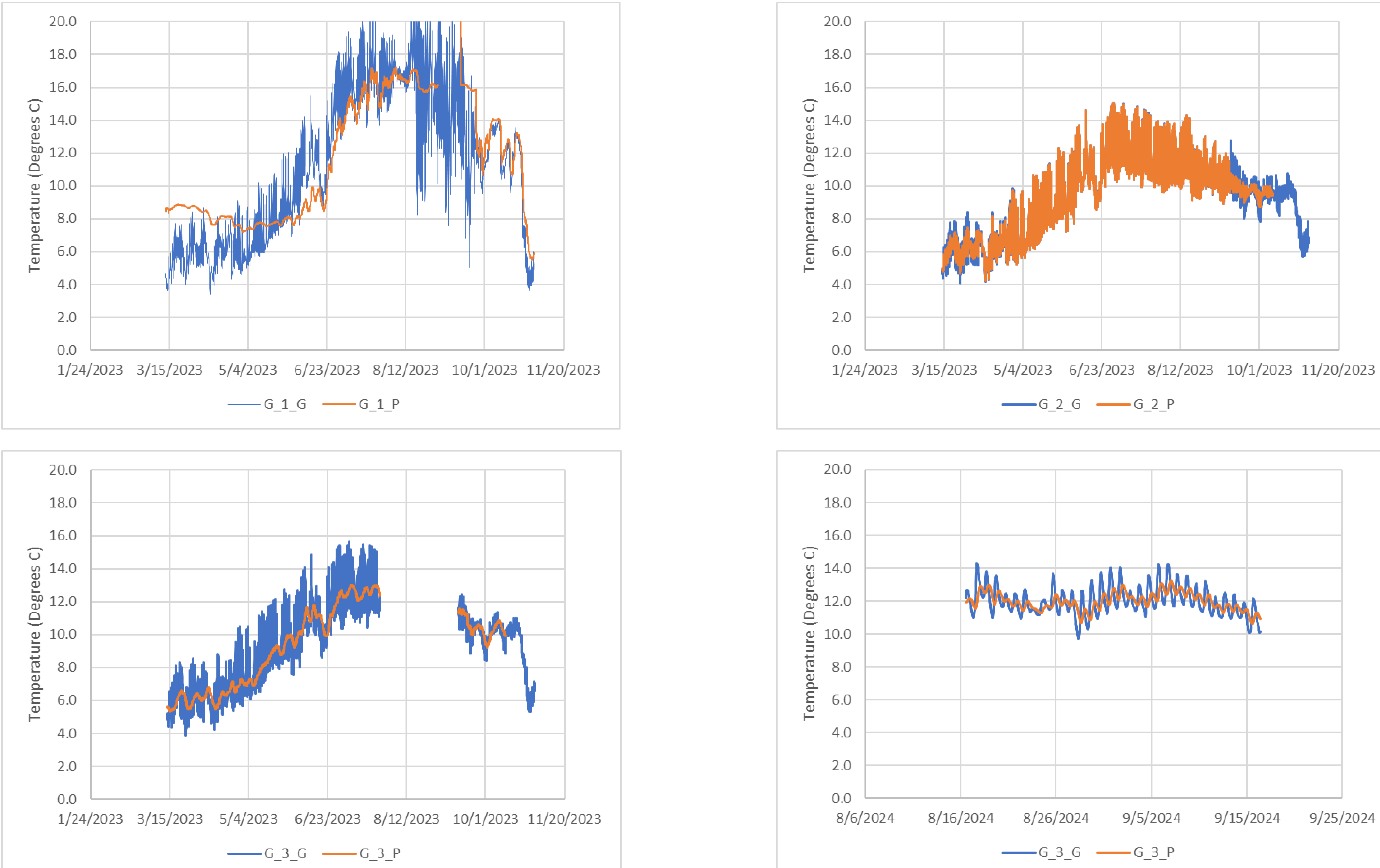


**Figure 7. Water temperature in stream gages (X_X_G) and piezometers (X_X_P) at locations Grandy 1 (top left), Grandy 2 (top right), and Grandy 3 (bottom left and bottom right)**

## 3.3 Muddy Creek

On September 15, 2023, Muddy Creek was in a seep-like condition at RM 3.7, with flows barely measurable at 0.1 cfs (Table 4; Appendix B). Flows continued to be in that seep-like condition until RM 2.3, where flows started to gain. The stream gained flow from GW for the next 0.2 mile to approximately RM 2.1. Flows were then neutral to the entrance of the valley, around RM 1.2. After exiting the valley, Muddy Creek lost flow as it crossed over the creek's alluvial fan and the Skagit River Valley alluvium.

**Table 4. Seepage run data of Muddy Creek in the Skagit River Valley**

| Reach begin (RM) | Reach end (RM) | Inferred GW gain/loss (cfs) | Inferred GW gain/loss rate (cfs per RM) | Gaining or losing |
|---|---|---|---|---|
| 3.7 | 3.61 | 0.01 | 0 | Neutral |
| 3.61 | 3.20 | -0.05 | 0 | Neutral |
| 3.20 | 2.31 | 0.10 | 0 | Neutral |
| 2.31 | 2.11 | 1.20 | 5.99 | Gaining |
| 2.11 | 1.53 | 0.00 | 0 | Neutral |
| 1.53 | 1.20 | -0.06 | 0 | Neutral |
| 1.20 | 0.98 | -0.33 | -1.52 | Losing |
| 0.98 | 0.67 | -0.48 | -1.55 | Losing |
| 0.67 | 0.10 | -0.46 | -0.81 | Losing |

Hydraulic gradient measurements generally corroborated with inferred seepage run results, with limitations. Muddy 0 (RM 2.3) was at a transition to recessional outwash and the beginning of the gaining reach This location had a neutral hydraulic gradient in the late summer (Figure 8; Appendix C; Appendix D). Muddy 1 (RM 2.2) was in a short gaining reach, as indicated by the seepage run results, and had a positive hydraulic gradient from spring through late summer. Muddy 2 (RM 1.7) was in a neutral reach, but had positive hydraulic gradient results from March through July, indicating a gaining location. Muddy 3 (RM 1.5) was in a neutral reach, but had slightly negative hydraulic gradient results in the late summer. Water temperature results at Muddy locations 1, 2, and 3 indicate that water in the piezometer generally tracked SW but with muted variation, indicating a representation of more hyporheic conditions (Figure 9). Muddy 0 had cooler and steady water temperature in the piezometer, indicating more representative GW conditions.

*This page intentionally left blank*

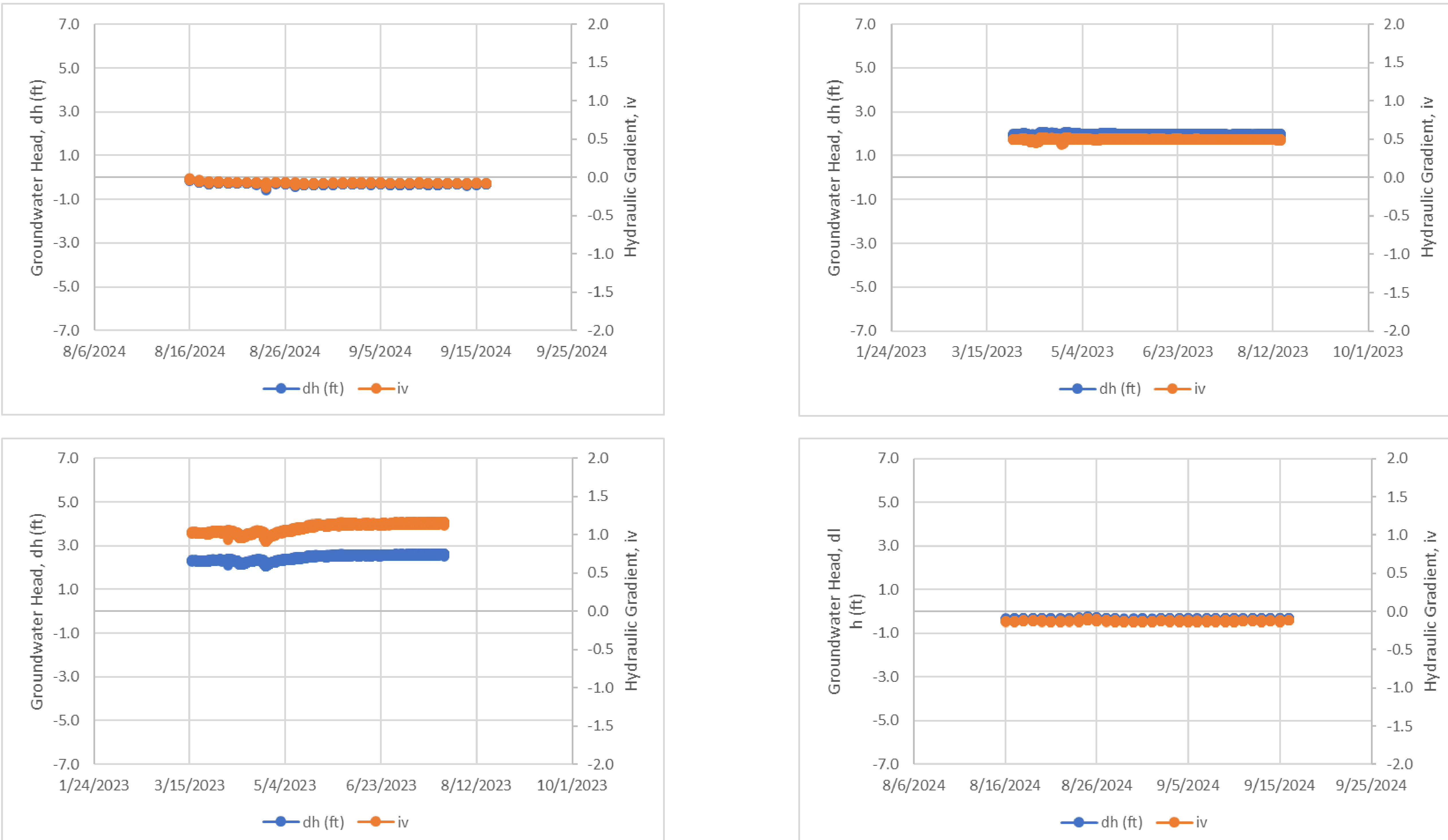


**Figure 8. Groundwater head (dh) and hydraulic gradient (iv) at locations Muddy 0 (top left), Muddy 1 (top right), Muddy 2 (bottom left) and Muddy 3 (bottom right)**

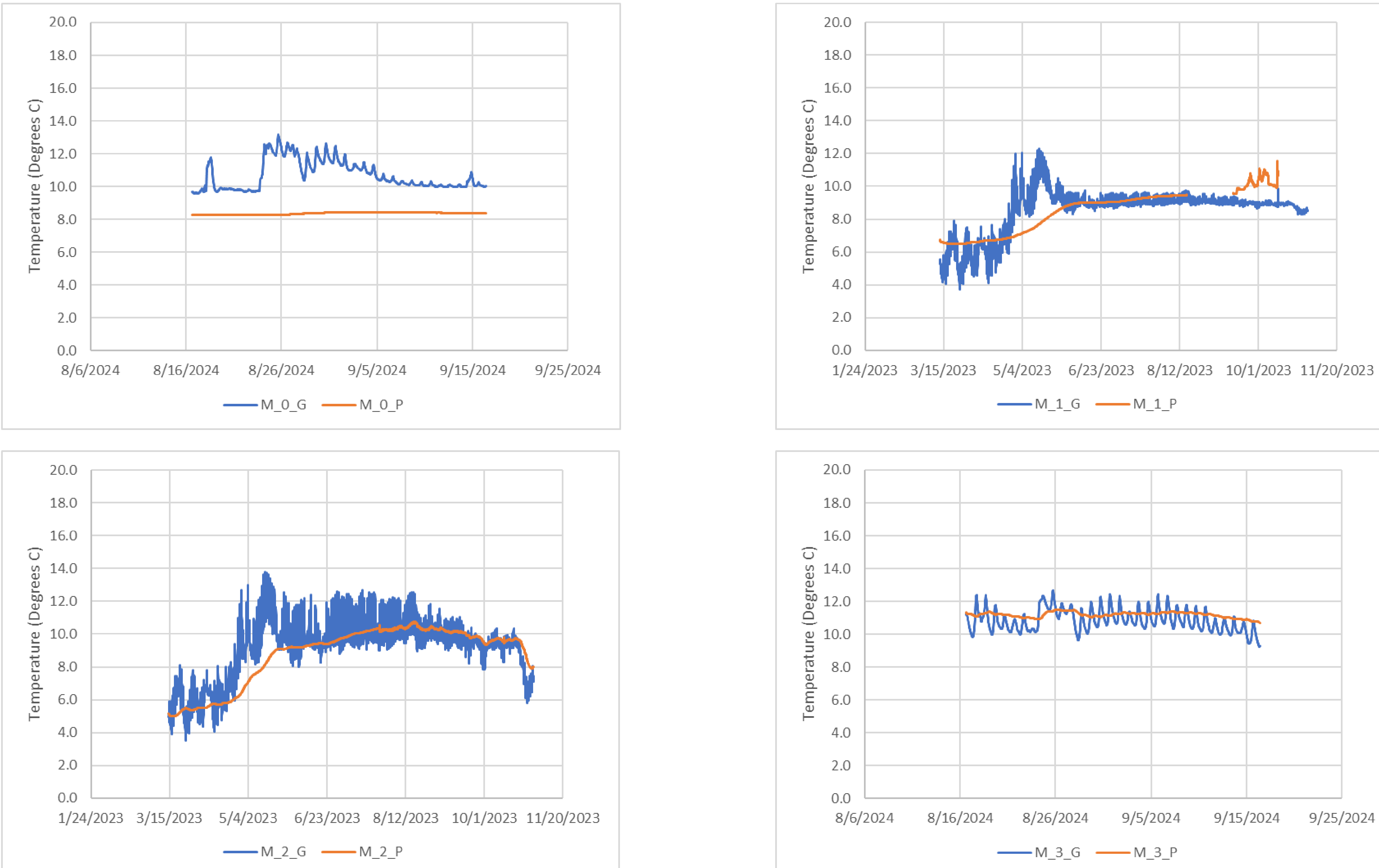


**Figure 9. Water temperature in stream gages (X_X_G) and piezometers (X_X_P) at locations Muddy 0 (top left), Muddy 1 (top right), Muddy 2 (bottom left) and Muddy 3 (bottom right)**

# 4 Discussion

The seepage run survey and hydraulic gradient data indicate variable GW-SW interactions. Grandy Creek is gaining GW mostly from the outwash deposits. The water table of the surrounding glacial terraces was much higher than the Grandy Creek streambed elevation in the valley. At various locations within the Grandy Creek study reach, Darrington Phyllite bedrock was observed in geologic cross-sections (part 1 of this study) (HDR 2024), particularly around RM 3.8 to RM 4.5. The areas where bedrock was near the surface could also cause the stream to be a gaining reach via inputs for the outwash along the banks and slopes of the valley wall. The tributary at RM 4.4 discharged into a bedrock channel. The only area in the confined valley that was not a gaining stream is between RM 3.3 and RM 3.8. This could possibly be because fine-grained lacustrine material is exposed on this part of the glacial terrace walls, preventing water seepage to this part of the stream, or it could be that the riverbed is underlain by outwash deposits and not bedrock, which would result in a recharging of the GW. Between RM 3.25 and RM 1.66, the stream was a gaining stream and was also likely supported by baseflow. The gaining stream is likely a result of the advance outwash being exposed at or near the surface of the stream and along the valley walls of the glacial terraces, allowing water to seep into the stream. If bedrock is near the surface along the reach that would also contribute to gaining reaches from SW from tributaries and GW seeps from the valley wall. This mechanism was supported by observations of water actively coming out of the glacial terrace walls on the western edges of Grandy Creek. Below RM 1.66, where the stream enters the floodplain, the stream is either neutral or losing water, indicating that the stream was discharging water to the Skagit River alluvial aquifer. This is likely because the water table is lower than the streambed elevation in the floodplain. These results in the Skagit River floodplain do not necessarily corroborate with streamflows previously collected by HDR (2017) that indicated a gaining reach between approximately RM 1.2 and RM 0.3. The differences could be due to seasonal fluctuations in Skagit River flows and the local alluvial GW elevation.

Muddy Creek was neutral between RM 3.7 and RM 2.3. As the stream passed through glacial terraces, the stream could have been gaining or losing water. Little is known about the character of this reach as neither the seepage run nor the hydraulic gradient measurements could evaluate this length of river because of inaccessibility. This is also an area where both advance glacial outwash and glaciolacustrine deposits could be exposed and providing both seepage to the stream through the outwash, and a lack of flow in other areas because of the glaciolacustrine deposits limiting water flow. The geological cross-sections from the 3D Hydrogeologic Framework Study (part 1 of this study) (HDR 2024) indicate that glacial outwash in the Muddy Creek vicinity is relatively shallow, which would limit the input and may cause the reach to maintain from initial inputs. At RMs 2.3 and 2.1, the stream is gaining and likely being supported by baseflow from the advance outwash. From RMs 2.1 and 1.2, the stream is a neutral stream again, which could be caused by till providing both baseflow in some areas and infiltration in other areas that are completely dry and unsaturated. Very few tributaries were observed along this reach, and this seems to indicate that the glacial outwash that blankets the surface of the terrace likely was able to infiltrate most of the precipitation into GW. The thickness of the outwash below the stream may have varied in such a way as to cause the stream to be both gaining and losing through this reach, which may have resulted in the neutral base flow between longitudinal measurement locations. Within the floodplain and from RMs 1.2 and 0.1, the stream is a losing flow (thus stream water is supplying the aquifer). These results corroborate with streamflows previously collected by HDR (2017) that lost 1.31 cfs between approximately RM 2.1 and RM 1.0. Bedrock seems to play less of a role in Muddy Creek than Grandy Creek, but in the upper portions of the reach bedrock was observed around RMs 3.67 and 3.61.

Based on these results, it appears that both Grandy and Muddy Creeks are losing streams within the floodplain during the low-flow period. Grandy Creek is a gaining stream overall within the glacial terraces, and Muddy Creek is neutral in the glacial terraces. Muddy Creek has more glacial till, glaciolacustrine deposits, and Chuckanut Formation exposed near the surface on the stream banks with the outwash, apparently balancing out water going both into the stream and infiltrating back into the aquifer. It should also be noted that Muddy Creek was far less accessible in the glacial terraces to take measurements (in particular between RM 2.31 and RM 3.20), resulting in potential data gaps; such issues did not exist at Grandy Creek.

# 5 References


Ecology (Washington State Department of Ecology)

2018a Standard Operating Procedure EAP056, Version 1.3. Measuring and Calculating Stream Discharge. Publication 18-03-203.

2018b Standard Operating Procedure EAP052, Version 1.2. Manual Well-Depth and Depth-to-Water Measurements. Publication 18-03-215.

2019 Standard Operating Procedure EAP074, Version 1.2. Use of Submersible Pressure Transducers During Groundwater Studies. Publication 19-03-205.

HDR (HDR Engineering, Inc.)

2017 Middle Skagit Valley Hydrogeologic Assessment, prepared for the Washington State Department of Ecology Technical Memorandum, 126 p.

2023 Groundwater Study Plan, WSU-WDOE Skagit River Basin Groundwater Study, Seepage Run and Hydraulic Gradient (Task 400). Prepared for the WSU Water Research Center. January 20.

2024 Three-Dimensional Hydrogeologic Framework. Skagit River Basin Groundwater Study. Lower Skagit River Valley from Sedro-Wooley to Birdsview, Washington.

Hidaka, F.T.

1973 Low-flow Characteristics of streams in the Puget Sound region, U.S. Geological Survey Open File Report to Washington Department of Ecology. https://doi.org/10.3133/ofr72163.

Riedel, J.L.

2017 Deglaciation of the North Cascade Range from the Last Glacial Maximum to the Holocene. Cuadernos de Investigación Geográfica, 43(2): 467–496.

Yoder, J., S. Chaudhary, B. Duarte, G. Greene, J. Jobe, G. LaHue, G. Maroney, G. Mauger, H. Morgan, J. Padowski, K. Rajagopalan, C. Raymond, M. Rogers, N. Rossman, N. Singh, B. Timpane-Padgham, C. Wiseman, and J. Won.

2021 Skagit Water Supply and Demand Synthesis. Story Map Series Prepared for the Washington State Joint Legislative Task Force on Water Supply. https://doi.org/10.7273/4n11-9k73.

# Appendix A. Quality Control Results

Table A-1. Seepage run discharge measurement field duplicate

Location: SR Grandy8

Date: 9/11/2023

Field Crew:
Cheyenne Ginther

MB OTT

| Distance (ft) | Depth (ft) | Velocity (ft/s) | Flow (ft³/s) |
|---|---|---|---|
| 20.6 | 0 | 0.00 | 0.00 |
| 19 | 0.4 | 0.00 | 0.00 |
| 18 | 0.5 | -0.01 | 0.00 |
| 16.8 | 0.4 | 0.33 | 0.13 |
| 16 | 0.5 | 0.22 | 0.10 |
| 15 | 0.7 | 0.01 | 0.01 |
| 14 | 0.8 | 0.03 | 0.02 |
| 13 | 0.7 | 0.40 | 0.28 |
| 12 | 0.7 | 0.43 | 0.30 |
| 11 | 0.8 | 0.32 | 0.25 |
| 10 | 0.9 | 0.11 | 0.10 |
| 9 | 1 | 0.05 | 0.05 |
| 8 | 1.1 | 0.34 | 0.38 |
| 7 | 1.3 | 0.41 | 0.53 |
| 6 | 1.5 | 0.48 | 0.72 |
| 5 | 1.5 | 0.63 | 0.95 |
| 4 | 1.4 | 0.46 | 0.64 |
| 3 | 1.3 | 0.55 | 0.54 |
| 2.5 | 1.2 | 0.73 | 0.48 |
| 1.9 | 0 | 0.00 | 0.00 |
| **Total** | | | **5.48** |

Location: SR Grandy8

Date: 9/11/2023

Field Crew:
Jeff Ninneman

Swoffer

| Distance (ft) | Depth (ft) | Velocity (ft/s) | Flow (ft³/s) |
|---|---|---|---|
| 20.6 | 0 | 0.00 | 0.00 |
| 19 | 0.4 | 0.00 | 0.00 |
| 18 | 0.5 | 0.00 | 0.00 |
| 16.8 | 0.4 | 0.35 | 0.14 |
| 16 | 0.4 | 0.24 | 0.09 |
| 15 | 0.4 | 0.00 | 0.00 |
| 14 | 0.8 | 0.00 | 0.00 |
| 13 | 0.7 | 0.39 | 0.27 |
| 12 | 0.7 | 0.48 | 0.34 |
| 11 | 0.7 | 0.30 | 0.21 |
| 10 | 0.8 | 0.08 | 0.06 |
| 9 | 0.9 | 0.00 | 0.00 |
| 8 | 1.1 | 0.29 | 0.32 |
| 7 | 1.3 | 0.47 | 0.61 |
| 6 | 1.5 | 0.50 | 0.75 |
| 5 | 1.5 | 0.66 | 0.99 |
| 4 | 1.4 | 0.38 | 0.53 |
| 3 | 1.3 | 0.63 | 0.61 |
| 2.5 | 1.2 | 0.71 | 0.47 |
| 1.9 | 0 | 0.00 | 0.00 |
| **Total** | | | **5.39** |

**%RPD** **1.5**

Table A-2. Hydraulic gradient field checks

| Date/ Time | Location | Measure-Down | Level Logger | Notes |
|---|---|---|---|---|
| 4/4/23 11:41 | Grandy 1 | 1.03 | 1.07 | |
| 8/17/23 13:53 | Grandy 1 | -0.67 | 0.99 | Stream is dry; residual pool |
| 4/4/23 12:08 | Grandy 2 | -0.05 | -0.05 | |
| 9/12/23 12:00 | Grandy 2 | -0.58 | -0.14 | |
| 4/4/23 12:24 | Grandy 3 (2023) | -1.62 | -1.62 | |
| 7/26/23 10:00 | Grandy 3 (2023) | -1.54 | -1.53 | |
| 9/16/24 10:00 | Grandy 3 (2024) | -1.13 | -1.13 | |
| 8/16/24 15:30 | Muddy 0 | 0.00 | -0.01 | |
| 9/16/24 11:00 | Muddy 0 | -0.08 | -0.08 | |
| 4/4/23 9:30 | Muddy 1 | 0.51 | 0.51 | |
| 4/4/23 13:30 | Muddy 2 | 1.04 | 1.04 | |
| 7/26/23 11:00 | Muddy 2 | 0.41 | 1.15 | |
| 9/16/24 12:25 | Muddy 3 | -0.13 | -0.12 | |

*This page is intentionally left blank.*

# Appendix B. Photos of Flow Sites

**Figure B-1. Grandy Creek at RM 5.3. No flow. Residual pool at piezometer 1.**

**Figure B-2. Dry tributary to Grandy Creek at RM 5.3 (Grandy Trib 1.1)**

**Figure B-3. Grandy Creek at RM 5.2; first measurable flow**

**Figure B-4 Tributary to Grandy Creek at RM 4.9**

**Figure B-5. Grandy Creek at RM 4.9**

**Figure B-6. Dry tributary to Grandy Creek at RM 4.4**

**Figure B-7. Grandy Creek at RM 4.2**

**Figure B-8. Grandy Creek at RM 3.8**

**Figure B-9. Grandy Creek at RM 3.3**

**Figure B-10. Grandy Creek at RM 2.9**

**Figure B-11. Grandy Creek at RM 2.8**

**Figure B-12. Grandy Creek at RM 2.3**

**Figure B-13. Tributary to Grandy Creek at RM 2.2**

**Figure B-14. Grandy Creek at RM 1.7**

**Figure B-15. Grandy Creek at RM 1.1**

**Figure B-16. Grandy Creek at RM 0.3**

**Figure B-17. Muddy Creek at RM 3.7**

**Figure B-18. Muddy Creek at RM 3.6**

**Figure B-19. Muddy Creek at RM 3.2**

**Figure B-20. Muddy Creek at RM 2.3**

**Figure B-21. Muddy Creek at RM 2.1**

**Figure B-22. Muddy Creek at RM 1.5**


**Figure B-23. Muddy Creek at RM 1.2**

**Figure B-24. Muddy Creek at RM 1.0, downstream of Hamilton Cemetery Road**

**Figure B-25. Muddy Creek at RM 0.7, downstream of Highway 20**

**Figure B-26. Muddy Creek at RM 0.1**

# Appendix C. Hydraulic Gradient Station Setup Calculations

## Table C-1. Grandy 1 site setup and tape down measurements (2023)

| Feature | Piezometer (ft below station) | Gage (ft below station) | Piezometer minus Gage Height (ft) |
|---|---|---|---|
| Top of Casing (TOC) | -2.88 | -4.99 | 2.11 |

| | |
|---|---|
| dl (ft) | 4.31 |

Tape Down Measurements

| Date | Piezometer (ft DTW) | Gage (ft DTW) | dh (ft) | $i_v$ |
|---|---|---|---|---|
| 3/13/23 17:00 | -1 | -3.34 | 4.45 | 1.03 |
| 3/14/23 14:10 | -0.88 | -3.40 | 4.63 | 1.07 |
| 4/4/23 11:41 | -0.98 | -3.31 | 4.44 | 1.03 |
| 8/17/23 13:53 | -8.31 | -3.30 | -2.90 | -0.67 |

Correction Factor:
Piezometer

| Date | LL Depth Piezometer (ft) | Piezometer (ft DTW) | TOC to LL (ft) |
|---|---|---|---|
| 3/14/23 14:10 | 4.80 | 0.88 | 5.68 |

Correction Factor: Gage

| Date | LL Depth Gage (ft) | Gage (ft DTW) | TOC to LL (ft) |
|---|---|---|---|
| 3/14/23 14:10 | 1.58 | 3.40 | 4.98 |

### Table C-2. Grandy 2 site setup and tape down measurements (2023)

| Feature | Piezometer (ft below station) | Gage (ft below station) | Piezometer minus Gage Height (ft) |
|---|---|---|---|
| Top of Casing (TOC) | -2.43 | -4.36 | 1.93 |

| | |
|---|---|
| dl (ft) | 3.1 |

Tape Down Measurements

| Date | Piezometer (ft DTW) | Gage (ft DTW) | dh (ft) | $i_v$ |
|---|---|---|---|---|
| 3/13/23 13:02 | -2.80 | -0.81 | -0.06 | -0.02 |
| 3/14/23 14:10 | -3.12 | -1.00 | -0.19 | -0.06 |
| 4/4/23 12:08 | -3.32 | -1.24 | -0.15 | -0.05 |
| 9/12/23 12:00 | -5.7 | -1.97 | -1.80 | -0.58 |
| 10/13/23 12:00 | -5.77 | -1.95 | -1.89 | -0.61 |

Correction Factor: Piezometer

| Date | LL Depth Piezometer (ft) | Piezometer (ft DTW) | TOC to LL (ft) |
|---|---|---|---|
| 4/4/23 12:08 | 2.91 | 3.32 | 6.23 |

Correction Factor: Gage

| Date | LL Depth Gage (ft) | Gage (ft DTW) | TOC to LL (ft) |
|---|---|---|---|
| 4/4/23 12:08 | 1.39 | 1.24 | 2.63 |

## Table C-3. Grandy 3 site setup and tape down measurements (2023)

| Feature | Piezometer (ft below station) | Gage (ft below station) | Piezometer minus Gage Height (ft) |
|---|---|---|---|
| Top of Casing (TOC) | -2.81 | -4.51 | 1.70 |
| | | | |
| dh (ft) | 3.4 | | |

Tape Down Measurements

| Date | Piezometer (ft DTW) | Gage (ft DTW) | dl (ft) | $i_v$ |
|---|---|---|---|---|
| 3/13/23 14:50 | -8.16 | -1.25 | -5.21 | -1.53 |
| 3/14/23 14:22 | -8.56 | -1.35 | -5.51 | -1.62 |
| 4/4/23 12:24 | -8.69 | -1.47 | -5.52 | -1.62 |
| 7/26/23 10:00 | -8.75 | -1.83 | -5.22 | -1.54 |
| 7/26/23 10:00 | | | 1.70 | 0.50 |

Correction Factor:
Piezometer

| Date | LL Depth Piezometer (ft) | Piezometer (ft DTW) | TOC to LL (ft) |
|---|---|---|---|
| 4/4/23 12:24 | 0.23 | 8.69 | 8.92 |

Correction Factor: Gage

| Date | LL Depth Gage (ft) | Gage (ft DTW) | TOC to LL (ft) |
|---|---|---|---|
| 4/4/23 12:24 | 1.54 | 1.47 | 3.01 |

## Table C-4. Grandy 3 site setup and tape down measurements (2024)

| Feature | Piezometer (ft below station) | Gage (ft below station) | Piezometer minus Gage Height (ft) |
|---|---|---|---|
| Top of Casing (TOC) | -1.95 | -2.18 | 0.23 |

| | |
|---|---|
| dh (ft) | 3 |

Tape Down Measurements

| Date | Piezometer (ft DTW) | Gage (ft DTW) | dl (ft) | $i_v$ |
|---|---|---|---|---|
| 8/16/24 11:20 | -5.2 | -2.59 | -2.38 | -0.79 |
| 9/16/24 10:00 | -6.19 | -2.58 | -3.38 | -1.13 |

Correction Factor:
Piezometer

| Date | LL Depth Piezometer (ft) | Piezometer (ft DTW) | TOC to LL (ft) |
|---|---|---|---|
| 9/16/24 10:00 | 0.07 | 6.19 | 6.26 |

Correction Factor: Gage

| Date | LL Depth Gage (ft) | Gage (ft DTW) | TOC to LL (ft) |
|---|---|---|---|
| 9/16/24 10:00 | 0.03 | 2.58 | 2.61 |

### Table C-5. Muddy 0 site setup and tape down measurements (2024)

| Feature | Piezometer (ft below station) | Gage (ft below station) | Piezometer minus Gage Height (ft) |
|---|---|---|---|
| Top of Casing (TOC) | -1.6 | -1.87 | 0.27 |
| | | | |
| dl (ft) | 4.25 | | |

Tape Down Measurements

| Date | Piezometer (ft DTW) | Gage (ft DTW) | dh (ft) | $i_v$ |
|---|---|---|---|---|
| 8/16/24 15:30 | -2.66 | -2.41 | 0.02 | 0.00 |
| 9/16/24 11:00 | -2.65 | -2.06 | -0.32 | -0.08 |

Correction Factor:
Piezometer

| Date | LL Depth Piezometer (ft) | Piezometer (ft DTW) | TOC to LL (ft) |
|---|---|---|---|
| 9/16/24 11:00 | 1.75 | 2.65 | 4.40 |

Correction Factor: Gage

| Date | LL Depth Gage (ft) | Gage (ft DTW) | TOC to LL (ft) |
|---|---|---|---|
| 9/16/24 11:00 | 0.58 | 2.06 | 2.64 |

**Table C-6. Muddy 1 site setup and tape down measurements (2023)**

| Feature | Piezometer (ft below station) | Gage (ft below station) | Piezometer minus Gage Height (ft) |
|---|---|---|---|
| Top of Casing (TOC) | -2.56 | -2.44 | -0.12 |

| | |
|---|---|
| dh (ft) | 3.95 |

Tape Down Measurements

| Date | Piezometer (ft DTW) | Gage (ft DTW) | dl (ft) | $i_v$ |
|---|---|---|---|---|
| 3/12/23 13:02 | -4.02 | -2.11 | -2.03 | -0.51 |
| 3/12/23 14:10 | -5.18 | -2.29 | -3.01 | -0.76 |
| 4/4/23 9:30 | -1.97 | -4.09 | 2.00 | 0.51 |
| 9/15/23 14:00 | -2.42 | -2.55 | 0.01 | 0.00 |

Correction Factor:
Piezometer

| Date | LL Depth Piezometer (ft) | Piezometer (ft DTW) | TOC to LL (ft) |
|---|---|---|---|
| 4/4/23 9:30 | 4.12 | 1.97 | 6.09 |

Correction Factor: Gage

| Date | LL Depth Gage (ft) | Gage (ft DTW) | TOC to LL (ft) |
|---|---|---|---|
| 4/4/23 9:30 | 1.24 | 4.09 | 5.33 |

### Table C-7. Muddy 2 site setup and tape down measurements (2023)

| Feature | Piezometer (ft below station) | Gage (ft below station) | Piezometer minus Gage Height (ft) |
|---|---|---|---|
| Top of Casing (TOC) | -12.76 | -14.86 | 2.10 |

| | |
|---|---|
| dl (ft) | 2.25 |

Tape Down Measurements

| Date | Piezometer (ft DTW) | Gage (ft DTW) | dh (ft) | $i_v$ |
|---|---|---|---|---|
| 3/14/23 12:20 | -6.56 | -1.75 | -2.71 | -1.20 |
| 3/14/23 12:35 | -6.55 | -1.75 | -2.70 | -1.20 |
| 3/14/23 13:30 | -4.03 | -1.77 | -0.16 | -0.07 |
| 4/4/23 13:30 | -1.00 | -1.25 | 2.35 | 1.04 |
| 7/26/23 11:00 | -3.33 | -2.15 | 0.92 | 0.41 |
| 9/15/23 15:24 | -4.91 | -2.14 | -0.67 | -0.30 |
| 10/13/23 15:24 | -5.01 | -2.15 | -0.76 | -0.34 |

Correction Factor: Piezometer

| Date | LL Depth Piezometer (ft) | Piezometer (ft DTW) | TOC to LL (ft) |
|---|---|---|---|
| 4/4/23 13:30 | 0.13 | 1.00 | 1.13 |

Correction Factor: Gage

| Date | LL Depth Gage (ft) | Gage (ft DTW) | TOC to LL (ft) |
|---|---|---|---|
| 4/4/23 13:30 | 0.82 | 1.25 | 2.07 |

## Table C-8. Muddy 3 site setup and tape down measurements (2024)

| Feature | Piezometer (ft below station) | Gage (ft below station) | Piezometer minus Gage Height (ft) |
|---|---|---|---|
| Top of Casing (TOC) | -1.51 | -2.45 | 0.94 |
| | | | |
| dl (ft) | 2.75 | | |

Tape Down Measurements

| Date | Piezometer (ft DTW) | Gage (ft DTW) | dh (ft) | $i_v$ |
|---|---|---|---|---|
| 8/16/24 13:27 | -4.76 | -2.22 | -1.60 | -0.58 |
| 9/16/24 12:25 | -3.47 | -2.18 | -0.35 | -0.13 |

Correction Factor:
Piezometer

| Date | LL Depth Piezometer (ft) | Piezometer (ft DTW) | TOC to LL (ft) |
|---|---|---|---|
| 9/16/24 12:25 | 2.84 | 3.47 | 6.31 |

Correction Factor: Gage

| Date | LL Depth Gage (ft) | Gage (ft DTW) | TOC to LL (ft) |
|---|---|---|---|
| 9/16/24 12:25 | 1.01 | 2.18 | 3.19 |

*This page intentionally left blank*

# Appendix D. Hydraulic Gradient: Photos of Sites

**Figure D-1. Hydraulic gradient site Grandy 1**

**Figure D-2. Hydraulic gradient site Grandy 2**

**Figure D-3. Hydraulic gradient site Grandy 3**

**Figure D-4. Hydraulic gradient site Muddy 0**

**Figure D-5. Hydraulic gradient site Muddy 1**

**Figure D-6. Hydraulic gradient site Muddy 2**

**Figure D-7. Hydraulic gradient site Muddy 3**

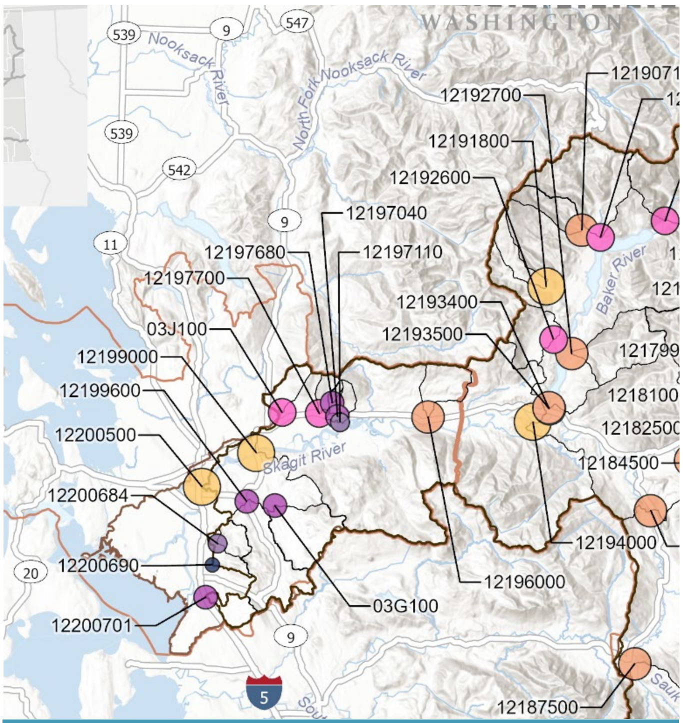


# FINAL Hydrograph Separation Report

## WSU-WDOE Skagit River Basin Groundwater Study

*Lower Skagit River Basin, Washington*

June 13, 2025

## Contents



## Tables

## Figures



## Appendices



.

# 1 Introduction

Determination of the baseflow component of the streamflow hydrograph is the primary concern of this part of the Skagit River Basin Groundwater Study, as described in this Task 300 Hydrograph Separation Report.

Streamflow in rivers can be separated into a relatively steady component, or baseflow, that is the portion of streamflow consisting of delayed subsurface flow that is generally maintained by groundwater (GW) discharge and represents reliably available surface water (Konrad 2022). Because baseflow (or GW discharge) typically accounts for most of the streamflow during dry periods, it plays a crucial role in maintaining and controlling water quality and aquatic ecosystems (Kang et al. 2022). Baseflow can be estimated through a variety of techniques that separate a streamflow hydrograph into stormflow (or quickflow) and baseflow components. The components of flow making up the streamflow hydrograph are used by hydrologists and hydrogeologists for quantifying GW discharge, GW recharge, estimating flooding potential, calibrating models, and assessing impacts of water development (Bradley et al. 2013), and are used as part of rainfall-runoff modeling (Jakeman and Hornberger 1993).

This section summarizes the background for the study as a whole and identifies the objectives for the specific efforts conducted under Task 300, Hydrograph Separation.

## 1.1 Background

The Washington State Joint Legislative Task Force on Water Supply identified development of information on GW as a major gap limiting management of water resources in the Skagit River basin (Basin). Subsequently, the Washington State Water Research Center (WRC) conducted a synthesis study covering water resources availability and use in the Basin and developed specific knowledge gaps associated with various disciplines, including GW (Yoder et al. 2021). As a result, Western Washington University and HDR, Inc. (HDR) have been authorized to conduct a three-part study seeking to gain understanding of GW resources in the Basin.

The first part of the study characterized the upland glacial outwash deposits in the lower Skagit River valley, between Sedro-Woolley and Birdsview in Skagit County, by evaluating well records, drilling and logging of a new deep borehole with installation of relatively deep well and GW-level monitoring and constructing hydrogeologic cross sections – see the Task 200 (HDR 2023) technical memorandum and Williams (2025). The second part of the study quantified GW discharge (baseflow) by performing hydrograph separation of existing streamflow gage records, as well as comparing baseflow to GW recharge and precipitation estimates, thereby providing an improved assessment and comparison of Basin water budget components (the Task 300 study documented herein). The third part of the study evaluated surface water (SW) and GW interaction in the same study area as the first part of the study – see the Task 400 HDR (2025) report.

This report is focused on the second part of the study, centered on hydrograph separation to quantify baseflow within an expanded study area (compared to the first and third parts of the study), including the Basin upstream of Mount Vernon within the United States, and another 43 subbasin drainage areas upstream of Mount Vernon (Figure 1). The additional subbasins, located outside of the study areas of the Tasks 200, 400, and 500 study area (green box on Figure 1), were analyzed to be comprehensive in terms of the water balance across the Basin since there is no field requirement for data collection and the analyses are relatively easy to repeat for a large number of gages.

## 1.2 Objectives

The primary objective of this Hydrograph Separation task was to quantify baseflow, as a proxy for GW discharge, over time at a variety of scales and sites using recorded streamflow at gaged locations across various parts of the Basin, including the Basin upstream from Mount Vernon, both on the Skagit mainstem and tributaries. A second objective was to calculate respective baseflow indices (BFI), calculated as the ratio of total volume of baseflow to total volume of streamflow, over the period of record at each site. A third objective was to compare the estimated long-term mean baseflow (GW discharge) rates to GW recharge and precipitation rate estimates for the 30-year period from 1/1/1981 through 12/31/2010, which were generated as part of the WRC synthesis study (Yoder et al. 2021). An additional, fourth objective was to compare results of baseflow separation between two different types of techniques, including performing a sensitivity analysis to help decide on the most appropriate digital filter parameter value to adopt for a commonly used hydrograph separation technique, namely the Lyne-Hollick (1979) one-parameter digital filter.

In addition to the stated objectives, this study also provides discussion about the results, particularly comparisons between the GW discharge and BFI estimates from the different baseflow separation techniques, as well as the possible causes for differences between GW discharge and GW recharge estimates (and precipitation), including methodological and temporal differences, along with potential accuracy concerns and possible influences caused by reservoir releases on the highly regulated Skagit and Baker Rivers. Furthermore, to conclude the report, a discussion of possible future studies is presented.

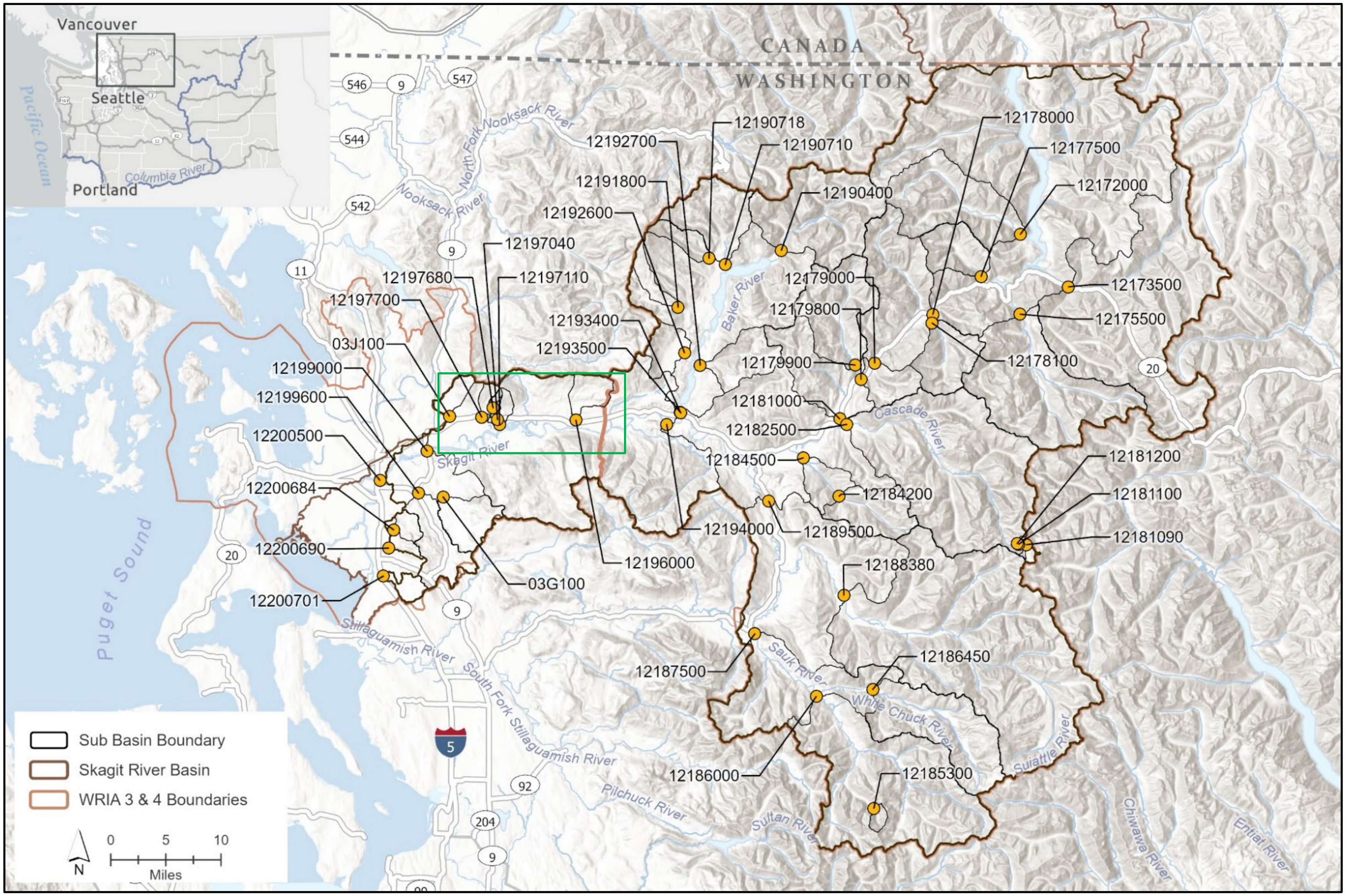


**Figure 1. Drainage basins and streamflow gages analyzed for baseflow within the Skagit River Basin, with the study area from Tasks 200, 400, and 500 shown as a green rectangle.**

# 2 Data Collection

This study utilized publicly available streamflow datasets from the United States Geological Survey (USGS) and the Washington State Department of Ecology (Ecology), in addition to spatial datasets of historic GW recharge and precipitation (1/1/1981 through 12/31/2010) generated as a part of the Skagit River Basin Water Supply and Demand Synthesis Study ("Synthesis Study") by Yoder et al. (2021), culminating in an ESRI Story Map Series. HDR downloaded daily streamflow data for the gages listed in Table 1.

Collection of daily streamflow data was initially limited to the time period of January 1, 1980, through December 31, 2021, regardless of current monitoring status (active or inactive). Gaging stations were screened to meet these criteria, barring a single outlier: USGS station 12196000 (Alder Creek near Hamilton); although the Alder Creek gage records end in 1971, an exception was made due to its location within the study area of the first and third parts (Tasks 200, 400, and 500) of the larger Skagit River Basin Groundwater Study.

The selected gaging stations were subsequently used to create two sets of streamflow data to serve different purposes. The first set of data includes available data for 44 gaging stations (1908 through 2021) to be used in the evaluation of BFI and comparison of two hydrograph separation techniques. More recent 2022 through 2023 data were mostly published as "provisional" and are therefore subject to revision and were not used in the analysis. A second set of data was created to compare the baseflow values directly against the long-term GW recharge estimates generated as a product of the Synthesis Study (Yoder et al. 2021). This comparison only utilized gages that have streamflow data records from 1/1/1981 through 12/31/2010. This date range was chosen to be consistent with that of the Synthesis Study to allow a direct comparison of baseflow (GW discharge) to GW recharge (and precipitation). A summary of the gages included in the second set of data is provided in Table 2. A total of six gages are located within the Tasks 200, 400, and 500 study area, including: 03J100, 12197700, 12197680, 12197040, 12197110, and 12196000, all of which have their station codes listed in bold in Table 1 and Table 2.

For the GW recharge to GW discharge comparison, there was a need to develop the subbasin boundaries associated with the analyzed gaging stations. The subbasin boundaries were generated using the USGS StreamStats interactive web interface (https://streamstats.usgs.gov/ss/) in most cases, and also a basin shapefile downloaded from the USGS Streamgage NHDPlus Version 1 Basins 2011 for Region 17 (https://water.usgs.gov/GIS/metadata/usgswrd/XML/streamgagebasins.xml). Gage location sources include those reported from USGS data downloads and also from the NHDPlus dataset. The two Ecology gaging station locations were used as reported from the Ecology website (Freshwater DataStream: https://apps.ecology.wa.gov/continuousflowandwq/).

**Table 1. Summary of all streamflow gaging stations analyzed for baseflow.**

| Station Code | Station Name | Stream Name | Agency | Monitoring Status | Drainage Area as Reported ($mi^2$) | Period of Record Analyzed | Duration of Records (years) | Percentage of the Period of Record with Measurements |
|---|---|---|---|---|---|---|---|---|
| **12196000** | Alder Creek near Hamilton, WA | Alder Creek | USGS | Inactive | 10.7 | 09/01/1943 – 09/29/1971 | 28.1 | 100 |
| 12179900 | Bacon Creek below Oakes Creek near Marblemount, WA | Bacon Creek | USGS | Active | 49.7 | 08/01/1943 – 12/31/2021 | 78.5 | 39 |
| 12190400 | Baker River above Blum Creek near Concrete, WA | Baker River | USGS | Active | 75.4 | 09/30/2012 – 12/31/2021 | 9.3 | 100 |
| 12193400 | Baker River at Henry Thompson Bridge at Concrete, WA | Baker River | USGS | Active | 297 | 09/11/1910 – 12/31/2021 | 111.4 | 74 |
| 12193500 | Baker River at Concrete, WA | Baker River | USGS | Inactive | 297 | 10/01/1910 – 04/30/2009 | 98.6 | 71 |
| 12192600 | Bear Creek below Tributaries near Concrete, WA | Bear Creek | USGS | Inactive | 14.4 | 04/01/1982 – 09/29/1986 | 4.5 | 100 |
| 12172000 | Big Beaver Creek near Newhalem, WA | Big Beaver Creek | USGS | Active | 63.2 | 03/01/1940 – 12/31/2021 | 81.9 | 23 |
| **12197680** | Black Creek near Minkler, WA | Black Creek | USGS | Inactive | 0.86 | 05/01/1975 – 06/30/1980 | 5.2 | 100 |
| 12200684 | Carpenter Creek near Bacon Rd near Mount Vernon, WA | Carpenter Creek | USGS | Inactive | 20 | 04/01/2007 – 09/29/2008 | 1.5 | 100 |
| 12200690 | Carpenter Creek near Conway, WA | Carpenter Creek | USGS | Inactive | 9.1 | 09/30/2006 – 04/01/2007 | 0.5 | 100 |
| 12181100 | Sf Cascade R at S Cascade Gl near Marblemount, WA | Cascade River | USGS | Inactive | 2.36 | 07/01/1957 – 09/29/1993 | 36.3 | 92 |
| 12182500 | Cascade River at Marblemount, WA | Cascade River | USGS | Active | 172 | 10/01/1928 – 12/31/2021 | 93.3 | 71 |
| 12185300 | Elliott Creek at Goat Lake outlet near Monte Cristo, WA | Elliott Creek | USGS | Inactive | 3.03 | 10/22/1982 – 09/29/1993 | 10.9 | 100 |
| 12200701 | Fisher Creek near Conway, WA | Fisher Creek | USGS | Inactive | 6.48 | 09/30/2006 – 09/29/2008 | 2.0 | 100 |
| **03J100** | Hansen Creek near Sedro Woolley, WA | Hansen Creek | Ecology | Active | 9.66 | 06/09/2005 – 10/01/2022 | 17.3 | 87 |
| 12184200 | Upper Illabot Creek near Rockport, WA | Illabot Creek | USGS | Inactive | 28.71 | 09/01/1982 – 09/29/1983 | 1.1 | 100 |
| 12184500 | Illabot Creek near Rockport, WA | Illabot Creek | USGS | Inactive | 42.4 | 08/23/1943 – 09/29/1985 | 42.1 | 10 |
| **12197110** | Minkler Creek near Lyman, WA | Minkler Creek | USGS | Inactive | 5.7 | 05/01/1974 – 06/30/1980 | 6.2 | 100 |
| 12178100 | Newhalem Creek near Newhalem, WA | Newhalem Creek | USGS | Active | 26.9 | 02/01/1961 – 12/31/2021 | 61.0 | 100 |
| 12199600 | Nookachamps Creek at Baker Heights, WA | Nookachamps Creek | USGS | Inactive | 25.51 | 07/07/2006 – 09/29/2008 | 2.2 | 100 |
| 03G100 | East Fork Nookachamps Creek at Beaver Lake Rd | Nookachamps Creek | Ecology | Active | 20.5 | 09/21/2000 – 10/01/2022 | 22.0 | 99 |
| 12190718 | Park Creek at Upper Bridge near Concrete, WA | Park Creek | USGS | Inactive | 10.5 | 06/01/1982 – 10/29/1990 | 8.4 | 100 |

| Station Code | Station Name | Stream Name | Agency | Monitoring Status | Drainage Area as Reported (mi$^2$) | Period of Record Analyzed | Duration of Records (years) | Percentage of the Period of Record with Measurements |
|---|---|---|---|---|---|---|---|---|
| 12173500 | Ruby Creek below Panther Creek near Newhalem, WA | Ruby Creek | USGS | Active | 206 | 10/01/1948 – 12/31/2021 | 73.3 | 25 |
| 12181200 | Salix Creek At S Cascade Gl near Marblemount, WA | Salix Creek | USGS | Inactive | 0.08 | 07/01/1961 – 03/20/2020 | 58.8 | 71 |
| 12186000 | Sauk River above White Chuck River near Darrington, WA | Sauk River | USGS | Active | 152 | 10/01/1917 – 12/31/2021 | 104.3 | 94 |
| 12187500 | Sauk River at Darrington, WA | Sauk River | USGS | Active | 293 | 07/01/1914 – 09/29/2016 | 102.3 | 21 |
| 12189500 | Sauk River near Sauk, WA | Sauk River | USGS | Active | 714 | 04/01/1911 – 12/31/2021 | 110.8 | 86 |
| 12178000 | Skagit River at Newhalem, WA | Skagit River | USGS | Active | 1175 | 12/21/1908 – 12/31/2021 | 113.1 | 94 |
| 12179000 | Skagit River above Alma Creek near Marblemount. WA | Skagit River | USGS | Active | 1274 | 10/01/1950 – 12/31/2021 | 71.3 | 65 |
| 12179800 | Skagit River above Bacon Creek near Marblemount. WA | Skagit River | USGS | Inactive | 1289 | 04/27/1977 – 10/25/1983 | 6.5 | 100 |
| 12181000 | Skagit River at Marblemount, WA | Skagit River | USGS | Active | 1381 | 09/01/1943 – 12/31/2021 | 78.4 | 66 |
| 12194000 | Skagit River near Concrete, WA | Skagit River | USGS | Active | 2737 | 10/01/1924 – 12/31/2021 | 97.3 | 100 |
| 12199000 | Skagit River near Sedro Woolley. WA | Skagit River | USGS | Active | 3015 | 05/01/1908 – 06/30/1980 | 72.2 | 28 |
| 12200500 | Skagit River near Mount Vernon, WA | Skagit River | USGS | Active | 3093 | 10/01/1940 – 12/31/2021 | 81.3 | 100 |
| 12181090 | South Cascade Middle Tarn near Marblemount. WA | South Cascade River | USGS | Inactive | 1.72 | 09/30/2002 – 10/09/2019 | 17.0 | 45 |
| 12177500 | Stetattle Creek near Newhalem, WA | Stetattle Creek | USGS | Inactive | 22 | 01/01/1914 – 11/23/1983 | 69.9 | 73 |
| 12188380 | Suiattle River above All Creek near Darrington. WA | Suiattle River | USGS | Inactive | 283 | 05/22/2013 – 09/29/2017 | 4.4 | 77 |
| 12191800 | Sulphur Creek near Concrete, WA | Sulphur Creek | USGS | Inactive | 8.36 | 03/01/1963 – 09/29/1982 | 19.6 | 63 |
| 12190710 | Swift Creek near Concrete, WA | Swift Creek | USGS | Inactive | 36.35 | 08/01/1982 – 09/29/1990 | 8.2 | 100 |
| **12197040** | Tank Creek near Lyman, WA | Tank Creek | USGS | Inactive | 2.5 | 04/24/1974 – 06/30/1980 | 6.2 | 100 |
| 12175500 | Thunder Creek near Newhalem, WA | Thunder Creek | USGS | Active | 105 | 10/01/1930 – 12/31/2021 | 91.3 | 100 |
| 12192700 | Thunder Creek near Concrete, WA | Thunder Creek | USGS | Inactive | 22.4 | 08/01/1982 – 09/29/1994 | 12.2 | 100 |
| 12186450 | White Chuck River above Crystal Creek near Darrington, WA | White Chuck River | USGS | Inactive | 66.4 | 10/01/2015 – 09/29/2016 | 1.0 | 100 |
| **12197700** | Wiseman Creek near Lyman, WA | Wiseman Creek | USGS | Inactive | 3 | 04/24/1974 – 06/30/1983 | 9.2 | 100 |

**Table 2. Streamflow gaging stations analyzed for the groundwater recharge and discharge comparison based on available records from 1/1/1981 through 12/31/2010.**

| Station Code | Station Name | Stream Name | Agency | Monitoring Status | Drainage Area as Reported ($mi^2$) | Period of Record Analyzed | Duration of Records (years) | Percentage of the Period of Record with Measurements |
|---|---|---|---|---|---|---|---|---|
| 12179900 | Bacon Creek below Oakes Creek near Marblemount, WA | Bacon Creek | USGS | Active | 49.7 | 10/01/1998 – 12/31/2010 | 12.3 | 100 |
| 12193400 | Baker River at Henry Thompson Bridge at Concrete, WA | Baker River | USGS | Active | 297 | 01/01/1981 – 12/31/2010 | 30.0 | 100 |
| 12193500 | Baker River at Concrete, WA | Baker River | USGS | Inactive | 297 | 01/01/1981 – 04/30/2009 | 28.3 | 100 |
| 12192600 | Bear Creek below Tributaries near Concrete, WA | Bear Creek | USGS | Inactive | 14.4 | 04/01/1982 – 09/29/1986 | 4.5 | 100 |
| 12200684 | Carpenter Creek near Bacon Rd near Mount Vernon, WA | Carpenter Creek | USGS | Inactive | 20 | 04/01/2007 – 09/29/2008 | 1.5 | 100 |
| 12200690 | Carpenter Creek near Conway, WA | Carpenter Creek | USGS | Inactive | 9.1 | 09/30/2006 – 04/01/2007 | 0.5 | 100 |
| 12181100 | Sf Cascade River at S Cascade Gl near Marblemount, WA | Cascade River | USGS | Inactive | 2.36 | 01/01/1981 – 09/29/1993 | 12.8 | 94 |
| 12182500 | Cascade River at Marblemount, WA | Cascade River | USGS | Active | 172 | 06/01/2006 – 12/31/2010 | 4.6 | 100 |
| 12185300 | Elliott Creek at Goat Lake outlet near Monte Cristo, WA | Elliott Creek | USGS | Inactive | 3.03 | 10/22/1982 – 09/29/1993 | 10.9 | 100 |
| 12200701 | Fisher Creek near Conway, WA | Fisher Creek | USGS | Inactive | 6.48 | 09/30/2006 – 09/29/2008 | 2.0 | 100 |
| **03J100** | Hansen Creek near Sedro Woolley, WA | Hansen Creek | Ecology | Active | 9.66 | 06/09/2005 – 12/31/2010 | 5.6 | 95 |
| 12184200 | Upper Illabot Creek near Rockport, WA | Illabot Creek | USGS | Inactive | 28.71 | 09/01/1982 – 09/29/1983 | 1.1 | 100 |
| 12184500 | Illabot Creek near Rockport, WA | Illabot Creek | USGS | Inactive | 42.4 | 03/22/1982 – 09/29/1985 | 3.5 | 100 |
| 12178100 | Newhalem Creek near Newhalem, WA | Newhalem Creek | USGS | Active | 26.9 | 01/01/1981 – 12/31/2010 | 30.0 | 100 |
| 12199600 | Nookachamps Creek at Baker Heights, WA | Nookachamps Creek | USGS | Inactive | 25.51 | 07/07/2006 – 09/29/2008 | 2.2 | 100 |
| 03G100 | East Fork Nookachamps Creek at Beaver Lake Rd | Nookachamps Creek | Ecology | Active | 20.5 | 09/21/2000 – 12/31/2010 | 10.3 | 100 |
| 12190718 | Park Creek at Upper Bridge near Concrete, WA | Park Creek | USGS | Inactive | 10.5 | 06/01/1982 – 10/29/1990 | 8.4 | 100 |
| 12181200 | Salix Creek at S Cascade Gl near Marblemount, WA | Salix Creek | USGS | Inactive | 0.08 | 01/01/1981 – 12/31/2010 | 30.0 | 66 |
| 12186000 | Sauk River above White Chuck River near Darrington, WA | Sauk River | USGS | Active | 152 | 01/01/1981 – 12/31/2010 | 30.0 | 100 |
| 12189500 | Sauk River near Sauk, WA | Sauk River | USGS | Active | 714 | 01/01/1981 – 12/31/2010 | 30.0 | 100 |
| 12178000 | Skagit River at Newhalem, WA | Skagit River | USGS | Active | 1175 | 01/01/1981 – 12/31/2010 | 30.0 | 100 |
| 12179000 | Skagit River above Alma Creek near Marblemount, WA | Skagit River | USGS | Active | 1274 | 01/01/1981 – 09/30/1995 | 14.8 | 100 |
| 12179800 | Skagit River above Bacon Creek near Marblemount, WA | Skagit River | USGS | Inactive | 1289 | 01/01/1981 – 10/25/1983 | 2.8 | 99 |
| 12181000 | Skagit River at Marblemount, WA | Skagit River | USGS | Active | 1381 | 01/01/1981 – 12/31/2010 | 30.0 | 100 |
| 12194000 | Skagit River near Concrete, WA | Skagit River | USGS | Active | 2737 | 01/01/1981 – 12/31/2010 | 30.0 | 100 |
| 12200500 | Skagit River near Mount Vernon, WA | Skagit River | USGS | Active | 3093 | 01/01/1981 – 12/31/2010 | 30.0 | 100 |
| 12181090 | South Cascade Middle Tarn near Marblemount, WA | South Cascade River | USGS | Inactive | 1.72 | 09/30/2002 – 12/14/2010 | 8.2 | 54 |

| Station Code | Station Name | Stream Name | Agency | Monitoring Status | Drainage Area as Reported ($mi^2$) | Period of Record Analyzed | Duration of Records (years) | Percentage of the Period of Record with Measurements |
|---|---|---|---|---|---|---|---|---|
| 12177500 | Stetattle Creek near Newhalem, WA | Stetattle Creek | USGS | Inactive | 22 | 01/01/1981 – 11/23/1983 | 2.9 | 100 |
| 12191800 | Sulphur Creek near Concrete, WA | Sulphur Creek | USGS | Inactive | 8.36 | 01/01/1981 – 09/29/1982 | 1.7 | 100 |
| 12190710 | Swift Creek near Concrete, WA | Swift Creek | USGS | Inactive | 36.35 | 08/01/1982 – 09/29/1990 | 8.2 | 100 |
| 12175500 | Thunder Creek near Newhalem, WA | Thunder Creek | USGS | Active | 105 | 01/01/1981 – 12/31/2010 | 30.0 | 100 |
| 12192700 | Thunder Creek near Concrete, WA | Thunder Creek | USGS | Inactive | 22.4 | 08/01/1982 – 09/29/1994 | 12.2 | 100 |
| **12197700** | Wiseman Creek near Lyman, WA | Wiseman Creek | USGS | Inactive | 3 | 01/01/1981 – 06/30/1983 | 2.5 | 100 |

# 3 Methods of Analysis

## 3.1 Baseflow Separation Techniques

Separating streamflow hydrographs into baseflow and quickflow (direct runoff) components is a common undertaking in hydrology. There are various manual and automated methods used for separating a hydrograph into baseflow and quickflow. This study utilized two automated methods: the Lyne and Hollick (1979) one-parameter, three-pass, digital filter method (cf. Ladson et al. 2013), and the USGS baseflow separation method (BFS Model; Konrad 2022).

Gaged streamflow data downloads, processing, and baseflow separation was completed via the R programming language (R Core Team 2022). All USGS streamflow gage records (42 out of 44 gages analyzed) were retrieved using the USGS' *dataRetrieval* package (De Cicco et al. 2022). Data from the two Ecology gages analyzed were supplied as fixed-width text files for each year and were imported and merged with the USGS datasets.

### 3.1.1 Lyne and Hollick Digital Filter

The Lyne and Hollick (1979) method is a one-parameter digital filtering technique that separates high-frequency signals (quickflow, or direct runoff) from low-frequency signals (baseflow). The equation is presented as follows:

$$q_t = \alpha * \; q_{t-1} + \frac{1+\alpha}{2} * \; (Q_t - Q_{t-1})$$

for $q_t > 0$, otherwise $q_t = 0$

where:

$q_t$ = the filtered direct runoff at the *t* time step

α = filter parameter ("alpha parameter")

$q_{t-1}$ = filtered direct runoff at the *t-1* time step

$Q_t$ = the total streamflow at the *t* time step

$Q_{t-1}$ = the total streamflow at the *t-1* time step

The total streamflow comes from stream gage measurement records, while the quickflow (direct runoff) is calculated, and the alpha parameter is a shape parameter that controls how the filter influences the attenuation of the streamflow hydrograph (Ladson et al. 2013). The baseflow component of streamflow is then calculated as the difference between the total streamflow ($Q_t$) and the quickflow (direct runoff; $q_t$) at the same time step.

The filter is generally run multiple times through a dataset; for example, for daily data three passes are commonly used and recommended (forward, backward, and forward with respect to time) (Ladson et al. 2013). The number of passes has been used as a calibration parameter in some studies with the objective being to match the appearance of baseflow derived from manual methods (Ladson et al. 2013). Over a single time step the $Q_t$ shifts to the calculated baseflow resulting from the first pass, then to the calculated baseflow resulting from the second pass, finally resulting in the final calculation of baseflow on the third pass. Three passes is warranted due to appearance of negative values of quickflow in some of the quickflow calculation from the first two passes, in which case those passes use the value of baseflow from the previous pass.

To reduce the warmup and cool down issues that arise as the recursive filter moves though the data, starting values were specified for each filter pass with the first and last 30 days of data being reflected at the start and end of the records, as described (with a worked example) by Ladson et al. (2013). Reflected values are just copies of the first and last 30 days of record added to the period analyzed in reverse order. The first and last measurement in the period of record are not copied/reflected. The reflected values were kept for the three filter passes, but they were excluded in the BFI calculations and calculation of summary statistics of the resulting baseflow rates. Where data are missing from the record there was no use of this reflection technique to smooth the transition of baseflow estimates for individual segments of data, but this would be a possibility. The effects of applying the reflection technique within streamflow data series where there are gaps of missing data is expected to be small overall for the gages analyzed, since a large majority of gages had either none or only a few data gaps.

For each gage, the sensitivity of baseflow quantities and BFI results to a range of alpha parameter values were tested. The Lynn-Hollick (1979) method was implemented using the R package *grwat* (Samsonov 2022) which was run for a set of six alpha parameters values (spanning nearly the same range as evaluated by Ladson et al. (2013)) according to:

$$\alpha \in \{0.900, 0.925, 0.950, 0.975, 0.980, 0.990\}$$

Resulting baseflow hydrographs with these six alpha parameter values were plotted against streamflow hydrographs at each analyzed gage and reviewed to see if baseflow estimates could be visually judged as relatively more reasonable with one alpha parameter value versus the others. The review considered whether the baseflow hydrographs were not too "spikey" during storm events and displayed smooth variation between storm events with values not sharply dropping at the end of storm events. This was utilized to aid in the determination of the most appropriate alpha value to adopt, along with review of results from a previous study (described in Ladson et al. (2013)). The most appropriate interpreted Lyne-Hollick singular alpha value to adopt has been selected as equal to 0.98, which was used in the analysis of baseflow for all 44 gages, over their entire period of record. Since the most appropriate alpha value to adopt remains an open question (cf. Ladson et al. 2013), the comparative analysis against the results from the USGS-developed Baseflow Separation Model (described in Section 3.1.2) retain the sensitivity analysis of the effects of altering the alpha value across the range from 0.90 to 0.99. In each analysis that uses a different alpha parameter value, the value was held constant across the entire analyzed period of record.

Summary statistics were prepared from the daily baseflow rates of the 44 analyzed gages for the entire period of record, resulting from implementing the Lyne-Hollick method. These statistics consist of mean daily flow, minimum daily flow, and maximum daily flow in cubic feet per second (cfs). In addition, box-and-whisker charts showing minimum, maximum, interquartile range (25th and 75th percentiles), and median (50th percentile) values of the daily baseflow rates have been generated. Total baseflow volume was divided by total streamflow volume over the period analyzed to calculate the BFI for each site. Daily statistics of BFI were also calculated and plotted as a time series on annual hydrographs for easy graphical comparisons of annual temporal-averages of seasonality in baseflow amongst the two different methods analyzed, and the various alpha parameter values tested. When calculating baseflow statistics, data were only used from days in which raw streamflow data were available.

### 3.1.2 USGS Baseflow Separation Model

The USGS-developed (Konrad 2022) Baseflow Separation (BFS) Model is the second technique employed to perform baseflow separation from daily streamflow data. The state-space method calculates baseflow as a non-linear function of upstream GW storage that allows relatively steady, non-zero baseflow. The BFS Model was originally intended to be used for forecasting baseflow (and streamflow when there is no direct runoff) for periods with no rainfall or snowmelt and estimation of residence times, in contrast to other hydrograph separation models (Konrad 2022).

The BFS Model was implemented in R (or R Studio) for this study, using code provided by the USGS (Chris Konrad, personal communication, 2023) and available at https://doi.org/10.5066/P9AIPHEP (Konrad 2020). The BFS Model relies on a set of gage-specific calibrated parameter values developed and explained in Konrad (2022). Thirteen streamflow gages analyzed in this study have not been subject to this calibration, and therefore baseflow separation using this method is not currently possible for these 13 gages.

Summary statistics were prepared from the daily baseflow rates of the 31 analyzed gages for the entire period of record, resulting from implementing the USGS BFS Model. These statistics consist of mean daily flow, minimum daily flow, and maximum daily flow in cfs. In addition, box-and-whisker charts showing minimum, maximum, interquartile range (25th and 75th percentiles), and median (50th percentile) values of the daily baseflow rates have been generated. Total baseflow volume was divided by total streamflow volume over the period analyzed to calculate the BFI for each site. Daily statistics of BFI were also calculated and plotted as a time series on annual hydrographs for easy graphical comparisons of annual temporal-averages of seasonality in baseflow—the same as was done for the Lyne-Hollick method—allowing for easy comparisons to be made between the results of the two methods. When calculating baseflow statistics, data were only used from days in which raw streamflow data were available.

## 3.2 Groundwater Recharge and Discharge Comparison

### 3.2.1 Background

Precipitation provides the vast majority of water recharging the GW system through infiltration that then percolates and reaches the water table (i.e., reaches the GW system). That water eventually travels through the GW system emerging either back to the surface via evapotranspiration (or pumping), out to sea along the coastline, or as the majority of the water does, back to surface water as GW discharge and baseflow in streams.

Based on previous studies by the USGS, an estimated 56 inches per year (in/yr) of precipitation occurs in tributary subbasins of the lower Skagit River basin (below Sedro-Woolley) with approximately 33 percent (18 in/yr) becoming recharge (Savoca et al. 2009). Groundwater recharge has also been estimated to exceed 50 in/yr in the alluvial valley around the town of Darrington (Thomas et al. 1997).

### 3.2.2 Analysis

Long-term mean baseflow (GW discharge) rates calculated in this study were compared directly to recently obtained GW recharge and precipitation rates generated as part of the Synthesis Study (Yoder et al. 2021) over the 30-year period from 1/1/1981 through 12/31/2010. Long-term gridded rates of precipitation were used in the Synthesis Study as the basis for estimating long-term, spatially explicit GW recharge, which is influenced by hydrogeologic units and surficial deposits near the land surface, and by the land cover (in this case the percentage of tree cover and impervious surface). For details on the methods used to estimate historic GW recharge rates and precipitation rates, refer to Yoder et al. (2021) and the methods document available on the "Groundwater" tab under the "Groundwater Recharge" section.

To extract data from the historic gridded GW recharge and precipitation datasets, first there was a need to delineate drainage basins associated with the gages analyzed for baseflow over the same time period (1/1/1981–12/31/2010), which is a total of 33 streamflow gaging stations (out of the 44 total gages analyzed for baseflow). Only 28 of the 33 gages could be analyzed for comparison with GW recharge using the USGS BFS Model since five (out of the 33) gages have not been calibrated by the USGS. The subbasin boundaries were generated largely using the USGS StreamStats interactive web interface (https://streamstats.usgs.gov/ss/). Gage locations were loaded to an ArcGIS Pro project on two separate layers, with 44 total gaging station locations. All data can be sourced back to the USGS and Ecology (see data sources in Section 2). On the StreamStats interface, the location of the gage was entered (latitude/longitude or gage ID if available). Then the basins were delineated based on the nearest stream location to each gage point and use of USGS 3D Elevation Program digital elevation data (with elevations conforming to the digital stream channels depicted in the high-resolution version of the National Hydrography Dataset) automatically by StreamStats, and a shapefile of each subbasin was exported. See the "User-Selected Sites" section of the USGS StreamStats "how-streamstats-works" webpage (https://www.usgs.gov/mission-areas/water-resources/how-streamstats-works) for more information. In most cases, the gage point contained a description of the stream location. During the review process, 14 gages were identified that needed verification due to misrepresented basins that did not appear to follow the expected topographic boundaries. In these cases, the subbasins were redrawn with StreamStats, using slightly varied gage locations. Using the historical USGS data, gage descriptions, and the updated coordinates, the probable pour points for each gaging station location were determined and expected drainage basin boundaries resulted. These were then compared against a world terrain basemap and listed sizes of each basin by the USGS for verification.

A spatial join was performed between each subbasin polygon and the polygon shapefile containing gridded values of GW recharge and precipitation, with the option to provide mean values selected using those grid cells that intersect subbasin polygons. The spatial join geoprocessing tool uses an input target feature: "Attributes of the target features and the attributes from the joined features will be transferred to the output feature class." The join feature input is the gridded GW recharge and precipitation polygon shapefile, where attributes from this layer are joined to the attributes of the target features; using one-to-one join operation and intersect as the match option, the attributes of the target feature were aggregated before being transferred to the output feature. Using the Field Map, the data have been aggregated using merge rules, in this case telling the tool to calculate the mean value of aggregated grid cells per intersection with each subbasin polygon.

Within each subbasin, the mean annual GW recharge from the gridded dataset was plotted against the GW discharge (baseflow) derived from the hydrograph separation of the two methods (Lyne-Hollick and BFS Model) with all six of the Lyne-Hollick alpha parameters analyzed. These comparisons provide the basis for identifying discrepancies in these important GW budget components, and the basis for initial interpretations of the causes of those discrepancies. Methods for the comparison of GW recharge and discharge follow closely from the analysis performed on 157 streamflow gaging stations in the Appalachian Valley and Ridge, Blue Ridge, and Piedmont physiographic provinces of the eastern United States, for the period of 1981 through 1990 by the USGS (Rutledge 1998).

# 4 Results

## 4.1 Streamflow and Separated Baseflow Rates

### 4.1.1 Streamflow Statistics

The basis by which baseflow rates are compared and derived is the measured streamflow. The summary statistics for streamflow rates, over the entire period of record, consist of mean daily flow, minimum daily flow, maximum daily flow, river regime coefficient (ratio of maximum and minimum flows), and coefficient of variation (ratio of standard deviation to the mean). Table 3 summarizes various flow statistics calculated using all of the available mean daily streamflow data (in cfs) for each analyzed gaging station. Refer to Table 1 for a listing of period of record, duration, and completeness of each gage’s records. The summary provided in Table 3 also includes results for both measured streamflow and estimated baseflow rates for the two techniques used—more detailed results are described in the following subsections. It is also noted that records displayed in Table 3 have been sorted first by stream name and then by station code (as they have been for Table 1 and Table 2). A total of six gages are located within the Tasks 200, 400, and 500 study area: 03J100, 12197700, 12197680, 12197040, 12197110, and 12196000, which have been identified in bold in Table 3.

A wide variety of subbasins exist within the Skagit River basin in terms of the subbasin sizes and streamflow rates. The mean daily streamflow rates among the 44 gages analyzed, over each gage’s entire period of record, range from 0.6 to over 16,600 cfs. These streamflow rates at the gaged subbasins generally correlate well with basin size, which range from 0.08 to 3,093 square miles. The streams analyzed also vary greatly with respect to their “flashiness,” as revealed by the large range of river regime coefficient and coefficient of variation statistics (Table 3). The maximum river regime coefficient is 7,300, with a mean of 635 (with four gages unable to yield calculations since the minimum measured streamflow rates were equal to zero). The maximum coefficient of variation is 2.15, with a mean of 0.98.

Table 3. Flow statistics for the analyzed period of record for all analyzed streamflow gaging stations.

| Station Code | River Regime Coefficient | Coefficient of Variation | Measured Streamflow (cfs) | | | Baseflow (cfs) (Lyne-Hollick, $\alpha$ = 0.98) | | | Baseflow (cfs) (USGS BFS Model) | | |
|---|---|---|---|---|---|---|---|---|---|---|---|
| | | | Mean | Min. | Max. | Mean | Min. | Max. | Mean | Min. | Max. |
| **12196000** | 128.2 | 0.94 | 35.4 | 4.5 | 577 | 19.5 | 1.1 | 45.8 | N/A | N/A | N/A |
| 12179900 | 133.5 | 0.92 | 448.1 | 56.8 | 12500 | 241.0 | 29.0 | 501.2 | 223.0 | 60.7 | 403.0 |
| 12190400 | 99.9 | 0.93 | 808.2 | 86.4 | 9670 | 386.1 | 86.4 | 797.0 | 638.2 | 54.7 | 1521.8 |
| 12193400 | 933.3 | 0.67 | 2662.7 | 30.0 | 28000 | 1550.3 | 30.0 | 3065.4 | 133.5 | 66.6 | 475.4 |
| 12193500 | 933.3 | 0.67 | 2636.1 | 30.0 | 28000 | 1543.7 | 30.0 | 3065.4 | 121.2 | 41.4 | 2013.3 |
| 12192600 | 200 | 1.15 | 84.8 | 5.1 | 1020 | 38.7 | 4.1 | 85.7 | 41.6 | 3.2 | 104.8 |
| 12172000 | 58.9 | 0.82 | 420.3 | 64.0 | 10800 | 227.0 | 56.0 | 471.6 | N/A | N/A | N/A |
| **12197680** | 7300 | 1.80 | 2.6 | 0.0 | 73 | 0.9 | 0.0 | 3.0 | N/A | N/A | N/A |
| 12200684 | 2457.1 | 2.15 | 6.4 | 0.1 | 172 | 1.8 | 0.1 | 6.5 | 1.8 | 0.1 | 9.0 |
| 12200690 | N/A (Min. flow: 0 cfs) | 1.77 | 20.2 | 0.0 | 233 | 2.9 | 0.0 | 9.6 | N/A | N/A | N/A |
| 12181100 | 3200 | 1.11 | 29.2 | 0.1 | 384 | 10.7 | 0.1 | 49.2 | 3.0 | 2.3 | 16.4 |
| 12182500 | 149.2 | 0.81 | 1049.0 | 118.0 | 17600 | 586.7 | 105.8 | 1411.0 | 562.4 | 111.9 | 1679.3 |
| 12185300 | 338.3 | 1.15 | 32.5 | 2.1 | 900 | 14.9 | 2.1 | 32.4 | 20.5 | 1.6 | 54.8 |
| 12200701 | 173.9 | 1.10 | 7.1 | 0.2 | 40 | 2.5 | 0.1 | 7.5 | 3.6 | 0.1 | 13.8 |
| **03J100** | 46.3 | 0.63 | 19.0 | 0.5 | 155 | 9.3 | 0.5 | 25.4 | N/A | N/A | N/A |
| 12184200 | 18.9 | 0.71 | 213.8 | 83.0 | 1570 | 113.1 | 16.3 | 191.5 | N/A | N/A | N/A |
| 12184500 | 32.4 | 0.75 | 259.7 | 66.0 | 2140 | 149.4 | 12.7 | 244.5 | 184.5 | 54.5 | 453.3 |

| Station Code | River Regime Coefficient | Coefficient of Variation | Measured Streamflow (cfs) | | | Baseflow (cfs) (Lyne-Hollick, $\alpha$ = 0.98) | | | Baseflow (cfs) (USGS BFS Model) | | |
|---|---|---|---|---|---|---|---|---|---|---|---|
| | | | Mean | Min. | Max. | Mean | Min. | Max. | Mean | Min. | Max. |
| **12197110** | N/A (Min. flow: 0 cfs) | 1.77 | 5.7 | 0.0 | 150 | 1.7 | 0.0 | 11.2 | N/A | N/A | N/A |
| 12178100 | 368.1 | 1.00 | 177.4 | 17.5 | 5300 | 89.5 | 17.5 | 234.9 | 89.0 | 15.8 | 225.6 |
| 12199600 | 4583.3 | 1.25 | 46.1 | 0.1 | 275 | 14.5 | 0.1 | 51.3 | 25.0 | 0.1 | 125.4 |
| 03G100 | 466.4 | 0.87 | 72.9 | 0.0 | 968 | 28.0 | 0.0 | 86.9 | N/A | N/A | N/A |
| 12190718 | 90.6 | 0.88 | 121.7 | 12.0 | 1350 | 61.7 | 12.0 | 128.4 | 91.9 | 22.5 | 159.5 |
| 12173500 | 140.4 | 1.17 | 702.9 | 49.0 | 6880 | 289.6 | 41.9 | 929.7 | N/A | N/A | N/A |
| 12181200 | N/A (Min. flow: 0 cfs) | 1.55 | 0.6 | 0.0 | 18.1 | 0.2 | 0.0 | 0.9 | 0.1 | 0.0 | 0.6 |
| 12186000 | 287.2 | 0.92 | 1134.0 | 90.0 | 40000 | 583.5 | 45.2 | 1537.1 | 643.6 | 74.0 | 2090.7 |
| 12189500 | 120.9 | 0.81 | 4376.2 | 578.0 | 69900 | 2526.4 | 352.9 | 5892.9 | 2301.6 | 521.8 | 5663.2 |
| 12178000 | 311.8 | 0.64 | 4470.6 | 136.0 | 42400 | 3004.2 | 136.0 | 5997.3 | 2523.5 | 1082.4 | 2534.9 |
| 12179000 | 31.4 | 0.51 | 5368.4 | 1110.0 | 38200 | 3878.1 | 610.7 | 6789.0 | 4480.8 | 1294.9 | 4749.7 |
| 12179800 | 23.3 | 0.48 | 4928.2 | 1080.0 | 25200 | 3393.9 | 381.8 | 5311.3 | 4085.9 | 1775.3 | 6506.3 |
| 12181000 | 46.0 | 0.50 | 6126.8 | 1190.0 | 54700 | 4495.4 | 378.4 | 8154.9 | 3830.7 | 1503.1 | 6839.9 |
| 12187500 | 103.1 | 0.93 | 2034.1 | 262.0 | 27000 | 1079.7 | 203.5 | 2388.9 | 1093.7 | 228.0 | 2264.4 |
| 12194000 | 55.9 | 0.60 | 15101.5 | 2360.0 | 135000 | 10145.1 | 1894.3 | 20342.7 | 11599.9 | 1588.7 | 33580.6 |
| 12199000 | 70.0 | 0.74 | 16035.0 | 2830.0 | 198000 | 9705.6 | 1976.7 | 18457.6 | N/A | N/A | N/A |
| 12200500 | 45.3 | 0.56 | 16661.3 | 3050.0 | 142000 | 11479.0 | 1958.1 | 21647.5 | 10614.5 | 3271.4 | 19720.5 |
| 12181090 | 748.7 | 0.75 | 32.5 | 0.4 | 277 | 16.6 | 0.4 | 34.7 | 6.8 | 0.1 | 11.8 |

| Station Code | River Regime Coefficient | Coefficient of Variation | Measured Streamflow (cfs) | | | Baseflow (cfs) (Lyne-Hollick, α = 0.98) | | | Baseflow (cfs) (USGS BFS Model) | | |
|---|---|---|---|---|---|---|---|---|---|---|---|
| | | | Mean | Min. | Max. | Mean | Min. | Max. | Mean | Min. | Max. |
| 12177500 | 460 | 0.98 | 183.8 | 9.0 | 4140 | 89.8 | 9.0 | 237.4 | 104.7 | 24.5 | 302.5 |
| 12188380 | 26.7 | 0.65 | 1740.3 | 351.0 | 9360 | 1017.0 | 258.6 | 1945.7 | 1228.3 | 355.5 | 2888.3 |
| 12191800 | 40 | 0.65 | 43.6 | 15.0 | 600 | 28.6 | 3.0 | 45.9 | 28.8 | 8.8 | 59.9 |
| 12190710 | 104.2 | 0.90 | 415.4 | 40.0 | 5000 | 209.0 | 40.0 | 412.0 | N/A | N/A | N/A |
| **12197040** | N/A (Min. flow: 0 cfs) | 1.71 | 2.3 | 0.0 | 65 | 0.8 | 0.0 | 3.7 | N/A | N/A | N/A |
| 12175500 | 180.6 | 0.88 | 624.3 | 50.0 | 9030 | 312.7 | 42.0 | 886.7 | 266.6 | 34.1 | 527.1 |
| 12192700 | 145.5 | 0.90 | 132.3 | 11.0 | 2300 | 68.7 | 7.1 | 157.3 | 68.3 | 8.1 | 188.6 |
| 12186450 | 24.9 | 0.75 | 570.9 | 126.0 | 3140 | 268.6 | 38.1 | 518.9 | N/A | N/A | N/A |
| **12197700** | 714.3 | 1.52 | 13.4 | 0.7 | 500 | 5.9 | 0.7 | 16.6 | 6.8 | 0.7 | 21.2 |

Note: N/A values cannot be calculated for the BFS Model because the model has not been calibrated at these gages.

### 4.1.2 Baseflow from the Lyne and Hollick Digital Filter

The Lyne and Hollick (1979) digital filter method was used to estimate baseflow rates for all 44 analyzed streamflow gages. Table 3 presents a listing of some key summary statistics (mean, minimum, maximum) of the total measured streamflow alongside the Lyne-Hollick estimates of baseflow in units of cfs, with alpha equal to 0.98, for each gage's available period of record. A wide variation of estimated baseflow rates result from the separation using the Lyne-Hollick digital filter (with alpha equal to 0.98). The estimated mean daily baseflow rates amongst the 44 gages analyzed, over each gage's entire period of record, range from 0.2 to over 11,400 cfs.

It is noted that the Lyne-Hollick estimated baseflow statistics presented in Table 3 only represent those derived using an alpha parameter value of 0.98. This value has been adopted as the most reasonable value of alpha based upon two points of consideration: 1) visual review of the plotted baseflow and streamflow hydrographs; and 2) The value of 0.98 for alpha has been adopted in a baseflow assessment of 141 streams in the Murray-Darling Basin (CSIRO and SKM 2010), and an alpha value of 0.98 produced a better match to BFI derived from chemical tracer estimates than the commonly adopted value of 0.925 (CSIRO and SKM 2012).

A sensitivity analysis of the Lyne-Hollick alpha parameter was completed for values within the range of 0.90 and 0.99. As an example, the sensitivity of BFI estimates for USGS station 12175500 (Thunder Creek near Newhalem), based on daily baseflow separation over the timer period from 1/1/1981 through 12/31/2010, are presented in Table 4, while year 2000 streamflow and baseflow estimates for the same gage with the various alpha parameter values are illustrated on a hydrograph in Figure 2. There is nothing particularly special about the gage presented in this example, other than it showcases well how the baseflow separation varies amongst the tested alpha parameter values. Calculated BFI values decline monotonically as alpha increases, as the portion of streamflow that is comprised of GW discharge (baseflow) decreases. There are instances, or portions of the annual hydrograph, where baseflow rates do not follow this relationship, such as during mid-March to mid-May in 2000, as shown in Figure 2, despite the BFI values decreasing with increasing alpha values.

Statistics of the daily estimates of baseflow rates for the Lyne-Hollick method, using all six different alpha parameter values, are presented on box and whisker charts in Appendix A for ease of comparison of the effects of varying alpha on the estimates of baseflow. The box and whisker plots provide the minimum, maximum, interquartile range (25th and 75th percentile), and median (50th percentile) values for each gage, including the entire period of record. These plots reveal at that there are not considerably drastic differences amongst estimated baseflow statistics caused by varying the alpha parameter. In addition, there are some findings that are nearly universal across all analyzed gaging stations: 1) the smallest alpha parameter value yields the largest baseflow estimates, and either 0.98 or 0.99—the two largest alpha parameter values—yield the smallest baseflow estimates; and 2) the largest range of baseflow estimates (as indicated by the interquartile range) results from the smallest alpha value.

**Table 4. Baseflow indices (BFI) estimates with various Lyne-Hollick alpha parameter ($\alpha$) values for the period from 1/1/1981 through 12/31/2010.** (USGS Station 12175500, Thunder Creek near Newhalem)

| $\alpha$ | BFI |
|---|---|
| 0.900 | 0.71 |
| 0.925 | 0.68 |
| 0.950 | 0.63 |
| 0.975 | 0.53 |
| 0.980 | 0.50 |
| 0.990 | 0.45 |

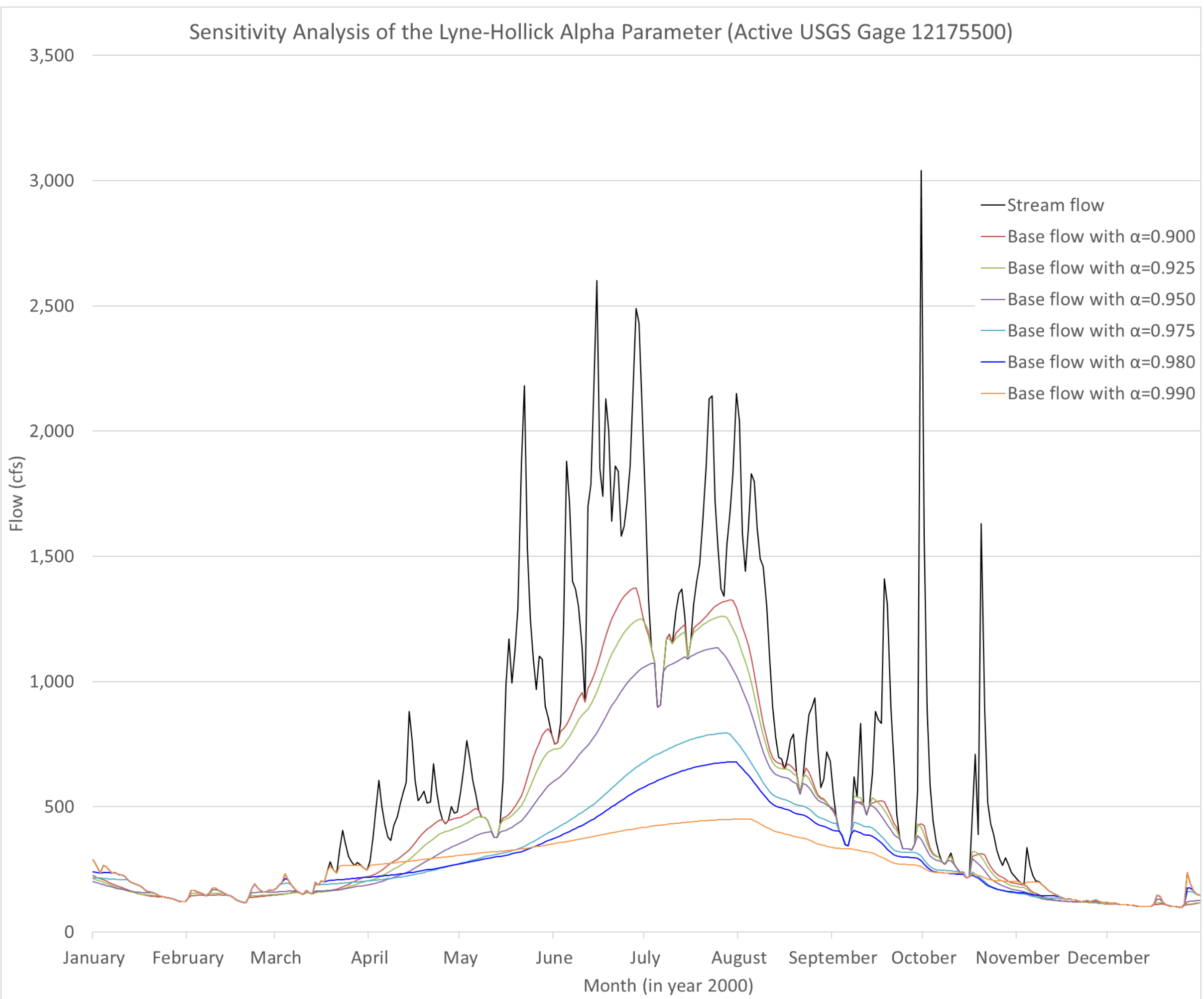


**Figure 2. Streamflow and separated baseflow hydrographs for USGS Station 12175500 (Thunder Creek near Newhalem) for year 2000 indicating the sensitivity of baseflow estimates to various Lyne-Hollick alpha parameter values.**

### 4.1.3 Baseflow from the USGS Baseflow Separation Model

The USGS (Konrad 2022) BFS Model was used to estimate baseflow rates and BFI for 31 analyzed streamflow gages. A total of 13 gages analyzed with the Lyne-Hollick digital filter method could not be analyzed using the BFS Model because BFS Model calibration parameters have not been developed (Chris Konrad, personal communication, 2023). Table 3 presents a listing of some key summary statistics (mean, minimum, maximum) of the total measured streamflow alongside the BFS Model estimates of baseflow in units of cfs and also compared alongside the Lyne-Hollick estimates of baseflow, for each gage's available period of record. A wide variation of estimated baseflow rates result from the separation using the BFS Model. The estimated mean daily baseflow rates amongst the 31 gages analyzed, over each gage's entire period of record, range from 0.1 to 11,600 cfs.

Statistics of the daily estimates of baseflow rates for the BFS Model (using calibration parameters generated by the USGS (Konrad 2022), are presented on box and whisker charts in Appendix A for ease of comparison against the Lyne-Hollick estimated baseflow (including the alpha parameter values evaluated). It is noted that the plots displayed in Appendix A have been sorted to be displayed the same as the gages are listed in Table 1 and Table 3, first by stream name and then by station code. Refer to Table 1 to see the stream and gaging stations names associated with each station code.

The box and whisker plots (Appendix A) provide the minimum, maximum, interquartile range (25th and 75th percentile), and median (50th percentile) values for each gage, including the entire period of record. These plots reveal at that in general the BFS Model generates baseflow estimates that are of similar magnitude and spread (interquartile range) as estimates generated using the Lyne-Hollick method, with little tendency for the median baseflow rates to be smaller than or larger than the rates from the Lyne-Hollick method. Out of the 31 gaging stations that allow for the methods to be compared directly, a small number (seven) have BFS Model median or interquartile ranges of estimated daily baseflow that differ substantially from the estimates using the Lyne-Hollick method, based solely on a visual comparison of the charts presented in Appendix A; these gaging stations are listed as follows:

- 12178000 (Skagit River at Newhalem)
- 12179000 (Skagit River above Alma Creek near Marblemount)
- 12181000 (Skagit River at Marblemount)
- 12181090 (South Cascade Middle Tarn near Marblemount)
- 12181100 (South Fork Cascade River at S. Cascade Gl. near Marblemount)
- 12193400 (Baker River at Henry Thompson Bridge at Concrete)
- 12193500 (Baker River at Concrete)

There exist some notable differences in minimum baseflow values generated using the BFS Model are much larger than those using the Lyne-Hollick method. These few notable gages where this discrepancy is largest are listed as follows:

- 12178000 (Skagit River at Newhalem)
- 12179000 (Skagit River above Alma Creek near Marblemount)

- 12179800 (Skagit River above Bacon Creek near Marblemount)
- 12181000 (Skagit River at Marblemount)
- 12200500 (Skagit River near Mount Vernon)

For the most downstream gage analyzed, station 12200500 (Skagit River near Mount Vernon), which represents the largest drainage area analyzed and nearly the entire Basin, the mean daily baseflow estimated from the BFS Model equals 10,615 cfs. This is only slightly lower than the mean baseflow estimate from the Lyne-Hollick method ($\alpha$ = 0.98), which is 11,479 cfs. More comparisons between the methods are described in the next section with respect to the baseflow index.

## 4.2 Comparison of Baseflow Index from the Lyne-Hollick Method and Baseflow Separation Model

A comparison of the BFI values calculated by both the Lynn-Hollick method (with various alpha parameters) and the USGS BFS Model is shown in Figure 3 and Table 5 by gaging station. For both methods, the BFI calculation was done over the entire period of record available at each gage, taken as the ratio between the total volume of baseflow divided by the total volume of streamflow. Gages are separated by their respective stream for ease of comparison in Figure 3 and have been grouped by stream in Table 5. A total of six gages are located within the Tasks 200, 400, and 500 study area: 03J100, 12197700, 12197680, 12197040, 12197110, and 12196000, which have been identified in bold in Table 5.

A wide variation of estimated BFI values result from the separations using the BFS Model and Lyne-Hollick method. The range of BFI values using the BFS Model (for the 31 gages analyzed) is from 0.09 to 0.87, with a mean value of 0.61. By way of comparison the range of BFI values using the Lyne-Hollick method (for the 31 gages that could be analyzed using the BFS Model), with alpha equal to 0.98, is from 0.27 to 0.73, with a mean value of 0.53. Amongst the entirety of gages (n = 44) analyzed using the Lyne-Hollick method, the range of BFI values, with alpha equal to 0.98, is from 0.15 to 0.73, with a mean value of 0.50.

In general, the resulting BFI from the two techniques compare relatively well with each other; the mean difference, taking the BFS Model minus the Lyne-Hollick (with alpha equal to 0.98) BFI values is 0.08. The mean of the absolute differences between BFI values from the two methods range from 0.14 to 0.20 across all six of the tested Lyne-Hollick parameter values. There are some notable exceptions where the two techniques yield vast differences in BFI values, particularly the Baker River gages downstream of the lowermost dam (12193400 and 12193500) where the Lyne-Hollick method yielded BFI values that are between 5.7 and 7.4 times larger than those resulting from the BFS Model. Three other gaging stations are exceptions, including those with relative percent differences between the two methods (again with the Lyne-Hollick alpha parameter value equal to 0.98) exceeding 50 percent; these gages include those on the South Fork Cascade River (12181100), South Cascade River (12181090), and Nookachamps Creek (12199600).

A comparison of the seasonality of the BFI on an annual basis is shown in Figure 4, which compares the median BFI calculated for each day in the period of record across all gages on a given stream using the BFS Model and the Lynn-Hollick method (alpha equal to 0.98). As is evident in Figure 4, some streams (e.g., Baker River and Elliot Creek) show relatively poor agreement between the two methods, whereas others (e.g., Bacon Creek and Salix Creek) show much higher agreement. A similar comparison of methods is shown in Figure 5, where a time series showing seasonality on annual hydrographs of the daily BFI statistics (median, interquartile range, and minimum and maximum range for all gages pooled together) comparing the BFS Model and the Lyne-Hollick method with all six tested alpha parameter values, including all gages. Appendix B provides method (and alpha parameter) comparison charts that are in the same format as presented in Figure 5, but that have been generated for each individual gaging station analyzed with results from both methods (a total of 31 gages with records analyzed over the entire period of record).

The charts in Appendix B, the same as in Figure 5, display the daily BFI statistics (median, interquartile range, and minimum and maximum range) comparing the BFS Model and the Lyne-Hollick method with all six tested alpha parameter values. Figure 4 and Figure 5, and the charts presented in Appendix B, indicate seasonality of the BFI that is marked by two periods with lower BFI, including the periods between about mid-May through August, and from about November through mid-December. These results generally agree with the findings of Savoca et al. (2009) that baseflow increases in the late summer and early fall when GW discharge sustains streamflow and also indicate that during periods of higher streamflow the BFI ratio is reduced. In addition, based on Figure 5, it is apparent how the sensitivity of the alpha parameter value alters the seasonal variability of the daily BFI values, with an increase in variability for higher alpha values.

The spatial variability of the calculated BFI values has been mapped to the gaging stations for both methods over the entire period of record analyzed (records between 1908 and 2021). Figure 6 displays the BFI results using the Lyne-Hollick method with alpha equal to 0.98, for the 44 gages analyzed. Figure 7 displays the BFI results using the BFS Model for the 31 gages analyzed. It becomes readily apparent from these maps that the BFI values from the BFS Model are generally higher than those resulting from the Lyne-Hollick method, which is in-line with the mean difference of BFI reported above.

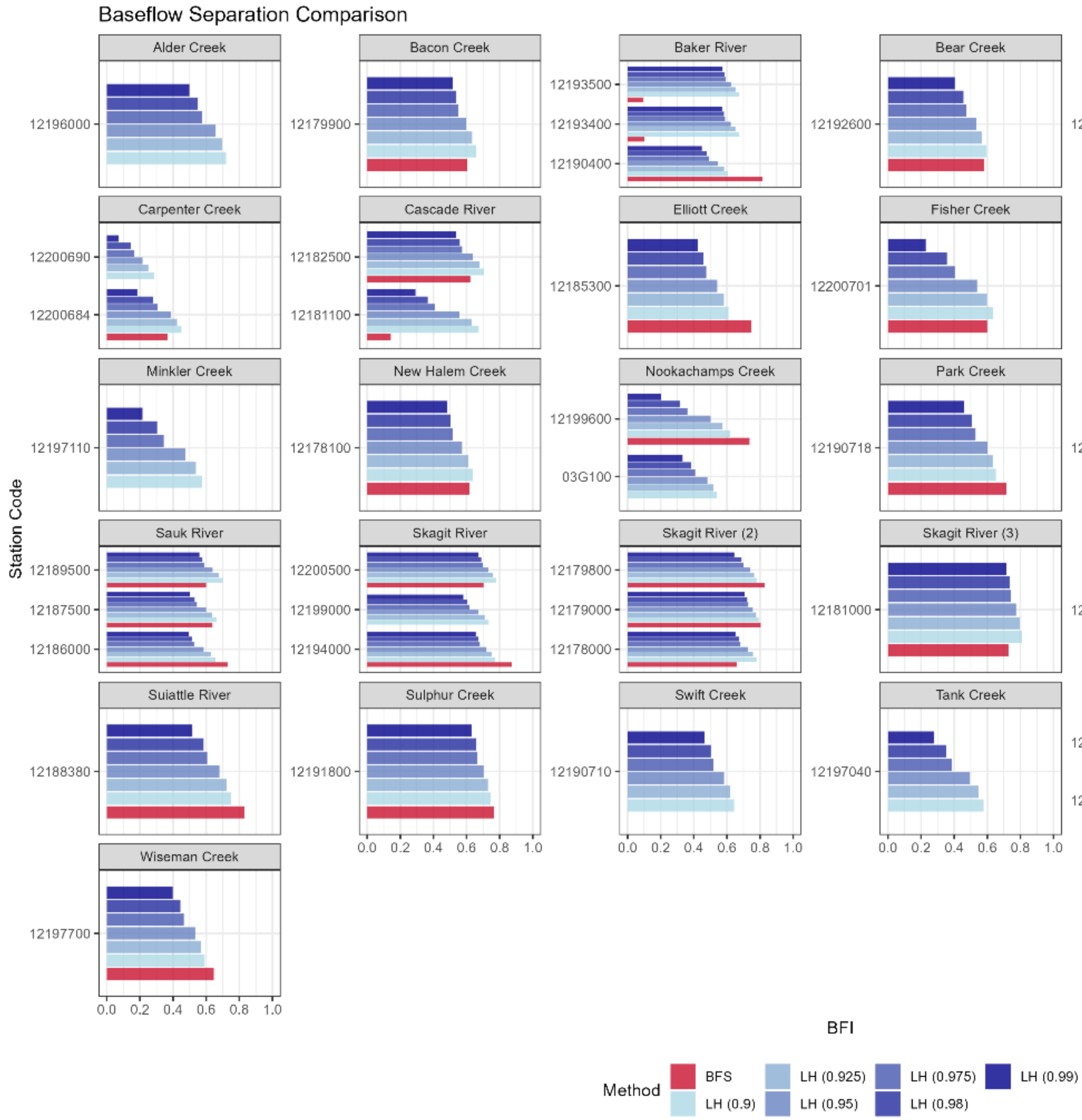


**Figure 3. Baseflow index method comparison by stream.**

**Table 5. Baseflow Indices by method for all streamflow gaging stations.**

| Station Code | Stream Name | Baseflow Index (Total Baseflow Divided by Total Streamflow) | | | | | | |
|---|---|---|---|---|---|---|---|---|
| | | BFS Model | Lyne and Hollick | | | | | |
| | | | α = 0.900 | α = 0.925 | α = 0.950 | α = 0.975 | α = 0.980 | α = 0.990 |
| **12196000** | Alder Creek | N/A | 0.72 | 0.70 | 0.66 | 0.58 | 0.55 | 0.50 |
| 12179900 | Bacon Creek | 0.60 | 0.66 | 0.63 | 0.60 | 0.55 | 0.54 | 0.52 |
| 12190400 | Baker River | 0.81 | 0.61 | 0.58 | 0.55 | 0.49 | 0.48 | 0.45 |
| 12193400 | Baker River | 0.10 | 0.67 | 0.65 | 0.62 | 0.59 | 0.58 | 0.57 |
| 12193500 | Baker River | 0.09 | 0.67 | 0.65 | 0.62 | 0.59 | 0.59 | 0.57 |
| 12192600 | Bear Creek | 0.58 | 0.59 | 0.57 | 0.53 | 0.47 | 0.46 | 0.40 |
| 12172000 | Big Beaver Creek | N/A | 0.70 | 0.68 | 0.63 | 0.56 | 0.54 | 0.51 |
| **12197680** | Black Creek | N/A | 0.50 | 0.47 | 0.44 | 0.38 | 0.36 | 0.31 |
| 12200684 | Carpenter Creek | 0.37 | 0.45 | 0.42 | 0.39 | 0.31 | 0.28 | 0.18 |
| 12200690 | Carpenter Creek | N/A | 0.28 | 0.25 | 0.22 | 0.17 | 0.15 | 0.07 |
| 12181100 | Cascade River | 0.14 | 0.67 | 0.63 | 0.56 | 0.41 | 0.37 | 0.29 |
| 12182500 | Cascade River | 0.62 | 0.71 | 0.68 | 0.64 | 0.57 | 0.56 | 0.54 |
| 12185300 | Elliott Creek | 0.75 | 0.61 | 0.58 | 0.54 | 0.48 | 0.46 | 0.42 |
| 12200701 | Fisher Creek | 0.60 | 0.63 | 0.60 | 0.54 | 0.40 | 0.36 | 0.23 |
| **03J100** | Hansen Creek | N/A | 0.69 | 0.66 | 0.62 | 0.52 | 0.49 | 0.43 |
| 12184200 | Illabot Creek | N/A | 0.73 | 0.70 | 0.67 | 0.57 | 0.53 | 0.37 |
| 12184500 | Illabot Creek | 0.83 | 0.71 | 0.69 | 0.65 | 0.59 | 0.58 | 0.52 |

| Station Code | Stream Name | Baseflow Index (Total Baseflow Divided by Total Streamflow) | | | | | | |
|---|---|---|---|---|---|---|---|---|
| | | BFS Model | Lyne and Hollick | | | | | |
| | | | α = 0.900 | α = 0.925 | α = 0.950 | α = 0.975 | α = 0.980 | α = 0.990 |
| **12197110** | Minkler Creek | N/A | 0.58 | 0.54 | 0.48 | 0.34 | 0.30 | 0.22 |
| 12178100 | Newhalem Creek | 0.62 | 0.64 | 0.61 | 0.57 | 0.52 | 0.50 | 0.48 |
| 12199600 | Nookachamps Creek | 0.74 | 0.62 | 0.57 | 0.50 | 0.36 | 0.32 | 0.20 |
| 03G100 | Nookachamps Creek | N/A | 0.54 | 0.52 | 0.48 | 0.41 | 0.38 | 0.33 |
| 12190718 | Park Creek | 0.71 | 0.65 | 0.63 | 0.60 | 0.53 | 0.51 | 0.46 |
| 12173500 | Ruby Creek | N/A | 0.67 | 0.62 | 0.54 | 0.43 | 0.41 | 0.38 |
| 12181200 | Salix Creek | 0.29 | 0.49 | 0.45 | 0.38 | 0.29 | 0.27 | 0.24 |
| 12186000 | Sauk River | 0.73 | 0.66 | 0.63 | 0.58 | 0.53 | 0.51 | 0.49 |
| 12189500 | Sauk River | 0.60 | 0.70 | 0.68 | 0.64 | 0.59 | 0.58 | 0.56 |
| 12178000 | Sauk River | 0.66 | 0.78 | 0.76 | 0.73 | 0.68 | 0.67 | 0.65 |
| 12179000 | Skagit River | 0.80 | 0.79 | 0.78 | 0.76 | 0.73 | 0.72 | 0.71 |
| 12179800 | Skagit River | 0.83 | 0.78 | 0.76 | 0.74 | 0.70 | 0.69 | 0.64 |
| 12181000 | Skagit River | 0.73 | 0.81 | 0.80 | 0.77 | 0.74 | 0.73 | 0.71 |
| 12187500 | Skagit River | 0.64 | 0.66 | 0.64 | 0.60 | 0.54 | 0.53 | 0.50 |
| 12194000 | Skagit River | 0.87 | 0.77 | 0.75 | 0.72 | 0.68 | 0.67 | 0.66 |
| 12199000 | Skagit River | N/A | 0.73 | 0.71 | 0.67 | 0.62 | 0.61 | 0.58 |
| 12200500 | Skagit River | 0.70 | 0.78 | 0.76 | 0.73 | 0.70 | 0.69 | 0.67 |
| 12181090 | South Cascade River | 0.31 | 0.67 | 0.64 | 0.59 | 0.53 | 0.51 | 0.47 |

| Station Code | Stream Name | Baseflow Index (Total Baseflow Divided by Total Streamflow) | | | | | | |
|---|---|---|---|---|---|---|---|---|
| | | BFS Model | Lyne and Hollick | | | | | |
| | | | $\alpha = 0.900$ | $\alpha = 0.925$ | $\alpha = 0.950$ | $\alpha = 0.975$ | $\alpha = 0.980$ | $\alpha = 0.990$ |
| 12177500 | Stetattle Creek | 0.66 | 0.63 | 0.61 | 0.57 | 0.50 | 0.49 | 0.46 |
| 12188380 | Suiattle River | 0.83 | 0.75 | 0.72 | 0.68 | 0.61 | 0.58 | 0.52 |
| 12191800 | Sulphur Creek | 0.76 | 0.75 | 0.73 | 0.70 | 0.67 | 0.66 | 0.63 |
| 12190710 | Swift Creek | N/A | 0.64 | 0.62 | 0.58 | 0.52 | 0.50 | 0.47 |
| **12197040** | Tank Creek | N/A | 0.58 | 0.55 | 0.50 | 0.39 | 0.35 | 0.28 |
| 12175500 | Thunder Creek | 0.54 | 0.71 | 0.68 | 0.63 | 0.53 | 0.50 | 0.45 |
| 12192700 | Thunder Creek | 0.62 | 0.66 | 0.64 | 0.60 | 0.54 | 0.52 | 0.48 |
| 12186450 | White Chuck River | N/A | 0.69 | 0.66 | 0.62 | 0.51 | 0.47 | 0.31 |
| **12197700** | Wiseman Creek | 0.65 | 0.59 | 0.57 | 0.53 | 0.46 | 0.44 | 0.40 |

Note: N/A values cannot be calculated for the BFS Model because the model has not been calibrated at these gages.


**Figure 4. Median daily BFI method comparison by stream including all gages and all years (the Lyne-Hollick method alpha parameter value equals 0.98).**

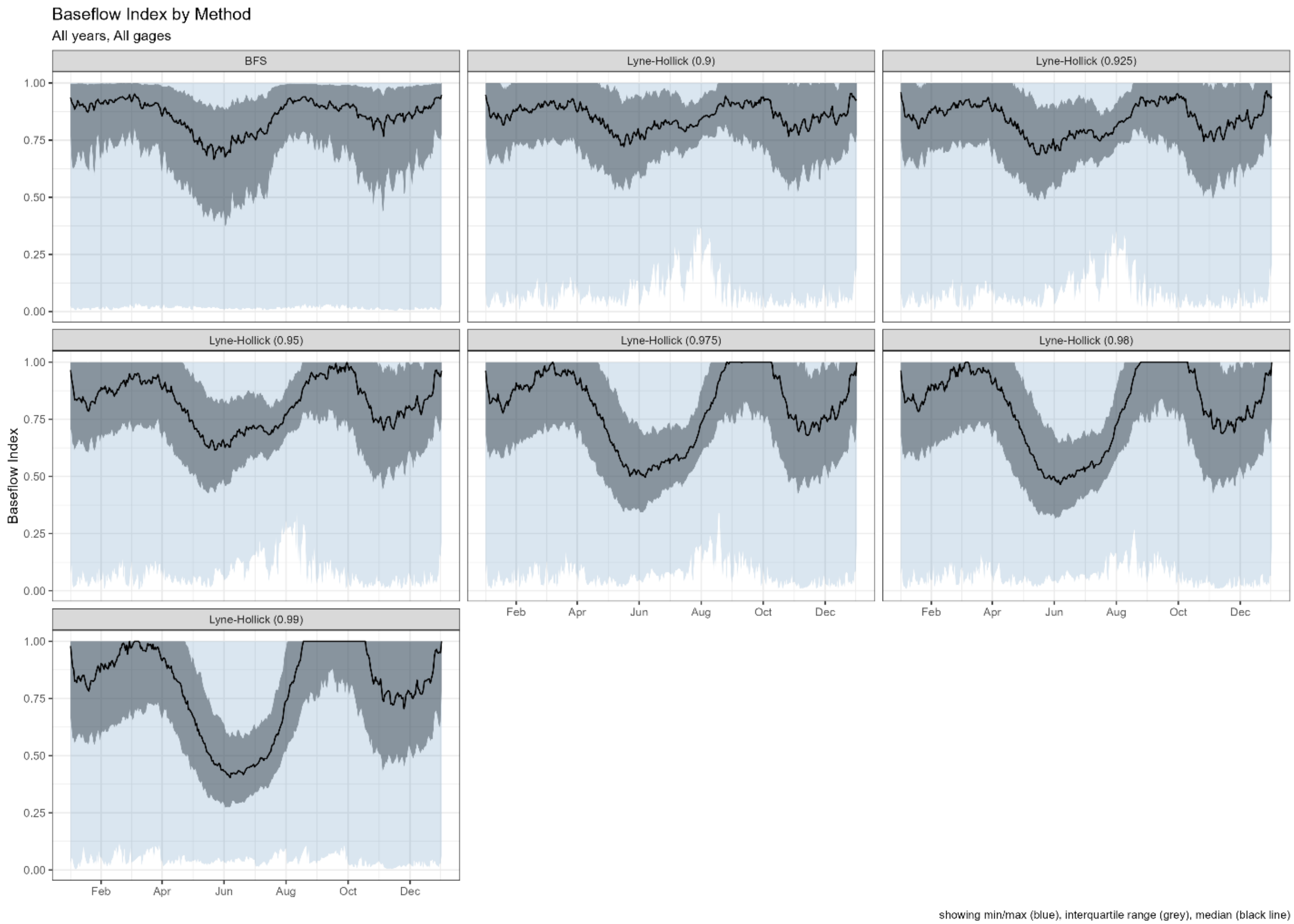


**Figure 5. Time series of annual hydrographs of daily BFI statistics comparing the BFS Model and Lyne-Hollick method with alpha ranging from 0.90 to 0.99 including all gages and all years.**

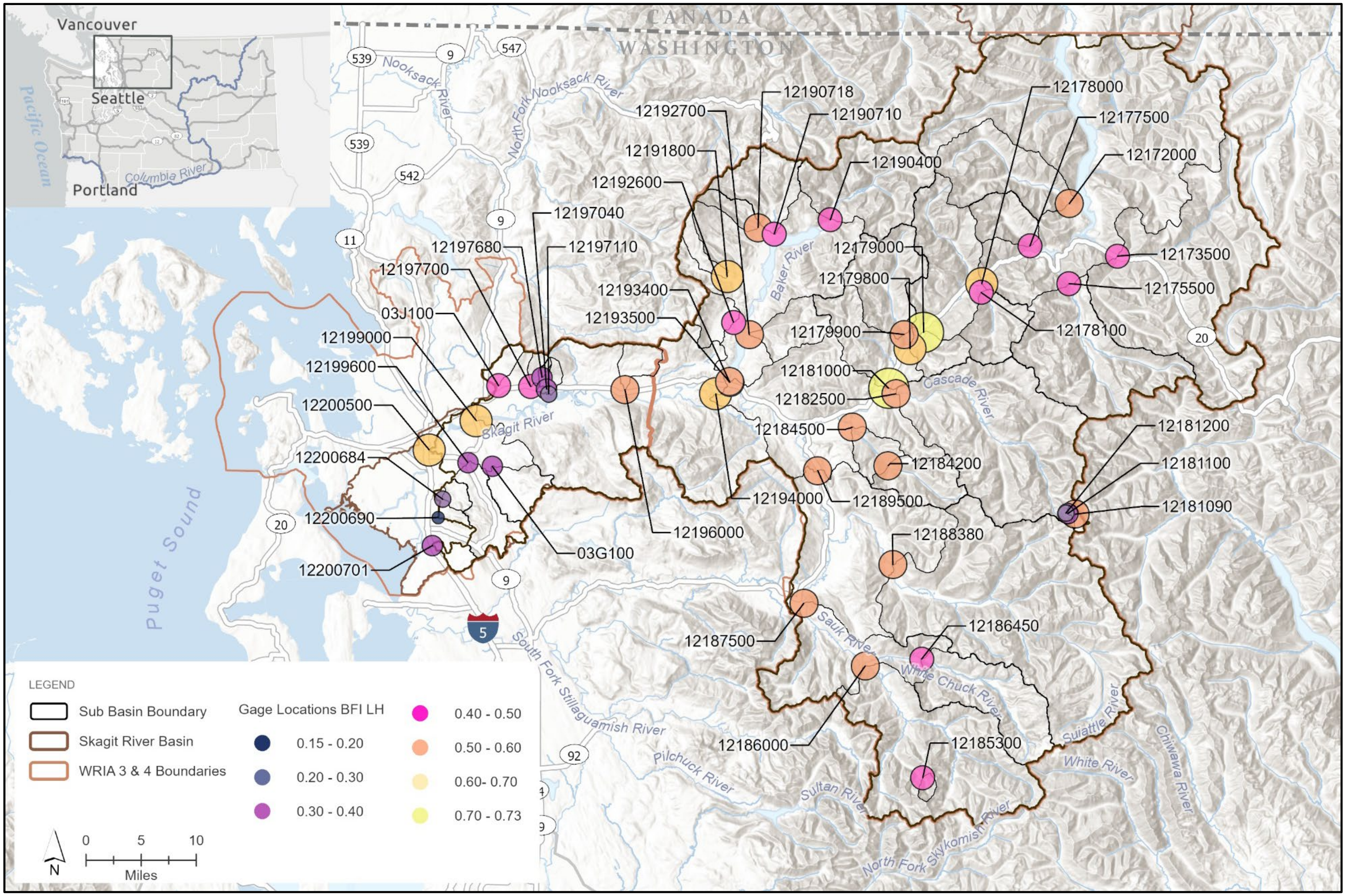


**Figure 6. Map of Baseflow Index (BFI) results by gage using the Lyne-Hollick method (alpha parameter equals 0.98) for the entire analyzed time period.**

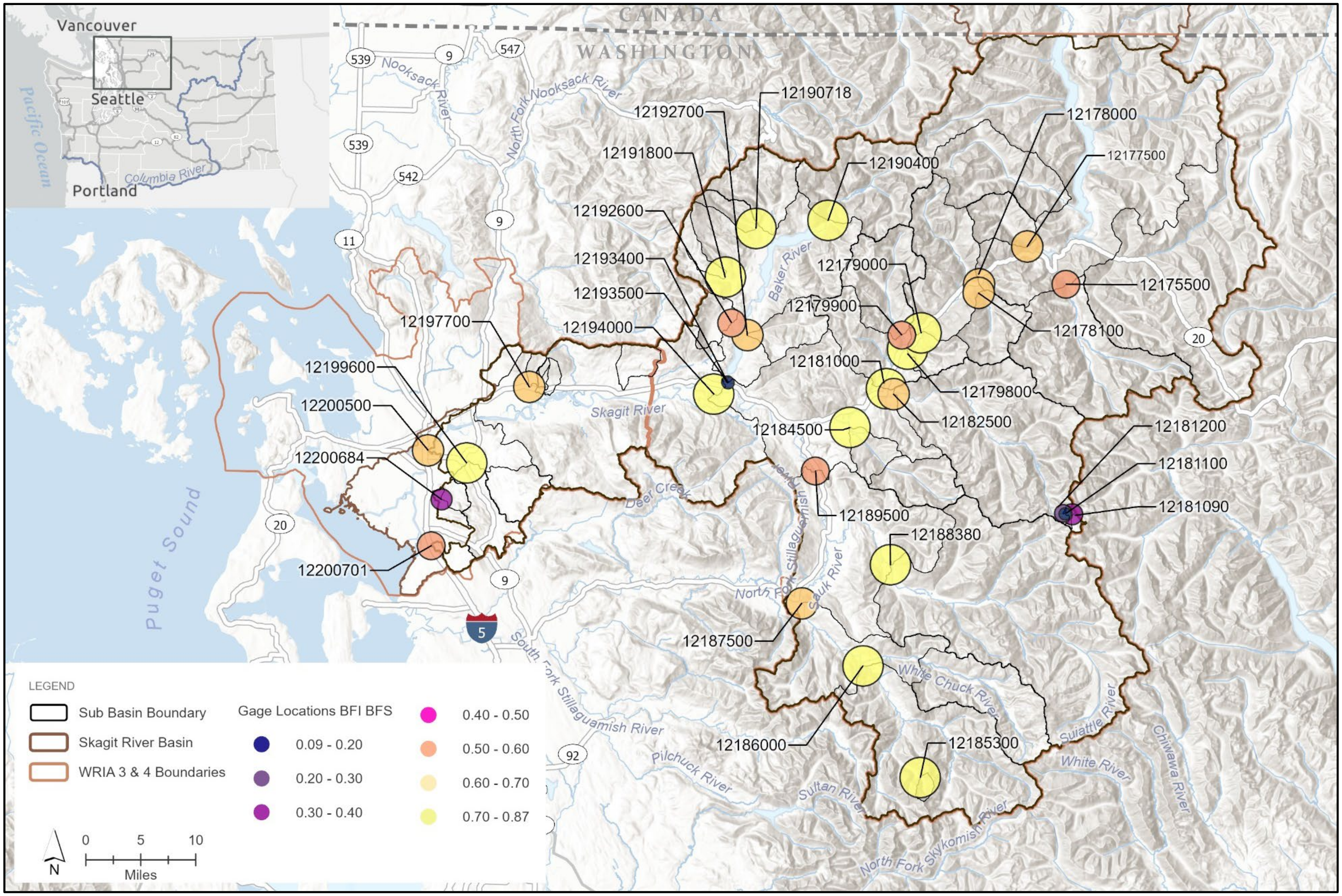


**Figure 7. Map of Baseflow Index (BFI) results by gage using the BFS Model for the entire analyzed time period.**

## 4.3 Comparison of Groundwater Recharge and Discharge

Long-term mean baseflow (GW discharge) rates calculated in this study were compared directly to recently obtained GW recharge and precipitation rates generated as part of the Synthesis Study (Yoder et al. 2021) over the 30-year period from 1/1/1981 through 12/31/2010. The evaluation includes a total of 33 streamflow gaging stations (out of the 44 total gages analyzed for baseflow). Only 28 of the 33 gages could be analyzed for comparison with GW recharge using the USGS BFS Model since five (out of the 33) gages have not been calibrated by the USGS.

Figure 8 shows the relationship between mean annual GW recharge and discharge, while Figure 9 shows the relationship between mean annual precipitation and GW discharge for the Lyne-Hollick method (alpha equal to 0.98). Similarly, Figure 10 shows the relationship between mean annual GW recharge and discharge, while Figure 11 shows the relationship between mean annual precipitation and GW discharge for the BFS Model. Groundwater recharge rates are generally much lower than GW discharge rates based on the hydrograph separation, with only 10 out of 33 gages having GW recharge within 20 in/yr of GW discharge for the Lyne-Hollick method, and 9 out of 28 gages for the BFS Model. Across the two methods, GW discharge is larger than GW recharge by a mean of 30.7 in/yr. Mean annual precipitation rates are mostly higher than mean annual GW discharge rates. There are, however, a few instances where the GW discharge rates are higher than the precipitation rates. The Lyne-Hollick method yielded one of these instances (see Figure 10) on the South Cascade River (12181090), while the BFS Model yielded three of these instances (see Figure 11), including two gaging stations on the Skagit River (12179800 and 12179000) and one gaging station on Park Creek (12190718).

The overall mean rates (across all gaging stations and their associated drainage basins) for the Lyne-Hollick method are 15.6 in/yr of recharge and 46.9 in/yr of discharge. This compares with a mean annual precipitation rate of 77.1 in/yr across all 33 drainage basins analyzed using the Lyne-Hollick method. The calculated percentage of recharge and discharge to precipitation for the 33 drainage basins using this method equals 20 percent and 61 percent, respectively. Since the two techniques used to estimate baseflow generally produced similar results, the differences in these mean values are small. The overall mean rates (across all gaging stations and their associated drainage basins) for the BFS Model are 15.3 in/yr of recharge and 45.3 in/yr of discharge. This compares with a mean annual precipitation rate of 77.9 in/yr across all 28 drainage basins analyzed using the BFS Model. The calculated percentage of recharge and discharge to precipitation for the 28 drainage basins using this method equals 20 percent and 58 percent, respectively.

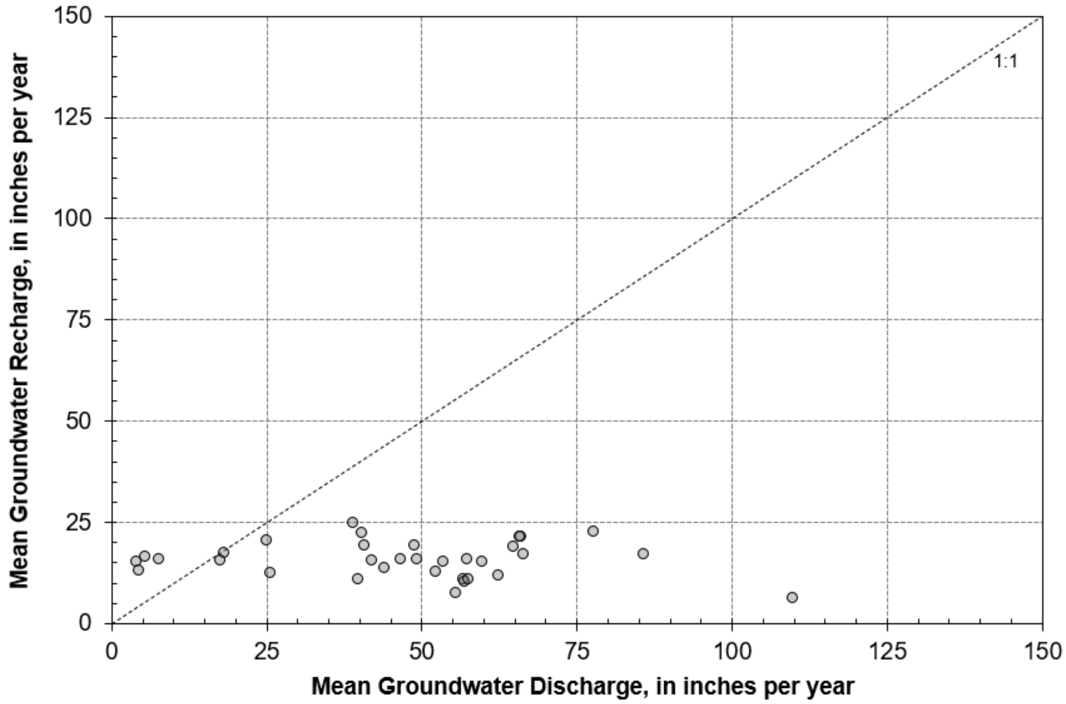


Figure 8. Relationship between mean groundwater recharge and mean groundwater discharge estimated using the Lyne-Hollick method (alpha parameter equals 0.98) for all analyzed gages for the period from 1/1/1981 through 12/31/2010.

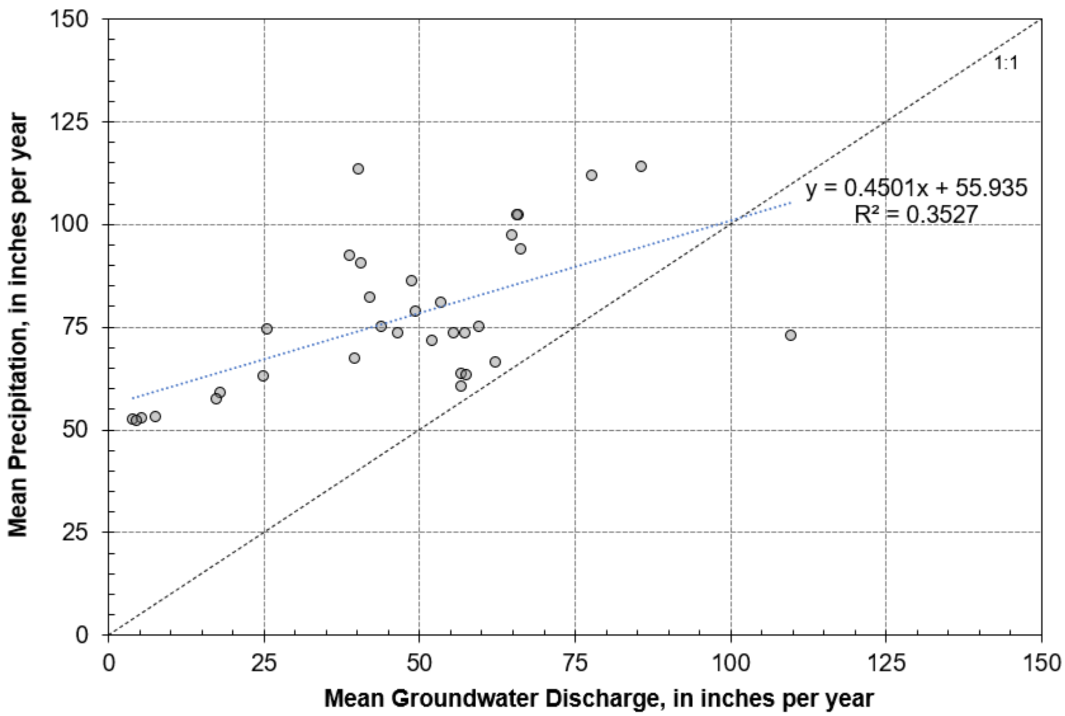


Figure 9. Relationship between mean precipitation and mean groundwater discharge estimated using the Lyne-Hollick method (alpha parameter equals 0.98) for all analyzed gages for the period from 1/1/1981 through 12/31/2010.

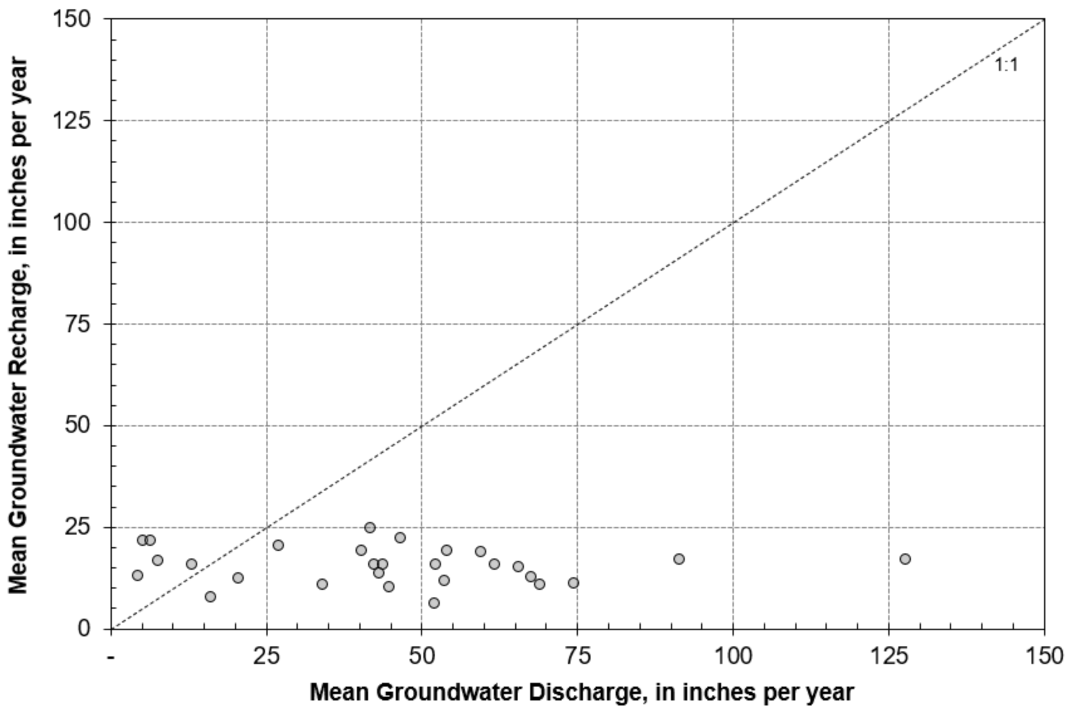


**Figure 10. Relationship between mean groundwater recharge and mean groundwater discharge estimated using the BFS Model for all analyzed gages for the period from 1/1/1981 through 12/31/2010.**

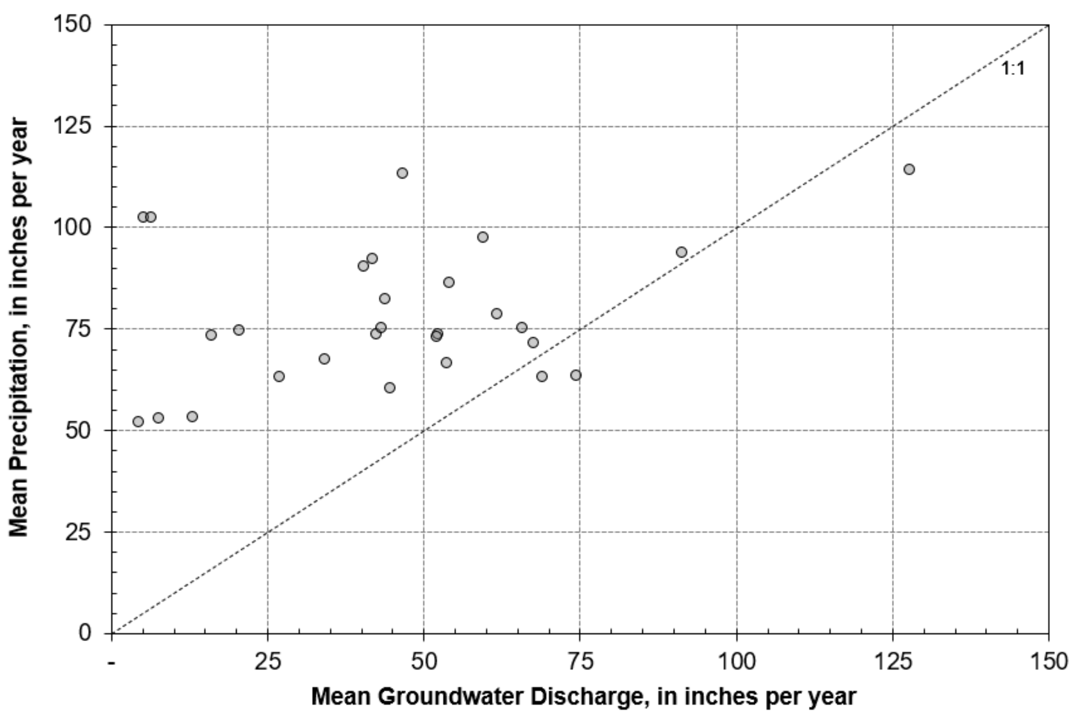


**Figure 11. Relationship between mean precipitation and mean groundwater discharge estimated using the BFS Model for all analyzed gages for the period from 1/1/1981 through 12/31/2010.**

# 5 Discussion of Findings

This study successfully completed baseflow quantification through hydrograph separation for 44 gaging stations using streamflow data collected between 1908 and 2021 based on publicly available data records from the USGS and Ecology. The results of this study can be used as a resource to better understand the complex hydrology of the Basin, as well as the gaged subbasins within the Tasks 200, 400, and 500 study area.

Streamflow rates were compared to the baseflow rates, including through the calculation and evaluation of BFI values. Two techniques were compared, including commonly employed one-parameter digital filter method (Lyne and Hollick 1979), and the state-space method calculating baseflow as a non-linear function of upstream GW storage that allows relatively steady non-zero baseflow. A sensitivity analysis of the Lyne-Hollick alpha parameter was successfully completed for values within the range of 0.90 and 0.99, and a preferred alpha value has been adopted (0.98).

This study provides a wide set of water balance data that can be reviewed, and hopefully utilized by practitioners, water managers, and other interested parties, within various parts of the Basin, or the Basin as a whole (above Mount Vernon). The focus here is on the components of the water budget from precipitation to basin runoff, including components partitioned into GW recharge, and streamflow, and the portion of streamflow moving through the GW system and emerging in streams as baseflow (presumably via GW discharge). There are some details regarding evapotranspiration (or other sinks such as pumping) that can also be gleaned through the direct comparison of long-term GW recharge with discharge.

The purpose of the comparisons (between the two GW discharge methods, and between both GW discharge methods and the associated GW recharge estimates) was to elucidate the magnitude of differences to help in understanding the magnitude of the issue in these estimation methods. Further discussion associated with the nuances and caveats of the analyses performed in this study are discussed in the following subsections, including some ideas about the future work that may stem from this study.

## 5.1 Comparison of BFS Model and Lyne-Hollick Digital Filter for Hydrograph Separation

Although the Lyne and Hollick (1979) recursive digital filtering method for baseflow separation is generally recognized as lacking a physical basis, the technique is particularly useful to characterize differences between drainage basins in a consistent manner, since it is easy to automate, objective, and repeatable (Nathan and McMahon 1991). The ability for the Lyne and Hollick (1979) method to provide the basis for making quantitative inferences is tested by direct comparison to the results from the BFS Model, thus providing potential for understanding both the usefulness of the Lyne-Hollick method and understanding details about the controlling physical parameters of individual drainage basins. This is possible at gages where the BFS Model has been calibrated (and results presented in this study), because the BFS Model is a spatially aggregated numerical time-series model that uses a state-space framework in which baseflow is a non-linear function of upstream storage. The findings from this study indicate there are a number of sites that show good agreement in baseflow rates and BFI values calculated from the two methods. More effort in determining the physical basis for differences amongst the smaller number of subbasins analyzed that have the largest discrepancy in resulting baseflow estimates amongst the two techniques investigated in this study would be interesting to study in more detail. While some efforts have been made to delve into the possible explanations for these differences, determination of the physical basis is not part of the scope of work of this study but could be the focus of future work, as discussed further in Section 5.5. Additional discussion about the details of the differences and similarities is provided in the remainder of this section.

The BFI time series charts on annual hydrographs show indicate two distinct periods with lower BFI, including the periods between about mid-May through August, and from about November through mid-December. This is indicated by the results from both techniques. In addition, based on Figure 5, it is apparent how the sensitivity of the alpha parameter value alters the seasonal variability of the daily BFI values, with an increase in variability for higher alpha values. While there are similarities between the resulting BFI values, there are also differences; BFI values from the BFS Model are generally higher than those resulting from the Lyne-Hollick method, and the Lyne-Hollick method generates more variability in the resulting baseflow and BFI values.

Calibration of the BFS Model has been performed prior to the current study (cf. Konrad 2022) through a four-step process developed to find a set of viable parameters that maximize the baseflow component within the constraints of the conceptual model (a first-order recession rate that decreases during dry periods). The largest differences between the baseflow fraction (BFF), which is based on the ratio of simulated baseflow to simulated streamflow rates, and BFI, where BFF is generally less than BFI, has been noted to occur in basins where streamflow in rivers are regulated and is generated predominantly by snowmelt (Konrad 2022). It is worth adding that Konrad (2020) developed BFF estimates using the BFS Model that also have rather high (>0.50) values that are comparable to the BFI values determined from this study.

Further discussion of some of the factors causing relatively large errors in baseflow estimates are provided by Konrad (2022), including: (1) the influence of reservoir releases (discussed in the Section 5.4); (2) high elevation basins where snowmelt is a dominant mechanism generating runoff (which does occur in several areas of the Basin); and (3) sites that have isolated, extremely low flows as a result of drying or freezing for example.

## 5.2 Lyne-Hollick Filter Alpha Parameter Sensitivity

In this study an alpha parameter value of 0.98 has been adopted as the preferred value (for analysis of the entirety of the period of record for the available 44 gage records; see Table 3) based upon two points of consideration: 1) visual review of the plotted baseflow and streamflow hydrographs, and 2) The value of 0.98 for alpha has been adopted in a baseflow assessment of 141 streams in the Murray-Darling Basin (CSIRO and SKM 2010), and an alpha value of 0.98 produced a better match to BFI derived from chemical tracer estimates than the commonly adopted value of 0.925 (CSIRO and SKM 2012). To be transparent, no attempt has been made in this study to assess how reasonable it would be to assume that the Murray-Darling basin is a suitable analog to the Skagit River basin. However, the use of chemical tracers to estimate baseflow at this scale is not common, and it provides an empirical measure not typically found. It was noted that BFI values increase as the alpha parameter value is decreased, and that the seasonal variability of the daily BFI values increases for higher alpha values. For purposes of evaluating the influence of the alpha parameter and comparing against the BFS Model baseflow values, the preferred alpha value of 0.98 was less important, and all six evaluated alpha values were carried through the analyses.

## 5.3 Groundwater Recharge and Discharge Estimates

The discrepancy between GW recharge and GW discharge rates was larger than anticipated for a majority of subbasins. About 85 percent of the subbasins analyzed have estimated GW discharge rates that are higher than the GW recharge rates derived from the Synthesis Study (Yoder et al. 2021). Furthermore, the range of mean GW recharge rates amongst the subbasins analyzed is much lower than the range of estimated mean GW discharge rates derived from hydrograph separation.

It is acknowledged that there could be an equal likelihood for the GW discharge and recharge rate estimates to have high degrees of error. To elucidate the possible magnitude of the error of the recharge rates used in this study, they have a basin-wide mean of approximately 22 percent of precipitation (Yoder et al. 2021) over the long-term, while the study of Savoca et al. (2009) reports a recharge rate that is 33 percent of precipitation (for the lower Skagit Basin). In addition, the study of Thomas et al. (1997) reports GW recharges rates exceeding 50 in./yr in the alluvial valley near Darrington, while the comparable basin is shown to have a mean GW recharge rate of approximately 19 in/yr in this study. These comparisons appear to indicate, along with comparison against the GW discharge rates determined in this study, that the GW recharge rates overall could be underestimated.

With regard to GW discharge rates, there are a total of four subbasins analyzed that have GW discharge estimates that exceed the precipitation estimates over the long-term (see Figure 10 and Figure 11). The estimated GW discharge rates are still less than the precipitation rates almost entirely, with four instances of exceptions where GW discharge is greater than precipitation (as pointed out in the second paragraph in Section 4.3). The cause of this could be due to physical processes such as ice melt or long-term losses from storage but also could be due to inaccuracies in precipitation rate estimates especially at high elevations, and errors in measurements of streamflow discharge rates, and also possibly the overestimation of GW discharge from the methods used. To expand on this last possibility, the minimum and maximum differences between the estimated long-term mean GW discharge and recharge rates amongst all subbasins analyzed with both GW discharge methods (n = 61) are -16.1 in./yr and 110.7 in./yr, with an average of 30.7 in./yr, and 13 of the largest estimates of GW discharge are greater than 50 percent of the mean difference of 30.7 in/yr, whereas only one of the smallest estimates of GW discharge have an absolute difference of greater than 50 percent of the mean. This indicates a bias toward large GW discharge estimates relative to GW recharge estimates.

The method of determining GW recharge and precipitation rates within each analyzed subbasin required the use of spatial data analysis tools to intersect gridded values with the subbasin polygons. The most efficient (default) method—spatial join with intersect as the selection method—has been used in the interest of time. Since some of the grid cells are on the edges of the subbasin polygons, there are some grid cells that have been selected multiple times (by neighboring subbasins) using the simple intersection method. While the “best,” or perhaps more precise, intersection methods could be explored further, we believe the resulting mean rates of GW recharge and precipitation within each subbasin from various intersection methods would be about equal to what has been reported in this study. However, it would be expected that the largest differences in results between different intersection methods would be for the smaller basins where the number of perimeter grid cells comprises a larger fraction of total grid cells intersecting the subbasin polygons.

## 5.4 Reservoir Releases

The lower Skagit River below the five major hydroelectric dams is considered heavily regulated, with Ross and Upper Baker Dams controlling runoff from about 39 percent of the drainage area of the Basin upstream of Mount Vernon (Puget Sound Energy 2006), but the five dams in the basin were not built primarily for flood control and provide only limited relief from the worst river flooding, which generally occurs in late fall when warm storm systems bring heavy rainfall, which can also melt early snowpack (Kunzler 2005).

While the results have not been presented in this study, the baseflow and streamflow hydrographs, statistics, and BFIs for a couple of the gages with the most regulated streamflow and an unregulated large river have been reviewed for comparison, including at the gages just downstream of the lowermost dams on the Baker River and the Skagit River (USGS stations 12193400 and 1217800, respectively) and on the unregulated Sauk River (USGS station 12189500). The Baker River at Henry Thompson Bridge appears much more affected by controlled reservoir releases than those of the Skagit River at the Newhalem gage, based on the observance of sharp declines in streamflow and resulting sharp declines in baseflow that result from the separation, with the Skagit River at Newhalem hydrographs appearing much more like those of the Sauk River gage. Much larger differences of BFIs between the Lyne-Hollick method and the BFS Model are noted at the Baker River gage than observed at the Skagit River or Sauk River gages.

In total there are nine gaging stations that have been analyzed in this study that are downstream of at least one of the five major dams in the Basin. These nine gaging stations are listed as follows:

- 12178000 (Skagit River at Newhalem)
- 12179000 (Skagit River above Alma Creek near Marblemount)
- 12179800 (Skagit River above Bacon Creek near Marblemount)
- 12181000 (Skagit River at Marblemount)
- 12193400 (Baker River at Henry Thompson Bridge at Concrete)
- 12193500 (Baker River at Concrete)
- 12194000 (Skagit River near Concrete)

- 12199000 (Skagit River near Sedro Woolley)
- 12200500 (Skagit River near Mount Vernon)

Some of these gages display large differences among the baseflow and BFI statistics when comparing the two methods, while others do not. An important additional finding is that these gages (all have baseflow estimated except for the Skagit River near Sedro Woolley) are among those with the largest differences between GW discharge and recharge, making up eight of the 15 gages with the largest differences for the Lyne-Hollick method and six of the 13 gages with the largest differences for the BFS Model. Delving into the explanations for these reasons is not part of the scope of work of this study but could be the focus of future work, as described further in Section 5.5.

## 5.5 Potential Future Work

It would be interesting to investigate objectively the relationships between BFI values resulting from the two techniques and other Basin hydrology-related characteristics, such as drainage area, average subbasin elevation, amount of glacial melt occurring, etc. For instance, while it was not analyzed statistically, this study does show that there is generally an increase in BFI values with increasing basin size. Going further, the spatial relationships, including how these characteristics relate to precipitation and a more thorough evaluation of how the results relate to hydrogeologic units could provide a better understanding of the underlying controlling processes responsible for variations amongst the BFI values of subbasins.

Selection of the Lyne and Hollick (1979) digital filter alpha parameter value is informed by comparison of two completely different conceptual approaches to separating baseflow from streamflow time series in this study. However, it has been recommended that the selection of the filter alpha parameter be informed by field studies wherever possible, using techniques such as chemical tracers and reach water balances (Ladson et al. 2013). Improved field investigation that aims to better understand the links between baseflow and physical factors is likely to be required in order to better reduce uncertainties in the adopted alpha parameter value. While the uncertainty of the alpha parameter values has been explored via sensitivity analysis (six different values of $\alpha$) in this study with respect to the Lyne-Hollick method, there remains the possibility of exploring the sensitivity of the various BFS Model parameter values and extending the BFS Model to the remaining gages within the Basin via calibration through steps outlined in Konrad (2022).

The discrepancy between GW recharge and GW discharge rates was, on the whole, larger than anticipated, providing the need for further evaluation and attempts to understand the reasons for large discrepancies in about two-thirds of the analyzed subbasins. There are also likely some issues related to the precipitation rates and not accounting directly for glacial melt, which could explain why GW discharge (and also streamflow) is larger than precipitation, particularly for the high-altitude subbasins. Further evaluation of recharge rates appears to be warranted, as the variability was much lower than the baseflow values derived from hydrograph separation. As noted in the ‘Knowledge Gaps’ of the Synthesis Study (Yoder et al. 2021), comparisons of recharge estimates generated from other studies and approaches could be made, such as using the cell-by-cell fluxes from applications of the Distributed Hydrologic Soil

Vegetation Model (DHSVM), or from studies applying the soil-water balance (SWB) method.

Of the nine gaging stations that have been analyzed in this study that are downstream of at least one of the five major dams in the Basin (listed above), some display large differences among the baseflow and BFI statistics when comparing the two methods, while others do not. The reservoir-controlled nature of the streamflow could be contributing to the high GW discharge estimates at some gages. Delving into the explanations could be the focus of future work.

Additionally, there remains some opportunities to analyze other historic gages, or more recently installed gages, within the Basin. While this study did provide an extensive analysis of gages beyond those analyzed by the USGS (Konrad 2022), there was not an attempt to comprehensively analyze all of the existing historic/inactive and most recent streamflow gage data.

# 6 References

Bradley, J.R., T. Kuntz, and R.R. Luckey

2013 Hydrograph Separation Methods Used to Estimate Groundwater Discharge for Assistance in Calibration of the Western Water Use Model. Nebraska Department of Natural Resources, 14 p., https://dnr.nebraska.gov/sites/dnr.nebraska.gov/files/doc/water-planning/BaseflowReport2013.pdf.

Chapman, T.G.

1991 Comment on "Evaluation of Automated Techniques for Base Flow and Recession Analysis" by R.J. Nathan and T.A. McMahon. *Water Resources Research* 27(7): 1783–1784.

Commonwealth Scientific and Industrial Research Organisation (CSIRO) and SKM

2010 *Baseflow Assessment for the Murray-Darling Basin*. Water for a Healthy Country National Research Flagship, 78 p.

2012 Methods for Estimating Groundwater Discharge to Streams: Summary of Field Trials. National Water Commission.

De Cicco, L.A., R.M. Hirsch, D. Lorenz, W.D. Watkins, and M. Johnson

2022 dataRetrieval: R packages for discovering and retrieving water data available from Federal hydrologic web services, v.2.7.12. doi:10.5066/P9X4L3GE.

Hagemann, M.

2023 StreamStats: R bindings to the USGS StreamStats API. R package version 0.0.3.

HDR

2023 Skagit River Hydrogeology Evaluation (Cross Sections). Skagit Groundwater Study Task 200: Hydrogeologic Characterization. Technical Memorandum Prepared for Washington State University. September 15.

2025 Surface Water and Groundwater Interaction. Skagit River Basin Groundwater Study, Lower Skagit River Valley from Sedro-Woolley to Birdsview, Washington. Report prepared for Washington State University. June.

Jakeman, A.J., G.M. Hornberger

1993 How Much Complexity Is Warranted in a Rainfall-Runoff Model? *Water Resources Research* 29 (8): 2637–49.

Kang, T., S. Lee, N. Lee, and Y. Jin

2022 Baseflow Separation Using the Digital Filter Method: Review and Sensitivity Analysis. *Water* 14, 485.

Konrad, C.P.

2020 Non-Linear Baseflow Separation Model with Parameters and Results (ver. 2.0, October 2022). U.S. Geological Survey Data Release, https://doi.org/10.5066/P9AIPHEP.

2022 *BFS—A Non-Linear, State-Space Model for Baseflow Separation and Prediction*. U.S. Geological Survey Scientific Investigations Report 2022–5114, 24 p., https://doi.org/10.3133/sir20225114.

Kunzler, L.

2005 Skagit River History, https://www.skagitriverhistory.com/PDFs/History%20of%20Skagit%20River.pdf.

Ladson, A.R., R. Brown, B. Neal, and R. Nathan

2013 A Standard Approach to Baseflow Separation Using the Lyne and Hollick Filter. *Australian Journal of Water Resources*, 17(1): 25–34.

Lyne, V., and M. Hollick.

1979 Stochastic Time-Variable Rainfall-Runoff Modeling. In *Institute of Engineers Australian National Conference*, 79: 89–92.

Nathan, R.J., and T.A. McMahon

1991 Reply (to Chapman, 1991). *Water Resources Research* 27(7): 1785–1786.

Puget Sound Energy

2006 Draft Environmental Impact Statement for Hydropower Relicensing: Baker River Hydroelectric Project. FERC Project No. 2150-033, Washington.

R Core Team

2022 R: A Language and Environment for Statistical Computing. R Foundation for Statistical Computing, Vienna, Austria. https://www.R-project.org.

Rutledge, A.T.

1998 Computer Programs for Describing the Recession of Ground-Water Discharge and for Estimating Mean Ground-Water Recharge and Discharge from Streamflow Records—Update. U.S. Geological Survey Water-Resources Investigations Report 98-4148, 43 p., https://pubs.usgs.gov/wri/wri984148/pdf/wri98-4148.pdf.

Samsonov, T.

2022 grwat: River Hydrograph Separation and Analysis. R package version 0.0.2, https://CRAN.R-project.org/package=grwat.

Savoca. M.E., K.H. Johnson, S.S. Sumioka, T.D. Olsen, E.T. Fasser, and R.L. Huffman

2009 Hydrogeologic Framework, Groundwater Movement, and Water Budget in Tributary Subbasins and Vicinity, Lower Skagit River Basin, Skagit and Snohomish Counties, Washington. U.S. Geological Survey Scientific Investigations Report 2009-5270. Tacoma, Washington.

Thomas, B.E., J.M. Wilkinson, and S.S. Embrey

1997 *The Ground-Water System and Ground-Water Quality in Western Snohomish County, Washington*. U.S. Geological Survey Water-Resources Investigations Report 96-4312. Tacoma, Washington.

Williams, H.

2025 Aquifer Characterization in the Lower Skagit River Valley, Northwest Washington State. Master’s Thesis. Western Washington University.

Yoder, J., S. Chaudhary, B. Duarte, C. Greene, J. Jobe, G. LaHue, C. Maroney, G. Mauger, H. Morgan, J. Padowski, K. Rajagopalan, C. Raymond, M. Rogers, N. Rossman, N. Singh, B. Timpane-Padgham, C. Wiseman, and J. Won.

2021 Skagit Water Supply and Demand Synthesis Story Map Series. Prepared for the Washington State Joint Legislative Task Force on Water Supply. https://doi.org/10.7273/4n11-9k73.

# Appendix A. Box and Whisker Charts of the Statistical Distribution of Mean Daily Baseflow for the Entire Period of Available Record of each Analyzed Gaging Station, Comparing the Lyne-Hollick Method and the BFS Model

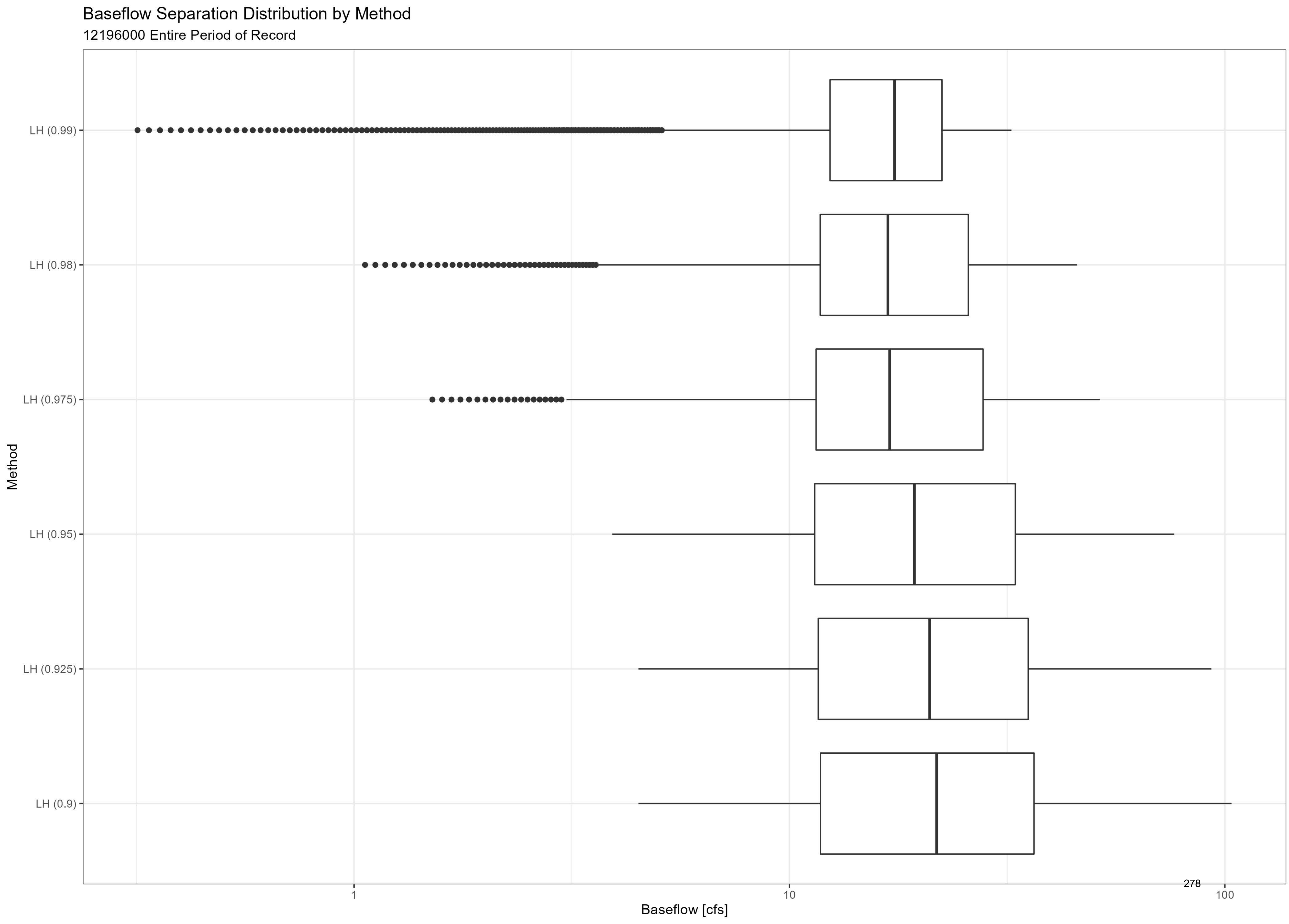

Baseflow Separation Distribution by Method
12196000 Entire Period of Record
Method
LH (0.99)
LH (0.98)
LH (0.975)
LH (0.95)
LH (0.925)
LH (0.9)
1
10
100
Baseflow [cfs]

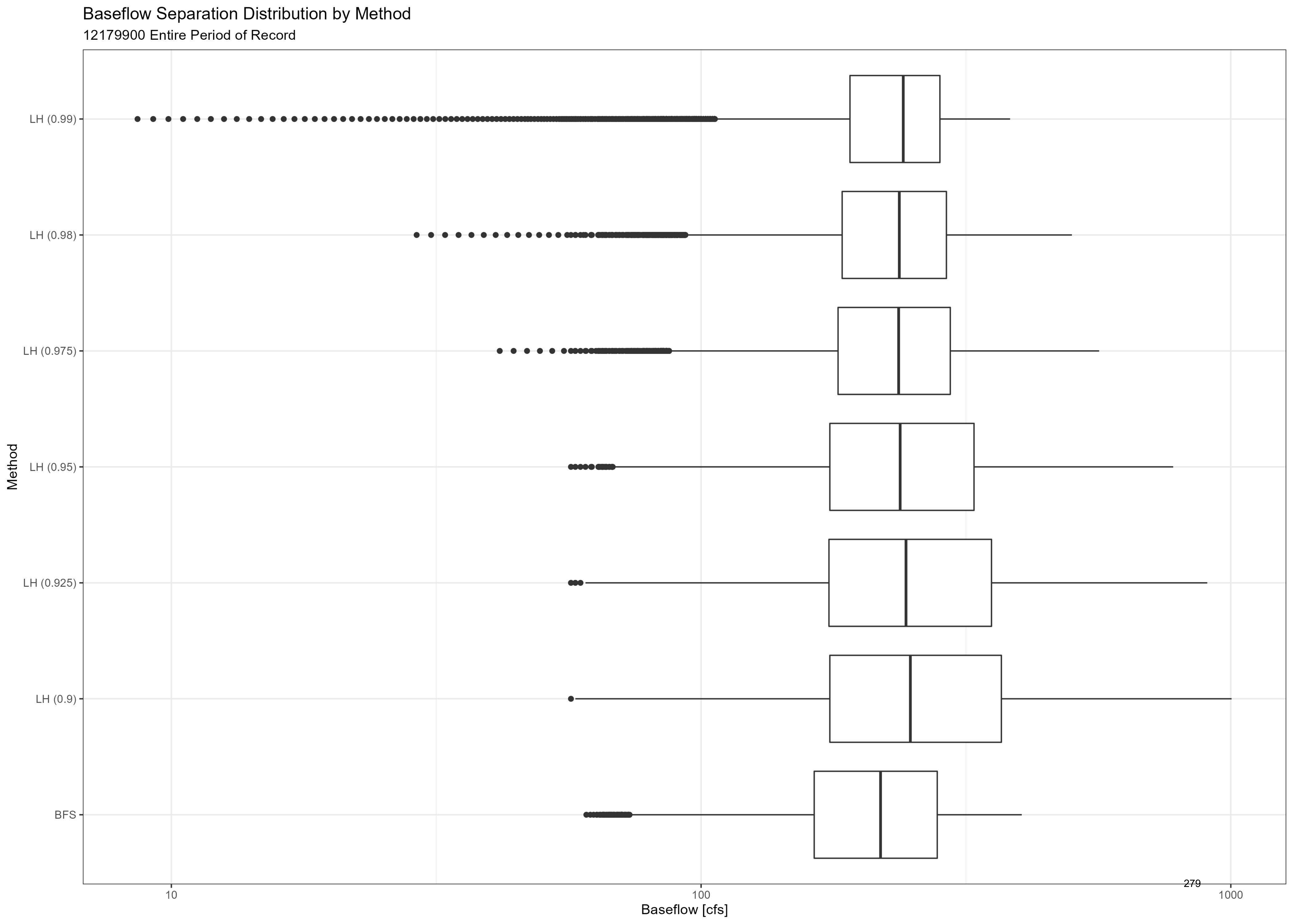
Baseflow Separation Distribution by Method
12179900 Entire Period of Record
LH (0.99)
LH (0.98)
LH (0.975)
LH (0.95)
LH (0.925)
LH (0.9)
BFS
Method
10
100
1000
Baseflow [cfs]

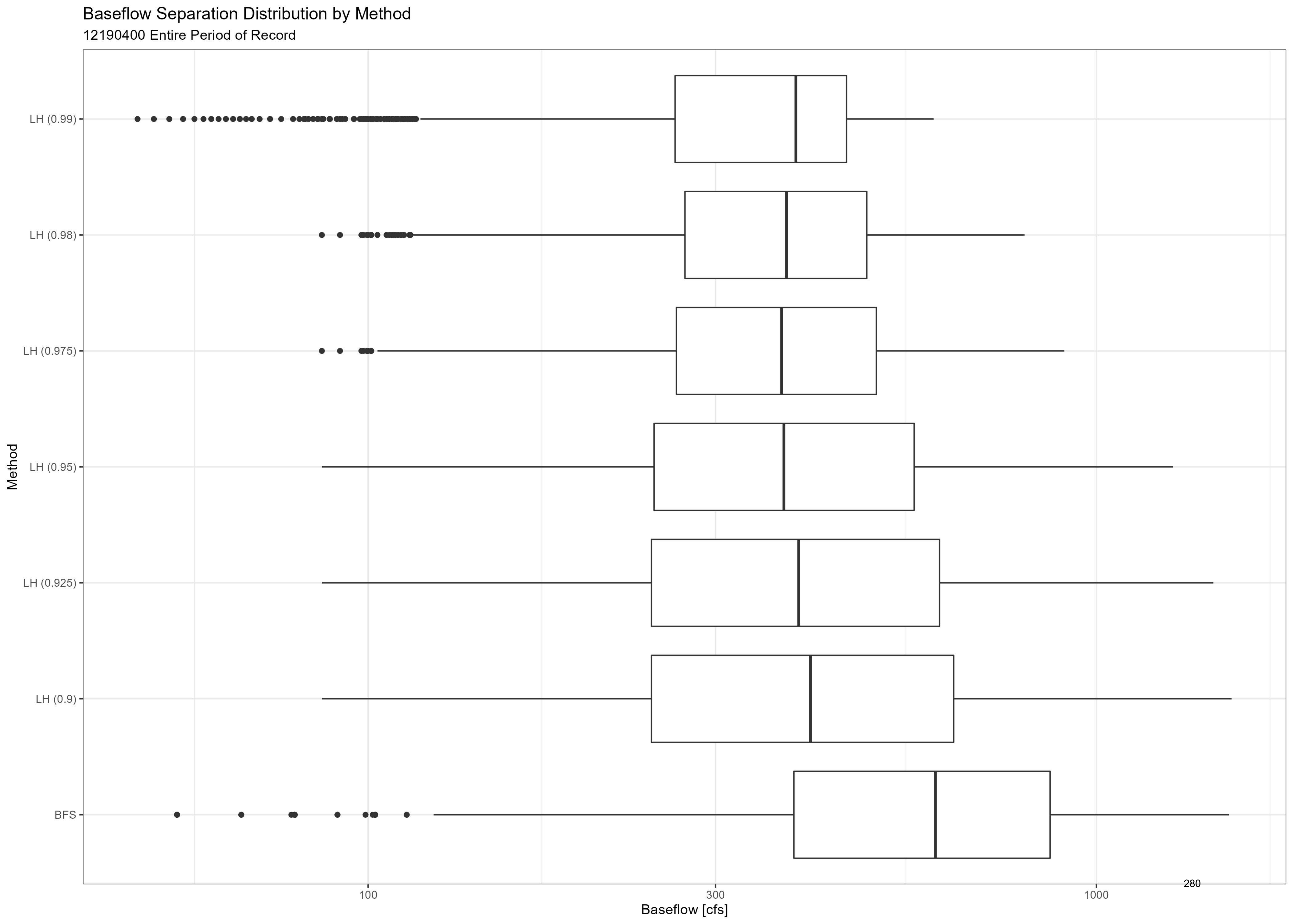
Baseflow Separation Distribution by Method
12190400 Entire Period of Record
Method
LH (0.99)
LH (0.98)
LH (0.975)
LH (0.95)
LH (0.925)
LH (0.9)
BFS
100
300
1000
Baseflow [cfs]

280

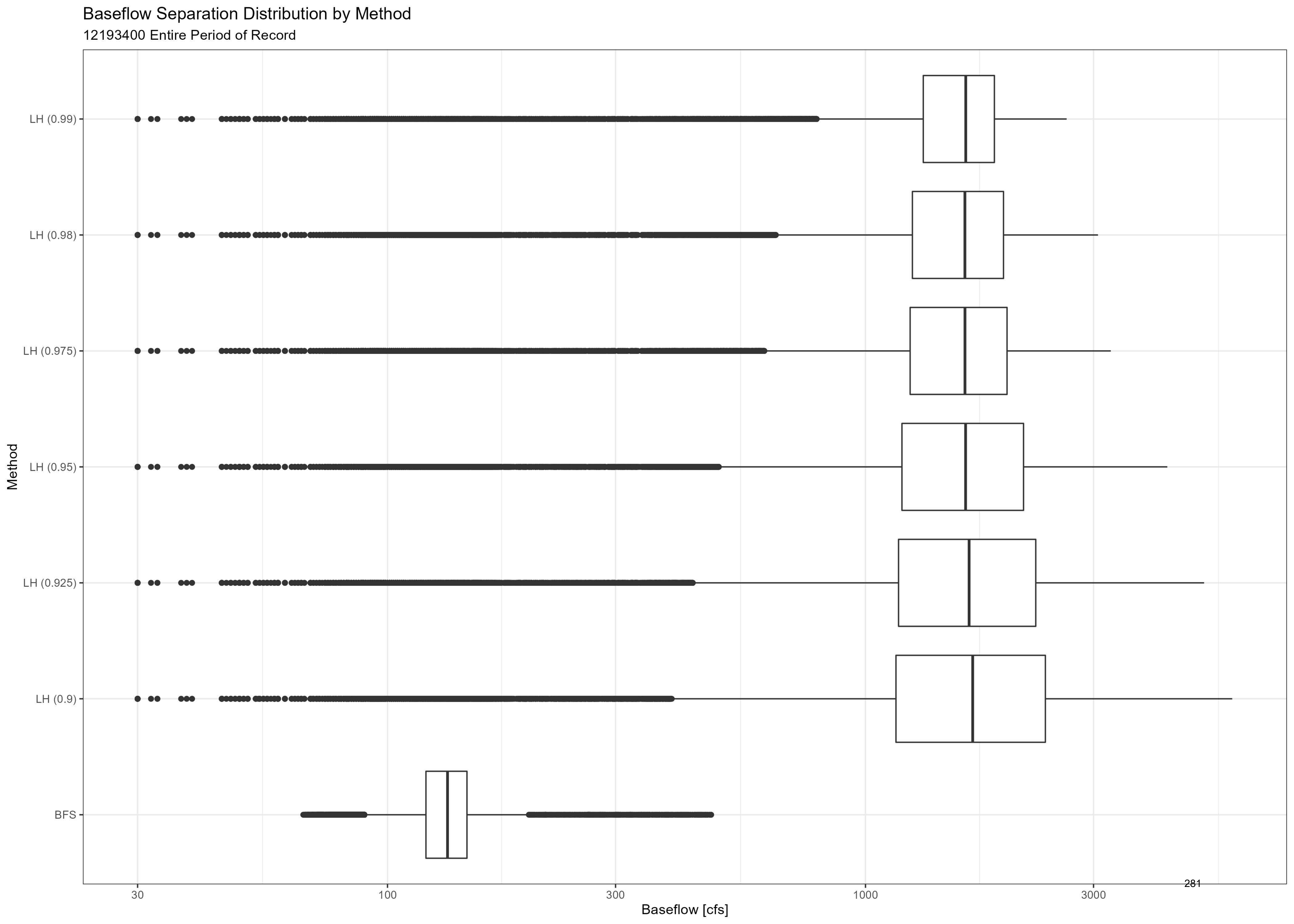
Baseflow Separation Distribution by Method
12193400 Entire Period of Record
LH (0.99)
LH (0.98)
LH (0.975)
LH (0.95)
LH (0.925)
LH (0.9)
BFS
Method
30
100
300
1000
3000
Baseflow [cfs]

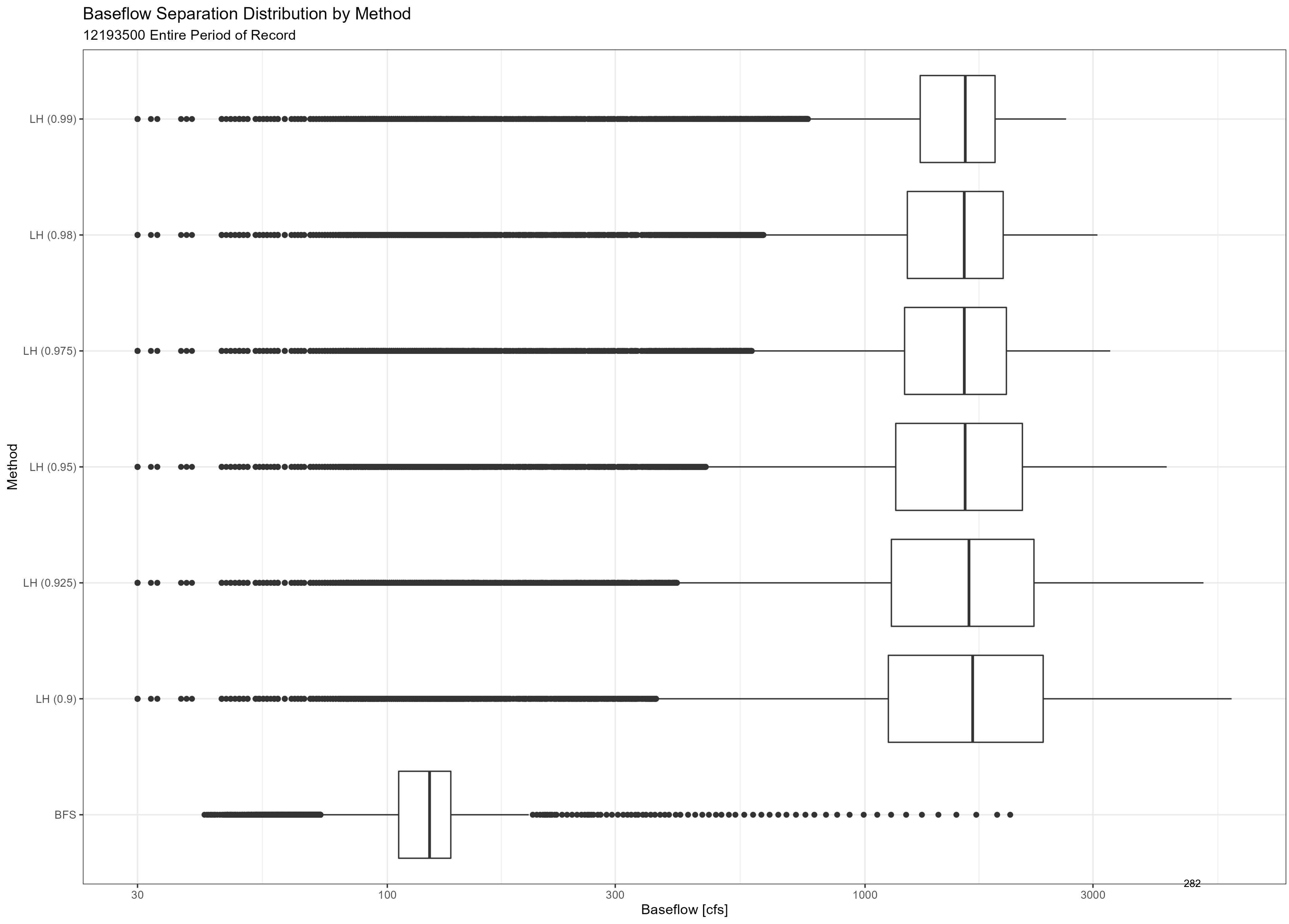

Baseflow Separation Distribution by Method
12193500 Entire Period of Record
Method
LH (0.99)
LH (0.98)
LH (0.975)
LH (0.95)
LH (0.925)
LH (0.9)
BFS
30
100
300
1000
3000
Baseflow [cfs]

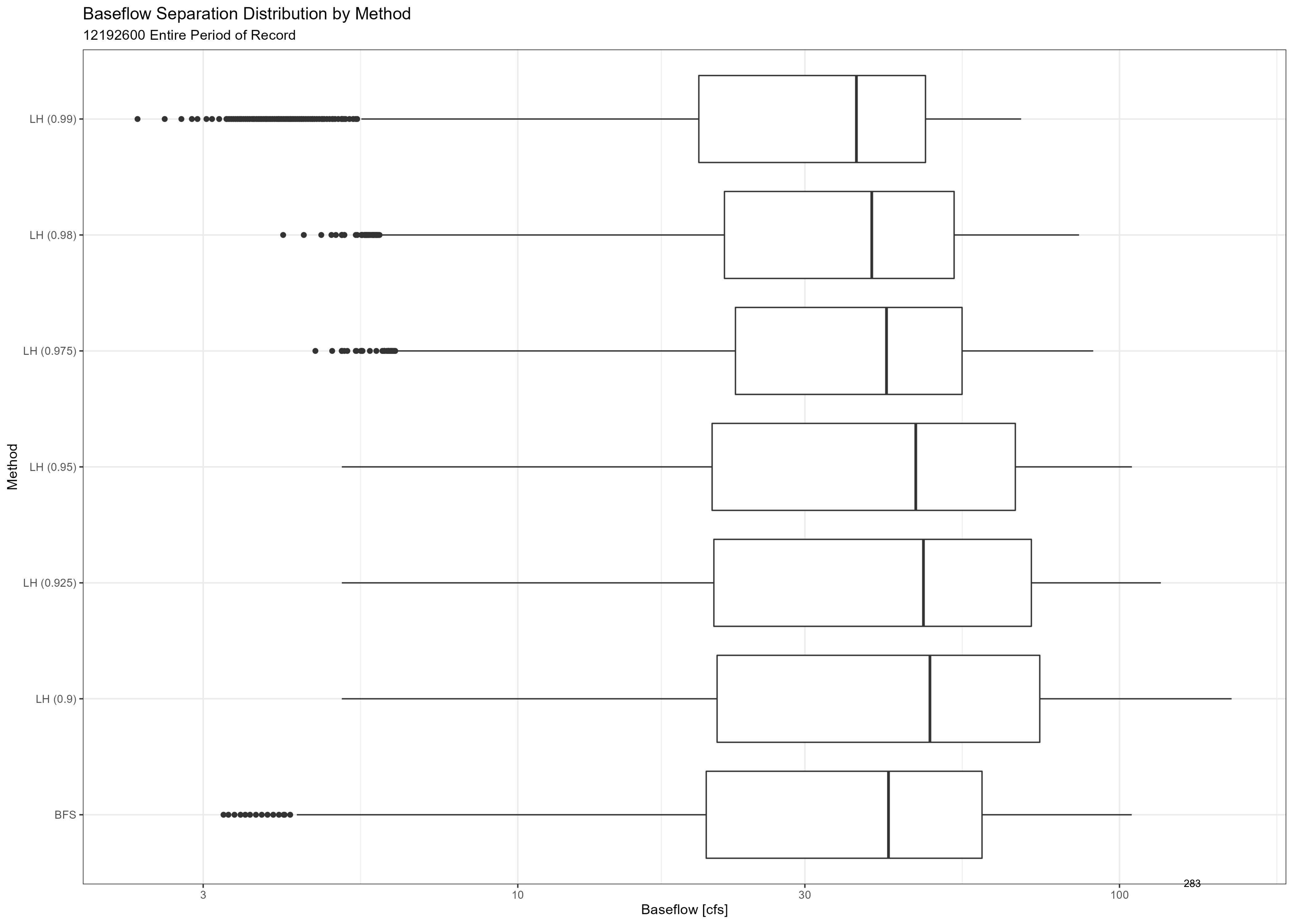
Baseflow Separation Distribution by Method
12192600 Entire Period of Record
LH (0.99)
LH (0.98)
LH (0.975)
LH (0.95)
LH (0.925)
LH (0.9)
BFS
Method
3
10
30
100
Baseflow [cfs]

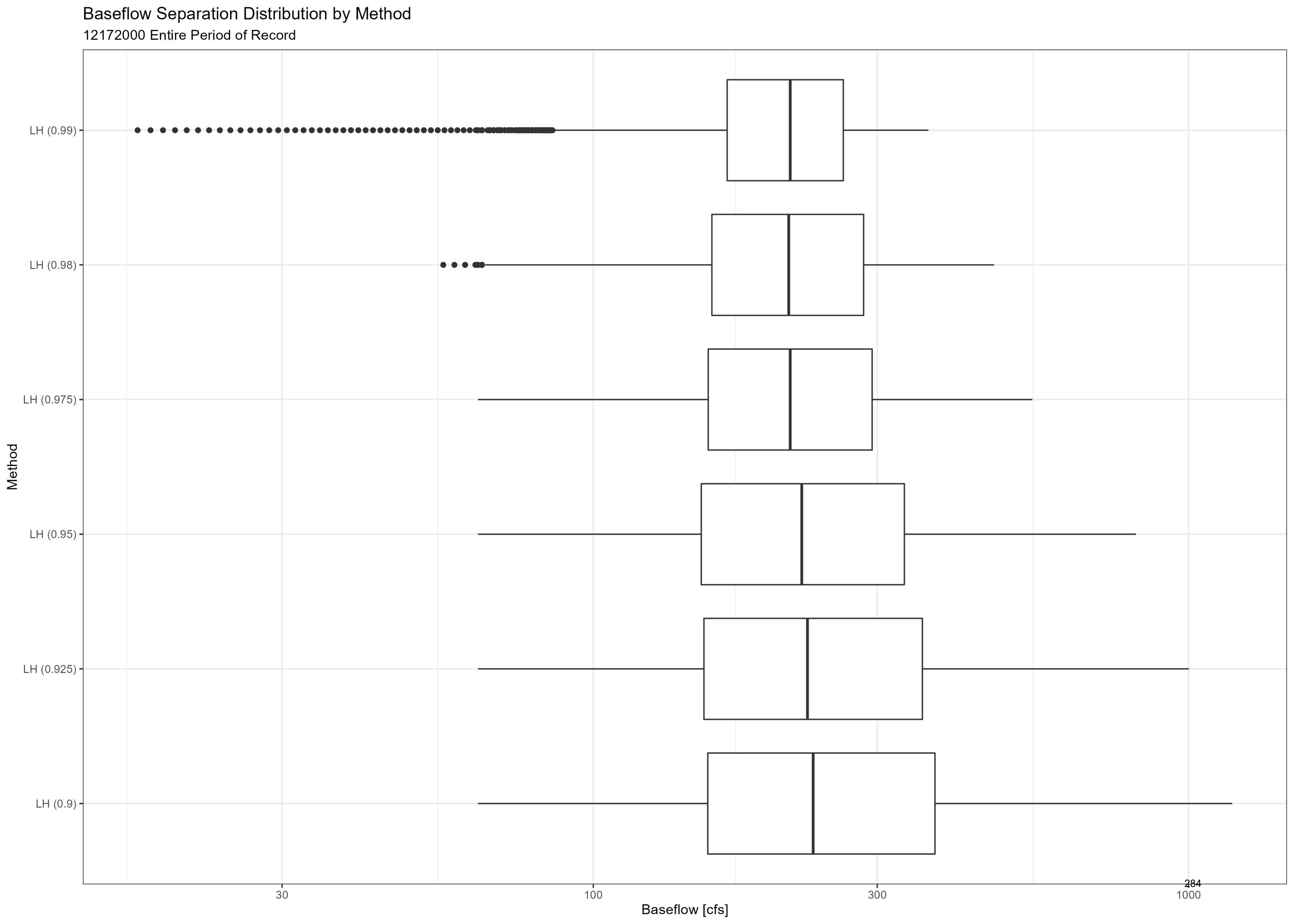
Baseflow Separation Distribution by Method
12172000 Entire Period of Record
LH (0.99)
LH (0.98)
LH (0.975)
LH (0.95)
LH (0.925)
LH (0.9)
Method
30
100
300
1000
Baseflow [cfs]
284

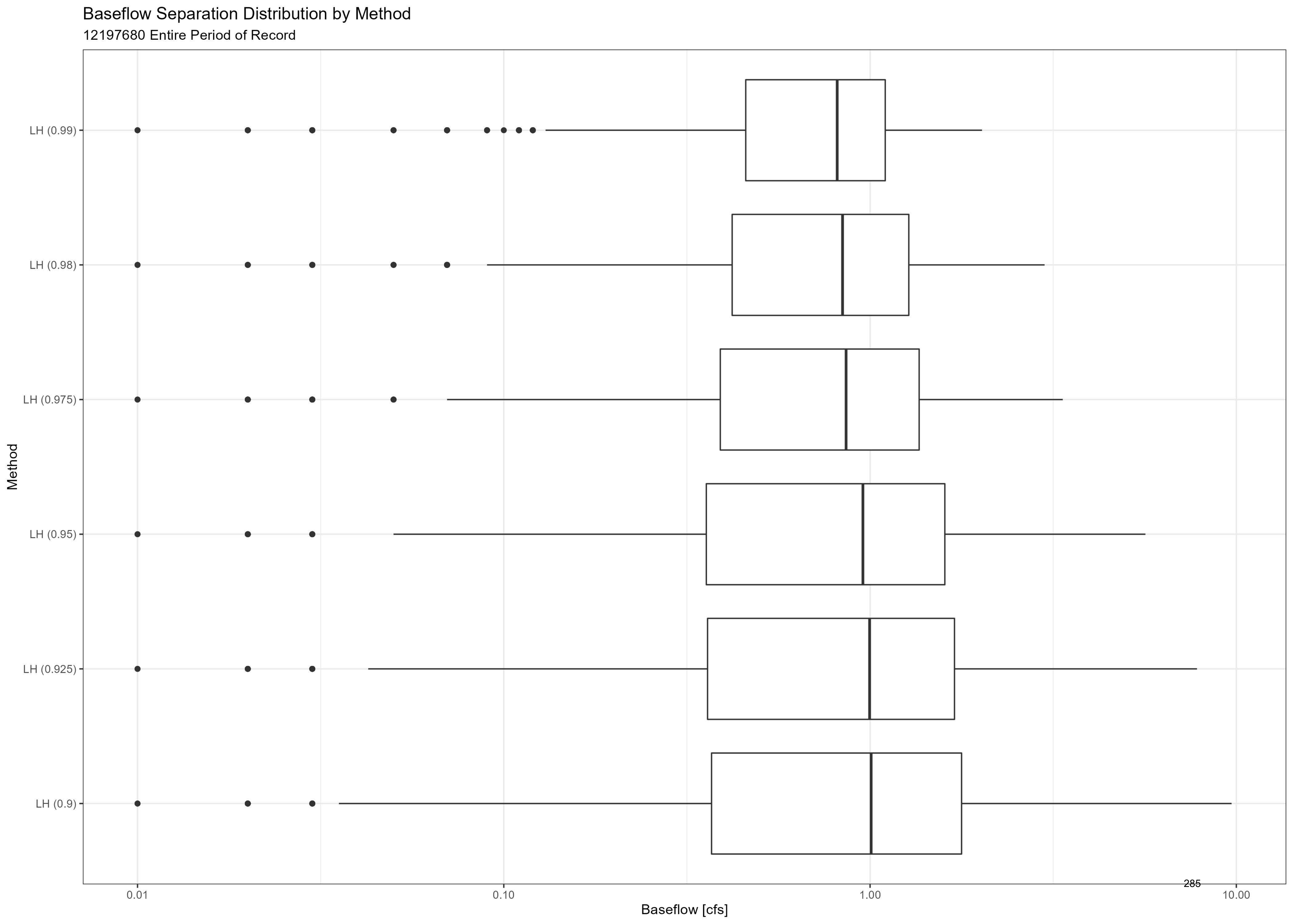

Baseflow Separation Distribution by Method
12197680 Entire Period of Record
LH (0.99)
LH (0.98)
LH (0.975)
LH (0.95)
LH (0.925)
LH (0.9)
Method
0.01
0.10
1.00
10.00
Baseflow [cfs]

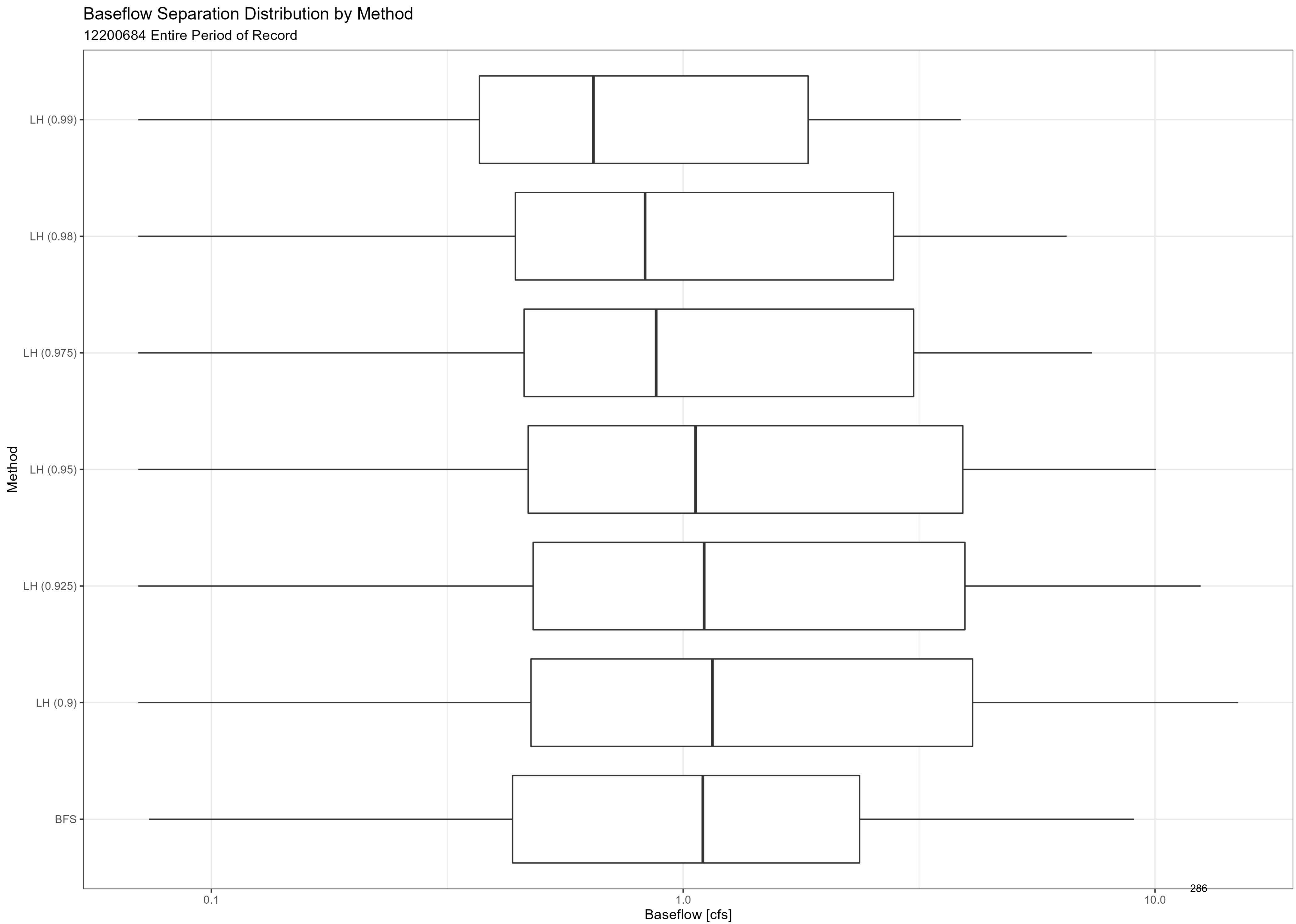
Baseflow Separation Distribution by Method
12200684 Entire Period of Record
LH (0.99)
LH (0.98)
LH (0.975)
LH (0.95)
LH (0.925)
LH (0.9)
BFS
Method
0.1
1.0
10.0
Baseflow [cfs]

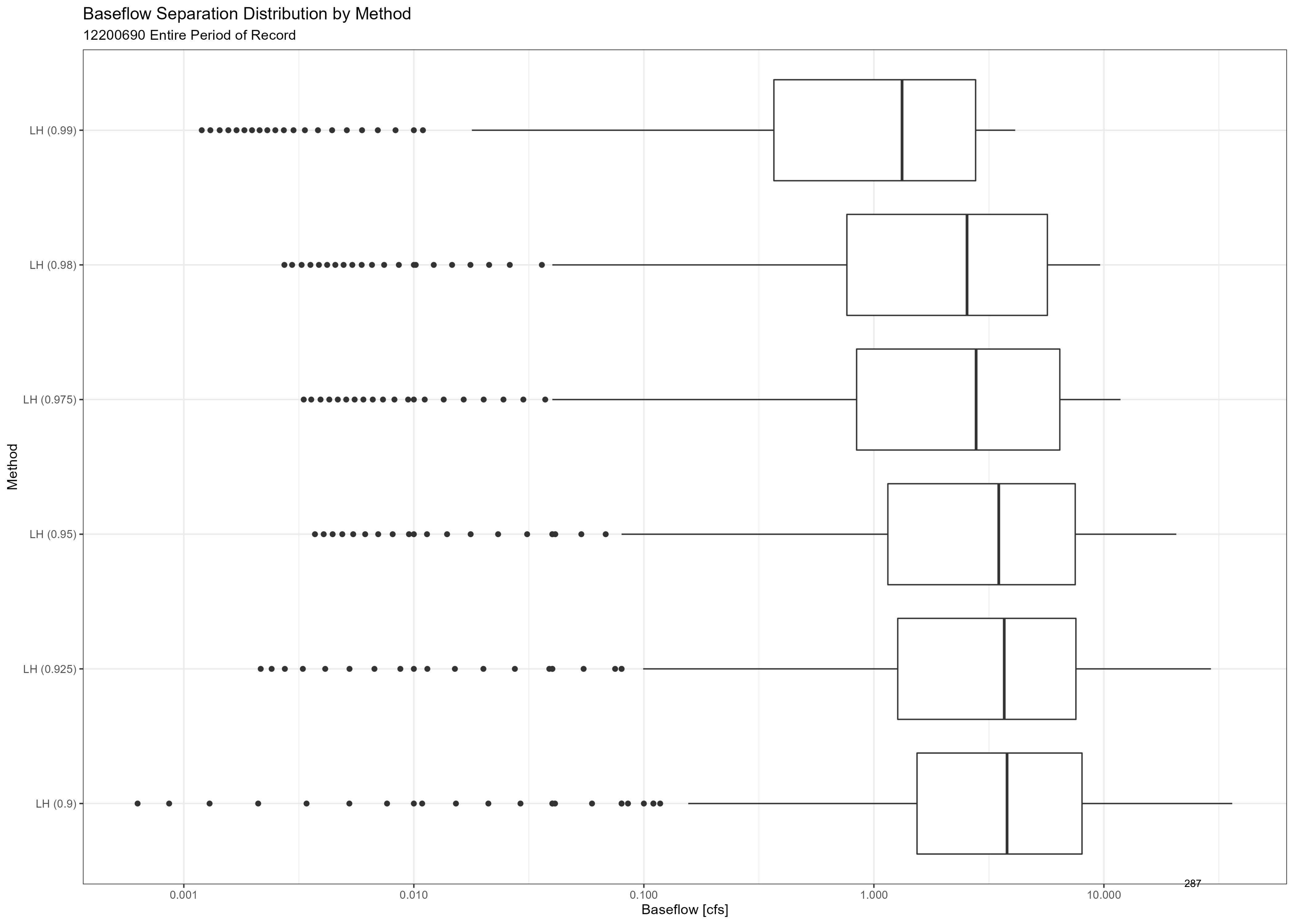

Baseflow Separation Distribution by Method
12200690 Entire Period of Record
Method
LH (0.99)
LH (0.98)
LH (0.975)
LH (0.95)
LH (0.925)
LH (0.9)
0.001
0.010
0.100
1.000
10.000
Baseflow [cfs]

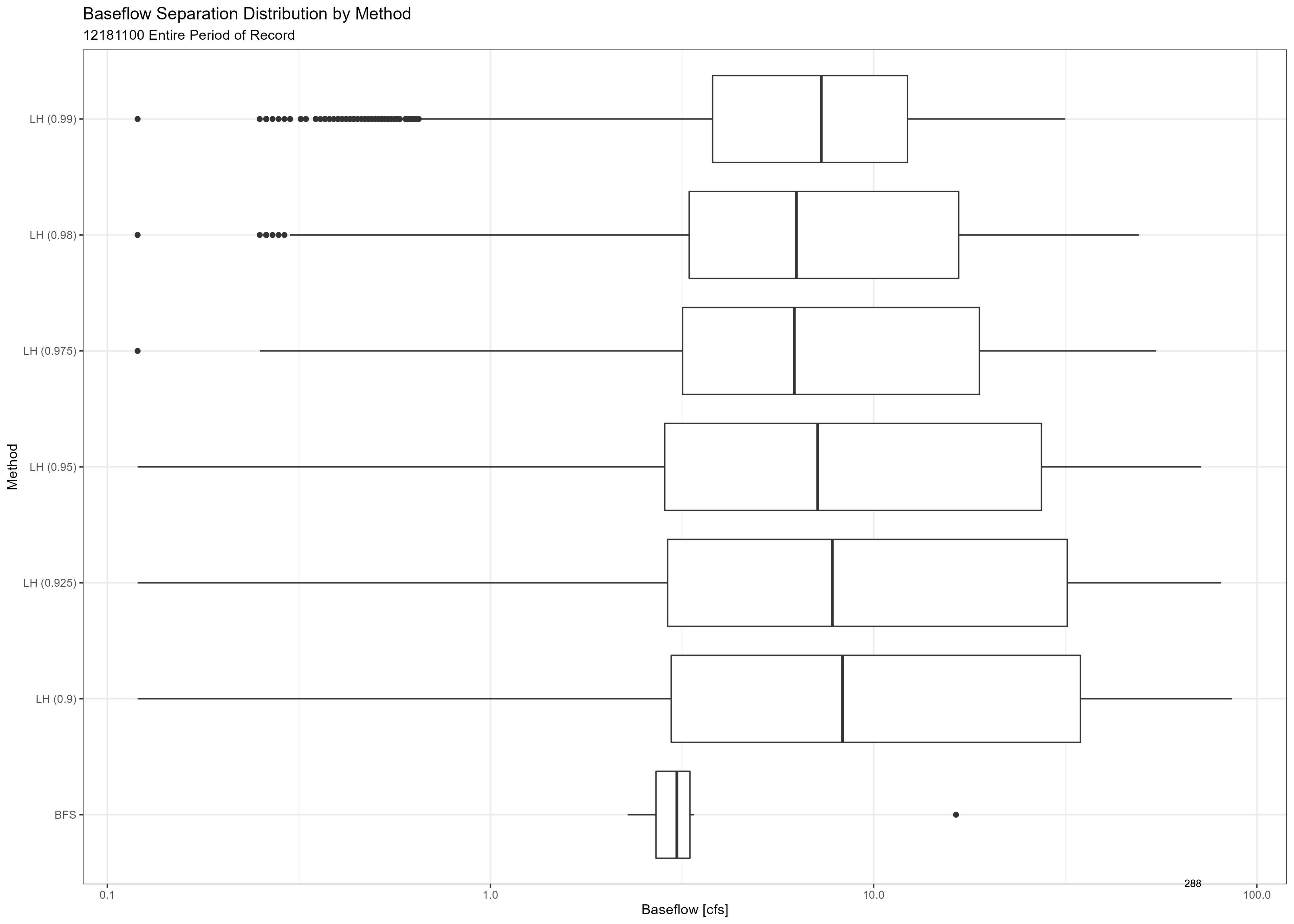
Baseflow Separation Distribution by Method
12181100 Entire Period of Record
Method
LH (0.99)
LH (0.98)
LH (0.975)
LH (0.95)
LH (0.925)
LH (0.9)
BFS
0.1
1.0
10.0
100.0
Baseflow [cfs]
288

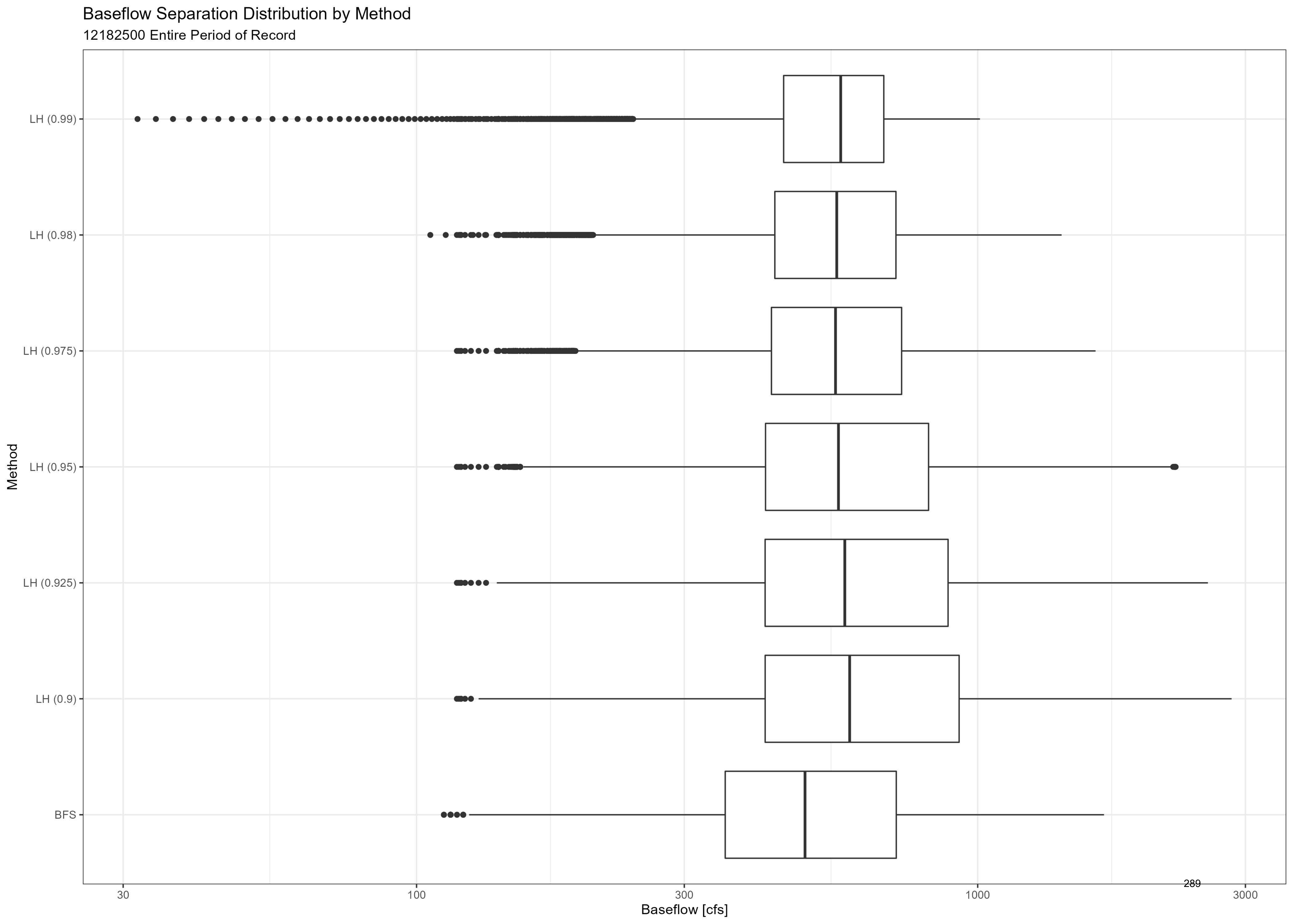
Baseflow Separation Distribution by Method
12182500 Entire Period of Record
Method
LH (0.99)
LH (0.98)
LH (0.975)
LH (0.95)
LH (0.925)
LH (0.9)
BFS
30
100
300
1000
3000
Baseflow [cfs]

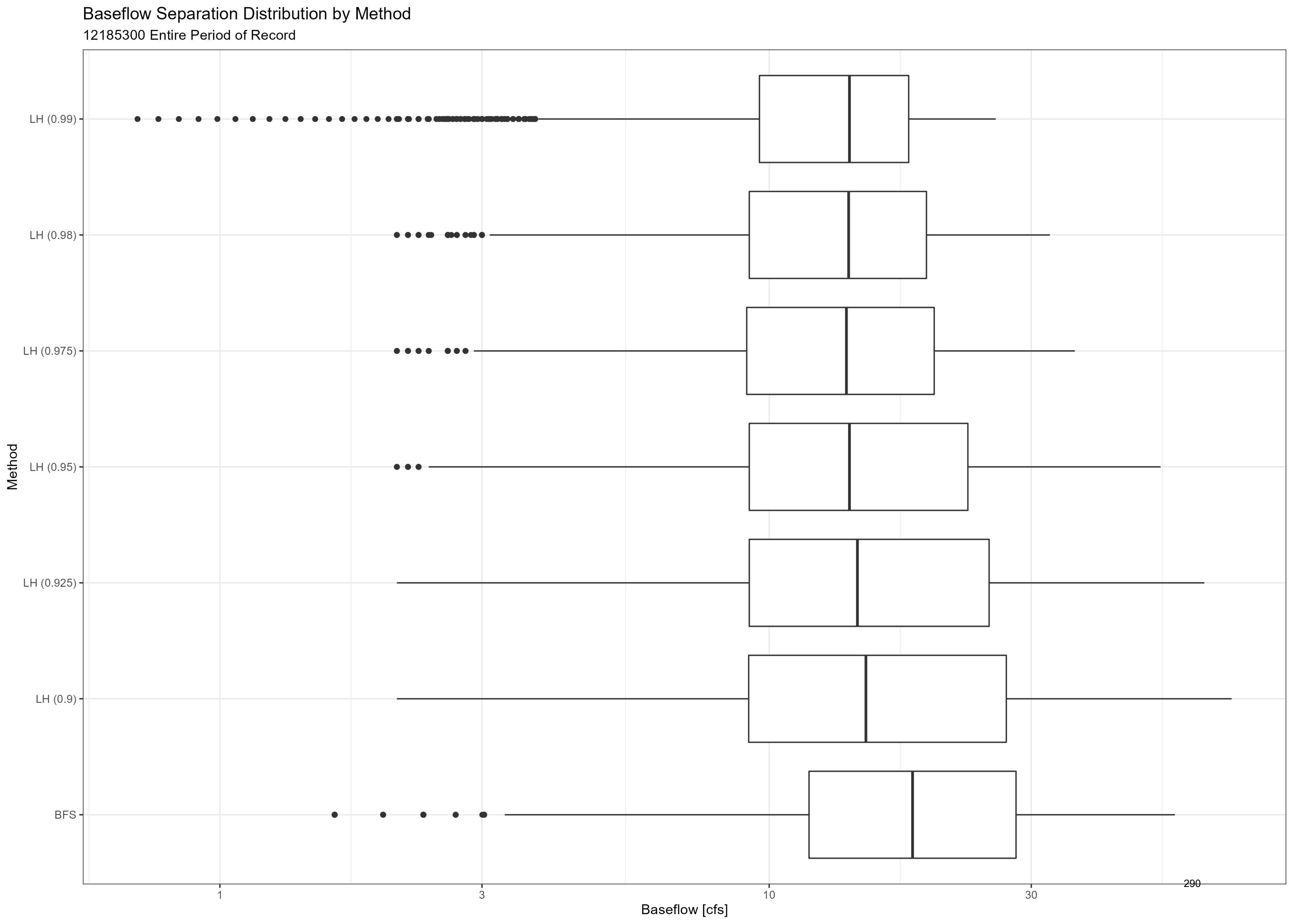

Baseflow Separation Distribution by Method
12185300 Entire Period of Record
LH (0.99)
LH (0.98)
LH (0.975)
LH (0.95)
LH (0.925)
LH (0.9)
BFS
Method
1
3
10
30
Baseflow [cfs]

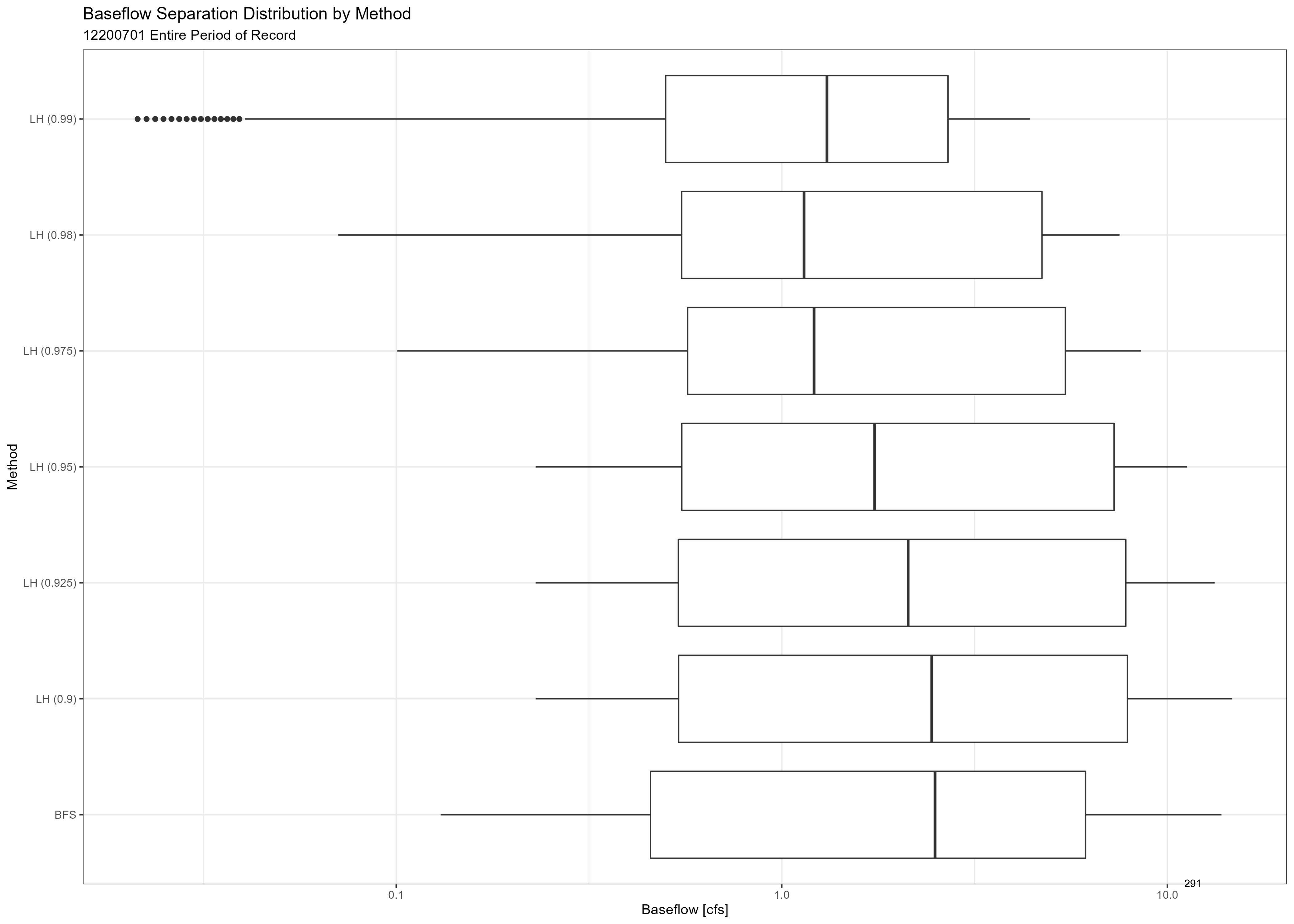

Baseflow Separation Distribution by Method
12200701 Entire Period of Record
Method
LH (0.99)
LH (0.98)
LH (0.975)
LH (0.95)
LH (0.925)
LH (0.9)
BFS
0.1
1.0
10.0
Baseflow [cfs]

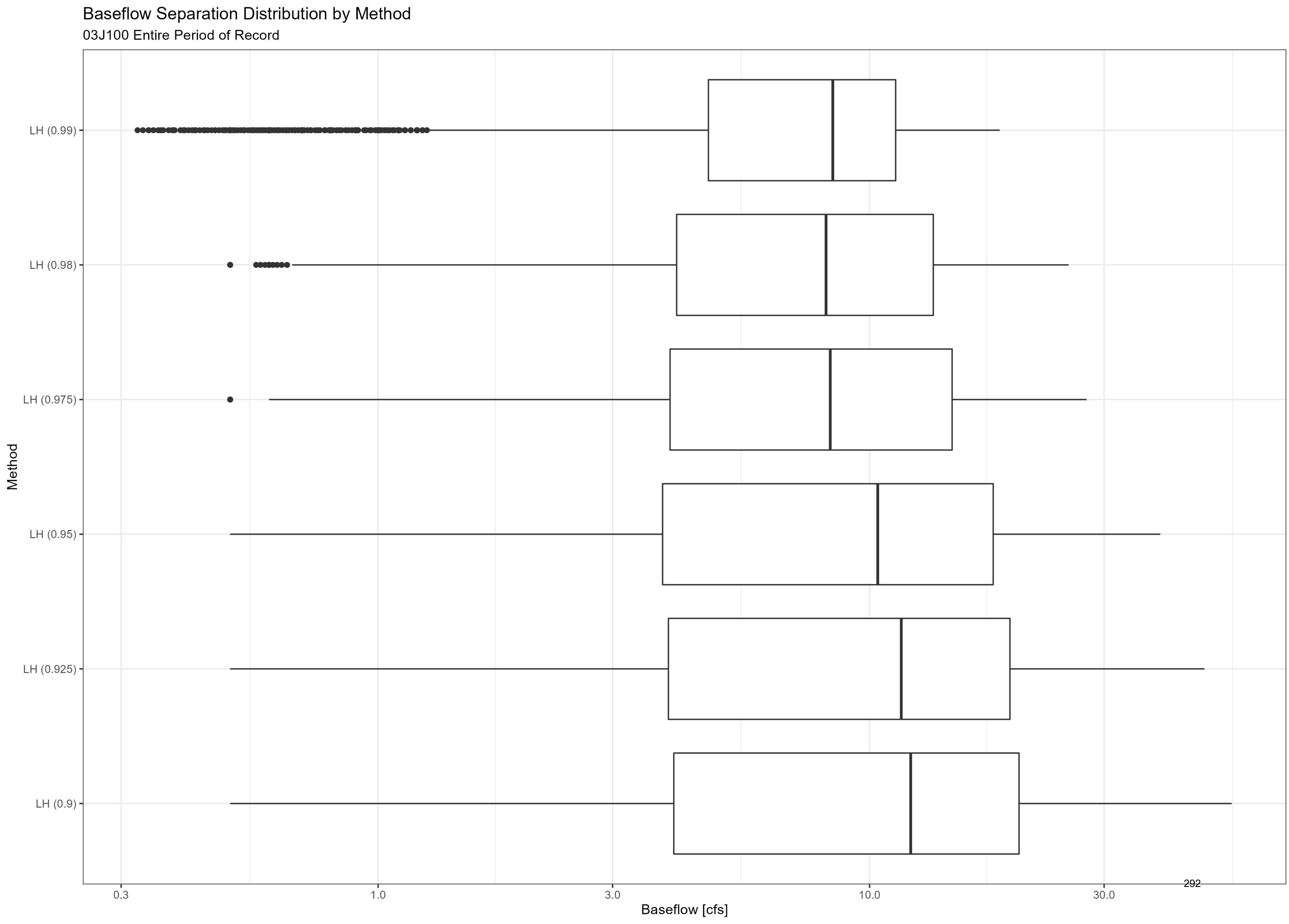
Baseflow Separation Distribution by Method
03J100 Entire Period of Record
Method
LH (0.99)
LH (0.98)
LH (0.975)
LH (0.95)
LH (0.925)
LH (0.9)
0.3
1.0
3.0
10.0
30.0
Baseflow [cfs]

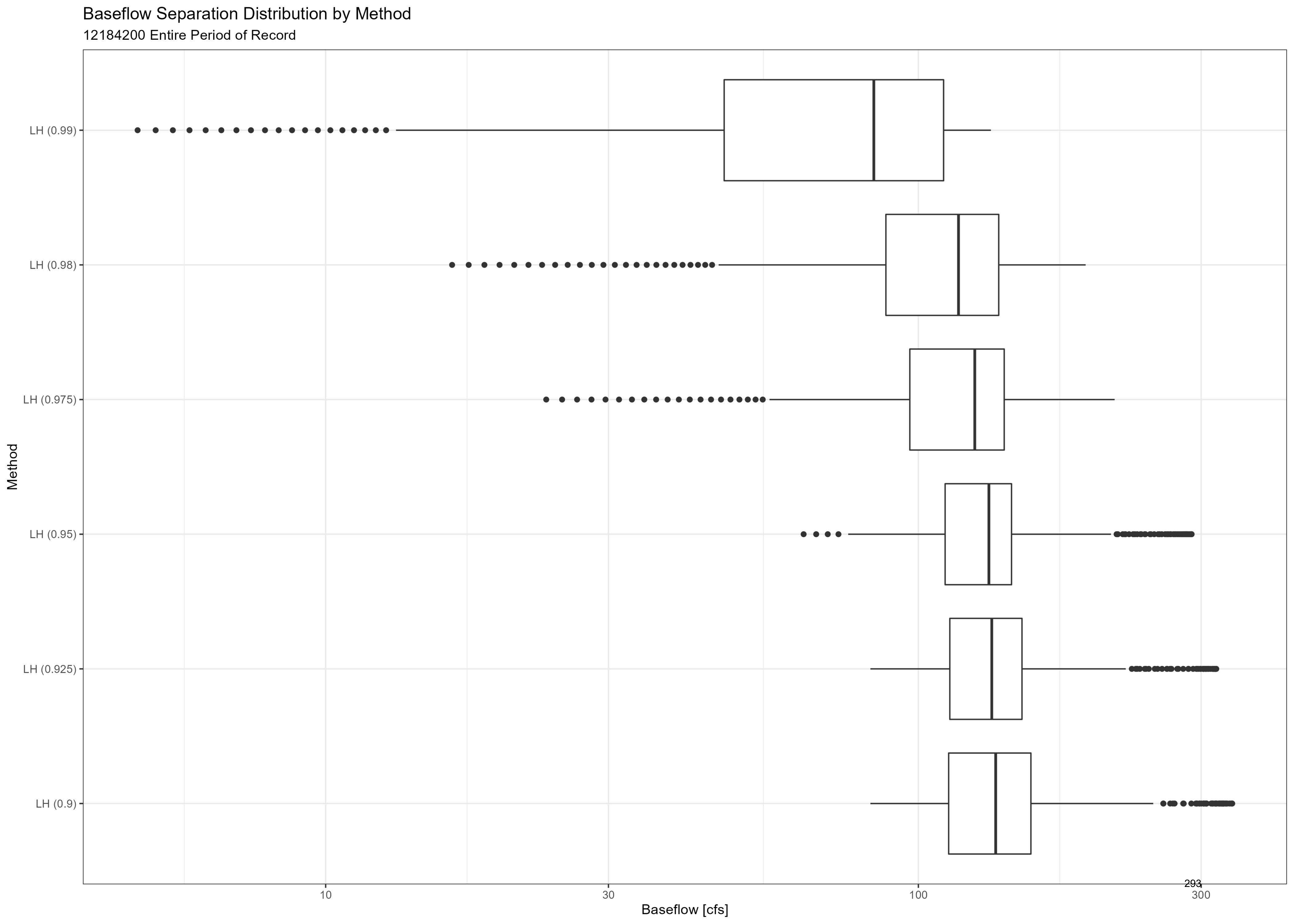

Baseflow Separation Distribution by Method
12184200 Entire Period of Record
Method
LH (0.99)
LH (0.98)
LH (0.975)
LH (0.95)
LH (0.925)
LH (0.9)
293
10
30
100
300
Baseflow [cfs]

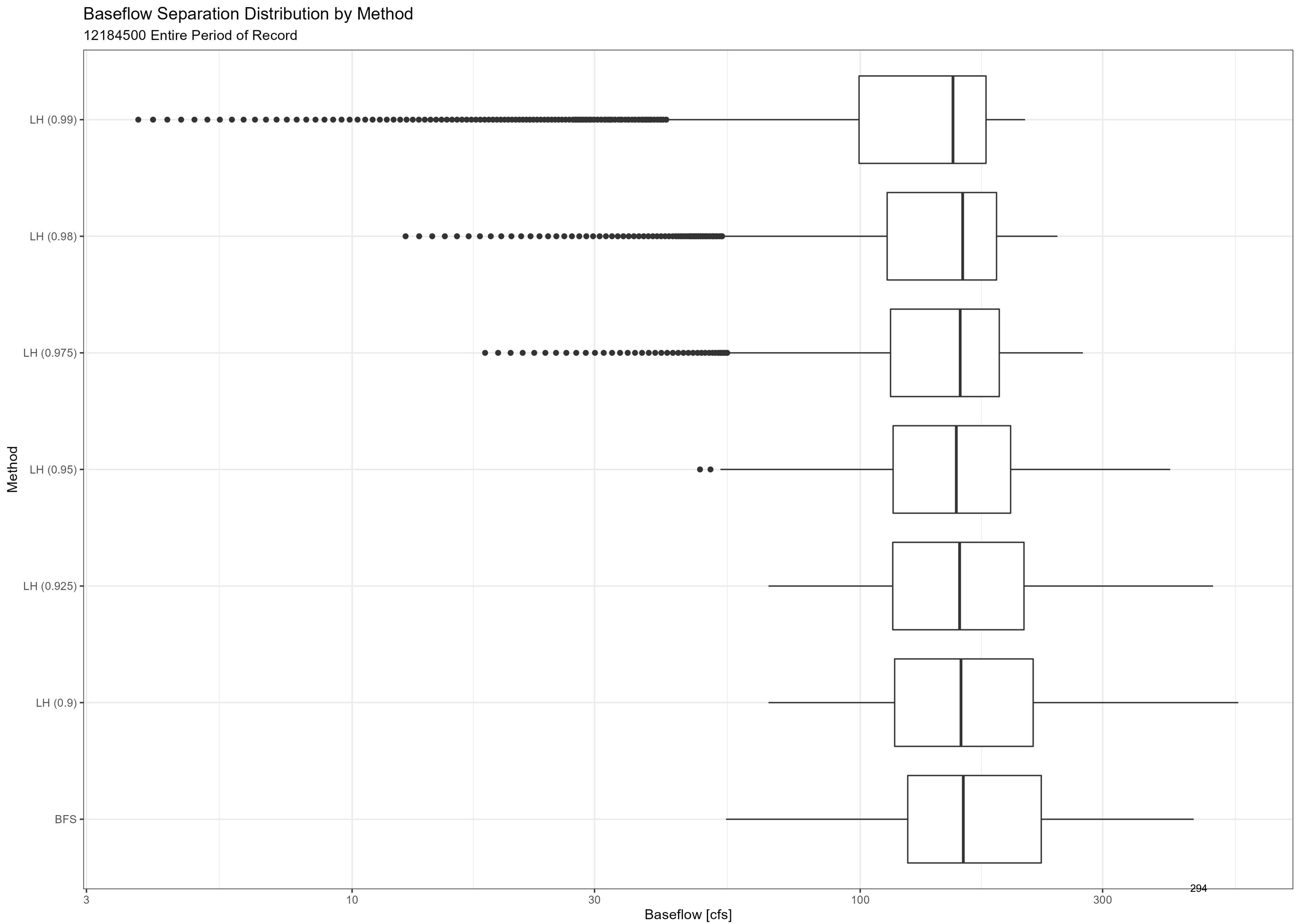

Baseflow Separation Distribution by Method
12184500 Entire Period of Record
Method
LH (0.99)
LH (0.98)
LH (0.975)
LH (0.95)
LH (0.925)
LH (0.9)
BFS
3
10
30
100
300
Baseflow [cfs]

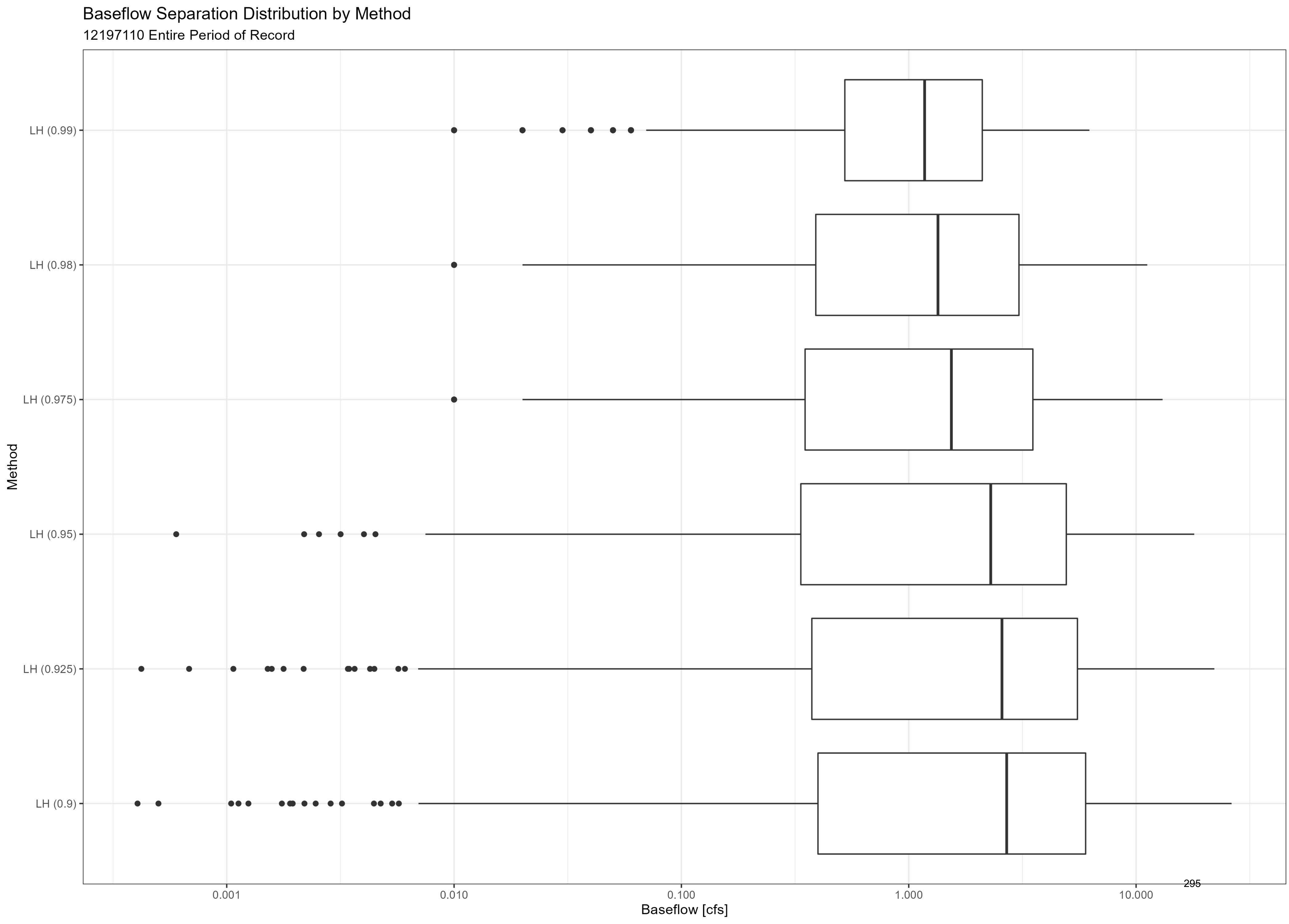

Baseflow Separation Distribution by Method
12197110 Entire Period of Record
Method
LH (0.99)
LH (0.98)
LH (0.975)
LH (0.95)
LH (0.925)
LH (0.9)
0.001
0.010
0.100
1.000
10.000
Baseflow [cfs]


295

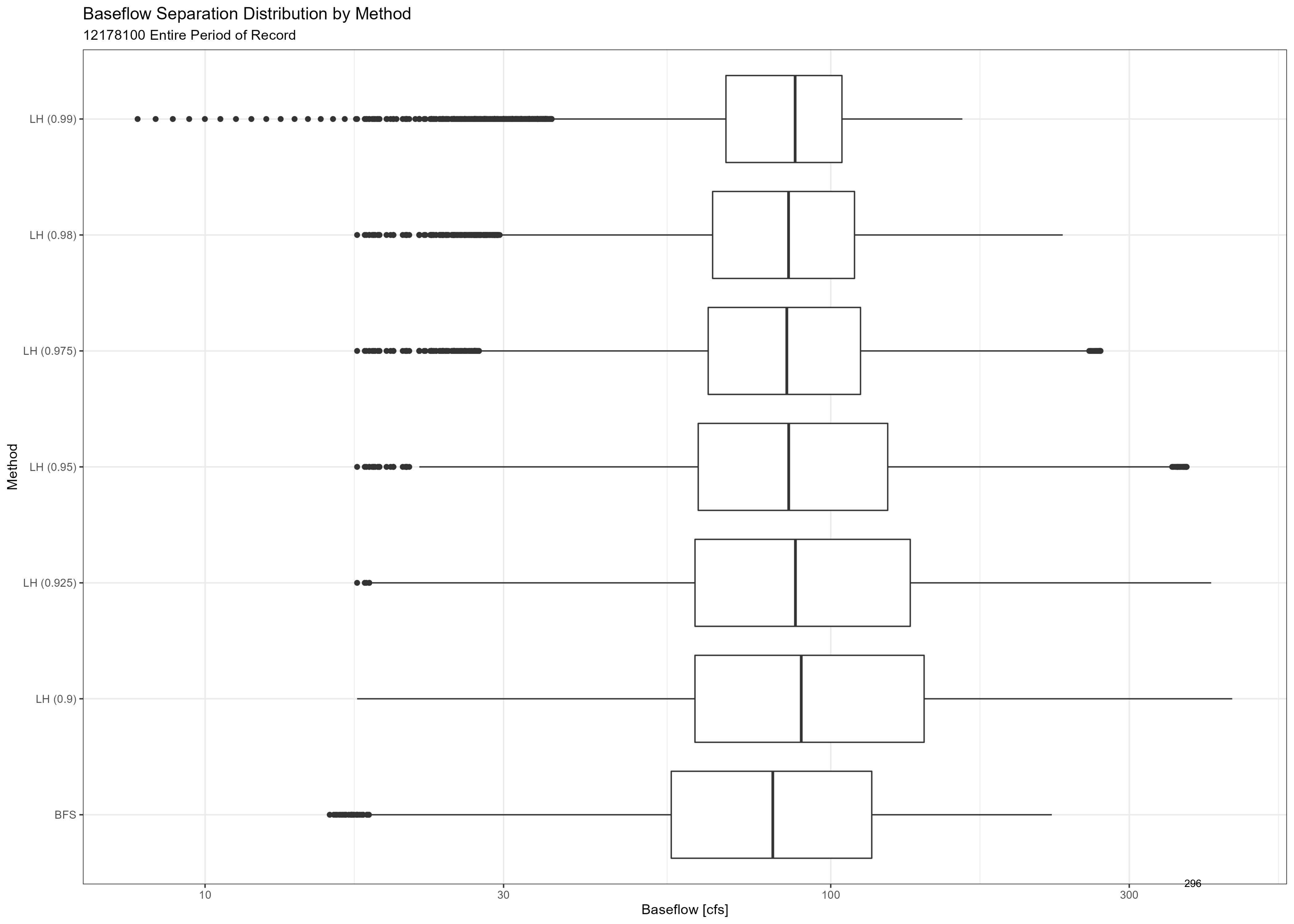
Baseflow Separation Distribution by Method
12178100 Entire Period of Record
LH (0.99)
LH (0.98)
LH (0.975)
LH (0.95)
LH (0.925)
LH (0.9)
BFS
Method
10
30
100
300
296
Baseflow [cfs]

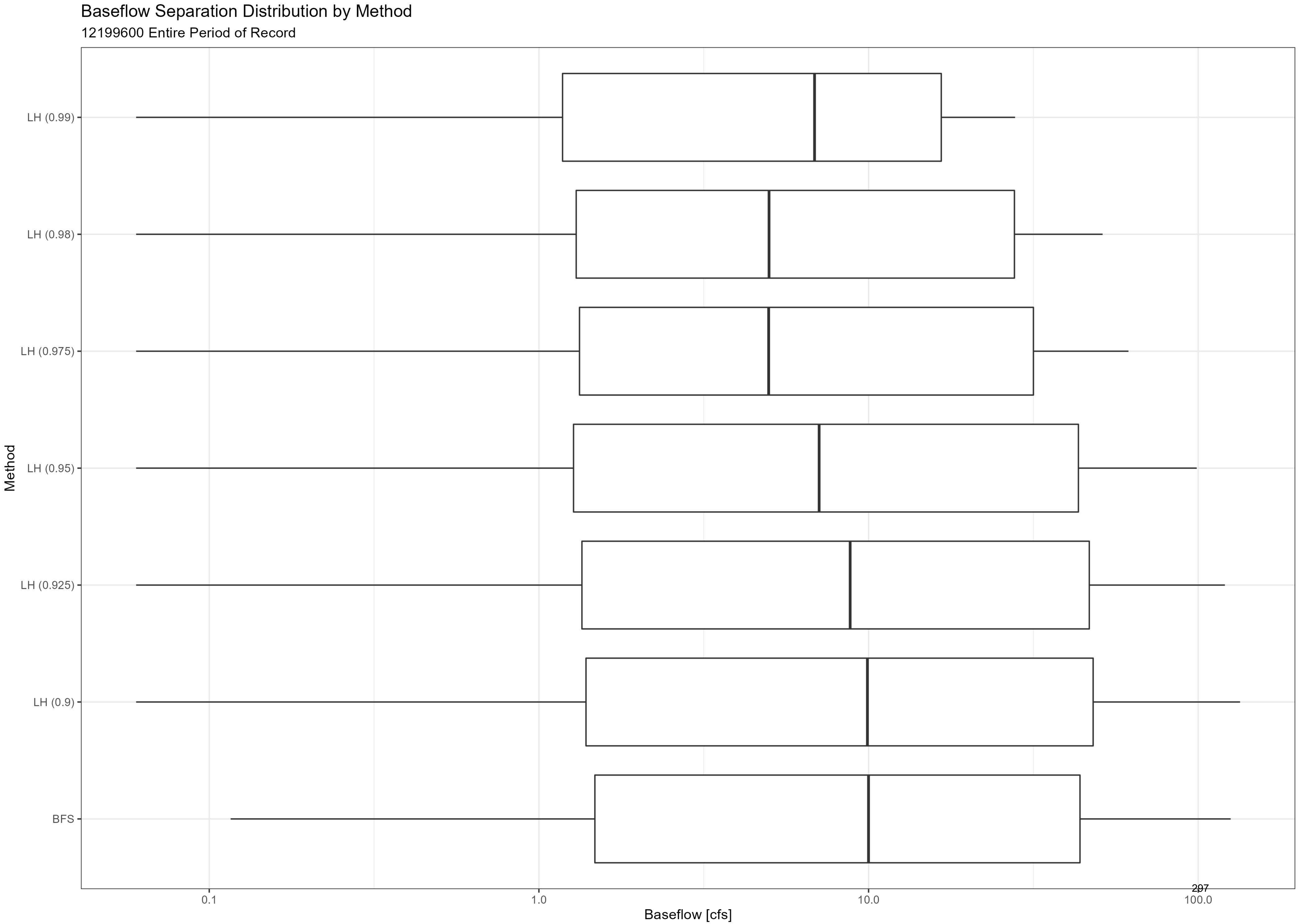
Baseflow Separation Distribution by Method
12199600 Entire Period of Record
Method
LH (0.99)
LH (0.98)
LH (0.975)
LH (0.95)
LH (0.925)
LH (0.9)
BFS
0.1
1.0
10.0
100.0
Baseflow [cfs]

Baseflow Separation Distribution by Method

03G100 Entire Period of Record

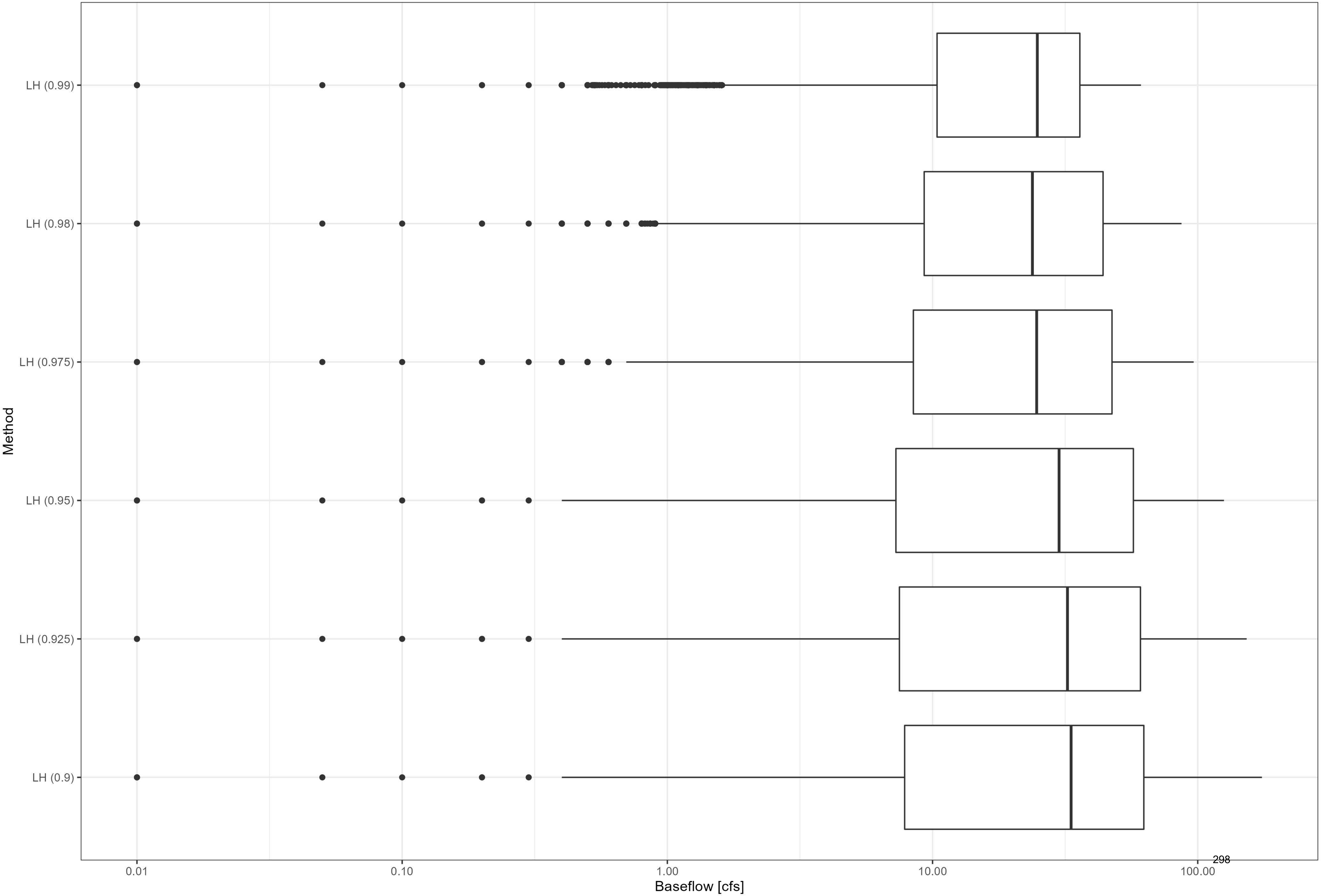

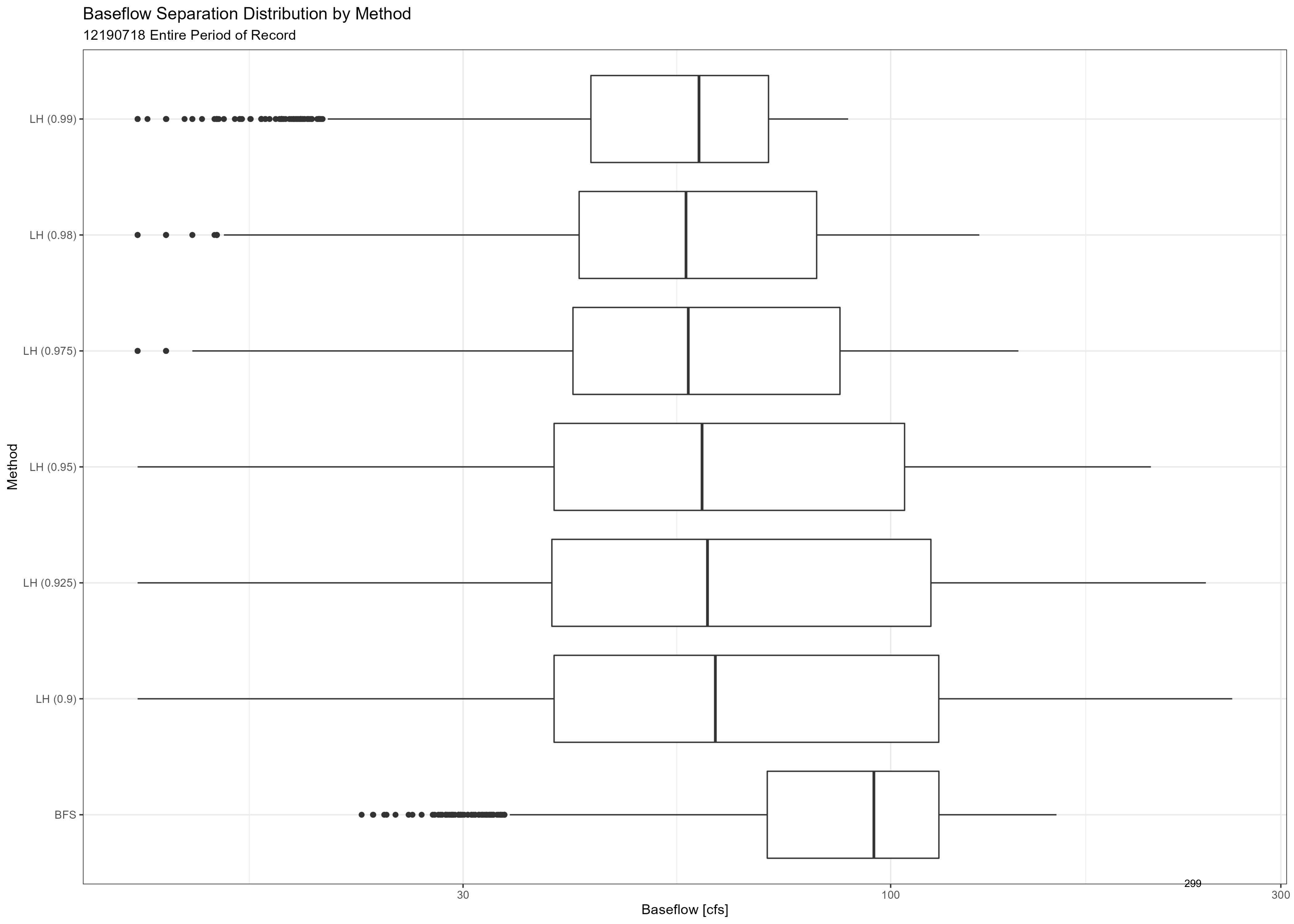

Baseflow Separation Distribution by Method
12190718 Entire Period of Record
Method
LH (0.99)
LH (0.98)
LH (0.975)
LH (0.95)
LH (0.925)
LH (0.9)
BFS
299
30
100
300
Baseflow [cfs]

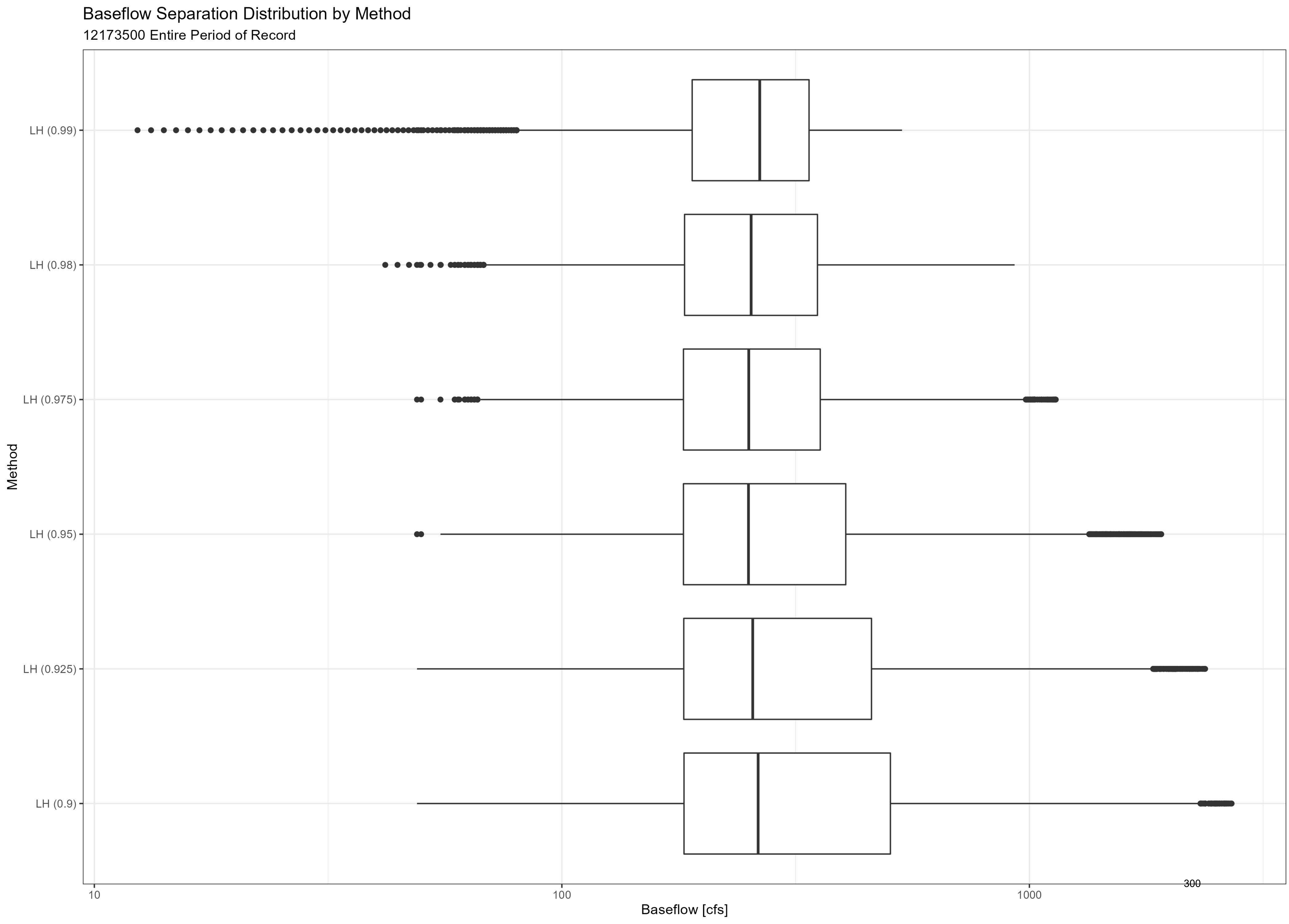

Baseflow Separation Distribution by Method
12173500 Entire Period of Record
Method
LH (0.99)
LH (0.98)
LH (0.975)
LH (0.95)
LH (0.925)
LH (0.9)
10
100
1000
Baseflow [cfs]


300

## Baseflow Separation Distribution by Method

12181200 Entire Period of Record

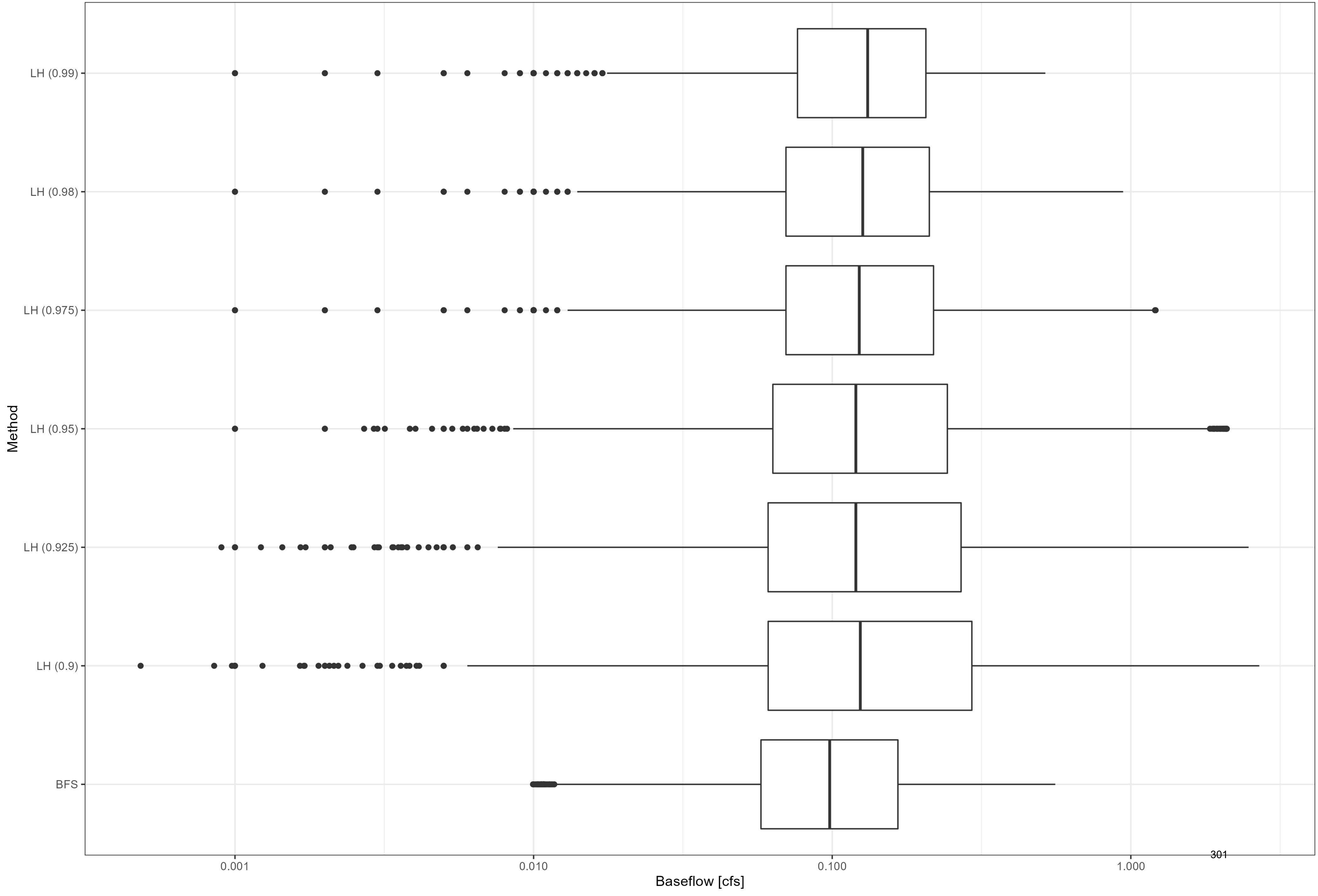

## Baseflow Separation Distribution by Method

12186000 Entire Period of Record

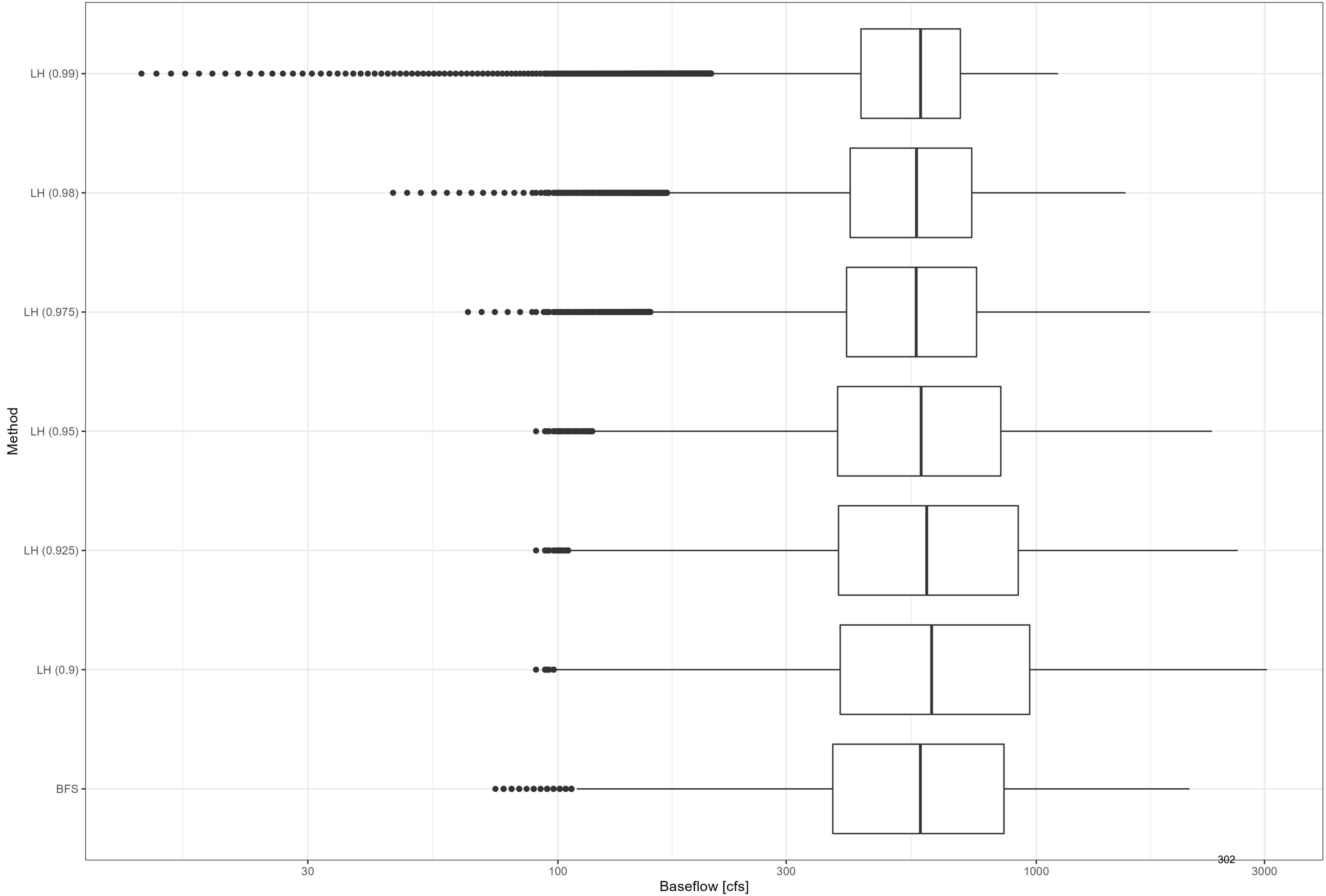

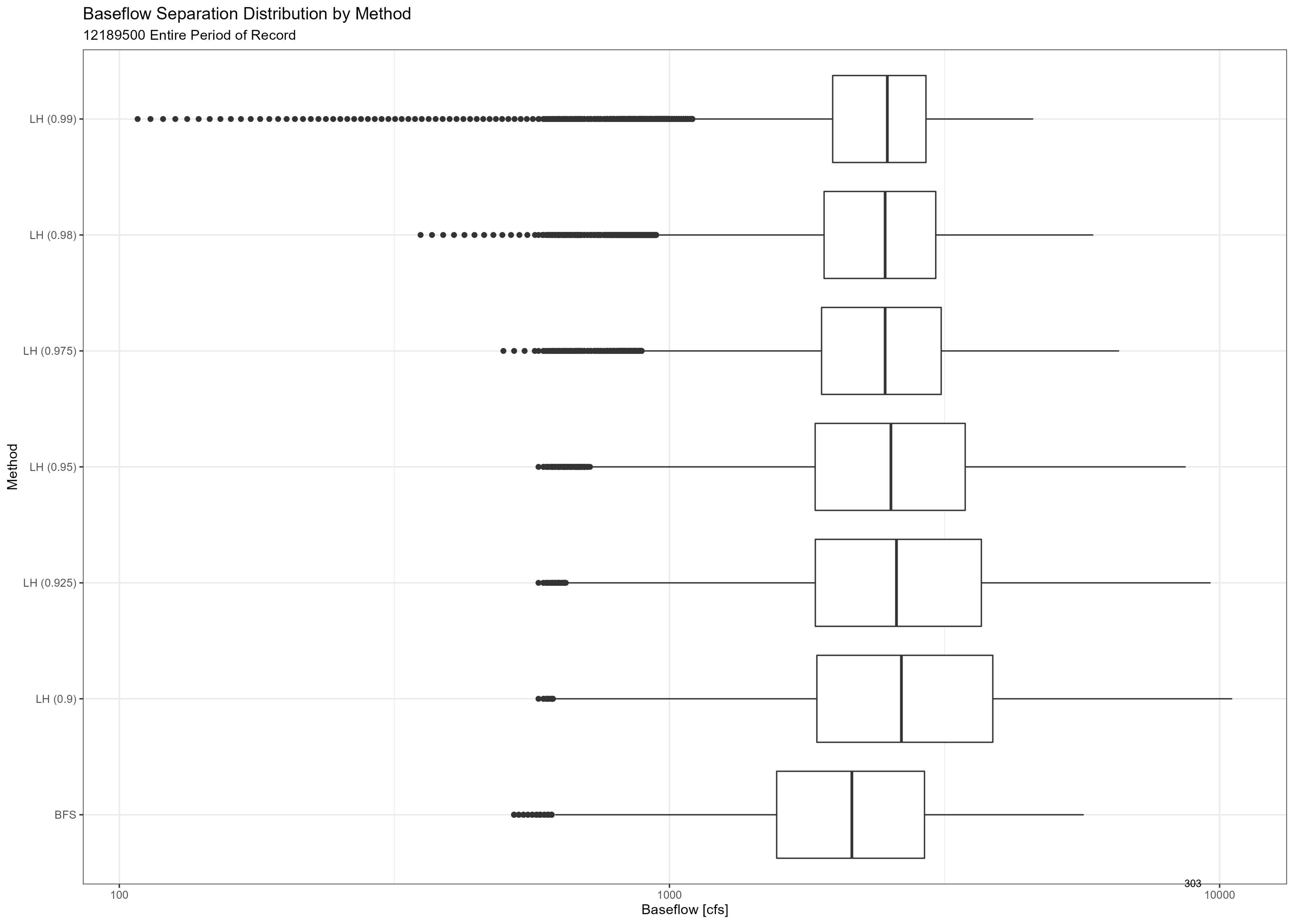
Baseflow Separation Distribution by Method
12189500 Entire Period of Record
Method
LH (0.99)
LH (0.98)
LH (0.975)
LH (0.95)
LH (0.925)
LH (0.9)
BFS
100
1000
10000
Baseflow [cfs]

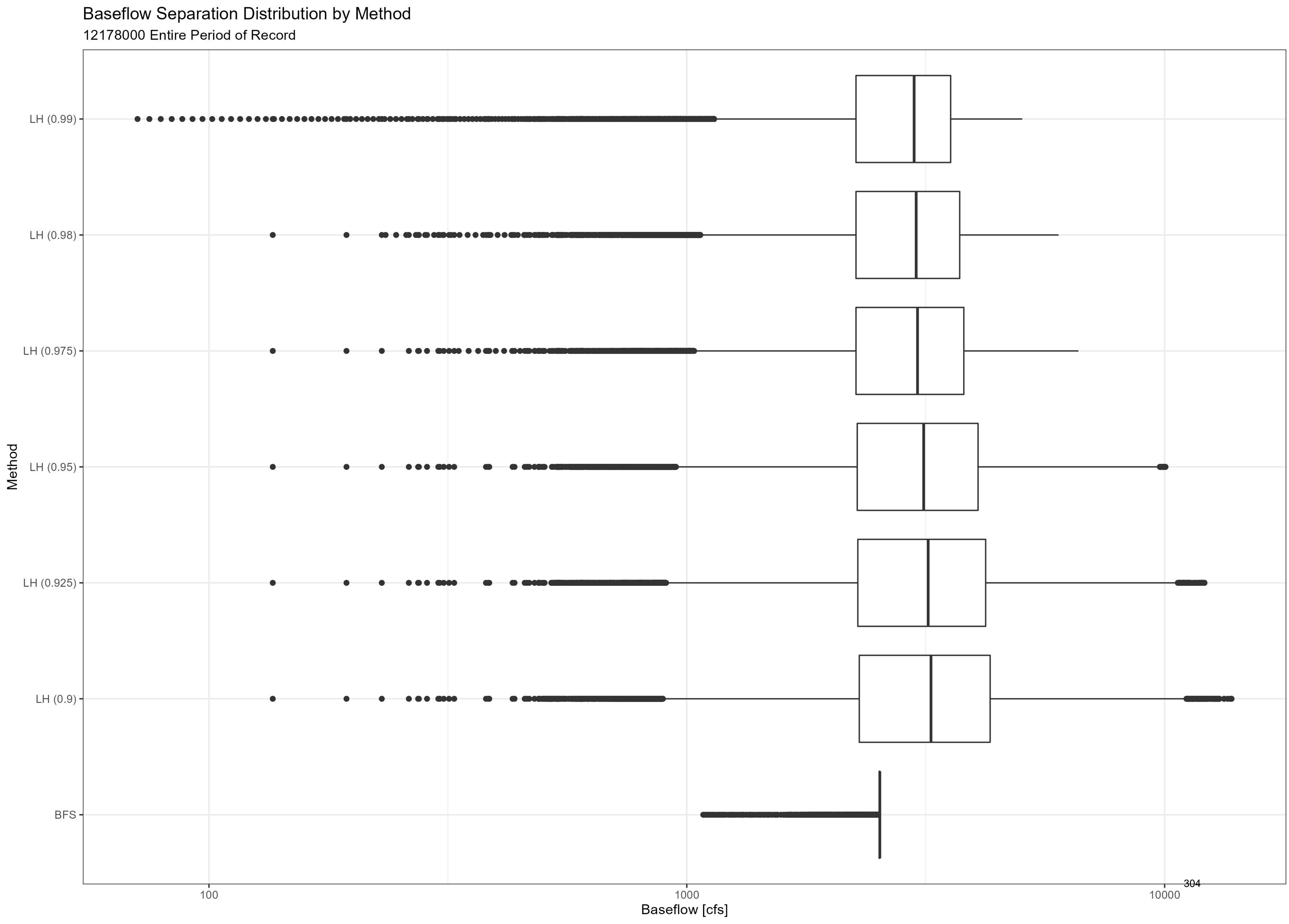
Baseflow Separation Distribution by Method
12178000 Entire Period of Record
Method
LH (0.99)
LH (0.98)
LH (0.975)
LH (0.95)
LH (0.925)
LH (0.9)
BFS
100
1000
10000
Baseflow [cfs]

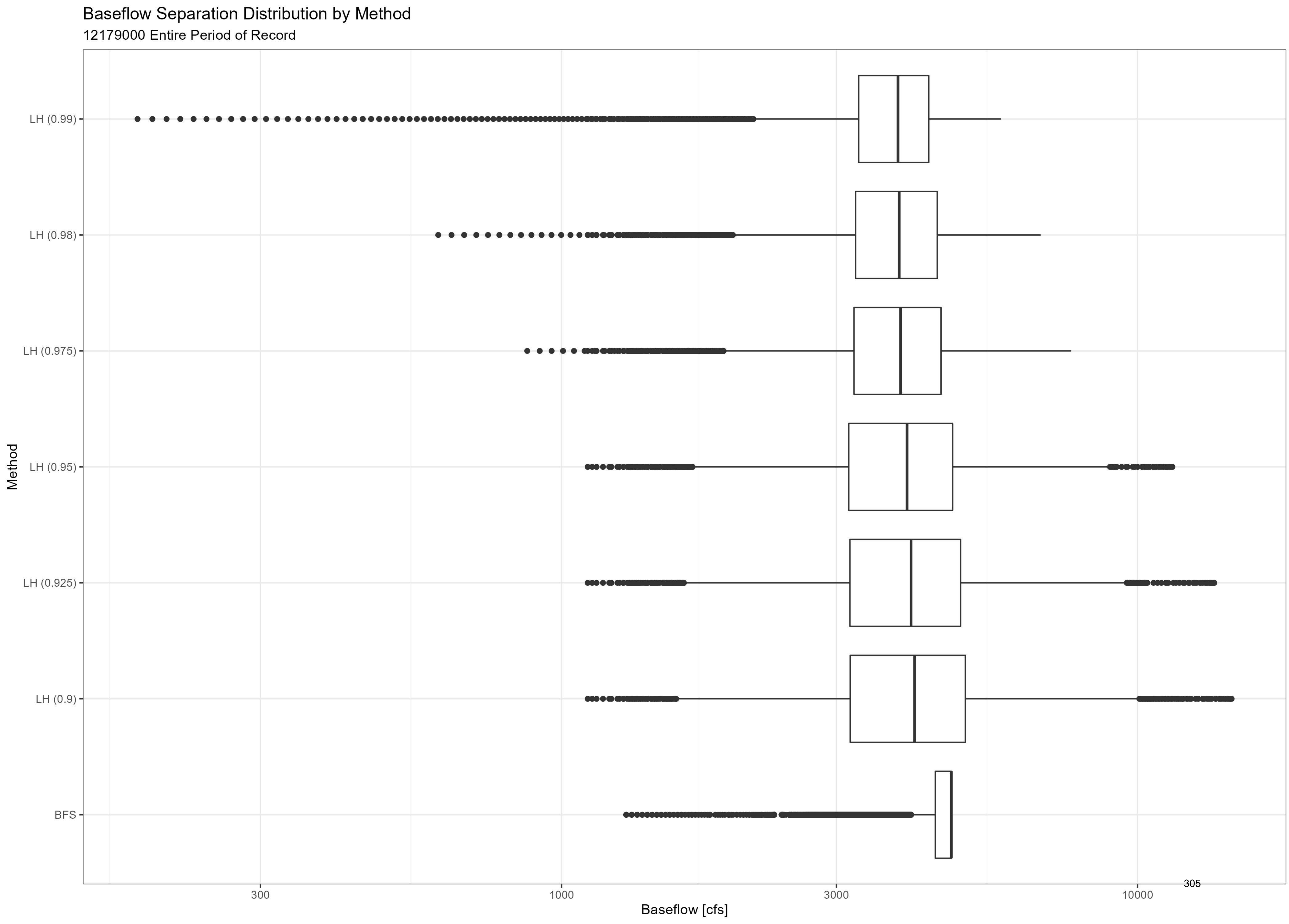
Baseflow Separation Distribution by Method
12179000 Entire Period of Record
Method
LH (0.99)
LH (0.98)
LH (0.975)
LH (0.95)
LH (0.925)
LH (0.9)
BFS
300
1000
3000
10000
Baseflow [cfs]

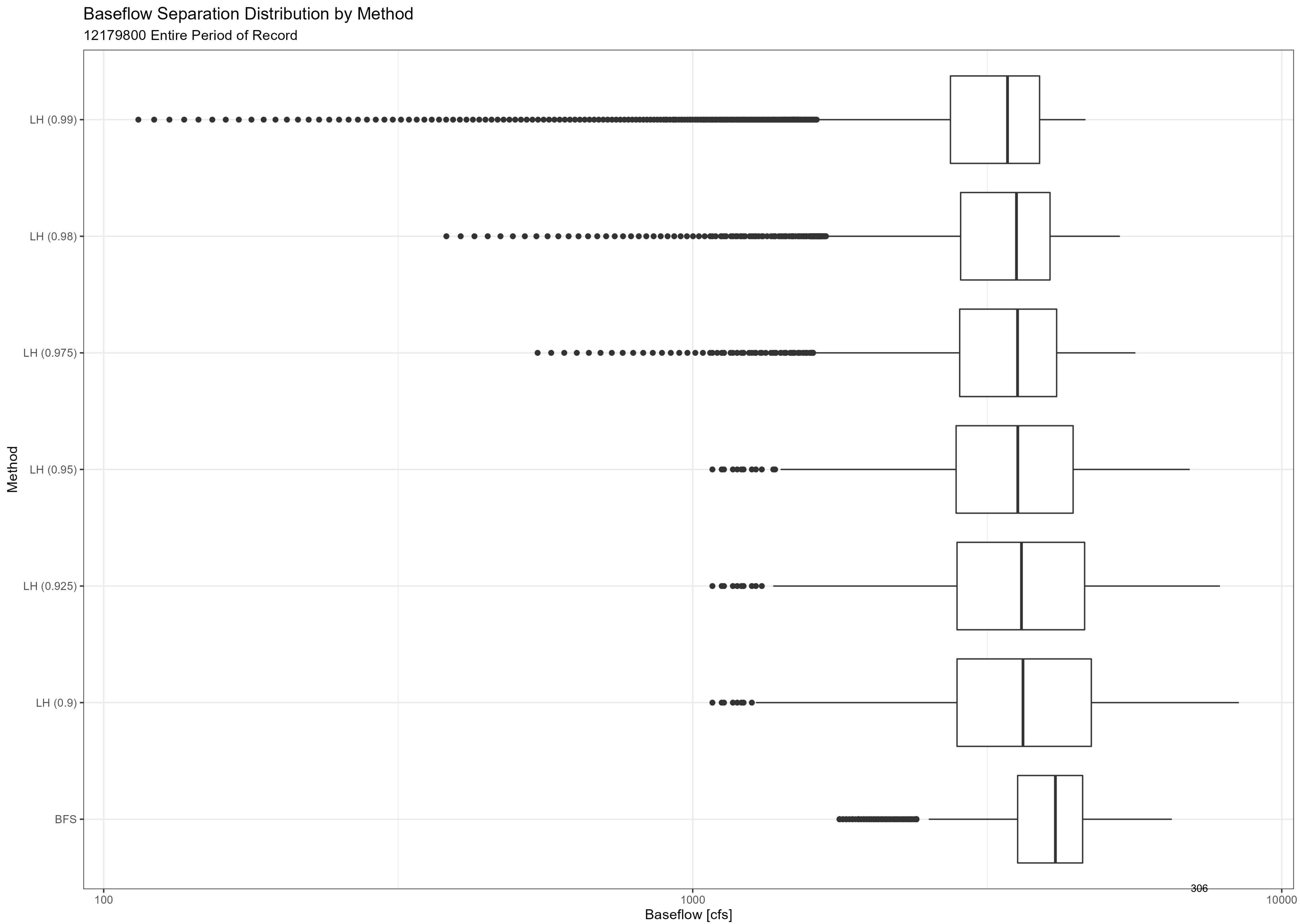
Baseflow Separation Distribution by Method
12179800 Entire Period of Record
LH (0.99)
LH (0.98)
LH (0.975)
LH (0.95)
LH (0.925)
LH (0.9)
BFS
Method
100
1000
10000
Baseflow [cfs]

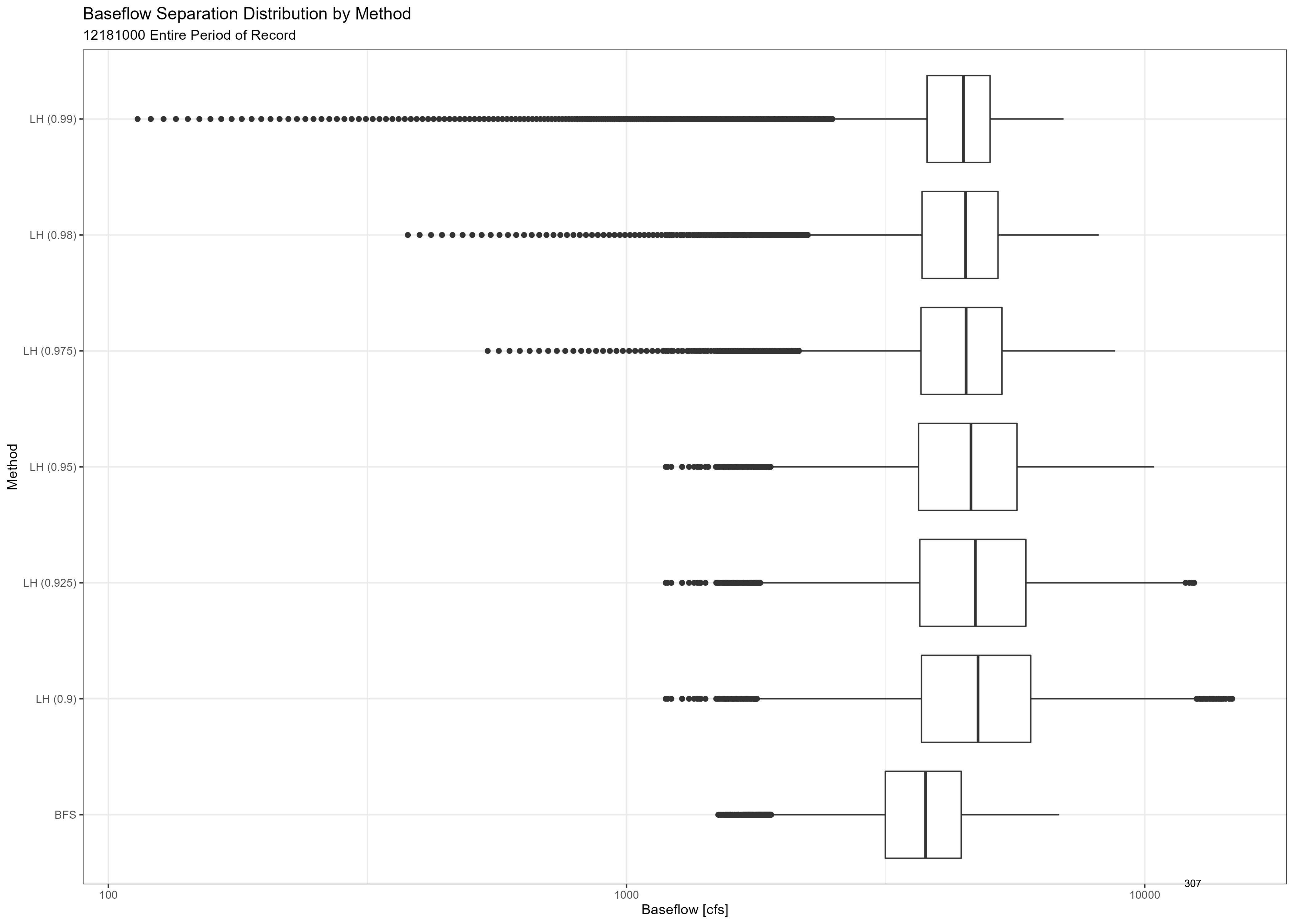
Baseflow Separation Distribution by Method
12181000 Entire Period of Record
Method
LH (0.99)
LH (0.98)
LH (0.975)
LH (0.95)
LH (0.925)
LH (0.9)
BFS
100
1000
10000
Baseflow [cfs]

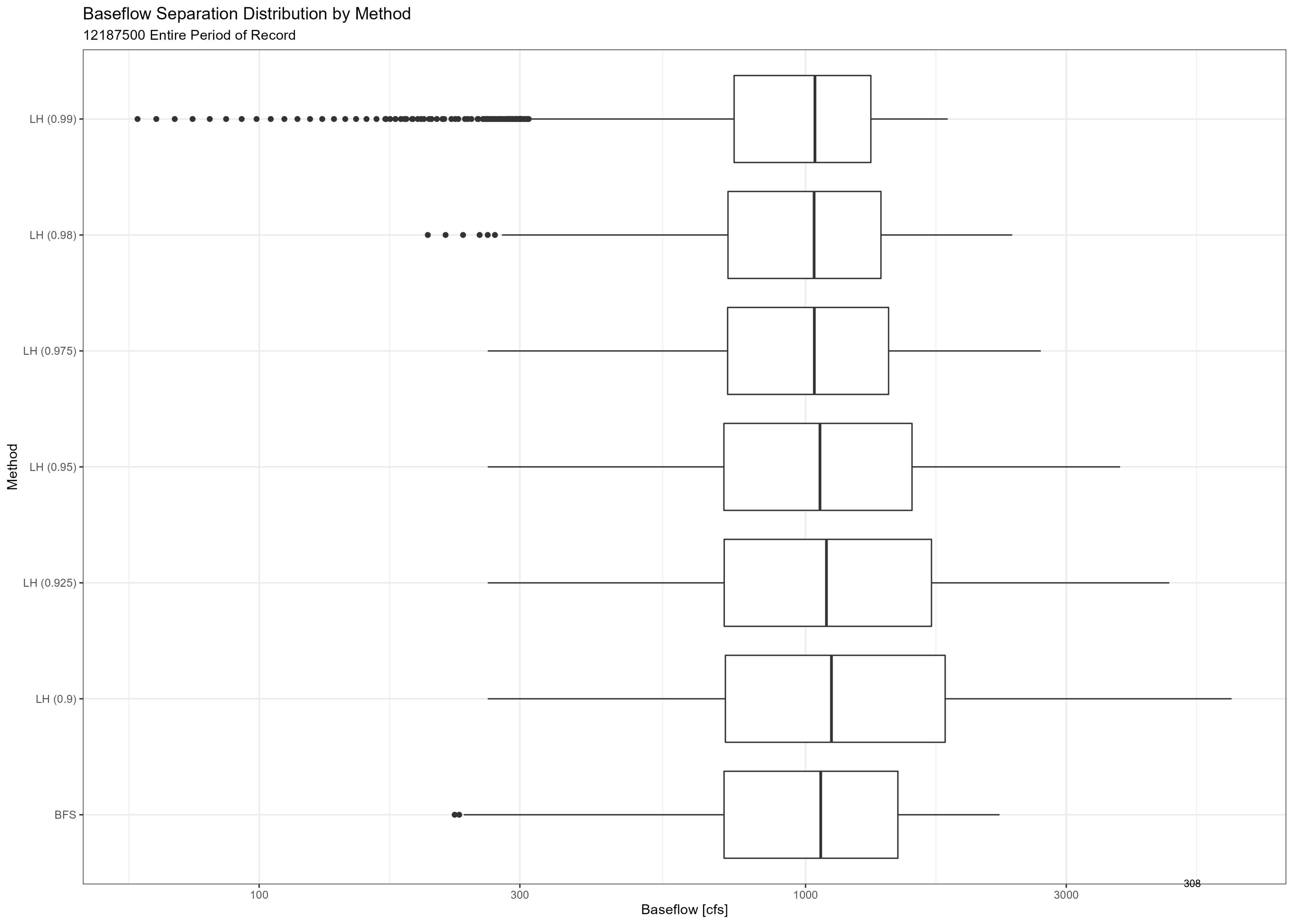
Baseflow Separation Distribution by Method
12187500 Entire Period of Record
LH (0.99)
LH (0.98)
LH (0.975)
LH (0.95)
LH (0.925)
LH (0.9)
BFS
Method
100
300
1000
3000
Baseflow [cfs]

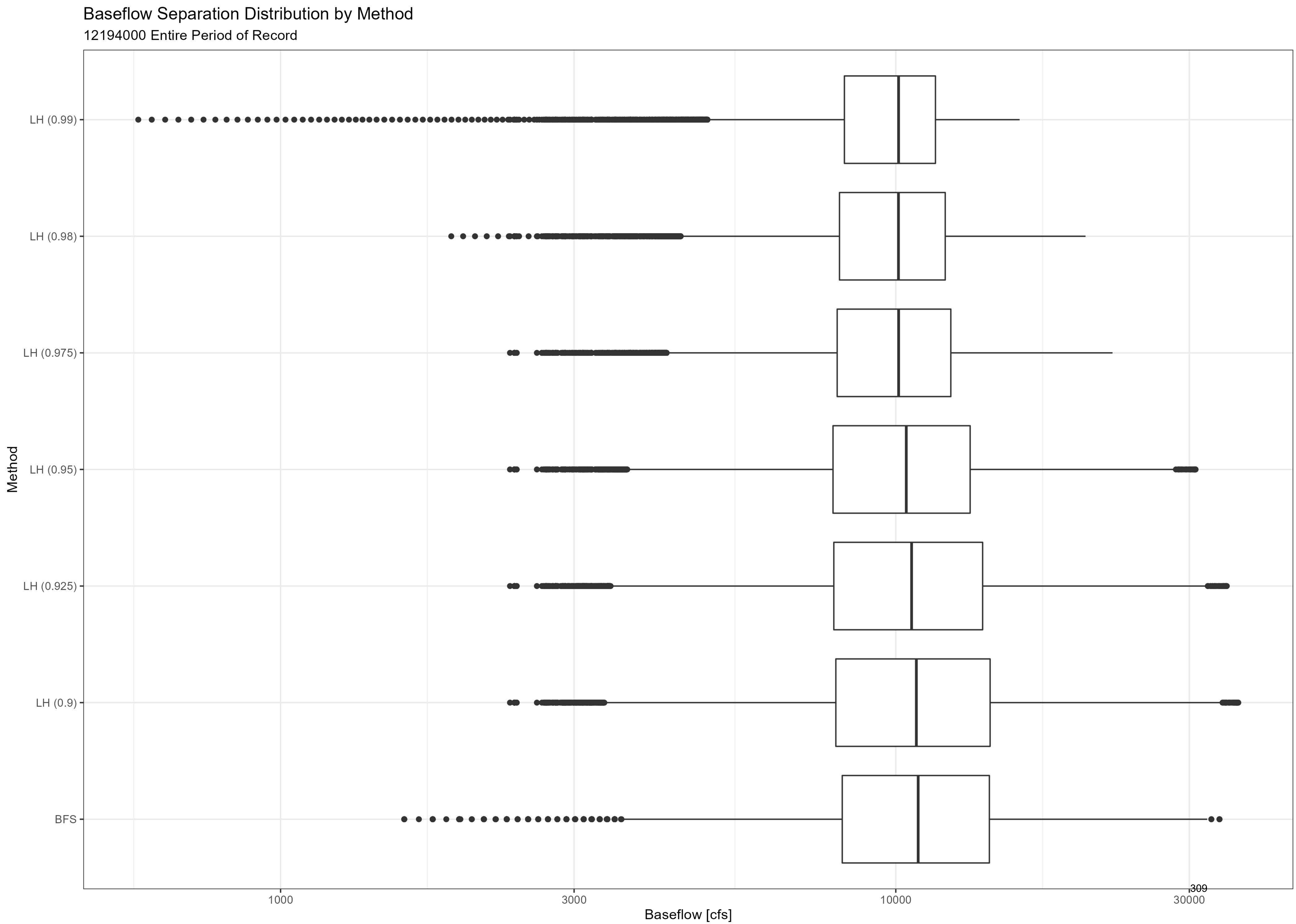
Baseflow Separation Distribution by Method
12194000 Entire Period of Record
Method
LH (0.99)
LH (0.98)
LH (0.975)
LH (0.95)
LH (0.925)
LH (0.9)
BFS
1000
3000
10000
30000
Baseflow [cfs]

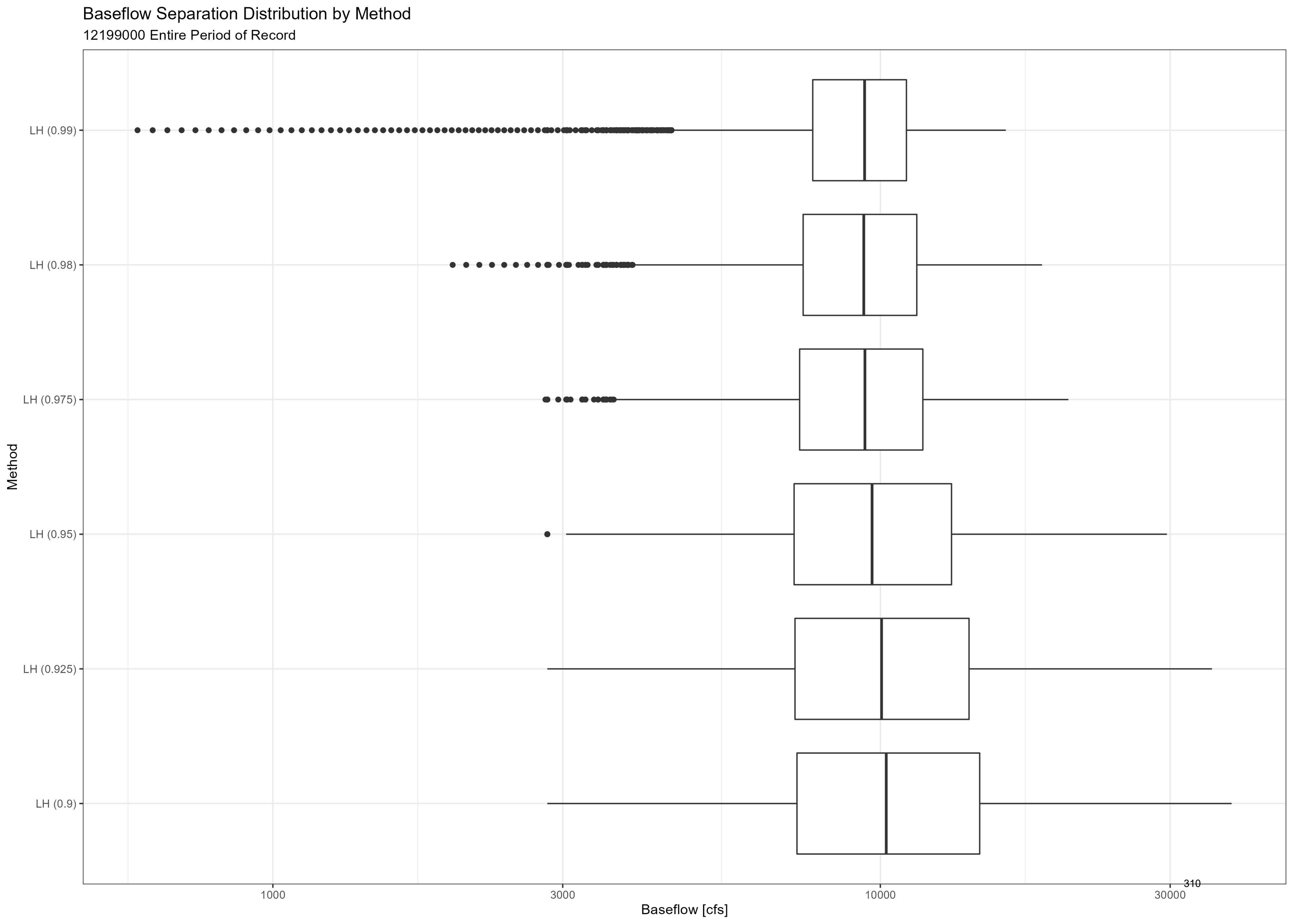

Baseflow Separation Distribution by Method
12199000 Entire Period of Record
LH (0.99)
LH (0.98)
LH (0.975)
LH (0.95)
LH (0.925)
LH (0.9)
Method
1000
3000
10000
30000
Baseflow [cfs]

Baseflow Separation Distribution by Method

12200500 Entire Period of Record

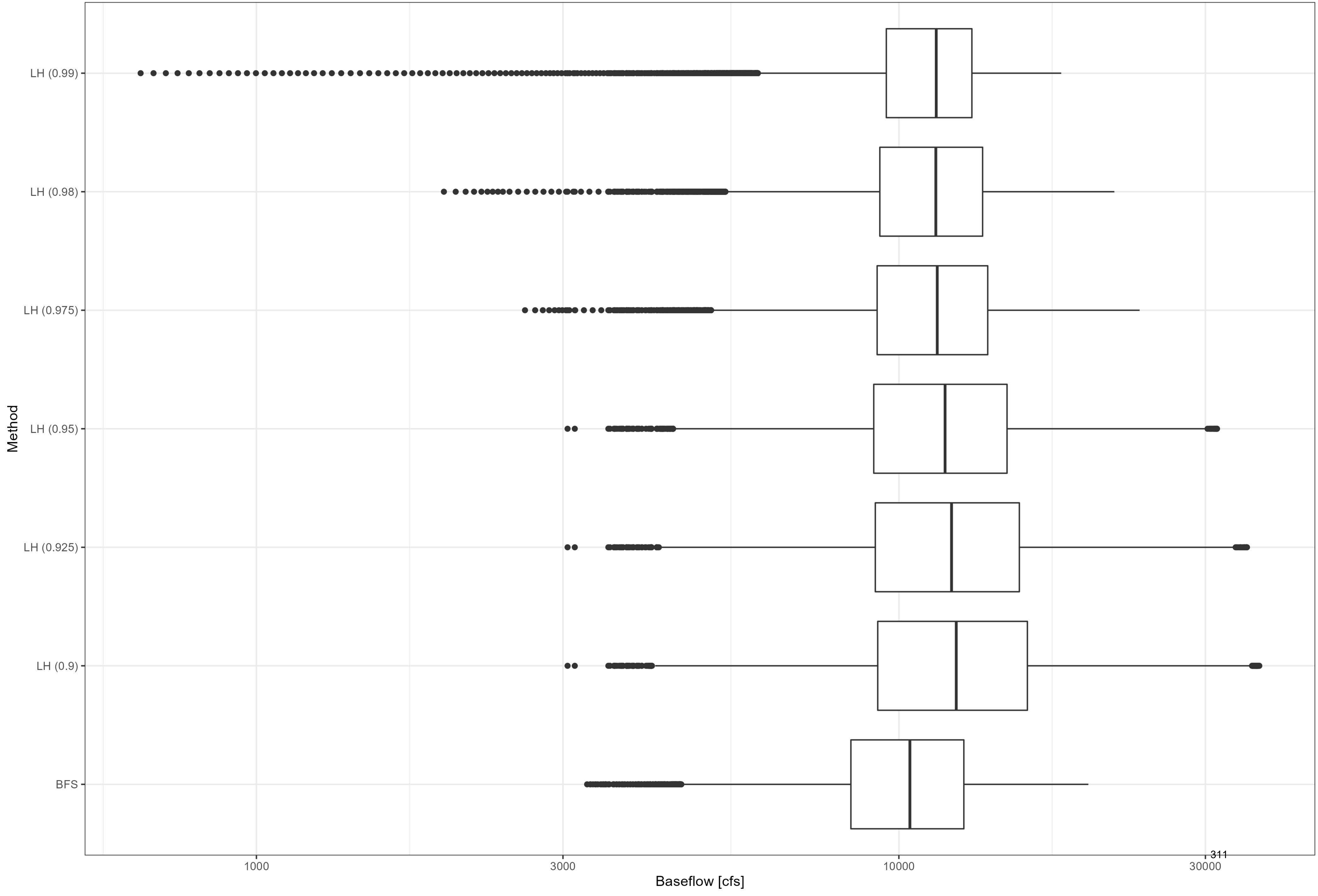

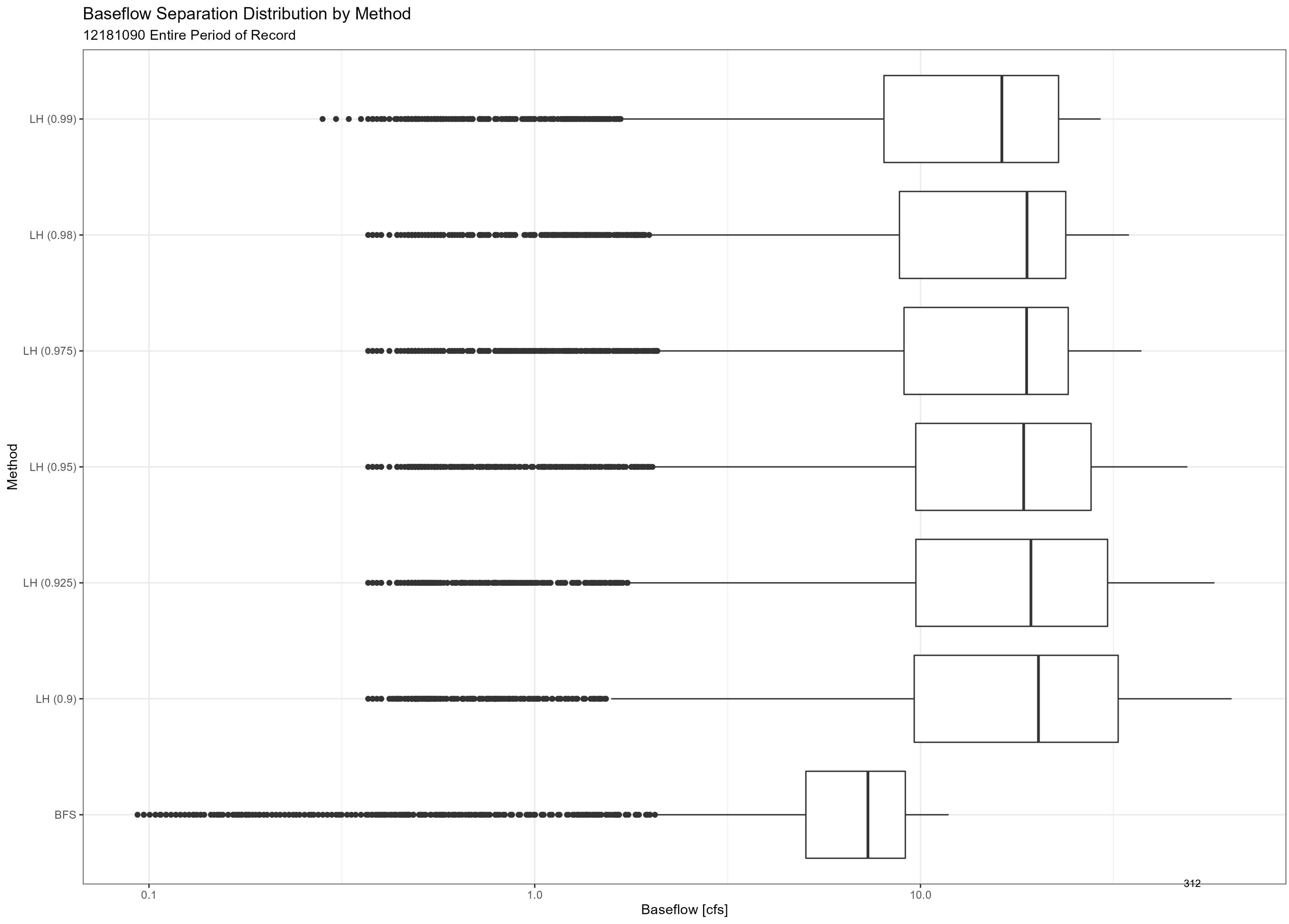
Baseflow Separation Distribution by Method
12181090 Entire Period of Record
Method
LH (0.99)
LH (0.98)
LH (0.975)
LH (0.95)
LH (0.925)
LH (0.9)
BFS
0.1
1.0
10.0
Baseflow [cfs]

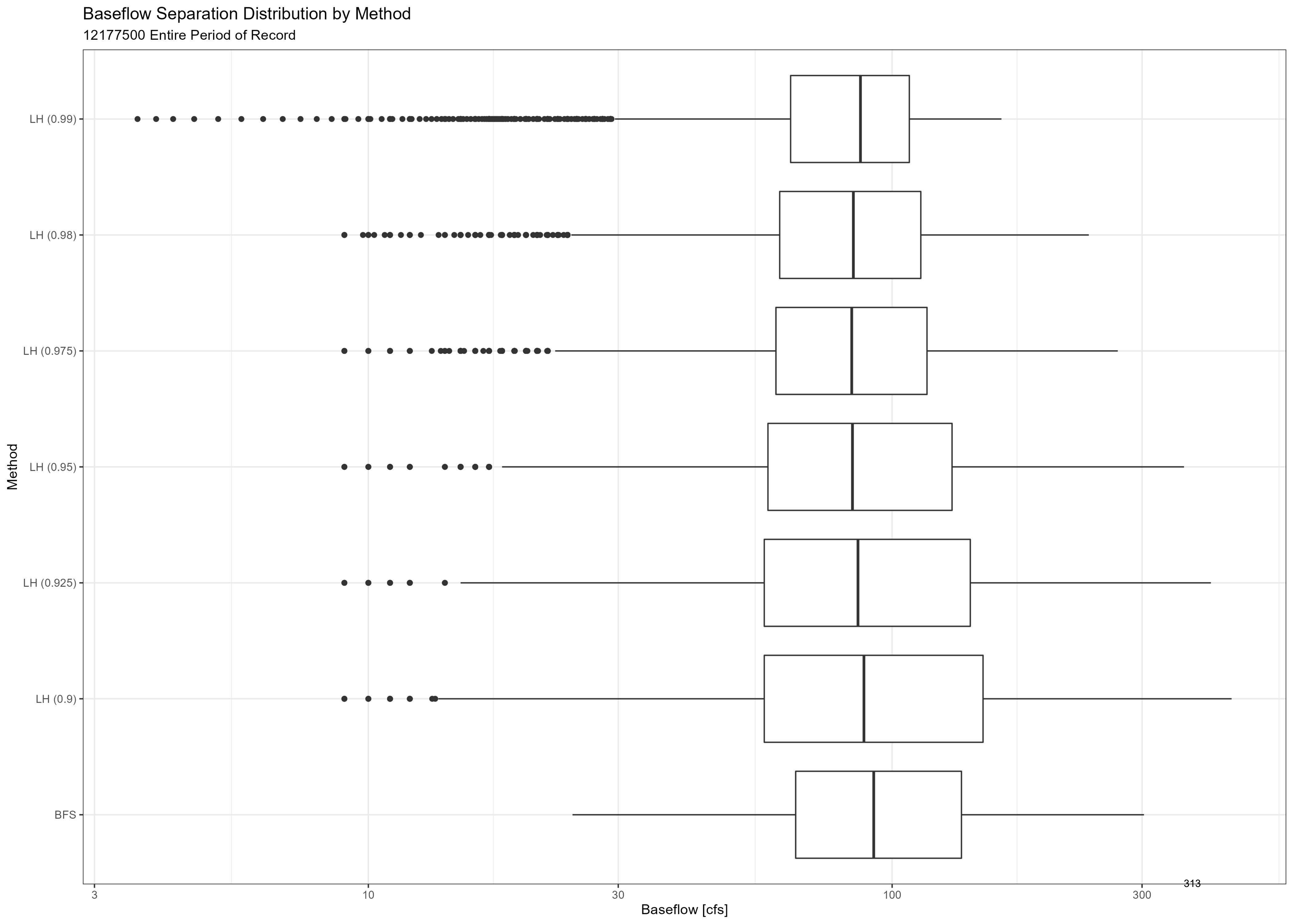
Baseflow Separation Distribution by Method
12177500 Entire Period of Record
Method
LH (0.99)
LH (0.98)
LH (0.975)
LH (0.95)
LH (0.925)
LH (0.9)
BFS
3
10
30
100
300
Baseflow [cfs]

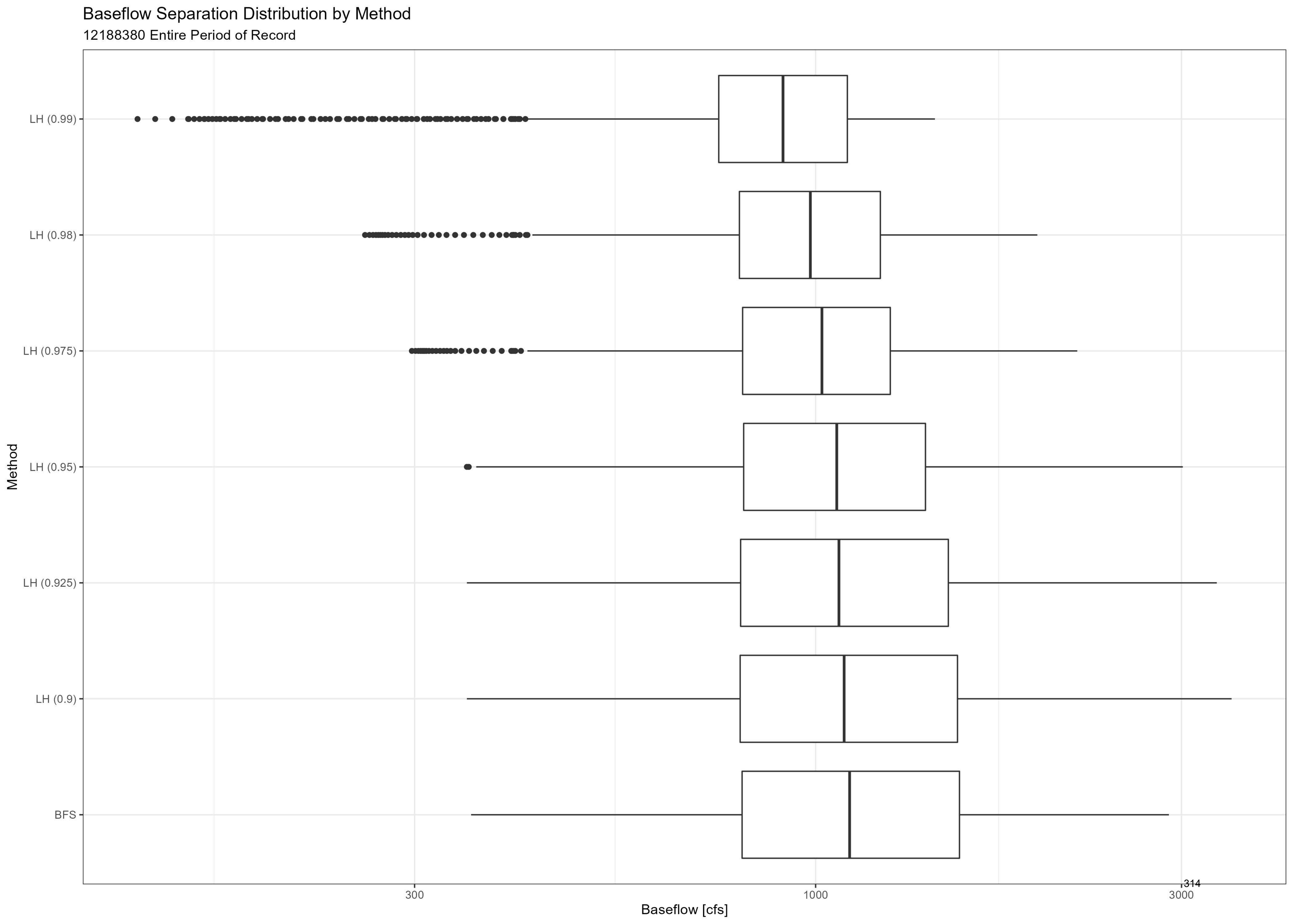
Baseflow Separation Distribution by Method
12188380 Entire Period of Record
Method
LH (0.99)
LH (0.98)
LH (0.975)
LH (0.95)
LH (0.925)
LH (0.9)
BFS
300
1000
3000
Baseflow [cfs]

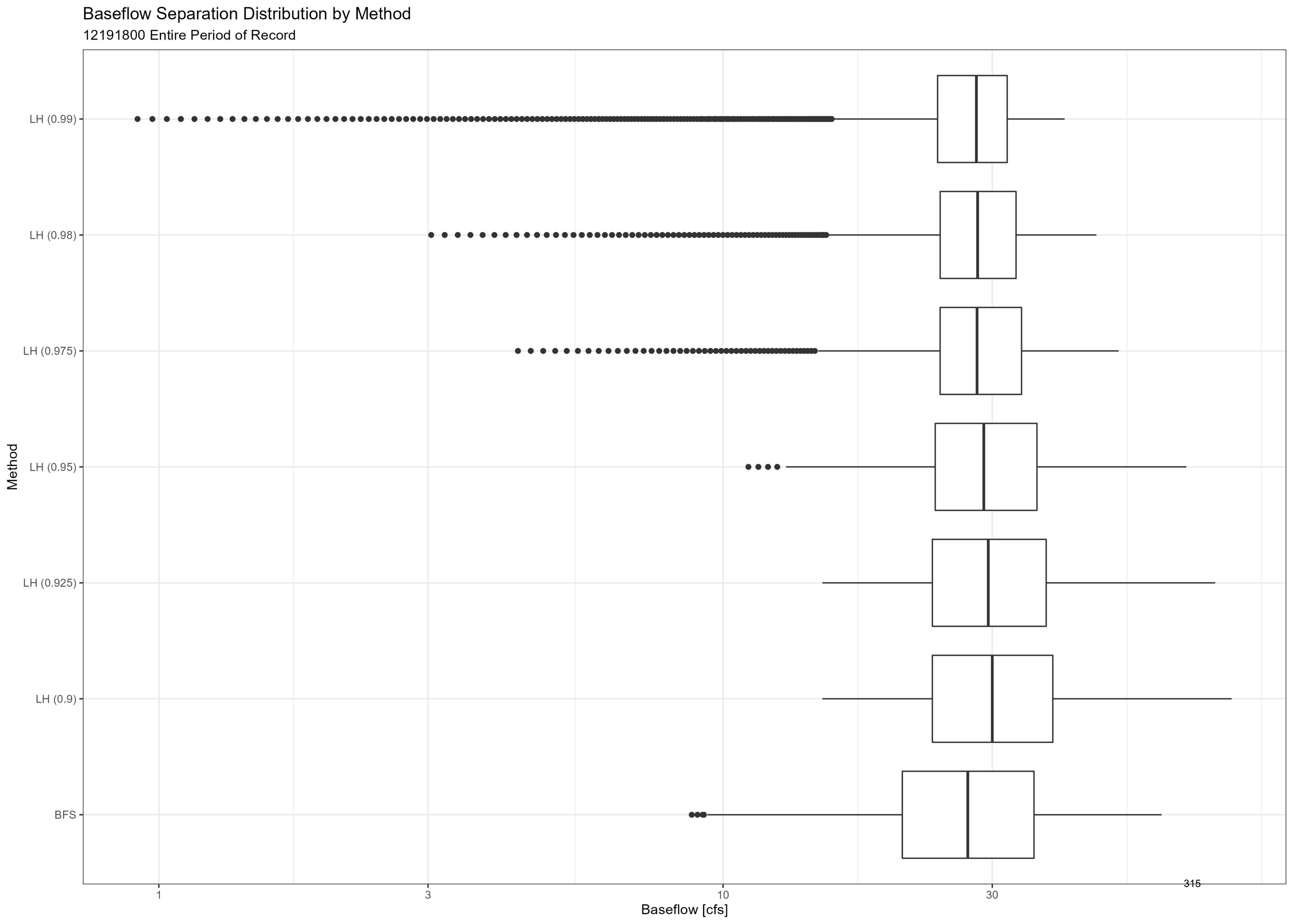
Baseflow Separation Distribution by Method
12191800 Entire Period of Record
LH (0.99)
LH (0.98)
LH (0.975)
LH (0.95)
LH (0.925)
LH (0.9)
BFS
Method
1
3
10
30
Baseflow [cfs]

Baseflow Separation Distribution by Method

12190710 Entire Period of Record

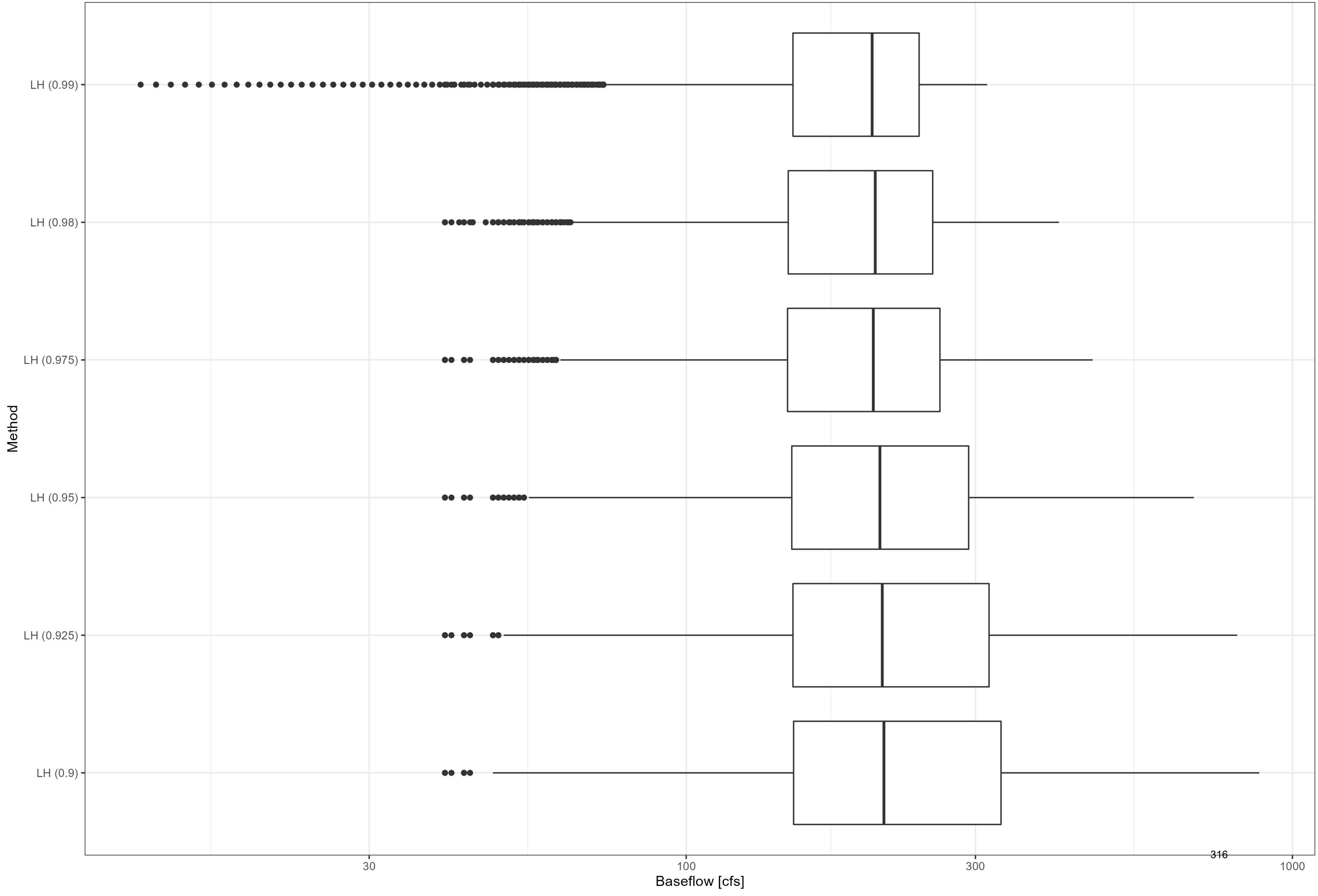


316

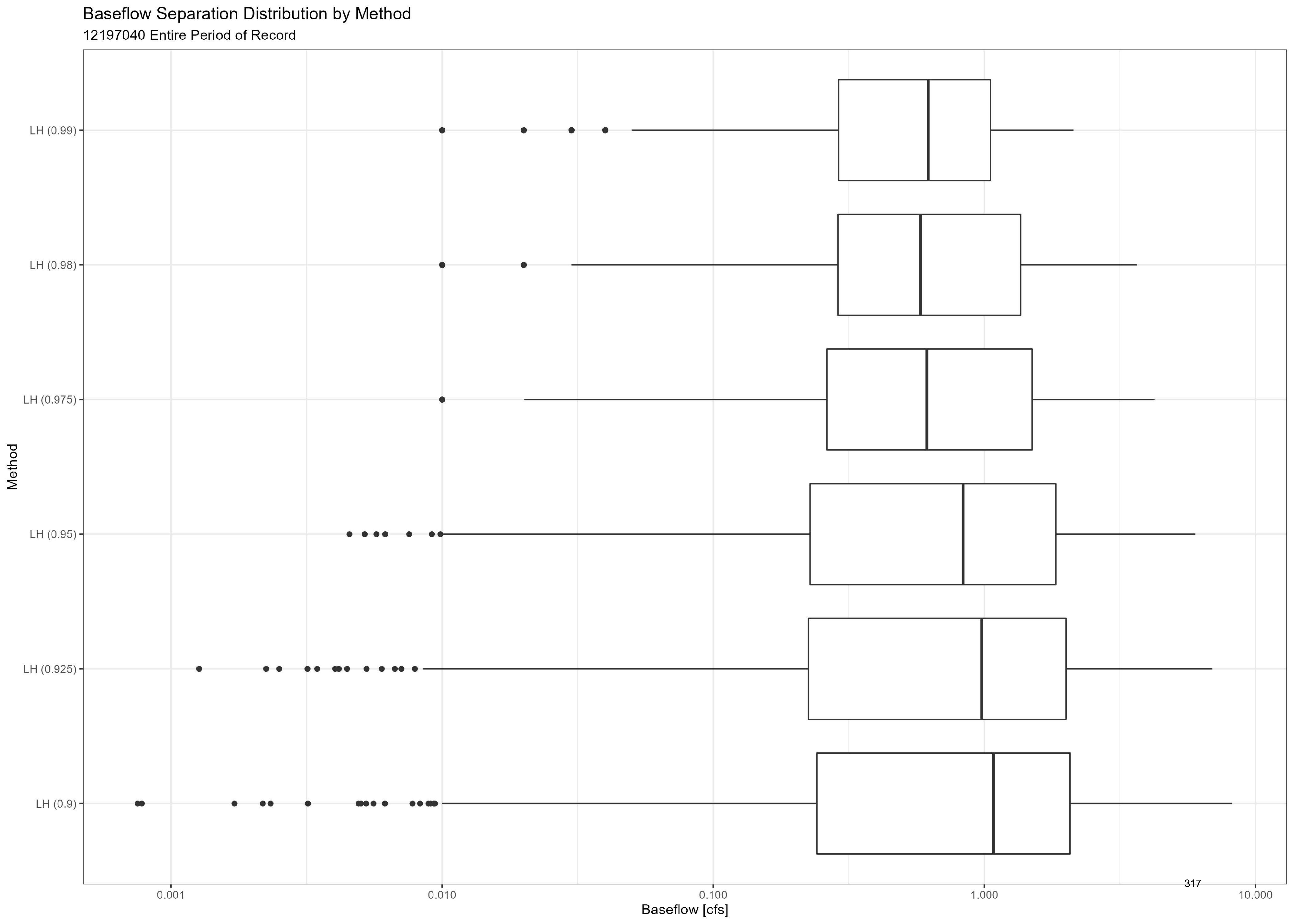
Baseflow Separation Distribution by Method
12197040 Entire Period of Record
Method
LH (0.99)
LH (0.98)
LH (0.975)
LH (0.95)
LH (0.925)
LH (0.9)
0.001
0.010
0.100
1.000
10.000
Baseflow [cfs]

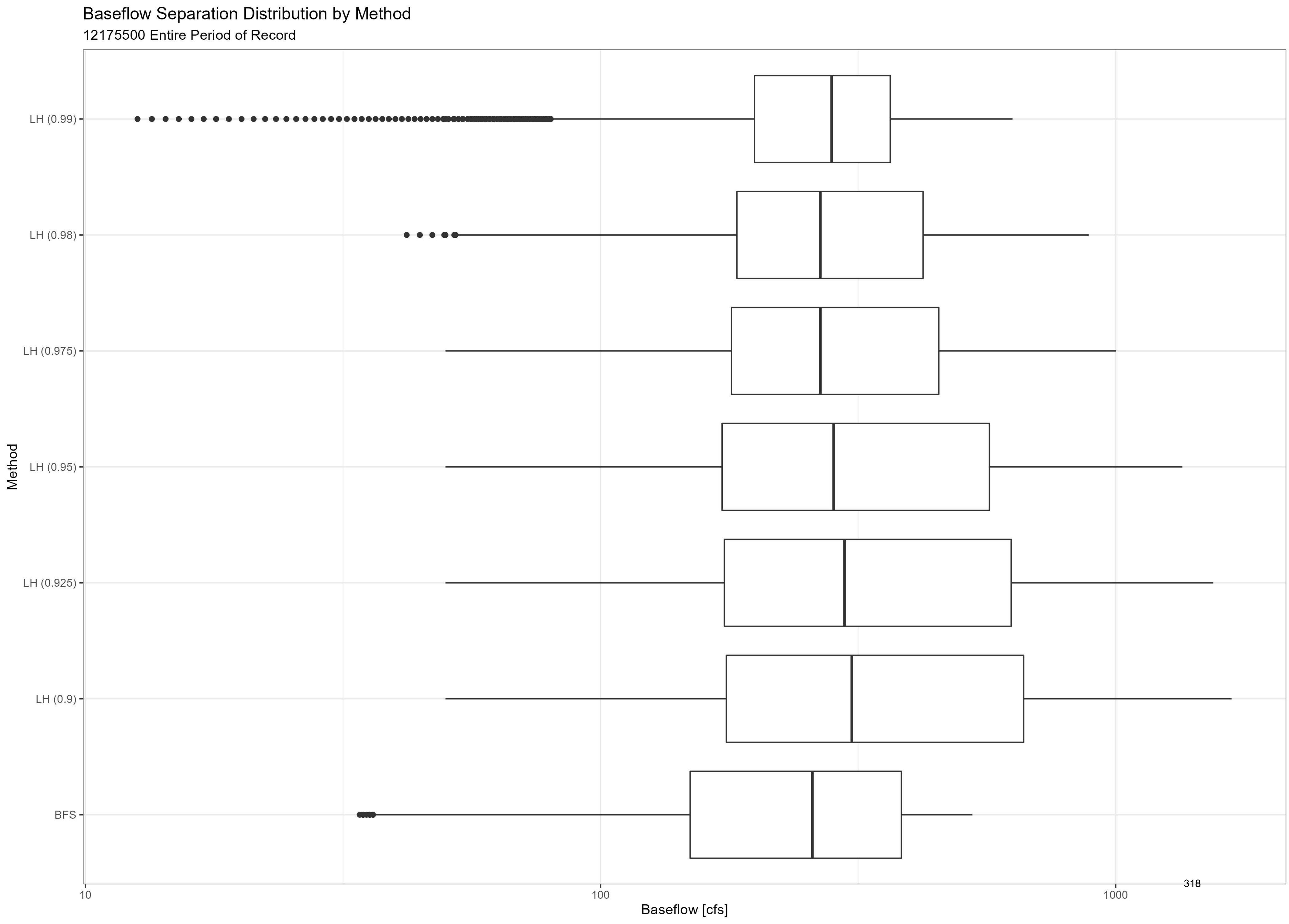

Baseflow Separation Distribution by Method
12175500 Entire Period of Record
Method
LH (0.99)
LH (0.98)
LH (0.975)
LH (0.95)
LH (0.925)
LH (0.9)
BFS
10
100
1000
Baseflow [cfs]

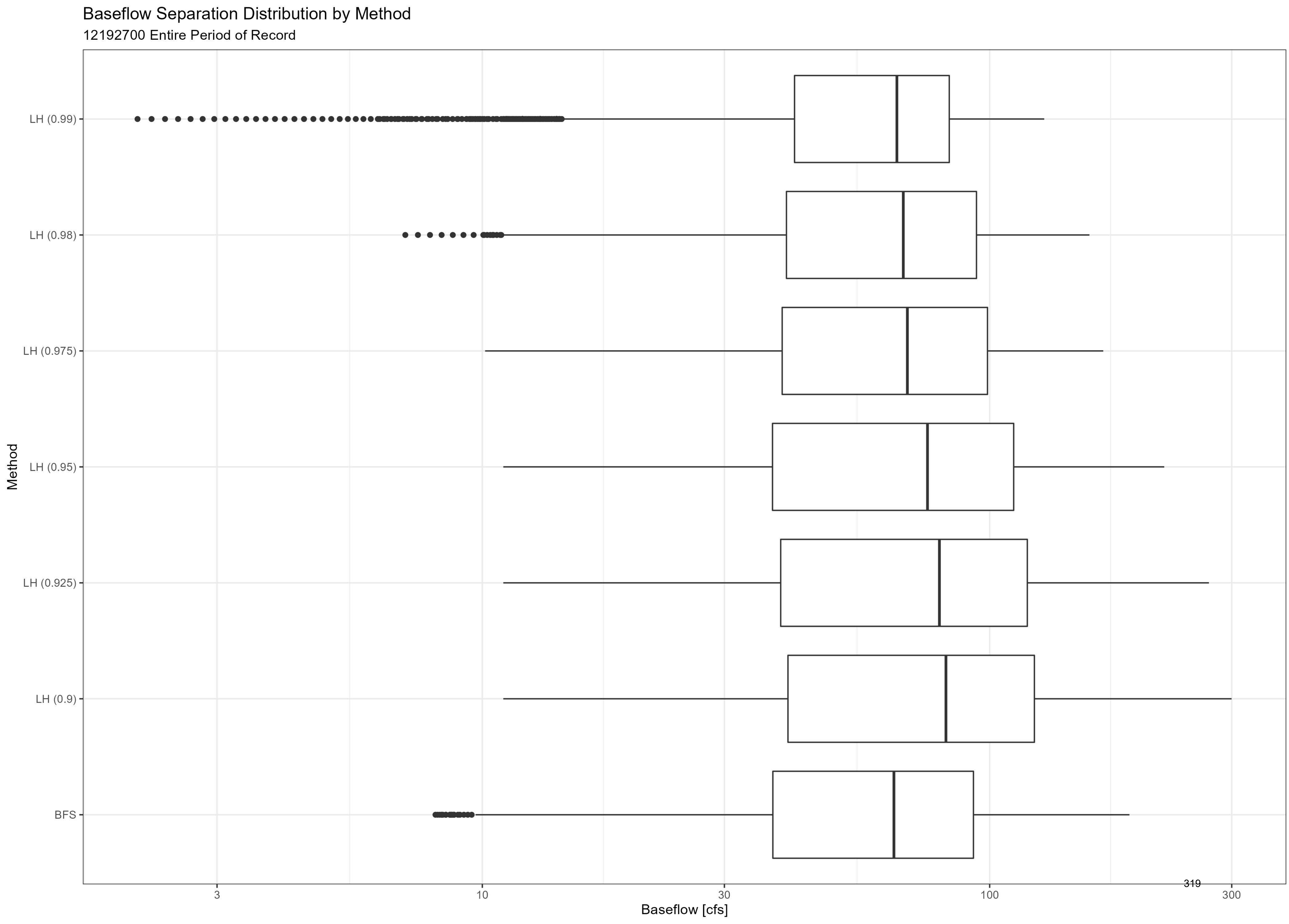
Baseflow Separation Distribution by Method
12192700 Entire Period of Record
Method
LH (0.99)
LH (0.98)
LH (0.975)
LH (0.95)
LH (0.925)
LH (0.9)
BFS
3
10
30
100
300
Baseflow [cfs]

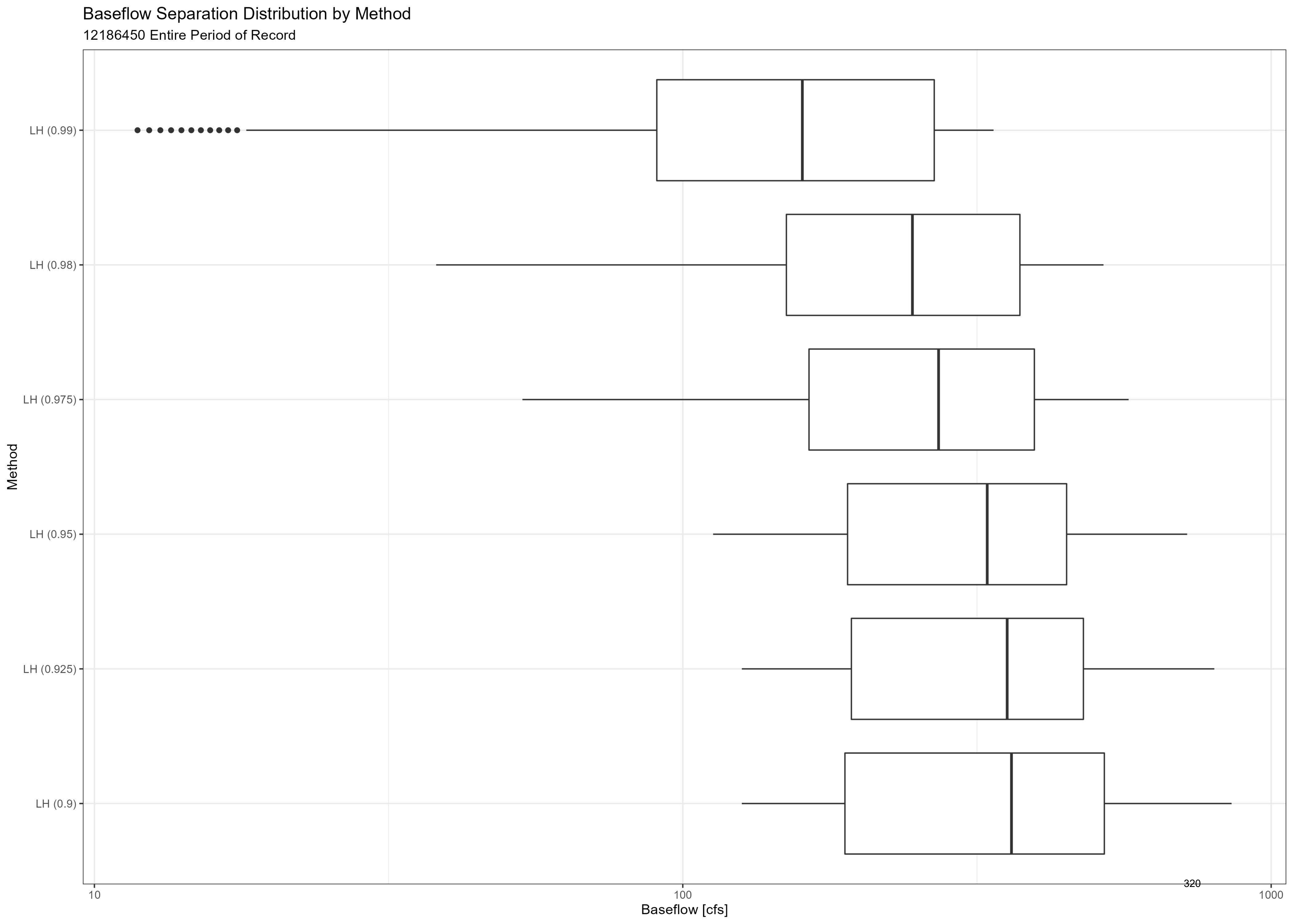

Baseflow Separation Distribution by Method
12186450 Entire Period of Record
LH (0.99)
LH (0.98)
LH (0.975)
LH (0.95)
LH (0.925)
LH (0.9)
Method
10
100
1000
Baseflow [cfs]

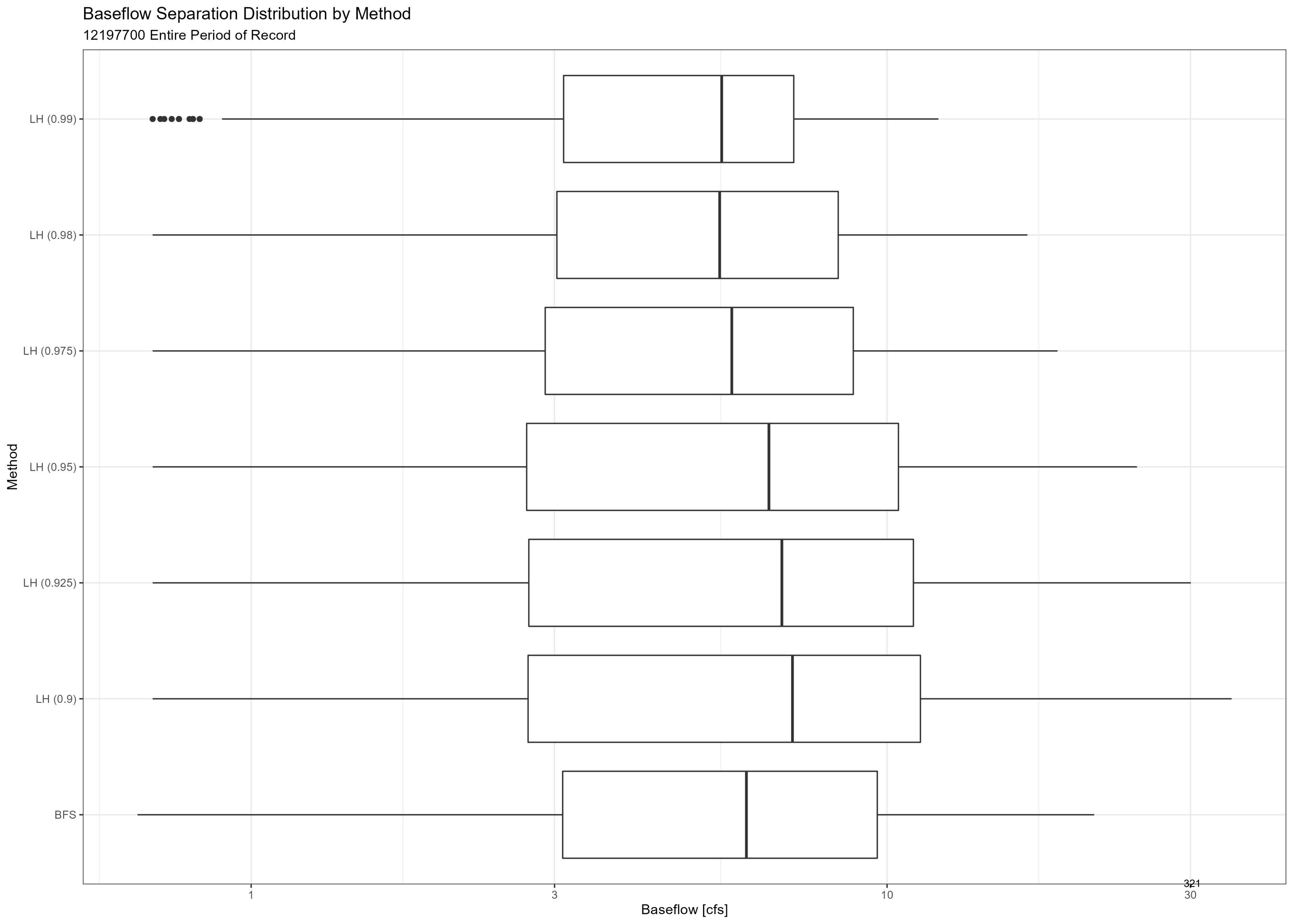

Baseflow Separation Distribution by Method
12197700 Entire Period of Record
Method
LH (0.99)
LH (0.98)
LH (0.975)
LH (0.95)
LH (0.925)
LH (0.9)
BFS
1
3
10
30
Baseflow [cfs]

# Appendix B. Time Series as Annual Hydrographs of Daily Baseflow Index (BFI) Statistics for the Entire Period of Available Record of each Analyzed Gaging Station, Comparing the Lyne-Hollick Method and the BFS Model

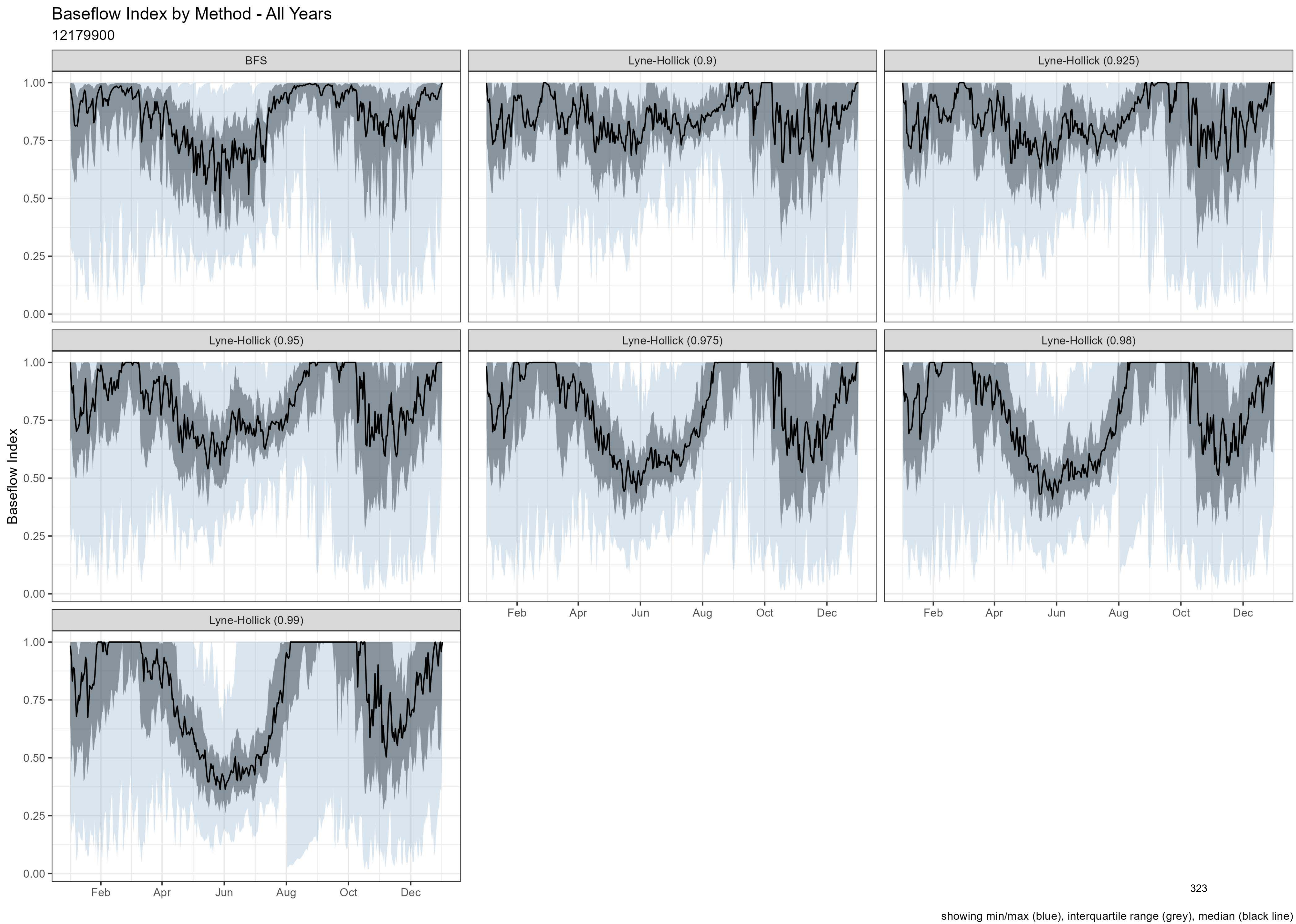
Baseflow Index by Method - All Years
12179900
BFS
Lyne-Hollick (0.9)
Lyne-Hollick (0.925)
Lyne-Hollick (0.95)
Lyne-Hollick (0.975)
Lyne-Hollick (0.98)
Lyne-Hollick (0.99)
Baseflow Index
1.00
0.75
0.50
0.25
0.00
Feb
Apr
Jun
Aug
Oct
Dec
showing min/max (blue), interquartile range (grey), median (black line)

# Baseflow Index by Method - All Years

12190400

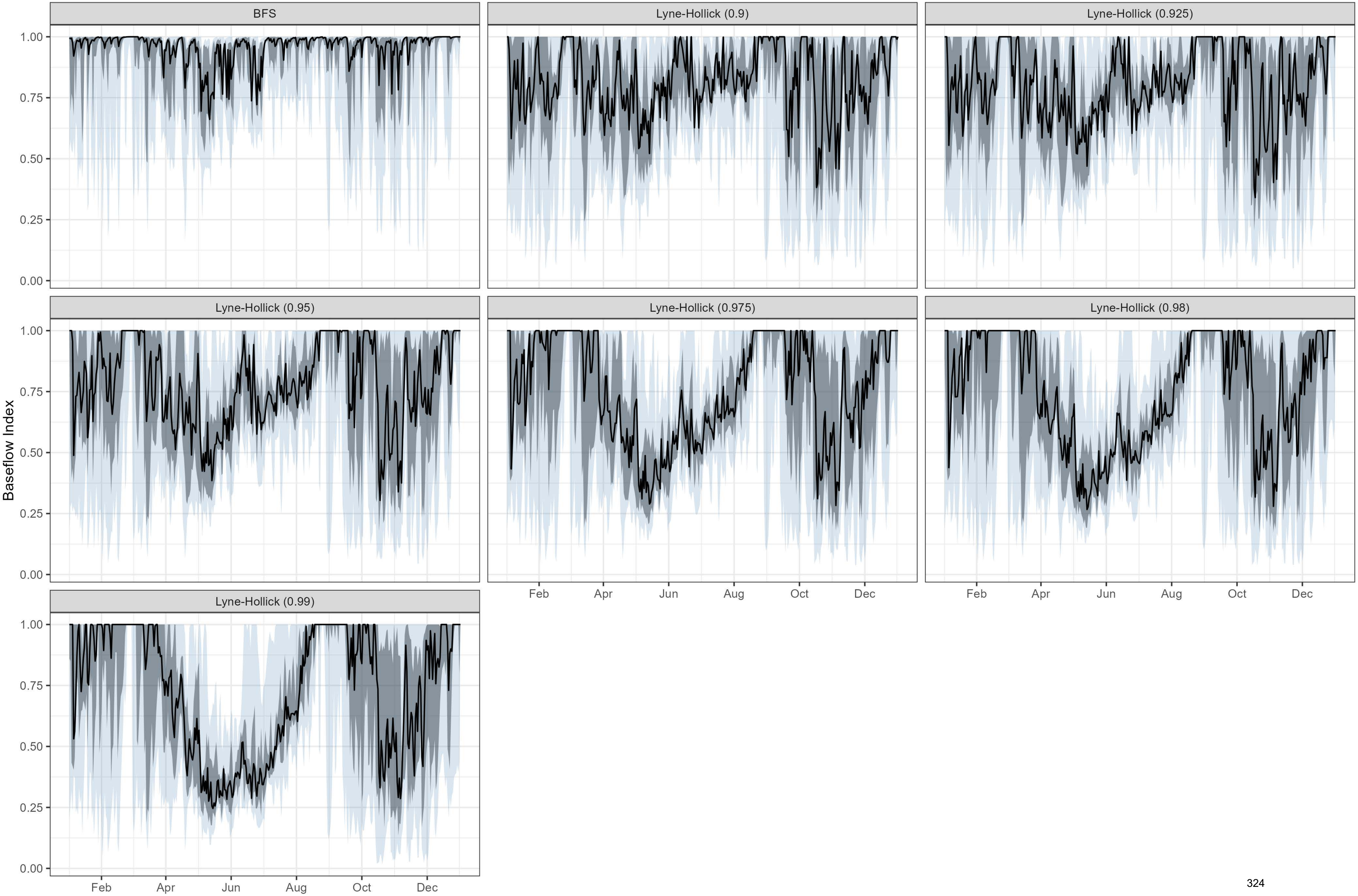




showing min/max (blue), interquartile range (grey), median (black line)

Baseflow Index by Method - All Years

12193400

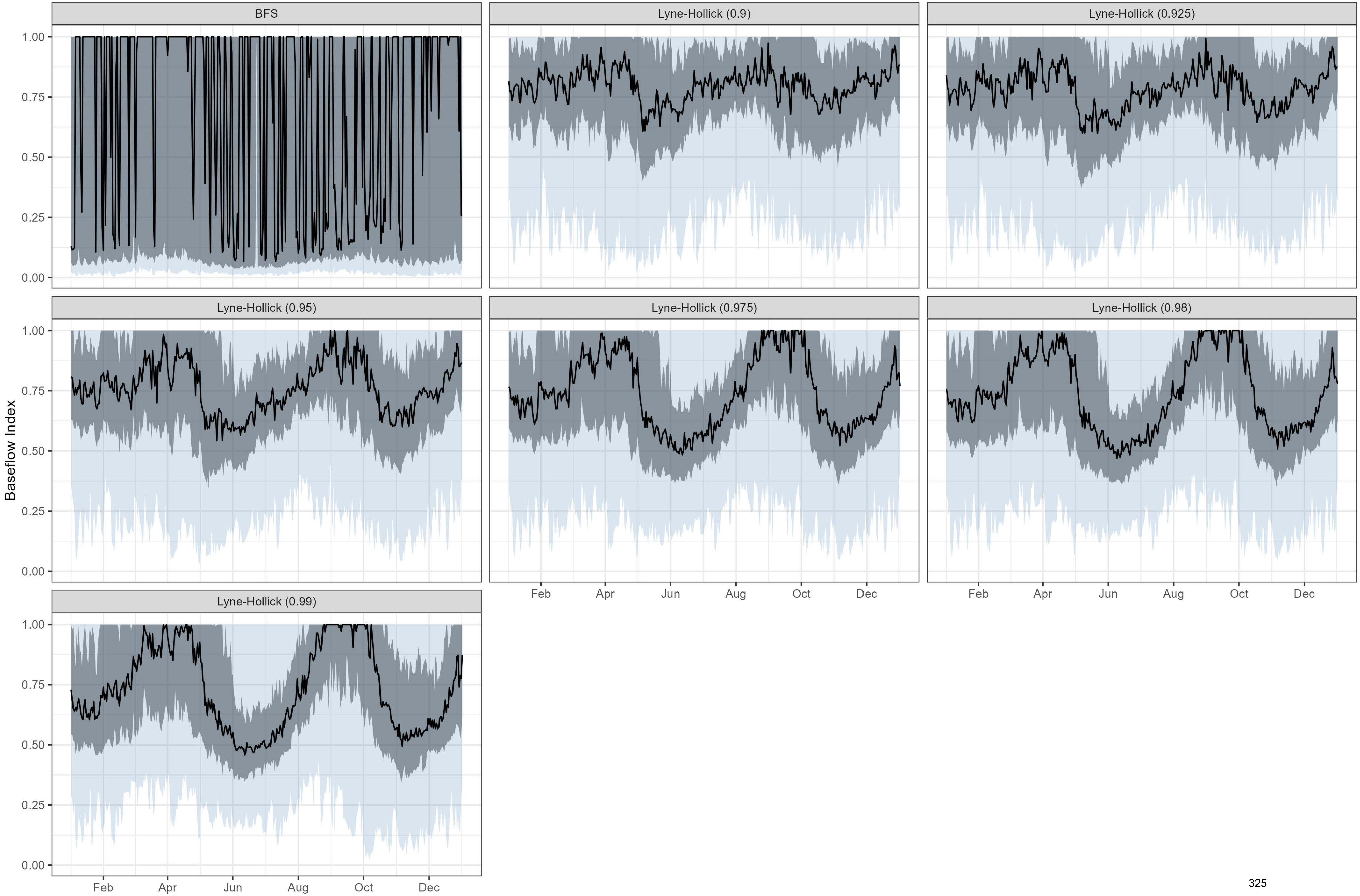




showing min/max (blue), interquartile range (grey), median (black line)

Baseflow Index by Method - All Years

12193500

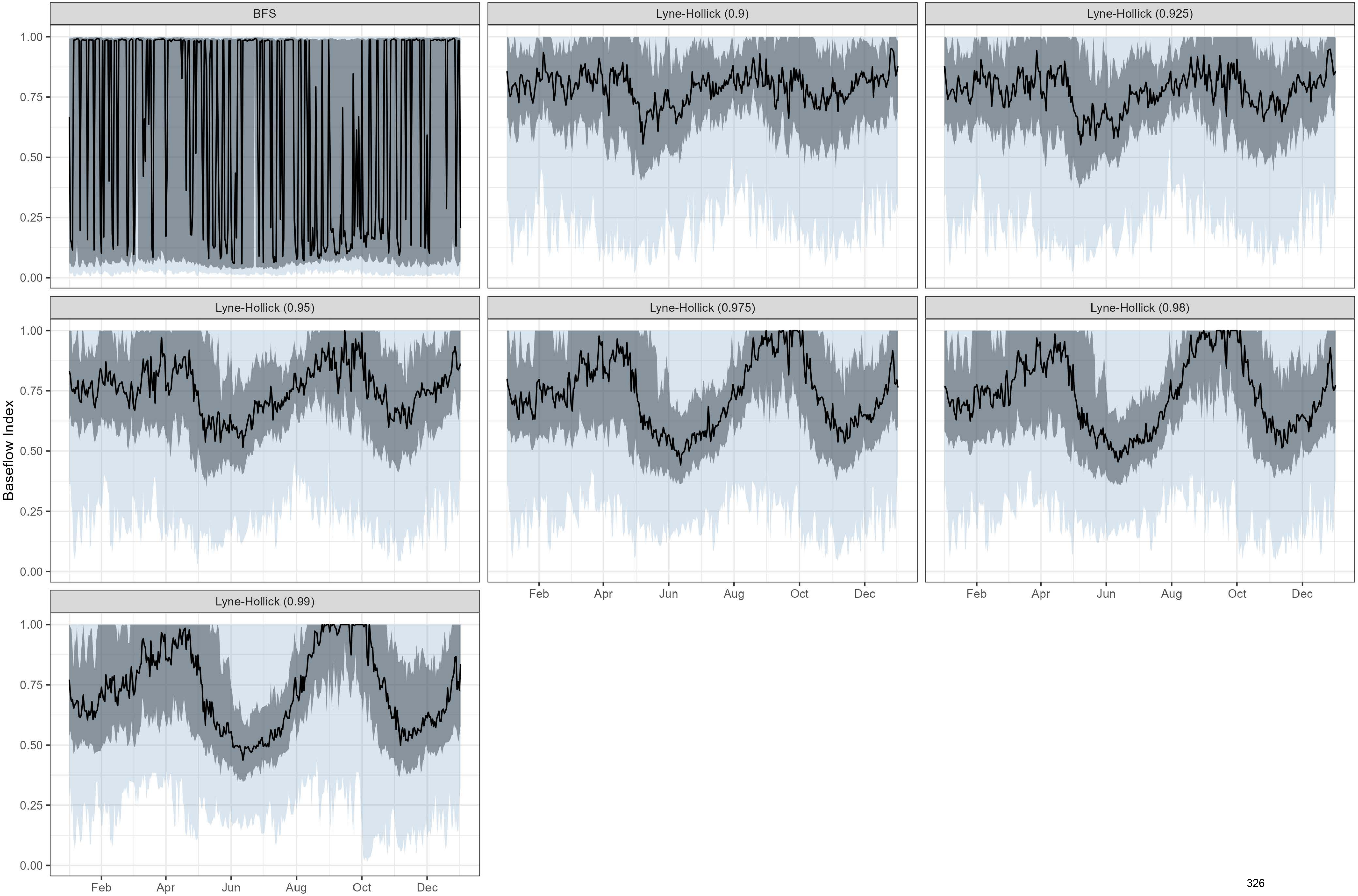




showing min/max (blue), interquartile range (grey), median (black line)

Baseflow Index by Method - All Years

12192600

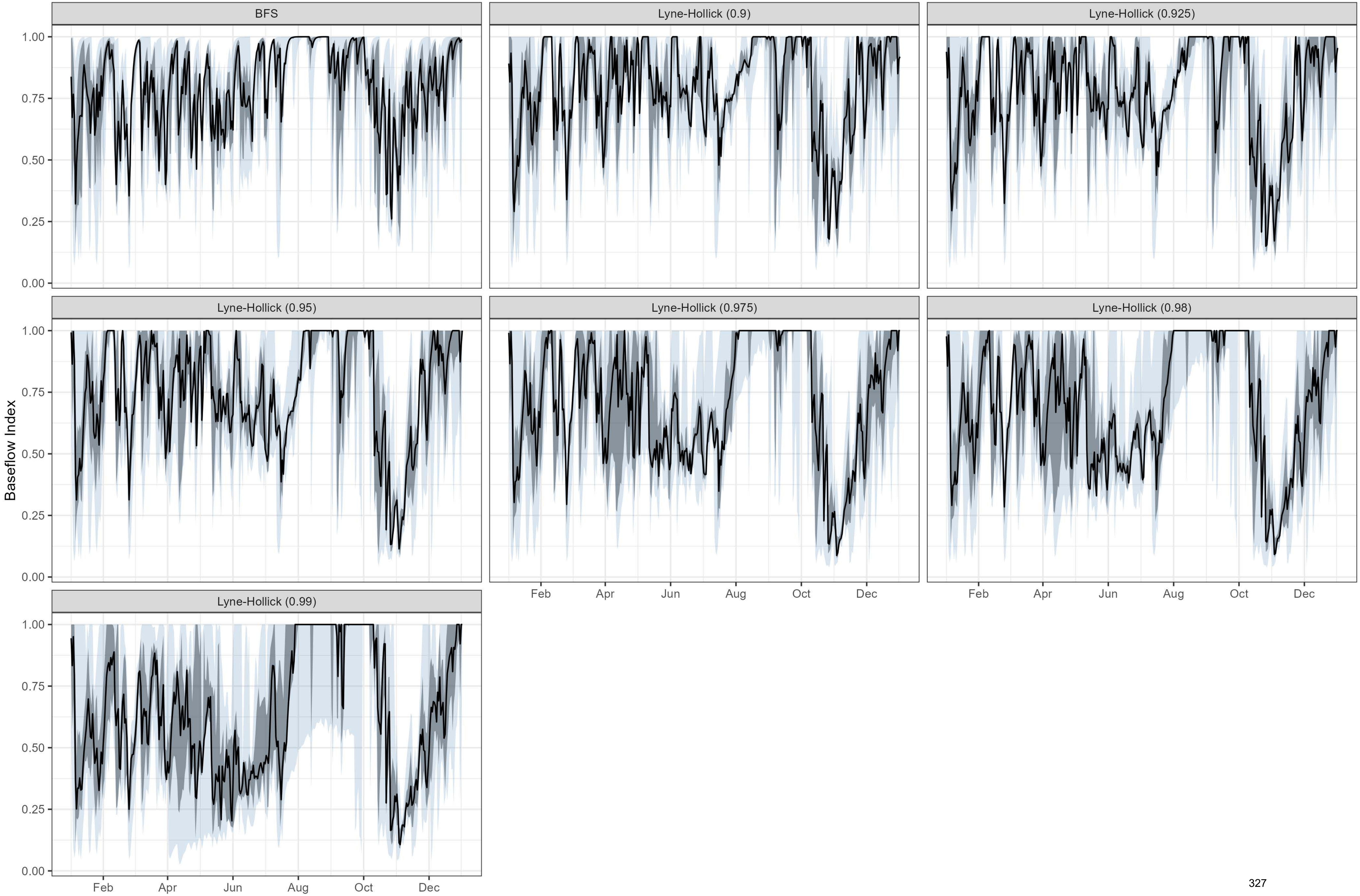


showing min/max (blue), interquartile range (grey), median (black line)

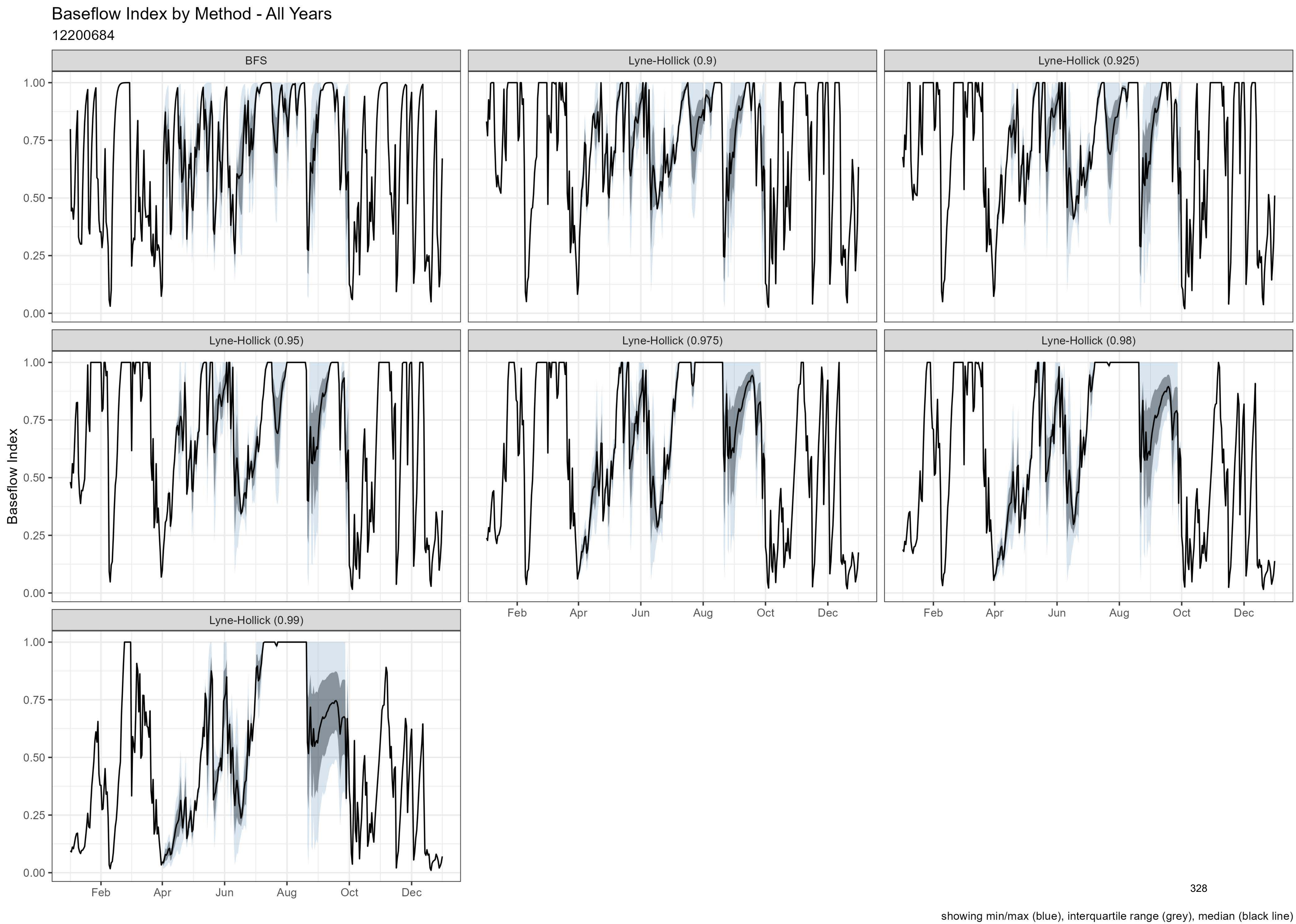
Baseflow Index by Method - All Years
12200684
BFS
Lyne-Hollick (0.9)
Lyne-Hollick (0.925)
Lyne-Hollick (0.95)
Lyne-Hollick (0.975)
Lyne-Hollick (0.98)
Lyne-Hollick (0.99)
Baseflow Index
1.00
0.75
0.50
0.25
0.00
Feb
Apr
Jun
Aug
Oct
Dec
showing min/max (blue), interquartile range (grey), median (black line)

# Baseflow Index by Method - All Years

12181100

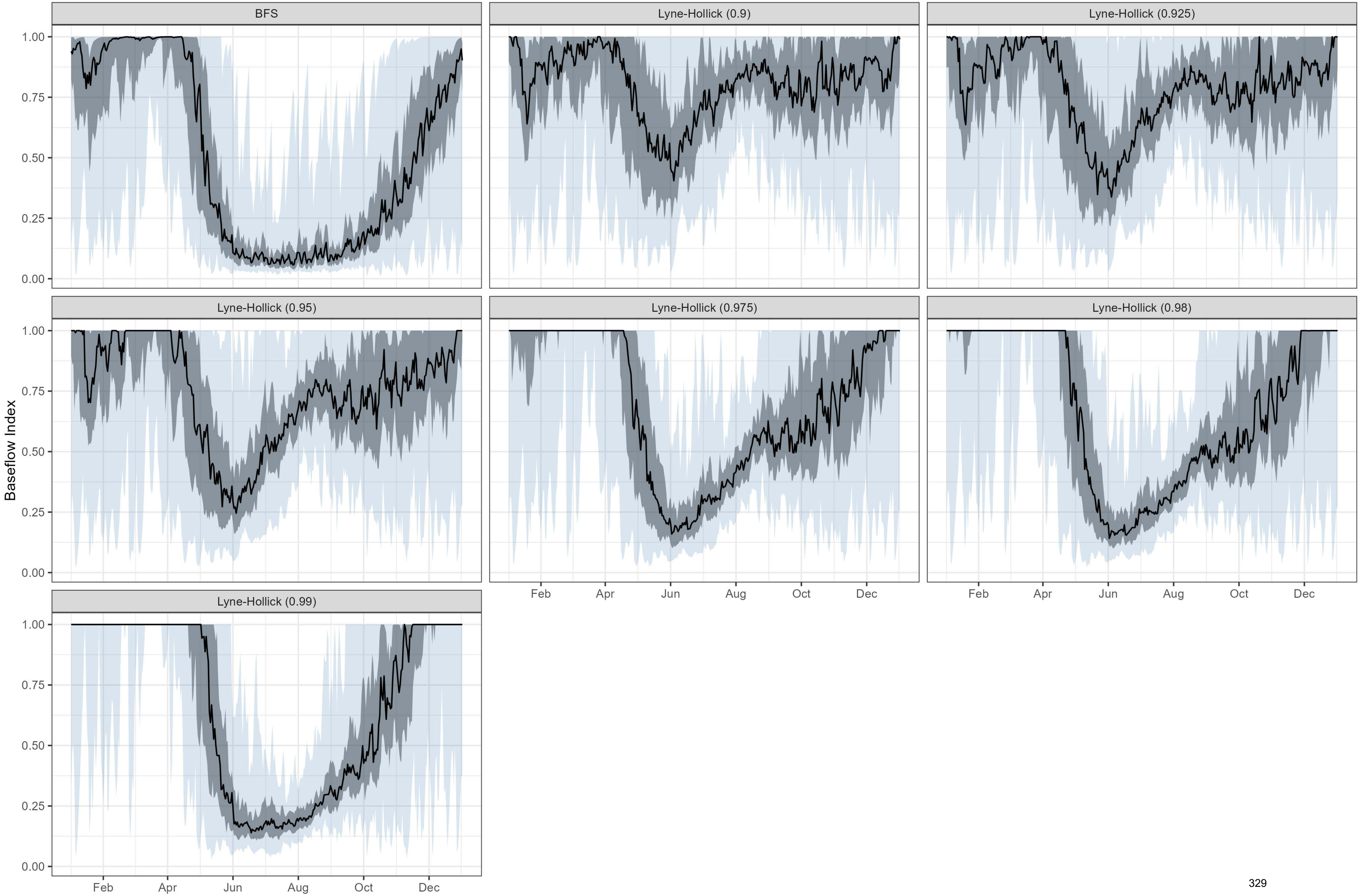




showing min/max (blue), interquartile range (grey), median (black line)

# Baseflow Index by Method - All Years

12182500

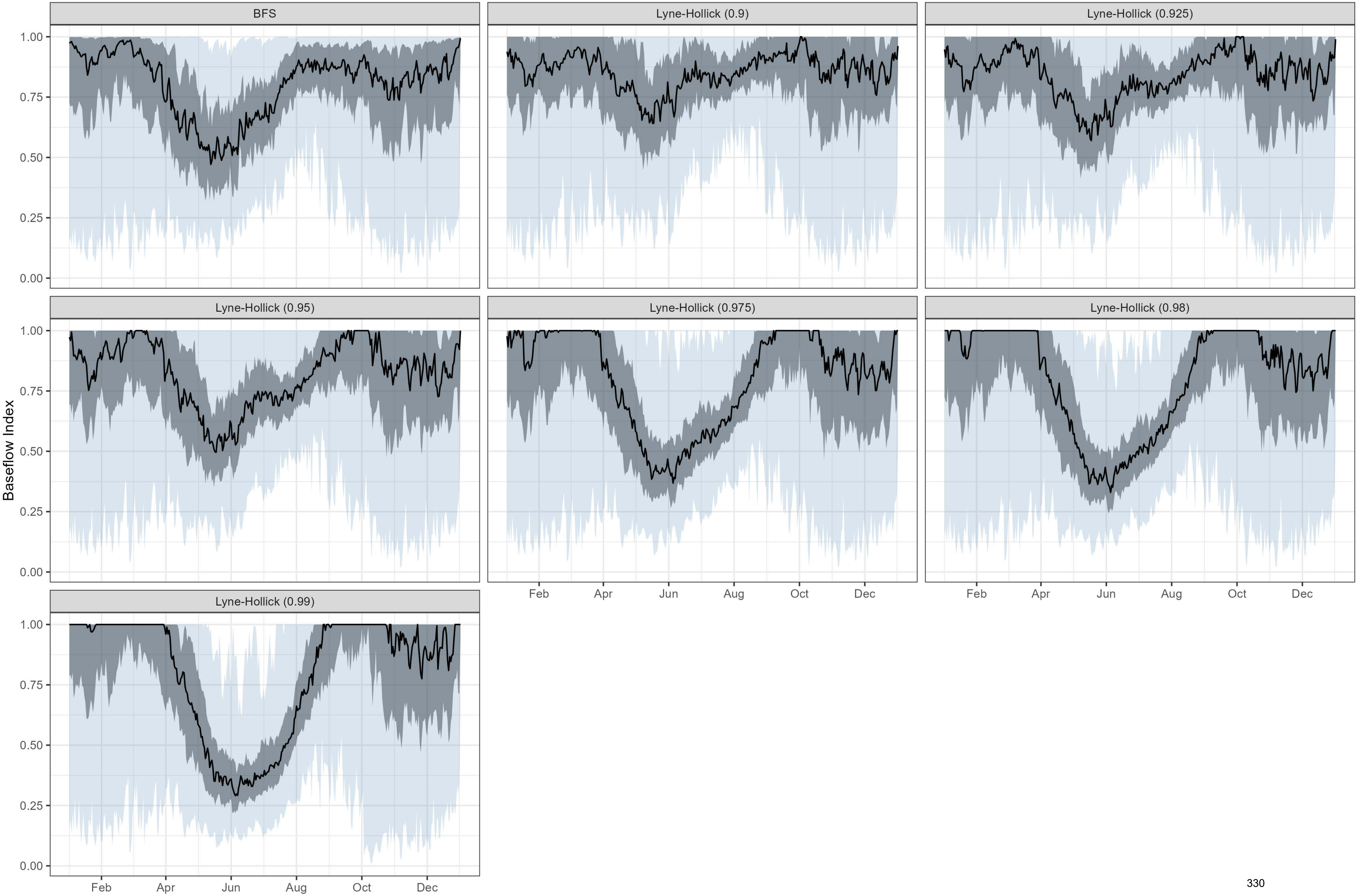




showing min/max (blue), interquartile range (grey), median (black line)

# Baseflow Index by Method - All Years

12185300

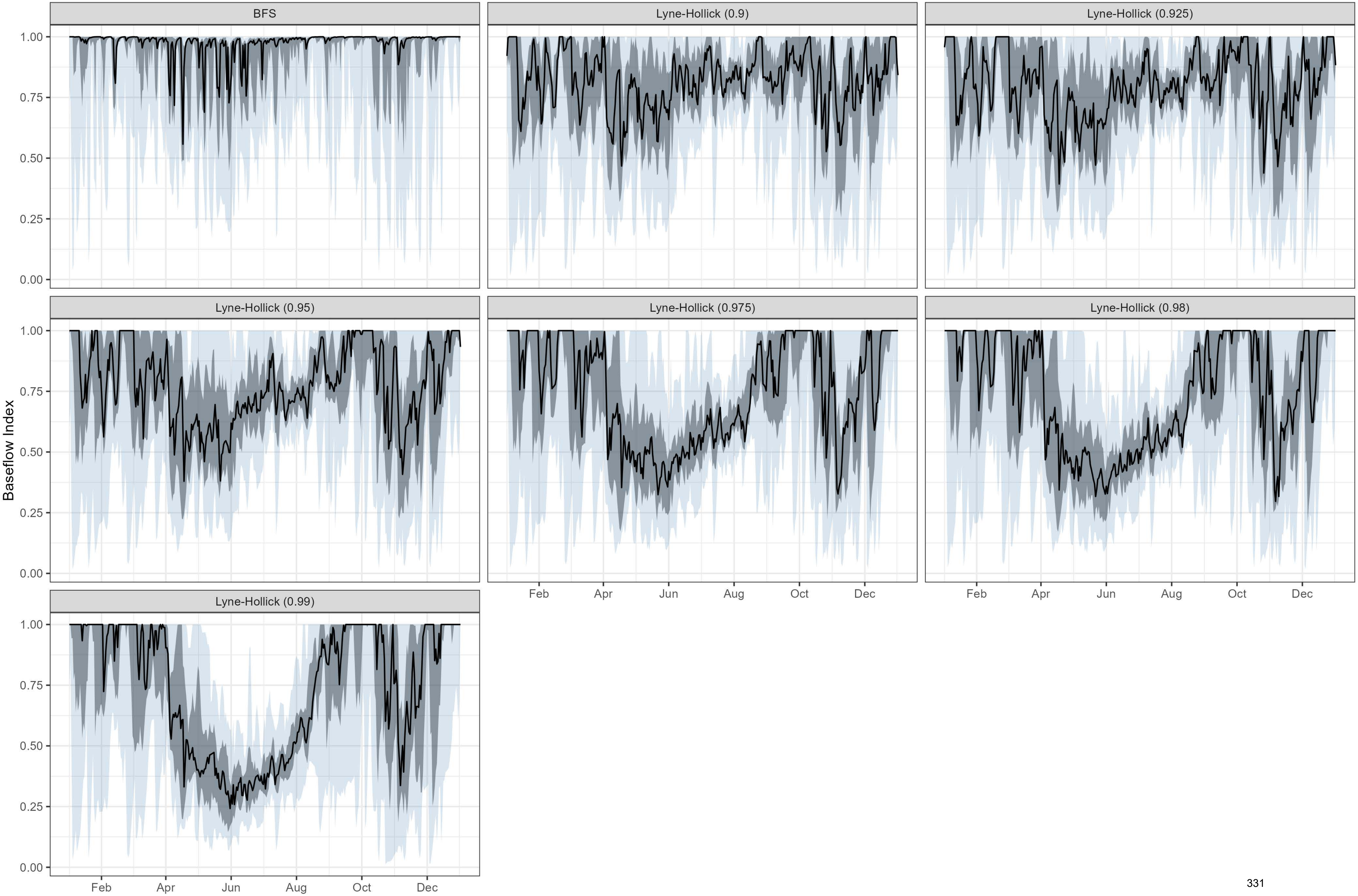




showing min/max (blue), interquartile range (grey), median (black line)

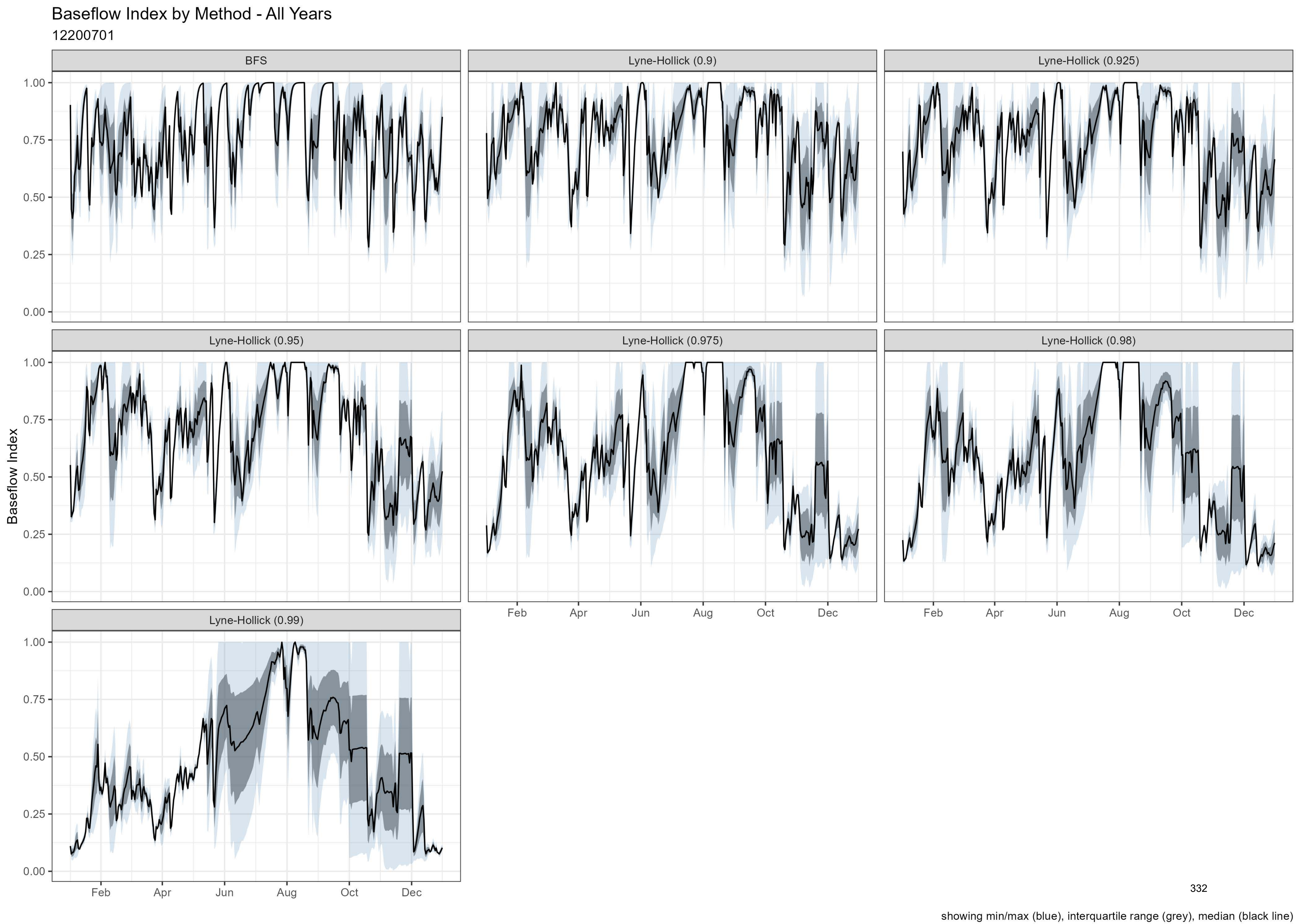
Baseflow Index by Method - All Years
12200701
BFS
Lyne-Hollick (0.9)
Lyne-Hollick (0.925)
Lyne-Hollick (0.95)
Lyne-Hollick (0.975)
Lyne-Hollick (0.98)
Lyne-Hollick (0.99)
Baseflow Index
1.00
0.75
0.50
0.25
0.00
Feb
Apr
Jun
Aug
Oct
Dec
showing min/max (blue), interquartile range (grey), median (black line)

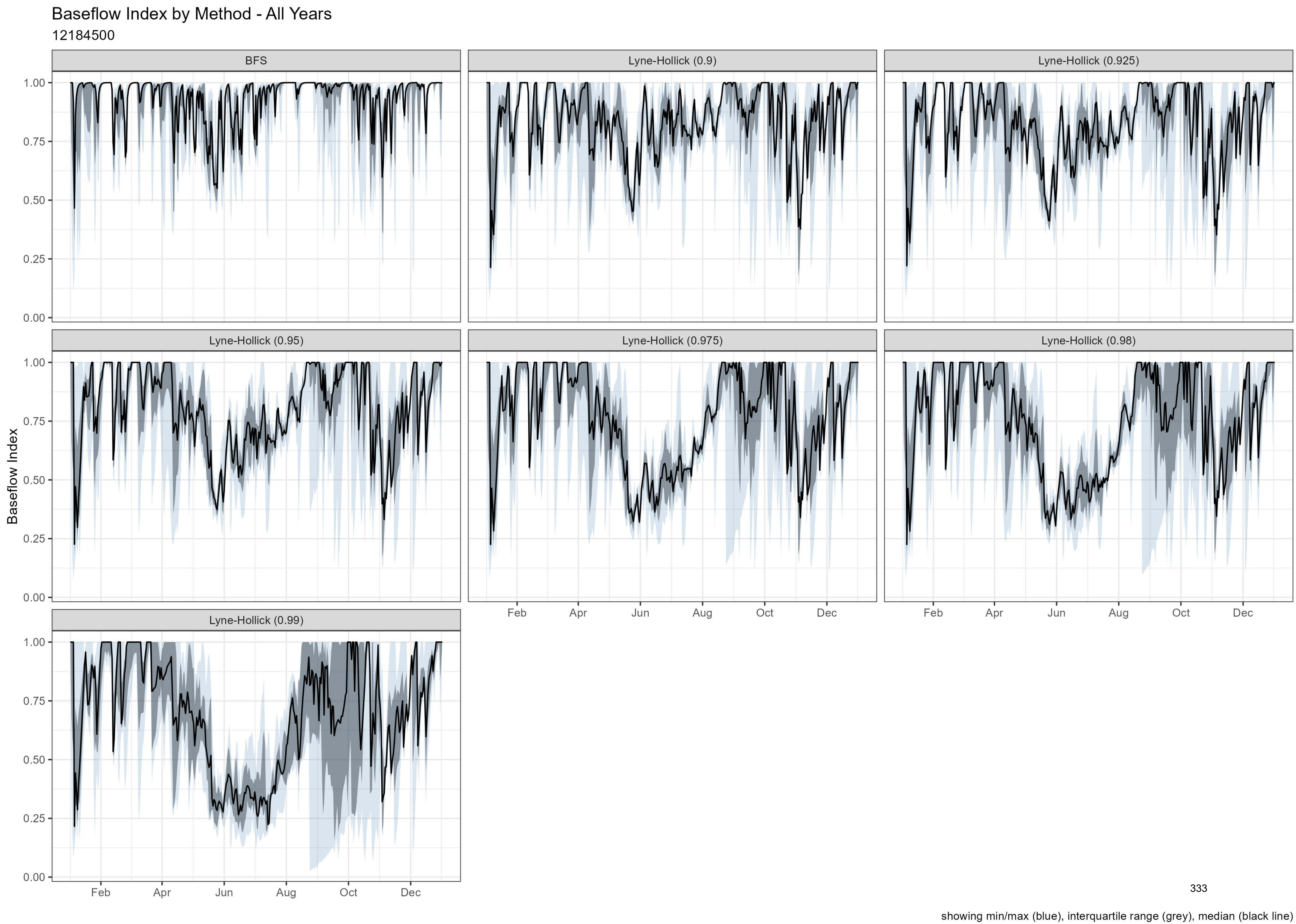
Baseflow Index by Method - All Years
12184500
BFS
Lyne-Hollick (0.9)
Lyne-Hollick (0.925)
Lyne-Hollick (0.95)
Lyne-Hollick (0.975)
Lyne-Hollick (0.98)
Lyne-Hollick (0.99)
Baseflow Index
1.00
0.75
0.50
0.25
0.00
Feb
Apr
Jun
Aug
Oct
Dec
showing min/max (blue), interquartile range (grey), median (black line)

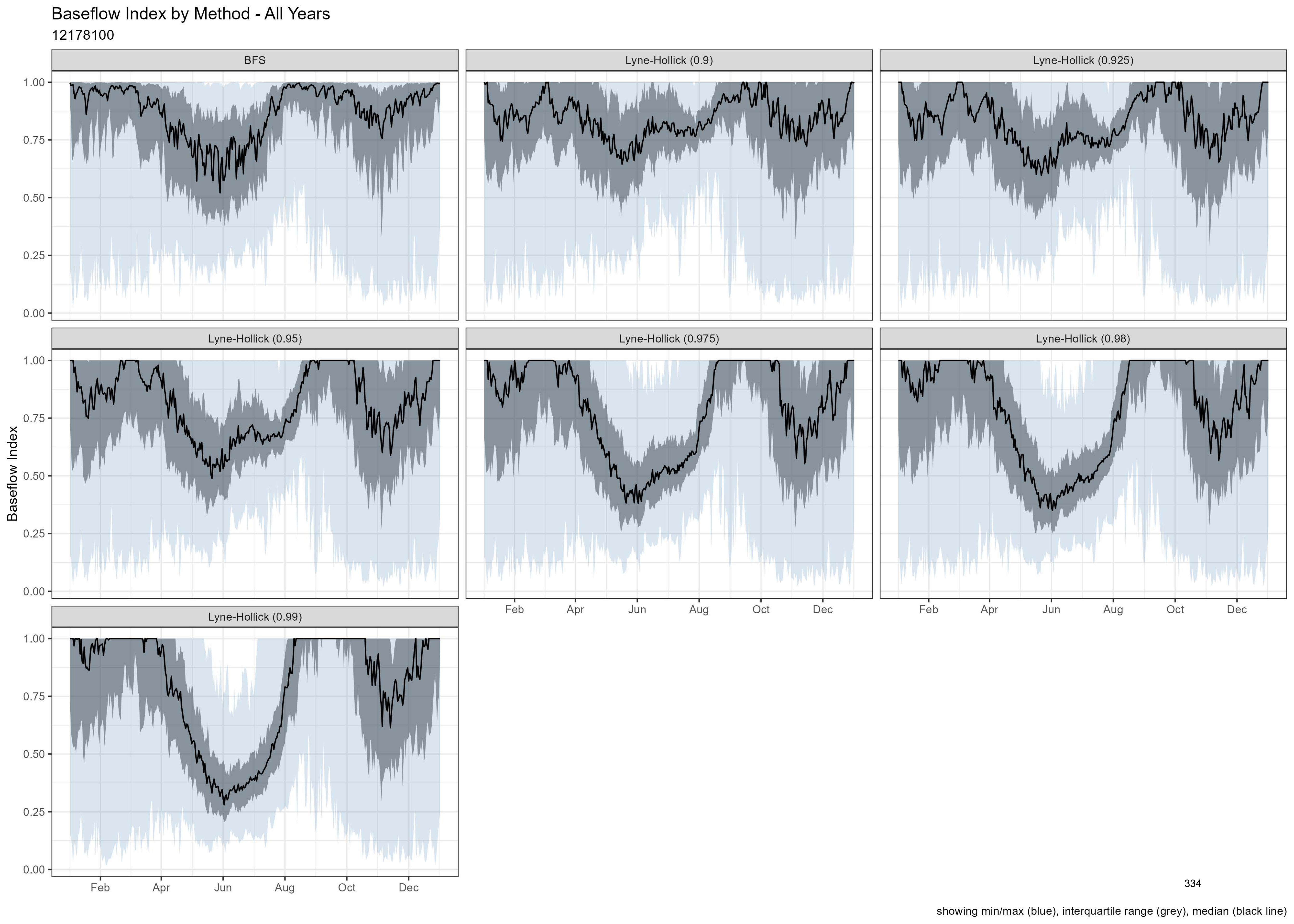

Baseflow Index by Method - All Years
12178100
BFS
Lyne-Hollick (0.9)
Lyne-Hollick (0.925)
Lyne-Hollick (0.95)
Lyne-Hollick (0.975)
Lyne-Hollick (0.98)
Lyne-Hollick (0.99)
Baseflow Index
1.00
0.75
0.50
0.25
0.00
Feb
Apr
Jun
Aug
Oct
Dec
showing min/max (blue), interquartile range (grey), median (black line)

# Baseflow Index by Method - All Years

12199600

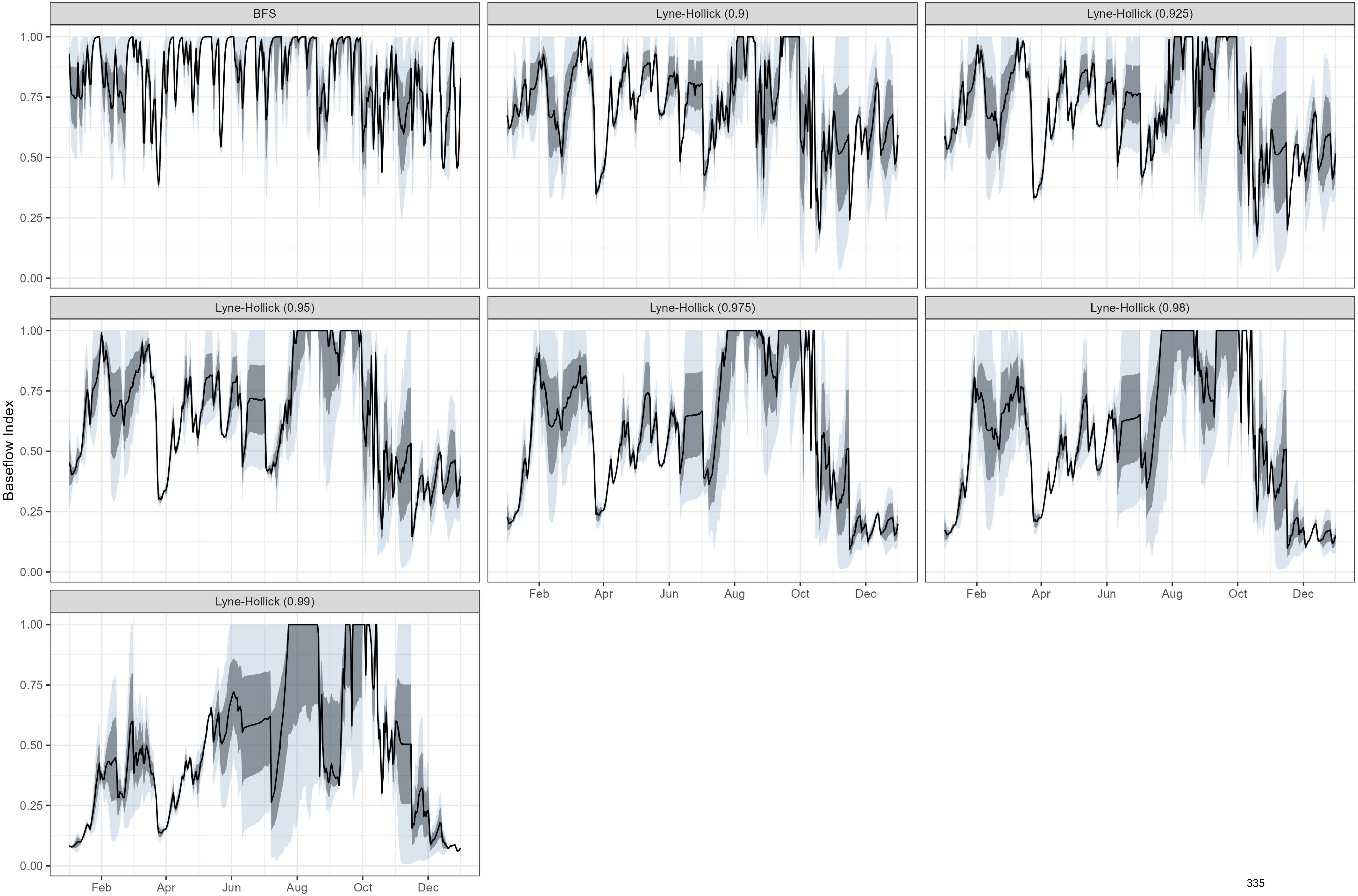




showing min/max (blue), interquartile range (grey), median (black line)

## Baseflow Index by Method - All Years

12190718

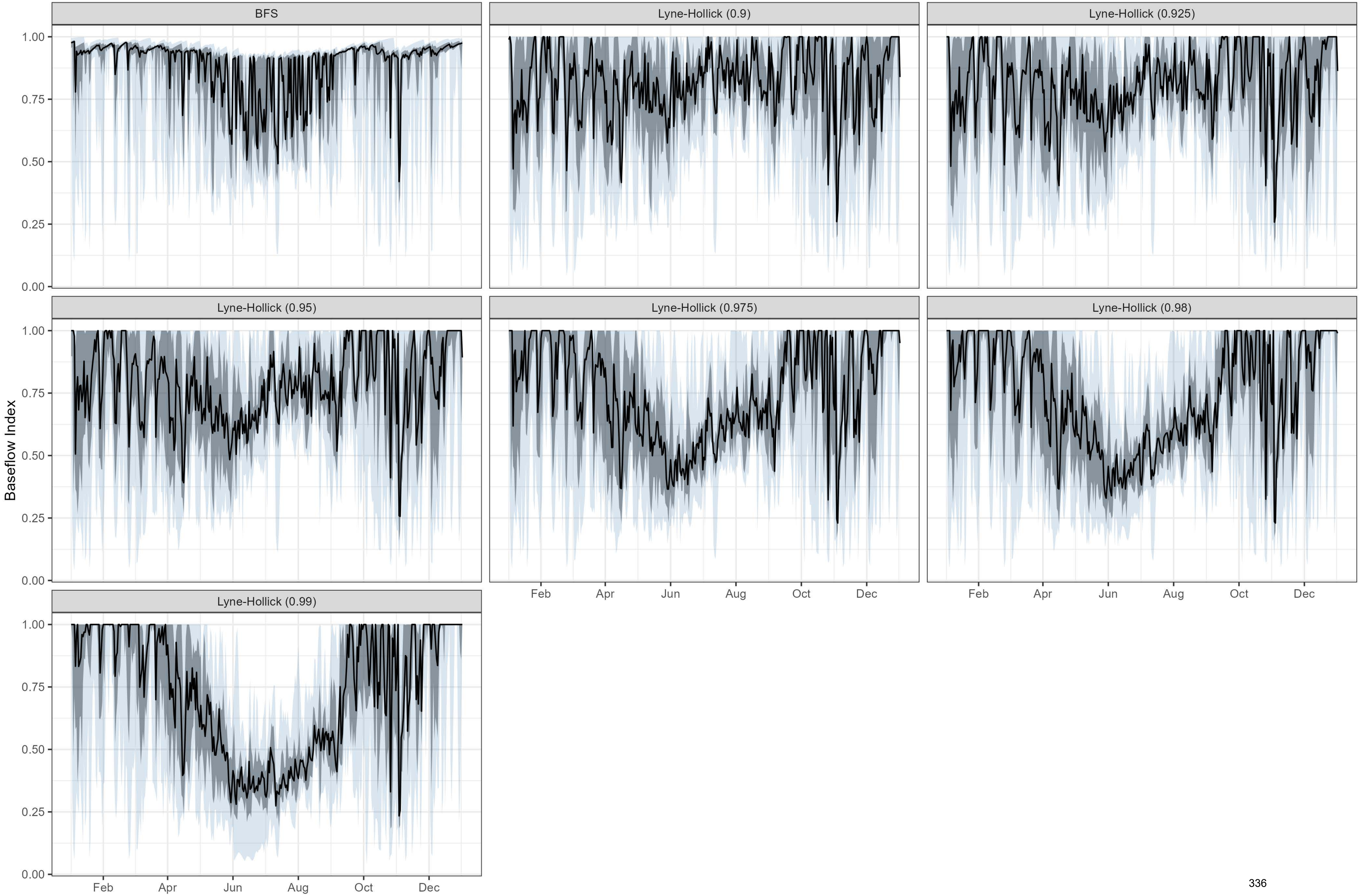


showing min/max (blue), interquartile range (grey), median (black line)

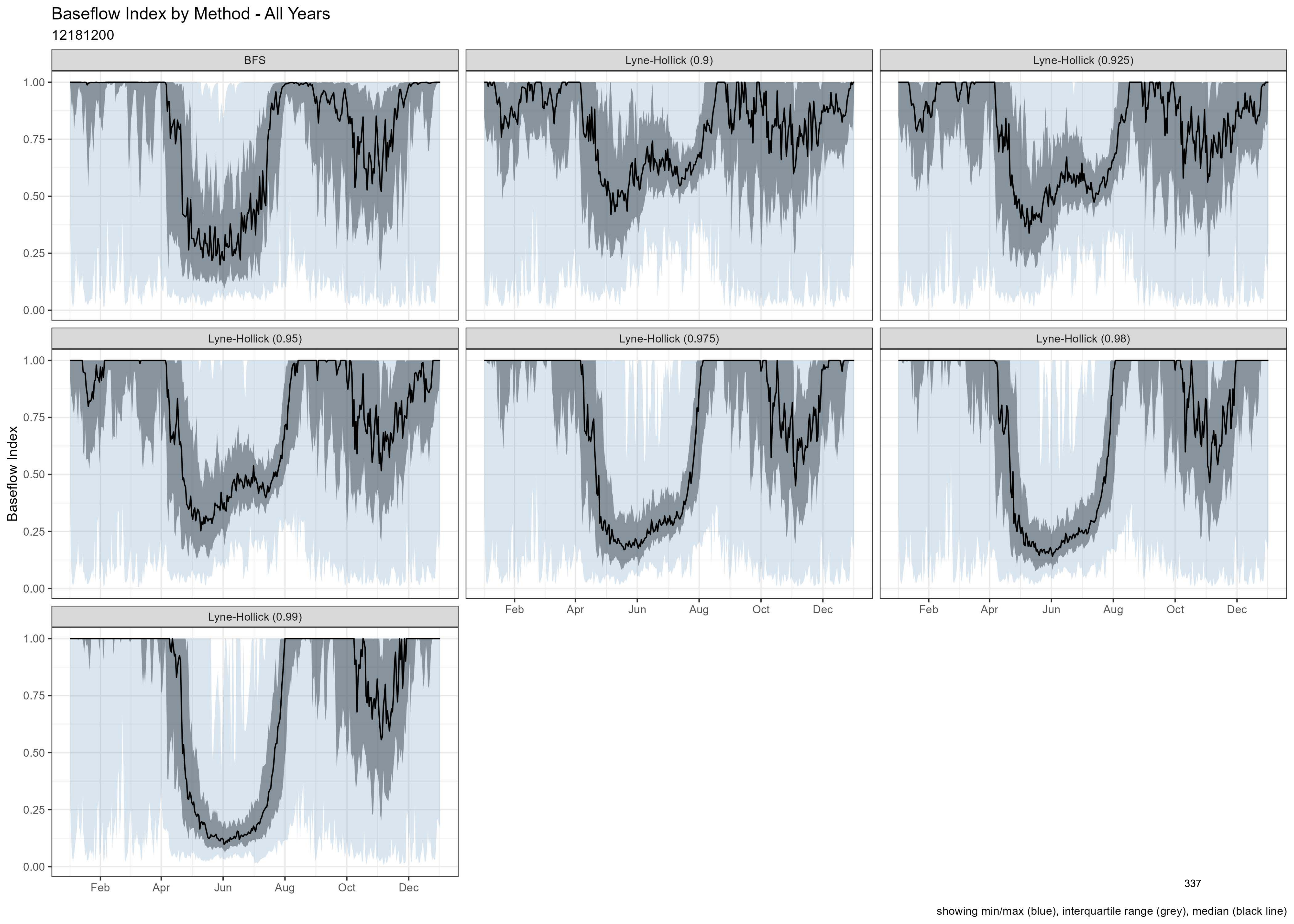
Baseflow Index by Method - All Years
12181200
BFS
Lyne-Hollick (0.9)
Lyne-Hollick (0.925)
Lyne-Hollick (0.95)
Lyne-Hollick (0.975)
Lyne-Hollick (0.98)
Lyne-Hollick (0.99)
Baseflow Index
1.00
0.75
0.50
0.25
0.00
Feb
Apr
Jun
Aug
Oct
Dec
showing min/max (blue), interquartile range (grey), median (black line)

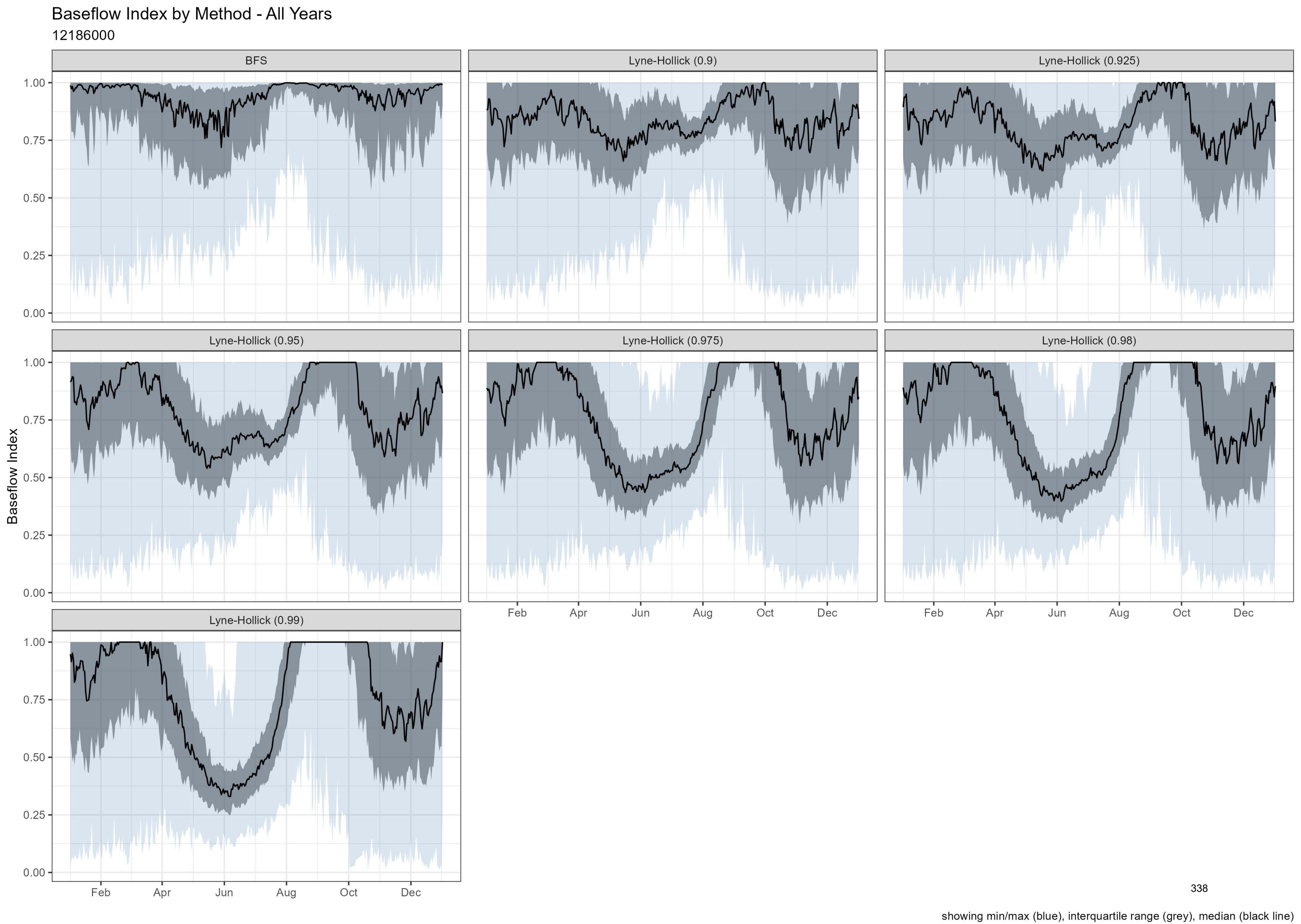

Baseflow Index by Method - All Years
12186000
BFS
Lyne-Hollick (0.9)
Lyne-Hollick (0.925)
Lyne-Hollick (0.95)
Lyne-Hollick (0.975)
Lyne-Hollick (0.98)
Lyne-Hollick (0.99)
Baseflow Index
1.00
0.75
0.50
0.25
0.00
Feb
Apr
Jun
Aug
Oct
Dec
showing min/max (blue), interquartile range (grey), median (black line)

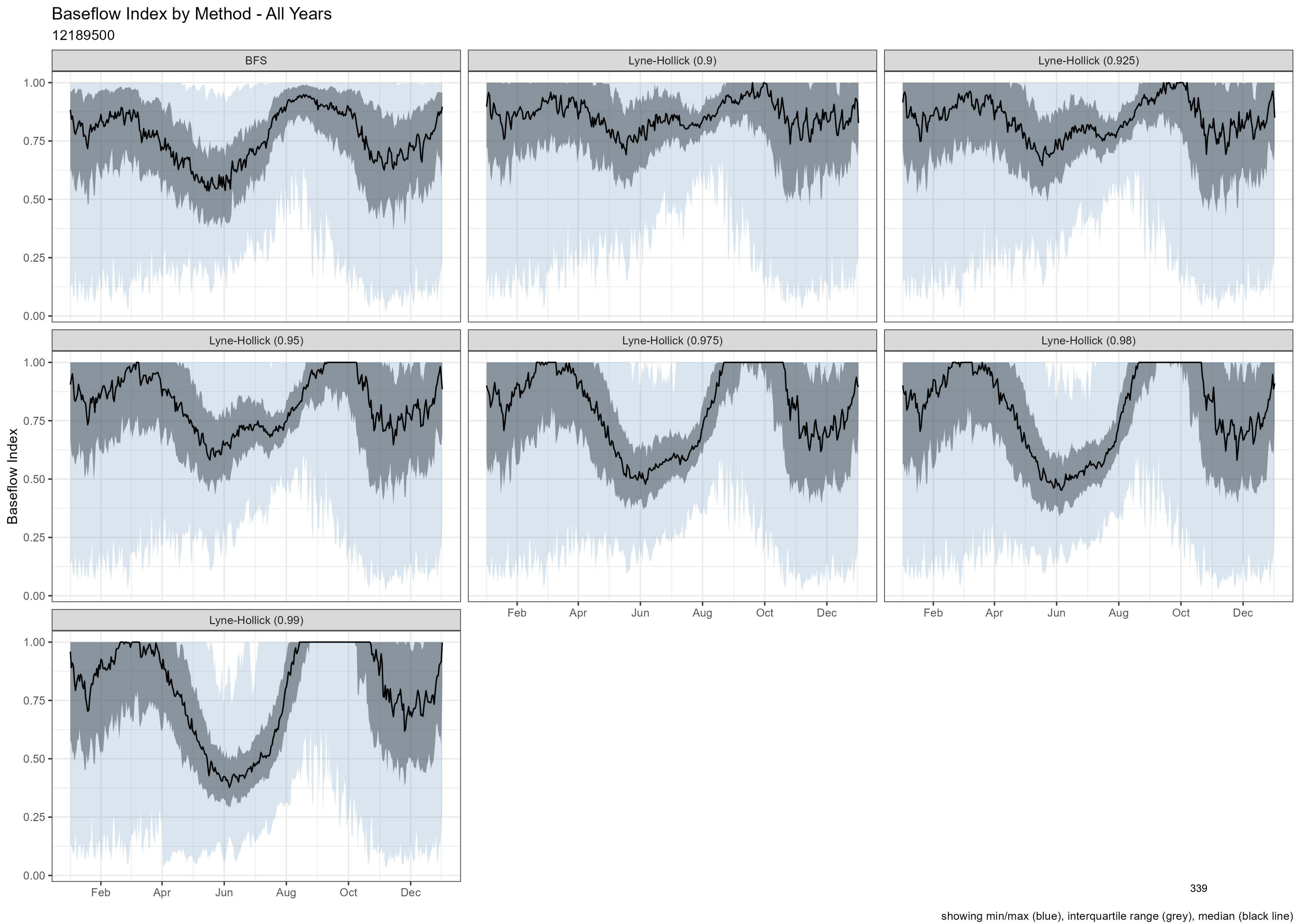
Baseflow Index by Method - All Years
12189500
BFS
Lyne-Hollick (0.9)
Lyne-Hollick (0.925)
Lyne-Hollick (0.95)
Lyne-Hollick (0.975)
Lyne-Hollick (0.98)
Lyne-Hollick (0.99)
Baseflow Index
1.00
0.75
0.50
0.25
0.00
Feb
Apr
Jun
Aug
Oct
Dec
showing min/max (blue), interquartile range (grey), median (black line)

## Baseflow Index by Method - All Years

12178000

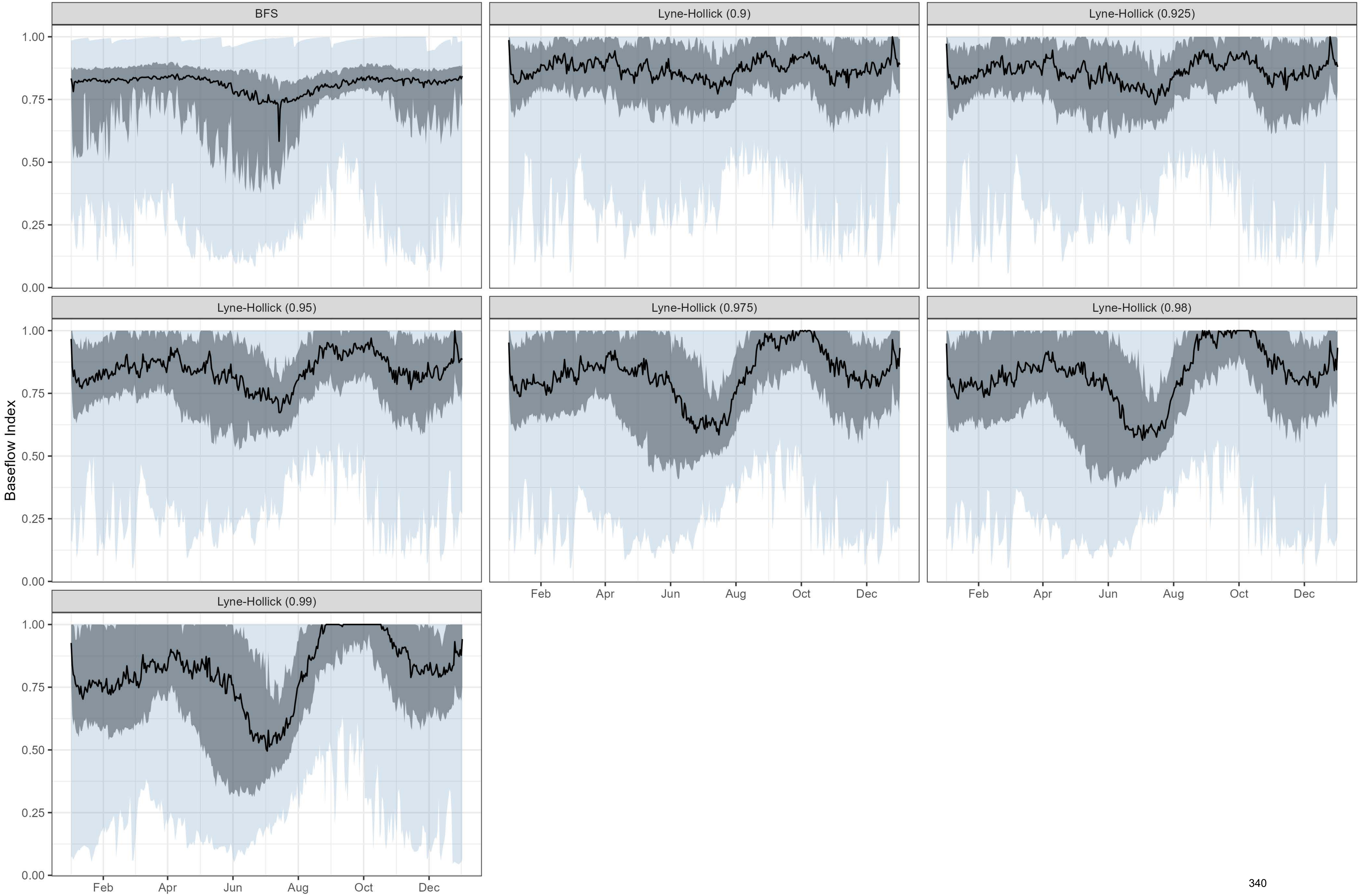


showing min/max (blue), interquartile range (grey), median (black line)

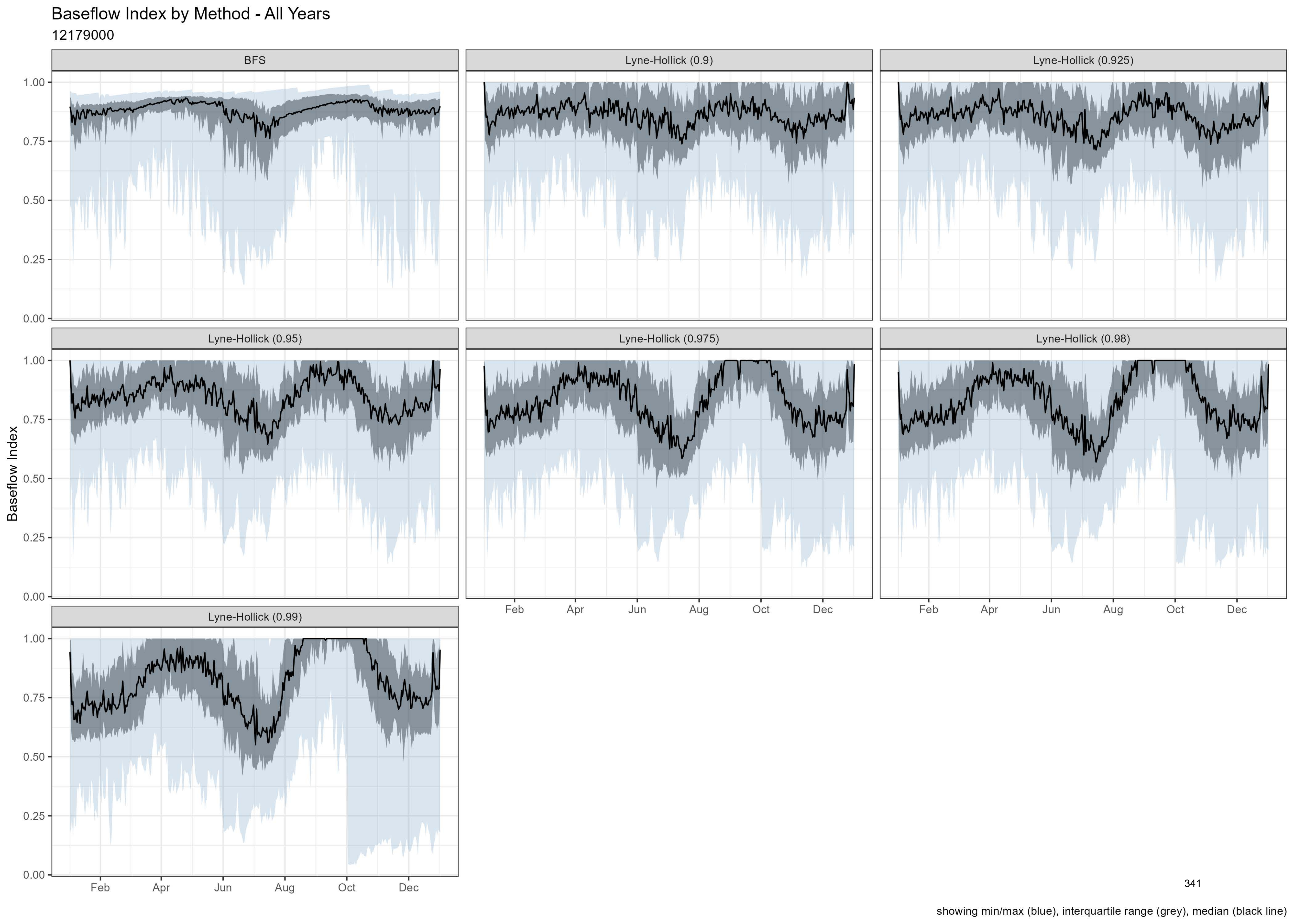
Baseflow Index by Method - All Years
12179000
BFS
Lyne-Hollick (0.9)
Lyne-Hollick (0.925)
Lyne-Hollick (0.95)
Lyne-Hollick (0.975)
Lyne-Hollick (0.98)
Lyne-Hollick (0.99)
Baseflow Index
1.00
0.75
0.50
0.25
0.00
Feb
Apr
Jun
Aug
Oct
Dec
showing min/max (blue), interquartile range (grey), median (black line)

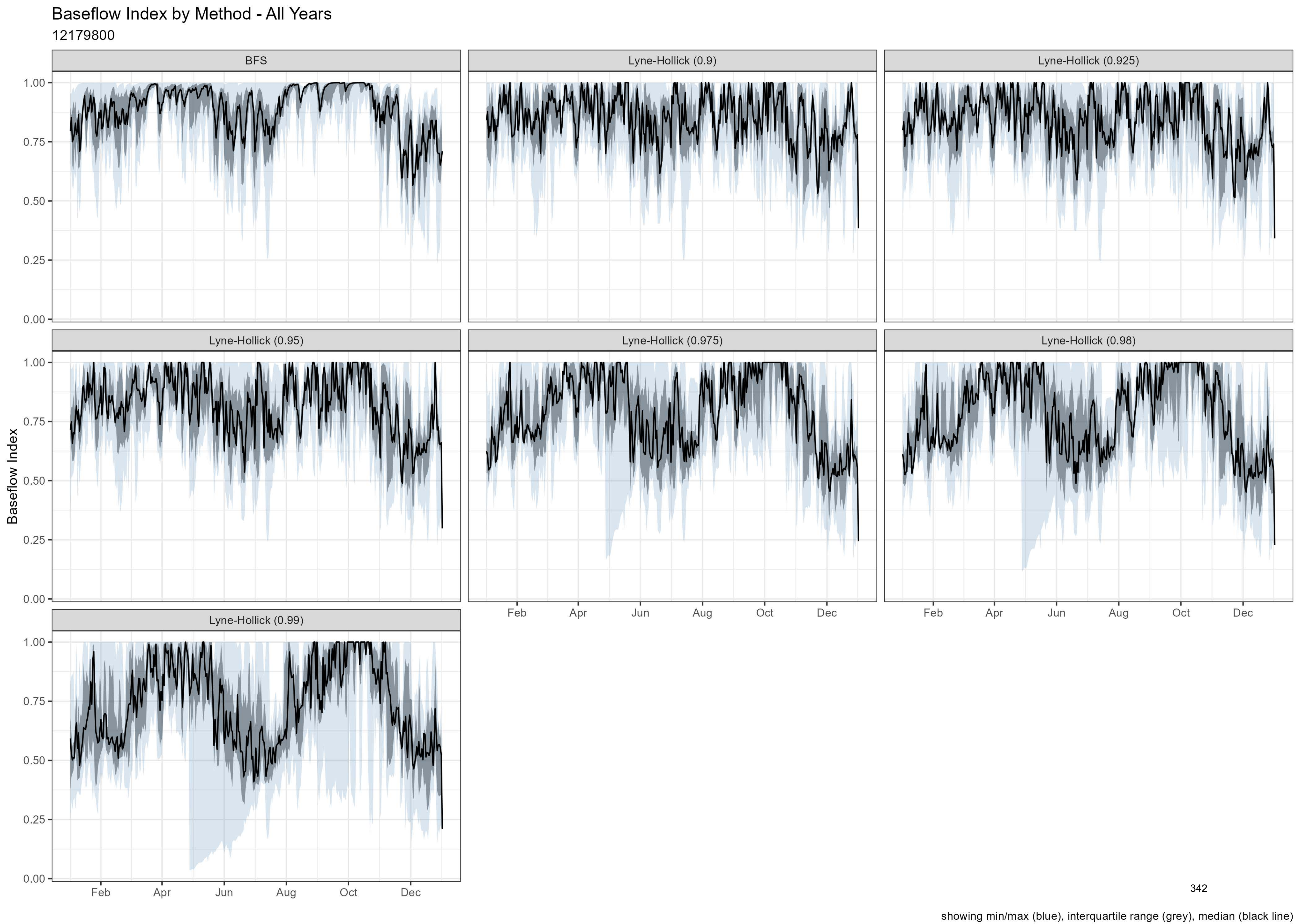
Baseflow Index by Method - All Years
12179800
BFS
Lyne-Hollick (0.9)
Lyne-Hollick (0.925)
Lyne-Hollick (0.95)
Lyne-Hollick (0.975)
Lyne-Hollick (0.98)
Lyne-Hollick (0.99)
Baseflow Index
1.00
0.75
0.50
0.25
0.00
Feb
Apr
Jun
Aug
Oct
Dec
showing min/max (blue), interquartile range (grey), median (black line)

Baseflow Index by Method - All Years

12181000

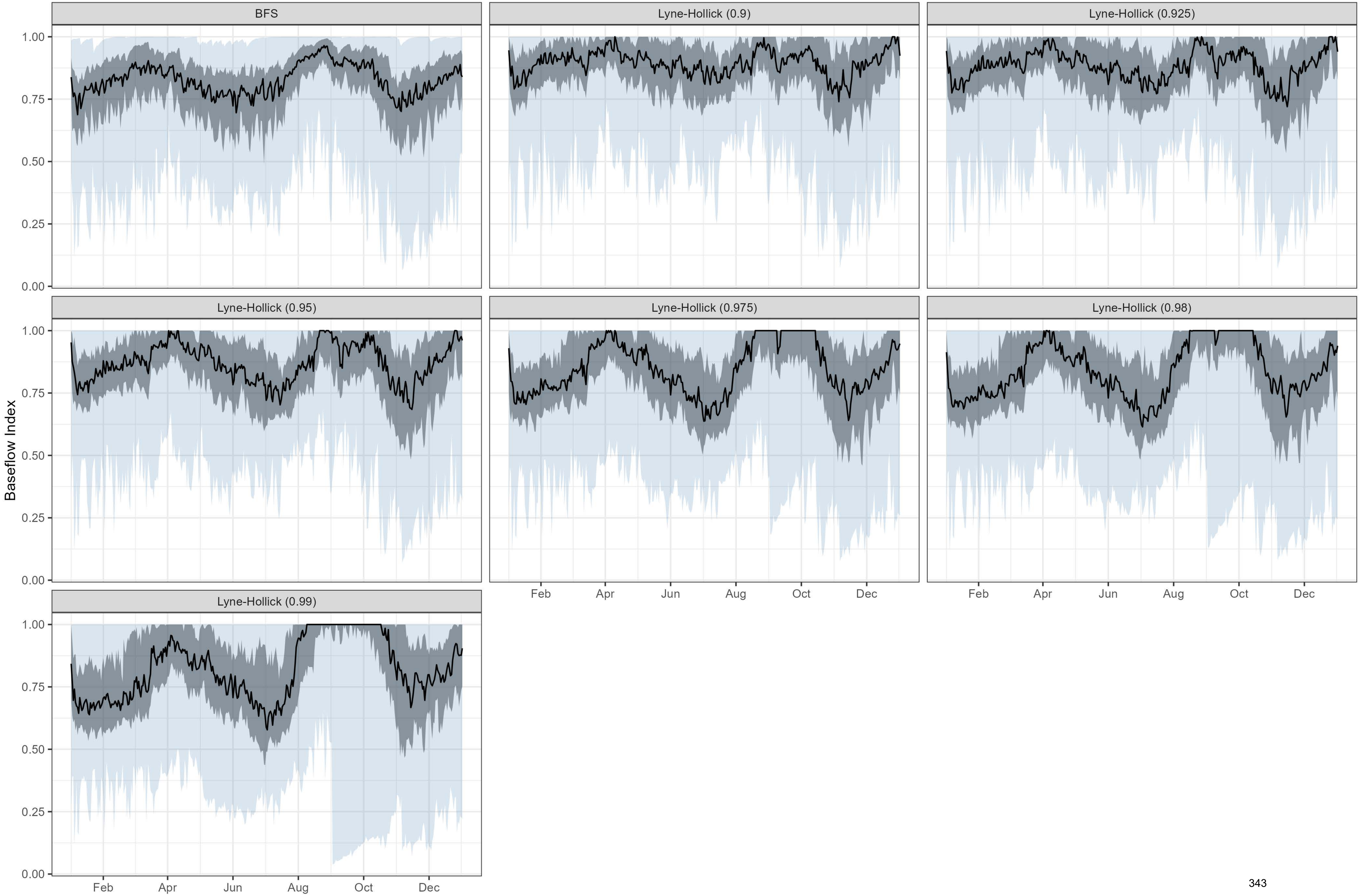




showing min/max (blue), interquartile range (grey), median (black line)

Baseflow Index by Method - All Years

12187500

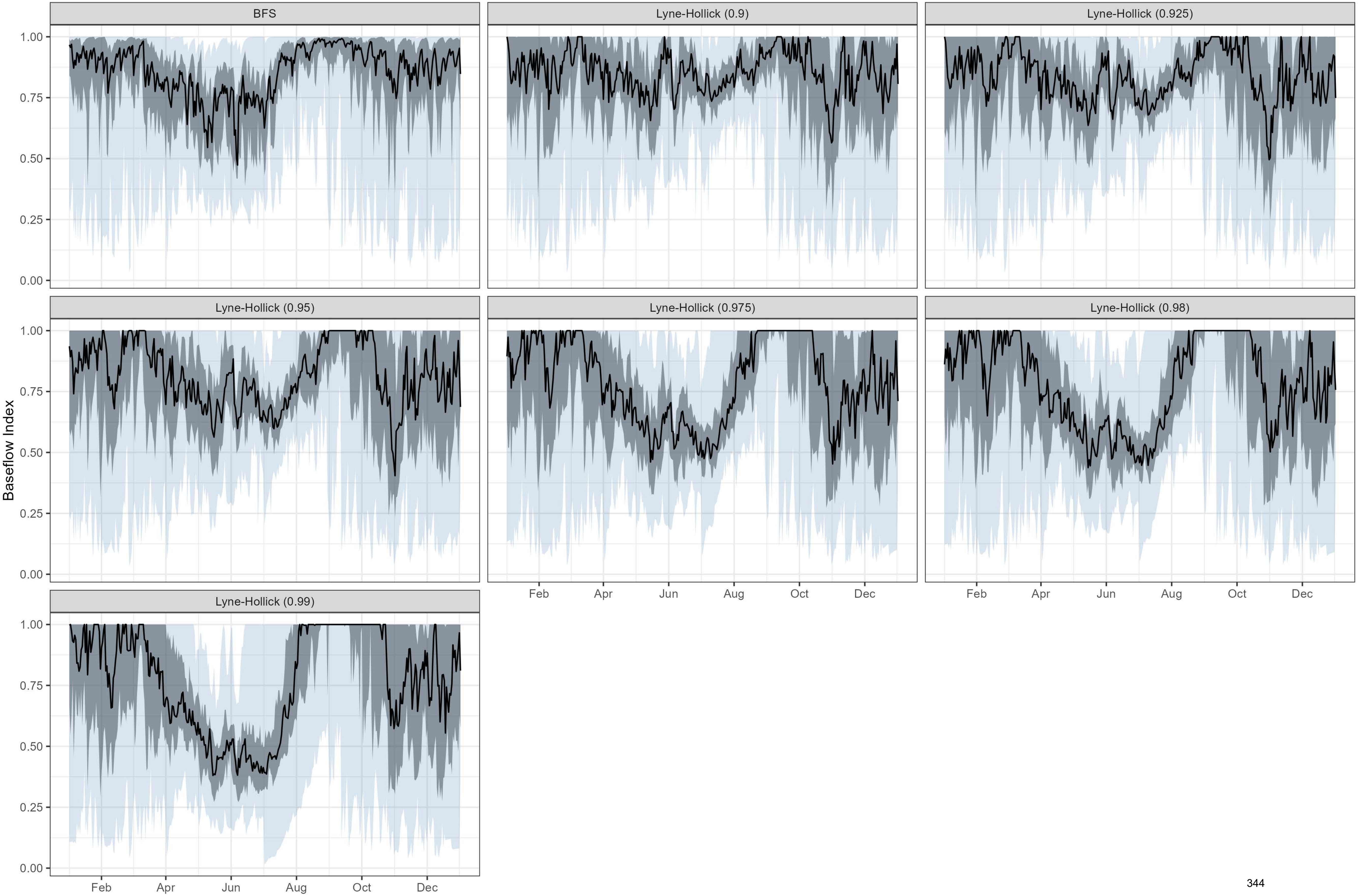


showing min/max (blue), interquartile range (grey), median (black line)

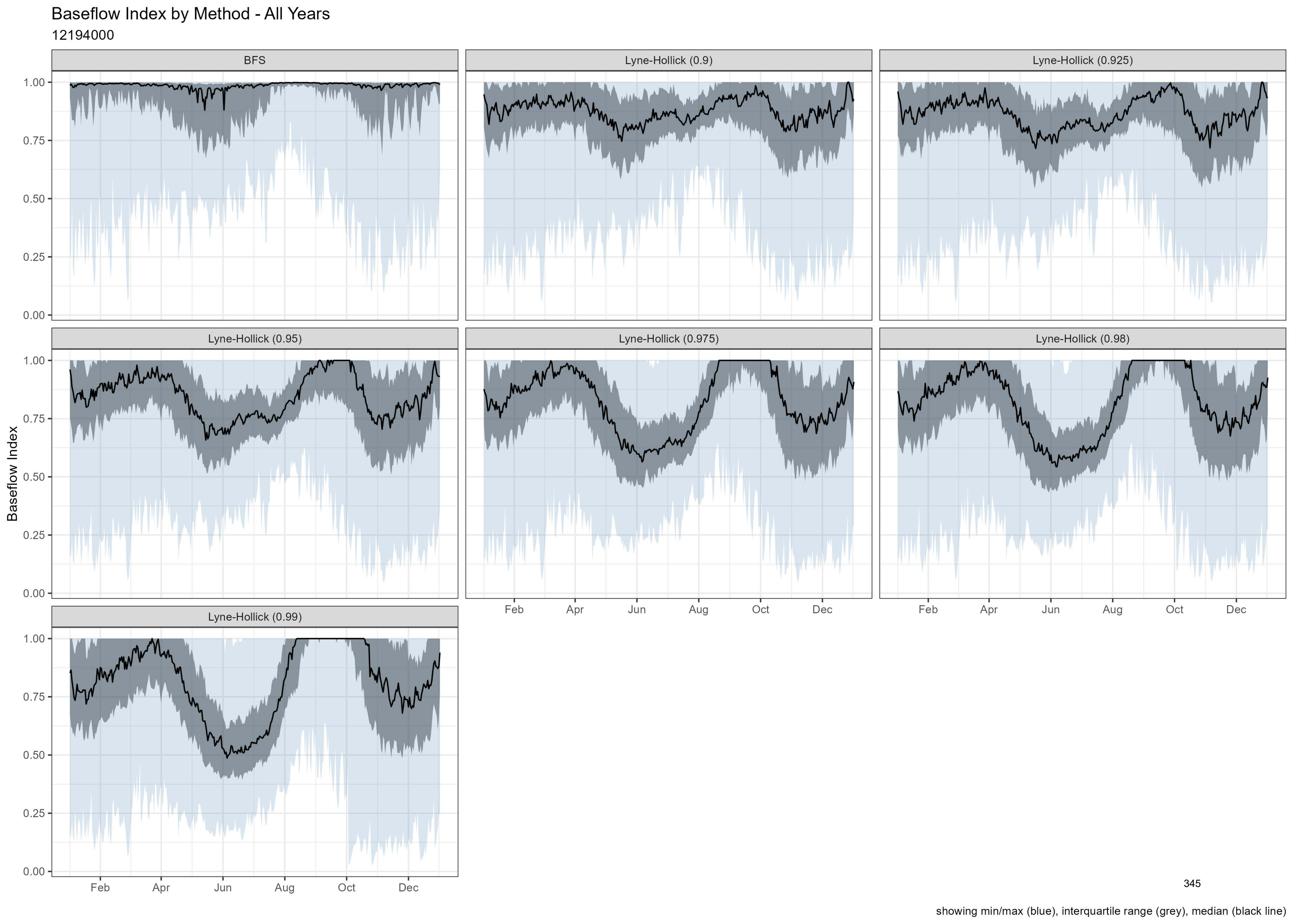

Baseflow Index by Method - All Years
12194000
BFS
Lyne-Hollick (0.9)
Lyne-Hollick (0.925)
Lyne-Hollick (0.95)
Lyne-Hollick (0.975)
Lyne-Hollick (0.98)
Lyne-Hollick (0.99)
Baseflow Index
0.00
0.25
0.50
0.75
1.00
Feb
Apr
Jun
Aug
Oct
Dec
showing min/max (blue), interquartile range (grey), median (black line)

## Baseflow Index by Method - All Years

12200500

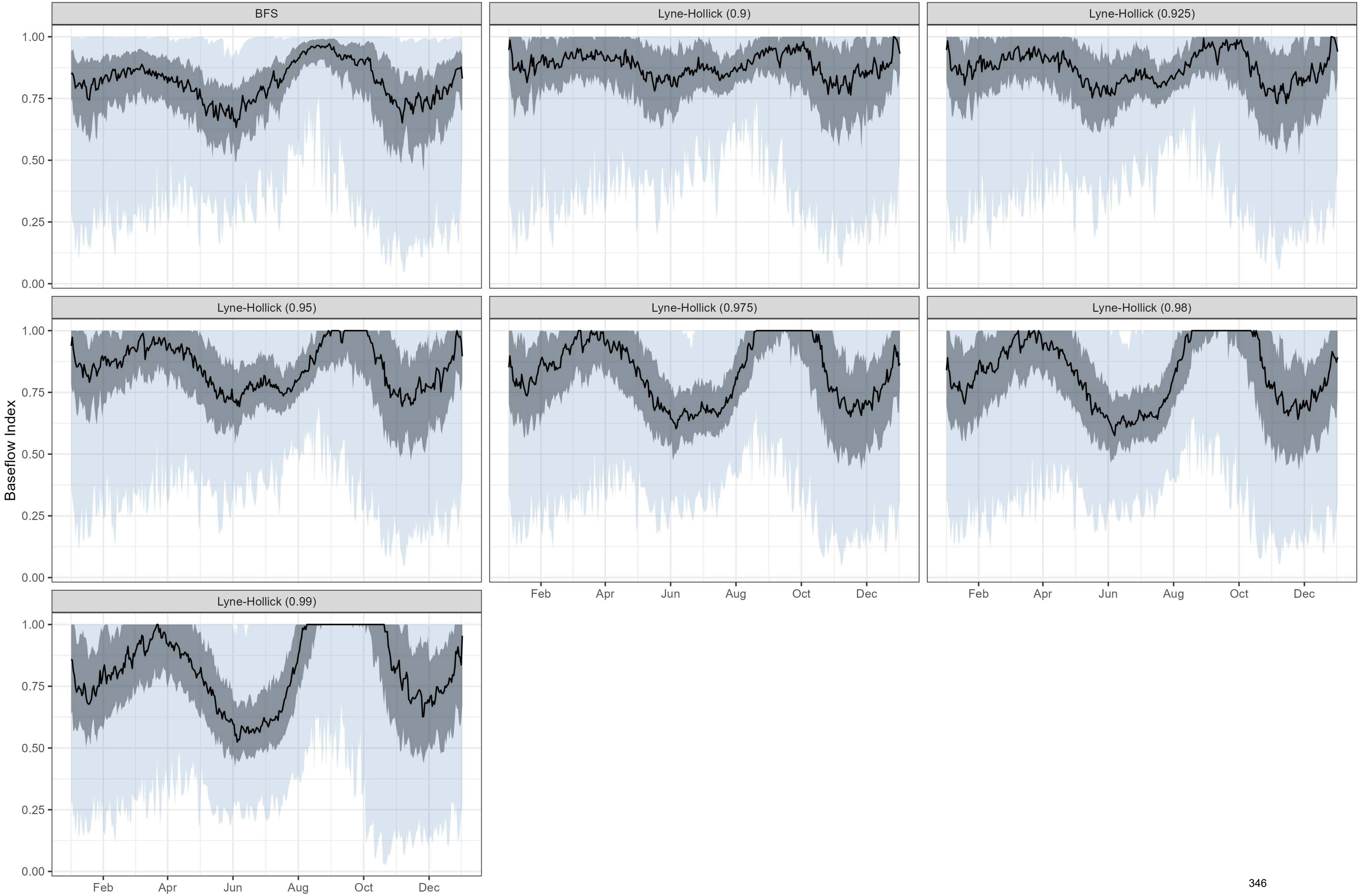


showing min/max (blue), interquartile range (grey), median (black line)

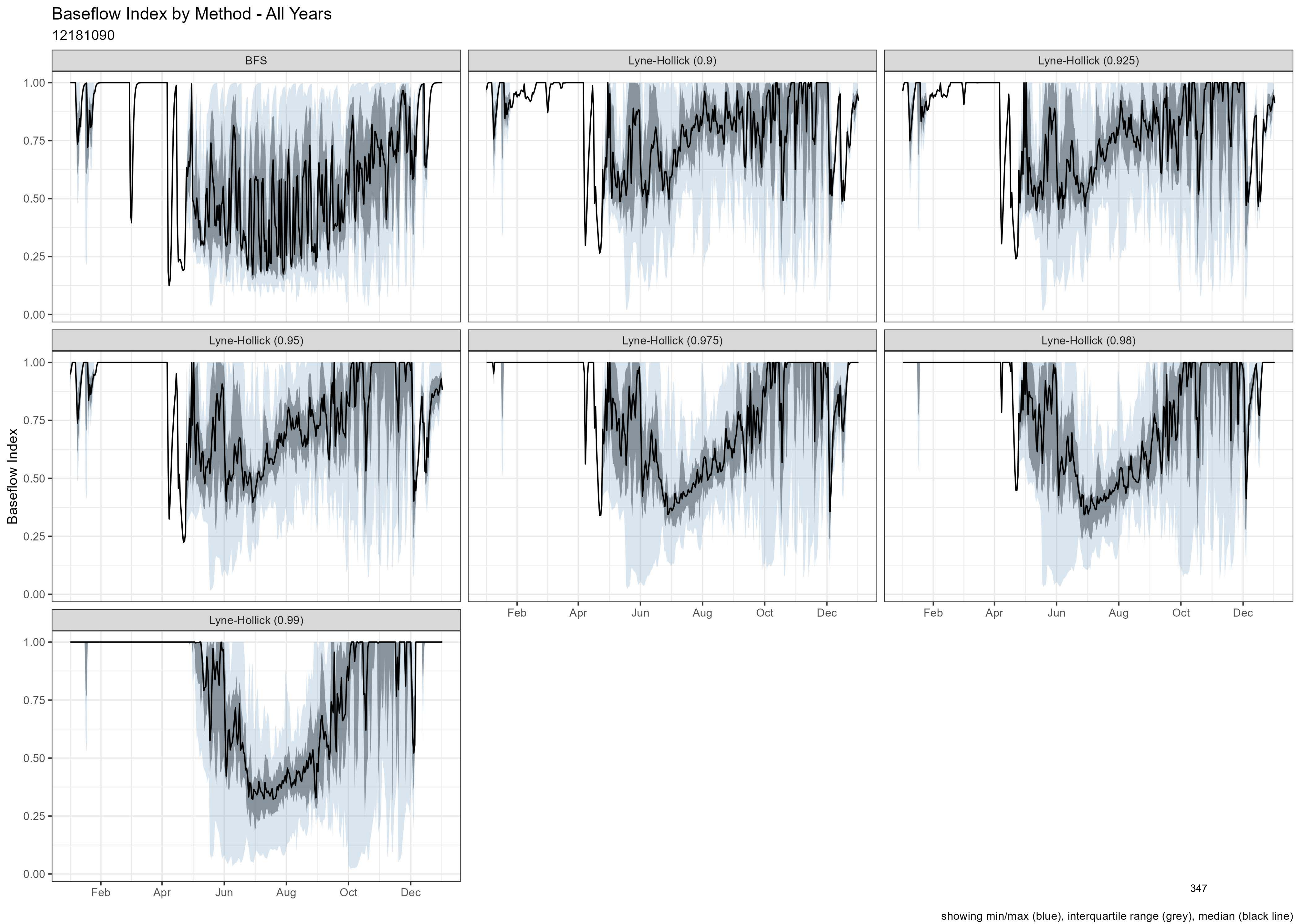
Baseflow Index by Method - All Years
12181090
BFS
Lyne-Hollick (0.9)
Lyne-Hollick (0.925)
Lyne-Hollick (0.95)
Lyne-Hollick (0.975)
Lyne-Hollick (0.98)
Lyne-Hollick (0.99)
Baseflow Index
1.00
0.75
0.50
0.25
0.00
Feb
Apr
Jun
Aug
Oct
Dec
showing min/max (blue), interquartile range (grey), median (black line)

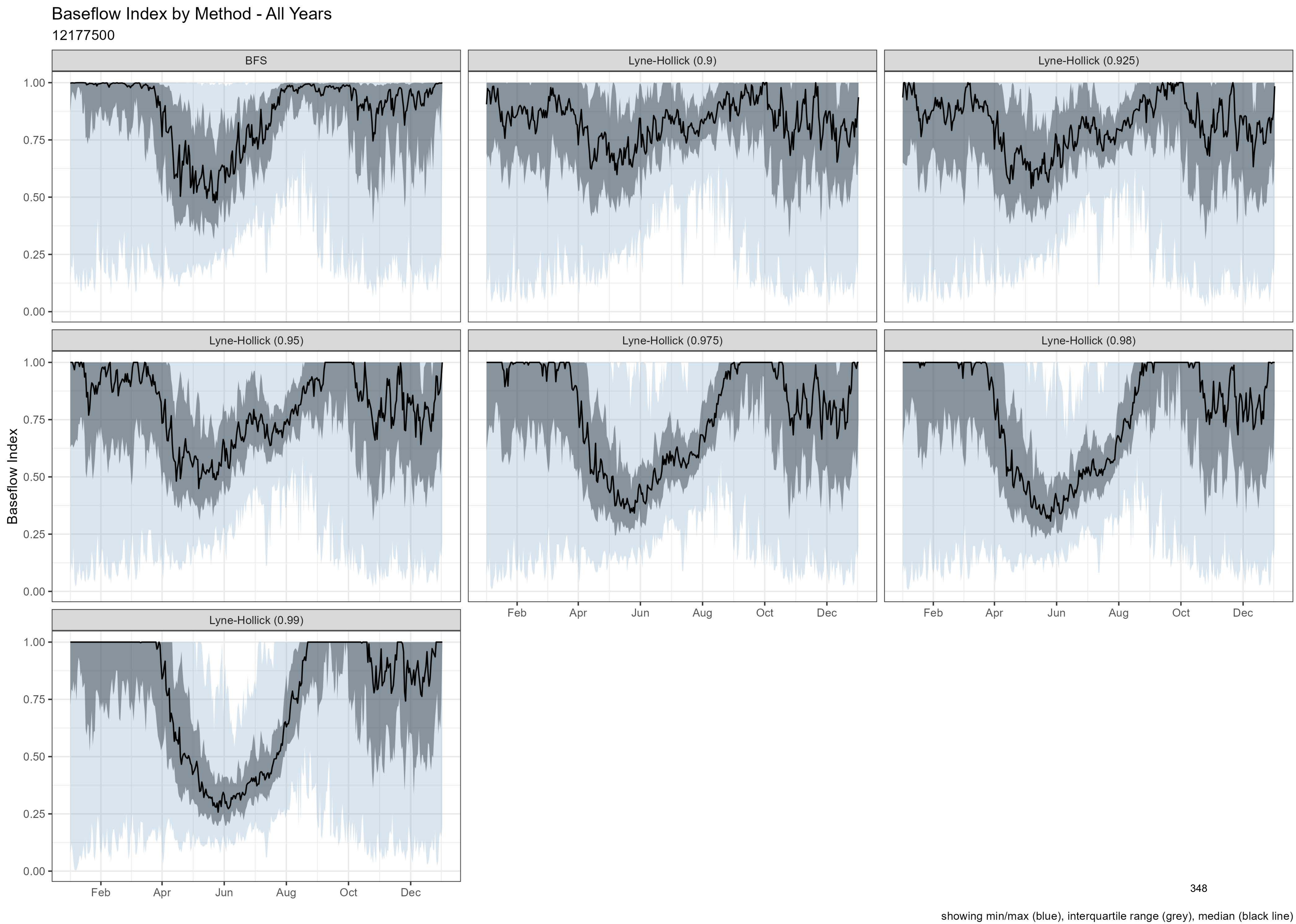
Baseflow Index by Method - All Years
12177500
BFS
Lyne-Hollick (0.9)
Lyne-Hollick (0.925)
Lyne-Hollick (0.95)
Lyne-Hollick (0.975)
Lyne-Hollick (0.98)
Lyne-Hollick (0.99)
Baseflow Index
1.00
0.75
0.50
0.25
0.00
Feb
Apr
Jun
Aug
Oct
Dec
showing min/max (blue), interquartile range (grey), median (black line)

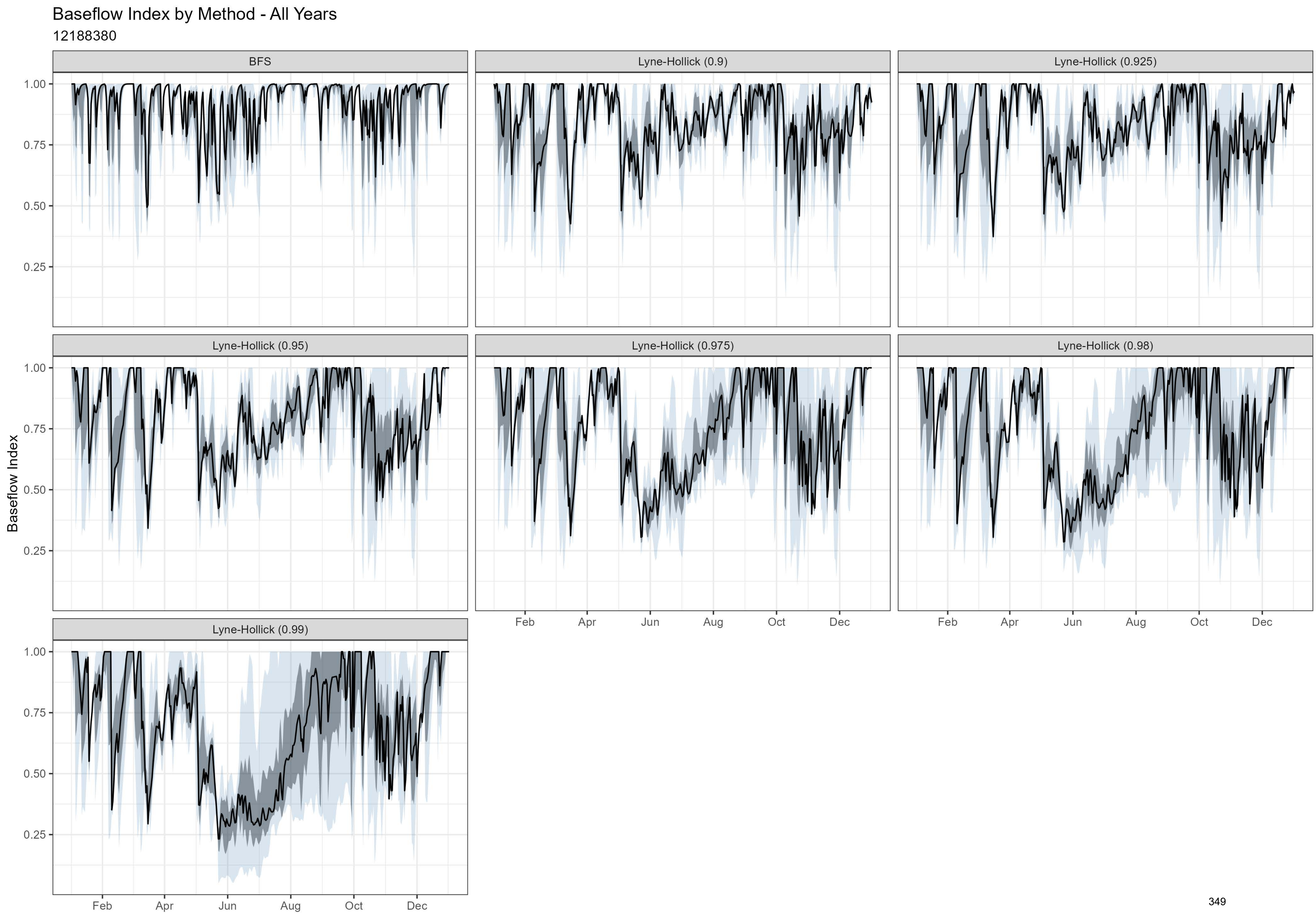




showing min/max (blue), interquartile range (grey), median (black line)

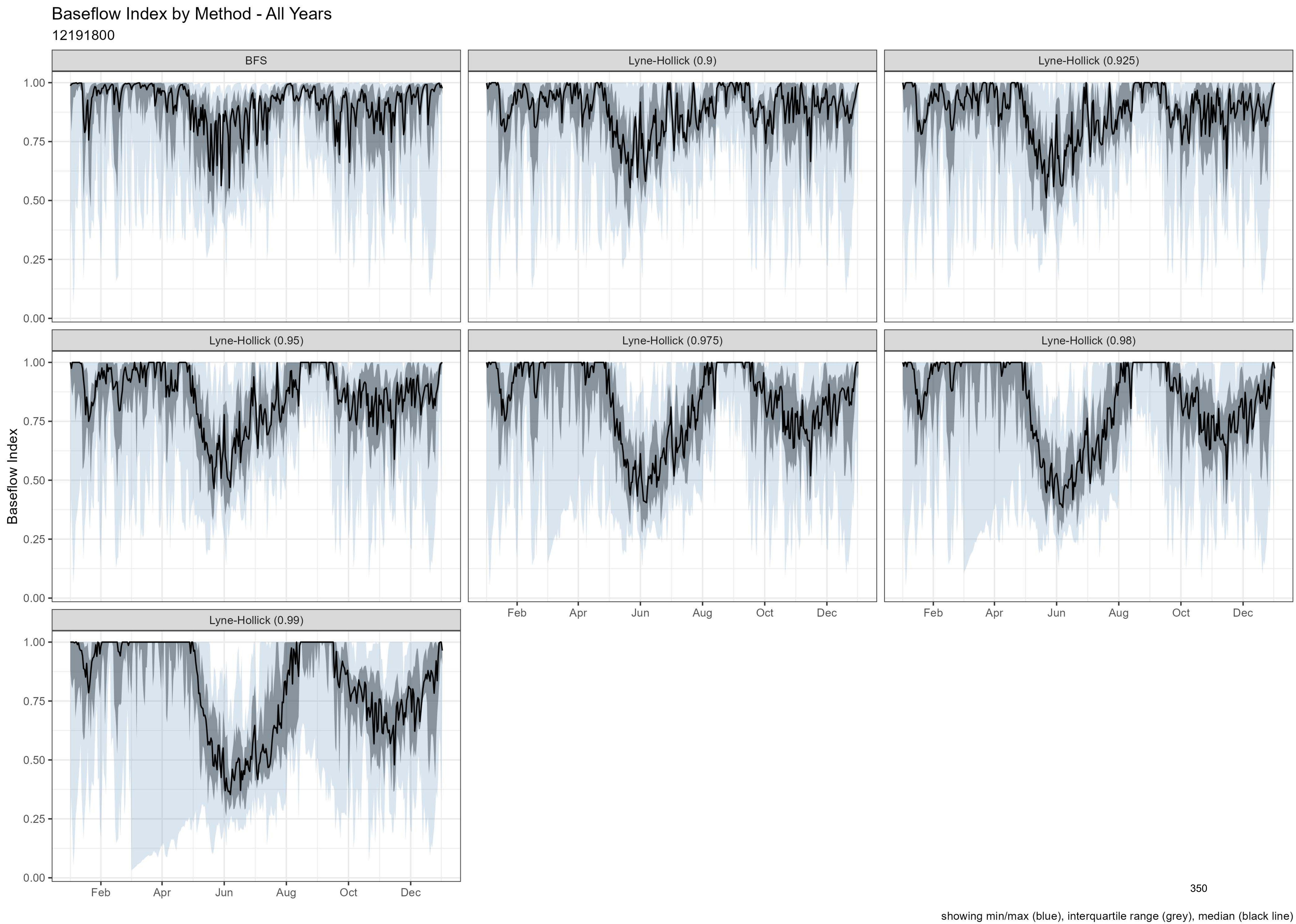

Baseflow Index by Method - All Years
12191800
BFS
Lyne-Hollick (0.9)
Lyne-Hollick (0.925)
Lyne-Hollick (0.95)
Lyne-Hollick (0.975)
Lyne-Hollick (0.98)
Lyne-Hollick (0.99)
Baseflow Index
1.00
0.75
0.50
0.25
0.00
Feb
Apr
Jun
Aug
Oct
Dec
showing min/max (blue), interquartile range (grey), median (black line)


Baseflow Index by Method - All Years
12175500
BFS
Lyne-Hollick (0.9)
Lyne-Hollick (0.925)
Lyne-Hollick (0.95)
Lyne-Hollick (0.975)
Lyne-Hollick (0.98)
Lyne-Hollick (0.99)
Baseflow Index
1.00
0.75
0.50
0.25
0.00
Feb
Apr
Jun
Aug
Oct
Dec
showing min/max (blue), interquartile range (grey), median (black line)

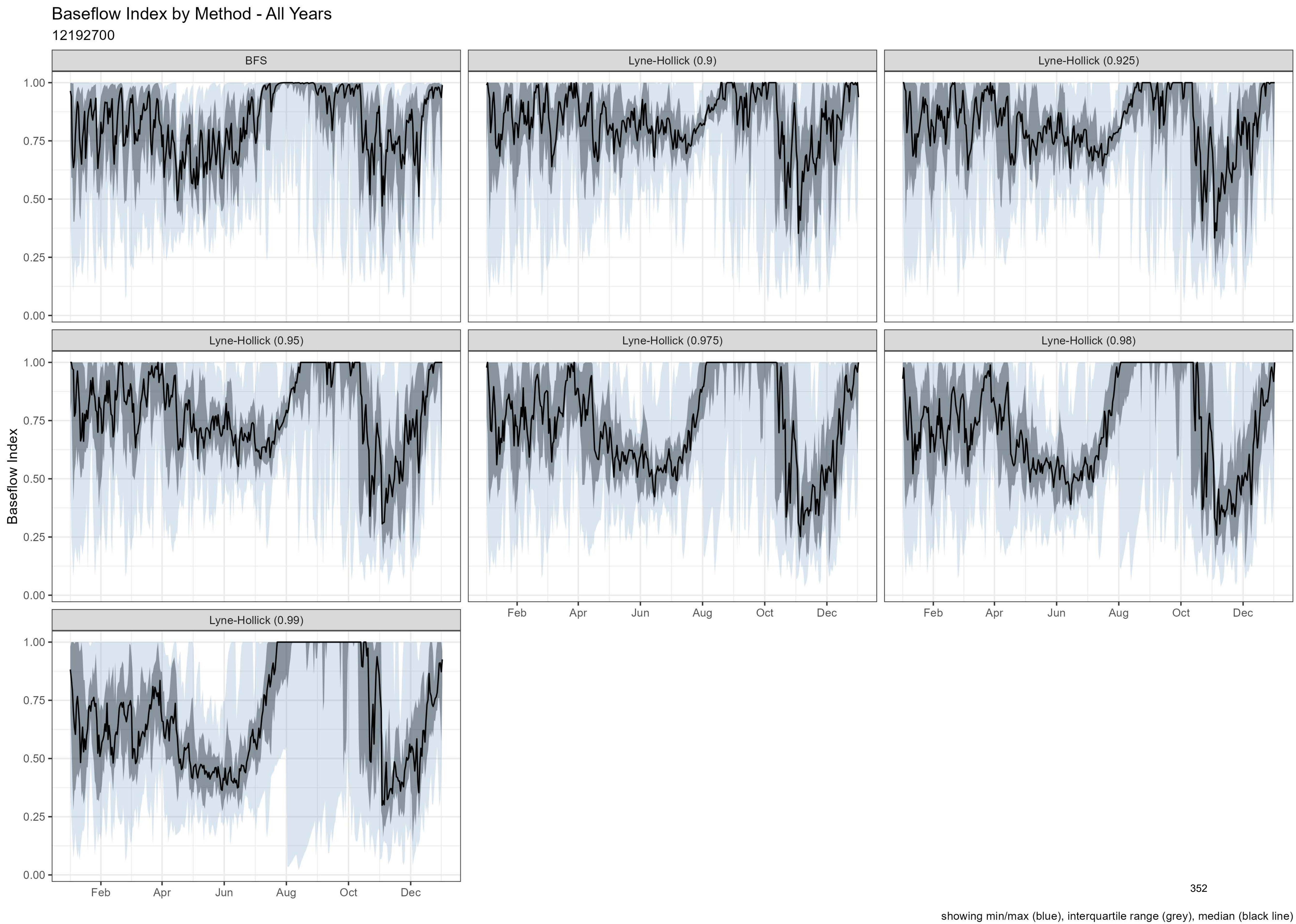

Baseflow Index by Method - All Years
12192700
BFS
Lyne-Hollick (0.9)
Lyne-Hollick (0.925)
Lyne-Hollick (0.95)
Lyne-Hollick (0.975)
Lyne-Hollick (0.98)
Lyne-Hollick (0.99)
Baseflow Index
1.00
0.75
0.50
0.25
0.00
Feb
Apr
Jun
Aug
Oct
Dec
showing min/max (blue), interquartile range (grey), median (black line)

# Baseflow Index by Method - All Years

12197700

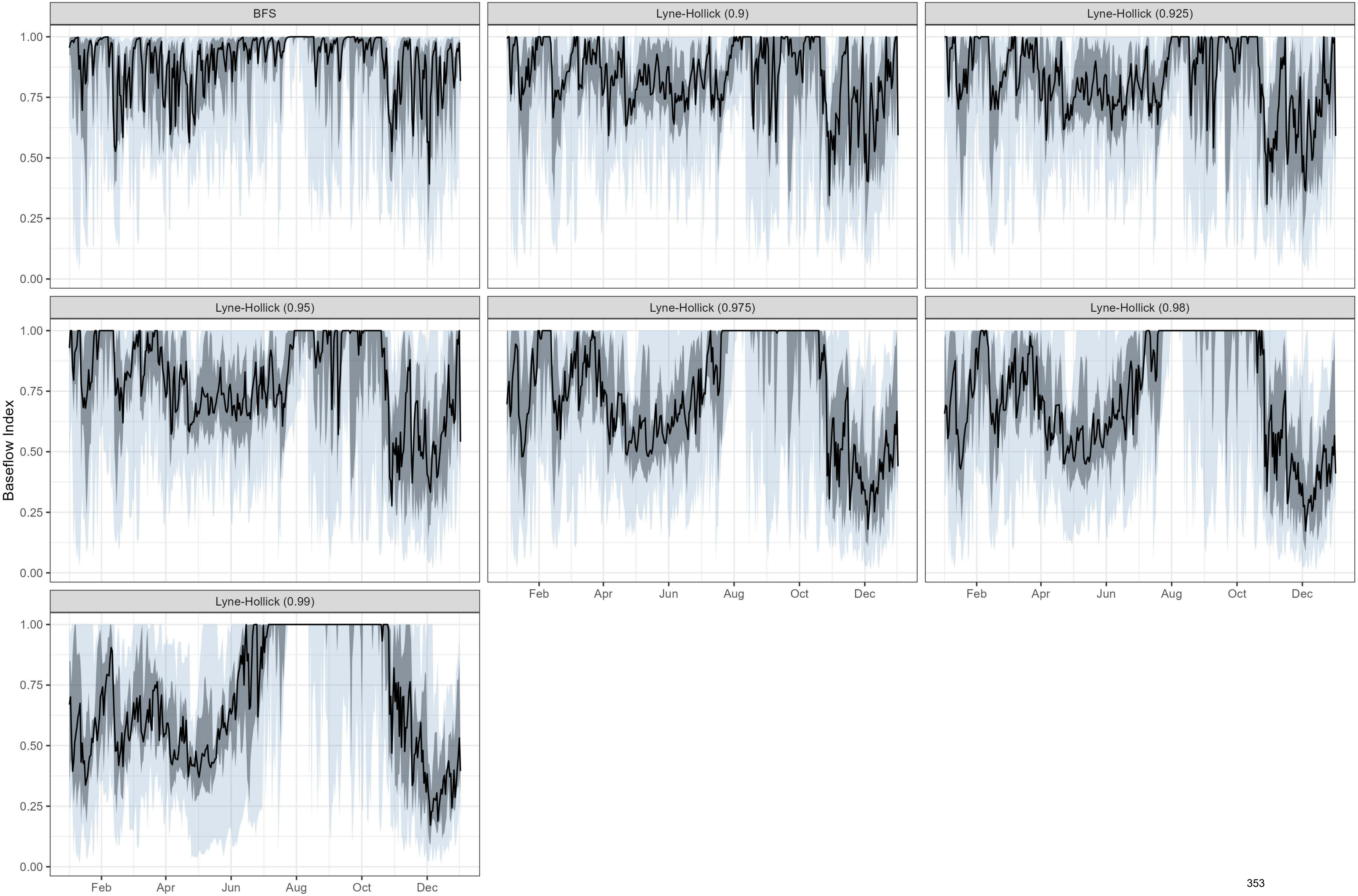




showing min/max (blue), interquartile range (grey), median (black line)

WASHINGTON STATE
Academy of Sciences
Science in the Service of Washington State

# Peer review of the draft report on the "Skagit River Basin Groundwater Study"

*A report for the Washington State Department of Ecology*

**April 2025**

## ABOUT THE WASHINGTON STATE ACADEMY OF SCIENCES

The Washington State Academy of Sciences (WSAS) is a nonpartisan, nonprofit organization established by the Washington State Legislature in 2005 to advise state agencies, the Legislature, the Governor's office and others on public policy issues involving science and technology. WSAS accomplishes its mission "Science in the Service of Washington State" through a structure that mirrors both the form and function of the National Academies wherein senior scientists and engineers are elected by their peers and agree to serve when they confirm their membership. WSAS mobilizes the research community in Washington and beyond to provide timely, credible expertise on issues that affect Washington state.

Learn more at www.washacad.org.

# TABLE OF CONTENTS

# EXECUTIVE SUMMARY

The Washington State Department of Ecology (“Department”) asked the Washington State Academy of Sciences (“WSAS”) to provide a peer review of the Groundwater Study, one of three studies commissioned by the Department at the direction of the Washington Joint Legislative Task Force on Water Supply (“Task Force”) through the Washington State Water Research Center at Washington State University. WSAS convened a panel of three reviewers, chaired by WSAS Board Member Michael F. Goodchild, to conduct the peer review. Reviewers were chosen for their interest and experience in areas covered by the report, and in the Skagit Basin generally. Reviewers were provided with the project’s report, asked to provide written commentaries on the study in response to guiding questions, and convened in a virtual discussion on April 2, 2025.

# BACKGROUND

This study on groundwater on the Skagit Basin is one of three studies undertaken to address knowledge gaps related to the Skagit River and its contributions to agriculture, urban development, fishery, and recreation identified in a 2022 WSAS report for the Task Force, titled “Proposed Scope for a Comprehensive Hydrologic Study of the Skagit Estuary.”

That study found one significant knowledge gap to be the proportion of stream water that was composed of baseflow groundwater, which could play a significant role in moderating temperatures. To address this gap, the Department of Ecology awarded a contract to HDR Engineering and Western Washington University, in collaboration with the State of Washington Research Center, to conduct an analysis of groundwater flows near Muddy, Alder, and Grandy Creeks between the towns of Hamilton and Concrete, WA. As described by the Washington State Water Research Center, the study was designed to:

*…characterize subsurface hydrogeologic units and groundwater resources, including investigation of groundwater/surface water interactions and will also evaluate basin-wide groundwater baseflow (groundwater discharge flowing to streams).*

*…produce a more complete understanding of the Skagit’s groundwater resources and aquifers and in doing so will help water resource managers with decision making.*

The project was divided into four tasks:

- Task 200 (Hydrogeologic Characterization, report delivered 9/15/23)
- Task 300 (Hydrograph Separation, report delivered 5/15/23
- Task 400 (Surface Water and Groundwater Interaction, report delivered 12/6/24), and
- and Task 500 (Three-Dimensional Hydrogeologic Framework, report delivered 10/31/24).

The Department asked WSAS to assess the quality of the research, whether it was effective at achieving the stated objectives, and areas that could benefit from additional context. WSAS recruited four well-respected researchers from different fields and institutions with multidisciplinary expertise in hydrology, fish biology, streamflow, and watershed management to review the study.

# SUMMARY OF COMMENTS

The contractor has provided a very detailed report on the project, with numerous tables, figures, appendices, and photographs. The Skagit Basin is an area of incredible geologic and hydrologic complexity, making it very difficult to characterize groundwater/surface water interactions and basin-wide groundwater flow in a way that could inform decision making. This study contributes data that could be useful for future decision making but is not sufficient by itself to provide a useful, explanatory model to inform decision making. Making the data and observations within this study useful for future investigators to test specific hypotheses would require better documenting, standardizing, and making the data available in a single source. In addition, there are numerous methodological and analysis issues that need to be addressed to validate or explain certain findings, and additional seasonal data would need to be collected to better understand low-flow periods.

What follows consists of two additional summary comments, and the detailed reviews by the three reviewers.

First, it would be helpful if the report could be placed into a broader context. The document on the history of the project that has been attached to the report is helpful, but this new report is not clearly linked into the history. What motivated this study, with its specific emphasis on the east side of the Skagit between Hamilton and Concrete? What has been learned from this study that contributes to our general knowledge of the entire basin? What parts of the report, including the extensive data and figures, might be most useful in later studies and in decisions about withdrawals from the river?

Second, all three reviewers raise concerns about the central conclusions of the study. Connections between upland snowmelt and baseflow are discussed, but is the evidence sufficiently compelling, and is the report consistent in its discussion of the connections? As Reviewer 3 notes in a discussion section, the report does a valiant job of sorting some simplicity out of a very complex environment, but are the caveats sufficiently explored and clearly stated? And is the experimental design optimal given the resource constraints and the central conclusions?

## REVIEWERS' COMMENTS

### REVIEWER 1

***General comments***

*History of Skagit Research Project*

This is full of jargon, and little hint of what the objectives and/or questions addressed by the various subprojects are/were. For instance, "[WSAS] was requested to review a series of three consultant reports …". Fine, but what were those reports intended to do? And so on …

*Task 200 (Hydrogeologic characterization)*

*The Task 200 report (submitted 9/2023) and Task 500 report (submitted 10/2024) were progress reports for an ongoing MS thesis for a geology student at Western Washington University to develop a hydrogeologic framework for the lower Skagit River basin. The MS thesis was completed in May 2025 and will serve as the final report encompassing tasks 200 and 500. Although the MS thesis was produced by Henry Willaims at Western Washington University, his thesis advisor, Robert Mitchell, and committee member Jon Riedel serve as coauthors for the project.*

*The MS thesis will satisfy most of the concerns expressed by the reviewers related to the 200 and 500 reports. For example, the MS thesis clearly states the motivation for the development of the hydrogeologic framework and emphasizes that the hydrogeologic framework is a generalized characterization of the lower Skagit valley and should not be used to make water management decisions. It will serve as a basis to guide future studies. The MS thesis Includes detailed maps, updated and additional cross sections and 3D conceptual models, a more detailed discussion, and conclusions and recommendations. Not included in the MS thesis are the 2D geology cross sections illustrated in the Task 200 report. The MS thesis focuses on the hydrogeologic units that lump geologic deposits.*

First off, this really needs a map showing the study area, and please reference river miles. Moreover though, it's very difficult to get an idea of the contribution of the work to better understanding linkages between groundwater (in the lowland and upland terrace areas) and the flow of the river, which is what I presume the contribution of the report is supposed to be. For instance:

1) The executive summary is obscured by details like "The cross sections were developed using the Xacto Section tool". This sort of thing should be in a methods section, not the executive summary.

See the new Introduction in the MS thesis.

2) “The well-log database includes information on well identification, location, depth, and logged formation materials”. Yes, that makes sense, but this sort of detail also should be in a methods section.

Rectified in the Methods section of the MS thesis.

3) The closest the executive summary comes to providing key information about the “big picture” is the statement “The cross sections and geology literature reviewed indicate the occurrence of unconfined aquifer materials in the upland (glacial) terrace that are potentially connected to unconfined aquifers in the Skagit River valley, therefore they are hypothesized to have hydraulic connections with the Skagit River or its tributaries.” That’s important, but how was the hypothesis tested? The following paragraph hints at this by saying “… initial basis of a more detailed conceptual hydrogeologic/ hydrostratigraphic framework that will be expanded on in the subsequent evaluations” but that doesn’t seem to me to be the same as testing the hypothesis.

The MS thesis Introduction clearly states the motivation for the development of the hydrogeologic framework.

*Comments on main text:*

1) Please provide a map, showing Alder Creek and other key attributes, with river miles.

Alder Creek is clearly illustrated in multiple figures in the MS thesis. The figures have scale bars rather than river miles.

2) The paragraph starting “Outcomes will provide the initial basis ..” basically is gobbledygook. I think what you’re after is an understanding of the extent to which the glacial terrace and valley aquifers are connect to each other, and the extent to which they control river low flows.

A more detailed analysis is provided in the MS thesis. Natural systems are complex, so yes inferences are made based on the best available information to offer some insight that may lead to further studies.

3) Please embed the key figures (like Figure 1) in the main text rather than an appendix. It’s very irritating to have to flip back and forth. Also, wrt Figure 1 provide a full size figure for the study area, with an inset to much smaller figure of the entire Skagit River basin. And be sure that key features, like the various creeks discussed in sections 4.1-4.3 are shown in the expanded figure of the study area.

Imbedding figures in the text is a matter of style. The authors prefer to maintain the style which is consistent with our academic institution for MS theses and manuscripts for peer review. Updated figures are provided in the MS thesis.

4) How many well logs were usable? Also, please assure that relevant figures (e.g., Figure 4) show the study area in the same way as Figure 1, and have key attributes (creeks, river miles, etc.) shown.

Clarified in the MS thesis. Most wells eliminated were shallow wells in the valley floor because they did not provide insight into the deeper stratigraphy. Updated figures are provided in the MS thesis.

5) It seems as though at least Figures 2 and 4, and perhaps 2, 3, and 4, could be combined. As a minimum,

Figure 4 needs to show the glacial terrace and the floodplain.

Illustrated in updated figures in the MS thesis.

6) In Figure 3, it's not clear what the numbers on the cross-sections mean. Are those existing pumped wells? And how was the decision made to put the one new deep well on the one particular transect? And how much value added is there for just one deep well? Finally, surface elevation contours would be useful on this figure.

Illustrated in updated figures in the MS thesis. Funding for the project allowed for the installation of one well. We chose a strategic location based on access on public land, a spatial gap in data, and site geology.

7) Figures 5-9 may be OK for an appendix, but they need to be synthesized into a single figure that helps the reader understand commonalities (or lack thereof) among the three cross-sections. It's too difficult to get that picture by flipping back and forth between five figures.

Illustrated in updated figures in the MS thesis.

8) I would argue that there are no conclusions at this point, and I would call that section "synthesis". But also, the statement "Some of the Task 200 results suggest that the GT between Hamilton and Concrete may be important sources of groundwater for the Skagit River". How is that statement substantiated? Is this just from the well logs? Not clear to me that you know at this point that the GT aquifer(s) are an important contributor to

low flows. And in fact, you even state "9) At this point, however, direct groundwater connections between the GT and the floodplain/river are not clear."

The MS thesis includes a detailed discussion, conclusions, and recommendations.

*Task 300 (Hydrograph separation)*

In general, this report is somewhat better written than the 200 report. It does have objectives clearly stated, although Section 1.1 should refer explicitly to the four reports (200-500). Thank you for embedding figures in the text (lengthy tables, however, like Tables 1 and 2, should go in an appendix – although locations of stream gauges should be shown on a map).

[Response: Citations and references added to the other three reports/technical memoranda (Task 200, 400, and 500). Tables 1 and 2 provide necessary information and are each only two-page tables, so they have been retained embedded in the main body text of the report. There is already a map of stream gage locations (see Figure 1).]

*Specific comments:*

1) Figure 1 needs to be rectified with Figure 1 in the 200 report (200 study area should be shown). It appears that the study area for the 300 report is larger? Why?

[Response: Figure 1 has been updated to include a box outlining the study area from the other tasks. Yes, the study area is larger for this Task 300 report, covering the extents of the entire Skagit River Basin within the United States. Additional text has been added to Section 1.1, stating "**The additional subbasins, located outside of the study areas of the Tasks 200, 400, and 500 study area (green box on Figure 1), were analyzed to be comprehensive in terms of the water balance across the Basin since there is no field requirement for data collection and the analyses are relatively easy to repeat for a large number of gages.**"]**In addition, based on this comment, the gages within the Tasks 200, 400, and 500 study area have been identified in bold text in Tables 2, 3, and 5, for ease of locating in the tables, and a note was added about this to Section 5.**]

2) Tables 1 and 2 might be condensed into figures showing e.g. periods of record for each of the gauges. As it is though (see above) the tables are too long for main text.

[Response: See response above (two above). There's quite a bit of information in Tables 1 and 2 that is better presented in table format.]

3) Most readers don't need the details of different baseflow separate methods, which can go in an appendix. What would be better is to include a conceptual figure, perhaps using a year's data from one of the gauges. The real question in doing this kind of analysis is what constitutes baseflow. My contention is that, for the issues faced here, this is primarily a summer dry period issue. The main issue with baseflow separation is that, if you get a dry period in winter following high flows, the dry period flow that follows isn't coming from the same stored water as it is in the summer. Stated otherwise, you tend to have wet weather storage that decays relatively more quickly than during the "real" dry periods in late summer. My hypothesis is that many of the differences between the two methods they use come about because of the low flow periods the different methods are using. See for example Figure 2. There's a lot of obvious snowmelt in the May-August period (and frankly, that's a complicated example because of the glacier contribution). Then there's a large rainstorm in October. So about the only period that's suitably dry in that year and basin is November-December. My guess is, for that basin, there are

much better years where you don't need elegant (and potentially error-prone) baseflow separation methods; just isolate the dry and snowmelt-free periods from multiple years.

[Response: The details of the methods are important to understand because the methods comparison is a primary aspect of the study, and the methods are presented succinctly.

A year's worth of data from one gage is already presented in Figure 2 with the streamflow and associated baseflow hydrographs using Lyne-Hollick with all six analyzed alpha values, providing a nice "conceptual figure." In addition to the November-December time period, it could easily be argued that there are several periods in the January-March months that can be representative of low-flow (streamflow) that represents baseflow. For all gages the results indicate that there is at least some time period analyzed where the daily BFI calculated (from one of the baseflow separation methods) is equal to 1.0, which does lend credence to the idea of analyzing low-flow streamflow periods to estimate baseflow. Task 400 does this with its seepage run survey, so the approach concept is the same and results should be comparable.

There is no difference in the periods analyzed and compared between the two methods (BFS Model and Lyne-Hollick), and they both estimate baseflow over the entire period of available record (year-round over multiple years). Conceptually there is not any issue with baseflow (GW discharge) increasing during wet periods, as there is more precipitation (and/or snow/glacial melt) that recharges the groundwater system and increases groundwater levels, which causes the driving heads to increase, that in turn increases GW discharge (and baseflow). Since the rivers are net sinks where GW discharge occurs, it stands to reason that GW discharge increases (on the whole over the basins analyzed, with obvious nuances locally around river meanders that cannot be captured). The filtering included with the baseflow separation methods represents the smoothing of the baseflow with the "decay" being represented as a result of the overall process.

Perhaps what is best to do is quote the first paragraph from Konrad (2022) in describing their BFS Model (which the first part has been added to Section 1 (Introduction):

> *Streamflow in rivers can be separated into a relatively steady component, or baseflow, that represents reliably available surface water and more dynamic components of runoff that typically represent a large fraction of total streamflow. A spatially aggregated numerical time-series model was developed to separate the baseflow component of a streamflow time-series using a state-space framework in which baseflow is a non-linear function of upstream storage, an unmeasured state variable. The state-space framework allows forecasting of baseflow for periods with no rainfall or snowmelt and estimation of residence times in contrast to other hydrograph separation models. The use of a non-linear relation between baseflow and storage maintains model performance over a wide range of time scales but will only provide reliable predictions for periods when the rate of streamflow recession as a fraction of streamflow decreases over time.*

It is also worth pointing out that baseflow estimates published by the USGS using the BFS Model (cf. Konrad (2020)) are comparable to those from this study (i.e., total baseflow is typically greater than 50% of total streamflow (BFI >0.50) when averaged over the entire period of record).]

4) In Table 3 (which is too long to be in main text) I assume coefficient of variation is for annual flows? In any event, another statistic I suggest including is some measure of baseflow (for instance, 7-day 10 year low flow) as a fraction of the mean annual flow. You also might want to plot that as a function of drainage area (log scale)

[Response: Table 3 provides necessary information and is only three pages long, so it has been retained embedded in the main body text of the report. The coefficient of variation is based on the ratio of the standard deviation to the mean from daily streamflow, so it's not annual – no change was made since the text in Section 4.1.1 already states, "Table 3 summarizes various flow statistics calculated using all of the available mean daily streamflow data (in cfs) for each analyzed gaging station."

While the suggested metrics to help establish low-flows for comparison against baseflows calculated via the other techniques presented, and comparing against drainage area in a plot, it would only add more information to an already crowded table and would not add a lot compared to the other information already provided.]

5) Table 5 results for "total baseflow/total streamflow" don't make sense to me. They are suggesting that most of the flow is baseflow. I simply don't believe that, and I think it's an artifact of their method which is trying to allocate runoff during periods of snowmelt and/or rainstorms to "direct" and baseflow. I strongly suspect that most of their "baseflow" is coming from the wet and/or snowmelt seasons. It they're trying to make decisions that involve connectivity of streamflow to the groundwater system, I suspect that during most of those periods, groundwater isn't supplying

[Response: **The definition of total baseflow and total streamflow was expanded to specify that it was the total volume of baseflow and volume of streamflow that were compared over the period analyzed (baseflow divided by streamflow) in Sections 3.1.1, 3.1.2, and 4.2 to clarify**. **Additional text has been added to Section 4.2 to make the point that the variability of the BFI values as shown in the report (Figure 4, Figure 5, and Appendix B) is quite dramatic throughout the year with values of baseflow increasing in the late summer and early fall when GW discharge sustains streamflow, results that agree with those described by Savoca et al. (2009), and also indicating that during periods of higher streamflow the BFI ratio is reduced.**

See also the additional responses to comment #6, since it is related to the possibility of GW discharge rates being overestimated. Furthermore, the comment here, stating that most baseflow comes from wet and/or snowmelt seasons is contradictory to the statement provided in comment #3 that the baseflow is a dry period issue.]

6) I don't understand in Figure 8 how mean groundwater discharge could be so much larger than mean recharge. Seems like those should be in balance. Otherwise, where's the groundwater coming from? It can't be crossing basin divides for all the gauges!

[Response: Agreed, we were anticipating better agreement on average, despite there being some sub-basins that do have a good match. Text already exists in the report in Section 5.3 stating: "The discrepancy between GW recharge and GW discharge rates was larger than anticipated for a majority of sub-basins." The estimated GW discharge rates are still less than the precipitation rates (almost entirely, except for the few instances pointed out in the second paragraph in Section 4.3), which could be due to physical processes such as ice melt or long-term losses from storage but also could be due to inaccuracies in precipitation rate estimates and errors in streamflow rates as well (also possibly the overestimation of GW discharge from the methods used). **Text has been added to Section 4.3 to call out the one instance of this from the Lyne-Hollick method. Furthermore, additional discussion of potential for underestimation of the GW recharge rates (and added text) to comment #7 on Task 300 for Reviewer 3, along with additional text addressing how GW discharge rates may be biased high in certain basins, to Section 5.3.** See also response to Reviewer 2 comments on Task 300 Section 4 Results.]

7) Overall, I think there's a major conceptualization problem here. I assume that where this is going is to try to understand how groundwater withdrawals affect low flows. But as indicated above, the analysis that's presented is completely dominated by the high flow times of year. I strongly suspect that much/most of what's being identified as baseflow really is being sustained by bank storage, which occurs quite close to the stream channel, and probably is pretty much independent of anything that happens in the groundwater flow field very far (e.g., tens to hundreds of meters) from the channel. It seems to me that more attention is needed to the low flow periods, in late summer, which are much more connected to for instance fish survival, water temperatures, and so on. I don't think the analysis that's been presented deals with these issues.

[Response: It is important to be cognizant of the objectives, with one related one that is copied here: "**In addition to the stated objectives, this study also provides discussion about the results, particularly comparisons between the GW discharge and BFI estimates from the different baseflow separation techniques, as well as the possible causes for differences between GW discharge and GW recharge estimates (and precipitation), including methodological and**

**temporal differences, along with potential accuracy concerns and possible influences caused by reservoir releases on the highly regulated Skagit and Baker Rivers."**

Perhaps the total period of record calculations of the BFI are the focus of this reviewer comment. The breadth of the results presented also include calculations of the daily statistics (including tables/plots) of the BFI from two methods (and six to seven different calculations for each gage). While it is common to use an alpha value of 0.925 for use of the Lyne-Hollick method, our preferred alpha value is 0.98, which overall reduces the BFI by comparison. There are increases in the BFI during low-flow periods and decreases in the BFI during high-flow periods, so the methods used intuitively make sense when viewed in this light (see for example Figures 2, 4, and 5, and Appendix B) and related discussion added to the text to Section 4.2. It has already been noted that higher variability in the results from the Lyne-Hollick method are generated as compared to the BFS Model.

*Task 400 (Surface/groundwater interaction)*

My take on this report is that it attempts to rectify the 200 (hydrogeologic characterization) and 300 (baseflow) reports. Its domain, however, is much smaller than the 200 report's, something that needs to be addressed (or at least acknowledged and justified).

[Response: The Surface/ groundwater interaction study objectives are related to Tasks 200 and 500 reports. However, this Task 400 study was spatially limited to a subset of the Task 500 aquifer modeling because of budget limitations. They findings are related to the other tasks but not dependent on them. Task 300 is basin scale and so the findings from this study are less directly applicable to the Task 300 study.]

In general, this report is better written than the 200 and 300 reports. It is, however, a little confusing as to what constituted the seepage run vs hydraulic gradient measurements. I believe (but am not certain) that hydraulic gradient measurements were based on pairings of piezometers and stream gauge water levels. However, this is not entirely clear in the report, as "seepage run" measurements were also made, and what they consist of isn't well stated (possibly difference in water levels between upstream and downstream piezometers?

[Response: The Seepage Run was simply the synoptic measurement of stream and tributary flows during the same day, which is used to construct a water balance. The hydraulic gradient measurements are indeed based on pairings of piezometers and stream gauge water levels. These differences will be clarified in the report.]

In any event, both sets of measurements (hydraulic gradient and seepage runs) were made at multiple locations along two Skagit River tributaries (both entering from the north side). Gaining reaches were identified when the piezometer water level was greater than the stream water level, and the reverse for losing reaches. They also took differences in stream discharge (I believe, also not clear from the report) between upstream and downstream locations, and after accounting for lateral inflows, determined gaining and losing reaches based on the signs of the differences.

[Response: This interpretation is correct.]

*Other comments:*

1) I don't understand what "manual tape-down measurements" means in section 3.1.

[Response: Updated for clarity. These indicate measurements from top of casing to the static water level.]

2) In Figure 8, it's not clear what's being plotted. The left axis label says "groundwater head, dh", but the dh implies a head difference (but between what and what)? The right axis is hydraulic gradient, which must be a head difference divided by a distance, but difference between what and distance aren't clear.

[Response: The values correspond to the explanation in section 2.3.3 and Figure 4. Groundwater head, dh, refers to the difference in water surface elevations between the piezometer and the stream.]

3) What are M_0_G and M_0_P etc. in Figure 9?

[Response: M_O_G = Muddy Creek, Station 0 , Stream gage; M_0_P = Muddy Creek, Station 0, Piezometer]

I don't get much from the discussion. For instance, at the beginning it says "Grandy Creek is gaining GW mostly from the outwash deposits", but then "it appears that both Grandy and Muddy Creeks are losing streams within the floodplain during the low-flow period". It's not at all clear how they get from one to the other. I am glad to see that they focus (at the very end) on the low flow period, as this should in my view be the main motivation for the analysis. But they need to be much more specific about that focus.

[Response: Additional interpretation will be added to the discussion The discussion relies on the aquifer characterization (Task 500) which was not completed until spring of 2025 (Williams 2025). Both documents now reference each other and provide a consistent discussion. Williams (2025) provides a more complete discussion of hydrogeology as related to seepage run results. This document summarizes their interpretation.]

4) It's also confusing that some of their gradient observations shown in Figures 6 and 8 are for late summer, where others go for 6-8 months. They need to do a much better job of interpretation.

[Response: An explanation has been added to the methods subsection 2.3.1. The original intent was to measure at least 1 month during late summer of 2023. Piezometers were installed in the spring of 2023, with the intent of validating that the piezometers were functioning and representing shallow groundwater conditions. However, suspect connectivity with local groundwater or non-functioning level loggers resulted in uneven periods of record and the need to re-install and measure hydraulic gradients in the summer of 2024.]

*Task 500 (Three-dimensional hydrogeologic framework)*

This report seems to be more or less unconnected with the previous (200-400) reports. This is apparent in the study site, which appears to be different than in, for instance, the 200 report? Why? Also, as in the other reports, figures should be embedded in the text; it's really irritating to flip back and forth. Also, please indicate river miles along the main stem of the Skagit at the upper and lower boundaries of the study area.

The Task 200 report (submitted 9/2023) and Task 500 report (submitted 10/2024) were progress reports for an ongoing MS thesis for a geology student at Western Washington University to develop a hydrogeologic framework for the lower Skagit River basin. The MS thesis was completed in May 2025 and will serve as the final report encompassing tasks 200 and 500. Although the MS thesis was produced by Henry Willaims at Western Washington University, his thesis advisor, Robert Mitchell, and committee member Jon Riedel serve as coauthors for the project.

The MS thesis will satisfy most of the concerns expressed by the reviewers related to the 200 and 500 reports. For example, the MS thesis clearly states the motivation for the development of the hydrogeologic framework and emphasizes that the hydrogeologic framework is a generalized characterization of the lower Skagit valley and should not be used to make water management decisions. It will serve as a basis to guide future studies. The MS thesis Includes detailed maps, updated and additional cross sections and 3D conceptual models, a more detailed discussion, and conclusions and recommendations. Not included in the MS thesis are the 2D geology cross sections illustrated in the Task 200 report. The MS thesis focuses on the hydrogeologic units that lump some geologic deposits.

*Some other issues:*

1) Are the well logs used in this report the same as in the 200 report? If not, how are they different

Task 200 was a preliminary report that was expanded upon in the Task-500 report. The well log database was expanded in the 500 report and in the MS thesis.

2) Some (perhaps all) of the information in section 2 could be in the 200 report. This would also help rectify study areas and so on and tie the reports together.

Updated in the final MS thesis.

3) As with the companion reports, there isn't much said about the "big picture" of the study. Section 2.4 is explicit about fish habitat and the possible effects of groundwater withdrawals on low flows, which I believe is the concern underlying all the reports. This provides even more motivation for putting this information (which frankly is better than the material in the other reports) into an overview document.

The MS thesis contains an updated motivation in the Introduction.

4) What was the motivation for selecting the upper and lower boundaries of the study area (and if different from the other reports, why)?

The MS thesis clearly states that our objective was to characterize the aquifers in the uplands and terraces and floodplain aquifers and to test the hypothesis that the upland aquifers are hydrogeologically connected to the floodplain aquifers.

5) It seems to me that the ultimate objective (determining the effects of groundwater withdrawals on low flows in the main stem lower Skagit and some of its tributaries) is not going to be addressable without a validated numerical model. The information collected and analyzed in this report would part and parcel of that process, as would the other reports. I suggest that be stated explicitly. If that is the case, archiving and documenting the data collected and analyzed will be critical, and there should be a section in the report that states how this has been done.

Given the limited budget for this study, our objective was to use domestic well logs to establish the basis of a 3D conceptual that would serve as a guide for future studies, including groundwater modeling.

6) How is the well log database created for this report different from the one created for the 200 report? Seems duplicative.

The Task 200 report was preliminary and expanded upon in the Task-500 report. The well log database was expanded upon in the 500 report and final MS thesis.

7) One has to be skeptical of the information content of the single deep well given the size of the domain. How transferable is this information? Would it be possible to compare well logs from some of the shallower wells (perhaps the deeper ones among them) to get an idea of how laterally persistent the stratigraphic characteristics are, so as to at least make a rough attempt at interpreting information from the single deep well in a broader context?

Funding for the project allowed for the installation of one well. We chose a strategic location based on access on public land, a spatial gap in data, and site geology. The creation of 2D and 3D models in Task 500 attempts to relate the deep well data to other wells in the domain. However, there are few wells in the upland areas of Boundaries C and D.

8) How do the seepage run surveys in this report relate to the ones in the 400 report? Very curious that no mention is made of that activity?

The authors will clarify in the updated 500 report that the seepage run information is a summary of those in the 400 report. The authors clarify in the MS thesis that the seepage run information is a summary of the results in the 400 report produced by HDR, Inc.

9) I'm confused by the recharge section which seems unrelated to the analysis done in the 300 report. Clearly these need to be linked, especially given the huge apparent imbalance in the 300 report.

Groundwater recharge was roughly estimated to generally illustrate its variability in the study area for the MS thesis. It is not intended for a thorough water budget or to predict groundwater flow. The Task 300 report provides more detail over a wider area but generally agrees with our recharge estimates.

10) The (lateral) hydraulic conductivity estimates from sections 3.3 and 4.4 aren't connected in any interpretation. Generally, the ones from pump tests seem to be in the 100s of ft/day,, whereas some of the ones in section 4.4 are much lower. Most likely, the reason is that wells are intended to draw from high yield aquifers. The key question is, do those high hydraulic conductivity estimates indicate connectivity of the groundwater and surface water systems, irrespective of the occasional lower values? My guess is yes, but this is something the report should discuss.

The hydraulic conductivity (K) estimates were based on driller well-log pump test data traditionally used for specific capacity analyses and were only used to group geological deposits with similar K ranges into hydrogeologic units. As clarified in the MS thesis, units with both low and high conductivity values are connected to aquifers in the floodplain and surface water.

## REVIEWER 2

***General comments***

*Task 200*

Overall I found the technical memorandum for Study Task 200 well written. I do have a few questions/comments regarding the methods and some larger concerns about the conclusions.

*Methods:*

The study team did a nice job of retrieving well information from existing databases and putting in the effort needed to make sure the retrieved data were properly located geospatially and to summarize the varied well log descriptions into consistent soil type categories.

My main question with the methods resides with which wells were chosen to be included in the study versus excluded, and why, when recharge to the tributaries was a focus of one of the study tasks (Task 400), were only north-south transects developed. Additional east-west transects could provide insight into aquifer existence for supporting ground-water surface water connections along these tributaries. It seemed from the report for this task that many wells exist in the area but only those that aligned with a perceived N-S transect and didn't overlap with previous transects developed by the consulting company (HDR) were used. There was no mention of the number of well excluded versus included in the development of transect, and I wonder if a greater understanding of the subsurface could have been developed if additional transects were generated.

Clarified in the MS thesis is that only wells illustrating deep stratigraphy were chosen but were not abundant. East-west transects are illustrated in the MS thesis

Page 4 states, "Only wells with relatively good locational accuracy and with reliable data were used for the creation of hydrogeologic cross sections." What defines reliable in this context? Was a strict criterion used?

Clarified in the MS thesis.

Page 5 states, "Hydrostratigraphic interpretations are limited in part by the number of wells used for each cross section (i.e., interpolating between large distances), the number of gravel pit exposures, and our interpretations of the textural descriptions in well-driller logs made by well drillers (who are commonly not geologists)." As mentioned above, I am curious how many wells were included versus excluded in the analysis. I am also not clear how the gravel pit exposures were used in the development of the cross sections. I don't think, based on my reading, that they were explicitly used within the transects.

Clarified in the MS thesis.

*Conclusions:*

It is not clear to me based on the figures in the report, and on the text of the report, why there are statements in the executive summary and in the conclusion section indicating the existence of connections between the GT and the tributaries or the GT and the lower valley aquifer. The established transects were focused N-S and cannot really provide much information about connections between the GT and the tributaries in the same way that E-W transects would help clarify. The N-S transects can identify if there are potential aquifers in the GT but not if these formation are connected with the tributaries – unless one assumes the N-S transect formations extend uniformly in the E-W direction, which is unlikely to be correct. There could be confining units between the transect and the tributaries, for example.

The N-S transects help with identifying connections between the GT aquifer and the lower valley aquifer. But throughout the report, it states that the available information is inconclusive and hard to interpret with regards to a direct connection between these two formations. Section 4.1 stated, "Based on these observations, it is not clear what groundwater connections there may be between the lower alluvium within the valley and that within the GT." Section 4.2 stated, "At this point, it is not clear how well connected the GT aquifers are to the floodplain aquifers. No aquifer units appear to be interconnected between the floodplain and GT." Section 4.3 stated, "At this point, however, it is not clear how well connected the two aquifer systems are."

Thus, I was surprised to read in the first sentence of the conclusion section state, "Some of the Task 200 results suggest that the GT between Hamilton and Concrete may be important sources of groundwater for the Skagit River interconnected to several tributaries, including Muddy, Alder, and Grandy Creeks, and possibly also to the Skagit River mainstem via hydraulic interconnections between the GT and the alluvial valley aquifer materials." Prior to this point in the report, I had thought that the report was pointing to the opposite conclusion.

I think the report should be revised to more clearly and carefully provide conclusions that align with the results. Currently, it feels like the report is conflicting itself. In the same paragraph in the conclusion one sentence states, "Grandy and Muddy Creek cross sections suggest connections between the upper glacial and lower floodplain aquifer materials based on hydrostratigraphic units of sand that underlie the entire north side of the Skagit River valley," while another sentence in a few lines later states, "At this point, however, direct groundwater connections between the GT and the floodplain/river are not clear."

After sitting with these two sentences for a long period of time and puzzling over them, it could be possible the authors are meaning to say that the transects indicate the possibility of a continuous sand unit across the GT and lower valley, but whether this sand unit represents a groundwater connection is uncertain. More careful use of the word 'connection' throughout the report and more clarification of what is meant with the use of that word (e.g., material connection versus groundwater connection) would help readers more easily understand the report and its conclusions.

The Task 200 report was a summary of preliminary work. The MS thesis provides more detailed analyses and inferences about the hydrogeologic continuity between the terraces and upland areas to the north and the aquifer systems in the Skagit valley floodplain. A detailed discussion, conclusions, and recommendations are in the MS thesis.

*Task 300*

Overall, I found the report for Task 300 hard to follow and I found the fact that the estimated rate of discharge exceeded estimated rates of recharge highly problematic. Below I outline my concerns.

*Section 3 – Methods of Analysis*

Upon reading this section I had many questions about the decisions and approaches used. Later in the report, some of my questions were answered and addressed, but in general, it is good practice to put all of the method information together so readers do not get frustrated by a lack of clarity and understanding.

[Response: There are some instance where some details of the methods are discussed briefly in the results and discussion sections, but it seems like the details are appropriate for the context in those sections. The primary, and required, details about the methods are described in the appropriate location (in the methods section). Overall, the description of methods provides a balance between readability, details, main points, and discussion pieces.]

The specific questions that arose for me while reading this section initially included:

*3.1.1 Lyne and Hollick Digital Filter*

It was not clear what parameters in the equation on Page 9 were data, fitted values, or calculated values. Later, it became clear that alpha was not fitted (which I thought it was initially), but simply assigned a value.

[Response: **Additional text was added to Section 3.1.1 to clarify that the streamflow comes from stream gage measurement records, the quickflow (and baseflow) are calculated, and the alpha parameter controls how the filter influences the attenuation of the streamflow hydrograph.**]

Page 9 states, "To reduce the warmup and cool down issues that arise as the recursive filter moves though the data, starting values were specified for each filter pass with the first and last 30 days of data being reflected at the start and end of the records, as described (with a worked example) by Ladson et al. (2013)." I am not familiar with this method, but the terms warmup and cool down issues are not clear to me. What does this mean? I also don't know what it means for data to be reflected at the start and end of the records. Is this repeated data?

[Response: Reflected values are copies of the record of measurements in reverse order copied to the start and end of the period of record. For instance, the set of streamflow values starts with recorded values from the 31st measurement day, then goes to the 30th, then the 29th, and so on until the 30th reflected value is a copy of the 2nd streamflow day record, and then the 31st value analyzed is actually the 1st measurement value in the record. The inverse logic is applied at the end of the record as well. **This sort of detail would be too much to add to the text, so instead the following text has been added instead to help clarify: "Reflected values are just copies of the first and last 30 days of record added to the period analyzed in reverse order. The first and last measurement in the period of record are not copied/reflected."**]

Page 10 – why were the six alpha values chosen? What is the justification for these values? As presented, it feels relatively random, though I imagine there was justification to the choice.

[Response: The range chosen appeared to be reasonable based on review of the Ladson et al. (2013) article and the range from 0.90 to 0.987 they evaluated—**text has been added to Section 3.1.1 to indicate this**. Additionally, as can be seen in the results presented in Section 4.1.2, for instance on Table 4 and Figure 2, that there is a relatively large range of results that can be derived for the example gage shown (0.45 to 0.71 in Table 4) that corresponds with a large difference in how the baseflow component compares to the overall streamflow hydrograph throughout the year (relatively "spikey" with changes in baseflow by over a factor of 10 times with an alpha of 0.90, and relatively subdued with changes of less than about 4 times with an alpha of 0.99). **This comment has caused us to clarify that the analyzed time period for the presentation of the BFI values in Table 4 was for the period from 1/1/1981 through 12/31/2010.**]

Page 10 – the described method of deciding which alpha value gave the best results was very qualitative and made me question the validity of the approach. The text indicates it was just a visual judgment to decide which alpha value performed best. By the end of the report, I understood that results from multiple alpha values were carried forward through the analysis. But in the method section, it seemed that a single alpha value was going to be used and decided upon by simple visual judgment. At this point, it also was not clear to me if a single alpha value was used for the entire study, or if each gage had its own alpha value, or even if each storm event at each gage had its own alpha value.

[Response: The alpha value does not have a straightforward way to select it, as it is generally recognized as lacking a physical basis, and therefore the most appropriate value does depend on judgement/interpretation. For these reasons (already described in the text) in our case the selection of the alpha parameter values was informed by a sensitivity analysis, indeed with analyses carried forward with the use of six different alpha values. This was done despite 0.98 being the one adopted as the best alpha value.

**To clarify the last point, additional text was added to Section 3.1.1, "The most appropriate interpreted Lyne-Hollick singular alpha value to adopt has been selected as equal to 0.98, which was used in the analysis of baseflow for all 44 gages, over their entire period of record. The comparative analysis against the results from the USGS-developed Baseflow Separation Model (described in Section 3.1.2) retain the sensitivity analysis of the effects of altering the**

**alpha value across the range from 0.90 to 0.99. In each analysis that uses a different alpha parameter value, the value was held constant across the entire analyzed period of record."** Furthermore, it is worth pointing out that more evaluation of why 0.98 was adopted as the most reasonable value is discussed in the second paragraph of Section 4.1.2, including reference to another study (CSIRO and SKM 2010) that had also selected 0.98 as the best alpha value that included comparison to chemical tracer estimates of the baseflow index. Despite all of this, the fourth paragraph states, "there are not ~~very~~ considerably drastic differences amongst estimated baseflow statistics caused by varying the alpha parameter."]

*Section 3.1.2.*

Page 11 – BFI was finally defined. But it was used multiple times in the report before this point.

[Response: BFI is first introduced in Section 1.2 with a brief/general definition of how it is calculated.]

*Section 3.2*

The numbers of wells used in the analysis was conflicting in this section of the report. In section 3.1.2. it said that 31 wells were analyzed with the USGS Baseflow Separation Model. In section 3.2 is said 28 of the 33 gages could be analyzed using the USGS BFS Model.

[Response: Section 3.1.1 and 3.1.2 discuss the box-and-whisker charts, and later those charts are mentioned as being plotted in Appendix A. Going through all 44 plots in Appendix A, one will find that there are only 31 plots that include analysis using the BFS Model method. At the beginning of Section 4.1.3 there is further discussion about how 13 of the total of 44 gages could not be analyzed using the BFS Model method because calibration parameters have not been developed. The difference between 31 gages (44 minus 13) and 28 gages analyzed with the USGS BFS model stems from the reduction in the time window (1/1/1981–12/31/2010) used for the comparative analysis of baseflow to GW recharge—see all the gages listed in Table 2. **In Section 3.2.2 and 4.3 language was added to clarify this ("for comparison with GW recharge")**.

The value of 33 gages is clear from the language in the first sentence of the second paragraph of Section 3.2.2, that reads, "To extract data from the historic gridded GW recharge and precipitation datasets, first there was a need to delineate drainage basins associated with the gages analyzed for baseflow over the same time period (1/1/1981–12/31/2010), which is a total of 33 streamflow gaging stations (out of the 44 total gages analyzed for baseflow)."]

Page 12 states, "Then the basins were delineated based on the nearest stream location automatically by StreamStats." I don't know what this means. What is meant by the nearest stream location? How is the stream location used in basin delineation? Is it used as a boundary condition somehow?

[Response: **The nearest stream location, "to each gage point," has been added to the text.** Earlier in the paragraph the web-link to the USGS StreamStats page is provided. We did not want to delve too deep into the methodology in our report, since the way that StreamStats works can be read/understood from that resource. **However, additional text and another website reference has been added to help clarify.**]

Page 12 states, "Within each subbasin, the mean annual GW recharge from the gridded dataset was plotted against the GW discharge (baseflow) derived from the hydrograph separation of the two methods (Lyne-Hollick and BFS Model) with all six of the Lyne-Hollick alpha parameters analyzed." The direct use of baseflow to estimate discharge assumes that the gage used to get baseflow sits at the outlet of the basin from which recharge is derived. If the gage is further up inside the basin, and not at the outlet, there would be discharge into the downstream segment not captured by the gage. I have to assume that the method for estimating the contributing area for recharge to each gage is treating the gage as the outlet/end-point for the contributing area. Clarification around this aspect would be helpful.

[Response: Text already exists that clarifies this point at the bottom of page 11, as follows: "To extract data from the historic gridded GW recharge and precipitation datasets, first there was a need to delineate drainage basins associated with the gages […].” It should also be clear from Figure 1 and text at the bottom page 1 that the gages sit at the outlet of the Skagit Basin and the upstream subbasins analyzed for baseflow.]

*Section 4 Results*

In Figure 4 and Figure 5 the caption states, “including all gages and all years.” But the presented data are different. In Figure 4, the data seem to be for individual rivers. In Figure 5, the data seem to be for the entire data set lumped together (I think). More clarity on what is actually being presented would be helpful.

[Response: In Figure 4 the gages are first grouped by stream and then the median BFI value of each stream grouping is plotted by method on annual hydrographs. Similarly, in Figure 5, all of the gages are grouped together and their quantiles (0%, 25%, 50%, 75%, 100%) are plotted for each method with BFI on a daily basis on annual hydrographs. **Some additional language to clarify has been added to the text describing these figures in Section 4.2.**]

My biggest concern with this report is the finding that discharge far exceeds recharge. This result does not make sense hydrologically and points to an error somewhere in the process, either in estimating recharge rates (a previous report), estimating contributing areas, or estimating baseflow. The report does not take any concrete steps to address this discrepancy other than to say this result was surprising. It is in fact physically impossible to have more discharge than recharge. The result causes me to question the validity of the entire study. It is good to see that discharge is generally less than precipitation, but in some locations, the estimated discharge rate is close to or in one case exceeds the precipitation rate. These locations could use further scrutiny with regards to the baseflow estimates.

[Response: See responses to comment #6 on Task 300 for Reviewer 2 and comment #7 on Task 300 for Reviewer 3.

The draft report text of Section 5.5 (Potential Future Work) outlines several concrete steps (or at the very least discusses possible steps) to address the discrepancies between GW discharge and GW recharge rates. Note also that this study does in fact have a good match for about one-third of the sub-basins, and it provides clear indications of which basins should be investigated further to achieve better overall water budget estimates (where it might be possible to have the biggest effect in terms of getting GW discharge and GW recharge rate estimates to align). Another thing to point out is that factors that have been attributed to causing large errors in baseflow estimates are listed out already in the text, including: (1) the influence of reservoir releases (as discussed in the Section 5.4); (2) high elevation basins where snowmelt is a dominant mechanism generating runoff (which does occur in several areas of the Basin); and (3) sites that have isolated, extremely low flows as a result of drying or freezing for example. The impact of reservoir releases are also discussed

**Additional text has been added to Section 5.3 where the source of possible additional errors are described, and to Section 5.4 and 5.5 related to the relationship between large GW discharge to recharge discrepancies at gages downstream of at least one of the five major dams in the Basin**.]

The linear fits that cross the origin in Figures 8-11 need to be removed. The data are not well fit by the applied line, and if the authors checked the residuals of the fit they would see that fit is not appropriate. In Figures 8 and 10, I see an almost flat line. In Figure 9, there could potentially be a linear relationship with an intercept closer to 50 in/year. The authors should check the appropriateness of the fit if they chose to try it. But in figure 11, I see no clear relationship.

[Response: **All four figures (8, 9, 10, and 11) have been updated, with only Figure 9 retaining the linear relationship line (with the adjustment to allow the y-intercept to be non-zero with a value equal to 55.935 in/yr).**]

*Section 5.4 – Reservoir Releases*

I was caught off guard by this section. It felt completely out of place in the discussion section when nothing previously in the results or methods touched on this aspect of reservoir releases. If the authors want to keep this in the report, it needs to be better integrated and supported by the previous sections. It is not good practice to bring in a new idea/result into the discussion section.

[Response: **Additional text was added to Section 1.2 (Objectives) to provide the needed introduction about the discussion**

**of reservoir releases being included in the report, in the context of potential accuracy concerns.**]

*Task 400*

Overall I found the report for Task 400 easy to follow and the analysis well done. I had only a few comments and questions.

My main question when reading about the study was why a dry period was chosen for the seepage run survey – I am guessing there was a rationale for this decision. Including that rationale in the report would make it stronger. I was also curious why the seepage survey was not repeated over the year to capture the seasonality with this measurement that was captured by the pressure transducers and vertical hydraulic gradient measurements. Given the seasonality captured by the pressure transducers and vertical hydraulic gradients, I think it could be possible to push the study a bit further and have a more nuanced conclusion about the gaining/losing/neutral state of the streams. Currently, it seems the report has assigned stream sections as losing/gaining/neutral (e.g., Figure 5) based largely on the seepage survey with the pressure transducer data being used only as an additional piece of information that either aligns or conflicts with the seepage survey. A more nuanced approach would be seeing if the pressure transducer data can help inform an understanding of GW-SW interactions across seasons as well as along the stream spatially. Maybe a stream section is gaining in the dry period but losing in the web period, or vice versa.

[Response: I agree that the groundwater/ surface water interaction and dynamics could vary by season. We chose to focus on the summer low-flow season under the premise that among all seasons, the summer low-flow period would be the most sensitive to changes to groundwater levels from future water withdrawals. I clarified this point in Section 2.1 (Study Design). Given limited budget, we chose to focus on this time period. We did deploy level loggers in the spring of 2023 to validate successful installation and representativeness of shallow groundwater. As it turned out, level logger failure and no groundwater communication (Grandy 3) required re-installation at some locations in 2024.This resulted in a “mixed bag” of piezometer and stream gage periods of record.]

*Task 500*

When reading the Task 500 report I was confused about what was new information specific to this task versus what was information gleaned from the previous tasks. I had the sense that a lot of the presented information was based on the previous tasks and not new results.

I suggest revising the report to clearly specify what is new work versus what is being pulled from the previous tasks. The bullet points listed section 3 Methodology include many aspects that I think are based on the previous tasks. Section 3.1 Well Log Database – is this the same databased developed in Task 200? If yes, referencing that report would be helpful. Section 3.2 Fieldwork and New Well – for the new well aspect in this section, is this the same deep well described in the Task 200 report? Section 3.4 & 3.5 – the 2D cross sections mentioned, are some of these cross sections the same as the Task 200 report? Section 3.7 Recharge – is this based on Task 300? Section 3.8 Seepage Run Survey – is this based on Task 400? It was hard for me to evaluate the report when I wasn't sure where the information was coming from.

This report seems like the culminating effort of the previous tasks and the goal of the larger study – the development of a conceptual 3D model of the area. However, the report had no discussion or conclusion section. I was left wondering what was actually learned and how this culminating conceptual model can or has been used to help inform groundwater resources or management in the Skagit.

The Task 200 report was a summary of preliminary, ongoing work that was built upon for Task 500 and the MS thesis. The Task 200 report was delivered 1.75 years ago and much more work has been conducted, and on task 500. The MS thesis is serving as the final report and includes a more robust discussion, conclusions, and recommendations

## REVIEWER 3

***General comments***

*"Task 200"*: the first phase of evaluation of the possibility of connections between upland glacial outwash terrace and Skagit River alluvial valley deposits.

The evaluation was done by developing 3 hydrostratigraphic cross sections using the "Xacto Section tool add-on to ArcMap" and are mostly based on domestic water well logs, geologic maps, LiDAR DEM, gravel pit exposures, previous reports, and one 310 foot deep monitoring well.

p1: "The cross sections and geology literature reviewed indicate the occurrence of unconfined aquifer materials in the upland (glacial) terrace that are potentially connected to unconfined aquifers in the Skagit River valley, therefore they are hypothesized to have hydraulic connections with the Skagit River or its tributaries. Aquifers in the GT are variable in terms of number and extents of possible physical connections with the aquifer materials in close proximity to the Skagit River in the alluvial valley." This is a lot of hypothesizing...

A more detailed analysis is provided in the MS thesis. Natural systems are complex, so yes, inferences are made based on the best available information to offer some insight that may lead to further studies.

p3: "Acceptable wells were used to identify..." What makes a well "acceptable"? Depths and more details (from the previous paragraph)?

Clarified in the MS thesis.

p5: "Cross sections were created using the hydrogeologic unit interpretations to connect units from neighboring wells along each section together." How were these connections made? By "expert judgment," or was some type of "automatic" process used (i.e., something in the ArcGIS software)?

Software was used to synthesize the well-log database and human judgement based on geologic maps and field observations was used to interpolate where information was lacking. This is clarified in the MS thesis.

p5: "Passage of the ice itself over the GT left a thin (less than 16 feet) veneer of glacial till on top of the lacustrine and advance outwash sequences..." This seems to imply confined groundwater conditions, rather than unconfined (WT), since till is usually considered (very) low-conductivity.

Clarified in the MS thesis

p7: "Organic debris recovered during drilling is postulated to have an age of at least 20,000 years and may be much older." On what basis?

The MS thesis states that the organic material was carbon dated to range between 29-31,000 calibrated years.

p8: "both cross sections display unconfined conditions within the floodplain." How do you evaluate unconfined conditions in this instance? Did you find soil mottling, indicative of changes in water table height? Or do you mean you observed unsaturated sediments beneath the overlying clay layers? Or...?

p9: "Despite this, the inclusion of silt is very important and should not be overlooked, because every interval in the well has silt logged." Agreed.

Agree. Clast size was used to combine geologic deposits into hydrogeologic units in the MS thesis.

p9: "As seen in , individual cross sections..." ??? Missing some information here.

Illustrated in updated figures in the MS thesis.

p9: "The variability in subsurface geology and spatial gaps in well logs makes the interpretation of the possible groundwater connections between the GTs and Skagit River floodplain tenuous..." Agreed. "until more data are collected and analyzed in subsequent evaluations..." Not sure I believe a reliable hydrostatigraphy can ever be sorted out of this type of complex glacial/fluvial mess. I'm especially not certain that a meaningful 3D framework can be established.

A more detailed analysis is provided in the MS thesis. Natural systems are complex, so yes inferences are made based on the best available information to offer some insight that may lead to further studies.

Figure 5: No offense to the consultants that drafted this figure, but I am skeptical about the continuity of the "Gravel Sand" layer shown on this cross-section. Other than seeing similar grain sizes in several wells, are there mineralogical/petrological similarities between the wells? I suppose this is unknown, because drillers typically don't make those kinds of determinations.

Best judgment along with geologic maps were used to infer the stratigraphy and stratigraphic connections. Further study will be required. The MS thesis provides a discussion of the limitations of our interpretations.

Figure 9: Similar to my comments on Figure 5, I would say the "sand" layer connection between the Glacial Terrace and Skagit River Floodplain deposits is highly speculative.

Best judgment along with geologic maps were used to infer the stratigraphy and stratigraphic connections. Further study will be required. The MS thesis provides a discussion of the limitations of our interpretations.

Appendix D: This is an outstanding well log. I would have liked to see the construction details of the monitoring well placed in this hole, though.

Not available.

*Hydrograph Separation Report (Task 300)*

p9: Lyne and Hollick Digital Filter: This is a very poor explanation of the Lyne and Hollick (1979) method. From what is written, it is difficult for me to understand how this method works, what the alpha parameter represents, or what the outcome of the filtering yields. How is it that multiple applications of the filter improve the output, and why is the filter run "forward, backward, and forward" (in time, or in space)? Why three times? Why are different values of alpha used, and how would an investigator choose between them? What is the physical meaning (if any) of alpha? What criteria are used to determine whether or not filtering (and therefore hydrograph separation) are complete? Consideration of "whether the baseflow hydrographs were not too 'spikey' during storm events..." hardly seems like a quantitative factor.

[Response: See responses to Reviewer 2 comments under *3.1.1 Lyne and Hollick Digital Filter*. Almost all of these questions are addressed there. I will add that Table 4 and Figure 2 (and related text in Section 4) were developed as examples with the intent of informing the reader about how the method works and how the alpha parameter acts to vary the resulting baseflows (i.e., its sensitivity).

On that isn't addressed there relates to running the filter forward, backward, and forward (in time, or in space)? The filter is run three times based on the method outlined by Ladson et al. (2013), and it is run directionally with respect to time. Ladson et al. (2013) provides a succinct discussion about the number of passes that reads: "The number of passes that are appropriate to separate baseflow depends on the time step of the flow values. For daily data, it has been common to use three passes, and our recommendation is that this be continued. … Passes should be in order, forward, backward, Forward," and adding, "The number of passes has also been used as a calibration parameter in some studies with the objective being to match the appearance of baseflow derived from manual methods." **Such language, and some additional language about the method has been added to the text in Section 3.1.1.**]

p11: "Thirteen streamflow gages analyzed in this study have not been subject to this calibration, and therefore baseflow separation using this method is not currently possible." Presumably, not possible for these thirteen stations. Otherwise, why bring this method up at all?

[Response: **Good point, text added to end of second paragraph of Section 3.1.2.**]

p17 and elsewhere: Is there any reason to think the Murray-Darling basin is a good analog to the Skagit River basin?

[Response: Hard to say, it could, but the discussion is not meant to imply that. **Clarification around this point has been made to the text in Section 5.2 in the Discussion of Findings section instead of the results (more appropriate here). Added text reads, "To be transparent, no attempt has been made in this study to assess how reasonable it would be to assume that the Murray-Darling basin is a suitable analog to the Skagit River basin. However, the use of chemical tracers to estimate baseflow at this scale is not common, and it provides an empirical measure not typically found."**]

p19: To what do you attribute the discrepancies between the two methods for these stations?

[Response: There is already a comparison presented between the calculated BFI values from the two baseflow separation methods in Section 4.2, and further discussion about the findings in Section 5.1.

Figures 8-11: The linear best-fit lines should not have been constrained to run through the (0,0) point. A constraint of this type causes an artifact in the fit; furthermore, it is clear that there does not need to be zero precipitation when the groundwater discharge is zero (for example). That is, there is no physical reason for the y-intercept of any of these plots to be forced to zero.

[Response: Agree, and in fact all linear relationship best-fit lines have been removed from the figures (except for Figure 9 where the y-intercept was not fixed at zero). See also the response to Reviewer 2 comment #4 under *Section 4 Results*]

pp33-34: "More effort in determining the physical basis for differences amongst the smaller number of sub-basins analyzed that have the largest discrepancy in resulting baseflow estimates amongst the two techniques investigated in this study." It looks as though this sentence was missed in proofreading, but the intent is clear: more work is needed to understand why some basins demonstrated large differences between the two methods. Too bad. I would be really interested in knowing why there were large discrepancies in some cases.

[Response: Thank you for pointing out this error missed during proofreading. The possible explanations for the differences (and similarities) have actually been explored and discussed, but to perform some of the work required to elucidate the physical basis for the findings is indeed out of scope work, and there could be a lot of debate about the most important areas within the Basin to study, and at what level of effort. **The text has been updated (at the end of the first paragraph of Section 5.1) to read, "More effort in determining the physical basis for differences amongst the smaller number of subbasins analyzed that have the largest discrepancy in resulting baseflow estimates amongst the two techniques investigated in this study would be interesting to study in more detail. While some efforts have been made to delve into the possible explanations for these differences, determination of the physical basis is not part of the scope of work of this study but could be the focus of future work, as discussed further in Section 5.5. Additional discussion about the details of the differences and similarities is provided in the remainder of this section."**]

p34: "estimated GW discharge rates that are higher [than] the GW recharge rates..." There is no reason these have to match on a short-term (e.g., annual) basis. There are a number of reasons why observed discharge may be higher than observed recharge. The most likely of these is that water is being removed from long-term storage (i.e., groundwater stored in aquifers is declining or glacial ice that contributes recharge is melting). Another possibility (also likely) is that the recharge estimates are wrong. Recharge is notoriously difficult to quantify, so this would not be very surprising.

[Response: We acknowledge that there are reasons why GW recharge would not be expected to match GW discharge on a short-term basis, but the time period was 30 years (1981 through 2010) that forms the basis of the comparison made. It could be argued that it is equally likely that GW discharge rates are wrong, and in fact there is likely error in estimates of GW recharge and GW discharge.

The purpose of the comparisons (between the two GW discharge methods, and between both GW discharge methods and the associated GW recharge estimates) was to elucidate the magnitude of differences to help in understanding the magnitude of the issue in these estimation methods—text has been added to Section 5 to focus attention on this point. In fact there is uncertainty in the alpha parameter used for the application of the Lyne-Hollick GW discharge estimation method, as outlined well in Table 4 and Figure 2 (Section 4.1.2).

**Text has been added to Section 5.3 to discuss the following results from other studies in comparison to the GW recharge rates reported from this study:**

**"It is acknowledged that there could be an equal likelihood for the GW discharge and recharge rate estimates to have high degrees of error. To elucidate the possible magnitude of the error of the recharge rates used in this study, they have a basin-wide mean of approximately 22 percent of precipitation (Yoder et al. 2021) over the long-term, while the study of Savoca et al. (2009) reports a recharge rate that is 33 percent of precipitation (for the lower Skagit Basin). In addition, the study of Thomas et al. (1997) reports GW recharges rates exceeding 50 in/yr in the alluvial valley near Darrington, while the comparable basin is shown to have a mean GW recharge rate of approximately 19 in/yr in this study. These comparisons appear to indicate, along with comparison against the GW discharge rates determined in this study, that the GW recharge rates overall could be underestimated.**

**With regard to GW discharge rates, there are a total of four subbasins analyzed that have GW discharge estimates that exceed the precipitation estimates over the long-term (see Figure 10 and Figure 11). The estimated GW discharge rates are still less than the precipitation rates almost entirely, with four instances of exceptions where GW discharge is greater than precipitation (as pointed out in the second paragraph in Section 4.3). The cause of this could be due to physical processes such as ice melt or long-term losses from storage but also could be due to inaccuracies in precipitation rate estimates especially at high elevations, and errors in measurements of streamflow discharge rates, and also possibly the overestimation of GW discharge from the methods used. To expand on this last possibility, the minimum and maximum**

**differences between the estimated long-term mean GW discharge and recharge rates amongst all subbasins analyzed with both GW discharge methods (n = 61) are -16.1 in/yr and 110.7 in/yr, with an average of 30.7 in/yr, and 13 of the largest estimates of GW discharge are greater than 50 percent of the mean difference of 30.7 in/yr, whereas only one of the smallest estimates of GW discharge have an absolute difference of greater than 50 percent of the mean. This indicates a bias toward large GW discharge estimates relative to GW recharge estimates."**]

*Surface Water Groundwater Interaction Study (Task 400)*

p3: "interactions will be evaluated by measuring the hydraulic gradient between paired GW...and SW...elevations..." I'm surprised the investigators didn't use seepage meters, either in place of or in addition to piezometers. I think seepage meters would be easier to use and interpret, and probably be just as accurate or more accurate than piezometer data.

[Response: Noted]

p3: If the seepage surveys were conducted only during low-flow periods, it is difficult to imagine they would be useful for a water balance, since seepage direction can reverse as the channel water level changes over the year.

[Response: It's true that these results are only applicable to the low flow period. This aspect of the study design has been updated in section 2.1]

p7: "when baseflow conditions were most prevalent." So, your data are biased. Since you are already anticipating baseflow (inflow from groundwater), you aren't really expecting a losing reach.

[Response: No. Baseflow conditions simply mean that the flow that is in the stream is from groundwater discharge, as opposed to surface and subsurface runoff. We expect to have both gaining and losing reaches during baseflow conditions. These results were only intended to be applicable to the low flow period, when baseflow conditions are most prevalent.]

p25: "This is likely because the water table is lower than the streambed elevation in the floodplain." It's not just likely--it is the only explanation physically possible. Water always moves from regions of higher head to lower head; therefore, if water is being lost out of the channel to groundwater, the piezometric surface (the water table) of the groundwater must be lower than the water level in the channel.

[Response: The word "likely" was the groundwater elevation was not directly measured. It was inferred from the lower downstream stream flow from the seepage run measurements.]

*Three-Dimensional Hydrogeologic Framework (Task 500)*

p3: "28 percent decrease in glacier contributions to summer streamflow, resulting in higher reliance on groundwater to support baseflows..." Are you sure about this? In some areas (e.g., the Chilean Andes) glacier melting contributes to higher recharge to groundwater and therefore increased baseflows--although, unfortunately, this is only temporary, and will cease when the glaciers finish melting.

We corrected the report to state that the reduction in glacial surface meltwater was 24% (Riedel and Larrabee 2016). We provide citations for historical glacier recession and projected due to climate change.

p9: Usually, drillers report specific capacity (pumping rate divided by observed drawdown). Also, equation 1 is a time-varying version of the Theis (1935) equation based on the Cooper-Jacob approximation, and drawdown data are generally evaluated using the Cooper straightline method, rather than assuming a storativity and iterating a transmissivity. It would be much more accurate and informative to use the Cooper straightline method--unless you didn't have time-series drawdown (i.e., all you had was specific capacity). It would have been proper to discuss these issues in your report.

The hydraulic conductivity (K) estimates were based on driller well-log pump-test data and were only used to group geological deposits with similar K ranges into hydrogeologic units. They were not used to determine groundwater flow rates or directions. When resources do not allow for long-term well tests, the three equations used to estimate K values are standard approaches used by the USGS in regional studies (e.g., Kahle and Olsen, 1995; Gendaszek, 2014). The estimated K values are consistent with hydraulic conductivities measured in similar glacial and alluvial deposits in Puget Sound aquifers.

p9 Equation 3 is a steady-state equation. Were the data you evaluated taken from a pumping well at steady state?

See reply to the comment above.

p10: Averaging estimates made from equations for which one or both may not be applicable does not result in an improved estimate. In statistics, this is known as the "emperor's nose fallacy."

The estimated K values were only used to group geological deposits having similar K ranges into hydrogeologic units. The estimated K values are consistent with the deposit types in other regional studies and were not used to determine groundwater flow rates or directions. This is clarified in the MS thesis.

p10: I am not a fan of "automated modeling" (i.e., Aquaveo and similar). This type of automatic generation of conceptual models cannot replace careful human judgment.

The modeling software was an efficient way to catalog and horizontally and vertically map the spatial distribution of nearly 150 well logs. We generated 38 cross sections, evaluated their quality and used our human judgment to interpolate and clarify the stratigraphy using geologic maps and field visits.

p11: Were the monitored wells pumping wells?

The wells monitored were domestic drinking water wells volunteered by landowners. Although the landowners were notified prior to field visits, the wells may have been operating their wells prior to the measurements (some were used for irrigation purposes). This is clarified in this in the MS thesis.

p11: Were the linear regression equations calibrated in any way?

No, the recharge relationships were not validated but are consistent with other regional studies by the USGS (e.g., Vaccaro et al. (1998). Groundwater recharge was roughly estimated to generally illustrate its variability in the study area, not for a thorough water budget or to predict groundwater flow.

p14: Alluvial fan deposits are distinct from fluivial (riverine) deposits, so the alluvial fans described here cannot be "deposited from the Skagit River tributaries via fluvial deposition."

We clarify in the MS thesis that the alluvial fans were formed by deposition from tributary streams. While the alluvial fans are typically composed of sand and gravel, some fans in the study area are finer-grained because of the glacial terrace geology they drain through.

p15: Was the area invaded by sea level rise at one time? I didn't know that (this is in reference to the "Glaciomarine Drift").

Yes, there was a marine transgression to about 100m elevation at the end of the last ice age. The weight of the continental glacier depressed the crust, and for a short time as sea levels rose lower Skagit Valley was inundated before isostatic rebound lifted the lower part of the valley above sea level.

p25: "This is likely due to the water table being lower than the st[r]eam depth in the floodplain, compared to the water table of the surrounding..." See my comment on groundwater flow direction in the Task 400 section.

Agreed. Both streams have gaining, losing, and neutral segments depending on geology. The seepage run analysis is detailed in the Task 400 report. We update our interpretations in the MS thesis.

p25: "The stream could be gaining water or losing water." If it is neutral, it is neither gaining nor losing.

Agreed. Both streams have gaining, losing, and neutral segments depending on geology. The seepage run analysis is detailed in the Task 400 report. We update our interpretations in the MS thesis.

I recognize the authors of this study were in a very difficult spot; that is, trying to discuss their observations and possible groundwater and surface water behaviors in a domain of incredible geologic and hydrologic complexity. I am grateful I didn't have to do this study. However, I dislike the ad hoc approach employed, by which I mean that every observation or potential finding is accompanied by a tailor-made explanation similar to "the stream is (gaining/losing/neutral) in this area, likely because (some possible thing)." It is better to sketch out a set of basic premises that control flow, then apply the basic premises to all the observations, noting whether or not they explain what is observed. If not, the conceptual model is probably not good. If they do explain the observations, the conceptual model may be good (more testing is, of course, desirable). By providing ad hoc explanations for every observation, every observation is made to fit, and there is no way of testing whether or not the underlying conceptual model is useful (i.e., has explanatory power). The ad hoc method is common, even in academic research, but it is not really helpful. Again, I do not envy the authors their position, in which they are forced to make a meaningful picture out of a jumble of noisy data (often collected for purposes other than developing a conceptual model). I think they have done a very credible job, considering the complexity of the site and the information they had to work with.

I think there was some very good information gained from these four tasks, and they have no doubt contributed to a body of knowledge on the Skagit River Basin groundwater. I also think it was premature to force the investigators to develop a 3D geologic and hydrogeologic model of the area. I think a very common response of agencies responsible for groundwater (or surface water) management is "we need a model." However, developing a model without having a very specific idea of exactly how it will be used and what questions it will be applied to answering is seldom, if ever, helpful. A model (geologic, hydrogeologic, or any other) should only be developed for a very specific purpose with a very narrow scope. I can't imagine the conceptual model developed in Task 500 will be useful for any purpose, and certainly not as a framework on which to develop a fully-integrated, basin-scale groundwater flow model. That is not, however, to say the work presented here is useless. In fact, I see great utility in the work they have done drawing together the data in this basin, checking it, putting the location information into a consistent format, and making it all available in a single source. This is an invaluable resource on which future investigators can draw on to make their own, very specialized, models (conceptual, geological, hydrological) for hypothesis testing.

The Conclusions and Recommendations section of the MS thesis summarizes the utility of the 3D conceptual hydrogeologic framework (the most extensive to date) as a basis to guide more detailed studies before groundwater management choices are made regarding water resources in the lower Skagit River Valley, including potential managed aquifer recharge (MAR) sites It also summarizes and limitations of the 3D framework because of the limited resources provided for the study.

Groundwater modeling would be the next logical step for examining the continuity of the aquifer systems and for determining recharge rates and groundwater flow directions and rates in the study area. However, applying Aquaveo's MODFLOW (USGS, 2025) extension to model groundwater flow would be challenging using the conceptual framework. We chose to break up the study area into four separate boundaries to capture and illustrate the complex nature of the hydrostratigraphy, whereas MODFLOW requires a single modeling domain. Also, the version of the Subsurface Analyst used to develop the conceptual models requires ESRI's ArcMap which is being phased out by ESRI. The conceptual models would have to be rebuilt using my well database and the ArcGIS Pro version of Aquaveo's Arc-Hydro Groundwater Subsurface Analyst.